Preface

Review of Pulmonary Physiology

David A. Kaminsky, MD[1] Kathryn A. Hibbert, MD[2] Andrew M. Luks, MD[3]

[1] Division of Pulmonary and Critical Care, University of Vermont Medical Center, University of Vermont Larner College of Medicine, Burlington, Vermont
[2] Division of Pulmonary and Critical Care, Massachusetts General Hospital, Harvard Medical School, Boston, Massachusetts
[3] Division of Pulmonary, Critical Care and Sleep Medicine, Harborview Medical Center, University of Washington School of Medicine, Seattle, Washington

Semin Respir Crit Care Med 2023;44:509–510.

David A. Kaminsky, MD

Kathryn A. Hibbert, MD

Andrew M. Luks, MD

It is our great honor and pleasure to present this special issue of Seminars in Respiratory and Critical Care Medicine devoted to pulmonary physiology. In this modern day of cell and molecular biology, the basics of pulmonary physiology are often overlooked and misunderstood by students and practitioners alike. These physiologic principles remain central to understanding human disease and treating patients, and while there are many excellent textbooks and other sources that cover the basics of pulmonary physiology, our goal was to provide a definitive source of information on not just the basics but also the wonderful complexities of the respiratory system.

We have had the great privilege to invite authors from around the world who are leading experts in each of the topic areas included. Dr. Ramon Farre starts the special edition with a discussion of the static mechanical properties of the respiratory system. Static lung volumes are determined by the pressure-volume characteristics of the mechanically linked lungs and chest wall, together with the surface tension forces modified by surfactant. The equation of motion relates pressure to drive airflow to static elastic forces as well as resistive forces, linking this first topic to the next article on the dynamic properties of the respiratory system by Drs. David Kaminsky, Don Cockcroft, and Beth Davis. This section examines how airway geometry determines airflow resistance during breathing, and why flow limitation develops due to the compressible nature of the bronchial tree. Consequences of flow limitation including airway obstruction, dynamic hyperinflation, and airway hyperresponsiveness are also discussed.

A number of highly specialized articles on the gas exchange functions of the lung follow. First, Drs. Susan Hopkins and Michael Stickland describe the intricate anatomy of the pulmonary vasculature, emphasizing its unique properties of recruitment and distension, the determinants of pulmonary vascular resistance, and its response to hypoxia. Next, Drs. Robb Glenny and Johan Petersson examine how gas exchange is influenced by the matching of ventilation and perfusion, and the role of gas diffusion. An extensive, two-part article written by Dr. Peter Wagner follows, which delineates the detailed steps involved in transport of oxygen and carbon dioxide and how these properties are uniquely determined by their respective binding curves with hemoglobin. Once oxygen reaches the tissue level, cellular respiration occurs, as described by Dr. Connie Hsai, who emphasizes the unique interactions of oxygen with hemoglobin and myoglobin and other molecules that optimize gas transport by convection and gas transfer by diffusion. Assessment of blood oxygenation and acid–base status is commonly accomplished by interpretation of arterial blood gases, which are discussed by Drs. Sarah Sanghavi and Erik Swenson. Such an analysis gives insight into how various blood gas disturbances are related to the bicarbonate/carbon dioxide buffer system and the effects of ventilation. Finally, Drs. Jerome Dempsey and Joseph

Address for correspondence David A. Kaminsky, MD, Pulmonary Disease and Critical Care Medicine, University of Vermont Larner College of Medicine, Given D-213, 89 Beaumont Avenue, Burlington VT 05405 (e-mail: david.kaminsky@uvm.edu).

Issue Theme Pulmonary Physiology; Guest Editors: David A. Kaminsky, MD, Kathryn A. Hibbert, MD, and Andrew M. Luks, MD

Thieme Medical Publishers, Inc.,
333 Seventh Avenue, 18th Floor,
New York, NY 10001, USA

DOI https://doi.org/10.1055/s-0043-1771162.
ISSN 1069-3424.

SHOUT
SHARE
IT

Welch discuss the mechanisms involved in the control of breathing, with an emphasis on the relationship between alveolar ventilation and CO_2 production, and how these mechanisms relate to common disorders of breathing control.

In the next section, Drs. Michael Pinsky and Natsumi Hamahata describe the global interaction of the heart and lungs, including an examination of the hemodynamic effects of intrathoracic pressure and ventilation under conditions of mechanical ventilation. The heart and lungs, of course, interact intricately during exercise, and the details of exercise physiology and measurement through cardiopulmonary exercise testing are described in the next article by Drs. Sietsma and Harry Rossiter.

We end this special edition with a survey of how the respiratory system performs in extreme environments. Drs. Marc Berger and Andrew Luks describe how hypobaric hypoxia and other environmental effects of high altitude affect the cardiorespiratory system. At the other extreme of pressure, Dr. Kay Tetzlaff discusses how the cardiorespiratory system copes with the high pressure and oxygen debt associated with diving. Finally, and particularly pertinent to the early 21st century, Drs. Jan Stepanek, Rebecca Blue, and Desmond Connolly take us on a journey to space and explain how microgravity, low ambient pressure, and other environmental stressors associated with space travel affect the functioning of the cardiorespiratory system.

The guest editors sincerely thank all of the contributing authors for providing such thorough and engaging discussion of each of the topics at the highest level of understanding. We hope this special edition not only provides a rich source of information on the physiology of the respiratory system but also challenges the reader to deepen their understanding of the inner workings of how we breathe and support cellular respiration both at rest and under various forms of stress.

Conflict of Interest
None declared.

Article published online: 2023-07-19

Ventilation Mechanics

Ramon Farré, PhD[1,2,3] Daniel Navajas, PhD[1,2,4]

[1] Unitat de Biofísica i Bioenginyeria, Facultat de Medicina i Ciències de la Salut, Universitat de Barcelona, Barcelona, Spain
[2] CIBER de Enfermedades Respiratorias, Madrid, Spain
[3] Institut Investigacions Biomediques August Pi Sunyer, Barcelona, Spain
[4] Institut de Bioenginyeria de Catalunya (IBEC), The Barcelona Institute of Science and Technology, Barcelona, Spain

Address for correspondence Ramon Farré, Unitat de Biofísica i Bioenginyeria, Facultat de Medicina i Ciències de la Salut, Casanova 143, 08036 Barcelona, Spain (e-mail: rfarre@ub.edu).

Semin Respir Crit Care Med 2023;44:511–525.

Abstract

A fundamental task of the respiratory system is to operate as a mechanical gas pump ensuring that fresh air gets in close contact with the blood circulating through the lung capillaries to achieve O_2 and CO_2 exchange. To ventilate the lungs, the respiratory muscles provide the pressure required to overcome the viscoelastic mechanical load of the respiratory system. From a mechanical viewpoint, the most relevant respiratory system properties are the resistance of the airways (R_{aw}), and the compliance of the lung tissue (C_L) and chest wall (C_{CW}). Both airflow and lung volume changes in spontaneous breathing and mechanical ventilation are determined by applying the fundamental mechanical laws to the relationships between the pressures inside the respiratory system (at the airway opening, alveolar, pleural, and muscular) and R_{aw}, C_L, and C_{CW}. These relationships also are the basis of the different methods available to measure respiratory mechanics during spontaneous and artificial ventilation. Whereas a simple mechanical model (R_{aw}, C_L, and C_{CW}) describes the basic understanding of ventilation mechanics, more complex concepts (nonlinearity, inhomogeneous ventilation, or viscoelasticity) should be employed to better describe and measure ventilation mechanics in patients.

Keywords
- resistance
- compliance
- elastance
- mechanical ventilation
- monitoring
- inhomogeneous ventilation
- viscoelasticity

The function of the respiratory system is to maintain the physiological partial pressures of O_2 and CO_2 in the blood to support tissue metabolism adequately. To achieve this aim, a fundamental task of the respiratory system is to operate as a mechanical pump generating ventilation, that is, ensuring that fresh air gets in close contact with the blood circulating through the lung capillaries. Alveolar ventilation, together with lung perfusion, makes possible the process of gas exchange through the alveolar–capillary membrane.

From a simplified mechanical viewpoint, the respiratory system is a reciprocating pump moving gas between ambient air and the alveoli.[1] Schematically, it consists of the airways, the alveolar compartment, the chest wall, and the respiratory muscles. The airways are a branching tree starting at the airway opening (nose and mouth) and the trachea, with approximately 23 subsequent bifurcations of progressively narrower bronchi, finishing in approximately 300 million alveoli. Each alveolus is a small air balloon (~100 µm radius) with a thin elastic wall separating the alveolar gas from the blood circulating through the lung capillaries lying at the external wall of the alveoli. Efficient gas exchange by passive diffusion through the alveolar–capillary membrane (~5 µm thick) requires that the alveolar gas is continuously renewed with atmospheric air. ►**Fig. 1** shows a diagram of the respiratory system from a simplified mechanical viewpoint. The airways are represented by a single tube (the trachea), and a bifurcation representing the bronchial tree, and the alveoli are represented by a homogeneous alveolar compartment. The lungs (airways and alveoli), with an air volume of V_L, are surrounded by an impermeable membrane (the visceral pleura) that is in contact with another similar membrane (the parietal pleura) which covers the inner

article published online
July 19, 2023

Issue Theme Pulmonary Physiology; Guest Editors: David A. Kaminsky, MD, Kathryn A. Hibbert, MD, and Andrew M. Luks, MD

Thieme Medical Publishers, Inc.,
333 Seventh Avenue, 18th Floor,
New York, NY 10001, USA

DOI https://doi.org/10.1055/s-0043-1770340.
ISSN 1069-3424.

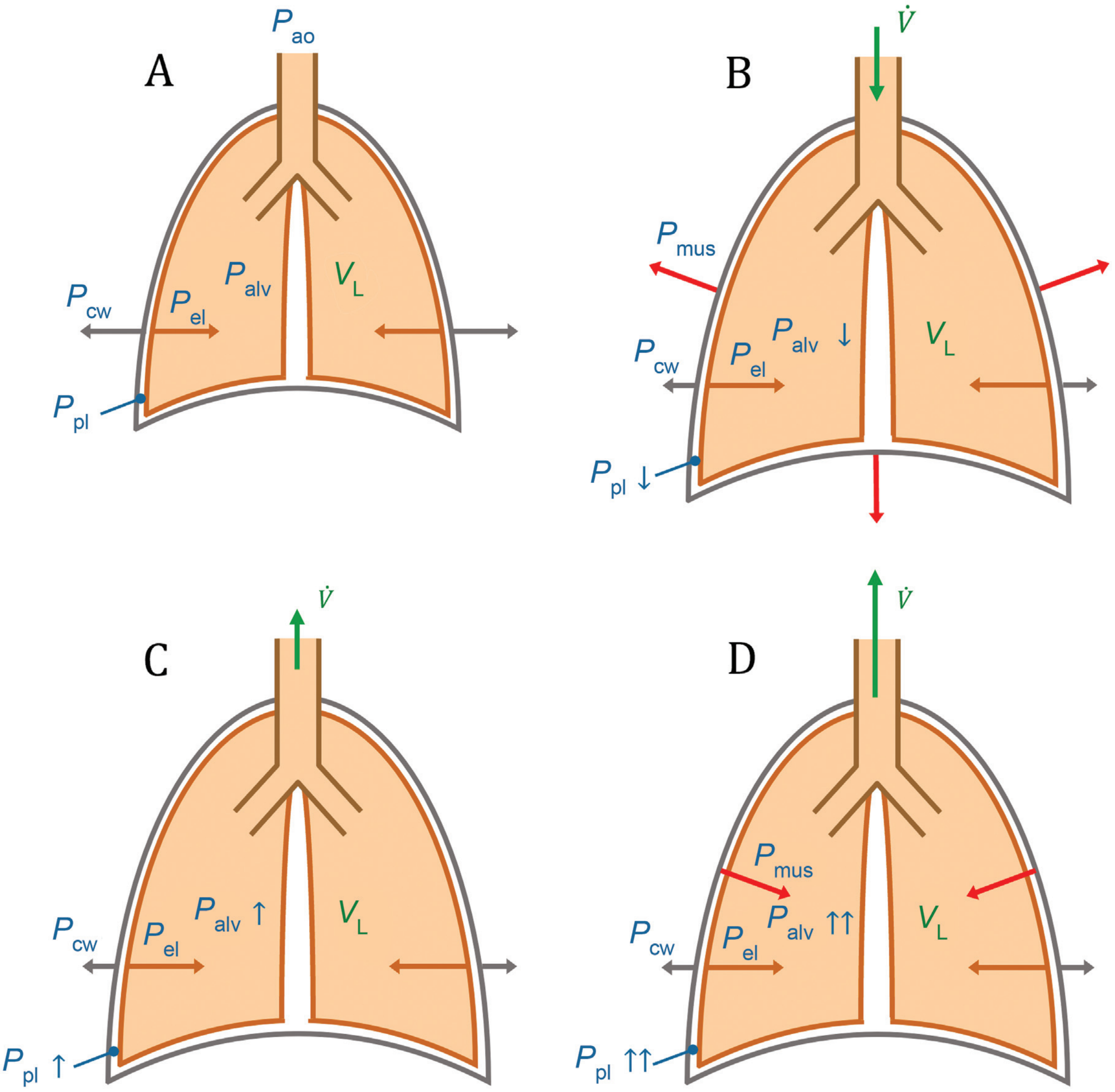

Fig. 1 Mechanical structure of the respiratory system. (**A**) Lung volume at end spontaneous resting expiration. (**B**) Inspiration. (**C**) Relaxed expiration. (**D**) Active expiration. P_{alv}, alveolar pressure; P_{ao}, pressure at the airway opening; P_{CW}, chest wall elastic pressure; P_{el}, lung elastic pressure; P_{mus}, muscular pressure, P_{pl}, pleural pressure; $\dot{V}$, flow; V, lung volume. Gray and brown arrows represent chest wall and lung elastic pressures, respectively.

part of the chest wall. The space between the two pleurae is an extremely thin liquid layer and plays the role of mechanically coupling the chest wall and lungs. Under normal conditions, the amount of gas between the two pleural membranes is negligible; hence, the volume of the pleural space does not change significantly with changes in pleural pressure. Due to this virtual adherence between the two pleural membranes, the lungs and the chest wall move together; therefore, the changes in lung and thoracic volumes are identical. The chest wall (rib cage and diaphragm) is an elastic compartment connected to the respiratory muscles. This anatomical structure is the mechanical pump allowing alveolar gas renewal for maintaining normoxia and normocapnia.

When the respiratory muscles are relaxed (►**Fig. 1A**), the lung–chest wall system is in mechanical equilibrium.[2] The pressure at the airway opening (P_{ao}) is usually the atmospheric pressure taken as the zero reference for pressure. V_L is the volume of the lungs, and P_{alv} and P_{pl} are the pressures at the alveolar gas and the pleural space, respectively. The volume at the end of the passive expiration is known as functional residual capacity (FRC); P_{alv} is equal to P_{ao}, and there is no airflow through the airways. As indicated by the arrows in ►**Fig. 1A**, at the equilibrium volume of the respiratory system, the lung is subjected to a certain degree of expansion: the elastic recoil pressure ($P_{el} = P_{alv} - P_{pl}$) is positive (and hence $P_{pl} < 0$). Moreover, the chest wall is partially compressed, so the elastic recoil pressures of the lung and chest wall (P_{CW}) are counterbalanced. Driving an inspiratory maneuver requires respiratory muscle contraction (mainly the diaphragm in resting breathing) to provide force, and thus pressure, for expanding the chest wall and the lung parenchyma (►**Fig. 1B**). The sealed pleural space experiences a reduction in pressure, inducing a decrease in alveolar pressure and thus expanding the lung above FRC. During inspiration, the flow through the airways ($\dot{V}$), which is the derivative of lung volume, is positive. End-inspiration is the point of the breathing cycle at which the recoil pressure of the lungs is maximal. In the second phase of the resting breathing cycle (expiration), the lung volume returns to FRC by exhaling the same air volume that entered the lung during inspiration. In normal resting breathing, expiration is started by the relaxation of the respiratory muscles, allowing the chest wall and lungs to recover the equilibrium volume of the respiratory system; expiratory flow is driven by potential energy that was stored during inhalation (►**Fig. 1C**). Under certain circumstances (e.g., exercise and chronic obstructive pulmonary disease [COPD]), expiratory muscle contraction contributes to increasing expiratory flow (►**Fig. 1D**).[3,4]

Mechanical Properties of the Respiratory System

Lung Volumes

Tidal volume (V_T), the change in lung volume during spontaneous breathing, is small compared with the range of lung volumes from maximal inspiration to maximal expiration.[5] ►**Fig. 2A** depicts V_L for several initial resting breathing cycles, ranging from FRC to FRC + V_T, followed by more intense breathing cycles where the subject increases V_T, with the end-expiratory lung volume below FRC. ►**Fig. 2B** shows resting breathing followed by the performance of a maximal inspiration to total lung volume (TLC) by the exertion of maximal contraction of inspiratory muscles, and by subsequent expiration to the minimum volume, the residual volume (RV), that the lung can achieve by maximal expiratory effort. IRV and ERV (►**Fig. 2A**) are the inspiratory and expiratory reserve volumes (i.e., the volume from end-inspiration to TLC and the volume from end-expiration to RV), respectively. Inspiratory capacity (IC) and vital capacity (VC; ►**Fig. 2B**) are the differences between TLC and FRC and RV, respectively. IRV, V_T, ERV, VC, and IC are changes in lung volume and, therefore, can be very easily measured while the subject is modifying his/her lung volume when connected to a mouthpiece and a volume spirometer (wearing nose clips). Alternatively, volume changes can be computed by integrating the flow signal measured by a pneumotachograph. By contrast, TLC, FRC, and RV are absolute volumes that cannot be assessed by simple spirometry. Interestingly, measuring only one of these absolute volume variables is sufficient to compute the others from the volume changes measured with a spirometer. In clinical practice, it is usual to measure FRC.[5]

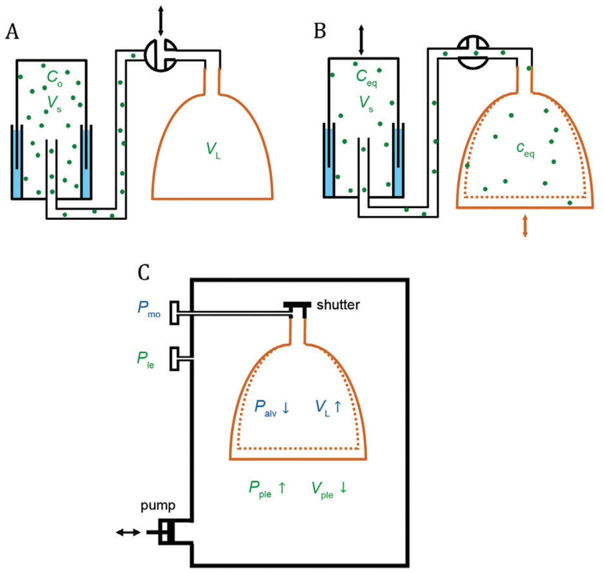

Fig. 3 Measurement of lung volume. (**A**, **B**) Helium dilution technique. (**C**) Body plethysmography. C_{eq}, concentration of He at equilibrium; C_o, initial concentration of He; P_{alv}: alveolar pressure; P_{mo}, mouth pressure; P_{ple}, plethysmograph pressure; V_{ple}, plethysmographic volume; V_s, spirometer volume; V_L, lung volume. The pump is used to calibrate the plethysmograph.

A clinical procedure to measure FRC is the helium dilution method.[6] As illustrated in ►**Fig. 3A**, the subject, having V_L, is

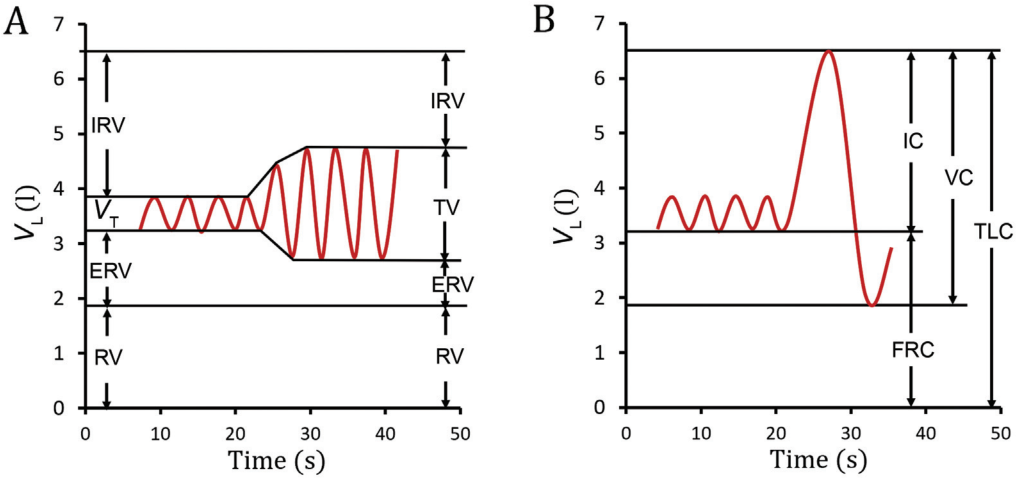

Fig. 2 Volumes and capacities of the respiratory system. ERV, expiratory reserve volume; FRC, functional residual capacity; IC, inspiratory capacity; IRV, inspiratory reserve volume; RV, residual volume, TLC, total lung capacity; VC, vital capacity, V_T, tidal volume.

connected to a volume spirometer through a three-way valve that is first open to ambient air. While the subject is breathing ambient air, the gas in the spirometer, with volume V_S, contains air with a known concentration of He (C_0). When the three-way valve connects the patient to the spirometer, the gas within the lung and the spirometer are mixed and, after several ventilation cycles, the concentration of He reaches an equilibrium (C_{eq}) at the spirometer and the lungs (►**Fig. 3B**), allowing the computation of V_L from V_S and C_{eq}. Another gas dilution approach to measure V_L is based on nitrogen washout.[7–10]An alternative method to measure V_L involves using a body plethysmograph, a closed box (~1,000 L in volume) where the subject sits and breathes spontaneously through a mouthpiece.[7,11] As schematically shown in ►**Fig. 3C**, the pressures at the mouthpiece (P_{mo}) and at the plethysmograph air (P_{ple}) are measured by pressure transducers. When the mouthpiece is occluded at end-expiration, an inspiratory effort of the patient against the closed airway induces a small increase in V_L (ΔV_L) by gas expansion and a reduction in P_{alv} (ΔP_{alv}). Applying Boyle's law to the gas enclosed in the lungs allows the computation of V_L.[4]

It is important to note that whereas the gas dilution techniques measure the lung volume that is ventilated during the breathing maneuver (i.e., mixing gas), the body plethysmograph technique measures all the thoracic gas in the lung regardless of whether it is ventilated. Accordingly, if there are areas of the lung with air trapped (e.g., by local bronchial occlusion by mucus), the lung volume measured by plethysmography is higher than by gas dilution.[12,13]

Elastic Properties of the Lungs

►**Fig. 4** shows the typical elastic properties of the lungs (volume-pressure relationship) and how they can be measured in clinical practice.[2,14] Exploring the compliance of the lungs requires determining the relationship between V_L and P_{el} ($P_{el} = P_{alv} - P_{pl}$). V_L can be computed by integrating the expiratory flow measured with a pneumotachograph and FRC determined by helium dilution or plethysmography. Since P_{pl} is difficult to measure directly, its value is estimated from the esophageal pressure (P_{es}), which is very close to P_{pl}. P_{es} can be measured by inserting a catheter with a small latex balloon attached to its end through the nose (or by similarly inserting a catheter-tip pressure transducer).[15–18] P_{alv} can be determined by measuring the pressure at the mouth (P_{mo}) during a brief interruption of airflow.

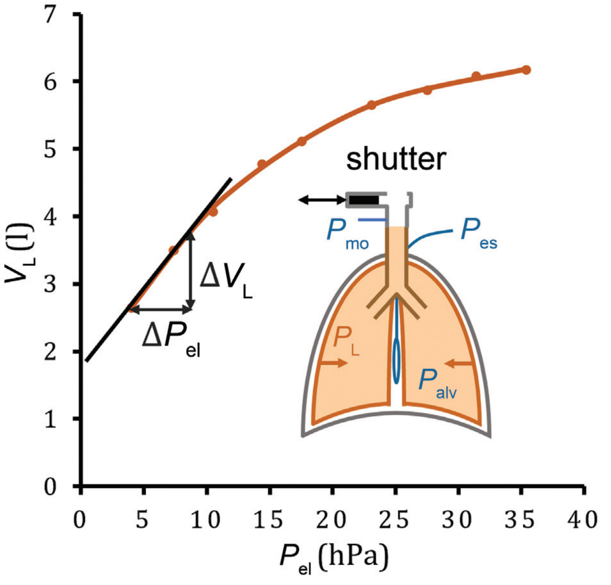

Fig. 4 Measurement of lung compliance. P_{alv}, alveolar pressure; P_{es}, esophageal pressure; P_{el}, elastic lung pressure; P_{mo}, mouth pressure; V_L, lung volume.

One procedure to determine the P_{el} – V_L curve is to perform a slow expiration from TLC to FRC. During this maneuver, airflow is briefly (1–2 seconds) occluded at regular volume intervals with a shutter placed at the mouthpiece. In this way, a pair of variables (V_L and P_{el}) is obtained for each shutter closure point (►**Fig. 4**). Lung compliance (C_L) is defined as the derivative (slope) of volume with respect to pressure ($C_L = dV_L/dP_{el}$) and quantifies how easy it is to expand the lungs. The slope of the resulting curve decreases with volume, indicating that the lung is less compliant, or more rigid, as its volume increases. It is possible to compute a linearized estimation for small volume changes as $C_L = \boldsymbol{\Delta} V_L/\boldsymbol{\Delta} P_{el}$. ►**Fig. 4** shows that the relationship is approximately linear at volumes close to FRC (P_{el} ~ 5 hPa). Accordingly, it is usual to take as the representative value of C_L the one calculated as the quotient $\boldsymbol{\Delta} V_L/\boldsymbol{\Delta} P_{el}$ for a volume increase from FRC to FRC + 0.5 L. The C_L value in healthy adults is approximately 0.2 L/hPa. (~ 0.2 L/cm H_2O). However, aging reduces the elastic recoil pressure and increases C_L. Notably, lung compliance depends on lung size. Indeed, applying the same pressure increase to two lungs with the same intrinsic elastic properties but of different sizes does not produce the same increase in volume. The C_L value calculated in the larger lung is higher since the absolute change in its volume is greater. To have an index accounting for the elastic properties of the lungs and not their size, the specific lung compliance (${}_SC_L$) is defined as the compliance per unit volume: ${}_SC_L = C_L/\text{FRC}$.

►**Fig. 4**, describing the expiratory pressure–volume relationship in the lung, was used to discuss the basic concept of compliance and thus only shows the elastic properties of the lung during an expiration from TLC to FRC. In an inspiratory and expiratory cycle measured in an isolated lung from the equilibrium volume of the lung (V_r) to TLC, a hysteresis loop is observed in the $P_{el} - V_L$ curve (►**Fig. 5**). Specifically, the elastic pressure is higher during inspiration than expiration for a given lung volume. This phenomenon contrasts with the behavior of a perfectly elastic system, such as a steel spring, characterized by superimposed deformation and recovery trajectories. Hysteresis is typical in complex elastic systems and involves energy dissipation since the energy required to inflate the lung is higher than the energy work recovered during its deflation.[2,19] ►**Fig. 5** also shows schematically the pressure–volume loop during spontaneous resting breathing, with lung volume varying from FRC to FRC + V_T.

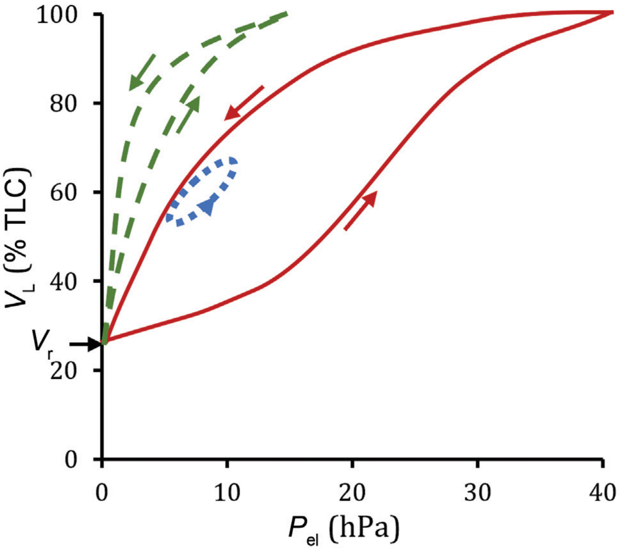

Fig. 5 Lung elasticity. Red line: Pressure-volume cycle of an isolated lung. Blue dotted line: Pressure-volume cycle of the lung corresponding to resting spontaneous breathing. Green dashed line: Pressure-volume cycle of the lung filled with saline. TLC, total lung capacity; P_{el}, elastic lung pressure; V_L, lung volume; V_r, equilibrium volume of the lung.

Tissue and Surface Forces in Lung Elasticity

Two main independent causes determine the most remarkable features of lung elasticity, nonlinearity and hysteresis: the elastic properties of the lung tissue and the surface forces in the air–liquid interface that covers the inner wall of alveoli. ►**Fig. 5** shows the typical $P_{el} - V_L$ loop in an isolated lung during air inspiration and expiration (the physiological condition) and when the same lung is inflated and deflated after the air is replaced by liquid. Filling the lung with liquid removes the air–liquid interface and thus the contribution of the surface forces. Therefore, the $P_{el} - V_L$ relationship in the liquid-filled lung exclusively corresponds to the lung tissue properties. Subtracting the pressure in the liquid-filled lung from that in the air-filled lung for each volume provides the pressure caused solely by the surface forces in the air–liquid interface. The considerable differences observed when comparing the loops in the figure illustrate that both lung tissue and surface forces have a relevant contribution to the elastic properties of the lung.

Lung tissue elasticity is determined by the intermolecular cohesive forces that oppose the extension of a complex three-dimensional framework of fibers (mainly elastin and collagen).[14] Notably, these elastic forces depend on the spatial arrangement of the fibers. Elastin fibers are highly distensible and, under physiological conditions, can increase their length up to twice their resting length, developing an elastic recoil force that opposes deformation. By contrast, collagen fibers can hardly be stretched. At low lung volumes, the collagen fibers are arranged in the network so that they are not subjected to stretch and thus do not contribute appreciably to the overall elastic recoil force of the lung. However, as the lung expands, the orientation of the collagen fibers progressively changes, increasing the fraction of the collagen fibers under tension. Hence, large pressures are required to increase lung volume toward TLC. Accordingly, collagen fibers act as a limiting factor for lung volume increase, with a low contribution to lung elasticity at the relatively low resting breathing lung volumes. Changes in the properties of elastin and collagen fibers or their spatial arrangement can explain the elastic alterations observed in aging or fibrotic lungs.

To better interpret the contribution of the surface forces in lung elasticity, the characteristics of the air–liquid interface could be interpreted by assuming that the alveoli are small spheres of radius (r) with the internal wall covered by a liquid layer. The relationship between transmural pressure (P_t: internal minus external pressure) and alveolar size can be estimated from Laplace's law ($P_t = 2\,T/r$), where T is tension at the alveolar wall. However, some of the predictions derived from this simple alveolar model are inconsistent with experimental facts. Indeed, the estimated pressure for an air–water interface ($T = 0.07$ N/m) with $r = 100$ µm is 14 hPa that seems an excessive value compared with the differences in the P_{el} between air- and saline-filled observed at reduced lung volumes, particularly in expiration (►**Fig. 5**). On the other hand, P_{el} should decrease with increasing alveolar radius, which is contrary to the data in ►**Fig. 5**. Finally, the model predicts a high alveolar instability since the larger alveoli would have more internal pressure if two alveoli had different volumes at any moment. Then, the air would flow from the smaller to the larger alveolus, which, far from balancing their volumes, would cause the collapse of the smaller one. All these model predictions, which are inconsistent with the experimental data, suggest that the simple model of an ideal air–water interface at the alveolar wall should be modified. Specifically, a reasonable model should allow that T of the alveolar interface is substantially lower than that of air-water, that the value of T increases with alveolar volume, and that, for a given volume, T is higher during inspiration than during expiration. These characteristics of surface forces can be in part explained by the presence of a tensioactive substance (surfactant) in the alveolar wall. Pulmonary surfactant, which is secreted by type-II alveolar epithelial cells, substantially reduces the surface tension of the liquid film that lines the alveolar walls and therefore diminishes the total recoil pressure of the lungs. Moreover, as the area of the interface increases, the surface density of surfactant molecules decreases, and thus the surface tension increases. This modulation of the interface forces contributes to stabilizing the alveoli, achieving a more synchronous air filling. The critical role played by surfactant is clinically manifested when its presence is reduced, either because of insufficient production (e.g., in immature preterm newborns) or because of pathologic alveolar epithelial dysfunction (e.g., in acute lung injury).[20–23]

Elastic Properties of the Chest Wall and the Total Respiratory System

The elastic forces developed passively by the chest wall tissues and the active forces exerted by the respiratory musculature are superimposed into the chest wall.[24]

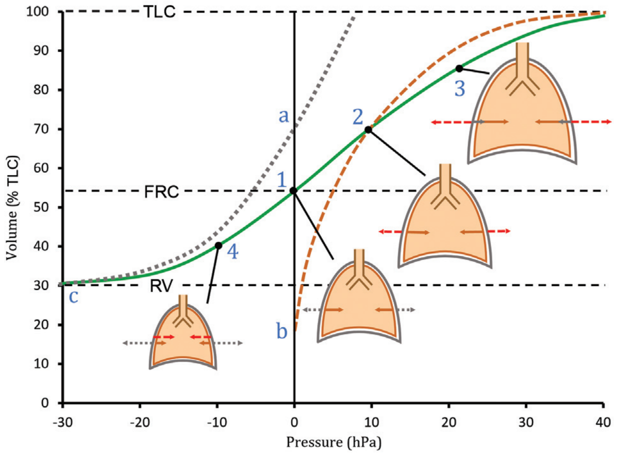

Fig. 6 Chest wall and respiratory system elasticity. Pressure-volume relationship of the lung (brown dotted line), chest wall (gray dotted line), and total respiratory system (green line). Gray dotted and brown dashed arrows represent chest wall and lung elastic recoil pressure, respectively. Red arrows represent muscle pressure. FRC, functional residual capacity; RV, residual volume, TLC, total lung capacity.

Transthoracic pressure, the pressure drop across the chest wall, is the difference between the pressure inside the thoracic cavity (P_{pl}) and the perithoracic pressure (usually the zero level of ambient pressure). Therefore, P_{pl} is the sum of the elastic pressure of the chest wall (P_{CW}) and the muscle pressure (P_{mus}), that is, $P_{pl} = P_{CW} + P_{mus}$. Hence, to assess the elastic properties of the chest wall, P_{pl} should be measured when the patient has his/her respiratory muscles fully relaxed ($P_{mus} = 0$). ►**Fig. 6** shows that P_{CW} increases with volume, remaining negative until the equilibrium volume of the chest wall is reached at approximately 70% TLC (point a on ►**Fig. 6**). The high equilibrium volume of the chest wall contrasts with that of the lungs (~15% TLC) (point b on ►**Fig. 6**). As indicated by the slope of the volume-pressure curves, the chest wall compliance (C_{CW}) increases with volume, which contrasts with the negative dependence of lung compliance on volume. C_{CW} at FRC in a healthy adult is approximately 0.2 L/hPa, similar to lung compliance. Below FRC, thoracic compliance decreases progressively and markedly, such that at volumes of approximately 30% of TLC, C_{CW} is so low that the volume can hardly be reduced (point c in ►**Fig. 6**). Thus, the RV of the lung is mainly determined by the elastic properties of the chest wall and the maximum expiratory muscle pressure. However, airway closure at low lung volumes can limit lung emptying, especially with advancing age. It should be mentioned that the chest wall elasticity also exhibits hysteresis, although of lower magnitude than the lung.[24]

►**Fig. 6** also shows the elastic properties of the total respiratory system by adding $P_{el} - V$ and $P_{CW} - V$ curves, where $P_{RS} = P_{el} + P_{CW}$ and the chest wall and lungs share a volume. The equilibrium volume of the respiratory system ($P_{RS} = 0$) is the volume (point 1 on ►**Fig. 6**) where the elastic recoil forces of the lung parenchmya and chest wall are equal and opposite to one another ($P_{el} = -\ P_{CW}$). For higher volumes, the elastic pressure of the chest wall is insufficient to compensate for that of the lungs and, hence, $P_{RS} > 0$. Therefore, to keep that volume, the inspiratory muscles must develop a negative pressure to counterbalance the elastic tissue recoil of the respiratory system. At a lung volume of approximately 70% of TLC the chest wall is in equilibrium, and inspiratory muscles should only compensate for the lung elastic recoil (point 2 in ►**Fig. 6**). The chest wall develops a positive elastic pressure for high volumes (>70% of TLC). Consequently, to keep these respiratory volumes, the inspiratory muscles must counteract both the tendencies of the lungs and the chest wall to compress (point 3 in ►**Fig. 6**). Accordingly, TLC is determined by the elastic properties of the respiratory system and the maximum inspiratory muscle pressure. At volumes below the equilibrium volume of the respiratory system, the elastic recoil pressure of the lungs is lower than that of the chest wall ($P_{RS} < 0$). Hence, the expiratory musculature should develop a positive pressure to maintain this low volume (point 4 in ►**Fig. 6**).

The lung and chest wall are two elastic compartments mechanically connected in series since the volume change experienced by each one is the same and the total pressure driving a given volume change is the addition of the pressures required to expand each of the compartments. Accordingly, the equivalent compliance of the respiratory system (C_{RS}) is $C_{RS} = C_L\ C_{CW}\ /\ (C_L + C_{CW})$.

However, by using elastance (E), defined as the reciprocal of compliance ($E = 1/C$), respiratory system elastance (E_{RS}) can be computed as $E_{RS} = E_L + E_{CW}$. Regarding the mechanical coupling between the lung and chest wall compartments, it is interesting to note that if air enters the pleural space (pneumothorax) through an abnormal pleural rupture (either visceral or parietal), the two pleural membranes are separated, the lungs contract, and the chest cavity expands, each compartment returning toward its equilibrium volume. In massive pneumothorax, contraction of inspiratory muscles expands the chest wall, but given the lack of mechanical coupling, the lung hardly expands, severely limiting the ventilatory capacity of the patient.

In diseased patients, E_{RS} can be altered by changes in E_L (e.g., in emphysema or fibrosis) or in E_{CW} (e.g., in chest wall deformities or morbid obesity).[13,25–30] However, E_{RS} is the variable that finally determines lung (and chest wall) volume. ►**Fig. 7** shows that in emphysema, characterized by loss of elastic fibers and destruction of interalveolar septa, there is an upward shift and steeper slope of the $P_{RS} - V_L$ curve, indicating increased respiratory system compliance. Furthermore, as the elastic recoil force of the respiratory system decreases, FRC increases since the equilibrium between the elastic forces of the chest wall and those of the lungs is reached at a higher volume. By contrast, in pulmonary fibrosis, characterized by stiffer lung tissue than in healthy lungs, the elastic recoil pressure of the total respiratory system is increased. Therefore, FRC is lower than in healthy subjects. ►**Fig. 7** also shows how abnormal changes in the lung (and thus in the total respiratory system) elastic properties in emphysema and fibrosis modify TLC. The colored area in the figure indicates the range of inspiratory pressures that normal respiratory muscles can exert for each lung volume. Maximal inspiratory pressure (>65 hPa, or

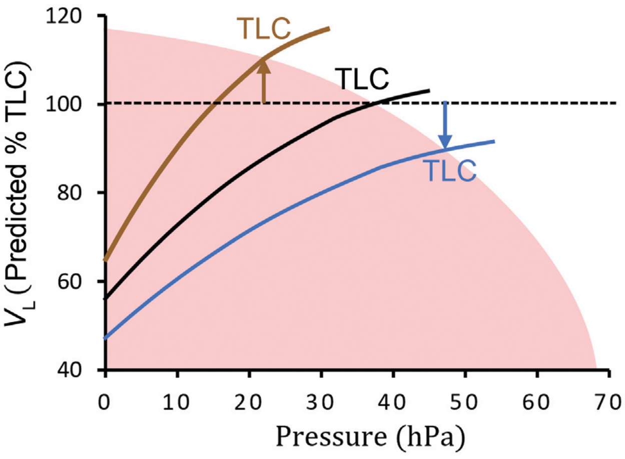

Fig. 7 Dependence of total lung capacity (TLC) on respiratory compliance. Solid lines depict the pressure-volume relationship of a normal respiratory system (black line), and with increased (brown line) and decreased (blue line) lung compliance. Pink area: range of possible inspiratory muscle pressures.

66 cm H_2O) is achieved for lung volumes around 40 to 50% of TLC. As lung volume increases above FRC, the maximum inspiratory force progressively decreases, approaching zero at a volume of approximately 120% of TLC. The colored area in the figure clearly shows that the inspiratory pump is not a constant-pressure pump. The loss in inspiratory pressure performance as lung volume increases can be explained by geometrical reasons. Indeed, as inspiration progresses, the muscle fibers considerably change their orientation (e.g., the diaphragm flattens) and thus the direction of the exerted force. The maximum volume the lung can achieve is determined by the intersection of the elastic pressure–volume relationship and the curve of maximum inspiratory pressure that the muscles can exert. In the case of the healthy lung, this intersection point defines TLC (100% of the predicted value) (►**Fig. 7**). In the case of emphysema (if the patient has intact inspiratory muscle force), TLC is increased. In contrast, TLC is lower in fibrosis than in a healthy lung.

Airways Resistance

The airway tree is composed by almost-cylindrical tubes (trachea, bronchi) each one presenting a resistance to air circulation.[31] As shown in detail elsewhere in this journal issue,[32] the pressure drop (ΔP) across a cylindrical conduit is proportional to the airflow ($\dot{V}$), and the conduit resistance ($R = \Delta P/\dot{V}$) is inversely proportional to the fourth power of its radius. The linear pressure–flow relationship is valid for a laminar flow regime, typical of low flows. However, at high flows the regime may be turbulent, and then the resistance increases with flow.

The trachea is the first generation of the airway tree splitting into the two lungs at the carina and successively bifurcates into bronchi and bronchioles (►**Fig. 8A**). The diameters of these tubes decrease as the generation progresses. However, as the number of parallel pathways is so high, the cross-section (S, sum of the cross-sections of all the airways of the same generation) increases remarkably, particularly when approaching the alveoli (►**Fig. 8B**). As the flow in each generation depends on its total cross-section and the mean air velocity of air (v) in the generation, the law of mass conservation (known as continuity equation when applied in this context) determines that air velocity ($v = \dot{V}/S$) decreases with airway generation. The flow regime during quiet breathing is laminar in almost all lung airways generations. The resistance of the airways (R_{aw}) can therefore be independent of flow during quiet breathing. However, during exercise, as flow and thus air velocity increase, the turbulences extend to more peripheral bronchi. Remarkably, R_{aw} is not distributed uniformly along the successive airway generations (►**Fig. 8C**). Given that the resistance of a conduit depends inversely on the fourth power of its radius and that the airway radius decreases (by ~15%) in each generation, the resistance of each of the parallel conduits in a generation increases progressively. However, since all the airways of the same generation operate in parallel, the equivalent resistance of the generation equals the resistance of one of the conduits divided by 2^N (N: generation number). As this exponential factor is so important quantitatively, it results

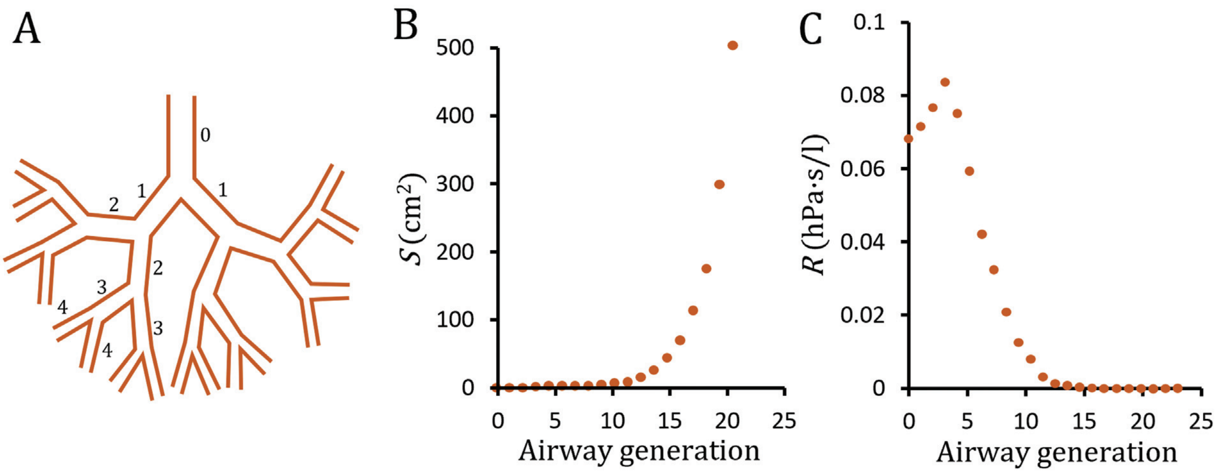

Fig. 8 Mechanics of the airways tree. (**A**) Diagram of airway architecture (five first generations). (**B**) Dependence of the airways cross-section area (S) on airway generation. (**C**) Dependence of flow resistance (R) on airway generation.

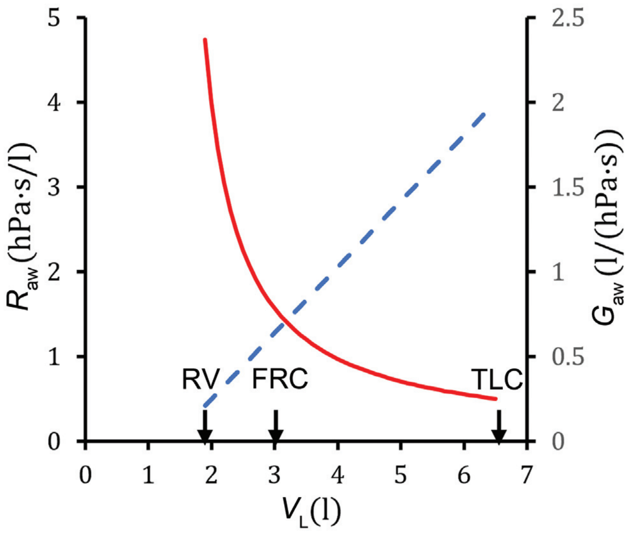

Fig. 9 Dependence of airways resistance and conductance on lung volume. Red line: airways resistance (R_{aw}), and blue dashed line: airways conductance (G_{aw}). FRC, functional residual capacity; RV, residual volume; TLC, total lung capacity; V_L, lung volume.

that the most peripheral generations, although with smaller airway diameters, have a modest contribution to R_{aw}. In healthy lungs, the central airways ($N \leq 7$–8, with $r > 0.2$ mm) contribute to approximately 80% of R_{aw}, thus peripheral airways contribute to only approximately 20% (►**Fig. 8C**). Considering that relevant lung diseases such as COPD involve the alteration of the most peripheral areas, assessment of changes in R_{aw} is not optimal for the early detection of these diseases. For instance, doubling the peripheral resistance (involved in gas exchange) barely represents a 20% increase in R_{aw}.

As R_{aw} depends on airway dimensions, a change in lung volume entails a variation in R_{aw}. Indeed, if lung volume increases, the elastic forces of expansion are transmitted throughout the whole tissues of the organ, augmenting airways dimensions, and consequently, R_{aw} decreases (►**Fig. 9**). For this reason, it is useful to define airway conductance (G_{aw}) as the reciprocal of R_{aw} ($G_{aw} = 1/R_{aw}$), which is a variable with an almost linear relationship with lung volume (►**Fig. 9**). Like in the case of normalizing compliance by lung size, to easily compare R_{aw} and G_{aw} for subjects having different lung sizes, it is common to normalize these variables by the corresponding lung volume (e.g., FRC) by computing the specific resistance (sR_{aw}) and conductance (sG_{aw}).[33]

The bronchial wall contains smooth muscles that may contract or relax depending on humoral and neural stimuli.[34,35] Contraction of bronchial wall smooth muscles generates a tension superimposed to the elastic recoil, reducing the radius and increasing R_{aw}. Similar to bronchoconstriction, relaxation of bronchial smooth muscles induces bronchodilation. Measurement of R_{aw} is therefore useful to test to what extent a patient (e.g., with COPD or asthma) is responsive to drugs or agents inducing bronchodilation or bronchoconstriction.[36–39] R_{aw} is usually measured using a body plethysmograph (like the one employed for measuring FRC).[8] For this application, when the subject breathes (with the shutter open), flow ($\dot{V}$) is measured by the pneumotachograph at the mouthpiece, and the pressure of the plethysmograph air (P_{ple}) is measured. As P_{alv} is estimated from P_{ple} using a plethysmograph calibration coefficient, R_{aw} is simply computed as $R_{aw} = P_{alv}/\dot{V}$. Interestingly, body plethysmography allows asking the patient to breathe at different levels of lung inflation to study how lung resistance depends on lung volume.

Spontaneous Breathing and Mechanical Ventilation

Spontaneous Breathing

The most simplified model of respiratory mechanics to describe spontaneous breathing assumes that: 1) the lung and pleural pressure are homogeneous; 2) the lung and chest wall are represented by their elastances (E_L and E_{CW}, respectively) at FRC, thus neglecting any viscoelastic and nonlinear behavior of these tissues; and 3) the viscous losses across the respiratory system are represented by the resistance of the airways (R_{aw}) at *FRC*, hence neglecting nonlinearities owing to turbulence and any resistive component of the respiratory tissues. Under such simplified assumptions, at any time (t) during inspiration, the driving pressure $P_{driv}(t)$ required to generate an inspiratory volume $\Delta V(t)$, being ($\Delta V(t) = V(t) -$ FRC), at flow $\dot{V}(t)$ has two components: a resistive pressure to account for the circulation of the viscous air through the airways and an elastic component to allow volume increase of the lung and chest wall (**Eq. 1**):

$$P_{driv}(t) = R_{aw} \cdot \dot{V}(t) + (E_L + E_{CW}) \cdot \Delta V(t) \quad \textbf{Eq. 1}$$

In general, $P_{driv}(t) = P_{ao}(t) - P_{mus}(t)$, and the respiratory system can be ventilated in three different ways: 1) spontaneous breathing ($P_{ao}(t) = 0$) by means of inspiratory muscles contraction ($P_{mus}(t) < 0$); 2) controlled mechanical ventilation in a patient with passive respiratory muscles ($P_{mus}(t) = 0$, $P_{ao}(t) > 0$); 3) assisted mechanical ventilation when the patient is breathing actively ($P_{mus}(t) < 0$) and a $P_{ao}(t) > 0$ is applied simultaneously by a support ventilator.

Thus, in spontaneous breathing, $P_{driv}(t) = 0 - P_{mus}(t)$ and therefore (**Eq. 2**),

$$P_{mus}(t) = -R_{aw} \cdot \dot{V}(t) - (E_L + E_{CW}) \cdot \Delta V(t) \quad \textbf{Eq. 2}$$

►**Fig. 10** shows the time course of the different mechanical variables computed in a resistance-elastance model from the resting flow recorded in a healthy subject. Lung volume ($V(t) = \text{FRC} + \int \dot{V}(t) \cdot dt$)) increases during inspiration from FRC up to FRC + V_T at end-inspiration. Alveolar pressure $P_{alv}(t)$ is negative and proportional to $\dot{V}(t)$ since the pressure drop across the airways ($P_{ao}(t) - P_{alv}(t)$) is simply equal to $-P_{alv}(t)$ because during spontaneous breathing airway opening pressure ($P_{ao}(t)$) is zero, and thus $P_{alv}(t) = -R_{aw} \cdot \dot{V}(t)$. At any time during inspiration, where the change in lung volume is $\Delta V(t)$, the elastic pressure ($P_{alv}(t) - P_{pl}(t)$) is the elastic pressure at FRC (P_L(FRC)) plus the change in pressure ($\Delta V(t) \times E_L$) required to increase lung volume by $\Delta V(t)$. Thus (**Eqs. 3** and **4**),

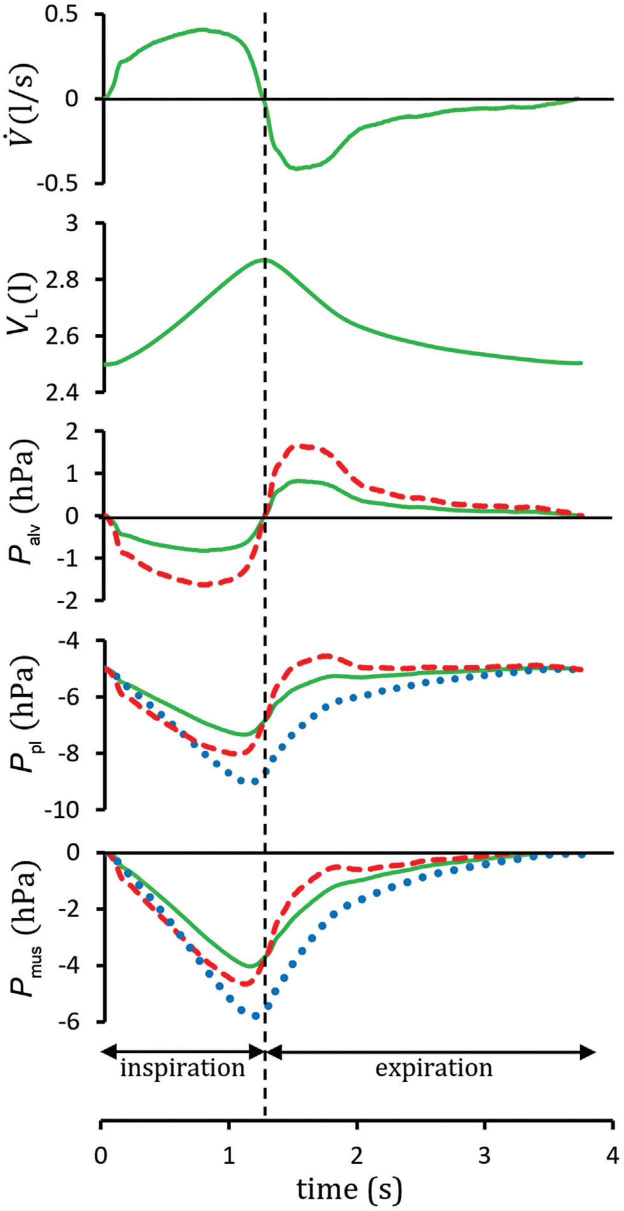

Fig. 10 Mechanics of the breathing cycle. Green solid lines: pressures computed from flow $\dot{V}$ recorded in a subject during a cycle of spontaneous resting breathing assuming normal airway resistance of 2 hPa·s/L, lung elastance of 5 hPa/L, chest wall elastance of 5hPa/l (green solid lines), and functional residual capacity (FRC) of 2.5 L. Model computation for an increased resistance of 4 hPa·s/L (red dashed lines) or increased lung elastance of 10 hPa/L (blue dotted lines). P_{alv}, alveolar pressure, P_{mus}, muscular pressure; P_{pl}, pleural pressure; V_L, lung volume. Note that in P_{alv}, red dashed and blue dotted lines coincide.

$$P_{alv}(t) - P_{pl}(t) = P_{el}(\mathrm{FRC}) + E_L \cdot \Delta V(t) \quad \textbf{Eq. 3}$$

and

$$P_{pl}(t) = -R_{aw} \cdot \dot{V}(t) - P_{el}(\mathrm{FRC}) - E_L \cdot \Delta V(t) \quad \textbf{Eq. 4}$$

$P_{pl}(t)$, which is already negative at *FRC* (typically approximately –5 hPa, or 5.1 cm H_2O) becomes more negative during inspiration. $P_{mus}(t)$ is the muscular pressure to generate the whole inspiration, that is, the addition of the pressure required to overcome airways resistance and to increase lung volume ($-R_{aw} \cdot \dot{V}(t) - E_L \cdot \Delta V(t)$) and the pulling (negative) pressure to increase the chest wall ($- E_{CW} \cdot \Delta V(t)$), as indicated by Eq. (2).

►**Fig. 10** also shows that the expiratory phase (negative $\dot{V}(t)$, and $V(t)$) decreasing to FRC) is characterized by an increase of $P_{pl}(t)$ up the value corresponding to FRC, and by a relaxing $P_{mus}(t)$ from the maximum pulling (negative pressure) at end-inspiration to a passive point ($P_{mus} = 0$) at end-expiration (FRC). As shown in ►**Fig. 10**, inspiratory muscles remain contracted in the first part of expiration, avoiding a sudden increase in expiratory flow. Expiratory muscles remain relaxed during expiration. However, the expiratory muscles can be activated during spontaneous breathing, particularly to reduce expiratory duration. For instance, during exercise requiring increased breathing frequency to augment ventilation or in patients with COPD. In this case, expiration through an increased airway resistance driven by the elastic pressure achieved during inspiration would result in low flow (and enlarged expiratory time). ►**Fig. 10** also shows how $P_{alv}(t)$, $P_{pl}(t)$, and $P_{mus}(t)$ change when there is an increase in R_{aw} (obstructive lung), or in E_L (restrictive lung) while maintaining the same ventilation ($\dot{V}(t)$ and $V(t)$). In the case of airway obstruction, the only change is in the resistive component of pressure ($P_{alv}(t)$) with no change in the elastic pressure component. In a restrictive lung, $P_{alv}(t)$ is not modified, and change in $P_{pl}(t)$ is caused by its elastic component.

Mechanical Ventilation

Patients with respiratory failure may be unable to maintain sufficient ventilation to ensure adequate gas exchange. The reason can be that considerably increased resistance and/or elastance do not allow the inspiratory muscles to generate enough pressure to induce the necessary ventilation to provide safe levels of blood gases, and/or that the high inspiratory effort required leads to muscle fatigue. A lifesaving treatment is to sedate the patient and provide mechanical ventilation: the action of the respiratory muscle pump is replaced by air pumping from an artificial ventilator.[40] Positive pressure ventilation is the most conventional modality in patients with severe respiratory failure. The patient's airway opening is connected to a positive pressure-generating cyclic pump through an endotracheal tube. Inspiratory flow is created by a positive pressure at the airway opening, thus inducing a positive alveolar pressure.

A mechanical ventilator is a servo-controlled cyclic pump that can be set to provide either predefined pressure- or volume/flow-controlled inspiratory waveforms.[41] In both cases, the ventilation variables are related by **Eq. 5**.

$$P_{ao}(t) - P_{mus}(t) = R_{RS} \cdot \dot{V}(t) + E_{RS} \cdot \Delta V(t) \quad \textbf{Eq. 5}$$

E_L and E_{CW} are added since the lung and chest wall are two elastic compartments connected in series ($E_{RS} = E_L + E_{CW}$).

In pressure control mode, $P_{ao}(t)$ is the controlled ventilator setting, and the resulting $\dot{V}(t)$ and $V(t)$ depend on the

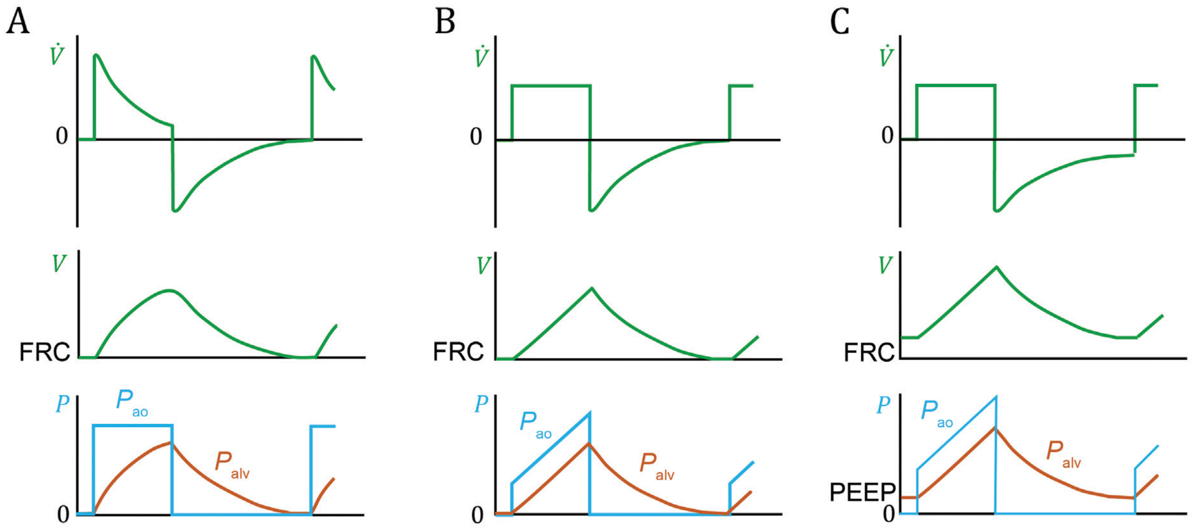

Fig. 11 Dynamics of positive pressure mechanical ventilation. Flow ($\dot{V}$), lung volume (V), airway opening pressure (P_{ao}), and alveolar pressure (P_{alv}) in a resistance-elastance linear model of a respiratory system ventilated with (**A**) constant pressure, (**B**) constant flow, and (**C**) constant flow in case of intrinsic positive end-expiratory pressure (PEEP). FRC, functional residual capacity.

values of R_{RS} and E_{RS} of the patient's respiratory system: inspiratory volume and flow change exponentially with a time constant $\tau = R_{RS}/E_{RS}$ (►**Fig. 11A**). Expiratory volume and flow are also exponential but in this case the time constant depends also on the mechanical properties of the expiratory line of the ventilator. In pressure-controlled mode, barotrauma can be avoided because $P_{ao}(t)$ is set, but there is a risk that ventilation is considerably reduced in case the patient's mechanical load (R_{RS} and/or E_{RS}) increases because of disease worsening (or accumulation of tracheal secretions). ►**Fig. 11B** shows an example of volume-controlled ventilation with constant flow inflation ($\dot{V}$). As $\dot{V}(t)$ and $V(t)$ are set, the value of $P_{ao}(t)$ applied by the ventilator depends on R_{RS} and E_{RS}. At the beginning of inspiration, there is a sudden step in pressure equal to $R_{RS} \cdot \dot{V}$. As inflation proceeds, this resistive pressure component is constant, and a linear elastic pressure component ($E_{rs}\dot{V}\,\Delta t$) is added as volume increases. The slope of this pressure ramp is determined by E_{RS}. With volume-controlled mode, ventilation is ensured, but in case of an increase in R_{RS} and/or E_{RS}, the pressure applied by the ventilator can be dangerously augmented. Pressure- and volume-controlled modes, each with their pros and cons, are widely applied in clinical practice and their selection depends on the patient's clinical status and the attending physician's criterion.[42]

Regardless of the control mode, the ventilator can be set to apply a positive end-inspiratory pressure (PEEP) to start inspiration when lung volume is slightly above the equilibrium volume, hence keeping some degree of lung hyperinflation which in some patients can be useful for avoiding partial lung collapse (atelectasis) and improving gas exchange.[43] In this case, Eq. 5 is modified to **Eq. 6** as follows:

$$P_{ao}(t) = \mathrm{PEEP} + R_{RS} \cdot \dot{V}(t) + E_{RS} \cdot \Delta V(t) \quad \textbf{Eq. 6}$$

In conventional ventilators, PEEP is applied by a built-in servo-controlled valve in the expiratory line that stops expiration when the airway pressure decreases to the PEEP value set. In more simple ventilators and resuscitation bags, PEEP can be set by connecting the expiratory line to a passive valve regulating pressure by the force exerted by a spring. In other cases, (e.g., pediatric bubble-CPAP), PEEP is set by placing a water column against the expiratory line.

Notably, regardless of the application of external PEEP, ventilation at a lung volume above the equilibrium volume of the respiratory system can occur under certain circumstances depending on the patient's respiratory mechanics and ventilation parameters. Indeed, dynamic hyperinflation appears when the expiratory phase is not sufficiently long to allow complete passive lung emptying until it achieves the equilibrium volume of the respiratory system. This can happen, for instance, when there is a considerable increase in expiratory resistance (either caused by lung obstruction or by the expiratory circuit), or when the ventilation frequency or the ratio between inspiration and expiration times is too high. Regardless of its specific cause, dynamic hyperinflation is associated with $P_{alv} > 0$ at the end of the expiration, which is known as intrinsic PEEP (PEEPi) or auto-PEEP. ►**Fig. 11B** and **C** compare an example of mechanical ventilation with ventilator, or extrinsic, PEEP set to zero and without and with dynamic hyperinflation, respectively. In the case of dynamic hyperinflation, inspiration starts when the expiratory flow has not reached zero. The existence of auto-PEEP can be realized by measuring the airway opening pressure after imposing an end-expiratory airway occlusion and finding a $P_{ao} >$ extrinsic PEEP.

Measurement of R_{RS} and E_{RS} in passive patients subjected to mechanical ventilation allows us to monitor respiratory mechanics and thus help evaluate the progression of the disease and the effectiveness of treatments. Such monitoring can be performed from the signals ($P_{ao}(t)$, $\dot{V}(t)$) recorded at the airway opening by sensors built-in the ventilator. A very simple procedure is based on applying a short end-inspiratory

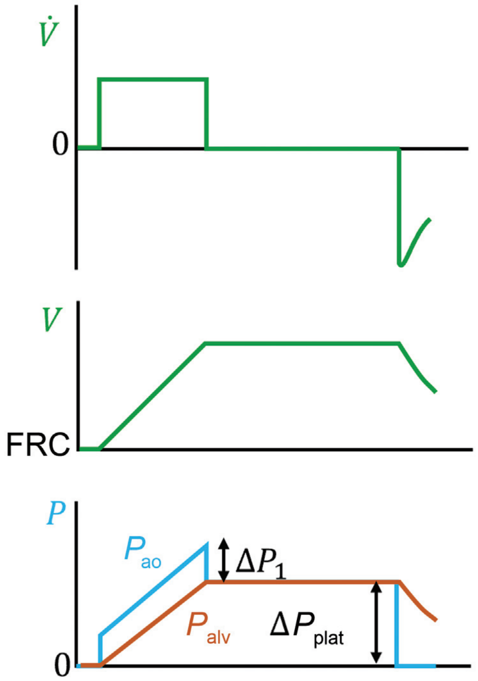

Fig. 12 Assessment of respiratory mechanics in mechanical ventilation with constant flow inflation by end-inspiratory airway occlusion. Sudden pressure drop (ΔP_1) and plateau pressure (ΔP_{plat}) after a short postinspiratory pause. FRC, functional residual capacity; P_{ao}, airway opening pressure; P_{alv}, alveolar pressure; $\dot{V}$, flow; V, lung volume.

pause (~5 second during controlled ventilation (V_T) with constant flow inflation ($\dot{V}$). As shown in ►**Fig. 12**, the application of an end-inspiratory pause allows for simple measurement of R_{RS} and E_{RS}.[44–47] Indeed, R_{RS} can be computed from the pressure drop (ΔP_1) ensuing just after flow interruption at end-inspiration. As this pressure drop equals $\Delta P_1 = R_{RS} \cdot \dot{V}$, then $R_{RS} = \Delta P_1/\dot{V}$. On the other hand, E_{RS} can be computed from plateau pressure (ΔP_{plat}). As ΔP_{plat} is the pressure change induced by a volume change V_T, $E_{RS} = \Delta P_{plat}/V_T$. The only correction required to refine the estimation of R_{RS} is to subtract the pressure contribution of the endotracheal tube for $\dot{V}$ from ΔP_1. As such a procedure to estimate respiratory mechanics virtually does not disturb ventilation, it can be applied periodically to monitor the patient's status in routine. Noteworthy, in the example of ►**Fig. 12** there is no *PEEP* (external or intrinsic). Performing an end-expiratory airway occlusion maneuver allows measurement of any intrinsic PEEP since then P_{ao} would equal P_{alv}. Then, E_{RS} would be computed as $E_{RS} = (\Delta P_{plat} - \text{PEEP})/V_T$.

Complex Features of Ventilation Mechanics

For the sake of simplicity, in the previous two sections describing the mechanics of spontaneous and mechanical ventilation, it has been assumed that the respiratory system is homogeneous, that is, composed of a monoalveolar compartment, a uniform pleural pressure applied around the lung, and a chest wall compartment. Moreover, it has been hypothesized that the model is linear, that is, R_{RS} and E_{RS} are constant regardless of lung volume and flow. Such simplifying assumptions can be reasonably applied to describe the main features of a healthy respiratory system during resting spontaneous breathing. However, the homogeneous linear model cannot satisfactorily explain the complex mechanical behavior of the respiratory system in patients during both spontaneous breathing and mechanical ventilation. Remarkable deviations from the homogeneous linear model are caused by flow limitation (addressed elsewhere in this journal issue),[32] nonlinearities, inhomogeneous ventilation, and tissue viscoelasticity.

Nonlinearities

When considering the whole range of possible lung volumes (from RV to TLC), the elastic properties of the lung depend on lung volume (►**Fig. 4**) and lung resistance depends on both lung volume (►**Fig. 9**) and flow (in turbulent regime). However, given that physiological ventilation occurs along a relatively narrow range of volume change (V_T) at FRC, it can be assumed that both the elastic and resistive properties can be linearized and thus a value of constant R_{RS} and E_{RS} can be considered for the volume range from FRC to FRC + V_T. Similarly, the nonlinear component of airways resistance caused by turbulences can be neglected for the relatively low values of airflow during spontaneous and mechanical ventilation ($\lesssim 1$ l/s). Accordingly, a linear approximation for R_{RS} and E_{RS} can be assumed for tidal ventilation. However, this hypothesis is questioned in some important ventilatory conditions in healthy subjects and particularly in patients.[48–60] A clear example in healthy subjects is exercise given the considerable flow values associated with high-amplitude and high-rate breathing.

In patients with severe respiratory disease subjected to mechanical ventilation, relatively high values of PEEP (>10 hPa, or 10.2 cm H_2O) can be applied to optimize gas exchange. A wide range of PEEP means that ventilation can be applied at different levels of lung volume. Consequently, the hypothesis of constant R_{RS} and E_{RS}, which can be reasonably assumed when breathing around the lung volume corresponding to $P_{ao} = 0$, can no longer be considered. Indeed, R_{RS} tends to be reduced and E_{RS} increased, respectively, as lung volume (and hence PEEP) is increased. Given that usually V_T tends to be maintained at relatively low levels, particularly in protective ventilation to prevent ventilator-induced lung injury, it is possible to follow a local linearization approach. Specifically, to consider that the respiratory system is linear within each ventilation cycle with V_T at a given PEEP, but that the R_{RS} and E_{RS} values depend on the specific value of PEEP. However, it could be possible that nonlinearities become apparent even within a single V_T maneuver, particularly at high PEEP values since the elastic properties are more nonlinear at high lung volumes.[48–51] In this case, the elastic nonlinearity is revealed by an upward curvature of the P_{ao} at the final phase of inspiration with constant flow.

Inhomogeneous Ventilation and Tissue Viscoelasticity

The simplest hypothesis to interpret ventilation mechanics is that the respiratory system is homogeneous. However, ►**Fig. 13** shows that in the normal standing position, and simply caused by the lung weight, there is a vertical

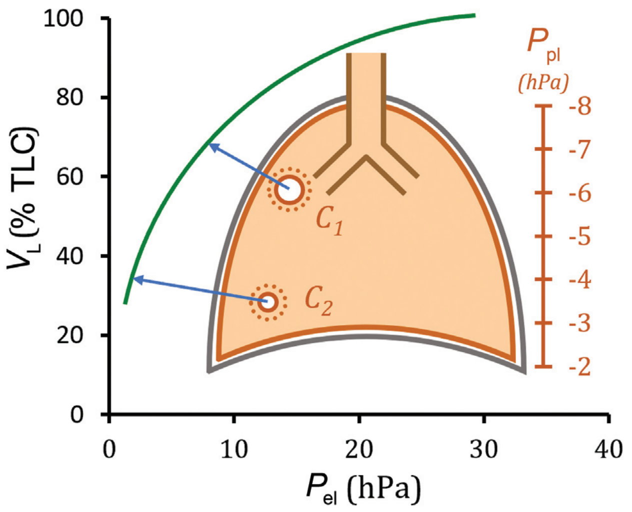

Fig. 13 Effect of gravity on pleural pressure. The green line is the pressure-volume curve of the lungs. C_1 and C_2 represent apical and basal alveoli, respectively. In C_1 and C_2, solid lines represent the alveoli size at functional residual capacity and dotted represent their volume for a given value of inspiratory alveolar pressure. P_{pl}, pleural pressure; P_L, lung elastic pressure; TLC, total lung capacity; V_L, lung volume.

distribution of pleural pressure.[52–54] The lower parts of the lungs are supporting the weight of their upper parts. As illustrated by ►**Fig. 13**, P_{pl} at FRC is not a unique value (typically assumed to be ~ -5 cm H_2O) but ranges from approximately −8 hPa at the lung apex to −2 hPa at the base of the lung. This P_{pl} gradient results in inhomogeneous ventilation. Indeed, at FRC, P_{alv} is zero at all the alveoli since there is no flow and no pressure drop across the airways. Therefore, the alveoli in the apical part of the lung are subjected to a transmural pressure P_{el} $(=P_{alv}-P_{pl})$ of approximately 8 hPa, whereas in the basal alveoli, it is only approximately 2 hPa. Assuming that lung compliance is homogeneous and described by the typical P_{el} – V_L curve, the alveoli have a lower volume at the basal than apical regions of the lung (►**Fig. 13**). Moreover, as the lung compliance is higher at $P_{el}=2$ hPa than at 8 hPa, any inspiratory change in P_{alv} induces a higher volume change in the basal than apical alveoli. The resulting inhomogeneous ventilation is more apparent if it is considered in relative terms since the higher change in inspiratory volume occurs in the alveoli that have the lower volume at FRC. The higher ventilation in the basal part of the lung, as compared with its apex, is physiological and in fact, is reduced when the subject is lying since at this body posture the regional gravitational differences are reduced. In patients, the ventilation changes induced by body position (sitting, semirecumbent, supine, prone) can have important consequences because the gravity field not only induces regional variation in ventilation but also in blood perfusion through the lung capillary bed, with a potential mismatch in the ventilation–perfusion relationship.

Besides gravity, inhomogeneous ventilation occurs, particularly in patients. The lungs are more complex than the simplest homogeneous mechanical model consisting of a resistance accounting for a uniform rigid-wall airway and elastance representing the pure elastic properties of a unique alveolar compartment (►**Fig. 14A**). Although this model is useful for interpreting ventilation mechanics in healthy subjects, it is too simplified for patients with severe respiratory diseases. There are two basic types of lung inhomogeneity.[55–58] A parallel inhomogeneity mechanism (►**Fig. 14B**) can be represented by two lung compartments (a and b) connected to a common parent airway, each compartment with its resistance (R_a, R_b) and elastance (E_a, E_b) and thus characterized with different time constants $\tau_a=R_a/E_a$ and $\tau_b=R_b/E_b$. In such a system, a given driving pressure at the airway bifurcation results in lower airflow and volume change in the compartment presenting a higher mechanical load. A trivial example of parallel homogeneity would be a patient with unilateral pneumonia in whom the healthy lung has normal mechanics, and the diseased lung has increased resistance and elastance. However, parallel inhomogeneities may appear at any lung generation. Serial lung inhomogeneity (►**Fig. 14C**) features airway wall compliance and a unique alveolar elastic compartment. Part of the airflow circulating through the central resistance (R_c) is shunted to expand the airways wall having an

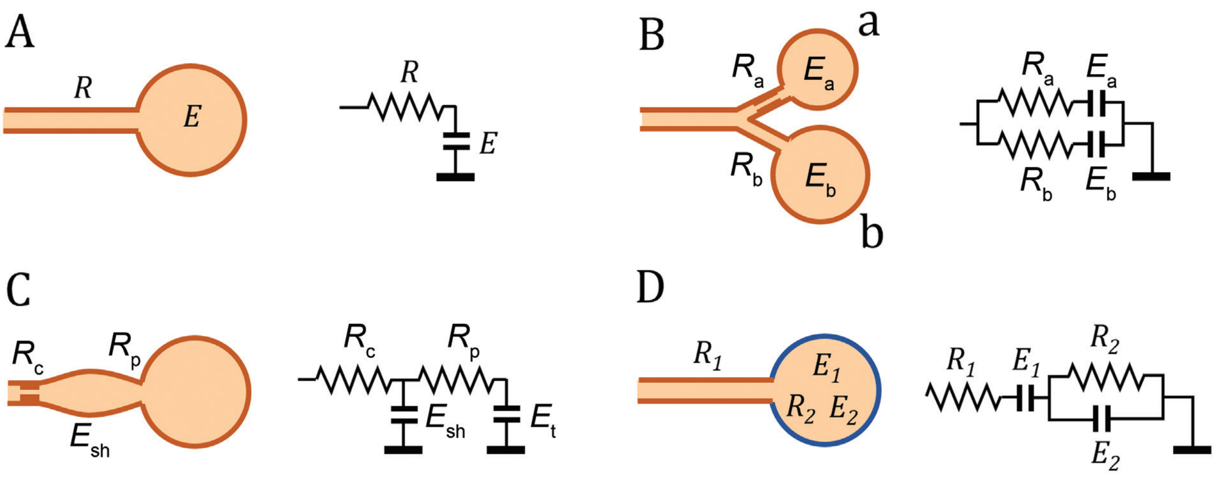

Fig. 14 Lung inhomogeneity and viscoelasticity models. Diagram of lung models and their electrical analog circuits. (**A**) Homogeneous model. (**B**) Parallel inhomogeneous model. (**C**) Series inhomogeneous model. (**D**) Viscoelastic tissue model (indicated by blue line). The different R and E are resistance and elastance parameters in the A–D models, respectively, as explained in the text.

elastance (E_{sh}), and thus the flow through the peripheral resistance (R_p) and the elastic tissue compartment (E_t) is reduced. Together with the mechanical scheme, **►Fig. 14** also represents the usual electrical circuit representation of the homogeneous model (A), parallel (B), and serial (C) inhomogeneities. There is a complete analogy between airway resistance and electrical resistance, mechanical elastance and condenser capacitance, changes in volume and in charge, and driving pressure and electric potential, respectively.

Lung inhomogeneity, either parallel or serial, makes the movement equation relating driving pressure $P(t)$ with flow $\dot{V}(t)$ and volume $V(t)$ more complex than the one for the simple homogeneous model. Indeed, the differential equation describing ventilation mechanics is (**Eq. 7**)

$$P(t) + \alpha \cdot \dot{P}(t) = \beta \cdot V(t) + \gamma \cdot \dot{V}(t) + \vartheta \cdot \ddot{V}(t) \quad \textbf{Eq. 7}$$

where parameters α, β, γ, and ϑ depend on the resistances and elastances of the parallel (R_a, R_b, E_a, E_b) and serial (R_c, R_p, E_{sh}, E_t) inhomogeneous models.[57,58] According to this equation, gas distribution among the elastances during inspiration is uneven, with different time constants, and if there is an end-inspiratory pause, internal air redistribution (pendelluft) occurs.[59,60] Whether a respiratory system is inhomogeneous is easily detected when respiratory mechanics is measured by conventional techniques. For instance, the application of Eq. 8 to the case of an end-inspiratory pause when a patient is ventilated with constant flow inflation shows that the measured airway opening pressure is as in **►Fig. 15**, thus differing from that in the simple homogeneous model (**►Fig. 12**).[45,61]

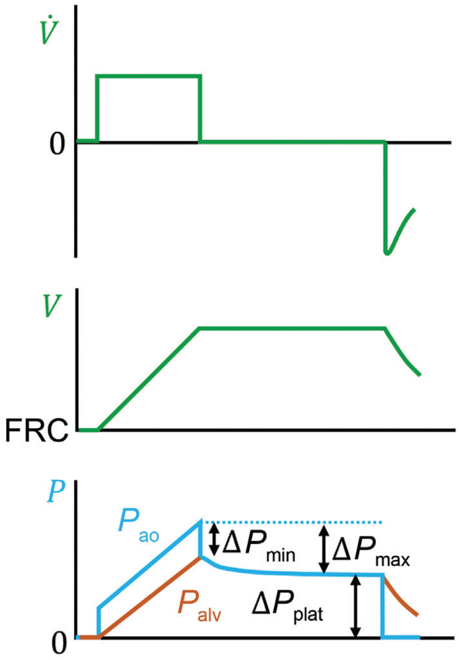

Fig. 15 Airway occlusion maneuver measurement in inhomogeneous lungs. End-expiratory pause during constant flow mechanical ventilation. FRC, functional residual capacity; P_{alv}, alveolar pressure; P_{ao}, airway opening pressure; ΔP_{max}, pressure drop down to the plateau; ΔP_{plat}, plateau pressure; ΔP_{min}, fast pressure drop after an end-inspiratory pause; $\dot{V}$, flow; V, lung volume.

Airway occlusion is followed by a first sudden drop in P_{ao} (ΔP_{min}) and a subsequent slow decay in P_{ao}, with time constant τ, down to a plateau resistive pressure drop (ΔP_{max}). Dividing ΔP_{min} and ΔP_{max} by the inspiratory flow $\dot{V}$ provides two resistance values, R_{min} and R_{max}, respectively. The values of R_{min}, R_{max}, and τ depend on the parameters in Eq. 7.

Both lung and chest wall tissues are not purely elastic but exhibit a viscoelastic behavior since there is frictional resistance when tissue fibers deform. Therefore, the alveolar and chest wall tissue cannot realistically be represented by single elastances as in the simple model considered in **►Figs. 14A–C**. Models with different complexity, and associated time constants, have been employed to describe the stress–strain deformation of respiratory tissues.[62–65] However, a simple representation of tissue viscoelasticity is shown in **►Fig. 14D**. The respiratory model consists of a simple airway resistance (R_1) and a viscoelastic tissue element, known as generalized Kelvin body of first order or linear standard solid.[66] The elastances (E_1 and E_2) represent a stress proportional to strain and the resistance (R_2) corresponds to a stress proportional to the time derivative of strain. Noteworthy, the mechanics of this model is also described by Eq. 7. Therefore, when techniques such as airway occlusion or oscillometry are applied for characterizing this viscoelastic model, the signals measured follow the same equations as for the parallel and series inhomogeneous models. Therefore, these easy-to-apply techniques do not allow us to ascertain whether ventilation inhomogeneity or alteration in lung tissue properties is the predominant abnormality. Additional more complex measurements are thus required to interpret respiratory mechanics in terms of alterations of gas distribution or viscoelasticity. Although some of them are not applicable in patients (e.g., measuring alveolar pressure with alveolar capsules[67]), others are feasible. For instance, carrying out the measurements when the patient is breathing gas mixtures with different viscosity (e.g., air, He-O_2, SF_6-O_2)[68] since flow resistance varies with gas viscosity, whereas tissue resistance does not.

Conflict of Interest

None declared.

References

1 Dynamics of Respiration. Supplement 12. Handbook of Physiology, The Respiratory System, Mechanics of Breathing. Joseph R Rodarte, Kai Rehder. First published: 01 January 2011
2 Static Behavior of the Respiratory System. Supplement 12. Handbook of Physiology, The Respiratory System, Mechanics of Breathing. Emilio Agostoni, Robert E Hyatt. First published: 01 January 2011 Accessed June 5, 2023 at: https://doi-org.sire.ub.edu/10.1002/cphy.cp030309
3 Ninane V, Rypens F, Yernault JC, De Troyer A. Abdominal muscle use during breathing in patients with chronic airflow obstruction. Am Rev Respir Dis 1992;146(01):16–21
4 Yan S, Sinderby C, Bielen P, Beck J, Comtois N, Sliwinski P. Expiratory muscle pressure and breathing mechanics in chronic obstructive pulmonary disease. Eur Respir J 2000;16(04):684–690
5 Wanger J, Clausen JL, Coates A, et al. Standardisation of the measurement of lung volumes. Eur Respir J 2005;26(03):511–522
6 Meneely GR, Kaltreider NL. The volume of the lung determined by helium dilution. description of the method and comparison with other procedures. J Clin Invest 1949;28(01):129–139

7 Rodarte JR, Hyatt RE, Westbrook PR. Determination of lung volume by single- and multiple-breath nitrogen washout. Am Rev Respir Dis 1976;114(01):131–136

8 Morris MG. The open circuit nitrogen washout technique for measuring the lung volume in infants: methodological aspects. Thorax 1999;54(09):790–795

9 Chiumello D, Cressoni M, Chierichetti M, et al. Nitrogen washout/washin, helium dilution and computed tomography in the assessment of end expiratory lung volume. Crit Care 2008;12 (06):R150. Doi: 10.1186/cc7139 Erratum in: Crit Care. 2009;13 (2):405. PMID: 19046447; PMCID: PMC2646315

10 Berger-Estilita J, Haenggi M, Ott D, Berger D. Accuracy of the end-expiratory lung volume measured by the modified nitrogen washout/washin technique: a bench study. J Transl Med 2021; 19(01):36

11 Stocks J, Godfrey S, Beardsmore C, Bar-Yishay E, Castile RERS/ATS Task Force on Standards for Infant Respiratory Function Testing. European Respiratory Society/American Thoracic Society European Respiratory Society/ American Thoracic Society. Plethysmographic measurements of lung volume and airway resistance. ERS/ATS Task Force on Standards for Infant Respiratory Function Testing. Eur Respir J 2001;17(02):302–312

12 Rodenstein DO, Stănescu DC. Reassessment of lung volume measurement by helium dilution and by body plethysmography in chronic air-flow obstruction. Am Rev Respir Dis 1982;126(06): 1040–1044

13 Ross JC, Copher DE, Teays JD, Lord TJ. Functional residual capacity in patients with pulmonary emphysema. A comparative study using gas dilution and plethysmographic techniques for measurement. Ann Intern Med 1962;57:18–28

14 Lung Parenchymal Mechanics. . Volume 1. Issue 3. July 2011. Béla Suki, Dimitrije Stamenović, Rolf Hubmayr. Published online: 1 July 2011. https://doi.org/10.1002/cphy.c100033.Published online: 1 October 2011 https://doi.org/10.1002/cphy.c100025

15 Milic-Emili J, Mead J, Turner JM, Glauser EM. Improved technique for estimating pleural pressure from esophageal balloons. J Appl Physiol 1964;19:207–211

16 Pasticci I, Cadringher P, Giosa L, et al. Determinants of the esophageal-pleural pressure relationship in humans. J Appl Physiol 2020;128(01):78–86

17 Zielinska-Krawczyk M, Krenke R, Grabczak EM, Light RW. Pleural manometry-historical background, rationale for use and methods of measurement. Respir Med 2018;136:21–28

18 Jiang J, Su L, Cheng W, et al. The calibration of esophageal pressure by proper esophageal balloon filling volume: a clinical study. Front Med (Lausanne) 2022;9:986982

19 Lung Mechanics in Disease Supplement 12. Handbook of Physiology, The Respiratory System, Mechanics of Breathing. N. B. Pride, Peter T. Macklem. Published online: 1 January 2011 https://doi.org/10.1002/cphy.cp030337

20 Wang S, Li Z, Wang X, Zhang S, Gao P, Shi Z. The role of pulmonary surfactants in the treatment of acute respiratory distress syndrome in COVID-19. Front Pharmacol 2021;12:698905

21 Hentschel R, Bohlin K, van Kaam A, Fuchs H, Danhaive O. Surfactant replacement therapy: from biological basis to current clinical practice. Pediatr Res 2020;88(02):176–183

22 Milad N, Morissette MC. Revisiting the role of pulmonary surfactant in chronic inflammatory lung diseases and environmental exposure. Eur Respir Rev 2021;30(162):210077

23 Härtel C, Glaser K, Speer CP. The miracles of surfactant: less invasive surfactant administration, nebulization, and carrier of topical drugs. Neonatology 2021;118(02):225–234

24 Passive Mechanical Properties of the Chest Wall. Supplement 12. Handbook of Physiology, The Respiratory System, Mechanics of Breathing. Jeffrey C Smith, Stephen H Loring. Published online: 1 January 2011. Accessed June 5, 2023 at: https://doi.org/10.1002/cphy.cp030325

25 Papandrinopoulou D, Tzouda V, Tsoukalas G. Lung compliance and chronic obstructive pulmonary disease. Pulm Med 2012; 2012:542769

26 Sansores RH, Ramirez-Venegas A, Pérez-Padilla R, et al. Correlation between pulmonary fibrosis and the lung pressure-volume curve. Lung 1996;174(05):315–323

27 Nava S, Rubini F. Lung and chest wall mechanics in ventilated patients with end stage idiopathic pulmonary fibrosis. Thorax 1999;54(05):390–395

28 Plantier L, Cazes A, Dinh-Xuan AT, Bancal C, Marchand-Adam S, Crestani B. Physiology of the lung in idiopathic pulmonary fibrosis. Eur Respir Rev 2018;27(147):170062

29 Pelosi P, Croci M, Ravagnan I, Vicardi P, Gattinoni L. Total respiratory system, lung, and chest wall mechanics in sedated-paralyzed postoperative morbidly obese patients. Chest 1996;109(01): 144–151

30 Redding G, Song K, Inscore S, Effmann E, Campbell R. Lung function asymmetry in children with congenital and infantile scoliosis. Spine J 2008;8(04):639–644

31 Kaminsky DA. What does airway resistance tell us about lung function? Respir Care 2012;57(01):85–96, discussion 96–99

32 Kaminsky DA, Cockcroft DW, Davis B. Respiratory system dynamics. Semin Respir Crit Care Med 2023;44(05):

33 Briscoe WA, Dubois AB. The relationship between airway resistance, airway conductance and lung volume in subjects of different age and body size. J Clin Invest 1958;37(09):1279–1285

34 Bossé Y, Riesenfeld EP, Paré PD, Irvin CG. It's not all smooth muscle: non-smooth-muscle elements in control of resistance to airflow. Annu Rev Physiol 2010;72:437–462

35 Bara I, Ozier A, Tunon de Lara JM, Marthan R, Berger P. Pathophysiology of bronchial smooth muscle remodelling in asthma. Eur Respir J 2010;36(05):1174–1184

36 Tattersfield AE, Keeping IM. Assessing change in airway calibre–measurement of airway resistance. Br J Clin Pharmacol 1979;8 (04):307–319

37 Kraemer R, Smith HJ, Matthys H. Normative reference equations of airway dynamics assessed by whole-body plethysmography during spontaneous breathing evaluated in infants, children, and adults. Physiol Rep 2021;9(17):e15027

38 Pressure-Flow Relationships in the Lungs. Supplement 12. Handbook of Physiology, The Respiratory System, Mechanics of Breathing. Roland H. Ingram Jr., T. J. Pedley. Published online: 1 January 2011. Accessed June 5, 2023 at: https://doi.org/10.1002/cphy.cp030318

39 Principles of Measurement: Applications to Pressure, Volume, and Flow. Supplement 12. Handbook of Physiology, The Respiratory System, Mechanics of Breathing. James P. Butler, David E. Leith, Andrew C. Jackson. First published: 01 January 2011. Accessed June 5, 2023 at: https://doi-org.sire.ub.edu/10.1002/cphy.cp030302

40 Laghi F, Tobin MJ. 2013Chapter 4. Indications for mechanical ventilation. Tobin M.J.(Ed.), Principles and Practice of Mechanical Ventilation, 3e. McGraw Hill. Accessed June 5, 2023 at: https://accessmedicine.mhmedical.com/content.aspx?bookid=520&sectionid=41692241

41 Chatburn RL. 2013Chapter 2. Classification of mechanical ventilators and modes of ventilation. In: Tobin MJ, ed., Principles and Practice of Mechanical Ventilation. 3rd ed. McGraw Hill

42 Holets SR, Hubmayr RD. 2013Chapter 5. Setting the ventilator. In: Tobin MJ, ed., Principles and Practice of Mechanical Ventilation. 3rd ed. New York, NY: McGraw Hill

43 Navalesi P, Maggiore S. 2013Chapter 10. positive end-expiratory pressure. Tobin M.J.(Ed.), Principles and Practice of Mechanical Ventilation, 3e. McGraw Hill. Accessed June 5, 2023 at: https://accessmedicine.mhmedical.com/content.aspx?bookid=520&sectionid=41692248

44 Hess DR. Respiratory mechanics in mechanically ventilated patients. Respir Care 2014;59(11):1773–1794

45 Bates JH, Baconnier P, Milic-Emili J. A theoretical analysis of interrupter technique for measuring respiratory mechanics. J Appl Physiol 1988;64(05):2204–2214

46 Lucangelo U, Bernabé F, Blanch L. Respiratory mechanics derived from signals in the ventilator circuit. Respir Care 2005;50(01): 55–65, discussion 65–67

47 Pelosi P, Cereda M, Foti G, Giacomini M, Pesenti A. Alterations of lung and chest wall mechanics in patients with acute lung injury: effects of positive end-expiratory pressure. Am J Respir Crit Care Med 1995;152(02):531–537

48 Radics BL, Makan G, Coppens T, et al. Effect of nasal airway nonlinearities on oscillometric resistance measurements in infants. J Appl Physiol 2020;129(03):591–598

49 Beck KC, Hyatt RE, Mpougas P, Scanlon PD. Evaluation of pulmonary resistance and maximal expiratory flow measurements during exercise in humans. J Appl Physiol 1999;86(04): 1388–1395

50 Lorino AM, Lofaso F, Abi-Nader F, et al. Nasal airflow resistance measurement: forced oscillation technique versus posterior rhinomanometry. Eur Respir J 1998;11(03):720–725

51 Peslin R, Rotger M, Farré R, Navajas D. Assessment of respiratory pressure-volume nonlinearity in rabbits during mechanical ventilation. J Appl Physiol 1996;80(05):1637–1648

52 Shi L, Herrmann J, Bou Jawde S, Bates JHT, Nia HT, Suki B. Modeling the influence of gravity and the mechanical properties of elastin and collagen fibers on alveolar and lung pressure-volume curves. Sci Rep 2022;12(01):12280

53 Bigler AH, Renzetti AD Jr, Watanabe S, Begin R, Clark J. Regional lung expansion and vertical pleural pressure gradients in normal human subjects. Bull Eur Physiopathol Respir 1979;15(05): 773–788

54 Lai-Fook SJ, Rodarte JR. Pleural pressure distribution and its relationship to lung volume and interstitial pressure. J Appl Physiol 1991;70(03):967–978

55 Similowski T, Bates JH. Two-compartment modelling of respiratory system mechanics at low frequencies: gas redistribution or tissue rheology? Eur Respir J 1991;4(03):353–358

56 Similowski T, Levy P, Corbeil C, et al. Viscoelastic behavior of lung and chest wall in dogs determined by flow interruption. J Appl Physiol 1989;67(06):2219–2229

57 Lorino AM, Lorino H, Harf A. A synthesis of the Otis, Mead, and Mount mechanical respiratory models. Respir Physiol 1994;97 (02):123–133

58 Lorino AM, Harf A. Techniques for measuring respiratory mechanics: an analytic approach with a viscoelastic model. J Appl Physiol 1993;74(05):2373–2379

59 Santini A, Mauri T, Dalla Corte F, Spinelli E, Pesenti A. Effects of inspiratory flow on lung stress, pendelluft, and ventilation heterogeneity in ARDS: a physiological study. Crit Care 2019;23(01): 369

60 Chi Y, Zhao Z, Frerichs I, Long Y, He H. Prevalence and prognosis of respiratory pendelluft phenomenon in mechanically ventilated ICU patients with acute respiratory failure: a retrospective cohort study. Ann Intensive Care 2022;12(01):22

61 Tsuzaki K, Hales CA, Strieder DJ, Venegas JG. Regional lung mechanics and gas transport in lungs with inhomogeneous compliance. J Appl Physiol 1993;75(01):206–216

62 Guérin C, Bayat S, Noury N, et al. Regional lung viscoelastic properties in supine and prone position in a porcine model of acute respiratory distress syndrome. J Appl Physiol 2021;131(01): 15–25

63 D'Angelo E, Calderini E, Tavola M, Pecchiari M. Standard and viscoelastic mechanical properties of respiratory system compartments in dogs: Effect of volume, posture, and shape. Respir Physiol Neurobiol 2019;261:31–39

64 Suki B, Bates JH. Lung tissue mechanics as an emergent phenomenon. J Appl Physiol 2011;110(04):1111–1118

65 Ganzert S, Möller K, Steinmann D, Schumann S, Guttmann J. Pressure-dependent stress relaxation in acute respiratory distress syndrome and healthy lungs: an investigation based on a viscoelastic model. Crit Care 2009;13(06):R199

66 Navajas D, Farré R, Canet J, Rotger M, Sanchis J. Respiratory input impedance in anesthetized paralyzed patients. J Appl Physiol 1990;69(04):1372–1379

67 Otis DR Jr, Petak F, Hantos Z, Fredberg JJ, Kamm RD. Airway closure and reopening assessed by the alveolar capsule oscillation technique. J Appl Physiol 1996;80(06):2077–2084

68 Rotger M, Farré R, Navajas D, Peslin R. Respiratory input impedance up to 256 Hz in healthy humans breathing foreign gases. J Appl Physiol 1993;75(01):307–320

Article published online: 2023-07-10

Respiratory System Dynamics

David A. Kaminsky, MD[1] Donald W. Cockcroft, MD[2] Beth E. Davis, PhD[3]

[1] Division of Pulmonary and Critical Care, Department of Medicine, University of Vermont Larner College of Medicine, Burlington, Vermont
[2] Division of Respirology, Critical Care and Sleep Medicine, University of Saskatchewan College of Medicine, Saskatoon Saskatchewan, Canada
[3] Division of Respirology, Critical Care and Sleep Medicine, University of Saskatchewan College of Medicine, Saskatoon Saskatchewan, Canada

Address for correspondence David A. Kaminsky, MD, Division of Pulmonary and Critical Care, Department of Medicine, University of Vermont Larner College of Medicine, Burlington, VT 05405 (e-mail: David.kaminsky@uvm.edu).

Semin Respir Crit Care Med 2023;44:526–537.

Abstract

Keywords

- work of breathing
- airway resistance
- flow–volume loop
- airflow limitation
- bronchodilator responsiveness
- dynamic hyperinflation
- airway hyperresponsiveness
- methacholine challenge

While static mechanical forces govern resting lung volumes, dynamic forces determine tidal breathing, airflow, and changes in airflow and lung volume during normal and abnormal breathing. This section will examine the mechanisms, measurement methodology, and interpretation of the dynamic changes in airflow and lung volume that occur in health and disease. We will first examine how the total work of breathing can be described by the parameters of the equation of motion, which determine the pressure required to move air into and out of the lung. This will include a detailed description of airflow characteristics and airway resistance. Next, we will review the changes in pressure and flow that determine maximal forced inspiration and expiration, which result in the maximal flow–volume loop and the clinically important forced expired volume in 1 second. We will also assess the mechanisms and interpretation of bronchodilator responsiveness, dynamic hyperinflation, and airways hyperresponsiveness.

The following section will explore the ways in which dynamic forces influence respiratory function, and how that function is measured. Specifically, we will examine the work of breathing as related to quiet, tidal breathing, determinants of airway resistance, the physiology of forced exhalation and airflow limitation, the response of flow and volume to inhaled bronchodilator administration, dynamic hyperinflation, and airways hyperresponsiveness.

Work of Breathing

During quiet breathing the inspiratory muscles are activated to raise intrathoracic volume, which decreases pleural pressure, increases transmural (alveolar minus pleural) pressure, and ultimately expands the alveoli outward from functional residual capacity (FRC). Since lung recoil is inward and chest wall recoil is outward at FRC, the work of the inspiratory muscles is mainly necessary to overcome increasing lung recoil as the lung expands to end-inspiratory lung volume. At the end of inspiration, the inspiratory muscles relax, and the passive recoil of the lung draws the lung and chest wall back toward FRC. The total work required to perform quiet, tidal breathing can be depicted by a Campbell Diagram, which displays the volume versus pressure (intrapleural) relationship, with the area of the inscribed inspiratory and expiratory loop equaling the total work involved (►**Fig. 1**).[1] The work can be broken down into its individual components related to resistive work due to the friction of moving gas through the airways and elastic work necessary to overcome the elastic forces of the lung parenchyma and chest wall. The Campbell Diagram illustrates how resistive work is increased in patients with increased airway resistance (e.g., obstructive lung disease), and elastic work is increased in patients with reduced lung compliance (e.g., restrictive lung disease). It is

article published online
July 10, 2023

Issue Theme Pulmonary Physiology; Guest Editors: David A. Kaminsky, MD, Kathryn A. Hibbert, MD, and Andrew M. Luks, MD

Thieme Medical Publishers, Inc.,
333 Seventh Avenue, 18th Floor,
New York, NY 10001, USA

DOI https://doi.org/10.1055/s-0043-1770058.
ISSN 1069-3424.

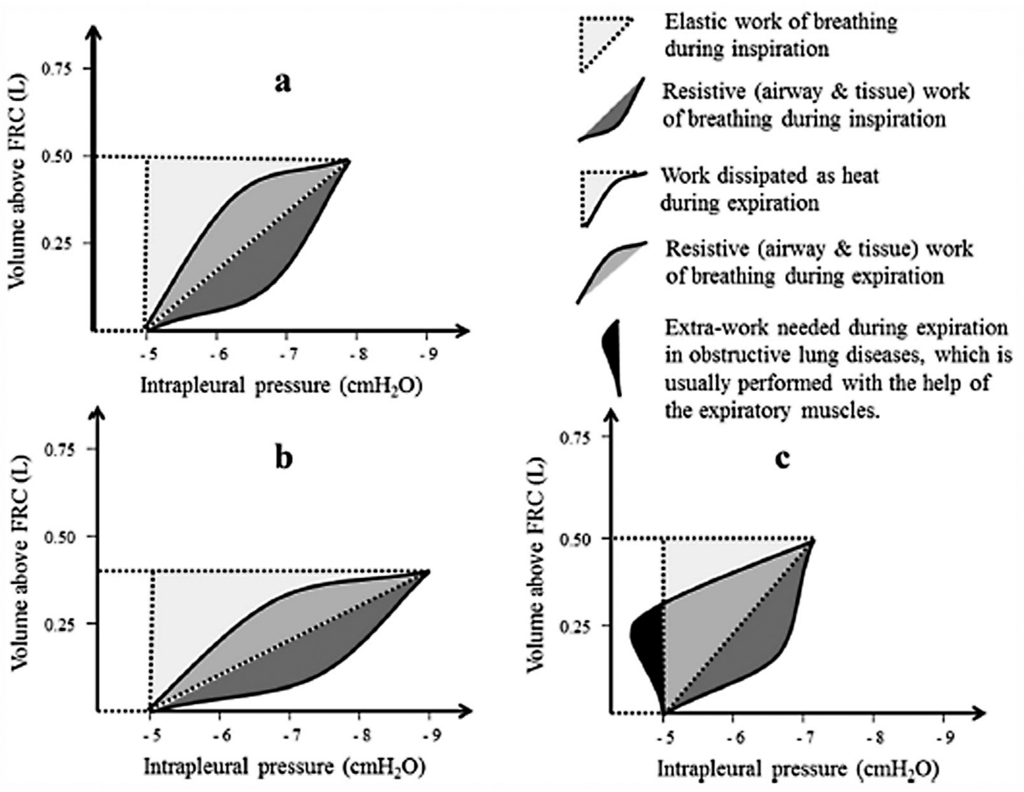

Fig. 1 Work of breathing in a healthy person (**A**) Compared with a person with increased lung elastance (**B**) or increased airway resistance (**C**). Notice for the person with increased elastance (**B**), the static, elastic work of breathing (area inscribed by diagonal dotted line) is increased as seen by the reduced slope of Volume versus Pressure, indicating decreased compliance, but there is relatively normal resistive work of breathing on both inspiration and expiration. Notice for the person with increased airway resistance (**C**), static, elastic work of breathing is normal (normal slope of volume vs. pressure), but there is increased resistive work during expiration due to airway narrowing from airflow obstruction. FRC, functional residual capacity. Reproduced with permission from Lufti 2017.[1]

also useful for assessing the contribution of intrinsic positive end-expiratory pressure to work of breathing in patients with obstructive lung disease.[2]

Let us examine each of the components of work separately, using the equation of motion describing the lung in its most simplified form, an inflatable balloon on a rigid pipe to represent a single compartment, linear system.[3] The equation of motion states that the pressure (P) necessary to move air into and out of the lung is determined by the sum of the associated forces involved, which include airway resistance (R), lung parenchymal elastance (E), and gas inertance (I):

$$P = E\Delta V + R\Delta\dot{V} + I\Delta\ddot{V}$$

where ΔV=change in lung volume, $\Delta\dot{V}$=airflow, and $\Delta\ddot{V}$ =gas acceleration. Airway resistance refers to the frictional forces that develop when air moves by bulk flow through the pipe. Elastance is the reciprocal of compliance and refers to the stiffness of the lung parenchyma that must overcome to expand the alveoli. Inertance is the force developed by the acceleration of the mass of gas within the system as it moves from mouth to alveoli and back again.

To accomplish airflow, a driving pressure must be provided to overcome airway resistance, which is related to pressure and flow as described by analogy to Ohm's law

$$R = \Delta P/\Delta\dot{V}.$$

Air flows in two general patterns: laminar, when the pathways of airflow are parallel to the side wall of the flow conduit, and turbulent, when airflow pathways are random and chaotic (►**Fig. 2**). Whether air flows in either of these patterns is described empirically by the Reynold's number (Re)

$$Re = \frac{\rho v d}{\mu}$$

where ρ = density, v = velocity, d = diameter, μ = viscosity

When Re < 2,000, airflow tends to be laminar, and when Re > 2,000 it is more likely to be turbulent. Under laminar conditions, the pressure required to achieve flow is described by Poiseuille' law

$$\Delta P = [8l\mu\dot{V}]/\pi r^4.$$

When flow is turbulent, the pressure required to achieve flow is greater (now $\Delta P \propto \dot{V}^2$ and gas density (ρ), rather than viscosity), which results in a higher work of breathing.[4]

$$\Delta P = [8l\rho(\dot{V}^2)]/\pi r^4.$$

Since laminar versus turbulent flow is related to the Reynold's number, laminar flow can be enhanced by either slower airflow, larger airways, or less dense or more viscous gas. When patients with asthma or chronic obstructive

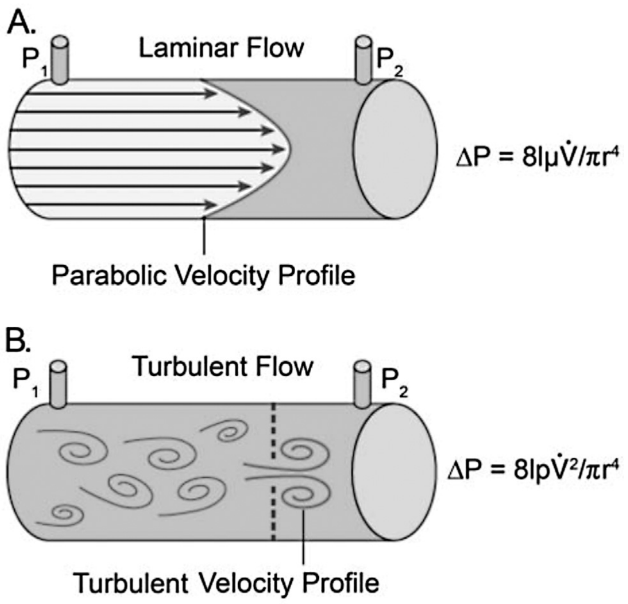

Fig. 2 The difference between laminar (**A**) and turbulent (**B**) flow. Notice that the change in pressure required to drive flow when flow is laminar is directly proportional to length (*l*), viscosity (μ), and flow $\Delta P \propto \dot{V}^2$, and inversely proportional to radius (*r*) to the fourth power, whereas for turbulent flow, pressure is proportional to similar parameters except density (ρ) instead of viscosity, and the square of flow ($\dot{V}^2$) rather than directly to flow. Reproduced with permission from Bossé et al 2010.[4]

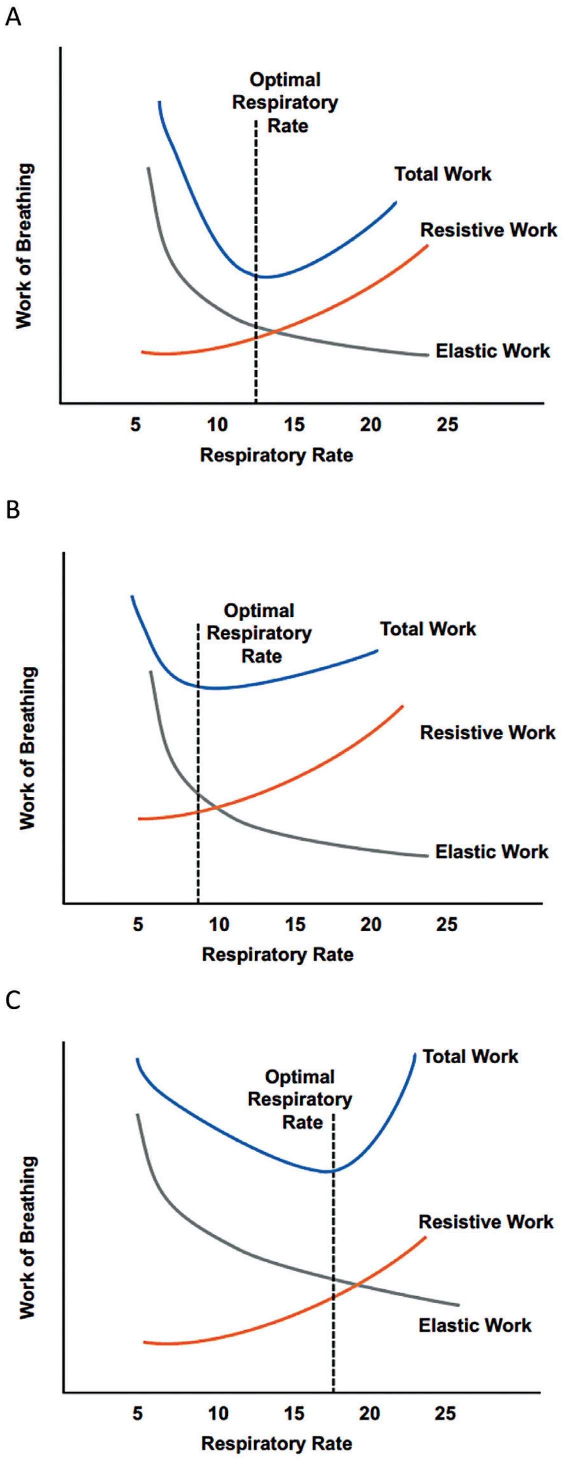

Fig. 3 Illustration of how optimal respiratory rate is determined by minimizing work of breathing. Three situations are shown: normal resistance and elastance (**A**), increased airway resistance (**B**), or increased elastance (**C**). For a given minute ventilation, elastic work increases at lower respiratory rates because larger tidal volumes, and hence lung stretch, are necessary. Likewise, airflow work is the highest at higher respiratory rates because airway resistance varies with airflow velocity. Adding together elastic and resistive work produces the total work curve. Notice how a person with increased airway resistance will adopt a lower respiratory rate (and higher tidal volume), whereas a person with increased elastance will adopt a higher respiratory rate (and consequently lower tidal volume) than a person with normal mechanics.

pulmonary disease (COPD) are struggling to breathe due to excessively turbulent airflow, the work of breathing can be reduced by dilating the airways with inhaled bronchodilators. One could also provide a gas with less density or more viscosity than air, such as the mixture of helium and oxygen (heliox), although this is not commonly used and is of uncertain clinical benefit.[5] Slower airflow is achieved by breathing at lower respiratory frequency, so for the same minute ventilation, a patient with obstructive lung disease will minimize their work of breathing by breathing at a low respiratory rate and a higher tidal volume (►**Fig. 3**).

The airways are arranged in a complex, branching system of series and parallel airways such that total airway resistance (R_{tot}) is the sum of the reciprocals of the resistances of each parallel pathway:

$$\frac{1}{R_{tot}} = \frac{1}{R_1} + \frac{1}{R_2} + \cdots \frac{1}{R_n}$$

where R_n = resistance of airway at the nth generation.

While airway diameter quickly decreases moving distally, the total cross-sectional area increases exponentially, resulting in the highest total airway resistance between the fourth and eighth generation of airways and less as one moves more distally (►**Fig. 4**). This concept is important in explaining why overall changes in airway resistance are very sensitive to changes in central airway diameter but markedly less sensitive to changes in peripheral airway diameter. It is estimated that at rest, the lung periphery only accounts for 10% of total airway resistance, explaining why this area is difficult to

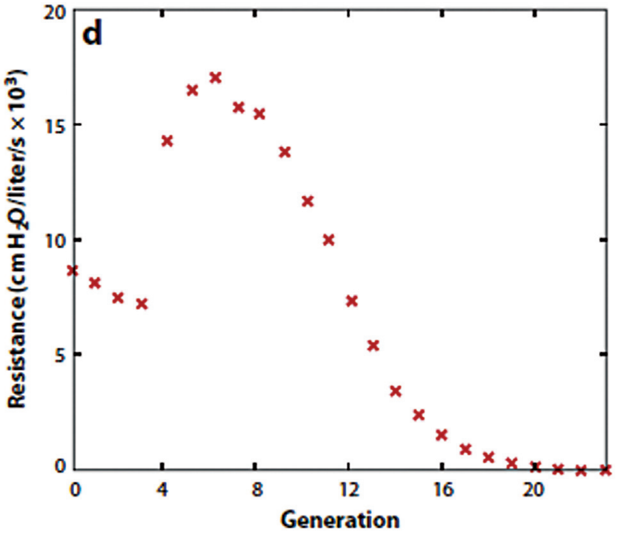

Fig. 4 Total airway resistance as a function of location within the airway tree as designated by airway generation. Notice that the highest resistance occurs at the segmental bronchial level (generations 4–8) and resistance falls with subsequent airway generations. Reproduced with permission from Bossé et al 2010.[4]

detect by conventional spirometry and hence dubbed “the quiet zone.”[6]

Since airway resistance is highly dependent on airway diameter, lung volume plays a key role in determining airway resistance because of the mechanical linkage of the airway wall to its surrounding lung parenchyma, known as airway–parenchymal interdependence.[7] Thus, as lung volume increases, so will airway diameter, which will greatly reduce airway resistance (►**Fig. 5**). Other factors that influence airway resistance by altering airway diameter, such as airway smooth muscle (ASM) tone, airway wall thickness and geometry, and airway inflammation, are discussed in the section on airway hyperresponsiveness.

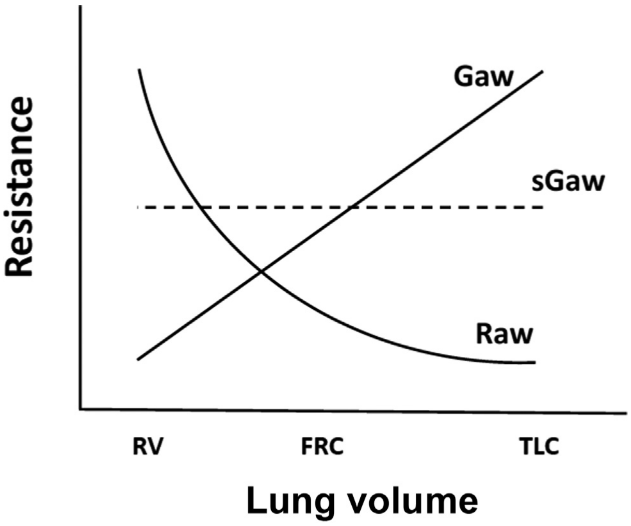

Fig. 5 Dependence of airway resistance on lung volume. While airway resistance (R_{aw}) varies inversely and hyperbolically with lung volume, its reciprocal, airway conductance (G_{aw}) varies linearly and directly with lung volume. Dividing G_{aw} by the volume at which it is measured results in specific G_{aw} (sG_{aw}), which is independent of lung volume. FRC, functional residual capacity; RV, residual volume; TLC, total lung capacity.

Airway resistance (R_{aw}) can be measured by several methods.[8] In the pulmonary function laboratory, R_{aw} is commonly measured during body plethysmography by relating mouth pressure to airflow via

$$R_{aw} = \frac{P_{mouth}}{P_{box}} x \frac{P_{box}}{Flow}.$$

Because of its important dependence on lung volume, R_{aw} is adjusted to lung volume by expressing it as its reciprocal, airway conductance (G_{aw}), divided by the lung volume at which it was measured to arrive at specific G_{aw} or sG_{aw} (►**Fig. 5**).

Respiratory system resistance can also be determined by oscillometry. Oscillometry, also known as the forced oscillation technique, involves having an individual breathe passively while a superimposed oscillatory flow of air is applied to the mouth. The resulting pressure oscillations measured at the mouth in response to the superimposed “forced” oscillatory flow are recorded and related in time to the applied oscillatory signal. Pressure in phase with flow reflects respiratory system resistance, whereas pressure out of phase with flow represents respiratory system reactance (the sum of elastance and inertance of the respiratory system). Conventionally, the flow signal is applied across a frequency range of ~5 to 40 Hz. At 5 Hz and greater, respiratory system resistance is predominantly comprised of airway resistance.[9]

A second important component of the work of breathing is the compliance of the lung and chest wall (usually described by its reciprocal, elastance, in the equation of motion). The elastic forces of these respiratory system components are discussed in the preceding chapter. Based on the Campbell diagram, one can see that there is substantially more pressure required to achieve a given lung volume when elastance is high (e.g., in idiopathic pulmonary fibrosis [IPF]) than when it is low (e.g., in emphysema; ►**Fig. 1**). There is no direct treatment that relieves the high elastance of lung tissue in diseases like IPF, so patients will try to minimize their work of breathing by breathing at a lower tidal volume (less lung stretch), therefore requiring a higher respiratory rate to achieve the same minute ventilation (►**Fig. 3**).

The third component of the equation of motion is inertance, related primarily to the acceleration of the gas column with the central airways.[10] Since this does not significantly contribute to increased work of breathing until relatively high frequencies (>12 Hz), inertance is usually not considered clinically important.

Physiology of the Flow–Volume Loop and Forced Expiratory Airflow

Flow–Volume Loop

The fundamental measure that characterizes lung function is the forced expiratory volume in 1 second (FEV_1). Surprisingly, this seemingly arbitrary assessment of lung function is highly reproducible, defines airflow obstruction (when related to the total amount of air exhaled, the forced vital

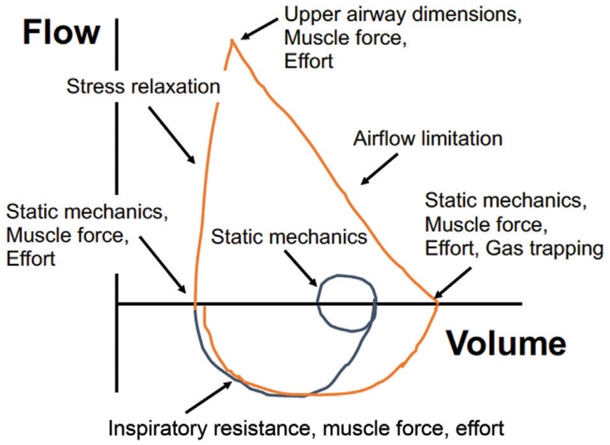

Fig. 6 Mechanical events involved in determining the key components of the maximal flow–volume loop. See text for details.

capacity, FVC, by the ratio FEV_1/FVC),[11] tracks disease severity, control, and progression over time, and is independently related to important patient outcomes such as symptoms, quality of life, and mortality.[12–15] FEV_1 is measured by spirometry, which requires a person to breathe on a mouthpiece, take in a full deep breath of air, and then, without hesitation, blast the air out as hard and as fast as they can until their lung empties. The FEV_1 is measured as the volume expired in the first second of an acceptable forced expiratory maneuver. The details of measuring and interpreting spirometry are discussed below, but before discussing these details, one must understand the physiological determinants of FEV_1 and FVC (►**Fig. 6**).

To achieve an acceptable FVC, an individual must be able to inspire fully to total lung capacity (TLC). This full, deep inspiration (DI) requires proper motivation and effort on the part of the individual, as well as sufficient inspiratory muscle strength and patency of the upper airway to achieve full deep inflation.[16] Once at TLC, the individual must blast the air out as hard and fast as possible, and this, once again, requires proper motivation and effort, sufficient muscle strength, and normal patency of the upper airway. Furthermore, it is important that there be no hesitation prior to the start of exhalation because of the tendency of the elastic elements in the lung to relax when held in distension, a property called "stress relaxation" that reduces the elastic recoil force of the exhalation and hence the resulting maximal flow.[17] As the lung empties, the volume of the lung decreases, and the airways diminish in size. In addition, the force of exhalation causes airway compression along the compliant, intrathoracic airways, resulting in airway narrowing. The end result is the development of expiratory flow limitation within the airways.

Expiratory flow limitation indicates that maximal expiratory flow is governed by the physical interactions of the compressible airway and the surrounding pleural pressure. Maximal flow is effort independent, because as more effort is applied, more airway narrowing takes place, limiting enhanced airflow. Expiratory flow limitation during forced exhalation has been described by two different but interrelated mechanisms. A simple view is the development of the equal pressure point (EPP), which is the location along the airway where the inside and outside pressures are equal and opposite (►**Fig. 7**).[18,19] From the EPP toward the mouth, the airway pressure is less than surrounding pleural pressure and so the airway wall will buckle and continue to narrow as flow approaches the mouth. The independent forces governing maximal flow ($\dot{V}_{max}$) in the collapsible airway are the elastic recoil of the lung (P_{el}) and the resistance of the airways upstream (i.e., toward the alveoli) from the EPP (R_{us}).[18]

$$\dot{V}_{max} = \frac{P_{el}}{R_{us}}.$$

As can be seen by this equation, maximal flow is reduced by loss of elastic recoil (lower P_{el}), such as seen in emphysema, or increase in (upstream) airway resistance (higher R_{us}), such as seen in asthma. As forced exhalation proceeds and the lung empties, the EPP will migrate deeper and deeper

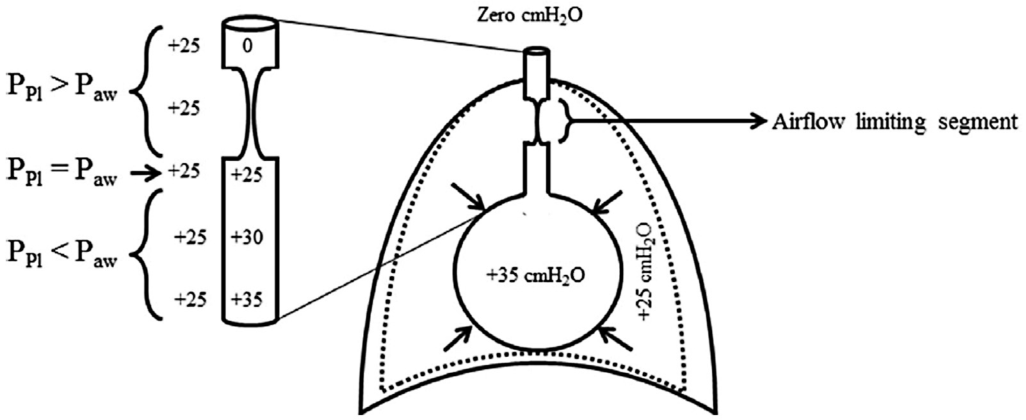

Fig. 7 Illustration of the equal pressure point (EPP) concept explaining expiratory airflow limitation. During forced exhalation, pleural pressure (P_{pl}) is positive (+25 cm H_2O), which together with lung elastic recoil (+10 cm H_2O) results in a markedly positive intra-alveolar pressure (+35 cm H_2O) well above atmospheric pressure. This results in expiratory airflow. The pressure within the airway (P_{aw}) drops from intra-alveolar to atmospheric and somewhere along the way becomes equal to the surrounding pleural pressure (the EPP), around 25 cm H_2O . At this point and beyond toward the mouth, the flexible airway will narrow, limiting airflow. Reproduced with permission from Lufti 2017.[1]

into the lung as the elastic recoil of the lung drops and the surrounding pleural pressure more quickly exceeds inside airway pressure.

While the EPP mechanism explains expiratory flow limitation on the basis of the viscous properties of a gas flowing through a collapsible tube, another mechanism explains airflow limitation on the basis of "wave speed" theory,[20] which depends on the density of the gas and airway collapsability.[21] By this mechanism, the flow ($\dot{V}$) of air through a collapsible tube can never exceed the speed at which a pressure wave can propagate through the wall of the tube, regardless of the driving force (alveolar pressure minus mouth pressure = atmospheric pressure, or zero) behind it. This theory of flow limitation is dependent on the cross-sectional area of the airways (A), the collapsibility of the airway under pressure (dP/dA), and density of the gas (ρ);

$$\dot{V}\,\mathrm{max} = A\sqrt{\frac{A}{\rho}\left(\frac{dP}{dA}\right)}.$$

This formula indicates that maximal flow ($\dot{V}_{max}$) varies (1) directly with the area (A) of the tube, such that narrowing of the tube results in reduced flow (as occurs in asthma); (2) directly with the stiffness (dP/dA) of the tube, such that a more collapsible (less stiff) tube results in reduced flow (as occurs in emphysema); and (3) inversely with the density of the gas. The latter effect is exemplified by the higher peak expiratory flow (PEF) in patients with status asthmaticus when breathing a mixture of helium and oxygen that has a lower density than air.[22] During pressure wave propagation, the sides of the tube oscillate inward and outward to accommodate the wave, and at some point the amplitude of the inward oscillation would approach the radius of the tube such that the two inner sides would meet, causing a choke point that would limit flow.[21] This is somewhat analogous to the EPP explained above.

Once airflow has diminished and no further lung volume is expired, the lung has reached residual volume (RV). As the name indicates, the lung is not empty of all air; instead, a residual amount of air remains. The volume at which this occurs is determined by the maximal strength and effort provided during exhalation as well as chest wall compliance, because the muscle force to reduce lung volume must overcome increasing outward chest wall recoil. In addition, as airways narrow at lower lung volume, some will narrow to the point of closure or near closure before the communicating distal airspace has fully emptied, resulting in trapped gas that contributes to the RV.[23]

Measurement of Airflow and Vital Capacity by Spirometry

Methodology of Measuring Spirometry

Technical details for performance of spirometry were initially developed in 1979[24] have been updated several times since[25–27] with most up-to-date version published jointly by the American Thoracic Society (ATS) and the European Respiratory Society (ERS) in 2019.[28] Electronic spirometers produce both a volume–time and a flow–volume curve (►**Fig. 8**).[28] Values obtained from the spirogram include the FEV_1, the FVC, and the forced expired flow between 25 and 75% of the FEV ($FEF_{25–75\%}$).[28] Additional values include the $FEV_{0.75}$ used in children under 6 years of age and the FEV_6, which can be used as a surrogate for FVC.[28] The FEV_3/FEV_6 ratio has also been studied.[28] From the flow–volume curve PEF and FEF at 25, 50, and 75% of vital capacity can be obtained.

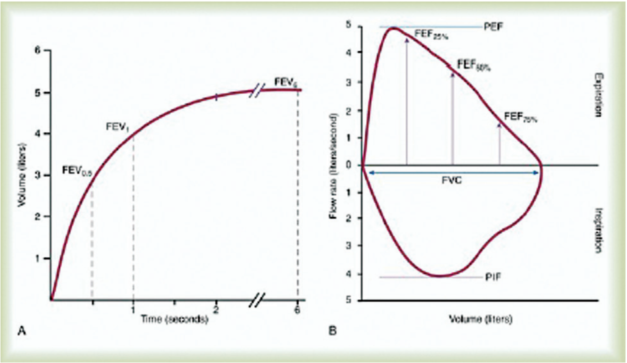

Fig. 8 (**A**) Maximal forced expiratory spirogram (volume time curve). Volume (L) is on the vertical axis and time (sec) on the horizontal axis. (**B**) Expiratory and inspiratory flow–volume curve. Flow rate (L/s) is on the vertical axis and volume (L) on the horizontal axis. Expiration and inspiration above and below the horizontal axis respectively. $FEF_{y\%}$, forced expiratory flow at y-percentage of the expired vital capacity; FEV_x, forced expiratory volume at x seconds; FVC, forced vital capacity; PEF, peak expiratory flow; PIF, peak inspiratory flow. Reproduced with permission from Douse.[29]

Interpretation of Spirometry

Obstruction

Airflow obstruction is identified by a reduced FEV_1/FVC ratio and its severity by the degree of FEV_1 reduction. The Global Initiative for Chronic Obstructive Lung Disease (GOLD) has recommended a fixed ratio of <0.7 to define obstruction,[30] but, since this is markedly age-dependent (falling with age),[31] the preferred approach is to use the lower limit of normal defined as the fifth percentile,[11] 1.645 standard deviation below the Global Lung Initiative (GLI) predicted values.[32] Schemes for quantification of severity of obstruction over the last 2 decades[11,29,32,33] are summarized in ►**Table 1**. The current ATS/ERS recommendation discourages use of FEV_1% predicted to grade severity and instead recommends using *z*-scores below the predicted FEV_1,[11] -1.645 to -2.5 mild, -2.5 to -4 moderate, and >-4 severe obstruction.[11] Disproportionate reduction of flows in the latter part of expiration (e.g., $FEF_{25–75\%}$, $FEF_{75\%}$) may signify distal airway obstruction.[33] The shape of the flow–volume curve can suggest intra- or extrathoracic variable obstruction or fixed obstruction.[33] Even though obstruction is typically characterized by a reduction in FEV_1 in the presence of a low FEV_1/FVC, obstruction may also result in a reduction in FVC from hyperinflation (see below).[23]

Table 1 Definitions and categorization of airflow obstruction using the FEV$_1$ and the FEV$_1$/FVC ratio

	Pauwels 2001[30] Ratio < 0.7	Pellegrino 2005[33] Ratio $<$ LLN[a]	Quanjer 2014[34] Ratio $<$ LLN	Stanojevic 2022[11] Ratio $<$ LLN
Obstruction: severity classification	FEV$_1$ (% predicted)	FEV$_1$ (% predicted)	FEV$_1$ (*z*-score)	FEV$_1$ (*z*-score)
Mild	$>80\%$	$>70\%$	< -2	-1.65 to -2.5
Moderate	50–80%	60–70%	-2 to -2.5	-2.5 to -4
Moderate–severe		50–60%	-2.5 to -3	
Severe	30–50%	35–50%	-3 to -4	> -4
Very severe	$<30\%$	$<35\%$	> -4	

Abbreviations: FEV1, forced expiratory volume in 1 second; FVC, forced vital capacity; GOLD, Global Initiative for Chronic Obstructive Lung Disease.
[a] LLN = lower limit of normal (5th percentile or *z*-score = − 1.645).

Restriction

Nonobstructive reduction in both FEV$_1$ and FVC (i.e., with a normal FEV$_1$/FVC) raises the possibility of restriction; measurements of lung volume are required to confirm this as restriction is defined by a low TLC.[11] While restriction is typically thought of in association with parenchymal lung disease causing reduced lung compliance, it may also be seen in any process that reduces TLC, such as space-occupying extrapulmonary disease (e.g., pleural effusion), reduced compliance of the chest wall (e.g., obesity, kyphoscoliosis), or neuromuscular disease resulting in muscle weakness (e.g., amyotrophic lateral sclerosis). Once pulmonary restriction is confirmed, the FVC is commonly used to monitor disease status.

Bronchodilator Response

A bronchodilator response is often tested at the time of spirometry to determine whether there might be significant ASM constriction contributing to airway narrowing. Because of the acute response being investigated, short-acting β agonists (SABA's) are the standard bronchodilator agent used. The mechanism of action of a β-agonist bronchodilator is related to stimulation of β2 adrenergic receptors on ASM resulting in smooth muscle relaxation. Other mechanisms may also be operative. For example, the very act of taking a deep breath may result in some bronchodilation by direct relaxation of ASM.[35] In addition, another action of β-agonists is stimulation of surfactant,[36] which could result in reduced airway fluid surface tension allowing airway widening. Interestingly, a deep breath is also a potent stimulus for surfactant secretion,[37] so taking a deep inhalation of SABA may have dual bronchodilator actions. The bronchodilator response allows faster and better lung emptying, resulting in a lower end-expiratory lung volume and less hyperinflation, as well as reduced gas trapping, both of which may have profound consequences for improvement in symptoms of shortness of breath.[38]

Bronchodilator response is assessed by repeat determination of FEV$_1$ and FVC 15 minutes following administration of a bronchodilator. While the choice of agent and dose is optional, a suggestion is salbutamol (albuterol) 100 µg 4 puffs.[33] Significant bronchodilator improvement was previously defined as a 12% and 200-mL increase in FEV$_1$ and/or FVC from baseline.[33] The ATS/ERS currently recommends that to minimize age and sex differences, a significant response is an increase in FEV1 or FVC of more than 10% of their respective predicted values.[11] This defines significant difference from normal but provides minimal distinction between different types of airway disease.[11] It is recommended against assessing bronchodilator response at various points in the FVC ($\text{FEF}_{25-75\%}$, $\text{FEF}_{50\%}$, $\text{FEF}_{75\%}$, etc.)[11] since they will be measured at different absolute lung volumes.[28,39,40] Of note, a bronchodilator response may also be defined by other criteria related to FEV$_1$ or FVC or changes in lung volumes[41] as well as changes in oscillatory resistance or reactance.[9]

Dynamic Hyperinflation

When airflow obstruction is present, a fundamental problem is insufficient time for full exhalation because expiratory flow is reduced. This may lead to a situation of incomplete lung emptying prior to the next inhalation, resulting in hyperinflation.[23] Another mechanism of hyperinflation is persistent inspiratory muscle activity during what would otherwise be a normal, passive exhalation through an open glottis. In this situation, FRC may not return to its fully relaxed level, resulting in hyperinflation.[42] If hyperinflation occurs during exercise or other reasons for increased ventilation, progressive elevation of end-expiratory lung volume may occur. This process is known as "dynamic hyperinflation" and is related to the degree of flow limitation as well as the time available for exhalation (►**Fig. 9**). Dynamic hyperinflation can also occur at rest during exacerbation of underlying disease such as COPD.[43] Dynamic hyperinflation results in severe dyspnea due to progressive flattening of the diaphragms and expansion of the chest, resulting in decreased mechanical advantage of the respiratory muscles. Progressive lung volume expansion also results in an increased work of breathing as the respiratory system now sits at a flatter position on its pressure–volume curve.[43] It also raises FRC to such a point that inspiratory capacity (IC) decreases, resulting in severe dyspnea.[44] The work of breathing is also increased because the respiratory muscles must generate enough inspiratory pressure to overcome any trapped, residual positive pressure within areas of gas trapping, similar to autopeep described in mechanical

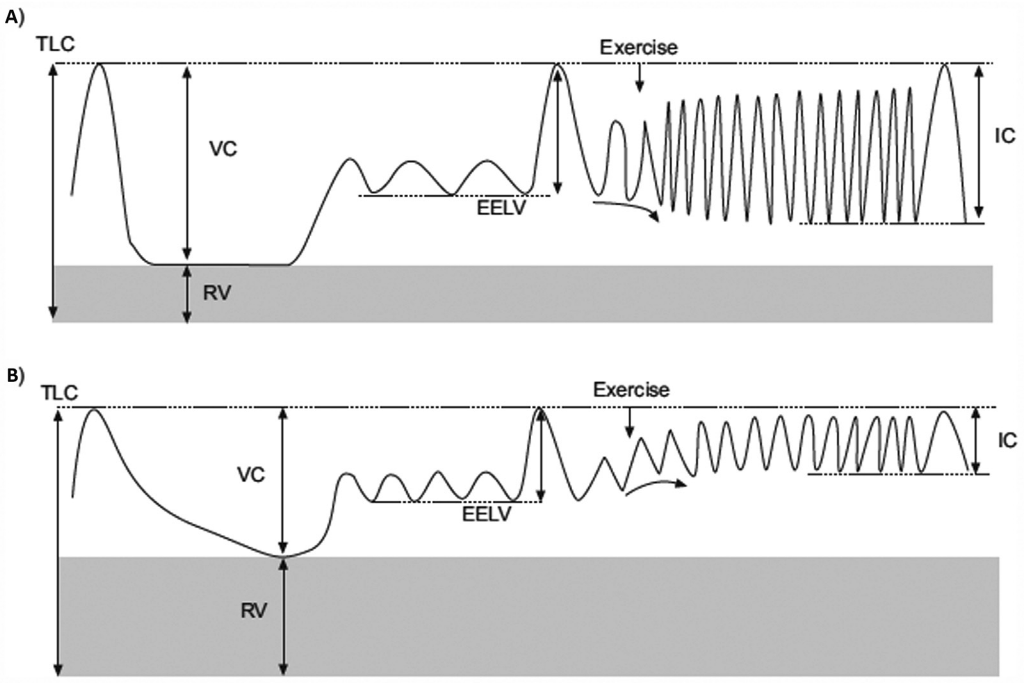

Fig. 9 Dynamic hyperinflation. Shown are typical volume versus time tracings in a healthy person (**A**) and a person with airflow obstruction (**B**), as they do a slow vital capacity maneuver (VC), breathe quietly at rest with end-expiratory lung volume (EELV) at functional residual capacity (FRC), and then take in a full deep inspiration (inspiratory capacity, IC) to total lung capacity (TLC). Exercise then starts as shown by the vertical downward arrow. In the healthy person, the IC during exercise becomes progressively larger as the EELV drops toward residual volume (RV) and the end-inspiratory lung volume rises toward TLC. In a person with airflow obstruction, who already starts off with a higher RV and EELV (FRC) at rest, limited time for exhalation only allows the IC to increase in the direction of TLC, not decrease toward RV, resulting in progressive elevation of the EELV, or dynamic hyperinflation. Reproduced with permission from O'Donnel DE.[45]

ventilation. Dynamic hyperinflation may also result in impaired gas exchange, since it is an uneven process resulting in more heterogeneous matching of ventilation and perfusion.[46] In addition, dynamic hyperinflation has been shown to have hemodynamic consequences since venous return through the pressurized, hyperinflated thoracic cavity may be compromised and result in reduced cardiac function and increased pulmonary artery pressures, further contributing to dyspnea.[46] Dynamic hyperinflation can be assessed using spirometry by tracking changes in IC before and after exercise.[47]

Airway Hyperresponsiveness

Airway hyperresponsiveness (AHR) refers to the increased sensitivity and response of the ASM to constrict following exposure to a stimulus. It is considered a defining feature of asthma, although AHR can also be observed in patients following upper respiratory tract infection (particularly due to viral causes), and in those with COPD,[48] cystic fibrosis,[49] and cardiac disease.[50]

The dual nature of increased sensitivity and response to a stimulus was first demonstrated in asthma by Woolcock et al,[51] who administered increasing doses of a bronchoconstrictor to healthy people and individuals with asthma and observed that AHR was characterized by both increased sensitivity (leftward shift in the dose–response curve) and increased maximal response. AHR is diagnosed when a lower dose of agonist causes a prespecified response, such as a 20% fall in FEV_1 when methacholine is the agonist.[52] Similarly, the fall in FEV_1 can be plotted on a linear dose axis to calculate the dose–response slope, providing a measure of AHR in all subjects, and not just those whose response meets the prespecified threshold.[53]

Mechanisms of Airway Hyperresponsiveness

Multiple mechanisms are implicated in the phenomenon of AHR (►**Fig. 10**).[54] Alterations in ASM function may result in increased contractile force[55,56] or speed.[57] Airway remodeling may result in increased airway wall thickness and thus geometric enhancement of any degree of ASM contraction on airway narrowing.[58,59] Airway remodeling may also disrupt the mechanical linkage of the airway wall to the surrounding lung parenchyma, reducing the tethering of the airway wall (airway–parenchymal interdependence) and thus enabling enhanced airway narrowing for any degree of ASM contraction.[60] The mechanical linkage of the airway to surrounding lung parenchyma is critical to understanding the effects of deep inflation and lung volume on ASM tone and AHR.[7] In health, periodic DI's result in stretch of ASM and cause bronchodilation.[7] DI's may also protect against subsequent bronchoconstriction.[61] In asthma, external ASM loads are thought to be decreased because of peribronchial inflammation and edema, which serve to uncouple the airway wall

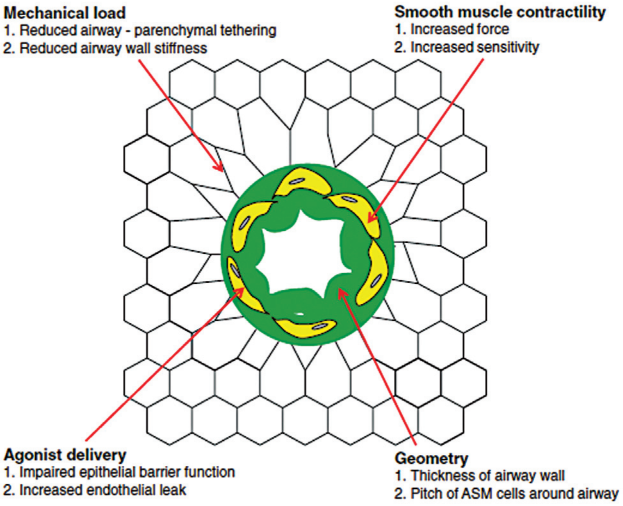
Mechanical load
1. Reduced airway - parenchymal tethering
2. Reduced airway wall stiffness
Smooth muscle contractility
1. Increased force
2. Increased sensitivity
Agonist delivery
1. Impaired epithelial barrier function
2. Increased endothelial leak
Geometry
1. Thickness of airway wall
2. Pitch of ASM cells around airway

Fig. 10 Mechanisms involved in airways hyperresponsiveness (AHR). Shown is a theoretical cross-section of an airway embedded in its surrounding parenchymal alveolar attachments. Major factors involved in AHR include altered airway smooth muscle (ASM) mechanical load or contractility, changes in airway wall geometry, and changes in agonist delivery. Not shown is the variability in subsequent regional airflow resulting in ventilation heterogeneity, which may also predispose to AHR. Reproduced with persmission from Bates.[62]

from the surrounding alveolar tethering units, a phenomenon referred to as loss of interdependence.[60] Loss of interdependence not only allows the ASM to constrict more for a given force, but also uncouples the airway wall from the lung parenchyma such that the airways dilate less in response to a DI. DI bronchoprotection is also lost in asthma,[63] which is thought to be a primary cause of AHR.

Resting lung volume can also play a role in determining AHR. Healthy individuals can develop AHR by voluntary breathing at low lung volume, lying supine, or increasing the external load on the chest wall, all of which result in a low volume state that can increase AHR.[64–66] Three mechanisms are thought to contribute. First, breathing at low lung volume may allow ASM to adapt to a shorter length thereby generating increased force and greater airway narrowing.[67] Second, a reduction in FRC would reduce the outward tethering forces exerted on the airways by the lung parenchyma,[68] allowing the airways to narrow more in response to a bronchoconstricting stimulus. Third, both voluntary low lung volume breathing[69] and chest wall strapping increase ventilation heterogeneity,[66] which computational modeling predicts would predispose to localized and exaggerated airway closure upon ASM stimulation[70] (see discussion of ventilation heterogeneity as a mechanism of AHR below). Indeed, chest wall strapping leads to exaggerated airway closure during bronchial challenge.[71]

Other mechanisms of AHR are also described. Since the airway epithelium acts as a barrier between the outside environment and the ASM underneath, any disruption in the airway epithelium may allow easier and quicker access of inhaled bronchoconstricting agents (e.g., methacholine) to the ASM, resulting in AHR.[72] Changes in environmental conditions at the airway epithelium surface, particularly low humidity, may result in local water loss and increased airway surface fluid osmolarity, triggering the release of bronchoconstricting mediators like histamine and cysteinyl leukotrienes from airway mast cells;[73] this is thought to be the primary stimulus for AHR in response to exercise. Even ventilation heterogeneity has been shown to contribute to AHR[74] and enhance AHR.[75] Computational modeling predicts that a positive feedback mechanism may develop that allows a small degree of induced bronchoconstriction on a heterogeneously narrowed airway tree to result in an "avalanche" effect of airway narrowing and closure throughout the tree.[70]

Table 2 PD_{20}^{a} diagnostic cut points

Classification	PD_{20}^{a} (μg)^{b}	Comparable English-Wright 2-min tidal breathing PC_{20}^{c} (mg/mL)
Normal	>400	>16
Borderline AHR	$>100–\leq 400$	$>4–\leq 16$
Mild AHR	$>25–\leq 100$	$>1–\leq 4$
Moderate AHR	$>6–\leq 25$	$>0.25–\leq 1$
Marked AHR	≤ 6	≤ 0.25

Abbreviations: AHR, airway hyperresponsiveness; FEV1, forced expiratory volume in 1 second.
$^{a}PD_{20}$ = provocative dose causing a 20% fall in FEV1.
$^{b}PD_{20}$ after taking into account evaporation if a jet nebulizer is used.
$^{c}PC_{20}$ = provocative concentration causing a 20% fall in FEV1.

Methodology of Measuring Airway Hyperresponsiveness

AHR may be measured by either direct or indirect airway challenge. In direct challenges, agents such as methacholine are administered that act directly on ASM to cause bronchoconstriction. Increasing doses of inhaled methacholine are administered in a standardized fashion to determine the provocative dose that causes a 20% fall in FEV_1 (PD_{20}-FEV_1, ►**Table 2**).[52] If the PD_{20}-$FEV_1 < 100$ μg, AHR is defined, whereas a PD_{20}-$FEV_1 > 400$ μg is considered normal (no AHR). PD_{20}-FEV_1 values between 100 and 400 μg are considered borderline. Due to the bronchodilating effect of a deep inhalation, it is recommended that methacholine challenge be performed using tidal breathing rather than 5 deep breaths to avoid overestimating the PD_{20}-FEV_1, which may miss mild AHR (►**Fig. 11**).[52] Indirect challenges involve inhalation of agents that act secondarily on ASM and thus mimic the more natural condition of asthma.[71] Common indirect challenges include exercise and mannitol, both of which result in ASM constriction through an osmotic stimulus as described above; standardized protocols for each have been published.[71] Differential features comparing indirect and direct challenges are summarized in ►**Table 3**. Indirect challenges reflect airway inflammation, whereas direct challenges reflect ASM function. Therefore, direct challenges are thought to be more sensitive but less specific for asthma, so are useful for ruling out asthma at the time of testing,

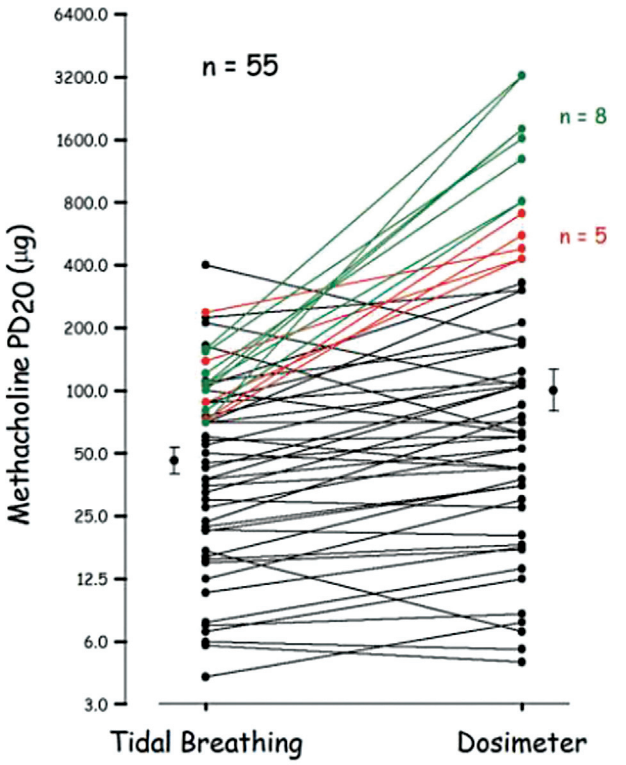

Fig. 11 Comparison of methacholine provocation dose causing a 20% FEV_1 fall (PD_{20}) performed in 55 asthmatics by the two allegedly equivalent methods outlined by the American Thoracic Society document in 2000 (Crapo et al[78]). The 2-minute tidal breathing PD_{20} is shown on the left and the deep inhalation dosimeter PD_{20} is shown on the right (both on a log scale). The geometric mean tidal breathing PD_{20} is 45 µg and the dosimeter PD_{20} 103 µg ($p < 0.00001$). The eight participants in green had dosimeter PD_{20}s between 800 and 3,200 µg and the five in red values between 400 and 800 µg. Reproduced in modified form (PC_{20} in mg/mL replaced with PD_{20} in µg) from Cockcroft and Davis.[79]

whereas indirect challenges are more specific but less sensitive for asthma.[76,77]

Conclusion

This chapter has highlighted the dynamics of the respiratory system. We need to understand the underlying principles governing airway resistance, lung elastance, and airflow to understand the events and work associated with tidal breathing. Likewise, a full appreciation of FEV_1 requires understanding the concept of airflow limitation during forced exhalation through collapsible airways. Important aspects of altered airflow and its consequences include bronchodilator responsiveness, dynamic hyperinflation, and airway hyperresponsiveness.

Conflict of Interest
None declared.

Acknowledgment
The authors thank Jacquie Bramley for assistance in preparing portions of this manuscript.

Table 3 Comparison of direct and indirect challenges

	Direct challenge e.g., methacholine	Indirect challenge e.g., mannitol
Muscle function	++++	++
Airway calibre	++++	±
Inflammation	Nil to ++	++++
Dose required	Low	Higher (1,000-fold)
Deep inhalations	Bronchoprotection	No effect
Refractory period	±	++++
Cromolyn inhibition	Nil	++++
Diagnostic sensitivity	High	Low
Diagnostic specificity	Low to moderate	High
Diagnostic value	Rule out	Rule in

Notes: + to ++++ = less to more highly associated.
± = equivocal.

References

1 Lutfi MF. The physiological basis and clinical significance of lung volume measurements. Multidiscip Respir Med 2017;12:3
2 Cabello B, Mancebo J. Work of breathing. Intensive Care Med 2006;32(09):1311–1314
3 Wagers S, Lundblad L, Moriya HT, Bates JH, Irvin CG. Nonlinearity of respiratory mechanics during bronchoconstriction in mice with airway inflammation. J Appl Physiol 2002;92(05):1802–1807
4 Bossé Y, Riesenfeld EP, Paré PD, Irvin CG. It's not all smooth muscle: non-smooth-muscle elements in control of resistance to airflow. Annu Rev Physiol 2010;72:437–462
5 Al-Subu AM, Rehder KJ. Heliox as adjunctive therapy for pediatric critical asthma: time to question its role? Respir Care 2022;67(05):624–626
6 Mead J. The lung's "quiet zone". N Engl J Med 1970;282(23):1318–1319
7 Paré PD, Mitzner W. Airway-parenchymal interdependence. Compr Physiol 2012;2(03):1921–1935
8 Kaminsky DA. What does airway resistance tell us about lung function? Respir Care 2012;57(01):85–96, discussion 96–99
9 Kaminsky DA, Simpson SJ, Berger KI, et al. Clinical significance and applications of oscillometry. Eur Respir Rev 2022;31(163):31
10 King GG, Bates J, Berger KI, et al. Technical standards for respiratory oscillometry. Eur Respir J 2020;55(02):55
11 Stanojevic S, Kaminsky DA, Miller MR, et al. ERS/ATS technical standard on interpretive strategies for routine lung function tests. Eur Respir J 2022;60(01):60
12 Hole DJ, Watt GC, Davey-Smith G, Hart CL, Gillis CR, Hawthorne VM. Impaired lung function and mortality risk in men and women: findings from the Renfrew and Paisley prospective population study. BMJ 1996;313(7059):711–715, discussion 715–716
13 Krishnan JK, Martinez FJ. Lung function trajectories and chronic obstructive pulmonary disease: current understanding and knowledge gaps. Curr Opin Pulm Med 2018;24(02):124–129
14 Mannino DM, McBurnie MA, Tan W, et al; BOLD Collaborative Research Group. Restricted spirometry in the Burden of Lung Disease Study. Int J Tuberc Lung Dis 2012;16(10):1405–1411
15 Mathew J, Nickel NP. Cardiovascular morbidity in individuals with impaired FEV1. Curr Cardiol Rep 2022;24(03):163–182

16 Quanjer PH, Tammeling GJ, Cotes JE, Pedersen OF, Peslin R, Yernault JC. Lung volumes and forced ventilatory flows. Eur Respir J 1993;6(suppl 16):5–40

17 Wanger JS, Ikle DN, Cherniack RM. The effect of inspiratory maneuvers on expiratory flow rates in health and asthma: influence of lung elastic recoil. Am J Respir Crit Care Med 1996;153(4 Pt 1):1302–1308

18 Hyatt RE. Expiratory flow limitation. J Appl Physiol 1983;55(1 pt 1):1–7

19 Pedersen OF, Butler JP. Expiratory flow limitation. Compr Physiol 2011;1(04):1861–1882

20 Dawson SV, Elliott EA. Wave-speed limitation on expiratory flow-a unifying concept. J Appl Physiol 1977;43(03):498–515

21 Bates J. Physics of Expiratory Flow Limitation. In: Hamid Q, Shannon J, Martin J, eds. Physiologic Basis of Respiratory Disease. Hamilton, ON, Canada: BC Decker, Inc.; 2005

22 Kass JE, Terregino CA. The effect of heliox in acute severe asthma: a randomized controlled trial. Chest 1999;116(02):296–300

23 Pellegrino R, Brusasco V. On the causes of lung hyperinflation during bronchoconstriction. Eur Respir J 1997;10(02):468–475

24 ATS statement–Snowbird workshop on standardization of spirometry. Am Rev Respir Dis 1979;119(05):831–838

25 Statement of the American Thoracic Society. Standardization of spirometry–1987 update. Am Rev Respir Dis 1987;136(05): 1285–1298

26 American Thoracic Society. Standardization of spirometry, 1994 update. Am J Respir Crit Care Med 1995;152(03):1107–1136

27 Miller MR, Hankinson J, Brusasco V, et al; ATS/ERS Task Force. Standardisation of spirometry. Eur Respir J 2005;26(02): 319–338

28 Graham BL, Steenbruggen I, Miller MR, et al. Standardization of spirometry 2019 update. An Official American Thoracic Society and European Respiratory Society Technical Statement. Am J Respir Crit Care Med 2019;200(08):e70–e88

29 Douce DH. Pulmonary Function Testing. Accessed June 6, 2023 at: https://thoracickey.com/pulmonary-function-testing-2/

30 Pauwels RA, Buist AS, Calverley PM, Jenkins CR, Hurd SSGOLD Scientific Committee. Global strategy for the diagnosis, management, and prevention of chronic obstructive pulmonary disease. NHLBI/WHO Global Initiative for Chronic Obstructive Lung Disease (GOLD) Workshop summary. Am J Respir Crit Care Med 2001;163(05):1256–1276

31 Stanojevic S, Wade A, Stocks J, et al. Reference ranges for spirometry across all ages: a new approach. Am J Respir Crit Care Med 2008;177(03):253–260

32 Quanjer PH, Stanojevic S, Cole TJ, et al; ERS Global Lung Function Initiative. Multi-ethnic reference values for spirometry for the 3-95-yr age range: the global lung function 2012 equations. Eur Respir J 2012;40(06):1324–1343

33 Pellegrino R, Viegi G, Brusasco V, et al. Interpretative strategies for lung function tests. Eur Respir J 2005;26(05):948–968

34 Quanjer PH, Pretto JJ, Brazzale DJ, Boros PW. Grading the severity of airways obstruction: new wine in new bottles. Eur Respir J 2014;43(02):505–512

35 Skloot G, Togias A. Bronchodilation and bronchoprotection by deep inspiration and their relationship to bronchial hyperresponsiveness. Clin Rev Allergy Immunol 2003;24(01):55–72

36 Mason RJ. Surfactant synthesis, secretion, and function in alveoli and small airways. Review of the physiologic basis for pharmacologic intervention. Respiration 1987;51(suppl 1):3–9

37 Nicholas TE, Power JH, Barr HA. The pulmonary consequences of a deep breath. Respir Physiol 1982;49(03):315–324

38 O'Donnell DE, Milne KM, James MD, de Torres JP, Neder JA. Dyspnea in COPD: new mechanistic insights and management implications. Adv Ther 2020;37(01):41–60

39 Cockcroft DW, Berscheid BA. Volume adjustment of maximal midexpiratory flow. Importance of changes in total lung capacity. Chest 1980;78(04):595–600

40 Olsen CR, Hale FC. A method for interpreting acute response to bronchodilators from the spirogram. Am Rev Respir Dis 1968;98 (02):301–302

41 Kaminsky DA. What is a significant bronchodilator response? Ann Am Thorac Soc 2019;16(12):1495–1497

42 Palecek F. Hyperinflation: control of functional residual lung capacity. Physiol Res 2001;50(03):221–230

43 O'Donnell DE, Laveneziana P. The clinical importance of dynamic lung hyperinflation in COPD. COPD 2006;3(04):219–232

44 Dempsey JA, Neder JA, Phillips DB, O'Donnell DE. The physiology and pathophysiology of exercise hyperpnea. Handb Clin Neurol 2022;188:201–232

45 O'Donnell D. Impacting patient-centered outcomes in COPD: breathlessness and exercise tolerance. Eur Respir Rev 2006; 15:37–41

46 Rossi A, Aisanov Z, Avdeev S, et al. Mechanisms, assessment and therapeutic implications of lung hyperinflation in COPD. Respir Med 2015;109(07):785–802

47 Marin JM, Carrizo SJ, Gascon M, Sanchez A, Gallego B, Celli BR. Inspiratory capacity, dynamic hyperinflation, breathlessness, and exercise performance during the 6-minute-walk test in chronic obstructive pulmonary disease. Am J Respir Crit Care Med 2001; 163(06):1395–1399

48 van den Berge M, Vonk JM, Gosman M, et al. Clinical and inflammatory determinants of bronchial hyperresponsiveness in COPD. Eur Respir J 2012;40(05):1098–1105

49 van Haren EH, Lammers JW, Festen J, Heijerman HG, Groot CA, van Herwaarden CL. The effects of the inhaled corticosteroid budesonide on lung function and bronchial hyperresponsiveness in adult patients with cystic fibrosis. Respir Med 1995;89(03): 209–214

50 Sasaki F, Ishizaki T, Mifune J, Fujimura M, Nishioka S, Miyabo S. Bronchial hyperresponsiveness in patients with chronic congestive heart failure. Chest 1990;97(03):534–538

51 Woolcock AJ, Salome CM, Yan K. The shape of the dose-response curve to histamine in asthmatic and normal subjects. Am Rev Respir Dis 1984;130(01):71–75

52 Coates AL, Wanger J, Cockcroft DW, et al; Bronchoprovocation Testing Task Force: Kai-Håkon Carlsen. ERS technical standard on bronchial challenge testing: general considerations and performance of methacholine challenge tests. Eur Respir J 2017;49(05): 49

53 Salome CM, Brown NJ, Reddel HK, Xuan W, Marks GB. Indices of bronchial reactivity and sensitivity. Thorax 2011;66(03):265-–266, author reply 266

54 Kaminsky DA, Chapman DG. Asthma and lung mechanics. Compr Physiol 2020;10(03):975–1007

55 Bai TR. Abnormalities in airway smooth muscle in fatal asthma. A comparison between trachea and bronchus. Am Rev Respir Dis 1991;143(02):441–443

56 Björck T, Gustafsson LE, Dahlén SE. Isolated bronchi from asthmatics are hyperresponsive to adenosine, which apparently acts indirectly by liberation of leukotrienes and histamine. Am Rev Respir Dis 1992;145(05):1087–1091

57 Solway J, Fredberg JJ. Perhaps airway smooth muscle dysfunction contributes to asthmatic bronchial hyperresponsiveness after all. Am J Respir Cell Mol Biol 1997;17(02):144–146

58 Moreno RH, Hogg JC, Paré PD. Mechanics of airway narrowing. Am Rev Respir Dis 1986;133(06):1171–1180

59 Lambert RK, Wiggs BR, Kuwano K, Hogg JC, Paré PD. Functional significance of increased airway smooth muscle in asthma and COPD. J Appl Physiol 1993;74(06):2771–2781

60 Macklem PT. Mechanical factors determining maximum bronchoconstriction. Eur Respir J Suppl 1989;6:516s–519s

61 Chapman DG, Brown NJ, Salome CM. The dynamic face of respiratory research: understanding the effect of airway disease on a lung in constant motion. Pulm Pharmacol Ther 2011;24(05): 505–512

62 Bates JH. Systems physiology of the airways in health and obstructive pulmonary disease. Wiley Interdiscip Rev Syst Biol Med 2016;8:423–437

63 Skloot G, Permutt S, Togias A. Airway hyperresponsiveness in asthma: a problem of limited smooth muscle relaxation with inspiration. J Clin Invest 1995;96(05):2393–2403

64 Ding DJ, Martin JG, Macklem PT. Effects of lung volume on maximal methacholine-induced bronchoconstriction in normal humans. J Appl Physiol 1987;62(03):1324–1330

65 Meinero M, Coletta G, Dutto L, et al. Mechanical response to methacholine and deep inspiration in supine men. J Appl Physiol 2007;102(01):269–275

66 Chapman DG, Berend N, Horlyck KR, King GG, Salome CM. Does increased baseline ventilation heterogeneity following chest wall strapping predispose to airway hyperresponsiveness? J Appl Physiol 2012;113(01):25–30

67 Pratusevich VR, Seow CY, Ford LE. Plasticity in canine airway smooth muscle. J Gen Physiol 1995;105(01):73–94

68 Mead J, Takishima T, Leith D. Stress distribution in lungs: a model of pulmonary elasticity. J Appl Physiol 1970;28(05):596–608

69 Hughes PJC, Smith L, Chan HF, et al. Assessment of the influence of lung inflation state on the quantitative parameters derived from hyperpolarized gas lung ventilation MRI in healthy volunteers. J Appl Physiol 2019;126(01):183–192

70 Venegas JG, Winkler T, Musch G, et al. Self-organized patchiness in asthma as a prelude to catastrophic shifts. Nature 2005;434 (7034):777–782

71 Pellegrino R, Pompilio PP, Bruni GI, et al. Airway hyperresponsiveness with chest strapping: A matter of heterogeneity or reduced lung volume? Respir Physiol Neurobiol 2009;166(01):47–53

72 Mitchell HW, Fisher JT, Sparrow MP. The integrity of the epithelium is a major determinant of the responsiveness of the dog bronchial segment to mucosal provocation. Pulm Pharmacol 1993;6(04):263–268

73 Kippelen P, Anderson SD, Hallstrand TS. Mechanisms and biomarkers of exercise-induced bronchoconstriction. Immunol Allergy Clin North Am 2018;38(02):165–182

74 Pascoe CD, Seow CY, Hackett TL, Paré PD, Donovan GM. Heterogeneity of airway wall dimensions in humans: a critical determinant of lung function in asthmatics and nonasthmatics. Am J Physiol Lung Cell Mol Physiol 2017;312(03):L425–L431

75 Gillis HL, Lutchen KR. Airway remodeling in asthma amplifies heterogeneities in smooth muscle shortening causing hyperresponsiveness. J Appl Physiol 1999;86(06):2001–2012

76 Hallstrand TS, Leuppi JD, Joos G, et al; American Thoracic Society (ATS)/European Respiratory Society (ERS) Bronchoprovocation Testing Task Force. ERS technical standard on bronchial challenge testing: pathophysiology and methodology of indirect airway challenge testing. Eur Respir J 2018;52 (05):52

77 Pauwels R, Joos G, Van der Straeten M. Bronchial hyperresponsiveness is not bronchial hyperresponsiveness is not bronchial asthma. Clin Allergy 1988;18(04):317–321

78 Crapo RO, Casaburi R, Coates AL, et al. Guidelines for methacholine and exercise challenge testing-1999. American Thoracic Society. Am J Respir Crit Care Med 2000;161:309–329

79 Cockcroft DW, Davis BE. The bronchoprotective effect of inhaling methacholine by using total lung capacity inspirations has a marked influence on the interpretation of the test result. J Allergy Clin Immunol 2006;117:1244–1248

The Pulmonary Vasculature

Susan R. Hopkins, MD, PhD[1] Michael K. Stickland, PhD[2]

[1] Department of Radiology, University of California, San Diego, California
[2] Department of Medicine, Faculty of Medicine and Dentistry, University of Alberta, Edmonton, Alberta

Address for correspondence Susan R. Hopkins, MD, PhD, Department of Radiology, University of California, San Diego, CA 92093 (e-mail: shopkins@ucsd.edu).

Semin Respir Crit Care Med 2023;44:538–554.

Abstract

The pulmonary circulation is a low-pressure, low-resistance circuit whose primary function is to deliver deoxygenated blood to, and oxygenated blood from, the pulmonary capillary bed enabling gas exchange. The distribution of pulmonary blood flow is regulated by several factors including effects of vascular branching structure, large-scale forces related to gravity, and finer scale factors related to local control. Hypoxic pulmonary vasoconstriction is one such important regulatory mechanism. In the face of local hypoxia, vascular smooth muscle constriction of precapillary arterioles increases local resistance by up to 250%. This has the effect of diverting blood toward better oxygenated regions of the lung and optimizing ventilation–perfusion matching. However, in the face of global hypoxia, the net effect is an increase in pulmonary arterial pressure and vascular resistance. Pulmonary vascular resistance describes the flow-resistive properties of the pulmonary circulation and arises from both precapillary and postcapillary resistances. The pulmonary circulation is also distensible in response to an increase in transmural pressure and this distention, in addition to recruitment, moderates pulmonary arterial pressure and vascular resistance. This article reviews the physiology of the pulmonary vasculature and briefly discusses how this physiology is altered by common circumstances.

Keywords
- gravity
- Zone model
- fractal
- hypoxic pulmonary vasoconstriction
- pulmonary vascular resistance

The Distribution of Pulmonary Blood Flow

Introduction

The primary function of the pulmonary circulation is to deliver blood to the alveolar capillaries for gas exchange.[1] The alveolar-capillary membrane is extremely thin to facilitate gas exchange, and as a result, pulmonary vascular pressures must remain low both to protect the thin blood–gas barrier and to allow for efficient diffusion of respiratory gases.[1] Many of the mechanisms determining regional pulmonary blood flow are thought to be passive, particularly in the healthy lung, with active mechanisms initiated in circumstances such as hypoxia to facilitate local control of pulmonary blood flow distribution.

Before reviewing the factors affecting the distribution of pulmonary blood flow, clarification of terminology may be helpful. This is particularly important in the lung because of the strong effects that gravity and posture have on the distribution of perfusion (►**Fig. 1**). The term "gravitationally non-dependent" refers to the highest plane under consideration that is perpendicular to the direction of the gravitational vector, and in the upright lung this region is located in the apex. Conversely "gravitationally dependent" refers to a region perpendicular to the direction of the gravitational vector that is in the lowest plane of consideration, i.e., the lung base in the upright lung. Isogravitational refers to lung regions that are in the same plane with respect to the gravitational vector.

West and Dollery performed the first measurements of the distribution of pulmonary blood flow in the upright human lung using inhaled radiolabeled CO_2.[2] The CO_2, a soluble gas, was cleared from the alveolar space proportional to blood flow, leading to the discovery that pulmonary blood flow was not uniform across the lung, but rather, was greater in the lung bases than in the lung apices. West later wrote "I still remember our

Issue Theme Pulmonary Physiology; Guest Editors: David A. Kaminsky, MD, Kathryn A. Hibbert, MD, and Andrew M. Luks, MD

Thieme Medical Publishers, Inc.,
333 Seventh Avenue, 18th Floor,
New York, NY 10001, USA

DOI https://doi.org/10.1055/s-0043-1770059.
ISSN 1069-3424.

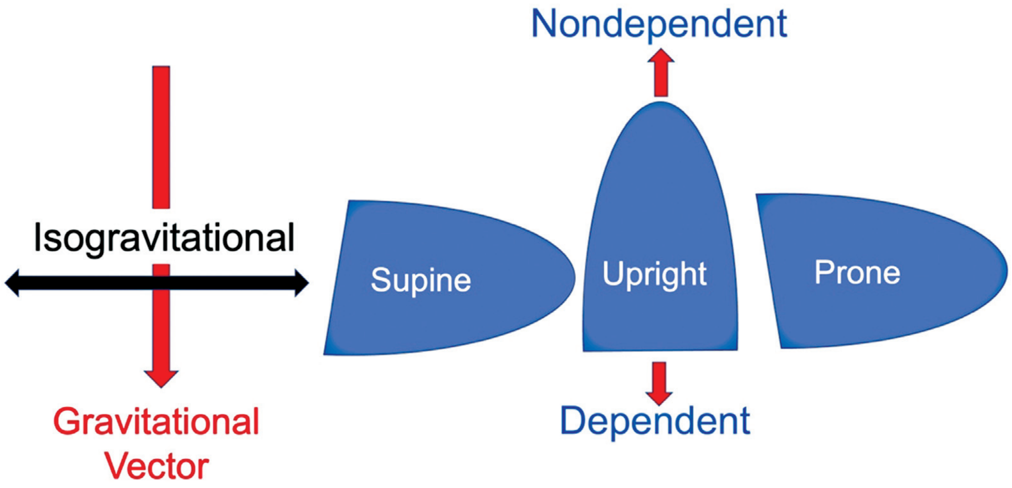

Fig. 1 Schematic diagram of gravitational relationships. The large red arrow indicates the direction of the gravitational vector, the black arrow perpendicular to the gravitational vector indicates the isogravitational direction, i.e., lung regions that are isogravitational are all in the same plane with respect to gravity. Gravitationally nondependent lung is the highest isogravitational plane under consideration whereas gravitationally dependent is lowest plane of consideration.

astonishment when measurements made in seated normal volunteers showed a striking increase in the clearance rate from the top to the bottom of the lung, because at that time there was little to suggest that it was not uniform."[3]

Since then, a great many studies have evaluated the distribution of pulmonary blood flow, but despite this, there are numerous unanswered questions and many conflicting studies. There are several factors that contribute to this uncertainty that should be kept in mind when reviewing the available literature. Many of these issues relate to the frame of reference of measurement. For example, heterogeneity is a function of spatial scale and increases as resolution increases, so studies conducted at different resolutions may return apparently conflicting results. In addition, the lung is a deformable structure and deforms under its own weight, resulting in a gravitational gradient in regional lung tissue density[4] and alveolar size,[5] such that alveoli in the gravitationally nondependent lung are larger than in dependent lung. In a hypothetical lung with uniform perfusion per alveolus, any gradient in alveolar size results in an apparent reversed gradient in perfusion when imaged externally because the perfusion occurs within the walls of the alveoli.[4] In other words, the deformation of the lung tissue means that the gravitationally dependent lung will have apparently greater perfusion in a given volume, because vessel density is greater; by correcting perfusion measurements for local tissue density, this apparent gradient is greatly reduced.[4] These gradients also affect local transpulmonary and transmural pressures, and therefore large blood vessel, and capillary diameters[5,6] and resistance to flow. Thus, lung volume of measurement affects not only interpretation of measures of heterogeneity, but also perfusion itself. Posture (discussed below) also has an effect on perfusion because the physical shape of the human lung is not symmetrical between postures, affecting transpulmonary pressure and lung stretch.[7]

In considering the distribution of blood flow in the lung, it would be a mistake to consider the pulmonary circulation in isolation. For example, local alveolar pressures influence the spatial distribution of pulmonary perfusion because the microcirculation of the lung is surrounded by alveoli, and the pressure within the alveoli exerts an external compressive force on the capillaries[1] (discussed below). Since pulmonary blood vessels and capillaries are distensible,[8,9] they respond in different ways to altered transpulmonary pressure. Lung expansion (i.e., increased transpulmonary pressure) stretches the capillaries, reducing their luminal diameter and increasing resistance. Two opposing effects act on the precapillary blood vessels as transpulmonary pressure increases: increased transmural pressure tends to increase the vessel diameter, whereas axial stretch of the vessel tends to decrease its diameter. The balance of radial and axial stretch determines the final vessel luminal size, and its resistance. The lung also undergoes large cyclical changes in volume with breathing. Regional changes in lung volume alter vascular diameters and hence regional resistances change throughout the breathing cycle. Importantly, the pulmonary circulation is a dynamic and integrated circuit where changes in flow within one region must influence flow elsewhere in the system.[1]

Structural Determinants of Pulmonary Blood Flow

The pulmonary vessels repeatedly branch, with a complete vascular tree created by repeatedly adding bifurcations at each terminal branch for up to 28 generations. A fractal structure is one that is composed of pieces that are similar to the structure as a whole, and the pulmonary vessels are considered a fractal tree/fractal network[10] due to the repetitive branching that is consistent in form from the initial branch, until the final terminal branches[11] (►**Fig. 2**).

Fractal structures are advantageous in that they appear to create the largest possible surface area within a given volume, while simultaneously minimizing the materials needed to construct the vascular tree, the volume of blood needed to fill the vascular tree, and the work needed to perfuse the tree.[11–14] The primary disadvantage of a fractal vascular tree is that it produces heterogeneous distributions of perfusion,[1]

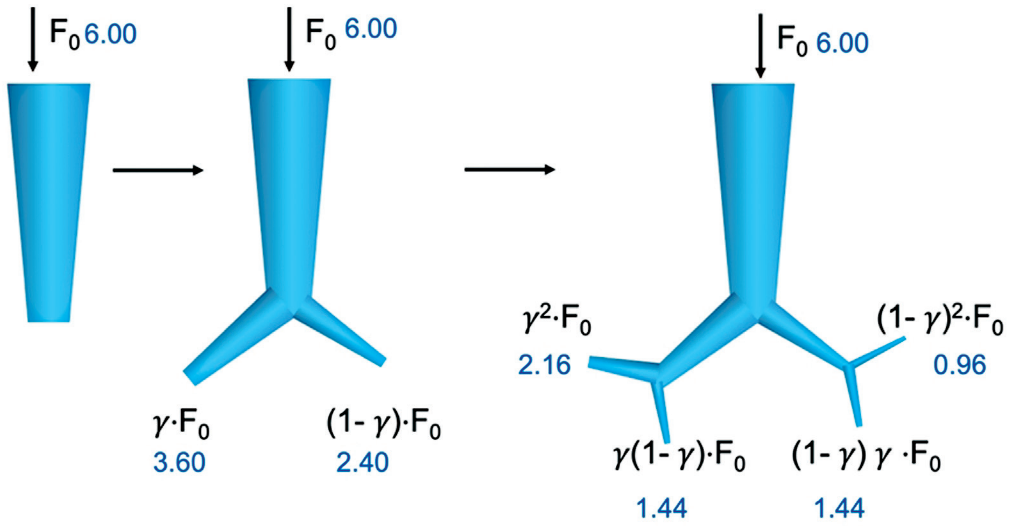

Fig. 2 A dichotomous branching model. The basic transformation is the dichotomous branching of each terminal element. The asymmetric branching of the terminal branch divides initial flow (F_0) into two fractions γ and $1-\gamma$ that are distributed to the daughter branches, where $\gamma = 0.5$ would be equal distribution between daughter branches. Following a second iteration in which all terminal nodes branch again, blood flow is now distributed to four terminal branches. Numbers in blue show calculated flow to each branch based on F_0 of 6 L/min and a γ of 0.6 and show how even relatively minor asymmetry in flow in the initial branches can give rise to large differences after a relatively small number of iterations. (Modified from Glenny and Robertson[11])

since slight asymmetries of branching angle and radii in these fractal trees result in significant heterogeneity of blood flow distribution at the level of gas exchange[1] (i.e., the acinus) (►**Fig. 2**). For efficient exchange gas, it is critical that regional ventilation be matched with regional perfusion. Structurally, the matching of ventilation to perfusion within the lung is supported by having a fractal airway tree similar to the vascular tree. Indeed, airways and pulmonary arteries branch in union with each other,[12,15] and while regional ventilation and perfusion are heterogeneous, they are closely correlated with each other (►**Fig. 3**), ensuring efficient gas exchange.[16,17]

Pulmonary Blood Flow Heterogeneity

Measurement of Pulmonary Blood Flow and Its Heterogeneity

A variety of techniques have been used to measure the distribution of pulmonary blood flow, including positron

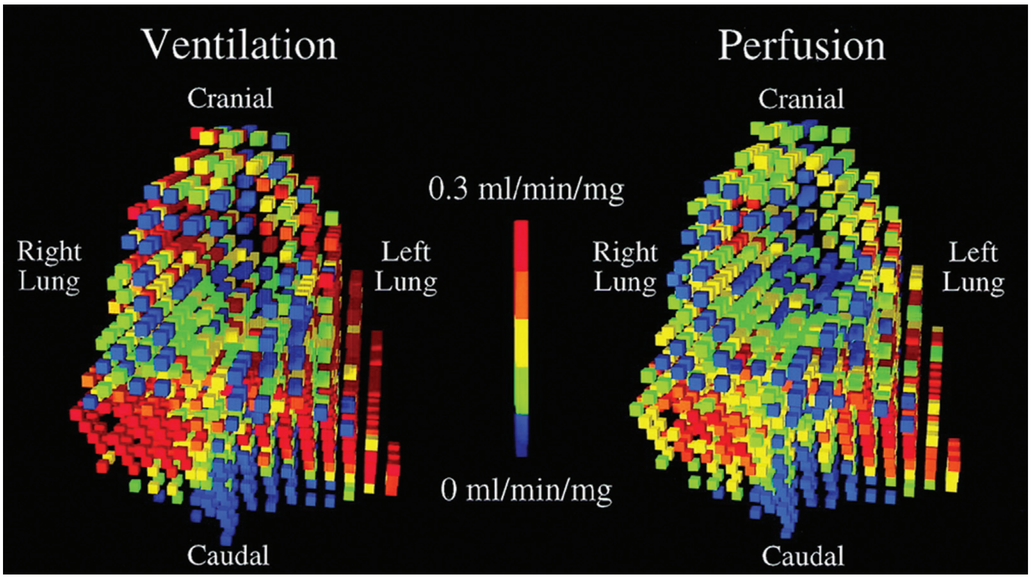

Fig. 3 Regional ventilation and perfusion scaled to the measured minute ventilation and cardiac output in prone posture. Data are from a microsphere study in mechanically ventilated pigs. Ventilation was measured by inhaled aerosolized fluorescent microspheres, and perfusion from injected fluorescent microspheres. These microspheres lodge in the small airways and capillaries proportional to ventilation and perfusion respectively and are quantified in approximately 1 cm cubes postmortem. Both ventilation and perfusion display regional clustering in which adjacent regions have similar flows. Note the strong spatial correlation in which regions that receive high ventilation receive high perfusion and regions that receive less ventilation receive less perfusion. (Reproduced with permission from Altemeier et al[17])

emission tomography (PET), single-photon emission computerized tomography (SPECT), computed tomography (CT), magnetic resonance imaging (MRI), and labeled microspheres (see Hopkins[18] and Hsia et al,[19] for review). Gravitational gradients as measures of heterogeneity are usually calculated as the slope of the relationship between perfusion and distance up the lung from the most gravitationally dependent surface.[4,20] Higher resolution studies of the distribution of pulmonary blood flow utilize two major indices of heterogeneity-relative dispersion (also known as the coefficient of variation) and fractal dimension. The relative dispersion is calculated as the ratio of the mean to standard deviation of signal intensity or blood flow. It is a global index of spatial heterogeneity without considering the specific anatomic location.[21] The advantage of the relative dispersion metric is that it is rather simple to calculate and does not require absolute quantification. Relative dispersion can be further broken down into an isogravitational component, which only considers variation across an isogravitational plane, and the variation in the direction of the gravitational vector.[22] Importantly, relative dispersion is scale-dependent, meaning that the value increases as the resolution increases, much in the way that when viewed from an aircraft, an expanse of beach may appear a uniform color, but when viewed through a microscope there is a multitude of colors of the grains of sand.

This change in heterogeneity with resolution is the basis of calculation of another metric, the fractal dimension. As described above, a fractal structure is composed of pieces that are similar to the structure as a whole. Fractal dimension is a scale-independent measure of perfusion heterogeneity[21] indicative of pulmonary vascular branching structure.[23] The fractal dimension can be calculated by calculating the relative dispersion at the highest resolution of measurement[21] and repeating this calculation in progressively larger blocks.[21,24] A plot of log-relative dispersion versus log piece size is constructed[21,24] with fractal dimension calculated as 1-slope of the relationship (►**Fig. 4**). In rats,[25] pulmonary perfusion heterogeneity has been shown to follow a fractal distribution to the level of the acinus. A fractal dimension of 1 represents a uniform distribution, whereas a fractal dimension of 1.5 represents a random distribution. The fractal dimension of pulmonary blood flow has been reported for several mammals—dogs, sheep, and horses,[24,26,27] ranging from 1.09 to 1.17. Fractal dimension measured in normal humans is similar (approximately 1.18[28]).

Large-Scale Effects on Regional Pulmonary Blood Flow: Gravitational Gradients and the Zone Model

Blood flow to a vascular bed is determined by the driving pressures and longitudinal resistances across the length of the circuit supplying and draining the region.[11] The resistance to flow for any region is a summation of the longitudinal resistances through the arteries, capillaries, and veins serving that region.[11] Most investigators identify the arterioles and venules as the highest resistance segments within the pulmonary circulation[11]; however, it is not well known which segments of the pulmonary vascular tree are the most important in determining regional flow. It is considered that all compartments (arterial, capillary, and venous) play a role in blood flow distribution.[11] It is important to recognize that the driving pressures—the difference between upstream pulmonary arterial pressure (P_a) and downstream venous pressure (P_v)—are not uniform in the lung. Pulmonary vascular resistance (PVR) is discussed in detail below.

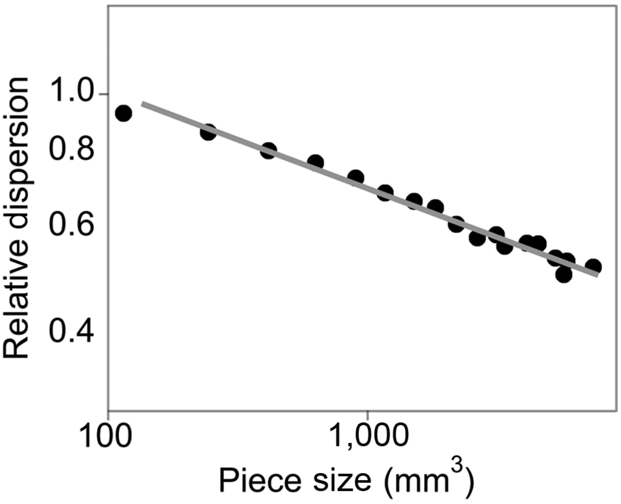

Fig. 4 Calculation of fractal dimension from imaging data. The relative dispersion (standard deviation/mean) is calculated at the highest resolution of measurement. This calculation is repeated by dividing the lung into progressively larger blocks, i.e., lower resolution. The fractal dimension is 1-slope of the relationship of the plot of log relative dispersion versus log piece size.

The low pressure of the pulmonary circulation ensures that there is just enough hydrostatic pressure to reach the apex of the upright lung, where the pressure is lower than at the lung base. In the lung, there is an additional complication compared with other vascular beds—the influences of alveolar pressure. Banister and Torrance[29] were the first to show that the alveolar pressure could influence pulmonary blood flow and likened this effect to a "Starling resistor."[1] With a Starling resistor, flow is dependent on the relative relationships between the upstream and downstream pressures and a surrounding pressure.[1] West et al subsequently advanced a simplified "Zone" model,[30] which described pulmonary blood flow as occurring in three distinct zones whereby blood flow is dictated by the relationship between pulmonary arterial (upstream), pulmonary venous (downstream), and alveolar (surrounding) pressures. This model has become the default approach that is taught in all medical schools/pulmonary physiology courses (►**Fig. 5**). In Zone III lung, the difference between upstream pulmonary arterial pressure (P_a) and downstream venous pressure (P_v) dictates flow just as it does in other organ circulations, because the alveolar (surrounding) pressure (P_A) is low and thus $P_a > P_v > P_A$. Regional flow is greatest in Zone III. Conversely when P_A is greater than both P_a and P_v (i.e., Zone I), there is no flow as the capillary is collapsed due to the greater surrounding P_A pressure. Zone II is an intermediate zone where $P_a > P_A > P_v$, the driving pressure is the difference between $P_a - P_A$, and flow is reduced relative to Zone III conditions. With the Zone model, the vertical height of the lung and the hydrostatic

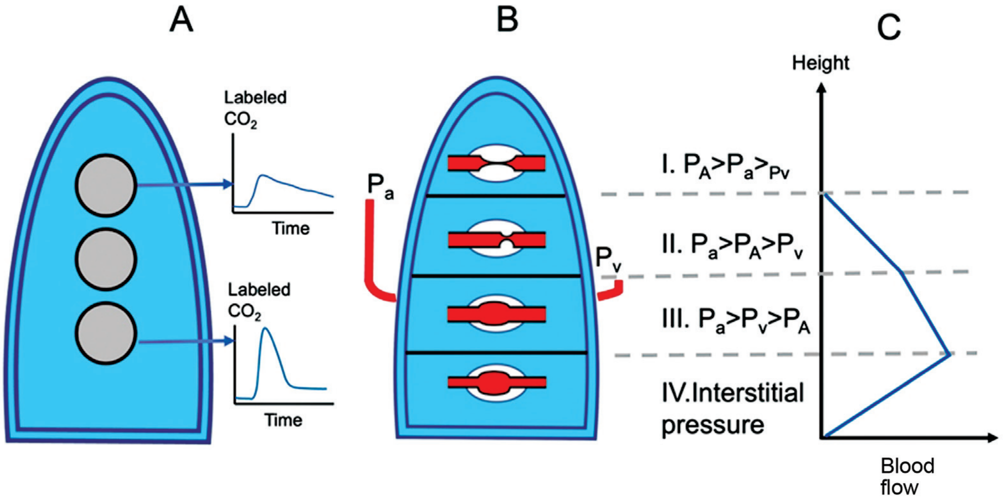

Fig. 5 The Zone model of pulmonary perfusion. **(A)** Schematic diagram of the original experiment. Detectors (gray circles) are placed on the chest wall. Radiolabeled CO_2, used as a tracer gas, is inhaled and time–activity curves constructed during a breath hold. The CO_2, a soluble and perfusion-limited gas, is cleared proportional to regional blood flow. In nondependent lung, clearance of the isotope is delayed compared with dependent lung. These observations led to the development of the Zone model of pulmonary perfusion[2] **(B, C)** that relates perfusion to the relationships between alveolar P_A, pulmonary arterial P_a, and pulmonary venous, P_v, pressure. In Zone I, when P_A is greater than both P_a and P_v, the capillary is collapsed and flow is zero. In Zone II the difference between P_A and P_a dictates flow, whereas in Zone III lung, the difference between P_a and P_v dictates flow since both are greater than alveolar pressure. Later, this model was modified to include a fourth Zone where perfusion was reduced with decreasing height. Zone IV was originally attributed to increased interstitial pressure increasing resistance in dependent lung vessels.[31]

pressures due to gravity dictate that Zone I conditions are primarily in the gravitationally nondependent apex of the upright lung, with Zone II being around heart level, and Zone III conditions located at the gravitationally dependent base. Later, this model was modified to include a fourth zone, a region in the most dependent lung where pulmonary perfusion decreased as a function of height,[31] which was originally ascribed to greater resistance in extra-alveolar vessels,[31] although this is unconfirmed.[32]

From the initial studies of West and Dollery mentioned above, work incorporating a large number of different experimental models confirms that there is a vertical gradient in perfusion from gravitationally nondependent to dependent lung that is present across multiple postures (e.g., prone/supine, right/left lateral decubitus[4,32–37]), imaging modalities (MRI, PET, SPECT, etc.) and species (reviewed in Glenny and Robertson[1]). Thus, there has been acceptance for more than 40 years that mean pulmonary blood flow with respect to the gravitational vector is influenced by the relations between P_a, P_A, and P_v as predicted by the Zone model, provided the lung is well expanded and PVR is normal.[30] While the effects of gravity on pulmonary blood flow distribution was initially suggested to be largest at total lung capacity (TLC) and absent at residual volume,[31] this effect largely disappears when lung tissue deformation is taken into account.[32] Instead, gravity affects the distribution of perfusion similarly irrespective of lung volume, except in the most nondependent portion of the lung, where it is reduced at TLC compared with other lung volumes.[32] In addition, the mechanism of Zone IV effects has been questioned[32] but local hypoxic pulmonary vasoconstriction (HPV) in regions of low alveolar PO_2[38] or local vascular branching structure patterns[39,40] may also play a role.

Smaller Scale Effects on the Distribution of Pulmonary Blood Flow and Measures of Spatial Heterogeneity

Despite the strengths of the simple Zone model to explain local pulmonary blood flow, marked heterogeneity of perfusion within isogravitational planes has been demonstrated by advanced measurement techniques, indicating that factors other than vertical height affecting hydrostatic gradients must also influence regional pulmonary perfusion.[1] While the zones of the lung must exist due to physical laws, as detailed by Glenny and Robertson,[1] it is suggested that the zones may not be vertically stacked in the lung. Rather, asymmetries in branching patterns and resistances within the vascular tree create differences in perfusion pressures, and ultimately capillary pressure. Because these heterogeneities in perfusion pressures may exist within horizontal planes, all three zones are proposed to exist within the same isogravitational plane,[1] with a greater probability of one zone favored over others dependent on vertical height. Indeed Glenny and colleagues have observed substantial blood flow heterogeneity within an isogravitational plane,[41,42] with greater variability often observed within a given isogravitational plane as compared with across different vertical heights of the lung.[43] Thus, the assumption that variability in capillary perfusion is solely due to gravity is an over-simplification and there is now general agreement that the spatial distribution of pulmonary blood flow is determined primarily by two factors; gravity and the geometry (i.e., fractal tree) of the vascular tree.[1]

Perfusion of the Pulmonary Microcirculation

Because of their intimate relationship with the local alveolar pressures, blood flow at the capillary level is influenced by the local zonal conditions, and small differences in regional driving pressures can open and close pathways at the capillary level.[1] Red blood cells (RBCs) pass through extensive networks of capillaries within the lung, switching between capillary branches as they reach junctions in the capillary network. The pathway of the RBCs, and the associated switching between capillaries appears somewhat random, and the perfusion of a single alveolar unit can fluctuate from no flow to partial and full recruitment within seconds.[44,45] This has the effect that in addition to spatial perfusion heterogeneity, there is also temporal heterogeneity, discussed further below.

The mechanisms responsible for this pattern of recruitment and de-recruitment of capillary perfusion are not well understood, and it is possible that there are active contractile fibers within the capillary walls that change local resistances.[11] However, Wagner et al recently demonstrated that RBC capillary flow switching patterns, number of perfused segments, and the fractal dimensions were not different in fresh lungs versus fixed lungs devoid of any contractile responses, and from these findings concluded that the flow switching patterns can be explained entirely by passive processes.[44] This passive switching may have many physiological advantages, in that it maintains all capillaries continuously ready for emergency recruitment without the need of a feedback loop. Further, with many redundant, autonomous, and independent passive components, the passive switching system is a simple and robust design that can function reliably for prolonged periods with little need for regulation.[44]

Morphological studies show that pulmonary capillaries are $\leq$13 microns in diameter, even under conditions of high perfusion pressure.[6] However, studies with agitated saline contrast echocardiography[46,47] and microspheres[48,49] suggests that increased cardiac output and/or pulmonary vascular pressures may recruit arteriovenous anatomic pathways in the mammalian lung. Notably, flow through these arteriovenous connections appears relatively small (i.e., $<$0.5% of cardiac output), with minimal impact on gas exchange.[50]

Temporal Heterogeneity

The pulmonary circulation is a dynamically regulated system with changes in vascular smooth muscle activity potentially affecting local perfusion.[51] Not only is there spatial heterogeneity, but heterogeneity can also vary spatially over time, so-called *spatial-temporal heterogeneity*. Data derived from microsphere studies in animals[20,52] and imaging studies in humans[53–55] have been helpful, and have largely confirmed the dynamic nature of the pulmonary circulation. In mechanically ventilated dogs, perfusion has been shown to vary over a time scale of several minutes,[52] but the extent is small (approximately 1/3) compared with the overall spatial heterogeneity. When measured over longer time scales, spatial-temporal heterogeneity is less.[20] Imaging studies in humans measured at short time scales (seconds)[53–55] confirm that the spatial-temporal heterogeneity is approximately one-third that of the overall spatial heterogeneity. In addition, in healthy subjects, spatial-temporal heterogeneity is affected by factors known to affect the pulmonary vasculature: it is increased by altered inspired oxygen, with hypoxia having a greater effect than hyperoxia,[54] and increased by inhaled nitric oxide.[53] Notably, spatial-temporal heterogeneity may be increased even when spatial measures of heterogeneity are unchanged[54]; however, this significance of this is unknown.

Active Regulation of the Distribution of Perfusion: Hypoxic Pulmonary Vasoconstriction

All circulations in the human body, including the brain, vasodilate in response to hypoxia except the pulmonary circulation, which vasoconstricts. It has been known since the middle of the 19th century in an animal model that if ventilation was interrupted, pulmonary arterial pressure increased.[56] Further work established that the rise in pulmonary artery pressure occurred, whether mechanical ventilation was suspended, the trachea obstructed, or anoxic gas administered.[57] However, it was not until the work of von Euler and Liljestrand[58] that this phenomenon was firmly linked to the direct effect of hypoxia on the pulmonary circulation. This phenomenon is termed hypoxic pulmonary vasoconstriction (HPV). HPV has been the subject of several reviews[59–64] including the exceptionally comprehensive one by Sylvester et al.[59] The focus of this section is on the effect of HPV in humans and intact animal models. The reader is directed elsewhere for a discussion of the cellular and molecular mechanisms of HPV.[59,63,65] von Euler and Liljestrand suggested that HPV was a mechanism to link local perfusion to the adequacy of local ventilation. Indeed, HPV is thought to be the most important active mechanism of ventilation–perfusion matching.[59] HPV is initiated by reduced partial pressure of oxygen (PO_2) near vascular smooth muscle, predominantly reduced alveolar PO_2. Since alveolar PO_2 is determined by the inspired PO_2 and the local ventilation–perfusion ratio (►**Fig. 6**), there are several ways local alveolar hypoxia may arise and stimulate HPV including local airway obstruction, alveolar filling, or ventilation–perfusion mismatch. Activation of HPV in a hypoxic region of the lung reduces local perfusion, which in turn raises the local ventilation–perfusion ratio and increases local alveolar PO_2 (►**Fig. 6**). At the same time, HPV redirects blood flow to nonhypoxic regions of the lung. Thus, the extent of regional HPV activity represents a dynamic equilibrium between PO_2 stimulus and response that minimizes the impact on pulmonary gas exchange. In the case of reduced inspired PO_2 causing global hypoxia, HPV activity also depends on the extent of the decrease in inspired PO_2 but may affect the distribution of local flow differently depending on regional differences in alveolar PO_2 or perhaps differences in local pulmonary arteriole smooth muscle response (discussed below). The site of HPV occurs primarily in the small precapillary pulmonary arterioles (30–50 μm); studies in animals largely in isolated lung models suggest that capillaries and pulmonary veins may also constrict,[66–70] but the role of

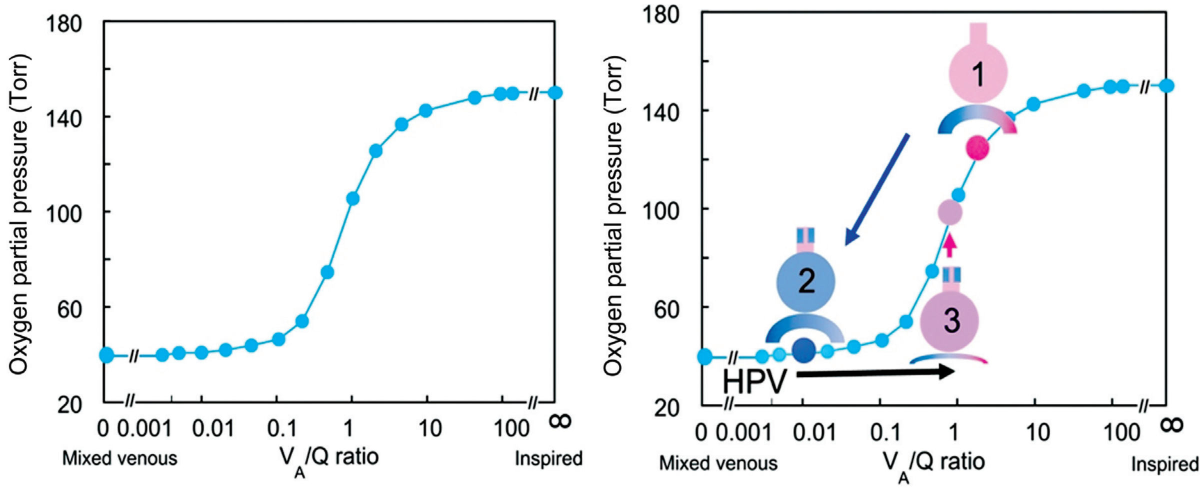

Fig. 6 Left: the relationship between alveolar PO_2 and the local ventilation–perfusion ($\dot{V}_A/\dot{Q}$) ratio in normoxia. Right: schematic representation of restoration of oxygenation by HPV in a lung unit. (1) When ventilation and perfusion are well matched, PO_2 is high (pink dot). (2) After ventilation is reduced to a lung region, in this case by partial airway obstruction, the ventilation–perfusion ratio decreases and PO_2 is reduced (dark blue dot). (3) Activation of HPV reduces local perfusion, matching ventilation and acting to restore the local ventilation–perfusion ratio towards baseline. This increases the alveolar PO_2 in the lung unit back to baseline (purple dot). HPV, hypoxic pulmonary vasoconstriction.

this in the intact lung is unclear. The precise mechanism of how low oxygen is sensed and the signal for constriction of pulmonary vascular smooth muscle is transduced has not been elucidated (see Strielkov et al[71] for review).

Assessing Hypoxic Pulmonary Vasoconstriction

It is difficult to fully evaluate HPV, though inferences can be made by evaluating changes in pulmonary arterial pressure and vascular resistance with hypoxia in humans[72,73] or animals.[74–76] However, this may be problematic particularly in patient populations. The interested reader is directed elsewhere where this is nicely discussed.[77] Briefly, pulmonary blood flow is affected by airway pressure in addition to the differences between arterial and venous pressures,[78,79] which may affect measurement, particularly in mechanically ventilated patients. Second, as mentioned previously, operating lung volumes affect the distribution of pulmonary blood flow and thus PVR.[32,80,81] Finally, pulmonary arterial pressure/vascular resistance is also affected by cardiac function, i.e., factors extrinsic to the lung. During exposure to high altitude or hypoxia, the extent of HPV has been also assessed by acute restoration of normoxia and evaluation of the decrease in pulmonary arterial pressure and PVR. However, after several days to weeks of hypoxia, administration of oxygen has little effect,[73,82,83] suggesting other mechanisms[84] maintain PVR and that vascular remodeling occurs.[85,86] All of these factors lend complexity to the task of evaluating HPV in humans. Alternate methods include imaging or microsphere studies during the administration of hypoxic or hyperoxic gas[87–90] or by gas exchange studies evaluating the effects of altered inspired O_2 on ventilation–perfusion relationships.[74,91] Postmortem studies,[92] studies in isolated lungs cells,[93] and using pulmonary arterial strips[66,67] have also provided important information.

Hypoxic Pulmonary Vasoconstriction Activation and Time Course

The reported time course of HPV is complex. Studies diverge depending on the extent of hypoxic stimulus, the experimental model, and the nature of the hypoxic exposure (i.e., regional or global hypoxia), see Sylvester et al[59] for details. HPV onset is rapid, beginning within seconds of a hypoxic stimulus with the rapidity of response related to the rate of decline in PO_2.[94] There is evidence for a multiphasic HPV response both in vitro[94] and in vivo[72,95,96] characterized by an initial rapid onset of increased PVR followed by a more gradual rise. Generally, in both humans and dogs, the increase in PVR in response to inspired hypoxic gas reaches a maximum by 15 to 20 minutes.[94,97,98] However, in the presence of atelectasis, the time course of redistribution of flow takes longer and reaches a maximum at approximately 60 minutes.[87] HPV is sustained for hours.[94,97,98] While alveolar hypoxia is the main stimulus for HPV, there is evidence that low mixed venous PO_2 as well as low bronchial arterial PO_2[99–101] can add to the vasoconstrictor response, as well as inducing vasoconstriction in and of themselves (see Sylvester et al[59] and Swenson[62] for review). Maximum HPV expressed as percentage change in local resistance from baseline is over 250 percent.[93] HPV begins to activate at an alveolar PO_2 of approximately 95 mm Hg and the response is 50% of the maximal response at a PO_2 of approximately 73 mm Hg and maximal at 37 mm Hg.[53,102]

Hypoxic Pulmonary Vasoconstriction Response

Even in young individuals with healthy lungs, there is a small amount of ventilation–perfusion mismatch and thus some HPV activity is expected. As assessed by the global increase in pulmonary arterial pressure and vascular resistance in response to acute hypoxia, the magnitude of the HPV response varies greatly between healthy individuals[103]: approximately one-quarter of healthy subjects have a minimal response to hypobaric hypoxia, whereas a minority may increase mean pulmonary arterial pressure to over 40 mm Hg.[61] HPV plays a critical role in the transition from life *in utero* to postnatal life. Before birth, the unventilated alveoli of the fetal lung have minimal perfusion, and HPV is fully activated. After the first breath, PVR rapidly falls (reviewed in Gao[and Raj104]) and pulmonary perfusion increases. It has been shown that the muscle mass of contracting elements of the pulmonary arteries decreases shortly after birth[92] suggesting that HPV may be reduced as part of normal growth and development in most lowland populations. The contractile elements of the pulmonary circulation are maintained in chronic exposure to hypoxia[92] and individuals born and raised at high altitude show medial hypertrophy and luminal narrowing of pulmonary arterioles.[105,106]

In the presence of lung disease such as chronic obstructive pulmonary disease, more regions of lung may have an alveolar PO_2 that is expected to activate HPV, while in patients with regions of atelectasis or alveolar flooding, HPV is expected to be maximal. In healthy individuals,[102] there is evidence that HPV corrects up to 40% of the decrease in alveolar PO_2 (PAO_2) that would otherwise occur in a theoretical passive system without HPV. Work in an animal model (dogs)[107] suggests that activation of HPV improves arterial PO_2 by approximately 15 to 20 mm Hg.

Effect of Hypoxic Pulmonary Vasoconstriction on Local Blood Flow

The absolute amount of flow to a particular region depends on both local resistance and total cardiac output. However, because the entire cardiac output passes through the lungs, blood flow in the lung is a zero-sum game: when flow is reduced in one region by HPV, then the flow is redistributed to regions of lower resistance, which will increase the fraction of the total cardiac output these areas receive. Thus, it is unsurprising that the redistribution of blood flow away from a local region of hypoxia is affected by the size of the region,[76,101] and smaller hypoxic regions experience a greater reduction in flow than larger ones. For example, when the hypoxic segment is 10% of the lung volume, there is approximately 80% reduction in flow to the area. This has a negligible effect on pulmonary artery pressure.[108] In contrast, in normal humans undergoing one lung ventilation, HPV has been shown to reduce the cardiac output to the hypoxic lung by up to 50%.[109] In global hypoxia, such as at high altitude, the main effect of HPV is to increase pulmonary arterial pressure, without a gross redistribution of flow since the entire lung is subject to HPV. This is not strictly accurate as there are minor increases in perfusion of the apical lung regions[88,110] consistent with Zone model effects associated with increased pulmonary arterial pressure.

There is evidence that HPV activity is not uniform in the mammalian lung. In pigs, for example, work using fluorescent microspheres has shown that there are anatomic clusters of the blood flow response to hypoxia[111]: regions of relatively high flow during hypoxia are adjacent to other high flow areas and, similarly, low flow areas are clustered near other low flow areas. In addition, MRI studies in individuals who have previously experienced high-altitude pulmonary edema, a noncardiogenic high permeability edema, that develops in otherwise healthy individuals following 24 to 72 hours exposure to altitudes above 2,400 m have shown evidence for spatially uneven HPV,[112,113] that is linked to the pathophysiology of the disease.[112,113] Exactly why HPV is uneven in these individuals is not established, but it does not appear to be due to a more uneven ventilation stimulus to HPV.[114]

Pulmonary Vascular Resistance and Distensibility

The pulmonary circulation is a high-flow and low-pressure circuit. Importantly, the low vascular pressures throughout the pulmonary circulation prevent fluid from moving into the interstitial space and allow the right ventricle to operate at minimal energy cost.[115] As a result of the low-pressure system, the right ventricle is thin-walled, and has difficulty with large increases in afterload.[116]

Measurement of Pulmonary Vascular Resistance

The pulmonary circulation is characterized by an inflow pressure (pulmonary artery pressure, P_a), an outflow pressure (left atrial pressure, P_{la}), and a flow rate ($\dot{Q}$, approximately equal to systemic cardiac output).[116] Measurements of P_a are typically obtained at end-expiration from a pulmonary artery catheter (►**Fig. 7**). Pulmonary artery wedge/occlusion pressure (P_{aOP}) is used an acceptable estimate of P_{la}, with an average gradient of approximately 3 mm Hg between the P_{aOP} and left-ventricular end-diastolic pressure.[117] Cardiac output is typically measured via thermodilution or the direct Fick equation. A systematic review by Kovacs et al summarizing invasive pulmonary artery catheter data conducted in healthy participants across 47 studies found that mean P_a was 14.0 ± 3.3 mm Hg, while mean P_{aOP} was 8.0 ± 2.9.[118]

PVR serves to describe the flow-resistive properties of the pulmonary circulation[115] and is calculated by the difference between mean P_a and P_{aOP} divided by $\dot{Q}$[115]:

$$PVR = (P_a - P_{AOP})/\dot{Q} \quad \textbf{Eq. 1}$$

Kovacs et al found that mean resting PVR in healthy supine adults is approximately 0.76 ± 0.29 Wood Units (WU) in adults <24 years, 0.86 ± 0.35 WU in adults 24 to 50, 1.08 ± 0.19 WU in adults 51 to 69, and 1.13 ± 0.49 WU in those over 70 years.[118]

Sometimes Paw cannot be obtained, and a *total* PVR (TPVR) is calculated as[115]:

$$TPVR = P_a/\dot{Q} \quad \textbf{Eq. 2}$$

Importantly, as P_{aOP} may be elevated in many conditions, TPVR is larger than PVR and this difference can be flow-dependent.[115] Therefore, it is not advisable to use TPVR to characterize the flow-resistive properties of the pulmonary

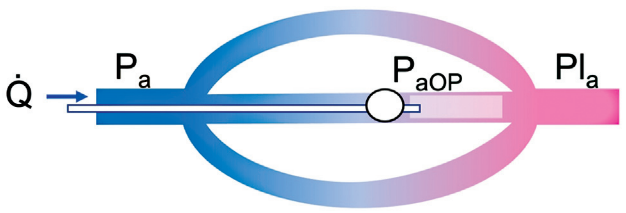

$$PVR = \frac{P_a - Pl_a}{\dot{Q}}$$

Fig. 7 Measurement of pulmonary vascular resistance (PVR). PVR is calculated from the inflow pressure, pulmonary artery pressure, P_a, the outflow pressure, left atrial pressure, P_{la}, and cardiac output, $\dot{Q}$ which is the flow rate. P_{la} is often estimated from pulmonary arterial occlusion pressure, P_{aOP}. This is measured via a catheter that is introduced into the pulmonary artery and manipulated distally in the pulmonary circulation where a balloon is inflated to occlude the vessel and prevent filling. P_{aOP} is measured distal to the balloon and reflects back pressure from the left atrium.

circulation.[115] When right heart catheterization is not available, pulmonary artery systolic pressure can be estimated with reasonable accuracy using Doppler echocardiography of the maximum velocity of the tricuspid regurgitant jet and echo-derived estimates of right atrial pressure.[119] Ultrasound can also been used to estimate resting left atrial pressure,[120] which combined with Doppler estimates of pulmonary artery systolic pressure allows for evaluation of PVR.

The longitudinal distribution of resistances in the pulmonary circulation has been estimated to be 60% precapillary and 40% postcapillary,[121] and micropuncture studies have shown that pulmonary capillary pressure is approximately halfway between arterial and venous pressures.[122] As outlined by Naeije,[116] according to the Hagen–Poiseuille law, resistance (R) is equal to:

$$R = (l \bullet \eta \bullet 8)/(\pi \bullet r^4) \quad \textbf{Eq. 3}$$

where l = length, η = viscosity, π = pi, r = radius. That radius is to the fourth power highlights that PVR is very sensitive to changes in vessel caliber.[116] Reeves and Taylor[123] illustrated that approximately 80% of the variance in P_a is explained by P_{aOP}, indicating that an increase in P_{la}/P_{aOP} is transmitted upstream to P_a. Chronic elevations in P_{la}/P_{aOP} can lead to vascular remodeling and an increase in PVR and P_a.[124] Clinicians often prefer to examine the transpulmonary pressure gradient ($P_a - P_{aOP}$) to help distinguish between a passive increase in P_a brought on by an increase in P_{aOP} versus an increase in P_a from pulmonary vascular disease.

Pulmonary Vascular Distensibility

While the pulmonary circulation has limited vasodilatory response, there is evidence of vascular distensibility across the pulmonary vasculature in response to an increase in transmural pressure. Vascular distention, in addition to recruitment, moderates pressure increases and thus helps to minimize right ventricular afterload. The distensibility of the pulmonary vessels can be defined by a coefficient α calculated as percentage change in diameter per mm Hg of pressure using a mathematical model of the pulmonary circulation.[125–127] Practically, for an individual, the coefficient can be determined using P_a, P_{aOP}, PVR, and $\dot{Q}$ data to solve for α (see Reeves et al[126] and Lalande et al[127] for further detail). The distensibility of pulmonary resistive vessels is approximately 2% of diameter change per millimeter of mercury of distending pressure over a wide range of vascular segments and species.[128] Similarly, Reeves et al calculated the distensibility coefficient in healthy participants at rest and during exercise in normoxia to be $2 \pm 0.2\%$/mm Hg.[126] The distensibility coefficient appears to be greater in women,[129] although PVR does not appear to be different between men and women.[118] It is unclear whether distensibility is altered with pregnancy; however, PVR may decrease in pregnancy, likely because of reduced blood viscosity and increased cardiac output resulting in capillary recruitment.[130,131] Pulmonary vascular distensibility decreases with aging[126,129] and decreases with chronic, but not acute hypoxia.[116]

Functional Measurements of Recruitment/Distention

Studies examining the intact pulmonary microcirculation have typically used fixed-diameter (approximately 15 µm) microspheres to examine perfusion[25,42,132–134]; however, this does not allow for the study of capillary recruitment/distention in the human. Radiolabeled macroaggregated albumin has been used in humans[135–138]; however, the size of these particles can be inconsistent, making accurate evaluation of perfusion difficult. Diffusing capacity for carbon monoxide (DLCO) can be partitioned into its components; capillary blood volume (Vc) and membrane diffusing capacity (Dm),[139] and DLCO, Vc, and Dm can be used as a functional evaluation of capillary recruitment/distention. Diffusing capacity of nitric oxide (DLNO) can also be used in combination with DLCO to determine Vc and Dm.[140] Membrane diffusing capacity reflects the available alveolar–capillary surface area for gas exchange, and is increased by unfolding and distention of alveolar septae during lung inflation, and recruitment of capillaries associated with previously un-perfused alveoli.[140] Vc increases as the number of perfused alveolar capillaries increases,[140] and capillaries become further distended with increased perfusion pressure. As gas exchange can only occur within a perfused alveolar/capillary unit, Dm is thought to describe capillary recruitment, while Vc reflects both recruitment and distention. First-pass pulmonary circulatory metabolism of [3H] benzoyl-Phe-Ala-Pro can also be used to calculate functional capillary surface area.[141,142] Pulmonary capillary recruitment and distention can be estimated from the surface area data in combination with pulmonary blood flow data (i.e., cardiac output).[141,142] Similar to DLCO, this technique provides a functional evaluation of pulmonary capillary recruitment/distention, and both of these techniques have been used recently to better understand recruitment/distention in various conditions.

Physiological Factors Affecting the Pulmonary Circulation

The previous sections have discussed the structure of the pulmonary circulation, determinants of the distribution of pulmonary blood flow and heterogeneity, PVR, and factors affecting recruitment and distension of the pulmonary vasculature. How these are affected under a variety of physiological circumstances is briefly discussed. In addition to the issues discussed below, diving and high-altitude exposure also result in changes in pulmonary circulation structure and function. These effects are discussed in more detail in other sections of this journal compilation.

Healthy Aging

Normal aging has several effects on the lung and pulmonary circulation. For example, it is well known that even in healthy individuals, pulmonary gas exchange efficiency worsens with age as a result of increasing ventilation–perfusion mismatch,[143] presumably because of an overall decline in lung function (see Janssens[144] for review) and increased ventilation heterogeneity.[145–147] In the pulmonary circulation, aging is associated with a reduction in pulmonary vascular distensibility.[126,129] Correspondingly, PVR, pulmonary arterial pressure, and the Pa/cardiac output index are elevated at rest and during exercise with age.[116,118,148] Elevated echo-derived pulmonary arterial systolic pressure is associated with mortality, and while P_a pressure may be influenced by left ventricular function and downstream pressure (i.e., P_{aOP}, discussed previously), these findings suggest that the age-associated changes in pulmonary resistance may have clinical significance.[148] Functionally, despite an increase in pulmonary arterial pressure with aging, DLCO, V_C, and Dm at rest are reduced with age.[149–152] Similarly, CT data demonstrate that pulmonary blood volume is also reduced with age, with an approximate linear decrement of 50 mL per 10 years of age.[153] The magnitude of the increase in DLCO when moving to the supine position is also blunted in elderly participants,[154,155] suggesting that aging-induced impairments in the pulmonary vasculature cannot be normalized with increasing perfusion pressure, consistent with decreased distensibility. DLCO, DLNO, V_C, and Dm are also reduced during exercise at a given cardiac output in older participants.[149,156] However, elderly participants demonstrate a similar expansion of the pulmonary capillary network with exercise (i.e., similar increase in DLCO, Dm, and Vc), suggesting that the changes in the pulmonary circulation that occur with healthy aging are insufficient to affect pulmonary vascular expansion and the recruitment of effective alveolar–capillary surface area during exercise.[149] The underlying mechanism(s) for the age-associated changes in pulmonary vascular function are unclear, but similar to the systemic circulation, may be related to arteriole remodeling or an increase in smooth muscle cell tone.[115,148]

There is some evidence of changes in the large-scale gravitational effects on perfusion with aging.[157] In male subjects aged 65 to 75 years, there was a relative increase in blood flow to lung apices in the upright posture compared with younger men (i.e., a smaller gravitational gradient). This may be explained in part by increased pulmonary vascular pressures,[158] leading to greater capillary recruitment (i.e., Zone model effects),[159,160] but this is not established. Also, since several subjects in this study had significant smoking histories, the significance of these findings is uncertain. Fractal dimension has not been shown to change with age in healthy nonsmokers, suggesting that vascular branching structure is unchanged,[161] but perfusion heterogeneity as measured by the relative dispersion increased significantly with increasing age.[161] The magnitude of the change (approximately 5% per decade of age) is similar to changes in ventilation–perfusion heterogeneity with age.[143] The reasons for increasing heterogeneity with age are unknown but may relate to nonuniform alveolar size changes[162] leading to an apparent heterogeneity in perfusion and/or an intrinsic alteration in the pulmonary vasculature consistent with changes in DLCO and pulmonary capillary blood volume.[149–152]

Alternatively, increased perfusion heterogeneity may represent increased HPV activity in response to regional alveolar hypoxia induced by the well-documented increase in heterogeneity of ventilation with aging.[147,157] While there is a great deal of research on HPV (see Sylvester et al[59] for review), it is important to recognize that it has largely been conducted in young subjects (both human and animal). The extent to which it changes with aging is unknown, largely because it has not been evaluated, in part due to concerns about making older individuals hypoxic, and the role of HPV optimizing ventilation–perfusion relationships in older subjects is presently unclear.

Exercise

Exercise represents a significant stress on the pulmonary circulation, as cardiac output can increase up to 5- to 7-fold with maximal exercise in trained individuals, and the pulmonary circulation must take the entire cardiac output while keeping the lungs dry and minimizing the increase in right ventricular stroke work.[115] The exercise-induced increases in P_a pressure facilitate capillary recruitment and distention, and as a result PVR decreases with incremental exercise.[46,123,163,164]

With exercise, DLCO, Vc, and Dm responses to exercise demonstrate a continuous rise up to peak exercise, with no apparent plateau in any component regardless of age or sex.[149,165–167] These findings indicate that capillary recruitment and distention continue to increase up to maximal exercise. Interestingly, endurance-trained athletes, who have a greater peak oxygen consumption, and thus a greater O_2 diffusion requirement demonstrate greater DLCO at peak exercise as compared with less-trained individuals secondary to greater Dm.[165] The larger Dm at peak exercise in endurance-trained individuals would suggest that athletes have enhanced capillary recruitment; however, the underlying physiology remains to be elucidated.

Using [3H]benzoyl-Phe-Ala-Pro, Langleben et al provided evidence that reductions in PVR during supine exercise in healthy humans were explained by both capillary recruitment and distention, with recruitment being predominant at moderate increases in flow and distention more likely with larger increases in flow.[141] In a follow-up study, Langleben et al examined potential species differences, and found that rabbits, dogs, and exercising humans all showed similar recruitment/distention patterns in response to increased blood flow, such that capillary recruitment is the dominant responses at low flow rates (up to approximately 2.5 to 3.7 times resting).[168] Thereafter, further rises in pulmonary blood flow were determined to be accommodated primarily by capillary distention.[135]

The [3H]benzoyl-Phe-Ala-Pro findings that capillary distention is the primary response at higher flow rates[141] is divergent from the DLCO data which indicate that both recruitment and distention occur up to peak exercise.[165,166] Although both approaches are based on measurement of functional area for gas exchange, differences may be explained by variations in experimental approach. The work to date using [3H]benzoyl-Phe-Ala-Pro has all been done while supine, whereas the DLCO data are typically collected during upright exercise. Supine posture reduces the height of the vertical hydrostatic column while increasing perfusion pressure. This would have the likely effect of increasing baseline capillary recruitment and thus altering the recruitment/distention response to incremental exercise.

As described by La Gerche et al, high-intensity exercise can present a significant hemodynamic challenge in which the right-sided heart chambers are exposed to a disproportionate increase in cardiac afterload and wall stress.[169] Mean left atrial pressure/P_{aOP} increases with exercise,[46,163,164] and as noted previously, approximately 80% of the variance in P_a is explained by P_{aOP}.[123] This increase in downstream P_{aOP} with exercise is transmitted through the pulmonary circulation, resulting in further elevation in P_a. As a consequence, relative to the left ventricle, increases in load are greater for the right ventricle during exercise and the contractile force may be insufficient to generate the increases in cardiac output required during intense exercise.[169] As highlighted by La Gerche et al, cardiac output is only as good as your worst ventricle, and therefore the coupling of the pulmonary circulation and the right ventricle may represent a limitation to maximal exercise. Consistent with this hypothesis, pulmonary arteriolar distensibility (α) is correlated with maximal oxygen uptake,[127] while resting and exercise DLCO, DLNO, Vc, and Dm (which reflect capillary recruitment and distention) are associated with greater exercise tolerance in health and disease.[127,165,166,170,171]

It is worth mentioning that recruitment and distension cannot increase in an unlimited fashion and with maximal recruitment and distension in combination with the elevation in P_a and P_{aOP}, pulmonary capillary pressure increases. Ultimately, high pulmonary capillary pressures may damage the thin blood–gas barrier that is a requirement to diffuse respiratory gases[172,173] (►**Fig. 8**). Stress failure of pulmonary capillaries is reported in horses which develop extremely high pulmonary vascular pressures during exercise.[174] There is also evidence that in some circumstances, the human pulmonary circulation may also develop breaks in capillary endothelium/alveolar epithelium sufficient to result in RBCs entering the airways.[172,173] This stress failure is more likely with maximal exercise[173,175] because of increased capillary pressure and lung stretch, which amplifies the mechanical forces on the lung. Stress failure may also be important in lung injury with mechanical ventilation with high airway pressures (reviewed in West[176]) and in the development of high-altitude pulmonary edema.[112]

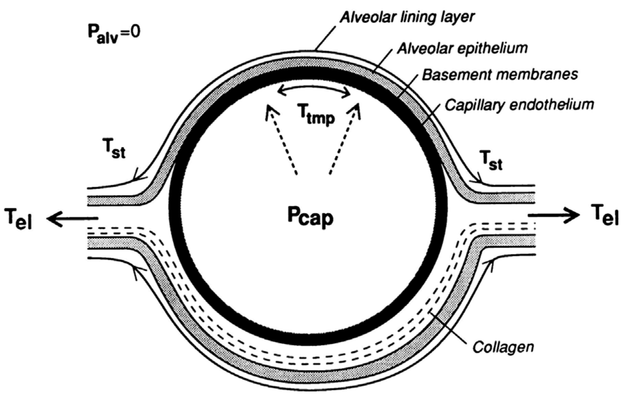

Fig. 8 Three forces acting on blood–gas barrier. Circumferential tension (T_{tmp}) is given by capillary transmural pressure X radius of curvature (*r*). In this example, alveolar pressure (P_{alv}) is atmospheric so that capillary transmural pressure is equal to capillary hydrostatic pressure (P_{cap}). Surface tension of alveolar lining layer (T_{st}) exerts an inward-acting force to support the capillary. Longitudinal tension in alveolar wall elements associated with inflation of lung (T_{el}) is presumably transmitted mainly by collagen fibers on the thick side of the capillary but may affect wall tension on the thin side, especially at high lung volumes. (Reproduced with permission from West et al[172].)

The picture of pulmonary blood flow heterogeneity with exercise is complex and depends on exercise intensity, species, and posture among other possible factors. Generally, exercise causes redistribution of flow against the gravitational gradient: with upright exercise in humans blood flow increases in the apical (nondependent) regions of the lung,[177–179] although the gravitational gradient in blood flow is not completely attenuated. These changes in the large-scale distribution of pulmonary blood flow may be due to local reactivity of the pulmonary vessels to exercise, local vascular structure creating nonuniform resistances in response to exercise, or Zone model-type hydrostatic behavior. In most quadruped animals, exercise redistributes blood flow to the most gravitationally nondependent lung, the dorsal caudal region.[180–182]

In humans undergoing mild supine exercise, pulmonary blood flow was redistributed to the nondependent lung,[22] and perfusion heterogeneity was reduced[22,183](►**Fig. 9**). The reduction in the spatial heterogeneity of pulmonary perfusion as measured by the relative dispersion[22] was present even after accounting for the effect of gravity. These findings are consistent with exercise DLCO and [3H]benzoyl-Phe-Ala-Pro work detailed above and suggest that lung perfusion follows a Zone-type model to some extent with greater recruitment of blood vessels during mild exercise.

Because of the difficulty in obtaining good-quality data during heavy exercise, there are few studies evaluating perfusion heterogeneity during high-intensity exercise, and a

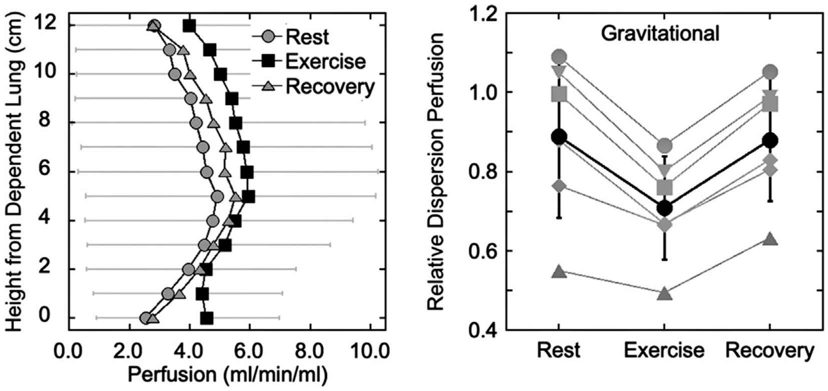

Fig. 9 The effect of mild exercise on the distribution of pulmonary blood flow. With exercise, blood flow is redistributed to the nondependent lung (left panel) and perfusion heterogeneity as measured by the relative dispersion is reduced (middle and right) even after accounting for the effect of gravity (right panel). (Modified with permission from Hall et al[22].)

consistent pattern is unclear. In some species such as dogs[184] and sheep,[181] perfusion heterogeneity does not decrease with exercise. Similarly, in horses perfusion heterogeneity is unchanged during exercise and redistribution of flow is small.[182] This has led to the suggestion that the primary determinant of pulmonary blood flow distribution in these animals is structural, rather than Zone model-type effects, but this has not been established. In humans, pulmonary perfusion heterogeneity is increased following heavy exercise,[185,186] and is positively correlated with the extent of ventilation–perfusion mismatch.[185] In addition, ventilation–perfusion mismatch occurred in a portion of the lung which was gravitationally dependent during exercise,[186] consistent with the development of local interstitial edema acting to disrupt local perfusion. Importantly, because of the rapid changes in pulmonary hemodynamics immediately following exercise, data obtained following exercise may not provide an accurate representation of perfusion heterogeneity during exercise.

Posture

In comparison to the upright position, the supine posture results in a translocation of blood centrally, while also lowering the vertical distance (hydrostatic column) of the lung. Previous work in healthy participants has demonstrated that the shift from upright to supine increases resting P_a and P_{aOP} by approximately 3 to 4 mm Hg,[46] which is expected to increase the amount of Zone III conditions within the lung. Consistent with greater capillary recruitment and distention, PVR is reduced by roughly 25% in young healthy when supine,[46] while DLCO is increased by 12 to 26%.[154,187]

The effects of postural changes on gravitational gradients in pulmonary perfusion are not fully established; some work suggests that they are smaller in the prone than in the supine posture,[161,188–190] but other studies do not find major differences.[35,188] The reasons are not entirely clear but may relate to whether (or how) redistribution of lung tissue is accounted for in measurements. Also, cardiac output is increased in prone compared with supine posture which may affect distribution of pulmonary blood flow.[191] As measured by the relative dispersion, the supine posture does not change heterogeneity relative to prone posture[161,190] in normal humans.

Positive Pressure Ventilation/Positive End-Expiratory Pressure

Alveolar pressure typically fluctuates from +1 cm H_2O during normal exhalation to −1 cm H_2O during inhalation; however, with positive pressure ventilation (PPV), alveolar pressure remains positive throughout the breathing cycle. Positive end-expiratory pressure (PEEP) is used to maintain alveolar patency and prevent alveolar collapse and de-recruitment; both PPV and PEEP can result in important direct and indirect effects on the pulmonary circulation.

With PPV, the intrathoracic pressure increases during inspiration causing a decrease in venous return, right ventricular output, and thus pulmonary blood flow.[192] Both PPV and PEEP increase alveolar pressure, compressing the capillaries, resulting in capillary de-recruitment (i.e., a shift from Zone II to Zone I, and Zone III to Zone II), and increased alveolar deadspace.[192,193] Any capillary de-recruitment is also expected to raise PVR. With a shift from Zone III to Zone II conditions, perfusion/cardiac output may be further reduced with PPV and PEEP, because driving pressure in affected regions changes from $P_a - P_V$ determining flow to P_a – PA. Importantly, both PPV and PEEP typically increase lung volumes, which may further increase PVR[194] as small blood vessels are axially elongated reducing their diameter and negatively impacting cardiac output.

In a supine animal model, PEEP increases the dorsal-to-ventral gradient in perfusion.[195] This is consistent with data in heathy supine mechanically ventilated human subjects, where PEEP also causes large-scale redistribution of pulmonary blood flow to gravitationally dependent (dorsal) lung, accompanied by corresponding changes in ventilation. These responses are different in the prone posture, where there were large changes in perfusion to the dependent ventral lung with mechanical ventilation, which were not matched by ventilation changes.[196]

Conclusion

The distribution of pulmonary blood flow is determined by several factors, including structural effects of vascular branching, gravity, as well as finer scale factors related to local control. HPV is a major vascular regulatory mechanism that constricts the pulmonary arterioles to divert blood toward oxygenated regions to optimize ventilation–perfusion matching. Factors such as aging, exercise, posture, and PPV alter vascular recruitment, distension, and, as a consequence, the distribution of pulmonary blood flow.

Conflict of Interest
None declared.

References

1 Glenny RW, Robertson HT. Determinants of pulmonary blood flow distribution. Compr Physiol 2011;1(01):39–59
2 West JB, Dollery CT. Distribution of blood flow and ventilation-perfusion ratio in the lung, measured with radioactive carbon dioxide. J Appl Physiol 1960;15(03):405–410
3 West JB. Distribution of pulmonary blood flow. Am J Respir Crit Care Med 1999;160(06):1802–1803
4 Hopkins SR, Henderson AC, Levin DL, et al. Vertical gradients in regional lung density and perfusion in the supine human lung: the Slinky effect. J Appl Physiol 2007;103(01):240–248
5 Glazier JB, Hughes JM, Maloney JE, West JB. Vertical gradient of alveolar size in lungs of dogs frozen intact. J Appl Physiol 1967;23(05):694–705
6 Glazier JB, Hughes JM, Maloney JE, West JB. Measurements of capillary dimensions and blood volume in rapidly frozen lungs. J Appl Physiol 1969;26(01):65–76
7 Tawhai MH, Nash MP, Lin CL, Hoffman EA. Supine and prone differences in regional lung density and pleural pressure gradients in the human lung with constant shape. J Appl Physiol 2009;107(03):912–920
8 Fung YC, Sobin SS. Theory of sheet flow in lung alveoli. J Appl Physiol 1969;26(04):472–488
9 Fung YC, Sobin SS. Pulmonary alveolar blood flow. Circ Res 1972;30(04):470–490
10 Mandelbrot BB. The Fractal Geometry of Nature. San Francisco, CA: W.H. Freeman; 1983
11 Glenny R, Robertson HT. Distribution of perfusion. Compr Physiol 2011;1(01):245–262
12 Glenny RW, Robertson HT. Spatial distribution of ventilation and perfusion: mechanisms and regulation. Compr Physiol 2011;1(01):375–395
13 Lefèvre J. Teleonomical optimization of a fractal model of the pulmonary arterial bed. J Theor Biol 1983;102(02):225–248
14 West GB, Brown JH, Enquist BJ. The fourth dimension of life: fractal geometry and allometric scaling of organisms. Science 1999;284(5420):1677–1679
15 Ochs M, Weibel ER. Functional design of the human lung for gas exchange. In: Grippi MA, Elias JA, Fishman JA, et al., eds. Fishman's Pulmonary Diseases and Disorders, 5th ed. New York, NY: McGraw-Hill Education; 2015
16 Galvin I, Drummond GB, Nirmalan M. Distribution of blood flow and ventilation in the lung: gravity is not the only factor. Br J Anaesth 2007;98(04):420–428
17 Altemeier WA, McKinney S, Glenny RW. Fractal nature of regional ventilation distribution. J Appl Physiol 2000;88(05):1551–1557
18 Hopkins SR. Ventilation/perfusion relationships and gas exchange: measurement approaches. Compr Physiol 2020;10(03):1155–1205
19 Hsia CCW, Bates JHT, Driehuys B, et al. Quantitative imaging metrics for the assessment of pulmonary pathophysiology: an official American Thoracic Society and Fleischner Society joint workshop report. Ann Am Thorac Soc 2023;20(02):161–195
20 Glenny RW, McKinney S, Robertson HT. Spatial pattern of pulmonary blood flow distribution is stable over days. J Appl Physiol 1997;82(03):902–907
21 Glenny RW. Heterogeneity in the lung: concepts and measures. In: Hlastala MP, Robertson HT, eds. Complexity in Structure and Function in the Lung. New York, NY: Marcel Dekker Inc.; 1998:571–609
22 Hall ET, Sá RC, Holverda S, et al. The effect of supine exercise on the distribution of regional pulmonary blood flow measured using proton MRI. J Appl Physiol 2014;116(04):451–461
23 Glenny RW, Robertson HT. Fractal modeling of pulmonary blood flow heterogeneity. J Appl Physiol 1991;70(03):1024–1030
24 Glenny RW, Robertson HT. Fractal properties of pulmonary blood flow: characterization of spatial heterogeneity. J Appl Physiol 1990;69(02):532–545
25 Glenny RW, Bernard SL, Robertson HT. Pulmonary blood flow remains fractal down to the level of gas exchange. J Appl Physiol 2000;89(02):742–748
26 Sinclair SE, McKinney S, Glenny RW, Bernard SL, Hlastala MP. Exercise alters fractal dimension and spatial correlation of pulmonary blood flow in the horse. J Appl Physiol 2000;88(06):2269–2278
27 Caruthers SD, Harris TR. Effects of pulmonary blood flow on the fractal nature of flow heterogeneity in sheep lungs. J Appl Physiol 1994;77(03):1474–1479
28 Levin DL, Buxton RB, Spiess JP, Arai T, Balouch J, Hopkins SR. Effects of age on pulmonary perfusion heterogeneity measured by magnetic resonance imaging. J Appl Physiol 2007;102(05):2064–2070
29 Banister J, Torrance RW. The effects of the tracheal pressure upon flow: pressure relations in the vascular bed of isolated lungs. Q J Exp Physiol Cogn Med Sci 1960;45(04):352–367
30 West JB, Dollery CT, Naimark A. Distribution of blood flow in isolated lung; relation to vascular and alveolar pressures. J Appl Physiol 1964;19:713–724
31 Hughes JM, Glazier JB, Maloney JE, West JB. Effect of lung volume on the distribution of pulmonary blood flow in man. Respir Physiol 1968;4(01):58–72
32 Hopkins SR, Arai TJ, Henderson AC, Levin DL, Buxton RB, Kim Prisk G. Lung volume does not alter the distribution of pulmonary perfusion in dependent lung in supine humans. J Physiol 2010;588(Pt 23):4759–4768
33 Amis TC, Jones HA, Hughes JM. Effect of posture on inter-regional distribution of pulmonary perfusion and VA/Q ratios in man. Respir Physiol 1984;56(02):169–182
34 Brudin LH, Rhodes CG, Valind SO, Jones T, Hughes JM. Interrelationships between regional blood flow, blood volume, and ventilation in supine humans. J Appl Physiol 1994;76(03):1205–1210
35 Jones AT, Hansell DM, Evans TW. Pulmonary perfusion in supine and prone positions: an electron-beam computed tomography study. J Appl Physiol 2001;90(04):1342–1348
36 Orphanidou D, Hughes JM, Myers MJ, Al-Suhali AR, Henderson B. Tomography of regional ventilation and perfusion using krypton 81m in normal subjects and asthmatic patients. Thorax 1986;41(07):542–551
37 Kaneko K, Milic-Emili J, Dolovich MB, Dawson A, Bates DV. Regional distribution of ventilation and perfusion as a function of body position. J Appl Physiol 1966;21(03):767–777
38 Petersson J, Rohdin M, Sánchez-Crespo A, et al. Paradoxical redistribution of pulmonary blood flow in prone and supine humans exposed to hypergravity. J Appl Physiol 2006;100(01):240–248
39 Burrowes KS, Hunter PJ, Tawhai MH. Evaluation of the effect of postural and gravitational variations on the distribution of pulmonary blood flow via an image-based computational model. Conf Proc IEEE Eng Med Biol Soc 2005;2005:6138–6140

40 Burrowes KS, Tawhai MH. Computational predictions of pulmonary blood flow gradients: gravity versus structure. Respir Physiol Neurobiol 2006;154(03):515–523

41 Glenny RW. Spatial correlation of regional pulmonary perfusion. J Appl Physiol 1992;72(06):2378–2386

42 Glenny RW, Bernard S, Robertson HT, Hlastala MP. Gravity is an important but secondary determinant of regional pulmonary blood flow in upright primates. J Appl Physiol 1999;86(02):623–632

43 Hlastala MP, Bernard SL, Erickson HH, et al. Pulmonary blood flow distribution in standing horses is not dominated by gravity. J Appl Physiol 1996;81(03):1051–1061

44 Wagner WW Jr, Jaryszak EM, Peterson AJ, et al. A perpetual switching system in pulmonary capillaries. J Appl Physiol 2019; 126(02):494–501

45 Wearn JT, Ernstene AC, Bromer AW, Barr JS, German WJ, Zschiesche LJ. The normal behavior of the pulmonary blood vessels with observations on the intermittence of the flow of blood in the arterioles and capillaries. Am J Physiol 1934;109(02): 236–256

46 Stickland MK, Welsh RC, Haykowsky MJ, et al. Intra-pulmonary shunt and pulmonary gas exchange during exercise in humans. J Physiol 2004;561(Pt 1):321–329

47 Bryan TL, van Diepen S, Bhutani M, Shanks M, Welsh RC, Stickland MK. The effects of dobutamine and dopamine on intrapulmonary shunt and gas exchange in healthy humans. J Appl Physiol 2012;113(04):541–548

48 Whyte MK, Peters AM, Hughes JM, et al. Quantification of right to left shunt at rest and during exercise in patients with pulmonary arteriovenous malformations. Thorax 1992;47 (10):790–796

49 Stickland MK, Lovering AT, Eldridge MW. Exercise-induced arteriovenous intrapulmonary shunting in dogs. Am J Respir Crit Care Med 2007;176(03):300–305

50 Stickland MK, Tedjasaputra V, Seaman C, et al. Intra-pulmonary arteriovenous anastomoses and pulmonary gas exchange: evaluation by microspheres, contrast echocardiography and inert gas elimination. J Physiol 2019;597(22):5365–5384

51 Aaronson PI, Robertson TP, Knock GA, et al. Hypoxic pulmonary vasoconstriction: mechanisms and controversies. J Physiol 2006; 570(pt. 1):53–58

52 Glenny RW, Polissar NL, McKinney S, Robertson HT. Temporal heterogeneity of regional pulmonary perfusion is spatially clustered. J Appl Physiol 1995;79(03):986–1001

53 Asadi AK, Sá RC, Kim NH, et al. Inhaled nitric oxide alters the distribution of blood flow in the healthy human lung, suggesting active hypoxic pulmonary vasoconstriction in normoxia. J Appl Physiol 2015;118(03):331–343

54 Asadi AK, Cronin MV, Sá RC, et al. Spatial-temporal dynamics of pulmonary blood flow in the healthy human lung in response to altered FI(O2). J Appl Physiol 2013;114(01):107–118

55 Asadi AK, Sá RC, Arai TJ, et al. Regional pulmonary perfusion patterns in humans are not significantly altered by inspiratory hypercapnia. J Appl Physiol 2019;127(02):365–375

56 Beutner A. Ueber die Strom- und Druckkräfte des Blutes in der Arteria pulmonalis. Z rationelle Med 1852;2:97–138

57 Plumier L. La circulation pulmonaire chez le chien. Arch Int Physiol 1904;1:176–213

58 Euler Uv, Liljestrand G. Observations on the pulmonary arterial blood pressure in the cat. Acta Physiol Scand 1946;12(04): 301–320

59 Sylvester JT, Shimoda LA, Aaronson PI, Ward JP. Hypoxic pulmonary vasoconstriction. Physiol Rev 2012;92(01):367–520

60 Naeije R, Brimioulle S. Physiology in medicine: importance of hypoxic pulmonary vasoconstriction in maintaining arterial oxygenation during acute respiratory failure. Crit Care 2001;5 (02):67–71

61 Bärtsch P, Gibbs JS. Effect of altitude on the heart and the lungs. Circulation 2007;116(19):2191–2202

62 Swenson ER. Hypoxic pulmonary vasoconstriction. High Alt Med Biol 2013;14(02):101–110

63 Dunham-Snary KJ, Wu D, Sykes EA, et al. Hypoxic pulmonary vasoconstriction: from molecular mechanisms to medicine. Chest 2017;151(01):181–192

64 Sommer N, Strielkov I, Pak O, Weissmann N. Oxygen sensing and signal transduction in hypoxic pulmonary vasoconstriction. Eur Respir J 2016;47(01):288–303

65 Grimmer B, Kuebler WM. The endothelium in hypoxic pulmonary vasoconstriction. J Appl Physiol 2017;123(06):1635–1646

66 Dawson CA, Grimm DJ, Linehan JH. Influence of hypoxia on the longitudinal distribution of pulmonary vascular resistance. J Appl Physiol 1978;44(04):493–498

67 Dawson CA, Grimm DJ, Linehan JH. Lung inflation and longitudinal distribution of pulmonary vascular resistance during hypoxia. J Appl Physiol 1979;47(03):532–536

68 Groh J, Kuhnle GE, Kuebler WM, Goetz AE. An experimental model for simultaneous quantitative analysis of pulmonary micro- and macrocirculation during unilateral hypoxia in vivo. Res Exp Med (Berl) 1992;192(06):431–441

69 Hakim TS, Michel RP, Minami H, Chang HK. Site of pulmonary hypoxic vasoconstriction studied with arterial and venous occlusion. J Appl Physiol 1983;54(05):1298–1302

70 Madden JA, Dawson CA, Harder DR. Hypoxia-induced activation in small isolated pulmonary arteries from the cat. J Appl Physiol 1985;59(01):113–118

71 Strielkov I, Pak O, Sommer N, Weissmann N. Recent advances in oxygen sensing and signal transduction in hypoxic pulmonary vasoconstriction. J Appl Physiol 2017;123(06):1647–1656

72 Dorrington KL, Clar C, Young JD, Jonas M, Tansley JG, Robbins PA. Time course of the human pulmonary vascular response to 8 hours of isocapnic hypoxia. Am J Physiol 1997;273(3, Pt 2): H1126–H1134

73 Groves BM, Reeves JT, Sutton JR, et al. Operation Everest II: elevated high-altitude pulmonary resistance unresponsive to oxygen. J Appl Physiol 1987;63(02):521–530

74 Domino KB, Hlastala MP, Eisenstein BL, Cheney FW. Effect of regional alveolar hypoxia on gas exchange in dogs. J Appl Physiol 1989;67(02):730–735

75 Hambraeus-Jonzon K, Bindslev L, Frostell C, Hedenstierna G. Individual lung blood flow during unilateral hypoxia: effects of inhaled nitric oxide. Eur Respir J 1998;11(03):565–570

76 Marshall BE, Marshall C, Benumof J, Saidman LJ. Hypoxic pulmonary vasoconstriction in dogs: effects of lung segment size and oxygen tension. J Appl Physiol 1981;51(06):1543–1551

77 Ryan D, Frohlich S, McLoughlin P. Pulmonary vascular dysfunction in ARDS. Ann Intensive Care 2014;4:28

78 West JB. Regional differences in the lung. Chest 1978;74(04): 426–437

79 West JB, Luks AM. West's Respiratory Physiology. Philadelphia, PA: Lippincott Williams & Wilkins; 2020

80 Whittenberger JL, McGREGOR M, Berglund E, Borst HG. Influence of state of inflation of the lung on pulmonary vascular resistance. J Appl Physiol 1960;15(05):878–882

81 Hakim TS, Michel RP, Chang HK. Effect of lung inflation on pulmonary vascular resistance by arterial and venous occlusion. J Appl Physiol 1982;53(05):1110–1115

82 Dubowitz G, Peacock AJ. Pulmonary artery pressure in healthy subjects at 4250 m measured by Doppler echocardiography. Wilderness Environ Med 2007;18(04):305–311

83 Canepa A, Chavez R, Hurtado A, Rotta A, Velasquez T. Pulmonary circulation at sea level and at high altitudes. J Appl Physiol 1956; 9(03):328–336

84 Voelkel NF, Mizuno S, Bogaard HJ. The role of hypoxia in pulmonary vascular diseases: a perspective. Am J Physiol Lung Cell Mol Physiol 2013;304(07):L457–L465

85 Grover RF. The fascination of the hypoxic lung. Anesthesiology 1985;63(06):580–582

86 Sommer N, Dietrich A, Schermuly RT, et al. Regulation of hypoxic pulmonary vasoconstriction: basic mechanisms. Eur Respir J 2008;32(06):1639–1651

87 Glasser SA, Domino KB, Lindgren L, Parcella P, Marshall C, Marshall BE. Pulmonary blood pressure and flow during atelectasis in the dog. Anesthesiology 1983;58(03):225–231

88 Dawson A. Regional pulmonary blood flow in sitting and supine man during and after acute hypoxia. J Clin Invest 1969;48(02):301–310

89 Arai TJ, Henderson AC, Dubowitz DJ, et al. Hypoxic pulmonary vasoconstriction does not contribute to pulmonary blood flow heterogeneity in normoxia in normal supine humans. J Appl Physiol 2009;106(04):1057–1064

90 Schuster DP, Anderson C, Kozlowski J, Lange N. Regional pulmonary perfusion in patients with acute pulmonary edema. J Nucl Med 2002;43(07):863–870

91 Wagner PD, Dantzker DR, Dueck R, Clausen JL, West JB. Ventilation-perfusion inequality in chronic obstructive pulmonary disease. J Clin Invest 1977;59(02):203–216

92 Naeye RL. Children at high altitude: pulmonary and renal abnormalities. Circ Res 1965;16:33–38

93 Sylvester JT, Harabin AL, Peake MD, Frank RS. Vasodilator and constrictor responses to hypoxia in isolated pig lungs. J Appl Physiol 1980;49(05):820–825

94 Weissmann N, Grimminger F, Walmrath D, Seeger W. Hypoxic vasoconstriction in buffer-perfused rabbit lungs. Respir Physiol 1995;100(02):159–169

95 Vejlstrup NG, Dorrington KL. Intense slow hypoxic pulmonary vasoconstriction in gas-filled and liquid-filled lungs: an in vivo study in the rabbit. Acta Physiol Scand 1993;148(03):305–313

96 Vejlstrup NG, O'Neill M, Nagyova B, Dorrington KL. Time course of hypoxic pulmonary vasoconstriction: a rabbit model of regional hypoxia. Am J Respir Crit Care Med 1997;155(01):216–221

97 Morrell NW, Nijran KS, Biggs T, Seed WA. Magnitude and time course of acute hypoxic pulmonary vasoconstriction in man. Respir Physiol 1995;100(03):271–281

98 Carlsson AJ, Bindslev L, Santesson J, Gottlieb I, Hedenstierna G. Hypoxic pulmonary vasoconstriction in the human lung: the effect of prolonged unilateral hypoxic challenge during anaesthesia. Acta Anaesthesiol Scand 1985;29(03):346–351

99 Marshall BE, Marshall C, Frasch F, Hanson CW. Role of hypoxic pulmonary vasoconstriction in pulmonary gas exchange and blood flow distribution. 1. Physiologic concepts. Intensive Care Med 1994;20(04):291–297

100 Marshall C, Marshall B. Site and sensitivity for stimulation of hypoxic pulmonary vasoconstriction. J Appl Physiol 1983;55(03):711–716

101 Marshall BE, Marshall C. A model for hypoxic constriction of the pulmonary circulation. J Appl Physiol 1988;64(01):68–77

102 Mélot C, Naeije R, Hallemans R, Lejeune P, Mols P. Hypoxic pulmonary vasoconstriction and pulmonary gas exchange in normal man. Respir Physiol 1987;68(01):11–27

103 Grünig E, Mereles D, Hildebrandt W, et al. Stress Doppler echocardiography for identification of susceptibility to high altitude pulmonary edema. J Am Coll Cardiol 2000;35(04):980–987

104 Gao Y, Raj JU. Regulation of the pulmonary circulation in the fetus and newborn. Physiol Rev 2010;90(04):1291–1335

105 Arias-Stella J, Saldana M. The terminal portion of the pulmonary arterial tree in people native to high altitudes. Circulation 1963; 28(05):915–925

106 Naeye RL. Hypoxemia, Effects on the Pulmonary Vascular Bed. Normal And Abnormal Pulmonary Circulation. Basel: Karger Publishers; 1963:302–309

107 Brimioulle S, LeJeune P, Naeije R. Effects of hypoxic pulmonary vasoconstriction on pulmonary gas exchange. J Appl Physiol 1996;81(04):1535–1543

108 Marshall BE, Marshall C. Continuity of response to hypoxic pulmonary vasoconstriction. J Appl Physiol 1980;49(02):189–196

109 Bindslev L, Jolin A, Hedenstierna G, Baehrendtz S, Santesson J. Hypoxic pulmonary vasoconstriction in the human lung: effect of repeated hypoxic challenges during anesthesia. Anesthesiology 1985;62(05):621–625

110 Neumann PH, Kivlen CM, Johnson A, Minnear FL, Malik AB. Effect of alveolar hypoxia on regional pulmonary perfusion. J Appl Physiol 1984;56(02):338–342

111 Hlastala MP, Lamm WJ, Karp A, Polissar NL, Starr IR, Glenny RW. Spatial distribution of hypoxic pulmonary vasoconstriction in the supine pig. J Appl Physiol 2004;96(05):1589–1599

112 Hopkins SR, Garg J, Bolar DS, Balouch J, Levin DL. Pulmonary blood flow heterogeneity during hypoxia and high-altitude pulmonary edema. Am J Respir Crit Care Med 2005;171(01):83–87

113 Dehnert C, Risse F, Ley S, et al. Magnetic resonance imaging of uneven pulmonary perfusion in hypoxia in humans. Am J Respir Crit Care Med 2006;174(10):1132–1138

114 Patz MD, Sá RC, Darquenne C, et al. Susceptibility to high-altitude pulmonary edema is associated with a more uniform distribution of regional specific ventilation. J Appl Physiol 2017;122(04):844–852

115 Naeije R, Chesler N. Pulmonary circulation at exercise. Compr Physiol 2012;2(01):711–741

116 Naeije R. Physiology of the pulmonary circulation and the right heart. Curr Hypertens Rep 2013;15(06):623–631

117 Halpern SD, Taichman DB. Misclassification of pulmonary hypertension due to reliance on pulmonary capillary wedge pressure rather than left ventricular end-diastolic pressure. Chest 2009;136(01):37–43

118 Kovacs G, Berghold A, Scheidl S, Olschewski H. Pulmonary arterial pressure during rest and exercise in healthy subjects: a systematic review. Eur Respir J 2009;34(04):888–894

119 Himelman RB, Stulbarg M, Kircher B, et al. Noninvasive evaluation of pulmonary artery pressure during exercise by saline-enhanced Doppler echocardiography in chronic pulmonary disease. Circulation 1989;79(04):863–871

120 Nagueh SF, Middleton KJ, Kopelen HA, Zoghbi WA, Quiñones MA. Doppler tissue imaging: a noninvasive technique for evaluation of left ventricular relaxation and estimation of filling pressures. J Am Coll Cardiol 1997;30(06):1527–1533

121 Cope DK, Grimbert F, Downey JM, Taylor AE. Pulmonary capillary pressure: a review. Crit Care Med 1992;20(07):1043–1056

122 Bhattacharya J, Nanjo S, Staub NC. Micropuncture measurement of lung microvascular pressure during 5-HT infusion. J Appl Physiol 1982;52(03):634–637

123 Reeves JT, Taylor AE. Pulmonary hemodynamics and fluid exchange in the lungs during exercise. In: Rowell LB, Shepherd, J.T, eds. Handbook of Physiology: A Critical, Comprehensive Presentation of Physiological Knowledge and Concepts. New York, NY: Oxford University Press; 1996:585–613

124 Moraes DL, Colucci WS, Givertz MM. Secondary pulmonary hypertension in chronic heart failure: the role of the endothelium in pathophysiology and management. Circulation 2000;102(14):1718–1723

125 Linehan JH, Haworth ST, Nelin LD, Krenz GS, Dawson CA. A simple distensible vessel model for interpreting pulmonary vascular pressure-flow curves. J Appl Physiol 1992;73(03):987–994

126 Reeves JT, Linehan JH, Stenmark KR. Distensibility of the normal human lung circulation during exercise. Am J Physiol Lung Cell Mol Physiol 2005;288(03):L419–L425

127 Lalande S, Yerly P, Faoro V, Naeije R. Pulmonary vascular distensibility predicts aerobic capacity in healthy individuals. J Physiol 2012;590(17):4279–4288

128 Krenz GS, Dawson CA. Flow and pressure distributions in vascular networks consisting of distensible vessels. Am J Physiol Heart Circ Physiol 2003;284(06):H2192–H2203

129 Argiento P, Vanderpool RR, Mulè M, et al. Exercise stress echocardiography of the pulmonary circulation: limits of normal and sex differences. Chest 2012;142(05):1158–1165

130 Sharma R, Kumar A, Aneja GK. Serial changes in pulmonary hemodynamics during pregnancy: a non-invasive study using Doppler echocardiography. Cardiol Res 2016;7(01):25–31

131 Singh I, Horn E, Haythe J. Pulmonary hypertension in pregnancy. Clin Chest Med 2021;42(01):91–99

132 Beck KC, Rehder K. Differences in regional vascular conductances in isolated dog lungs. J Appl Physiol 1986;61(02):530–538

133 Greenleaf JF, Ritman EL, Sass DJ, Wood EH. Spatial distribution of pulmonary blood flow in dogs in left decubitus position. Am J Physiol 1974;227(01):230–244

134 Reed JH Jr, Wood EH. Effect of body position on vertical distribution of pulmonary blood flow. J Appl Physiol 1970;28(03): 303–311

135 Atwood RM, Burchell HB, Tauxe WN. Pulmonary scans achieved with macroaggregated radioiodinated albumin: use in diagnosis of pulmonary artery agenesis. Am J Med Sci 1966;252(01):84–88

136 Friedman WF, Braunwald E. Alterations in regional pulmonary blood flow in mitral valve disease studied by radioisotope scanning. A simple nontraumatic technique for estimation of left atrial pressure. Circulation 1966;34(03):363–376

137 Tauxe WN, Burchell HB, Chaapel DW, Sprau A. Quantitating the effect of gravity on lung scans of macroaggregates of albumin-I-131. J Appl Physiol 1966;21(04):1381–1386

138 Lovering AT, Haverkamp HC, Romer LM, Hokanson JS, Eldridge MW. Transpulmonary passage of 99mTc macroaggregated albumin in healthy humans at rest and during maximal exercise. J Appl Physiol 2009;106(06):1986–1992

139 Roughton FJ, Forster RE. Relative importance of diffusion and chemical reaction rates in determining rate of exchange of gases in the human lung, with special reference to true diffusing capacity of pulmonary membrane and volume of blood in the lung capillaries. J Appl Physiol 1957;11(02):290–302

140 Hsia CCW. Recruitment of lung diffusing capacity: update of concept and application. Chest 2002;122(05):1774–1783

141 Langleben D, Orfanos SE, Giovinazzo M, et al. Pulmonary capillary surface area in supine exercising humans: demonstration of vascular recruitment. Am J Physiol Lung Cell Mol Physiol 2019; 317(03):L361–L368

142 Orfanos SE, Langleben D, Khoury J, et al. Pulmonary capillary endothelium-bound angiotensin-converting enzyme activity in humans. Circulation 1999;99(12):1593–1599

143 Cardús J, Burgos F, Diaz O, et al. Increase in pulmonary ventilation-perfusion inequality with age in healthy individuals. Am J Respir Crit Care Med 1997;156(2, pt 1):648–653

144 Janssens JP. Aging of the respiratory system: impact on pulmonary function tests and adaptation to exertion. Clin Chest Med 2005;26(03):469–484, vi–vii

145 Holley HS, Milic-Emili J, Becklake MR, Bates DV. Regional distribution of pulmonary ventilation and perfusion in obesity. J Clin Invest 1967;46(04):475–481

146 Frerichs I, Braun P, Dudykevych T, Hahn G, Genée D, Hellige G. Distribution of ventilation in young and elderly adults determined by electrical impedance tomography. Respir Physiol Neurobiol 2004;143(01):63–75

147 Verbanck S, Thompson BR, Schuermans D, et al. Ventilation heterogeneity in the acinar and conductive zones of the normal ageing lung. Thorax 2012;67(09):789–795

148 Lam CS, Borlaug BA, Kane GC, Enders FT, Rodeheffer RJ, Redfield MM. Age-associated increases in pulmonary artery systolic pressure in the general population. Circulation 2009;119(20): 2663–2670

149 Coffman KE, Carlson AR, Miller AD, Johnson BD, Taylor BJ. The effect of aging and cardiorespiratory fitness on the lung diffusing capacity response to exercise in healthy humans. J Appl Physiol 2017;122(06):1425–1434

150 Chang SC, Chang HI, Liu SY, Shiao GM, Perng RP. Effects of body position and age on membrane diffusing capacity and pulmonary capillary blood volume. Chest 1992;102(01):139–142

151 Stam H, Hrachovina V, Stijnen T, Versprille A. Diffusing capacity dependent on lung volume and age in normal subjects. J Appl Physiol 1994;76(06):2356–2363

152 Georges R, Saumon G, Loiseau A. The relationship of age to pulmonary membrane conductance and capillary blood volume. Am Rev Respir Dis 1978;117(06):1069–1078

153 Hermann EA, Motahari A, Hoffman EA, et al. Pulmonary blood volume among older adults in the community: the MESA Lung Study. Circ Cardiovasc Imaging 2022;15(08):e014380

154 Huang YC, Helms MJ, MacIntyre NR. Normal values for single exhalation diffusing capacity and pulmonary capillary blood flow in sitting, supine positions, and during mild exercise. Chest 1994;105(02):501–508

155 Ross BA, Brotto AR, Fuhr DP, et al. The supine position improves but does not normalize the blunted pulmonary capillary blood volume response to exercise in mild COPD. J Appl Physiol 2020; 128(04):925–933

156 Johnson RL Jr, Spicer WS, Bishop JM, Forster RE. Pulmonary capillary blood volume, flow and diffusing capacity during exercise. J Appl Physiol 1960;15:893–902

157 Holland J, Milic-Emili J, Macklem PT, Bates DV. Regional distribution of pulmonary ventilation and perfusion in elderly subjects. J Clin Invest 1968;47(01):81–92

158 McQuillan BM, Picard MH, Leavitt M, Weyman AE. Clinical correlates and reference intervals for pulmonary artery systolic pressure among echocardiographically normal subjects. Circulation 2001;104(23):2797–2802

159 Anthonisen NR, Milic-Emili J. Distribution of pulmonary perfusion in erect man. J Appl Physiol 1966;21(03):760–766

160 West JB. Importance of gravity in determining the distribution of pulmonary blood flow. J Appl Physiol 2002;93(05):1888–1889, author reply 1889–1891

161 Prisk GK, Yamada K, Henderson AC, et al. Pulmonary perfusion in the prone and supine postures in the normal human lung. J Appl Physiol 2007;103(03):883–894

162 Fain SB, Altes TA, Panth SR, et al. Detection of age-dependent changes in healthy adult lungs with diffusion-weighted 3He MRI. Acad Radiol 2005;12(11):1385–1393

163 Higginbotham MB, Morris KG, Williams RS, McHale PA, Coleman RE, Cobb FR. Regulation of stroke volume during submaximal and maximal upright exercise in normal man. Circ Res 1986;58 (02):281–291

164 Wagner PD, Gale GE, Moon RE, Torre-Bueno JR, Stolp BW, Saltzman HA. Pulmonary gas exchange in humans exercising at sea level and simulated altitude. J Appl Physiol 1986;61(01): 260–270

165 Tedjasaputra V, Bouwsema MM, Stickland MK. Effect of aerobic fitness on capillary blood volume and diffusing membrane capacity responses to exercise. J Physiol 2016;594(15): 4359–4370

166 Bouwsema MM, Tedjasaputra V, Stickland MK. Are there sex differences in the capillary blood volume and diffusing capacity response to exercise? J Appl Physiol 2017;122(03):460–469

167 Hsia CC, McBrayer DG, Ramanathan M. Reference values of pulmonary diffusing capacity during exercise by a rebreathing technique. Am J Respir Crit Care Med 1995;152(02):658–665

168 Langleben D, Fox BD, Orfanos SE, Giovinazzo M, Catravas JD. Pulmonary capillary recruitment and distention in mammalian lungs: species similarities. Eur Respir Rev 2022;31(163):210248

169 La Gerche A, Rakhit DJ, Claessen G. Exercise and the right ventricle: a potential Achilles' heel. Cardiovasc Res 2017;113 (12):1499–1508

170 Zavorsky GS, Smoliga JM. The association between cardiorespiratory fitness and pulmonary diffusing capacity. Respir Physiol Neurobiol 2017;241:28–35

171 Elbehairy AF, Faisal A, Guenette JA, et al; Canadian Respiratory Research Network (CRRN) Resting physiological correlates of reduced exercise capacity in smokers with mild airway obstruction. COPD 2017;14(03):267–275

172 West JB, Tsukimoto K, Mathieu-Costello O, Prediletto R. Stress failure in pulmonary capillaries. J Appl Physiol 1991;70(04): 1731–1742

173 Hopkins SR, Schoene RB, Henderson WR, Spragg RG, Martin TR, West JB. Intense exercise impairs the integrity of the pulmonary blood-gas barrier in elite athletes. Am J Respir Crit Care Med 1997;155(03):1090–1094

174 West JB, Mathieu-Costello O, Jones JH, et al. Stress failure of pulmonary capillaries in racehorses with exercise-induced pulmonary hemorrhage. J Appl Physiol 1993;75(03):1097–1109

175 Hopkins SR, Schoene RB, Henderson WR, Spragg RG, West JB. Sustained submaximal exercise does not alter the integrity of the lung blood-gas barrier in elite athletes. J Appl Physiol 1998;84 (04):1185–1189

176 West JB. Invited review: pulmonary capillary stress failure. J Appl Physiol 2000;89(06):2483–2489, discussion 2497

177 Bake B, Bjure J, Widimsky J. The effect of sitting and graded exercise on the distribution of pulmonary blood flow in healthy subjects studied with the 133Xenon technique. Scand J Clin Lab Invest 1968;22(02):99–106

178 Harf A, Pratt T, Hughes JM. Regional distribution of VA/Q in man at rest and with exercise measured with krypton-81m. J Appl Physiol 1978;44(01):115–123

179 Mohsenifar Z, Ross MD, Waxman A, Goldbach P, Koerner SK. Changes in distribution of lung perfusion and ventilation at rest and during maximal exercise. Chest 1985;87(03):359–362

180 Hopkins SR, Kleinsasser A, Bernard S, et al. Hypoxia has a greater effect than exercise on the redistribution of pulmonary blood flow in swine. J Appl Physiol 2007;103(06):2112–2119

181 Melsom MN, Flatebø T, Sjaastad OV, Aulie A, Nicolaysen G. Minor redistribution of ventilation and perfusion within the lung during exercise in sheep. Acta Physiol Scand 1999;165(03): 283–292

182 Bernard SL, Glenny RW, Erickson HH, et al. Minimal redistribution of pulmonary blood flow with exercise in racehorses. J Appl Physiol 1996;81(03):1062–1070

183 Kuikka JT, Länsimies E. A fractal approach for evaluation of pulmonary circulation in man at rest and during exercise. Clin Physiol 1999;19(02):107–110

184 Parker JC, Ardell JL, Hamm CR, Barman SA, Coker PJ. Regional pulmonary blood flow during rest, tilt, and exercise in unanesthetized dogs. J Appl Physiol 1995;78(03):838–846

185 Burnham KJ, Arai TJ, Dubowitz DJ, et al. Pulmonary perfusion heterogeneity is increased by sustained, heavy exercise in humans. J Appl Physiol 2009;107(05):1559–1568

186 Tedjasaputra V, Sá RC, Anderson KM, Prisk GK, Hopkins SR. Heavy upright exercise increases ventilation-perfusion mismatch in the basal lung: indirect evidence for interstitial pulmonary edema. J Appl Physiol 2019;127(02):473–481

187 Stokes DL, MacIntyre NR, Nadel JA. Nonlinear increases in diffusing capacity during exercise by seated and supine subjects. J Appl Physiol 1981;51(04):858–863

188 Musch G, Layfield JD, Harris RS, et al. Topographical distribution of pulmonary perfusion and ventilation, assessed by PET in supine and prone humans. J Appl Physiol 2002;93(05): 1841–1851

189 Nyrén S, Mure M, Jacobsson H, Larsson SA, Lindahl SG. Pulmonary perfusion is more uniform in the prone than in the supine position: scintigraphy in healthy humans. J Appl Physiol 1999;86 (04):1135–1141

190 Henderson AC, Sá RC, Theilmann RJ, Buxton RB, Prisk GK, Hopkins SR. The gravitational distribution of ventilation-perfusion ratio is more uniform in prone than supine posture in the normal human lung. J Appl Physiol 2013;115(03):313–324

191 Rohdin M, Petersson J, Sundblad P, et al. Effects of gravity on lung diffusing capacity and cardiac output in prone and supine humans. J Appl Physiol 2003;95(01):3–10

192 Soni N, Williams P. Positive pressure ventilation: what is the real cost? Br J Anaesth 2008;101(04):446–457

193 Nieman GF, Paskanik AM, Bredenberg CE. Effect of positive end-expiratory pressure on alveolar capillary perfusion. J Thorac Cardiovasc Surg 1988;95(04):712–716

194 Luecke T, Pelosi P. Clinical review: positive end-expiratory pressure and cardiac output. Crit Care 2005;9(06):607–621

195 Kallas HJ, Domino KB, Glenny RW, Anderson EA, Hlastala MP. Pulmonary blood flow redistribution with low levels of positive end-expiratory pressure. Anesthesiology 1998;88(05): 1291–1299

196 Petersson J, Ax M, Frey J, Sánchez-Crespo A, Lindahl SG, Mure M. Positive end-expiratory pressure redistributes regional blood flow and ventilation differently in supine and prone humans. Anesthesiology 2010;113(06):1361–1369

Gas Exchange in the Lung

Johan Petersson, MD, PhD[1,2] Robb W. Glenny, MD[3,4]

[1] Section of Anesthesiology and Intensive Care Medicine, Department of Physiology and Pharmacology, Karolinska Institutet, Stockholm, Sweden
[2] Department of Anaesthesiology, Surgical Services and Intensive Care, Karolinska University Hospital, Stockholm, Sweden
[3] Division of Pulmonary, Critical Care and Sleep Medicine, Department of Medicine, University of Washington, Seattle, Washington
[4] Department of Physiology and Biophysics, University of Washington, Seattle, Washington

Address for correspondence Johan Petersson, MD, PhD, Department of Anaesthesiology, Surgical Services and Intensive Care, Karolinska University Hospital, 17176 Stockholm, Sweden
(e-mail: johan.petersson@regionstockholm.se).

Semin Respir Crit Care Med 2023;44:555–568.

Abstract

Keywords
- ventilation-perfusion ratio
- respiratory dead space
- respiratory physiology
- pulmonary ventilation
- hypoxia
- hypercapnia

Gas exchange in the lung depends on tidal breathing, which brings new oxygen to and removes carbon dioxide from alveolar gas. This maintains alveolar partial pressures that promote passive diffusion to add oxygen and remove carbon dioxide from blood in alveolar capillaries. In a lung model without ventilation and perfusion ($\dot{V}_A/\dot{Q}$) mismatch, alveolar partial pressures of oxygen and carbon dioxide are primarily determined by inspiratory pressures and alveolar ventilation. Regions with shunt or low $\dot{V}_A/\dot{Q}$ ratios worsen arterial oxygenation while alveolar dead space and high $\dot{V}_A/\dot{Q}$ lung units lessen CO_2 elimination efficiency. Although less common, diffusion limitation might cause hypoxemia in some situations. This review covers the principles of lung gas exchange and therefore mechanisms of hypoxemia or hypercapnia. In addition, we discuss different metrics that quantify the deviation from ideal gas exchange.

Oxygen (O_2) is required for cellular respiration in all multicellular organisms. In humans, the first step in delivering O_2 to the cellular level is via uptake from air through the lungs. Carbon dioxide (CO_2), the byproduct of cellular metabolism, must continuously be eliminated from the body via the lungs to maintain homeostasis. Blood carries O_2 to the tissues for metabolism and delivers CO_2 from these tissues to the lungs for elimination. Ventilation brings O_2 to the blood while concurrently removing CO_2 from the blood. Efficient respiratory gas exchange therefore requires the intimate matching between blood flow and ventilation in the lung. Clinically, most cases of impaired gas exchange are caused by a reduced correlation between regional lung ventilation and blood flow, known as $\dot{V}_A/\dot{Q}$ mismatch ($\dot{V}_A$ alveolar ventilation; $\dot{Q}$ total lung blood flow), i.e., lung regions that are either over- or under-ventilated in proportion to regional blood flow. The main part of this review will therefore discuss how different forms of $\dot{V}_A/\dot{Q}$ mismatch affect gas exchange efficiency for O_2 and CO_2. To adequately describe basic principles that are equally important in situations where $\dot{V}_A/\dot{Q}$ mismatch is present, we will start with gas exchange in an ideal lung with no $\dot{V}_A/\dot{Q}$ mismatch. Because there is only limited $\dot{V}_A/\dot{Q}$ mismatch in normal lungs, gas exchange in healthy individuals comes close to this model.

Gas Exchange in a Lung without $\dot{V}_A/\dot{Q}$ Mismatch

The active part of pulmonary uptake of O_2 is tidal breathing that brings air with a high inspiratory partial pressure of oxygen (P_IO_2) to the lung alveoli (►**Fig. 1**). When breathing air (20.9% O_2), P_IO_2 is 159 mm Hg if barometric pressure (P_B) is 760 mm Hg, often taken as normal P_B at sea level, (0.209×760 mm Hg = 159 mm Hg). During passage through the conducting airways, inspired gas is heated to body temperature and humidified to 100% relative humidity, corresponding to a partial pressure of water vapor (P_{H_2O}) of 47 mm Hg. The addition of water vapor dilutes inspired air,

Issue Theme Pulmonary Physiology; Guest Editors: David A. Kaminsky, MD, Kathryn A. Hibbert, MD, and Andrew M. Luks, MD

Thieme Medical Publishers, Inc.,
333 Seventh Avenue, 18th Floor,
New York, NY 10001, USA

DOI https://doi.org/10.1055/s-0043-1770060.
ISSN 1069-3424.

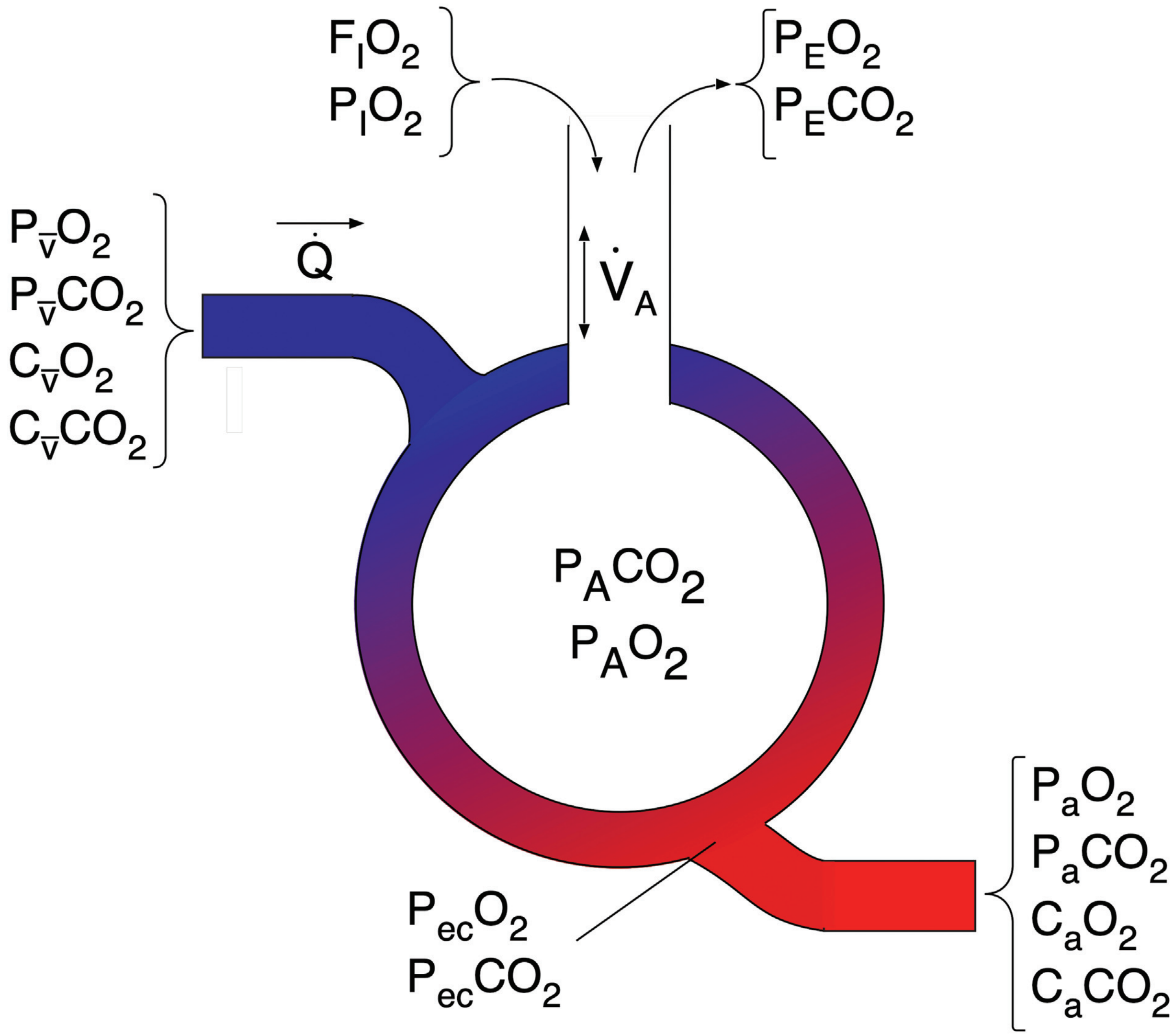

Fig. 1 Model of single alveolus (gas exchanging unit) displaying the traditional nomenclature used to describe fractions (F), partial pressures (P) and content (C) of gases (O_2 and CO_2) in venous blood (v), end-capillary blood (ec), inhaled gas (I), exhaled (E) gas, and alveolar gas (A). $\dot{Q}$ and $\dot{V}_A$ represent blood flow and ventilation, respectively.

reducing partial pressures of other inspired gases. During the conditions assumed above, PO_2 of inspired gas reaching the distal airways is therefore 149 mm Hg (0.209 × [760 mm Hg – 47 mm Hg]). Alveolar PO_2 (P_AO_2) is then further reduced by continuous uptake of O_2 from alveolar gas to blood in the alveolar capillaries. Although lower than P_IO_2, P_AO_2 is much greater than PO_2 of mixed venous blood ($P_{\bar{v}}O_2$), at rest in a normal subject ~ 40 mm Hg, entering the alveolar capillaries causing oxygen to diffuse from alveolar gas into the blood. This is a passive process driven solely by partial pressure differences as there is no active transport of O_2 across the alveolar capillary membrane. In most situations, the result is equilibration between P_AO_2 and PO_2 of end-capillary blood ($P_{ec}O_2$) leaving the alveoli (►**Fig. 1**). The diffusion and equilibration of gas partial pressures is facilitated by several structural components in the lung: (1) the exceptionally thin membrane, only 1 µm,[1,2] separates the alveolar gas and blood compartments, (2) the large surface area for gas exchange (140 $m^{2,3}$), (3) exposure of blood to several gas-exchanging units, and (4) the relatively large blood volume within the alveolar capillaries which slows blood flow, allowing more time for gas exchange (►**Fig. 2**). At rest, transit time through the alveolar capillaries is normally 0.25 to 0.75 second. In this theoretical model of a lung without $\dot{V}_A/\dot{Q}$ mismatch, P_AO_2 and hence $P_{ec}O_2$ are identical for all lung regions. Oxygenation of arterial blood is therefore primarily dependent on P_AO_2. P_AO_2 can be estimated from the ideal alveolar gas equation in which the delivery of O_2 to the alveolar compartment is represented by the first part of the equation (explained below in Box 1) and the removal of O_2 from the alveolar space is represented by the second part of the equation where the term P_aCO_2/R represents the amount of oxygen being removed.[4–6] As shown in Box 1, with a normal arterial PCO_2 (P_aCO_2) and during the conditions stated, the alveolar gas equation results in a

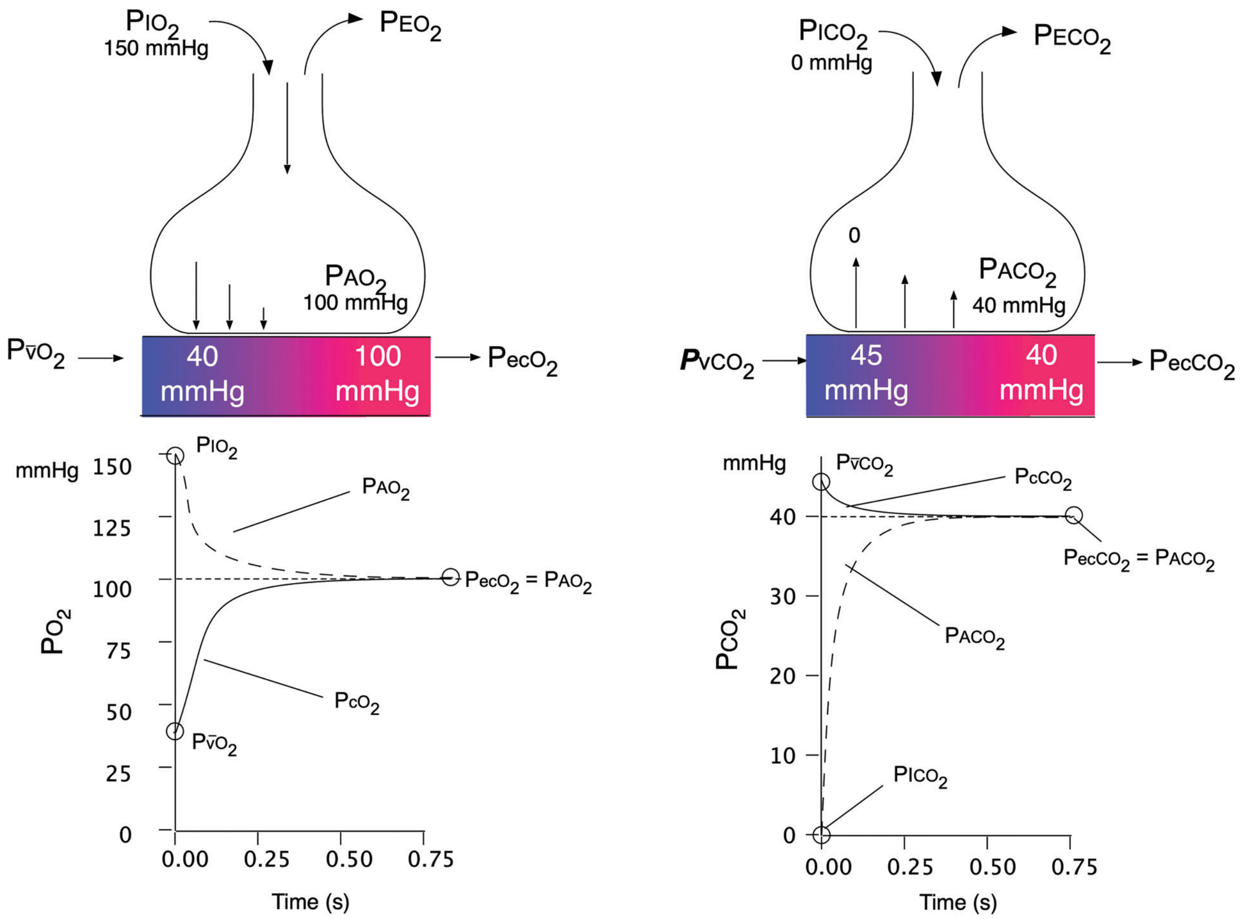

Fig. 2 Time course of PO_2 and PCO_2 as they rapidly reach equilibration through passive diffusion across the alveolar-capillary membrane. The figures demonstrate that there is no difference between the alveolar and end-capillary pressures within the time it takes for blood to traverse the gas-exchanging lung regions. At rest the normal transit time is 0.25 to 75 seconds. Notations are explained in ►**Fig. 1**.

P_AO_2 of approximately 102 mm Hg. Note that in this idealized lung model, the difference between alveolar and arterial PO_2 ($P_{A\text{-}a}O_2$) is zero. We will come back to how the $P_{A\text{-}a}O_2$ difference can be used to assess gas exchange impairment.

Elimination of carbon dioxide (CO_2) occurs in a similar manner but of course in the opposite direction. In a normal subject at rest, partial pressure of carbon dioxide in mixed venous blood ($P_{\bar{v}}O_2$) is approximately 45 mm Hg, which is greater than PCO_2 in alveolar gas (P_ACO_2; ►**Fig. 1**). CO_2 therefore diffuses from blood in the alveolar capillaries to the alveolar space. Tidal breathing eliminates alveolar gas with a high PCO_2 and replaces it with fresh gas with PCO_2 close to zero, which maintains P_ACO_2 lower than $P_{\bar{v}}O_2$ (►**Figs. 2** and **3**). The equilibration between PCO_2 in blood and alveolar gas is even more rapid than for O_2 because the resistance to diffusion is even less than for O_2. Therefore, $P_{ec}CO_2$ and P_aCO_2 become equilibrated with the P_ACO_2. As with O_2, there is no active transport of CO_2 across the alveolar capillary membrane.

We have greatly simplified the concepts of gas exchange above. With tidal breathing, P_AO_2 and P_ACO_2 will rise and fall with each breath. These fluctuations are not reflected in temporal variations in arterial gases due to differences in regional blood transit times and ventilation across the lung that act as a mixing or smoothing process. When we speak about the partial pressures of gases in various compartments, we therefore ignore any temporal fluctuations and present mean values over multiple respiratory cycles.

Delivery of O_2 to peripheral tissues and CO_2 to the lungs is covered in detail elsewhere (see Chapter 5), and depends on cardiac output, tissue perfusion, and the amount of each gas in blood. O_2 is carried in blood bound to hemoglobin (Hgb) and dissolved in plasma. Each hemoglobin molecule has four binding sites for O_2 and the affinity for each of these binding sites is influenced by several factors including the number of bound oxygen sites, P_aCO_2, pH, and temperature of the blood. The resultant hemoglobin–O_2 saturation and content curves are shown in ►**Fig. 4**. The sigmoidal shape of these curves plays an important role in O_2 uptake in the lungs and offloading of O_2 to the peripheral tissues. The amount of O_2 dissolved in plasma is relatively small and directly proportional to P_aO_2. The O_2 content of arterial blood ($C_{a_{O_2}}$) is the sum of the O_2 bound to Hgb and dissolved in plasma. For a normal P_aO_2 and Hgb, there is typically around 20 mL of O_2 in

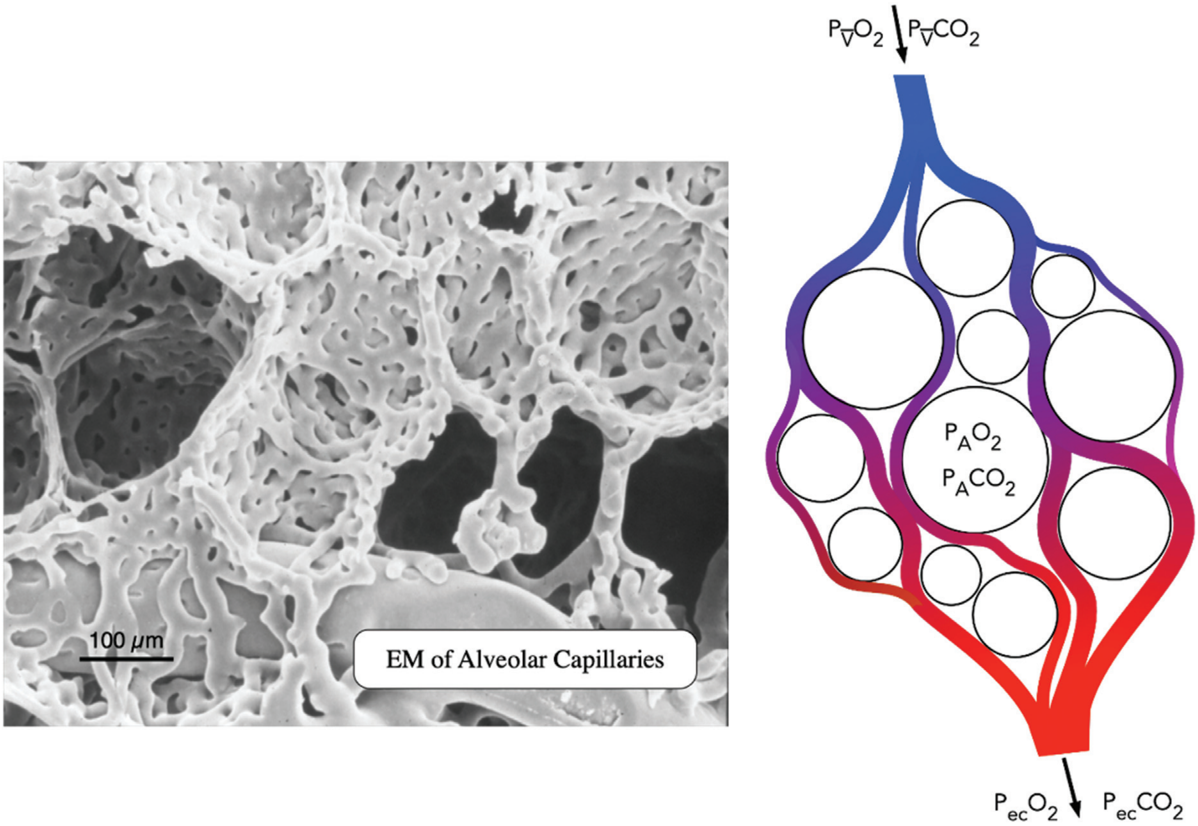

Fig. 3 Left: scanning electron micrograph of alveolar capillaries demonstrating the network of capillaries that surround the alveoli.[46] Right: schematic demonstrating the blood exchanging gas with multiple alveoli as it traverses the gas-exchanging regions in the lungs. Notations are explained in ►**Fig. 1**.

100 mL of blood (20 mL/dL). CO_2 is carried in blood bound to Hgb, as bicarbonate (HCO_3^-) and dissolved in plasma. The binding of CO_2 to hemoglobin does not change the affinity of Hgb for CO_2 as happens with O_2, resulting in a more linear relationship between P_aCO_2 and the content of CO_2 (C_{ao_2}) in blood (►**Fig. 4**). For a normal P_aCO_2 and Hgb, there is typically around 50 mL of CO_2 in 100 mL of blood (50 mL/dL). The arterial to venous content differences for O_2 and CO_2 are similar (∼5 mL/dL), hence the alveolar uptake of O_2 ($\dot{V}_{O_2}$, mL/min) is approximately as much as the elimination of CO_2

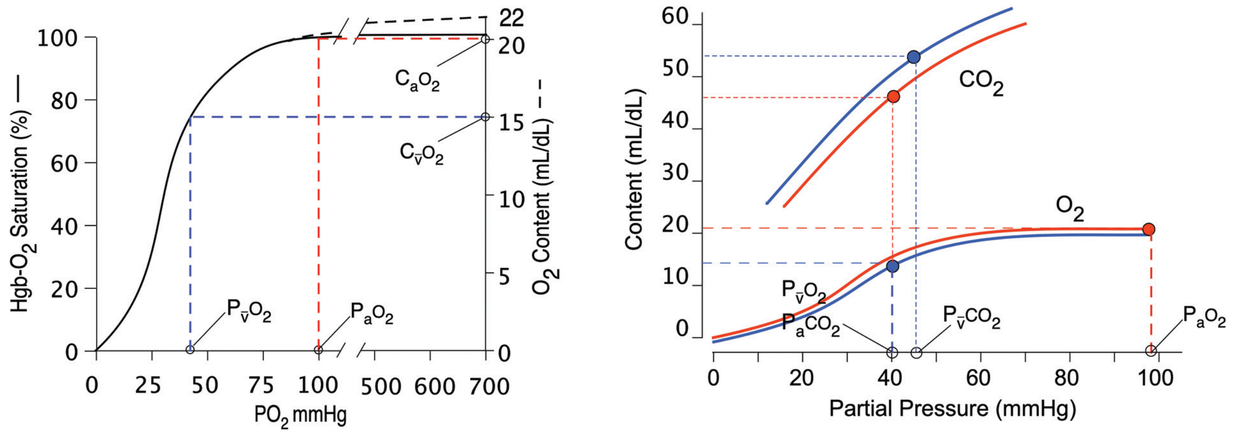

Fig. 4 Left: the hemoglobin–oxygen dissociation curve, content calculated for a hemoglobin concentration of 15 g/dL. The sigmoidal shape explains the nonlinear relationship between P_aO_2 and C_aO_2, nearly all of which is bound to hemoglobin. Note the small increase in C_aO_2 when P_aO_2 is greater than 100 mm Hg, which is one reason why high $\dot{V}_A/\dot{Q}$ regions add very little O_2 to arterial blood. Right: content of O_2 and CO_2 in blood as a function of the partial pressure of each gas in arterial (red curve) and mixed venous (blue curve). The arterial and venous curves differ in positions due to the Bohr (oxygen) and Haldane (carbon dioxide) effects. Dashed lines and markers correspond to normal values. Note the steeper curve for CO_2, the pressure difference between mixed venous and arterial blood is very different for oxygen and carbon dioxide despite very similar difference in content. Notations are explained in ►**Fig. 1**.

($\dot{V}_{CO_2}$, mL/min), which is described by the respiratory exchange ratio ($R = \dot{V}_{CO_2}/\dot{V}_{O_2}$, also called the respiratory quotient), at steady state, 0.7 to 1.0. The different relationships between partial pressures and contents mean that the drop in PCO_2 between mixed venous and end-capillary blood is approximately 5 mm Hg, while the increase in PO_2 is approximately 60 mm Hg (►**Fig. 4**).

In summary, ventilation maintains alveolar gas with PO_2 greater and PCO_2 lower than partial pressures in the mixed venous blood. The differences in partial pressure results in diffusion of oxygen and carbon dioxide across the alveolar-capillary membrane so that, in the absence of diffusion limitation (discussed later), end-capillary partial pressures equilibrate with those in alveolar gas (►**Fig. 2**). In a model with no $\dot{V}_A/\dot{Q}$ mismatch and no diffusion limitation, P_AO_2 and P_ACO_2 are uniform across the lung and $P_{A\text{-}a}O_2$ and $P_{a\text{-}A}CO_2$ differences are zero. It is important to understand that the absence of $\dot{V}_A/\dot{Q}$ mismatch does not require a homogeneous distribution of regional ventilation and blood flow throughout the lung. Even with heterogeneous distributions, there will be no mismatch if the regional variation in $\dot{V}_A$ and $\dot{Q}$ match each other.

Box 1: The ideal alveolar gas equation

$$P_AO_2 = P_IO_2 - \frac{P_aCO_2}{R} = F_IO_2 \times (P_B - P_{H_2O}) - \frac{P_aCO_2}{R}$$

$$P_AO_2 = P_IO_2 - \frac{P_aCO_2}{R} \times [1 - F_IO_2(1 - R)]$$

Box 1 The ideal alveolar gas equation exists in several forms, two are shown here. The upper equation is often used in clinical practice. The lower, more complex, equation takes into account that the inspiratory and expiratory minute volumes differ when the respiratory exchange ratio, R, does not equal 1.0. The effect is small but dependent on F_IO_2, with a normal R of = 0.8 and $P_aCO_2 = 40$ mm Hg the difference in calculated P_AO_2 is 2 mm Hg breathing air but 10 mm Hg with $F_IO_2 = 1.0$. Derivation of the equations is well described.[4–6] The equation defines what P_AO_2 would be in all lung regions if $\dot{V}_A/\dot{Q}$, and therefore gas exchange, is homogeneous throughout the lung, with the assumption that perfect equilibrium between P_A and P_{ec} is reached across all regions.[4] The P_AO_2 given by the equation has therefore been referred to as P_AO_2 of "ideal" alveolar gas and it can be used as a reference to quantitatively estimate the impact of $\dot{V}_A/\dot{Q}$ mismatch on P_aO_2, which corresponds to the alveolar-arterial PO_2 difference ($P_{A\text{-}a}O_2$). P_IO_2: partial pressure of O_2 in inspired gas reaching the alveoli, calculated as $P_IO_2 = F_IO_2 \times (P_B - P_{H_2O})$; F_IO_2: fraction of O_2 in inspired gas; P_B: barometric pressure; P_{H_2O}: saturated vapor pressure of water at body temperature, 47 mm Hg at 37°C; R: the respiratory exchange ratio defined as the ratio between the amount of CO_2 and O_2 exchanged across the alveolar-capillary barrier. P_B must be known or estimated for the appropriate altitude; at sea level it is commonly estimated as 760 mm Hg. If not measured, R is usually assumed to be 0.8. Using these values at sea level, the fraction of O_2 in air ($F_IO_2 = 0.21$) and a normal P_aCO_2 of 40 mm Hg, the upper equation results in $P_AO_2 = 102$ mm Hg.

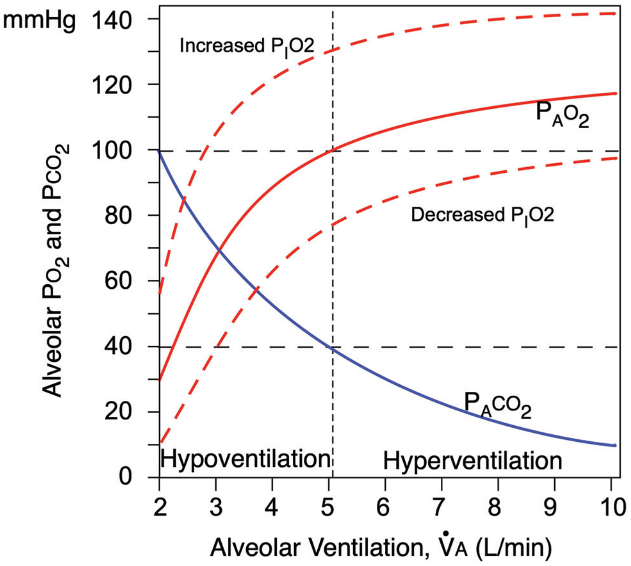

Fig. 5 Graph demonstrating the inverse relationships between P_AO_2 and P_ACO_2 as a function of alveolar ventilation. Remember that in a lung without $\dot{V}_A/\dot{Q}$ mismatch and diffusion limitation, the alveolar pressures equal P_aO_2 and P_aCO_2. Normal values for $\dot{V}_A$, P_AO_2, and P_aCO_2 are indicated by the dashed lines. The upper dashed red curve illustrates the effect of increasing F_IO_2 which raises P_IO_2. The lower dashed curve illustrates the effect of decreased P_IO_2, e.g., at high altitude. The curves are derived assuming unchanged cardiac output, O_2 consumption and CO_2 production and with mixed venous values changing with changes in P_aO_2 and P_aCO_2. For example, with hypoventilation $P_{\bar{v}}O_2$ is lower and $P_{\bar{v}}CO_2$ higher than normal. Hypoventilation results in both hypoxemia and hypercapnia. An increase in F_IO_2 results in an upward shift of the PO_2 curve while the PCO_2 curve remains fixed. An increase in $\dot{V}O_2$ and $\dot{V}_{CO_2}$ would shift the P_AO_2 curve downward and the P_ACO_2 curve upward which illustrates the corresponding changes in alveolar and arterial partial pressures if $\dot{V}_A$ remains unchanged. Notations are explained in ►**Fig. 1**.

Effects of Changes in alveolar ventilation ($\dot{V}_A/\dot{Q}$), $\dot{V}_{O_2}$, and $\dot{V}_{CO_2}$

Above we described a theoretical lung without $\dot{V}_A/\dot{Q}$ mismatch, P_AO_2 and $P_aO_2 \sim 102$ mm Hg and normal P_ACO_2 and $P_aCO_2 \sim 40$ mm Hg. By definition this also corresponds to a normal alveolar ventilation ($\dot{V}_A$; we discuss the relationship between $\dot{V}_A$ and minute ventilation ($\dot{V}_E$) later). ►**Fig. 5** illustrates how P_AO_2 and P_ACO_2 vary with $\dot{V}_A$ if $\dot{V}_{O_2}$ and $\dot{V}_{CO_2}$ remain unchanged. Greater alveolar ventilation (i.e., hyperventilation) increases P_AO_2 and lowers P_ACO_2. P_aO_2 and P_aCO_2 shift accordingly because our model assumes equilibration between alveolar and capillary blood partial pressures. Lower $\dot{V}_A$ (i.e., hypoventilation) reduces P_AO_2 and P_aO_2 but increases P_ACO_2 and P_aCO_2. Hypo- and hyperventilation are here in fact defined not by minute ventilation but by P_aCO_2 being outside the normal range. The relationship between P_ACO_2, alveolar minute ventilation, and $\dot{V}_{CO_2}$ is described by the alveolar ventilation equation:

$$P_ACO_2 = K \times \frac{\dot{V}_{CO_2}}{\dot{V}_A}$$

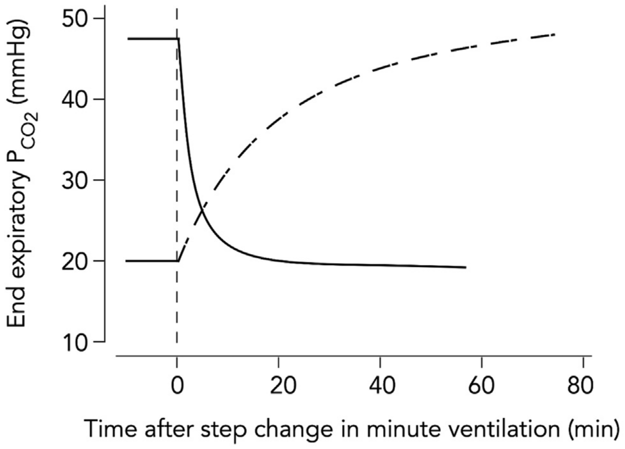

Fig. 6 Changes in P_ACO_2 (using end-expiratory CO_2 as a surrogate measure) with a step change in ventilation from 14 to 3.3 L/min (solid line) and conversely from 3.3 to 14 L/min (dashed line); P_aCO_2 follows a similar pattern. Note how much more quickly the P_ACO_2 reaches a new steady state when ventilation is increased compared with decreased because in the latter situation it takes time to build up the body stores of CO_2. For clarity the diagram illustrates a big change in ventilation, for a more realistic change the shift in partial pressure and the time course shorter. (Reproduced with permission from Lumb[21].)

where $\dot{V}_A$ refers to alveolar ventilation, the part of minute $\dot{V}_E$ that participates in gas exchange (explained further below), K is a constant (= 0.863 if P_ACO_2 in mm Hg, $\dot{V}_{CO_2}$ in mL STPD*/min, and $\dot{V}_A$ L BTPS*/min). For example, if $\dot{V}_A$ is reduced by 50% and $\dot{V}_{CO_2}$ remains unchanged, P_ACO_2 will double. This does not happen immediately, at first when $\dot{V}_A$ is reduced CO_2 *elimination* will be reduced to the same degree. The imbalance between unchanged CO_2 *production* at the cellular level but reduced elimination means that P_ACO_2 (and therefore P_aCO_2) will increase gradually until a new steady state between CO_2 production and elimination is reached at a higher P_ACO_2. Higher P_ACO_2 means that more CO_2 is eliminated per unit alveolar ventilation. Depending on gas exchange efficiency of an individual's lungs, it takes 10 to 20 minutes to reach this steady state, reflecting the time required for the body storage of CO_2 to build up to the new equilibrium (►**Fig. 6**). This time frame roughly applies to all sudden changes in $\dot{V}_A$ or $\dot{V}_{CO_2}$. Because the body stores of O_2 are much smaller than for CO_2, P_aO_2 reaches a steady state much faster after changes in $\dot{V}_A$, F_IO_2, or $\dot{V}_{O_2}$. If, instead, $\dot{V}_{O_2}$ and $\dot{V}_{CO_2}$ are increased but $\dot{V}_A$ remains unchanged, P_AO_2 and P_aO_2 will decrease and P_ACO_2 and P_aCO_2 increase. With unchanged $\dot{V}_A$ and decreases in $\dot{V}_{O_2}$ and $\dot{V}_{CO_2}$, the partial pressures change in the opposite directions. Because of the respiratory control system, which maintains a constant $\dot{V}_{CO_2}/\dot{V}_A$ ratio, this does normally not correspond to a situation in a spontaneously breathing subjects. It can however be observed, for example, in a patient who is receiving neuromuscular blockade on controlled mechanical ventilation and who has a significant increase or decrease in body temperature which corresponds to an increase or decrease in $\dot{V}_{O_2}$ and $\dot{V}_{CO_2}$. Hypoventilation is one example of how hypoxemia might occur without any lung pathology. If we calculate the $P_{A\text{-}a}O_2$ for this situation, the difference will be zero for the ideal lung model. Even in a healthy individual, $P_{A\text{-}a}O_2$ is somewhat greater than zero, but during hypoventilation not increased compared with a situation with normal $\dot{V}_A$. This differentiates hypoxemia caused by hypoventilation from hypoxemia due to $\dot{V}_A/\dot{Q}$ mismatch (see below).

Effect of Changes in F_IO_2 and P_IO_2

The first term of the alveolar gas equation states that P_IO_2, and therefore F_IO_2 and P_B, are determinants of P_AO_2. For example, an increase in F_IO_2 shifts the P_AO_2 versus $\dot{V}_A$ curve in ►**Fig. 5** upward. This corresponds to the clinical situation when administration of O_2 to a patient who is hypoventilating results in increased P_aO_2. Similarly, lower P_B at a high altitude moves this curve downward, illustrating the effect of altitude on P_AO_2. This demonstrates that although the fraction of O_2 in air is always 0.21, decreasing P_B causes a proportional decrease in P_IO_2. Although the response to high altitude might include hyperventilation, which increases P_aO_2, curves for different P_B illustrate that for a certain $\dot{V}_A$, P_AO_2 and therefore P_aO_2 are reduced with a lower P_B. Again, raising F_IO_2 corresponds to an upward shift of the P_AO_2 versus $\dot{V}_A$ curve, demonstrating that administration of supplemental O_2 is an additional strategy to mitigate the effect of high altitude on P_aO_2. Remember that it is P_B and F_IO_2 that determine P_IO_2. In summary, lower P_B results in lower P_AO_2 which might lead to hypoxemia even if the lung is normal, but this is influenced by any change in $\dot{V}_A$ and F_IO_2. If $P_{A\text{-}a}O_2$ is calculated for these situations, it would again be zero if the lung is without $\dot{V}_A/\dot{Q}$ mismatch and there is no diffusion limitation (discussed next).

Diffusion Limitation

So far, we have assumed equilibration between P_A and P_{ec} for both O_2 and CO_2, which is accurate for individuals with normal lungs in most situations. In contrast, diffusion limitation refers to a situation where P_{ec} fails to fully equilibrate with P_A. Fick's law of diffusion states that the rate of net transfer of a gas ($\dot{V}_{gas}$) across the alveolar-capillary membrane by diffusion is determined by molecular size, the difference in partial pressure across the membrane (the driving pressure for diffusion, ΔP), membrane area (A), membrane thickness (T), and the solubility of the gas in the membrane:

$$\dot{V}_{gas} = D \times \Delta P \times \frac{A}{T}$$

where D is a constant referring to properties of the gas and the membrane according to

---

* STPD, standard temperature and pressure dry (excluding any contribution water vapor to the measured volume); BTPS, body temperature and pressure saturated (saturated meaning 100% relative humidity). BTPS is used to relate, e.g., a tidal volume to the volume it would occupy in the lungs and airways. STPD is used to relate volume or flow to the quantitative (e.g., mmol) uptake or elimination of a gas.

$$D \propto \frac{S}{\sqrt{MV}}$$

S is the solubility of the gas in the membrane and MW is the molecular weight of the gas. The rate of uptake of O_2 from alveolar gas to blood per unit driving pressure (e.g., mL/min/mm Hg) is termed lung diffusing capacity for oxygen $D_{L_{O_2}}$.

$$D_{L_{O_2}} = \frac{\dot{V}_{O_2}}{\Delta P}$$

Here $\boldsymbol{\Delta}$P refers to the difference in PO_2 between alveolar gas and capillary plasma. Hemoglobin acts as an O_2 sink by rapidly binding the O_2 from the plasma, reducing PO_2, and increasing the driving pressure of O_2 from the alveolus to the blood. The pathway for oxygen includes not only the actual alveolar-capillary membrane but also the pathway through plasma to the erythrocytes. The chemical reaction when O_2 is bound to Hb takes time and this is also an important determinant for the rate of O_2 uptake. Roughton and Forster[7] showed that the resistance to diffusion of oxygen can be divided in two components in series so that

$$\frac{1}{D_L} = \frac{1}{D_M} + \frac{1}{\theta V_c}$$

D_M is the resistance to diffusion across the alveolar-capillary membrane and plasma to the erythrocytes, V_c is the blood volume in the lung capillaries, and $\boldsymbol{\theta}$ is a constant describing the amount of gas taken up by the hemoglobin per unit time and unit driving pressure. The equation takes this form because diffusing capacity is analogous to conductance and resistance is the reciprocal of conductance.

As stated above, one determinant of the diffusion capacity is the area available for gas exchange. Because gas exchange will only occur in perfused alveolar regions, the area depends on both lung volume and the distribution of blood within the lung capillaries. An increased number of alveoli that are either not ventilated or not perfused decreases diffusion capacity. From this, it follows that $\dot{V}_A/\dot{Q}$ mismatch might affect diffusion capacity, which means that whole lung decreased diffusion capacity does not require diffusion limitation, defined as failure of equilibration between P_A and P_{ec}. The multiple inert gas elimination method can be used to calculate the P_aO_2 expected with the observed degree of $\dot{V}_A/\dot{Q}$ mismatch.[8] The difference between the expected and measured P_aO_2 has been used an estimate of the real effect of diffusion limitation. Using this approach in patients with idiopathic pulmonary fibrosis, Agustí et al demonstrated that 20% of the hypoxemia observed at rest could be ascribed to diffusion limitation while the remainder was due to $\dot{V}_A/\dot{Q}$ mismatch.[8] With exercise, diffusion limitation caused 40% of the observed hypoxemia. This demonstrates that, although not dominant, the properties of the alveolar-capillary membrane might be an important determinant of diffusion capacity in patients with some lung diseases. The relationship between lung volume and the surface area available for gas exchange means that diffusion capacity is maximal at total lung capacity. In diseases that cause destruction of alveoli, e.g., emphysema, reduction of the area available for gas exchange is one cause of reduced diffusion capacity. In clinical medicine, measurements of diffusion capacity for carbon monoxide or nitric oxide are used to evaluate and monitor lung function. These methods have been discussed in detail in several excellent reviews.[9,10]

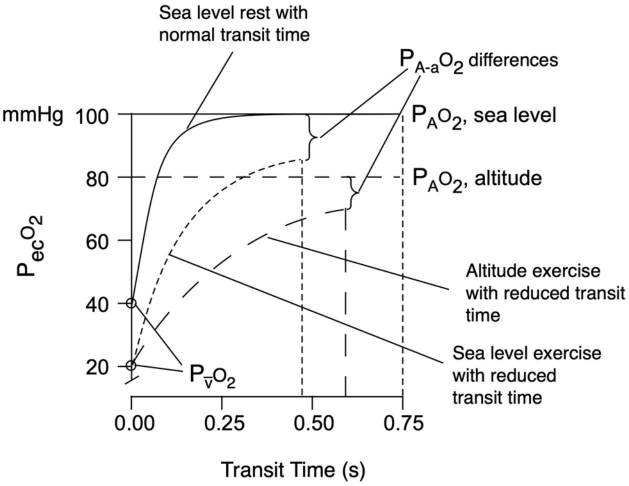

Fig. 7 Time course of capillary PO_2 as blood traverses the alveolar capillaries. At rest and sea level, there is more than enough time for the $P_{ec}O_2$ to equilibrate with the P_AO_2. With increased blood flow (decreased transit time) during exercise, there may not be enough time for the $P_{ec}O_2$ to equilibrate with the P_AO_2, i.e., diffusion limitation, resulting in an increased $P_{A\text{-}a}O_2$ difference. The lower $P_{\bar{v}}O_2$ during exercise means that more O_2 needs to be taken up by the blood to reach P_AO_2, higher altitude lowers P_AO_2 and hence the driving pressure for oxygen diffusion into the blood. Both these factors add to the tendency to diffusion limitation. Notations are explained in ►**Fig. 1**.

The solubility of CO_2 in water or tissue is approximately 30 times greater than for O_2 while the molecular weight of CO_2 is slightly greater than O_2, resulting in the resistance to diffusion across the membrane for CO_2 being roughly 20 times less than for O_2. The chemical reactions eliminating CO_2 from the blood limit the rate of CO_2 transfer from the blood to the alveolar gas so that the total resistance to diffusion between blood and alveolar gas has been estimated as roughly half of that for O_2. Diffusion limitation is therefore not of importance for the elimination of CO_2. It is also worth considering that even without equilibration between P_ACO_2 and $P_{ec}CO_2$, this would have little effect on P_aCO_2 due to the small difference between $P_{\bar{v}}CO_2$ and P_aCO_2.

►**Fig. 7** illustrates that the equilibration of $P_{ec}O_2$ with P_AO_2 depends on (1) the low resistance to diffusion with a rapid increase in $P_{ec}O_2$ to P_AO_2, (2) the transit time through the alveolar capillaries, and (3) the pressure difference between $P_{\bar{v}}O_2$ and P_AO_2, i.e., how much O_2 needs to diffuse across the alveolar-capillary membrane to reach equilibrium. Changes in these factors might result in diffusion limitation. In fact, significant hypoxemia caused by diffusion limitation is often the result of a combination of two or all three of these mechanisms. One example is increased resistance due to interstitial lung disease in combination with exercise, which decreases the transit time due to increased cardiac output and tends to reduce $P_{\bar{v}}O_2$, which in turn means that more O_2

must be taken up by the blood to reach a $P_{ec}O_2$ that equals P_AO_2. Hypoxemia due to diffusion limitation responds nicely to supplemental O_2. Of course, this does not correct the diffusion limitation, instead increased F_IO_2 raises both P_AO_2 and P_aO_2 although $P_{A\text{-}a}O_2$ remains increased (see legend to ►**Fig. 7**).

Effect of $\dot{V}_A/\dot{Q}$ Mismatch on Gas Exchange

So far, we have discussed gas exchange in a lung without $\dot{V}_A/\dot{Q}$ mismatch. This corresponds to a model with a single gas-exchanging unit, since with just one unit there can be no mismatch. The gas exchange capacity of the lung rests however on a design with a very large number of parallel gas-exchanging units. This design creates a very large surface area for the alveolar-capillary membrane encompassed within a comparably small volume. The drawback is that gas exchange efficiency decreases if each lung region does not receive equal proportions of the total blood flow and ventilation, i.e., if regional ventilation and perfusion do not match. Note that perfect matching does not require uniform distributions of regional ventilation and perfusion but it does require that regions that receive a lower fraction of total ventilation also receive an equally lower fraction of total blood flow, and that a region that receives a greater fraction of total blood flow also receives a greater fraction of total ventilation. Perfect matching thus means that the $\dot{V}_A/\dot{Q}$ ratio is uniform across all lung regions. Conversely, if the ratio varies between regions there is $\dot{V}_A/\dot{Q}$ mismatch, which causes P_aO_2 to be lower and P_aCO_2 to be higher than they would have been with perfect matching and other conditions unchanged. $\dot{V}_A$ and $\dot{Q}$ are usually of the same magnitude, approximately 5 L/min in a normal individual at rest. This means that the global $\dot{V}_A/\dot{Q}$ ratio is 1.0, and in the situation of perfect $\dot{V}_A/\dot{Q}$ match it means that the $\dot{V}_A/\dot{Q}$ ratio is 1.0 in all lung regions.

$\dot{V}_A/\dot{Q}$ Mismatch in the Normal Lung

Regional ventilation and perfusion are in fact not uniform in the normal lung. This has been ascribed to the influence of lung structure and the effect of gravity on regional lung compliance and vascular pressures.[11–15] The traditional model[14] is based on the observations that both regional ventilation and perfusion increase in the direction of gravity in upright subjects. The increase in perfusion is greater than for ventilation with $\dot{V}_A/\dot{Q}$ ratios, therefore decreasing down the lung. Higher resolution measurements used in animal studies have shown heterogeneous perfusion within isogravitational planes,[12] which cannot be explained by the influence of gravity. A fractal model has been suggested in which perfusion heterogeneity is explained by asymmetries in the vascular tree.[16,17] Regional ventilation and perfusion are influenced by lung volume, posture, and positive airway pressures among other factors.[12,13,18] Despite heterogeneous ventilation and perfusion, gas exchange is efficient due to the close matching of ventilation and perfusion, which has been explained by the shared influence of structure and gravity.[11] Even so, the matching is not perfect, $\dot{V}_A/\dot{Q}$ ratios, P_AO_2, and P_ACO_2 vary between regions (►**Fig. 8**) even in normal individuals.[11,19] In young normal individuals, ventilation and perfusion are mostly distributed to regions with $\dot{V}_A/\dot{Q}$ ratios between 0.3 and 2.0,[20] which corresponds to an approximate P_AO_2 range between 90 and 130 mm Hg.[19] With aging, the range of $\dot{V}_A/\dot{Q}$ ratios increases even in healthy

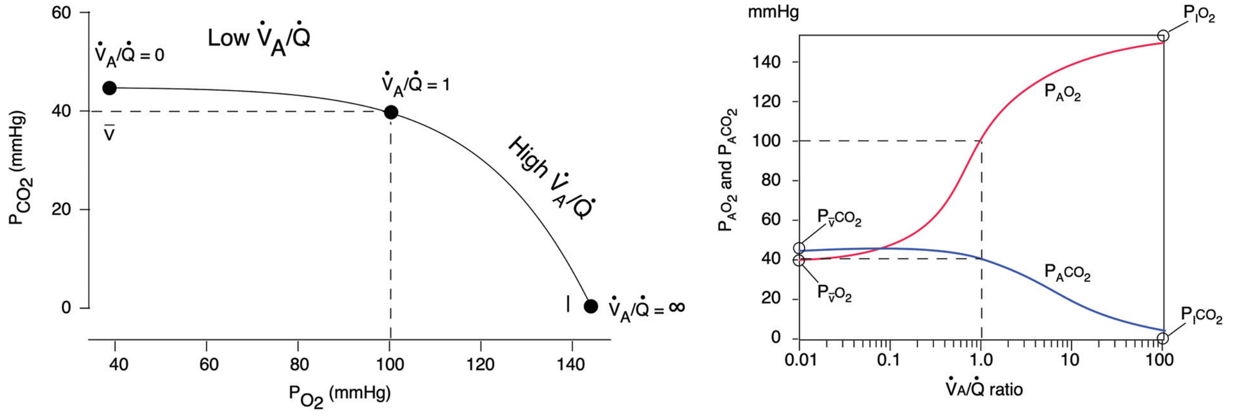

Fig. 8 Left: the classical O_2–CO_2 diagram,[41,47] showing the relationships between PO_2, PCO_2, and the $\dot{V}_A/\dot{Q}$ ratio. Right: a different representation of P_AO_2 and P_ACO_2 as determined by the $\dot{V}_A/\dot{Q}$ ratio. Both diagrams show the possible different combinations of alveolar PO_2 and PCO_2 and how these may vary across lung regions depending on their $\dot{V}_A/\dot{Q}$ ratio. Curves are constructed assuming normal values for P_IO_2, P_ICO_2 (the rightmost extremes, P_ICO_2 assumed to be zero), $P_{\bar{v}}O_2$, and $P_{\bar{v}}CO_2$(the leftmost extremes). These assumptions are not realistic for a whole lung because changes in P_aO_2 and P_aCO_2 will cause secondary changes in mixed venous values (►**Fig. 6** is more realistic in this regard), but the diagrams illustrate the influence of the $\dot{V}_A/\dot{Q}$ ratio on alveolar pressures for regional lung units in a situation when total ventilation to blood flow is sufficient to maintain normal mixed venous values. Other values for these parameters would reposition the extremes of the curves but the shape would remain similar. Starting at $\dot{V}_A/\dot{Q} = 1$, which also corresponds to the P_AO_2 given by the ideal alveolar gas equation (Box 1), moving left toward illustrates the effect of a decreasing $\dot{V}_A/\dot{Q}$ ratio on P_AO_2 and P_ACO_2. Perfusion in excess of ventilation results in a sharp decrease in P_AO_2 but much less increase in P_ACO_2. The extremes to the left correspond to a shunt ($\dot{V}_A/\dot{Q} = 0$) with alveolar PO_2 and PCO_2 identical to those in mixed venous blood. In contrast, $\dot{V}_A/\dot{Q} > 1$ results in an increase in PO_2 and a decrease in PCO_2, approaching the inspired values at the rightmost extremes, which correspond to a lung region with $\dot{V}_A/\dot{Q} = \infty$, i.e., alveolar dead space. Notations are explained in ►**Fig. 1**.

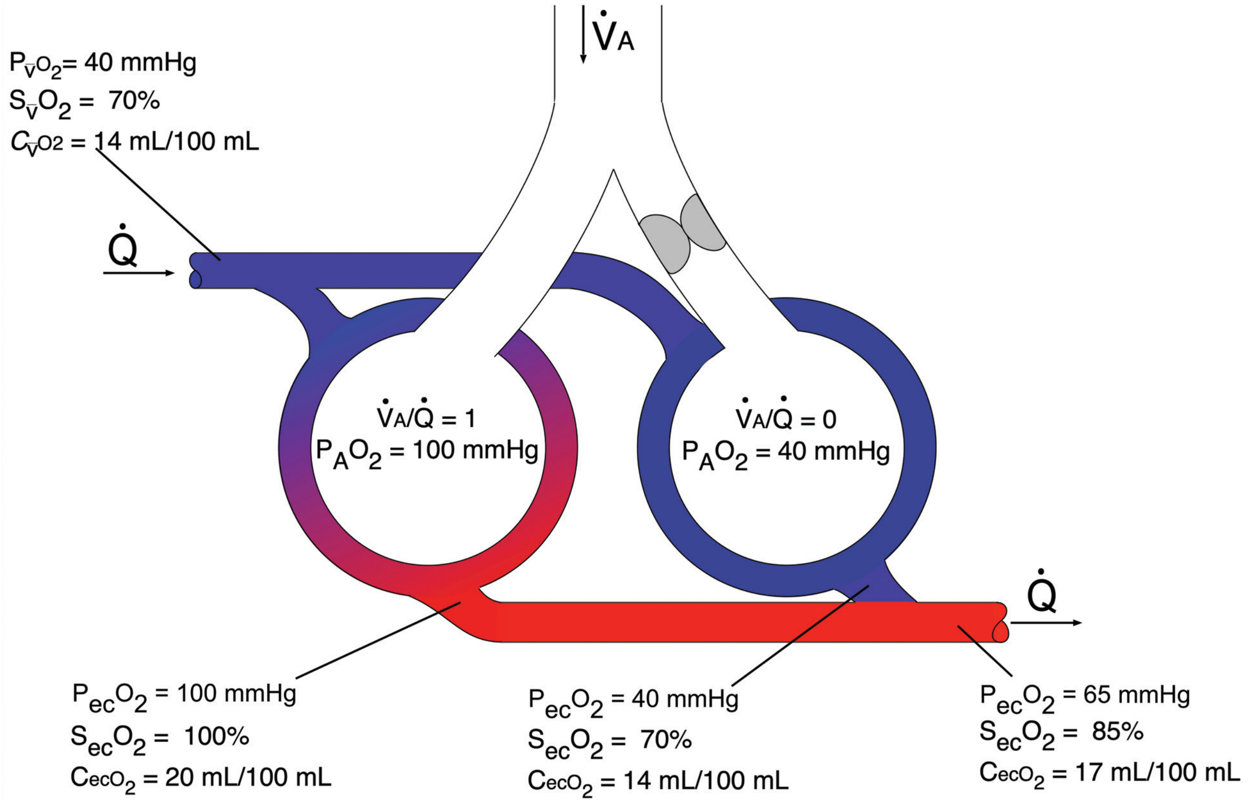

Fig. 9 Shunt illustrated by a lung model with two units, blood flow is equal for the two units but one is entirely without ventilation which constitutes a shunt, $\dot{V}_A/\dot{Q} = 0$. Because there is no gas exchange, the end-capillary partial pressures for the shunt equal those in mixed venous blood. C_aO_2 is the flow-weighted average of the content for blood from both units. The corresponding P_aO_2 is determined by the hemoglobin–oxygen dissociation curve, here calculated assuming a hemoglobin concentration of 15 g/dL. S_{ec}, end-capillary hemoglobin oxygen saturation; other notations are explained in ►**Fig. 1**.

individuals. For example, increasing airway closure causes reduced ventilation of dependent lung regions resulting in more perfusion being distributed to low $\dot{V}_A/\dot{Q}$ regions.[21,22] The result is that normal P_aO_2 decreases and normal $P_{A\text{-}a}O_2$ increases with advancing age.

Effect of Shunt on Gas Exchange

End-capillary blood from a lung region without ventilation ($\dot{V}_A/\dot{Q} = 0$) will have the same $P_{ec}O_2$ and $P_{ec}CO_2$ as mixed venous blood, which will decrease PO_2 of arterial blood (►**Fig. 9**). Quantitatively, the effect of blood from lung regions with different $\dot{V}_A/\dot{Q}$ ratios is determined by end-capillary blood O_2 content ($C_{ec}O_2$) rather than $P_{ec}O_2$. Arterial O_2 content (C_aO_2) is the flow-weighted average of blood from all lung regions (►**Fig. 9**). Shunt can be quantified as the fraction of total lung blood flow (Q_s/Q_t) that is distributed to nonventilated lung regions. The effect of shunt on P_aO_2 depends on this fraction and the O_2 content of mixed venous blood ($C_{\bar{v}}O_2$). For example, in a normal lung with $PecO_2 = 100$ mm Hg ($CecO_2 = 20.4$ mL/dL), a 20% shunt will reduce P_aO_2 to approximately 70 mm Hg ($CecO_2 = 19.3$ mL/dL) with a normal Hgb and $P_{\bar{v}}O_2 = 40$ mm Hg ($C_{\bar{v}}O_2 =$ 15 mL/dL). A $P_{\bar{v}}O_2$ of 27 mm Hg ($C_{\bar{v}}O_2 = 10$ mL/dL) would result in a PaO_2 of 55 (mm Hg). Thus, for a certain Q_s/Q_t, lower $C_{\bar{v}}O_2$ results in lower P_aO_2 and conversely higher $C_{\bar{v}}O_2$ results in higher P_aO_2. In the presence of a large shunt, P_aO_2 might improve with interventions that increase $C_{\bar{v}}O_2$, e.g., increasing cardiac output or hemoglobin concentration, or decreasing $\dot{V}_{O_2}$. However, it has been demonstrated that Q_s/Q_t may increase with increasing cardiac output, which will mitigate the benefit of increased blood flow.[23,24] Increased $P_{\bar{v}}O_2$ and pulmonary arterial pressure, counteracting hypoxic vasoconstriction, have been speculated to explain the effect of cardiac output on shunt.

With increasing Q_s/Q_t, raising F_IO_2 is progressively less effective in improving P_aO_2. An F_IO_2 of 1.0 has only a small effect on P_aO_2 if there is a large shunt fraction, which is illustrated by the iso-shunt diagram (►**Fig. 10**). The explanation for this is twofold, (1) increased F_IO_2 cannot improve P_AO_2 in unventilated regions and (2) little O_2 can be added to blood-perfusing regions with a normal, or increased, $\dot{V}_A/\dot{Q}$ ratio because the blood in these regions is already fully saturated with O_2. The effect of raised F_IO_2 is however different for regions with a $\dot{V}_A/\dot{Q}$ ratio that is low but >0, see below. An extrapulmonary right-to-left shunt has the same effect on P_aO_2 as an intrapulmonary shunt. In normal individuals, venous blood from bronchial and Thebesian veins is combined with arterial blood in an amount corresponding to a shunt of 2 to 3%.[21] This is one of the mechanisms causing the normal $P_{A\text{-}a}O_2$ difference to be greater than 0, the other being the small $\dot{V}_A/\dot{Q}$ mismatch in normal lungs. The effect of shunt on CO_2 elimination is discussed below.

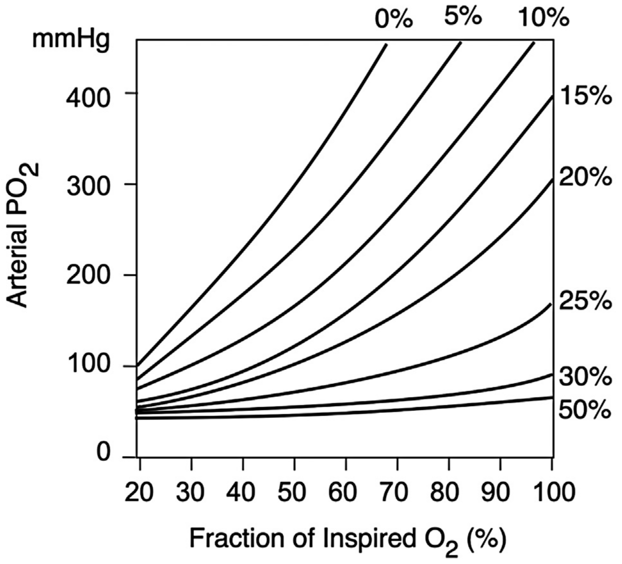

Fig. 10 The iso-shunt diagram which illustrates the theoretical relationship between F_IO_2 and P_aO_2 with shunt corresponding to different percentages of cardiac output. With no shunt, PaO_2 increases almost linearly with F_IO_2, with increasing shunt the response is increasingly less. That is, with a large shunt, increasing F_IO_2 has limited to almost no effect on P_aO_2. Modelling is based on an arterial-mixed venous oxygen content difference of 5 mL/dL and a hemoglobin concentration of 14 g/dL. (Modified from Benatar et al[48])

Effect of Low $\dot{V}_A/\dot{Q}$ Regions on Gas Exchange

Although shunt regions correspond to regions with the lowest possible $\dot{V}_A/\dot{Q}$ ratio, the term "low $\dot{V}_A/\dot{Q}$ region" often refers to regions with perfusion out of proportion to ventilation, but with $\dot{V}_A/\dot{Q} > 0$. ►**Fig. 8** shows that P_AO_2 and $P_{ec}O_2$ for these regions decrease progressively with lower $\dot{V}_A/\dot{Q}$ ratios. The effect on P_aO_2 is thus similar to that for a shunt, but weaker. Note that even a ratio of 0.5 results in substantially lower P_AO_2 than a ratio of 1.0, which emphasizes the effect of $\dot{V}_A/\dot{Q}$ mismatching on gas exchange efficiency. The effect on P_ACO_2 is less, which is clearly shown in ►**Fig. 8**. Note the part of the curve that corresponds to low $\dot{V}_A/\dot{Q}$ is almost horizontal and a substantial drop in P_AO_2 corresponds to a small increase in P_ACO_2. The reason for this is the much smaller difference between $P_{\bar{v}}CO_2$ and P_ACO_2 than between $P_{\bar{v}}O_2$ and P_AO_2; note that the extremes of the curves to the left correspond to $P_{\bar{v}}CO_2$ and $P_{\bar{v}}O_2$. Because low $\dot{V}_A/\dot{Q}$ regions are in fact ventilated, increasing F_IO_2 is comparatively effective in raising P_aO_2 (►**Fig. 5**). Consequently, low $\dot{V}_A/\dot{Q}$ cannot be the dominant cause of low P_aO_2 in a patient whose P_aO_2 does not increase significantly with the addition of supplemental O_2.

Effect of Increased Dead Space

Anatomical dead space is that part of each inspired tidal volume that is retained in the conducting airways and consequently fails to participate in gas exchange. This volume is approximately 150 mL (2–3 mL/kg predicted body weight) or 1/3 of a normal tidal volume.[21,25] The normal dead space fraction of the tidal volume is thus approximately 0.3. A lung region that is ventilated but lacks perfusion ($\dot{V}_A/\dot{Q} = \infty$) influences gas exchange in a way similar to the anatomical dead space and is therefore called alveolar dead space. The term "apparatus dead space" refers to the volume of any equipment, e.g., a face mask or tubing, that functions as an extension of the anatomical dead space. Total dead space (V_D) is the sum of anatomical dead space and any alveolar or apparatus dead space. Total dead space can be used to divide the minute ventilation (total volume expired per minute, $\dot{V}_E$) into one part that participates in gas exchange (alveolar ventilation, $\dot{V}_A$) and dead space ventilation ($\dot{V}_D$), which does not contribute to gas exchange. Thus

$$\dot{V}_A = \dot{V}_E - \dot{V}_D$$

which can be written as

$$\dot{V}_A = \dot{V}_E \times \left(1 - \frac{V_D}{V_T}\right)$$

where V_D/V_T is the total dead space as a fraction of the tidal volume. V_D/V_T therefore expresses the fraction of minute ventilation that does not contribute to gas exchange. Note that effective ventilation, and therefore CO_2 elimination, is determined by both $\dot{V}_E$ and V_D/V_T. For example, increased V_D/V_T means that greater $\dot{V}_E$ is necessary to maintain effective alveolar ventilation adequate for a normal P_aCO_2. It is important to understand that the control of breathing usually maintains P_aCO_2 at a constant level, the primary consequence of increased V_D/V_T is thus increased $\dot{V}_E$ and work of breathing. Increased V_D/V_T results in increased P_aCO_2 and decreased P_aO_2 when $\dot{V}_E$ is not sufficiently increased due to inability to do so or in a situation where $\dot{V}_E$ is not controlled by the respiratory center. This is illustrated by ►**Fig. 5**. Note that the horizontal axis shows $\dot{V}_A$, not $\dot{V}_E$, an increase in V_D/V_T with unchanged $\dot{V}_E$ corresponds to a shift to the left (decreased $\dot{V}_A$), and a subsequent increase in $\dot{V}_E$ (increasing $\dot{V}_A$ back to the original value) will result in a shift to the right, lowering P_aCO_2 back to the original level. Also note that if V_D/V_T increases from 0.3 to, for example, 0.6, $\dot{V}_A$ decreases from 4.2 to 2.4, which would have a large effect on P_AO_2 and P_ACO_2. Maintaining a normal P_aCO_2 in this situation would require an increase in $\dot{V}_E$ from 6 to 10.5 L/min.

Effect of Low $\dot{V}_A/\dot{Q}$ Regions on Gas Exchange

High $\dot{V}_A/\dot{Q}$ refers to regions that are overventilated in proportion to perfusion but not totally without blood flow. Ventilation in excess of perfusion influences gas exchange similarly to alveolar dead space. ►**Fig. 8** shows that a progressive increase in $\dot{V}_A/\dot{Q}$ ratio results in both P_AO_2 and P_ACO_2 moving toward P_IO_2 and P_ICO_2. Lower P_ACO_2 means that less CO_2 is removed by ventilation of a high $\dot{V}_A/\dot{Q}$ region than for a region with perfusion in proportion to ventilation. High $\dot{V}_A/\dot{Q}$ regions therefore mean that a greater $\dot{V}_E$ is needed to maintain adequate CO_2 elimination but, depending on the actual $\dot{V}_A/\dot{Q}$ ratio, the effect is less pronounced than for a region with $\dot{V}_A/\dot{Q} = \infty$. ►**Fig. 8** also shows that high $\dot{V}_A/\dot{Q}$ regions have a high P_AO_2 but for two reasons this has limited effect on P_aO_2. First, by definition the contribution from these regions to total blood flow is small. Second, even with a normal P_AO_2, $P_{ec}O_2$ corresponds to nearly complete oxygen saturation of hemoglobin and increased P_AO_2, therefore adds little oxygen content to the end-capillary blood (►**Fig. 4**). Hence high $\dot{V}_A/\dot{Q}$ regions cannot compensate for the hypoxemia caused by low $\dot{V}_A/\dot{Q}$ regions. In contrast, however, because the CO_2 dissociation curve is linear (does not plateau), increasing high $\dot{V}_A/\dot{Q}$ regions can compensate for the inefficient CO_2 removal of low $\dot{V}_A/\dot{Q}$ regions.

The Overall Effect of $\dot{V}_A/\dot{Q}$ Mismatch

We started with a discussion of gas exchange in a lung without $\dot{V}_A/\dot{Q}$ mismatch. When there is $\dot{V}_A/\dot{Q}$ mismatch and fixed minute ventilation, there must be regions with both low and high $\dot{V}_A/\dot{Q}$ ratios relative to total lung ventilation and blood flow. If one region receives perfusion in excess of ventilation, another region must be ventilated out of proportion to perfusion. The content of O_2 and CO_2 in arterial blood is the flow-weighted average of the content of end-capillary blood from all lung regions. Low $\dot{V}_A/\dot{Q}$ regions inherently make a larger contribution to the total flow, which cause P_aO_2 to be lower than it would have been in the absence of $\dot{V}_A/\dot{Q}$ mismatch. How much lower depends on the actual $\dot{V}_A/\dot{Q}$ ratio and the fraction of total blood flow that perfuses shunt and low $\dot{V}_A/\dot{Q}$ regions. This is the reason why low $\dot{V}_A/\dot{Q}$ regions increase the $P_{A\text{-}a}O_2$ difference even in the absence of diffusion limitation. Alveolar dead space and high $\dot{V}_A/\dot{Q}$ regions make a larger contribution to expired gas, which causes CO_2 content in expired gas to be lower, and CO_2 elimination less efficient than it would have been without $\dot{V}_A/\dot{Q}$ mismatch. It is more difficult to discern the effect of $\dot{V}_A/\dot{Q}$ mismatch on CO_2 elimination than the effect on P_aO_2. One reason is that the numerical changes in PCO_2 are much smaller than for PO_2, but more importantly the effect of inefficient CO_2 elimination on P_aCO_2 is often counteracted by an increase in $\dot{V}_E$ due to sensitivity of central chemoreceptors to any increase in PCO_2. This explains why patients with lung disease causing $\dot{V}_A/\dot{Q}$ mismatch so often have a low P_aO_2 in combination with a normal P_aCO_2. High $\dot{V}_A/\dot{Q}$ regions might thus be reflected by increased P_aCO_2, increased $\dot{V}_E$, or a combination of both. As explained above, high $\dot{V}_A/\dot{Q}$ regions have little effect on P_aO_2. In summary, $\dot{V}_A/\dot{Q}$ mismatch always results in reduced gas exchange efficiency. For a fixed F_IO_2 and $\dot{V}_E$, greater mismatch always results in lower P_aO_2 and higher P_aCO_2 but the effect on P_aCO_2 is in fact often attenuated or eliminated by an increase in $\dot{V}_E$

Quantitative Estimates of $\dot{V}_A/\dot{Q}$ Mismatch

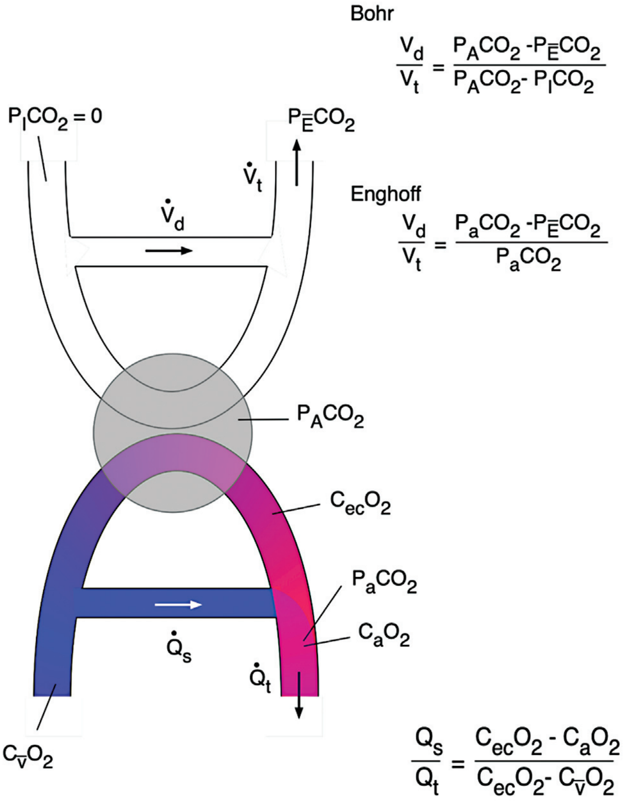
Bohr
$\frac{V_d}{V_t} = \frac{P_ACO_2 - P_{\bar{E}}CO_2}{P_ACO_2 - P_ICO_2}$
$P_ICO_2 = 0$
$P_{\bar{E}}CO_2$
$\dot{V}_t$
$\dot{V}_d$
Enghoff
$\frac{V_d}{V_t} = \frac{P_aCO_2 - P_{\bar{E}}CO_2}{P_aCO_2}$
P_ACO_2
$C_{ec}O_2$
P_aCO_2
C_aO_2
$\dot{Q}_s$
$\dot{Q}_t$
$C_{\bar{v}}O_2$
$\frac{Q_s}{Q_t} = \frac{C_{ec}O_2 - C_aO_2}{C_{ec}O_2 - C_{\bar{v}}O_2}$

Fig. 11 An illustration of Riley and Cournand's three compartment model.[4] The Bohr, Enghoff, and shunt equations are explained in Boxes 2 and 3. Note that with this model all gas exchange is assumed to occur in one compartment with perfect $\dot{V}_A/\dot{Q}$ match. Vd, dead space volume; Vt, tidal volume; Qs, shunt blood flow; Qt, total lung blood flow. The remaining notations are explained in ►**Fig. 1**.

The effect of $\dot{V}_A/\dot{Q}$ mismatch on O_2 and CO_2 exchange in the lung can be quantified using the "three-compartment model" suggested by Riley and Cournand[4] (►**Fig. 11**). In this model, the lungs consist of only three compartments with different $\dot{V}_A/\dot{Q}$ ratios. One compartment with uniform, ideal, $\dot{V}_A/\dot{Q}$ matching where all gas exchange occurs, one with blood flow and no ventilation ($\dot{V}_A/\dot{Q} = 0$, shunt), and one with ventilation without blood flow ($\dot{V}_A/\dot{Q} = \infty$, dead space) (►**Fig. 11**). The model estimates the effect of $\dot{V}_A/\dot{Q}$ mismatch on P_aO_2 as venous admixture, i.e., as the percentage of cardiac output directed to the compartment with $\dot{V}_A/\dot{Q} = 0$. The effect on CO_2 elimination is estimated as wasted ventilation, the fraction of $\dot{V}_E$ that ventilates the compartment with $\dot{V}_A/\dot{Q} = \infty$.

Venous Admixture

Venous admixture is calculated using the "shunt equation" (Box 2), which calculates the right-to-left shunt of mixed venous blood that would result in the observed P_aO_2. Remember that the model assumes only three $\dot{V}_A/\dot{Q}$ regions, and the venous admixture compartment must account for all of the observed hypoxemia, lumping together both low $\dot{V}_A/\dot{Q}$ and shunt. Hence the shunt equation provides an estimate of venous admixture even in the absence of true shunt (regions with $\dot{V}_A/\dot{Q} = 0$). Venous admixture is sometimes called physiologic shunt, which gives the name to the equation. We prefer the term venous admixture because this is not a measure of true shunt and also because "physiologic shunt" might be misunderstood as referring to the small amount of right-to-left shunt in normal individuals. Calculating venous admixture for values obtained when breathing 100% O_2 does provide an estimate of true shunt because in this situation the P_AO_2 in low $\dot{V}_A/\dot{Q}$ regions is so high that they have no effect on P_aO_2.[21] This approach to estimate true shunt is compromised by the tendency of breathing 100% O_2 to cause absorption atelectasis, which increases shunt. True shunt can also be measured using inert gases with very low solubility in blood.[19,26] The low solubility means that these gases are eliminated effectively even in regions with low $\dot{V}_A/\dot{Q}$ ratios. Any retention of the gas in arterial blood after intravenous administration is therefore an estimate of the fraction of lung blood flow through regions without ventilation. Off note, in contrast with venous admixture, using inert gas also excludes the effect of venous blood added to arterial blood by Thebesian and bronchial veins.

Wasted Ventilation

Wasted ventilation, also called physiological dead space, is calculated with the physiologic dead space equation (also known as the Bohr equation, ox 3), which estimates the total dead space ventilation, as a fraction of total $\dot{V}_E$, that would cause the observed efficiency of CO_2 elimination. Remember that this fraction is identical to the total dead space to tidal volume ratio (V_D/V_T) and that effective alveolar ventilation can be described as $\dot{V}_A = \dot{V}_E \times (1 - V_D/V_T)$. We prefer to use the term wasted ventilation as it better describes the meaning of this "as if" measure. In normal individuals wasted ventilation is close to the anatomical dead space fraction of tidal volume but the wasted ventilation includes the effect any apparatus or alveolar dead space and the effect of high $\dot{V}_A/\dot{Q}$ if present. Wasted ventilation can be viewed as a measure of the effect of $\dot{V}_A/\dot{Q}$ mismatch on the minute ventilation needed to maintain normal gas exchange. In a normal individual wasted ventilation, V_D/V_T is roughly 0.3, which means that a $\dot{V}_E = 7.5$ L/min results in $\dot{V}_A = 5.25$ L/min. In severe chronic lung disease, V_D/V_T might be in the order of 0.6[27] and in severe, acute respiratory failure, V_D/V_T might exceed 0.8, which means that a $\dot{V}_E > 25$ L/min is required to reach an effective alveolar ventilation of 5. 25 L/min.[28–30] Blood from shunt regions will have the same $P_{ec}CO_2$ as mixed venous blood which raises both P_aCO_2 and the calculated wasted ventilation, which has been coined shunt dead space.[24] The effect of shunt on the calculated wasted ventilation is an effect of using P_aCO_2 as a surrogate for P_ACO_2 according to the Enghoff modification of the Bohr equation (Box 3).[31] Although not an effect of alveolar dead space or high $\dot{V}_A/\dot{Q}$ regions, "shunt dead space" also represents impaired CO_2 elimination due to $\dot{V}_A/\dot{Q}$ mismatch.

Box 2: The shunt equation

$$\frac{Q_s}{Q_t} = \frac{C_{ec}O_2 - C_aO_2}{C_{ec}O_2 - C_{\bar{v}}O_2}$$

Box 2 Q_s/Q_t is the venous admixture quantified in the three-compartment model, expressed as the fraction of the total lung blood flow (Q_t, cardiac output) that reaches the systemic circulation without exchanging any gas. C_aO_2, $C_{\bar{v}}O_2$, and $C_{ec}O_2$ are the oxygen content of arterial, mixed venous, and end-capillary blood, respectively. C_aO_2 and $C_{\bar{v}}O_2$ are obtained from blood samples while $C_{ec}O_2$ is derived assuming that $P_{ec}O_2$ equals the P_AO_2 calculated by the ideal alveolar gas equation and the oxygen saturation of Hgb is obtained from the O_2–Hgb dissociation curve.

Box 3: Physiological dead space (Bohr–Enghoff) equation

$$\frac{V_D}{V_T} = \frac{P_aCO_2 - P_{\bar{E}}CO_2}{PaCO_2}$$

Box 3 V_D is the physiological dead space or wasted ventilation in the three-compartment model expressed as a fraction of tidal volume (V_T). The equation is derived from mass balance calculations which use the alveolar partial pressure of carbon dioxide (P_ACO_2), which is here replaced with P_aCO_2 (the Enghoff modification of the original Bohr equation[31]). In normal individuals the expired gas (P_ACO_2) from the gas-exchanging compartment is diluted by gas from the anatomical dead space which lowers the PCO_2 of mixed expired gas ($P_{\bar{E}}CO_2$), and in situations with additional alveolar or apparatus dead space $P_{\bar{E}}CO_2$, is reduced further. The difference between P_aCO_2 (the surrogate for P_aCO_2) and P_aCO_2 (divided by $P_{\bar{E}}CO_2$) is therefore proportional to the dead space fraction of total ventilation.

Hypoxic Pulmonary Vasoconstriction

Hypoxic pulmonary vasoconstriction (HPV) is precapillary vasoconstriction in lung regions with low P_AO_2, approximately <60 mm Hg. The effect is that blood flow is diverted from regions with low or no ventilation toward better ventilated regions, i.e., regions with a higher P_AO_2, which improves $\dot{V}_A/\dot{Q}$ matching and therefore P_aO_2. For example, in humans HPV reduces blood flow to atelectatic regions by up to 50%.[32,33] The beneficial effect on P_aO_2 from a similar reduction in shunt can be read from the iso-shunt diagram (►**Fig. 8**). One important aspect of HPV is that the beneficial effect on P_aO_2 decreases with the extent of the hypoxic lung regions, i.e., when the fraction of the lung vasculature with vasoconstriction increases. If we assume similarly low P_AO_2 and similar vasoconstriction in all regions (the latter is not necessarily true even with uniformly low P_AO_2), there will be no redistribution of blood flow. In this situation the consequence of HPV will be increased pulmonary vascular resistance (PVR) and increased pulmonary arterial pressure. There is therefore an inverse relationship between the proportion of lung that is hypoxic and the effect of HPV on P_aO_2; conversely, the effect of HPV on PVR is proportional to the amount of lung with low P_AO_2. Two examples of pathologic responses to global alveolar hypoxia are obstructive sleep apnea and living at high altitude, which can both present with right heart failure due to increased PVR. Animal and human experiments suggest that HPV does not contribute to the $\dot{V}_A/\dot{Q}$ matching in normal lungs.[34–36] The importance of HPV is greater in patients with disease causing regional alveolar hypoxia, in which HPV might improve P_aO_2 by up to 20 mm Hg.[37]

Assessment of Gas Exchange

Besides clinical evaluation and noninvasive measures such as pulse oximetry, assessment of gas exchange rests on arterial blood gases. In addition to venous admixture and wasted ventilation, which require measurements that often are difficult to obtain, several other indices can be used to quantify and differentiate between causes of gas exchange impairment. Here we will mention some of them briefly, further reading is found in a prior review.[38]

Using P_aO_2 to evaluate gas exchange is more difficult when F_IO_2 is raised above 0.21. The $P_{A\text{-}a}O_2$ difference is increased by shunt, $\dot{V}_A/\dot{Q}$ mismatch, and diffusion limitation but not when hypoxemia is caused by low P_IO_2 (e.g., at high altitude) or by hypoventilation. The difference found in normal individuals increases with age and is very dependent on F_IO_2. The P_aO_2/F_IO_2 ratio is often used in clinical medicine because it is easily calculated, and it is included in the definition of the adult respiratory distress syndrome.[39] Even with unchanged $\dot{V}_A/\dot{Q}$ mismatch the ratio varies with changes in F_IO_2 and also with changes in arterial-venous O_2 extraction.[40–42] It is therefore not a perfect index for comparing the impairment of arterial oxygenation between two situations.

When P_aCO_2 is used to evaluate CO_2 elimination efficiency, it is necessary to take the minute ventilation into account. End-tidal PCO_2 ($P_{ET}CO_2$) is the PCO_2 of expired gas at the end of expiration, in practice the highest value recorded at the proximal airways during a respiratory cycle. $P_{ET}CO_2$ is used as a measure of mixed alveolar gas and as a surrogate measurement of P_aCO_2. With perfect $\dot{V}_A/\dot{Q}$ matching the P_aCO_2 to $P_{ET}CO_2$ difference is expected to be zero and in normal individuals the difference is low (<4 mm Hg) but increases with increased wasted ventilation. $P_aCO_2 - P_{ET}CO_2$ is however also dependent on several other parameters which might lead to both over- and underestimation of wasted ventilation.[38,43] Although $P_{ET}CO_2$ provides an estimate of PCO_2 in mixed alveolar gas, it does not correspond to the PCO_2 of mixed expired gas ($P_{\bar{E}}CO_2$), which is used in the calculation of wasted ventilation. Due to the contribution of gas from the anatomical dead space ($PCO_2 \approx 0$), is much lower than $P_{ET}CO_2$. The ventilatory ratio (VR) is a relatively new measure that is calculated according to:

$$VR = \frac{\dot{V}_E \times P_aCO_2}{0.1 \times PBW \times 40}$$

where $0.1 \times PBW$ represents predicted $\dot{V}_E$ per kg predicted body weight and 40 is the normal P_aCO_2.[44] The ratio is therefore an aggregate estimate of CO_2 elimination efficiency that incorporates both minute ventilation and P_aCO_2. Remember that if $\dot{V}_A$ is halved, P_aCO_2 is expected to double. In theory this corresponds to an unchanged VR, i.e., it is consistent with unchanged CO_2 elimination efficiency, ignoring that doubled $\dot{V}_E$ might not equal doubled $\dot{V}_A$. VR is significantly influenced by $\dot{V}_{CO_2}$ and, similar to wasted ventilation, the effect of venous admixture on P_aCO_2, which hampers the use of VR to follow changes in dead space and high $\dot{V}_A/\dot{Q}$ regions.[45] VR has been reported for invasively ventilated patients with values from <1 to >5.[44,45]

Conclusion

Exchange of respiratory gases in the lung is facilitated by the large surface area over which blood and the alveolar space are in close proximity through the very thin membrane separating them. Variations in regional ventilation and perfusion that would make gas exchange less efficient are mitigated by the close matching of local perfusion and ventilation including by active matching of perfusion to ventilation through HPV. Venous admixture created by shunt and low $\dot{V}_A/\dot{Q}$ regions primarily causes hypoxemia while wasted ventilation due to dead space and high $\dot{V}_A/\dot{Q}$ regions results in inefficient ventilation and removal of CO_2. In comparison to an ideal situation with perfect match, $\dot{V}_A/\dot{Q}$ mismatch therefore leads to lower P_aO_2 and higher P_aCO_2 for a given minute ventilation, but the body responds by increasing minute ventilation to compensate for these cardinal signs of acute and chronic respiratory failure. Increased work of breathing is therefore a third, and sometimes the dominant, sign of acute and chronic respiratory failure.

Conflict of Interest
None declared.

References

1 Weibel ER, Federspiel WJ, Fryder-Doffey F, et al. Morphometric model for pulmonary diffusing capacity. I. Membrane diffusing capacity. Respir Physiol 1993;93(02):125–149

2 Weibel ER. What makes a good lung? Swiss Med Wkly 2009;139 (27–28):375–386

3 Gehr P, Bachofen M, Weibel ER. The normal human lung: ultrastructure and morphometric estimation of diffusion capacity. Respir Physiol 1978;32(02):121–140

4 Riley RL, Cournand A. Ideal alveolar air and the analysis of ventilation-perfusion relationships in the lungs. J Appl Physiol 1949;1(12):825–847

5 Cruickshank S, Hirschauer N. The alveolar gas equation. Contin Educ Anaesth Crit Care Pain 2004;4:24–27

6 Wang MC, Corbridge TC, McCrimmon DR, Walter JM. Teaching an intuitive derivation of the clinical alveolar equations: mass balance as a fundamental physiological principle. Adv Physiol Educ 2020;44(02):145–152

7 Roughton FJ, Forster RE. Relative importance of diffusion and chemical reaction rates in determining rate of exchange of gases in the human lung, with special reference to true diffusing capacity of pulmonary membrane and volume of blood in the lung capillaries. J Appl Physiol 1957;11(02):290–302

8 Agustí AG, Roca J, Gea J, Wagner PD, Xaubet A, Rodriguez-Roisin R. Mechanisms of gas-exchange impairment in idiopathic pulmonary fibrosis. Am Rev Respir Dis 1991;143(02):219–225

9 Hughes JM, Bates DV. Historical review: the carbon monoxide diffusing capacity (DLCO) and its membrane (DM) and red cell (Theta.Vc) components. Respir Physiol Neurobiol 2003;138(2–3):115–142

10 Hughes JM, Pride NB. In defence of the carbon monoxide transfer coefficient Kco (TL/VA). Eur Respir J 2001;17(02):168–174

11 Glenny RW. Determinants of regional ventilation and blood flow in the lung. Intensive Care Med 2009;35(11):1833–1842

12 Glenny RW, Lamm WJ, Albert RK, Robertson HT. Gravity is a minor determinant of pulmonary blood flow distribution. J Appl Physiol 1991;71(02):620–629

13 Glenny RW, Bernard S, Robertson HT, Hlastala MP. Gravity is an important but secondary determinant of regional pulmonary

blood flow in upright primates. J Appl Physiol 1999;86(02):623–632
14 West JB, Dollery CT, Naimark A. Distribution of blood flow in isolated lung; relation to vascular and alveolar pressures. J Appl Physiol 1964;19:713–724
15 Hlastala MP, Glenny RW. Vascular structure determines pulmonary blood flow distribution. News Physiol Sci 1999;14:182–186
16 Glenny RW, Polissar L, Robertson HT. Relative contribution of gravity to pulmonary perfusion heterogeneity. J Appl Physiol 1991;71(06):2449–2452
17 Glenny RW, Robertson HT. Fractal properties of pulmonary blood flow: characterization of spatial heterogeneity. J Appl Physiol 1990;69(02):532–545
18 Petersson J, Rohdin M, Sánchez-Crespo A, et al. Regional lung blood flow and ventilation in upright humans studied with quantitative SPECT. Respir Physiol Neurobiol 2009;166(01):54–60
19 Wagner PD, Laravuso RB, Uhl RR, West JB. Continuous distributions of ventilation-perfusion ratios in normal subjects breathing air and 100 per cent O2. J Clin Invest 1974;54(01):54–68
20 West JB. Regional differences in gas exchange in the lung of erect man. J Appl Physiol 1962;17:893–898
21 Lumb AB. Nunn's Applied Respiratory Physiology. 8th ed. Oxford: Elsevier; 2017
22 Janssens JP, Pache JC, Nicod LP. Physiological changes in respiratory function associated with ageing. Eur Respir J 1999;13(01):197–205
23 Dantzker DR, Lynch JP, Weg JG. Depression of cardiac output is a mechanism of shunt reduction in the therapy of acute respiratory failure. Chest 1980;77(05):636–642
24 Fredén F, Cigarini I, Mannting F, Hagberg A, Lemaire F, Hedenstierna G. Dependence of shunt on cardiac output in unilobar oleic acid edema. Distribution of ventilation and perfusion. Intensive Care Med 1993;19(04):185–190
25 Hedenstierna G, Sandhagen B. Assessing dead space. A meaningful variable? Minerva Anestesiol 2006;72(06):521–528
26 Pesenti A, Riboni A, Marcolin R, Gattinoni L. Venous admixture (Qva/Q) and true shunt (Qs/Qt) in ARF patients: effects of PEEP at constant FIO2. Intensive Care Med 1983;9(06):307–311
27 Chuang ML, Hsieh BY, Lin IF. Resting dead space fraction as related to clinical characteristics, lung function, and gas exchange in male patients with chronic obstructive pulmonary disease. Int J Gen Med 2021;14:169–177
28 Aubier M, Murciano D, Milic-Emili J, et al. Effects of the administration of O2 on ventilation and blood gases in patients with chronic obstructive pulmonary disease during acute respiratory failure. Am Rev Respir Dis 1980;122(05):747–754
29 Nuckton TJ, Alonso JA, Kallet RH, et al. Pulmonary dead-space fraction as a risk factor for death in the acute respiratory distress syndrome. N Engl J Med 2002;346(17):1281–1286
30 Kallet RH, Lipnick MS. End-tidal-to-arterial p_{co2} ratio as signifier for physiologic dead-space ratio and oxygenation dysfunction in acute respiratory distress syndrome. Respir Care 2021;66(02):263–268
31 Enghoff H. Volumen inefficax. Bemerkungen zur Frage des schädlichen Raumes. Upsala Lak Forhandl 1938;44:191–218
32 Morrell NW, Nijran KS, Biggs T, Seed WA. Magnitude and time course of acute hypoxic pulmonary vasoconstriction in man. Respir Physiol 1995;100(03):271–281
33 Morrell NW, Nijran KS, Biggs T, Seed WA. Regional matching of ventilation and perfusion during lobar bronchial occlusion in man. Clin Sci (Lond) 1995;88(02):179–184
34 Sylvester JT, Shimoda LA, Aaronson PI, Ward JP. Hypoxic pulmonary vasoconstriction. Physiol Rev 2012;92(01):367–520
35 Arai TJ, Henderson AC, Dubowitz DJ, et al. Hypoxic pulmonary vasoconstriction does not contribute to pulmonary blood flow heterogeneity in normoxia in normal supine humans. J Appl Physiol 2009;106(04):1057–1064
36 Frostell CG, Blomqvist H, Hedenstierna G, Lundberg J, Zapol WM. Inhaled nitric oxide selectively reverses human hypoxic pulmonary vasoconstriction without causing systemic vasodilation. Anesthesiology 1993;78(03):427–435
37 Naeije R, Brimioulle S. Physiology in medicine: importance of hypoxic pulmonary vasoconstriction in maintaining arterial oxygenation during acute respiratory failure. Crit Care 2001;5(02):67–71
38 Petersson J, Glenny RW. Gas exchange and ventilation-perfusion relationships in the lung. Eur Respir J 2014;44(04):1023–1041
39 Ranieri VM, Rubenfeld GD, Thompson BT, et al; ARDS Definition Task Force. Acute respiratory distress syndrome: the Berlin Definition. JAMA 2012;307(23):2526–2533
40 Wagner PD. The physiological basis of pulmonary gas exchange: implications for clinical interpretation of arterial blood gases. Eur Respir J 2015;45(01):227–243
41 Aboab J, Louis B, Jonson B, Brochard L. Relation between PaO2/FIO2 ratio and FIO2: a mathematical description. Intensive Care Med 2006;32(10):1494–1497
42 Gowda MS, Klocke RA. Variability of indices of hypoxemia in adult respiratory distress syndrome. Crit Care Med 1997;25(01):41–45
43 Kreit JW. Volume capnography in the intensive care unit: physiological principles, measurements, and calculations. Ann Am Thorac Soc 2019;16(03):291–300
44 Sinha P, Fauvel NJ, Singh S, Soni N. Ventilatory ratio: a simple bedside measure of ventilation. Br J Anaesth 2009;102(05):692–697
45 Maj R, Palermo P, Gattarello S, et al. Ventilatory ratio, dead space, and venous admixture in acute respiratory distress syndrome. Br J Anaesth 2023;130(03):360–367
46 Guntheroth WG, Luchtel DL, Kawabori I. Pulmonary microcirculation: tubules rather than sheet and post. J Appl Physiol 1982;53(02):510–515
47 Rahn H, Fenn WO. Graphical Analysis of the Respiratory Gas Exchange: The O2 CO2 Diagram. Bethseda, MD: American Physiological Society; 1955
48 Benatar SR, Hewlett AM, Nunn JF. The use of iso-shunt lines for control of oxygen therapy. Br J Anaesth 1973;45(07):711–718

Article published online: 2023-08-11

Blood Gas Transport: Carriage of Oxygen and Carbon Dioxide in Blood

Peter D. Wagner, MD[1]

[1] Department of Medicine, University of California San Diego, La Jolla, California

Address for correspondence Peter D. Wagner, MD, Department of Medicine, University of California San Diego, La Jolla, CA 92093 (e-mail: pdwagner@health.ucsd.edu).

Semin Respir Crit Care Med 2023;44:569–583.

Abstract

The ways in which oxygen (O_2) and carbon dioxide (CO_2) are carried in the blood are well known and well understood, with a plethora of textbooks, both general and lung specific, all presenting the topic in a very similar manner. This first of two companion chapters similarly summarizes this information. First, carriage of gases by physical solution is described, followed by discussion of O_2, carbon monoxide, and CO_2 transport in that order. However, what available texts have not emphasized is why knowing how gases are carried in blood matters, and the second, companion, chapter specifically addresses that critical aspect of gas exchange physiology. In fact, each of the chapters in this volume describes physiological behavior that depends more or less directly on the dissociation curves of O_2 and CO_2.

Keywords
- hemoglobin
- solubility
- partial pressure
- concentration
- dissociation curves
- O_2–CO_2 interactions

General Principles of Gas Carriage in Blood

There are many published descriptions of how oxygen (O_2) and carbon dioxide (CO_2) are carried in the blood. General textbooks of physiology[1–8] and smaller textbooks devoted to the respiratory system[9–13] are just some examples, and all address the topic in detail. The wording may differ across these texts, but the information remains the same because the field is well established. The present essay necessarily recapitulates these same details. A second, companion, chapter then moves beyond this presentation of facts to explain how the physics and chemistry of gas transport influence the principal functions that enable O_2 and CO_2 to move between the air and the mitochondria, as these gases negotiate the several diffusive and convective steps that constitute the gas transport system between the air and the tissues.[14] It is hoped that in this way, the reader will be better able to appreciate why the details of O_2 and CO_2 carriage in blood are physiologically and clinically important.

Partial Pressure and Concentration of a Gas in Blood

This chapter begins by describing how O_2 and CO_2 are carried in the blood. However, for this to make sense, it is essential to first understand the concepts of both partial pressure and concentration of a gas in both the gas phase (such as alveolar gas in the lungs) and in a liquid, be it water, blood, or some other liquid such as plasma. To facilitate this understanding, the discussion will begin with a benchtop experiment using an “inert” gas as the example. For gases transported in liquids, an inert gas is here defined as any gas transported only in physically dissolved form, that is, a gas that does not combine chemically with any other molecule in the liquid or transform chemically into another molecule or ion. Thus, “inert” here does not exclude any potential biological activity, as occurs for many anesthetic “inert” gases, which are carried in the blood only in physical solution but which have major central nervous system effects. While the same principles apply to gases that do undergo chemical binding or transformation (in particular, O_2 and CO_2), it is simpler to begin with an inert gas because of its single mode of transport in blood: physically dissolved.

Suppose we start the experiment with one closed syringe containing several milliliters of blood, and a second closed syringe of gas containing nitrogen spiked with an inert gas, which is completely absent from the syringe of blood. Suppose further that the syringes are kept at normal body temperature and atmospheric pressure. The benchtop

article published online
August 11, 2023

Issue Theme Pulmonary Physiology; Guest Editors: David A. Kaminsky, MD, Kathryn A. Hibbert, MD, and Andrew M. Luks, MD

Thieme Medical Publishers, Inc.,
333 Seventh Avenue, 18th Floor,
New York, NY 10001, USA

DOI https://doi.org/10.1055/s-0043-1771160.
ISSN 1069-3424.

experiment is simply to transfer the blood and gas volumes from the two separate syringes into a single closed syringe and gently agitate the combination for a few minutes. Molecules of the inert gas, initially present only in the gas phase, will start to move into the blood within the combined syringe. In this way, the inert gas concentration in the gas phase must fall while that in the blood phase must rise. However, being a closed syringe, all inert gas molecules remain trapped inside it, conserving inert gas mass within the syringe. After a few minutes of agitation, equilibrium will have been established between the blood and gas phases. Equilibrium means that there is no longer *net* movement of inert gas molecules between gas and blood phases within the syringe. Molecular diffusion of the inert gas will continue randomly both from gas to blood and blood to gas (fueled by thermally derived kinetic energy), but the concentrations of inert gas in each phase will remain constant over time, a concept known as dynamic equilibrium.

►**Fig. 1** shows this experiment schematically, with inert gas molecules as red dots, before combining the two syringes (panel A); immediately after combination but before any molecules have moved from gas to blood (panel B); and after equilibration (panels C and D). Panel C shows the molecular distribution at equilibrium between blood and gas phases for a *poorly* soluble gas, whereas panel D shows the molecular distribution at equilibrium between blood and gas phases for a *highly* soluble gas. The following discussion will refer only to panel C, but the reasoning applies to all inert gases, and thus, it works for panel D as well, although the numbers will be different due to the different solubility of the gas shown in D.

In the *gas* phase in panel C, the amounts of inert (and other) gases are quantified by two parameters: concentration (commonly expressed as mL gas/100 mL total gas volume), which in ►**Fig. 1** panel C will be called **C1**, and partial pressure in mm Hg, here called **P1** in the same panel. Note that **C1** and **P1** are related as follows:

$$P1 = C1 \times (PB - PH_2O) / 100 \qquad \textbf{Eq. 1}$$

where PB is atmospheric pressure and PH_2O is saturated water vapor pressure at body temperature, both in mm Hg. This equation is simply the expression of Dalton's Law of Partial Pressures.

In the blood, concentration and partial pressure are also used to quantify the amounts of gas present. Concentration in blood can also be expressed in the units of mL inert gas/100 mL, but of course it is now mL inert gas/100 mL blood, (termed **C2** for panel C). But what about partial pressure in blood? With reference to panel C, here is the fundamental point: the partial pressure of the gas in blood is defined as equal to the partial pressure in the gas phase above it (i.e., as in **Eq. 1**) when the blood–gas system is in (dynamic) equilibrium as defined above. Thus, partial pressure of the gas in the blood in panel C is **P1** mm Hg, the same as that in the gas phase.

The need to understand concentration and partial pressure in both gas and liquid (blood) cannot be overemphasized.

Physical Solubility of a Gas in Blood

Still confining discussion to an inert gas, Henry's Law states that the concentration of an inert gas in a liquid is equal to the product of the partial pressure of the gas in the liquid and the physical solubility of that gas in that liquid. If that solubility is termed **S** (commonly expressed as mL gas/100 mL liquid/mm Hg partial pressure), **C2** (in mL gas/100 mL liquid), and **P1** (mm Hg) are related as follows (Henry's Law):

$$\mathbf{C2 = S \times P1} \qquad \textbf{Eq. 2}$$

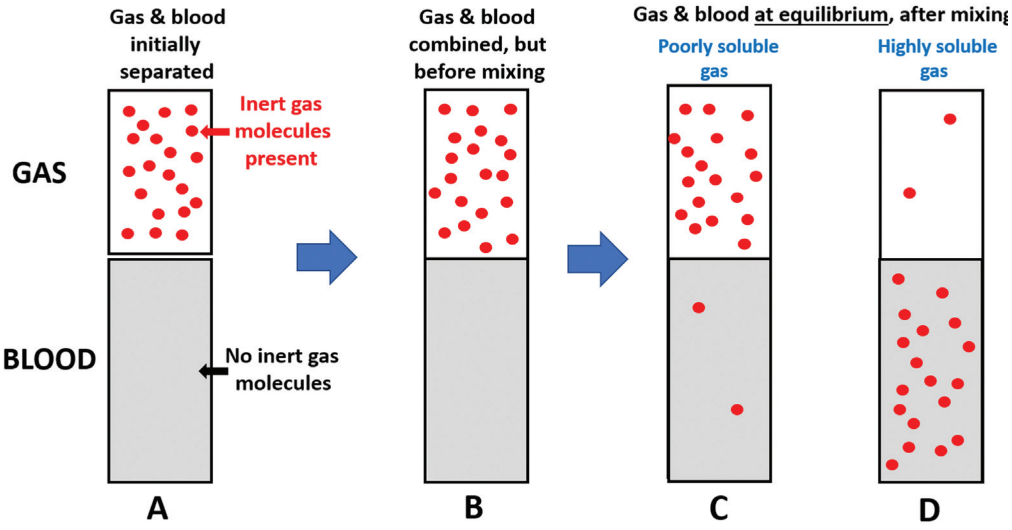
Gas & blood initially separated
GAS
BLOOD
Inert gas molecules present
No inert gas molecules
Gas & blood combined, but before mixing
Gas & blood at equilibrium, after mixing
Poorly soluble gas
Highly soluble gas
A
B
C
D

Fig. 1 Benchtop experiment to understand the concepts of gas concentration and gas partial pressure in both the gas and liquid (blood) phases. Moving from left to right (**A–D**), the panels show the sequence of gas molecular movement from gas to blood until equilibrium is reached. Panels C and D differ only in the solubility of the gas considered (poorly soluble in C; highly soluble in D).

This means that for an inert gas in blood, its concentration is proportional to its partial pressure, with the slope of the relationship between **C2** and **P1** representing its solubility, **S**.

Combining **Eqs. 1** and **2** results in this:

$$\mathbf{C2} = \mathbf{S} \times \mathbf{C1} \times (PB - PH_2O) / 100$$

which can be rearranged as follows:

$$\mathbf{C2/C1} = \mathbf{S} \times (PB - PH_2O) / 100$$

At sea level, **PB** averages 760 mm Hg and $\mathbf{PH_2O}$ 47 mm Hg (at 37°C) so that the term $\mathbf{(PB - PH_2O)/100}$ becomes a constant, 7.13. The product of 7.13 and **S** is commonly referred to as the blood:gas partition coefficient and is traditionally denoted by the Greek symbol **λ**.

Thus, the equation can be simplified to this:

$$\mathbf{C2/C1} = 7.13 \times \mathbf{S} = \boldsymbol{\lambda} \qquad \mathbf{Eq.\ 3}$$

Eq. 3 is important to understand:

- First, the blood:gas partition coefficient (**λ**) of an inert gas is the dimensionless ratio of its concentration in the blood (**C2**) to that in the gas (**C1**) *with which it is in equilibrium.*
- Second, the blood:gas partition coefficient is numerically equal to 7.13 × its solubility, **S** (when PB = 760 mm Hg and $PH_2O = 47$ mm Hg and **S** is expressed in mL gas/100 mL blood/mm Hg).

Returning to ►**Fig. 1**, 20 molecules in total are shown in each of the four panels (i.e., mass is conserved across all panels). Panel C shows how the equilibrium distribution of inert gas molecules might appear for a *poorly* soluble gas. Only 2 of 20 molecules have dissolved in the blood, leaving 18 remaining in the gas. The (dimensionless) partition coefficient (assuming equal gas and blood volumes for simplicity), is therefore 2/18, or 0.11, and the solubility is 0.11/7.13, or 0.016 mL gas/100 mL blood/mm Hg. In panel D, 18 of the 20 molecules have dissolved in the blood at equilibrium, leaving just 2 in the gas phase. This yields a partition coefficient of 18/2 or 9 for this much more soluble gas, whose solubility comes to 9/7.13 or 1.26 mL gas/100 mL blood/mm Hg.

As this chapter moves to a discussion of O_2 and CO_2 carriage in blood, the importance of the preceding analysis will become apparent as a foundation for understanding the more complex transport of O_2 and CO_2 in blood. The greater complexity stems from the fact that both gases undergo chemical reactions with other molecules in the blood as well as physically dissolving just as inert gases discussed above.

Oxygen Carriage in Blood

O_2 is carried in the blood simultaneously in two forms: as physically dissolved molecules (just as described above for inert gases) and as molecules bound to hemoglobin (Hb) within the red blood cells. In a blood sample taken from an artery (or vein), these two forms are considered to be in equilibrium with each other as defined in reference to ►**Fig. 1** above.

Oxygen Transport by Physical Solution

The solubility of O_2 in blood at normal body temperature is usually given as 0.003 mL/100 mL blood/mm Hg partial pressure of O_2 (PO_2).[15] It will be a little lower if body temperature increases, and a little higher if body temperature falls, but in the narrow, survivable range of temperatures encountered in humans, this variation can be ignored.

O_2 of course reaches the organs and tissues via the arterial blood stream. Arterial PO_2 in a normal young subject at rest is about 90 to 100 mm Hg breathing air at sea level. Thus, using **Eq. 2**, the amount of O_2 physically dissolved in the arterial blood is 0.003 × 100, or 0.3, mL O_2/100 mL blood (►**Fig. 2**). This comes to 3 mL/L blood. At rest, total systemic arterial blood flow (i.e., cardiac output) is about 6 L/min in a normal resting young subject. This means that 3 × 6, or 18, mL O_2 is delivered to the entire body per minute in physically dissolved form. At rest, the body consumes about 300 mL/min O_2, so it is clear that physically dissolved O_2 cannot come close to supporting the metabolic need for O_2: 18 mL/min is just 6% of 300 mL/min. Said differently, resting cardiac output would need to reach 100 L/min for physically dissolved O_2 to just supply resting metabolic needs.

During peak exercise, when cardiac output may reach 24 L/min and O_2 consumption rises to 4 L/min (or more) in the same healthy young subject, the amount of physically dissolved O_2 delivered to the tissues is 3 × 24 or 72 mL/min. This is just 2% of the 4 L/min O_2 needed. Cardiac output would have to reach over 1,300 L/min to supply the tissues with O_2 if the gas were transported only as physically dissolved. Clearly, transporting O_2 in physically dissolved form in blood is woefully insufficient as a means of providing the tissues with adequate O_2.

However, when 100% O_2 is breathed, as commonly occurs in critically ill patients in intensive care, physically dissolved O_2

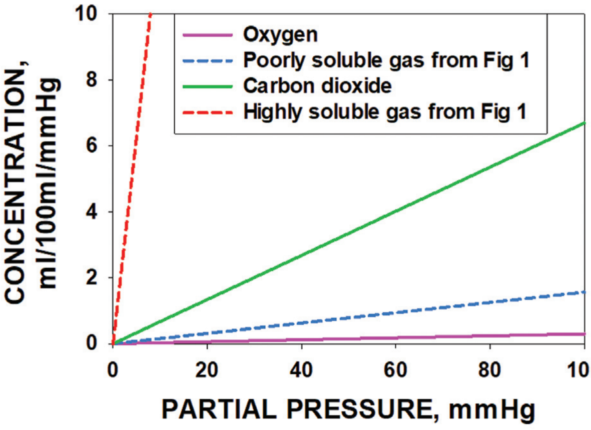

Fig. 2 Henry's Law for gases physically dissolved in a liquid. There is a linear relationship between concentration and partial pressure, the slope of which defines physical solubility. Four examples are shown: O_2 in pink; poorly soluble gas in ►**Fig. 1C** in blue (dashed line); CO_2 in green; highly soluble gas in ►**Fig. 1D** in red (dashed line). Solubility of CO_2 is more than 20 times that of O_2 in plasma/water. CO_2, carbon dioxide; O_2, oxygen.

contributes a greater share of O_2 delivered to the tissues. In a normal subject breathing 100% O_2 at sea level, with no alveolar nitrogen present, arterial PO_2 should, under ideal measurement conditions, reach about 650 mm Hg, and from **Eq. 2**, this means that 20 mL O_2 is present dissolved in every liter blood. With the same 6 L/min cardiac output, 120 mL of physically dissolved O_2 reaches the tissues/minute. This is about 40% of resting O_2 consumption. However, a critically ill patient would like to exhibit a lower arterial PO_2, and the contribution of physically dissolved O_2 to tissue O_2 delivery will be accordingly less, whereas metabolic rate may be raised from fever or other factors. For example, a critically ill patient breathing O_2-enriched gas who has an arterial PO_2 of 200 mm Hg, cardiac output elevated at 8 L/min and O_2 consumption increased to 600 mL/min will have 48 mL/min O_2 reaching the tissues in dissolved form (which is quite a bit higher than the above normal subject breathing room air), but this is still just 8% of metabolic need in this particular example.

Hyperbaric O_2 is used in certain clinical therapies, especially for postdiving decompression sickness, for carbon monoxide (CO) toxicity and for skin wound healing. By calculation, 2.3 atmospheres of pure O_2 would just suffice to fully support resting metabolic rate by physically dissolved O_2 transport in a subject with normal lungs: This atmospheric pressure equates to 2.3 × 760, or 1,748 mm Hg. Inspired PO_2 would then be about 1,700 mm Hg (after subtracting water vapor pressure of 47 mm Hg), and alveolar PO_2 would be slightly less at about 1,660 mm Hg (due to the presence of CO_2 at about 40 mm Hg). If arterial PO_2 were then also 1,660 mm Hg, arterial blood would carry 50 mL O_2/L, supplying the tissues with 300 mL O_2/min (cardiac output 6 L/min), just enough to support metabolism, assuming all the O_2 delivered could be extracted from the blood.

Oxygen Transport by Binding to Hemoglobin

Overview

As is well known, Hb has evolved as the primary method for carrying O_2 in the blood. The above normal subject at rest with an arterial PO_2 of 100 mm Hg and normal [Hb] will carry about 20 mL O_2 bound to Hb per 100 mL arterial blood (see below). With the same 6 L/min cardiac output, this means that 1,200 mL O_2 are delivered to the tissues each minute, well in excess of the resting metabolic requirement of 300 mL/min, and some 70-fold more than available by dissolved O_2 alone. During peak exercise, using the same example as above, 4,800 mL O_2 are delivered to the tissues/min (if cardiac output is 24 L/min and arterial $[O_2]$ remains at 20 mL O_2/100 mL blood), which exceeds the 4,000 mL/min metabolic need for O_2. This 4,800 mL/min is also about 70 times that available from dissolved O_2.

Clearly, Hb binding of O_2 is essential as the principal mechanism for cellular access to O_2. The Hb molecule is one of the most well studied in biology. The current chapter is not the platform to review the biochemistry of Hb but rather is intended to focus on the physiology of O_2 (and CO_2) transport. Therefore, the biochemical elements of Hb will be minimally discussed, and the reader interested in the biochemistry and genetics of Hb should seek texts that focus on those aspects. Hemoglobin, as its name proclaims, is a molecule consisting of a heme group bound to globin proteins. The globin of normal adult Hb (i.e., Hb A) has two alpha chains, each consisting of 141 amino acids, and two beta chains, each consisting of 146 amino acids, per molecule, and these four subunits form the scaffolding that holds a heme complex, which is a porphyrin ring containing Fe ions that are the (reversible) binding sites for O_2. Although there are several types of Hb, and many variants, the most commonly accepted formula appears to be $C_{2932}H_{4724}N_{828}O_{840}S_8Fe_4$ resulting in a computed molar mass of 65, 495 g/mol. Importantly, only Fe^{++} and not Fe^{+++} can bind O_2.

Each Hb molecule can bind four O_2 molecules, so each mole of Hb can bind 4 moles of O_2. Avogadro's Law describes the volume of a gas per mole under specified temperature and pressure: 22.7 L at "STPD" (standard temperature and pressure) conditions (dry; i.e., 760 mm Hg and 273°C without water vapor present). From this volume and the molar mass, given as 65,495 g/mol, it becomes apparent that 1 mole of Hb, or 65,495g can bind 4 × 22.7 L of O_2 STPD. This comes to 1.39 mL O_2/g Hb. It is important to understand that 1.39 mL O_2/g Hb is the amount of O_2 present when every O_2 binding site is occupied: That is, when Hb is said to be fully saturated with O_2.

It is interesting that the value of this important "constant" is not universally agreed to. Commonly, one will see 1.34 used rather than 1.39. It is unclear why such a range of values appears in the literature, but there may be two reasons: First, some of the Hb is bound by CO from inhaling air containing small amounts of CO from fossil fuel combustion. In addition, smoking tobacco produces CO, which is inhaled and binds to Hb in the blood. Since CO binds to heme groups far more tightly than does O_2, any CO present reduces the availability of heme for binding O_2. Second, some of the heme groups contain Fe ions in the oxidized (Fe^{+++}) state, producing a form of Hb that is termed methemoglobin. Since Fe^{+++} cannot bind O_2, any such heme groups are unavailable for O_2 transport. Together, these phenomena effectively reduce the constant to less than 1.39. It seems that the exact value will vary among individuals according to their CO exposure and methemoglobin levels.

It is also well known that Hb is not distributed uniformly in the blood. Rather, all of the Hb is confined within red blood cells, whose volume is normally 40 to 45% of the blood. The remaining 55 to 60% of the blood is Hb-free plasma. In sum, the red cells carry O_2 bound to Hb and also in physical solution, whereas the plasma carries O_2 only in physical solution. This nonuniformity has the potential for transient disequilibrium in PO_2 between plasma and the red cell interior. This is because O_2 diffusing from the alveolar gas into the pulmonary capillaries must first dissolve in (and diffuse through) the plasma before further diffusing into the red blood cell to combine with Hb. Such disequilibrium may exist during the short time (~0.75 s at rest) a red cell spends in the pulmonary capillaries loading O_2. This also occurs in the tissue capillaries as O_2 diffuses out of the red cells, through the plasma and finally out of the capillaries to reach the tissue mitochondria. However, with circulation times of around 1 minute to travel from lung to tissues and back to the lungs, such transient disequilibria are generally considered to be of little practical consequence for O_2 transport.

The Oxygen–Hemoglobin Dissociation Curve

Recall that ►**Fig. 2** shows the relationship between concentration and PO_2 present in blood only in physical solution. The amount of Hb-bound O_2 in the blood is described by the same parameters: concentration of O_2 in mL O_2/100 mL blood and PO_2 in blood in mm Hg. Therefore, it is possible to plot Hb-bound O_2 concentration and partial pressure on the same graph as that for dissolved O_2.

In so doing, it is important to realize that the total O_2 *concentration* in the blood is the *sum* of the physically dissolved and Hb-bound components; however, the PO_2 in the blood remains defined as that of a gas phase with which the blood is in equilibrium, which as mentioned above develops very quickly as O_2 is added to capillary blood (lungs) or removed from capillary blood (tissues). Said differently, there is but one PO_2 in any given blood sample despite the O_2 being carried in two distinct forms. There will be equilibrium between Hb-bound and physically dissolved O_2 molecules inside and outside the red cell, meaning that there is no net movement of O_2 molecules from dissolved to Hb-bound or vice versa, except as stated during the very short time of active loading/unloading, which we can neglect in this discussion. *Therefore, the same PO_2 exists in plasma as inside the red cells*, even though the O_2 concentrations are hugely different (much higher inside the red cell because of Hb).

We may now consider the relationship between O_2 concentration and O_2 partial pressure in a blood sample. Recall that the physically dissolved component obeys Henry's Law such that the concentration of dissolved O_2 is a linear and proportional function of the partial pressure (►**Fig. 2**).

The relationship between Hb-bound O_2 concentration and O_2 partial pressure is commonly called the oxygen–hemoglobin (O_2Hb) dissociation curve, but it could equally be called the O_2Hb association curve: O_2 molecules bind to Hb while in the pulmonary capillaries (association) and leave Hb in the tissue capillaries (dissociation). The first question might be whether this relationship is also a straight line, just one of hugely greater slope (because 70 times more O_2 is carried by Hb than by physical solution)? The answer is no, the relationship is nonlinear. It is steeper at low PO_2 and less steep as PO_2 increases. Eventually, when PO_2 is high enough that every heme binding site contains four O_2 molecules, there can be no further increase in Hb-bound O_2 concentration no matter how high the PO_2 goes, and the relationship must therefore become a horizontal one. In practice, about 97 to 98% of heme binding sites are occupied with O_2 molecules at a normal arterial blood PO_2 of 90 to 100 mm Hg, and $>$ 99% are occupied with O_2 molecules above a blood PO_2 of 200 mm Hg, which is that seen at roughly 30% inspired O_2 concentration in a normal lung.

Even so, the relationship is more than just a straight line of positive slope below this 200 mm Hg PO_2 coupled to a horizontal line above 200 mm Hg. The binding of four O_2 molecules to each heme molecule makes for a complex relationship, but insight can be had from examining the dissociation curve for myoglobin, which binds only a single O_2 molecule, not 4, making its O_2 binding less complex to consider than with Hb. When the myoglobin concentration/partial pressure relationship is examined, it turns out to follow a hyperbolic trajectory. This comports with Michaelis–Menten kinetics showing that simple chemical reactions often follow a hyperbolic pathway when plotted as we do for O_2 using concentration versus partial pressure. Is the O_2Hb dissociation curve also a simple hyperbola? The answer is no. The reason has to do with the fact that each heme molecule binds four O_2 molecules. It turns out that for O_2 to bind to the first of the four heme O_2 binding sites, it takes a higher PO_2 than for the next O_2 molecule to bind to the second site. The third and fourth O_2 molecules bind even more easily. This means that the O_2Hb dissociation curve at very low PO_2 has a somewhat shallow slope, which increases markedly as PO_2 is raised and subsequent heme sites become O_2-occupied. The behavior of increasing ease in binding the second, third, and fourth O_2 molecules is called "cooperativity" and the interested reader should seek biochemical texts to better understand the biochemical basis of this behavior. However, remember that the O_2Hb dissociation curve must eventually become flat at high PO_2 values when all binding sites become O_2-occupied.

Cooperativity is considered to happen through a conformational change in the O_2 binding site with heme, making that site more accessible to additional O_2 molecules after the first O_2 molecule has bound. It can be thought of as four people passing sequentially through an initially closed doorway. The first person has to do work to open the door, creating conformational change, to allow them to squeeze through, so that the second person has less work to do to get through because the first person has already opened the door. The result of this cooperativity is a dissociation curve that is even more nonlinear than a simple hyperbola. It is sigmoid (meaning that it has a shallow slope at low PO_2, which steepens as PO_2 rises, and then flattens again at higher PO_2). Several different mathematical expressions have been developed over the years to describe the O_2Hb dissociation curve. The Hill equation[16] is perhaps the most famous and is presented immediately below.

The Oxygen–Hemoglobin Dissociation Curve as a Function of Oxygen Saturation

The Hill equation brings in the concept of O_2 saturation of Hb, which is nothing more than the percentage (or fraction, whichever is preferred) of the total number of heme binding sites available to bind O_2 in the sample at hand that are actually occupied by O_2 molecules. Recall that if the blood PO_2 is 100 mm Hg (as for normal arterial blood), saturation is 97 to 98% (0.97 or 0.98 as a fraction). Thus, at this PO_2, 97 to 98% of heme binding sites are occupied with O_2. Normal mixed venous blood (in the pulmonary artery) has a PO_2 of around 40 mm Hg (at rest), which corresponds to a saturation fraction of about 0.75, meaning that 75% of the heme binding sites remain occupied with O_2 even after the tissues have taken all the O_2 they need.

The Hill equation looks like this:

$$O_2\ \text{saturation} = PO_2^{n} / [PO_2^{n} + P_{50}^{n}] \qquad \textbf{Eq. 4}$$

This gives saturation as a fraction, not a %. More importantly saturation is defined by the PO_2 of the blood sample plus two parameters, **n** and $\mathbf{P_{50}}$, where **n** is called the Hill coefficient and carries a value of about 2.7 for normal Hb. Note that were $\mathbf{n} = 1$, the Hill equation elegantly simplifies to a hyperbola, matching the myoglobin dissociation curve profile. As the value of **n** increases, the dissociation curve becomes more and more sigmoid in shape, which reflects increasing cooperativity in the binding of O_2 to Hb. In **Eq. 4**, $\mathbf{P_{50}}$ is the PO_2 when 50% of heme binding sites are occupied with O_2, and in normal adult subjects, $\mathbf{P_{50}}$ is commonly stated to average about 27 mm Hg under standard conditions (760 mm Hg barometric pressure, 37°C temperature, and partial pressure of CO_2 [PCO_2] 40 mm Hg). While this value is remarkably invariant across the normal population, such that values less than 26 or more than 28 mm Hg are rarely encountered, genetic variants in Hb (of which there are many) can result in very different values for $\mathbf{P_{50}}$ and thus the conformation of the dissociation curve and how much O_2 can bind to Hb at a given PO_2. The standard O_2Hb dissociation curve for Hb A derived from the Hill equation is depicted in ►**Fig. 3** where O_2 saturation is plotted as a function of PO_2.

In utero, normal fetal Hb (Hb F) has a lower $\mathbf{P_{50}}$ than normal Hb A due to the presence of alternate globin chains. Hb F has two alpha and two gamma amino acid subunits. The $\mathbf{P_{50}}$ of Hb F is about 19 mm Hg.[17] Over the weeks and months after birth, Hb F levels fall and are replaced by Hb A. ►**Fig. 4** compares the dissociation curves for Hb A and Hb F based on the Hill equation and the $\mathbf{P_{50}}$ values stated above (19 mm Hg [fetal]; 27 mm Hg [adult]). At first sight, it might seem that a $\mathbf{P_{50}}$ of 19 mm Hg (Hb F) would not result in very different O_2 binding metrics than when $\mathbf{P_{50}}$ is 27 mm Hg (Hb A), but ►**Fig. 4** shows that this small difference in $\mathbf{P_{50}}$ has a large influence on O_2 saturation, especially at the low PO_2 values to which the fetus is exposed in utero. For example, at 27 mm Hg PO_2, saturation of Hb A is about 0.5, whereas that for Hb F is almost 0.75, which means 50% more O_2 is carried by fetal than Hb A at this PO_2, making more O_2 available to fetal tissues despite its relatively low PO_2 environment.

The Oxygen–Hemoglobin Dissociation Curve as a Function of Oxygen Concentration

Plotting the dissociation curve as O_2 saturation versus PO_2 (as in ►**Figs. 3** and **4**) means that it will look similar no matter the actual [Hb] and total O_2 concentration. It also ignores the O_2 carried in physical solution, so it is not an accurate depiction of the overall relationship between O_2 concentration and partial pressure.

The O_2Hb dissociation curve is therefore also presented as O_2 concentration (mL/100 mL blood) versus PO_2 (mm Hg), where two subjects with different [Hb] will appear to have quite different dissociation curves even when **n** and $\mathbf{P_{50}}$ are the same. To do this requires converting O_2

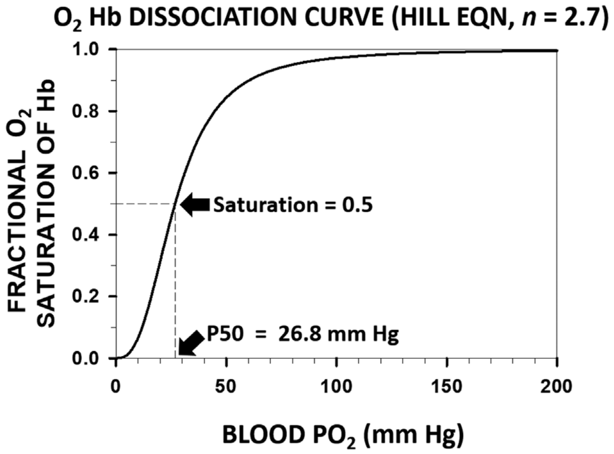

Fig. 3 The O_2Hb equilibrium dissociation curve displayed as O_2 saturation as a function of PO_2. P_{50} (about 27 mm Hg in normal blood) occurs when 50% of the heme binding sites for O_2 are occupied with O_2 and is indicated. This example was drawn using the Hill equation (see text). O_2, oxygen; O_2Hb, oxygen–hemoglobin; P_{50}, PO_2 when 50% of heme binding sites are occupied with O_2; PO_2, partial pressure of O_2.

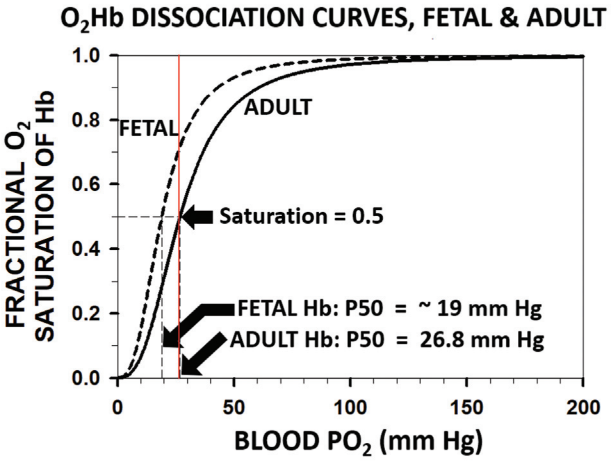

Fig. 4 Comparison of the dissociation curves for fetal and adult Hb. Fetal Hb is left-shifted with P_{50} about 8 mm Hg lower than for adult Hb. The solid red vertical line shows that O_2 saturation at a PO_2 of 27 mm Hg would be about 70% for fetal Hb but only 50% for adult Hb. This large increase clearly enhances O_2 availability for the fetus, which is helpful because the uterine environment results in much lower arterial PO_2 than in the adult. Hb, hemoglobin; O_2, oxygen; P_{50}, PO_2 when 50% of heme binding sites are occupied with O_2; PO_2, partial pressure of O_2.

saturation to O_2 concentration ($[O_2]$), and the following equation does this:

$$[O_2] = 1.39 \times [Hb] \times \text{fractional } O_2 \text{ saturation} \qquad \textbf{Eq. 5}$$

The number 1.39 was derived earlier as the number of mL that 1 g of Hb can carry when fully saturated with O_2; [Hb] is the concentration of Hb in g/100 mL; fractional O_2 saturation is the fraction of available heme binding sites actually occupied by O_2. The units of $[O_2]$ are therefore mL O_2/100 mL blood. The point is that two subjects with the same O_2 saturation may have very different blood O_2 concentrations simply because of [Hb] differences.

Eq. 5 does not, however, include the contribution of physically dissolved O_2 to total O_2 concentration and must be expanded using Henry's Law (**Eq. 2**) to add dissolved O_2:

$$[O_2] = 1.39 \times [Hb] \times \text{fractional } O_2 \text{ saturation} + 0.003 \times PO_2 \qquad \textbf{Eq. 6}$$

►**Fig. 5A** shows the O_2 dissociation curve for a subject with normal [Hb], Hill coefficient (**n**) and $\mathbf{P_{50}}$, plotted as concentration versus partial pressure. Bot the Hb-bound and dissolved components are shown (dashed lines) separately along with their sum, total O_2 concentration (solid line). It is clear that Hb-bound O_2 is by far the major carrier mechanism under normal sea-level conditions. ►**Fig. 5B** compares the dissociation curves for two subjects, one with normal [Hb] and one with anemia ([Hb] = 8 g/100 mL). While these two subjects might show identical dissociation curves when using O_2 saturation on the ordinate as in ►**Fig. 3**, the influence of the differences in [Hb] on O_2 concentration are apparent, as expected from **Eq. 6**.

The importance of showing the dissociation curves as in ►**Fig. 5** becomes clear when comparing the normal and anemic subjects in terms of their "operating points": the PO_2 and $[O_2]$ in both arterial and venous blood under resting conditions. This is shown in ►**Fig. 6**. Both subjects are presumed to have normal lungs and thus the same arterial PO_2 (solid red circles). As also shown in ►**Fig. 5**, the arterial $[O_2]$ is much lower in the anemic subject at the same arterial PO_2 due to lower [Hb]. If one assumes the same metabolic rate and cardiac output in the two subjects, their arteriovenous $[O_2]$ differences will be the same as shown (about 5 mL O_2/100 mL blood). Thus, the normal subject still has about 15 mL O_2/100 mL "in reserve" in the venous blood. However, the anemic subject has only about 6 mL O_2/100 mL in their venous blood, and venous PO_2 is considerably lower at approximately 30 mm Hg in the anemic subject than the normal subject ($PO_2 \sim 40$ mm Hg). This means a much lower "O_2 reserve." This may not matter at rest, when O_2 supply remains in excess of metabolic need despite anemia. However, the significance of this "reserve" is in exercise when, compared to rest, much more O_2 is required to be extracted from the blood and delivered to the tissues to sustain that exercise. Supposing venous PO_2 fell to the same value of 20 mm Hg, the arteriovenous $[O_2]$ difference in the anemic subject could not be much more than half of that in the normal subject, as depicted in ►**Fig. 7**. Coupled with likely similar peak cardiac output, the anemic subject cannot

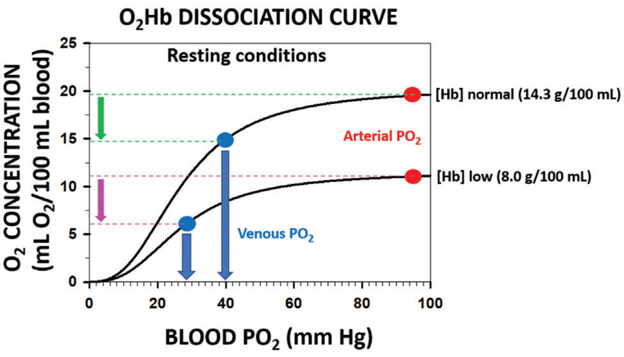

Fig. 6 Consequences of the [Hb] differences in Fig. 5 on arterial and venous O_2 concentration and PO_2. Arterial PO_2 is the same for both Hb levels (red circles), but with assumed similar arteriovenous $[O_2]$ differences of 5 mL O_2/100 mL, it is evident how venous $[O_2]$ and PO_2 must differ between the two curves. A low [Hb] leads to a lower venous PO_2 and $[O_2]$, which if severe enough, puts the tissues at risk of insufficient O_2 supply, especially during exercise. Hb, hemoglobin; O_2, oxygen; PO_2, partial pressure of O_2.

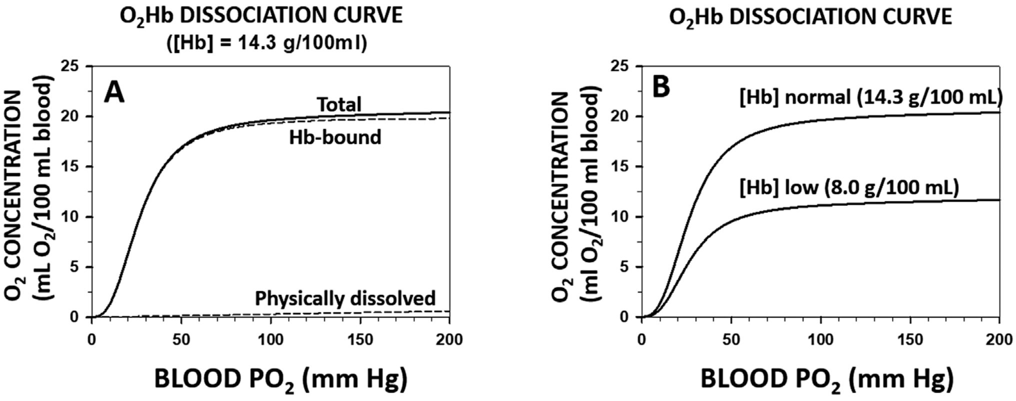

Fig. 5 Panel A: the O_2Hb dissociation curve displayed as the sum of Hb-bound O_2 and physically dissolved O_2 (uppermost solid curve) as well as its two separate components (Hb-bound and physically dissolved, dashed lines). Panel B: Illustration of how the O_2Hb dissociation curve depends on Hb concentration. Hb, hemoglobin; O_2, oxygen; O_2Hb, oxygen–hemoglobin; PO_2, partial pressure of O_2.

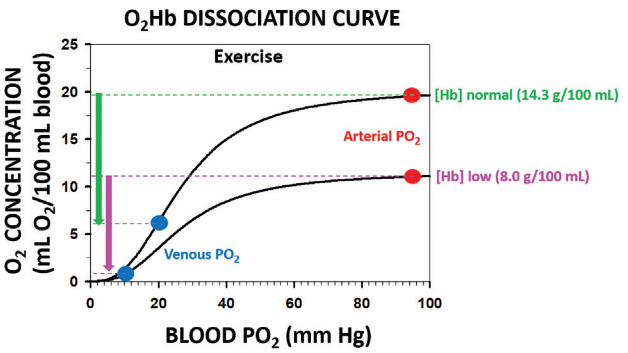

Fig. 7 Extension of Fig. 6 to show how exercise when [Hb] is reduced compromises O_2 availability to the tissues, which will reduce exercise capacity, increasingly so as [Hb] falls lower. Hb, hemoglobin; O_2, oxygen; O_2Hb, oxygen–hemoglobin; PO_2, partial pressure of O_2.

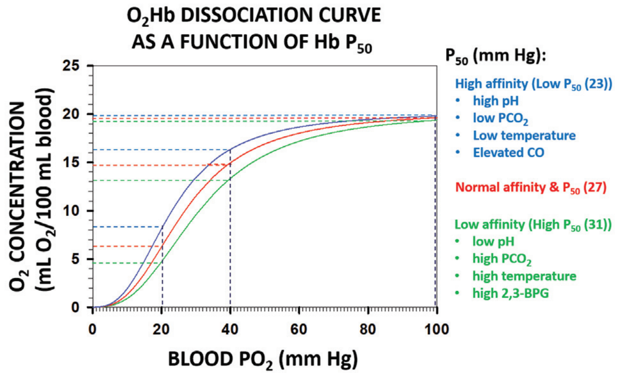

Fig. 8 Factors that affect Hb P_{50}, and the consequences for O_2 concentration in blood indicated by the various dashed lines. Three PO_2 points are exemplified: (A) 100 mm Hg corresponding to normal arterial PO_2, where P_{50} differences have little effect on [O_2]; (B) 40 mm Hg, corresponding to normal resting venous PO_2; and (C) 20 mm Hg, corresponding to venous PO_2 during exercise. As the dissociation curves steepen, changes in P_{50} increasingly affect [O_2] at a given PO_2. 2,3-BPG, 2,3-Bisphosphoglycerate; CO, carbon monoxide; Hb, hemoglobin; O_2, oxygen; O_2Hb, oxygen–hemoglobin; P_{50}, PO_2 when 50% of heme binding sites are occupied with O_2; PCO_2, partial pressure of carbon dioxide; PO_2, partial pressure of O_2.

provide the tissues with more than about half of the O_2 per minute as could the normal subject, considerably limiting endurance exercise capacity.

Factors Affecting the Oxygen–Hemoglobin Dissociation Curve

►**Figs. 5**–**7** show that there is no single O_2Hb dissociation curve, even considering only population differences in [Hb]. There are several other factors that alter the relationship between O_2 concentration and PO_2 in the blood at a given [Hb]. These are well known and include:

- pH.
- PCO_2.
- Blood temperature.
- 2,3-Bisphosphoglycerate (2,3-BPG) - also known as 2,3-Diphosphoglycerate.
- CO.

Each has a different mechanism for affecting the dissociation curve, but they all have a common outcome, i.e., altering the affinity of Hb for O_2. All five factors can act simultaneously and independently as their values change from one condition to another, with the net effect on affinity reflecting the sum of their separate effects. Depending on how pH, PCO_2, and blood temperature change directionally from normal, affinity of Hb for O_2 may increase or decrease. Decreases in affinity result from a reduced pH, increased PCO_2, and increased blood temperature. Increases in affinity result from an increased pH, decreased PCO_2, and decreased blood temperature.

The role of 2,3-BPG was defined by Benesch and Benesch in 1967.[18] Elevated 2,3-BPG levels (normally present in the red cell at about 5 mmol/L) decrease Hb affinity for O_2. 2,3-BPG increases in concentration when [Hb] is reduced as in anemia and, separately, at high altitude and in chronic lung disease when arterial PO_2 is reduced. Conversely, 2,3-BPG is depleted in stored bank blood, so that after blood transfusion the O_2Hb dissociation curve will be left-shifted until 2,3-BPG levels rise again. CO, normally present in only very small amounts throughout the body, increases Hb affinity for O_2[19] This is especially important in CO poisoning.

This plethora of factors affecting the dissociation seems overwhelming but can be handled fairly simply when it is realized that all of the factors and their effects can be thought of as shifting the dissociation curve (►**Fig. 3**) rightward or leftward. In concept, this means that changes in affinity can be understood as if $\mathbf{P_{50}}$ were altered, no matter which of the five named factors is in play. This is shown in ►**Fig. 8**. When the dissociation shifts rightward from its normal position (higher $\mathbf{P_{50}}$, reduced affinity, red to green in ►**Fig. 8**), O_2 saturation is lower at a given PO_2; when the dissociation curve shifts leftward (lower $\mathbf{P_{50}}$, increased affinity, red to blue in ►**Fig. 8**), O_2 saturation is higher at a given PO_2. This is true no matter which one or more of the above factors is at play.

Effects of Temperature, pH, and Partial Pressure of Carbon Dioxide on the Oxygen–Hemoglobin Dissociation Curve

►**Fig. 9** shows how temperature, pH, and PCO_2 individually shift the dissociation curve, based on calculations using digital algorithms published by Kelman several decades ago.[20–22] Both temperature and pH have significant effects on O_2 binding as the figure shows. While it is accepted that changes in PCO_2 will also shift the O_2Hb dissociation curve as stated, ►**Fig. 9** shows that there is little effect of PCO_2 itself (when pH remains constant), and that most of the effects of changes in PCO_2 come through the associated changes in pH, which in turn result from CO_2 in blood forming carbonic acid, which then dissociates into protons and bicarbonate ions, as described in more detail below. In other words, as PCO_2 increases, pH falls (and vice versa) and it is this pH change that causes most of the rightward shift from PCO_2.

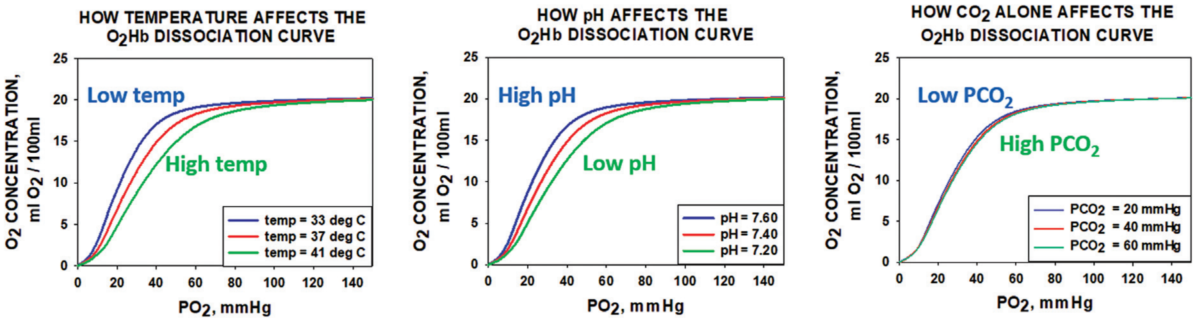

Fig. 9 Effects of individual factors affecting the O_2Hb dissociation curve (temperature, pH and PCO_2 respectively, left to right). PCO_2 effects are those occurring when pH is held constant and are minimal. In vivo, a change in PCO_2 will cause an immediate change in pH which will have a larger effect as implied by the center panel. O_2, oxygen; O_2Hb, oxygen–hemoglobin; PCO_2, partial pressure of carbon dioxide; PO_2, partial pressure of O_2.

It is usually stated that a rightward shift impairs O_2 loading in the lung capillaries (which is then reflected in arterial blood) because at a given PO_2 there is less O_2 bound to Hb. In corresponding fashion, a leftward shift enhances O_2 loading in the lung capillaries, because at a given PO_2 there is more O_2 bound to Hb.

Similarly, it is also reasoned that a rightward shift enhances O_2 unloading in the tissue capillaries because at a given PO_2 there is less O_2 bound to Hb, allowing more O_2 release to the tissues at any PO_2. In corresponding fashion, a leftward shift impairs O_2 unloading in the tissue capillaries, because at a given PO_2, more O_2 remains bound to Hb and not released to the tissues. What this means is that a shift in either direction from a change in Hb P_{50} results in opposing effects on O_2 transport that offset each other, such that no net improvement or reduction in O_2 transport may occur.

Under resting conditions sufficient O_2 is available to the tissues that the consequences of shifts in the O_2Hb dissociation curve are of little importance to tissue O_2 availability (recall that 1,200 mL/min O_2 are normally delivered to the tissues while only 300 mL/min are needed to support metabolism). There is thus a large excess in available O_2, and any impairment in loading or unloading from dissociation curve shifts is easily accommodated by this four-fold excess.

However, during heavy exercise, especially under hypoxic conditions, the consequences can be significant. Exercise (1) increases muscle vascular PCO_2 because of higher CO_2 production; (2) reduces muscle vascular pH both because of that higher PCO_2 and because of lactate efflux into the blood; and (3) increases muscle vascular temperature due to the high metabolic rate. As a result, the O_2Hb dissociation curve rapidly and transiently shifts rightward within the muscle blood vessels, enhancing O_2 unloading from the muscle microvascular blood. When that warm, acidic, and hypercarbic venous blood returns to the pulmonary capillaries, the dissociation curve rapidly shifts leftward as (1) lung capillary PCO_2 falls and pH rises; (2) vascular temperature cools a little due to fresh air being inhaled at high rates. The leftward shift enhances O_2 loading into the pulmonary capillaries. Thus, the normal physiological responses to exercise lead to constant oscillation the P_{50} of the blood in the lungs and tissues, favoring both O_2 loading in the lungs and unloading at the muscles, allowing for greater O_2 availability and exercise capacity than if those shifts did not occur.

Effects of 2,3-Bisphosphoglycerate on the Oxygen–Hemoglobin Dissociation Curve

While 2,3-BPG clearly affects Hb affinity for O_2, an important question is whether the increased 2,3-BPG seen at high altitude, causing a rightward shift of the dissociation curve, has any *net* effect on peak exercise O_2 availability, or not. The higher 2,3-BPG will act to shift the dissociation curve rightward in both the lung and muscle blood. This will enhance O_2 unloading in the exercising muscles, but it will also impair loading of O_2 into the pulmonary capillaries. Which wins out? In silico simulation[23] shows the muscle extraction benefit is almost exactly balanced by the pulmonary loading impairment such that there is no significant net change in O_2 availability to the muscles or enhancement of exercise capacity from the higher 2,3-BPG.

This is consistent with experimental data from measurements made at sea level and then in a hypobaric chamber after gradual "ascent" to 25,000 ft.[24] There was an increase in 2,3-BPG of 2.1 mmol/L and in Hb P_{50} of 4.9 mm Hg, with calculations suggesting that this increase in P_{50} had no net effect on exercise capacity at altitude. However, a definitive experiment to acutely alter 2,3-BPG and observe the effects on exercise capacity in man does not seem currently possible.

Effects of Carbon Monoxide on the Oxygen–Hemoglobin Dissociation Curve

CO is especially problematic for tissue O_2 availability. This molecule binds competitively to the same Fe^{++} sites in heme as does O_2, but with about 200 to 270 times the affinity compared with O_2. The carbon monoxide–hemoglobin (COHb) dissociation curve has the same shape as the O_2Hb dissociation curve, but with a P_{50} some 200 to 270 times lower than the 27 mm Hg P_{50} of O_2. This means COHb P_{50} is only about 0.1 mm Hg, such that half of all Hb binding sites will be unavailable to O_2 should blood PCO be just 0.1 mm Hg. This commonly happens in CO poisoning and is a major reason for the lethality of CO.

There is, however, an additional problem contributing to the lethality of CO in that its presence on Hb raises the affinity of the remaining non-CO bound heme sites for O_2. This affords little benefit in raising $[O_2]$ in arterial blood because the O_2Hb dissociation curve is almost insensitive to P_{50} when PO_2 is normal at 100 mm Hg and is already almost fully saturated (►**Fig. 8**). The main effect of the higher affinity is to impair tissue unloading of O_2, because at a given venous PO_2, O_2 saturation remains higher than normal and less O_2 is released to supply the tissues. With reference to ►**Fig. 8**, this leftward shift of the O_2Hb curve demands a fall in venous PO_2 to achieve adequate unloading of O_2 for metabolic sufficiency. However, the low venous PO_2 implies reduced upstream tissue capillary PO_2, which reduces the rate of O_2 movement by diffusion from the blood vessels to the mitochondria. If tissue vascular PO_2 falls too drastically, diffusive transport of O_2 may be insufficient to support normal metabolic rate. Combined with the occupation of Hb binding sites by CO reducing arterial $[O_2]$, CO thus causes a "double hit" on tissue O_2 availability, and with enough CO inhaled and in the blood, fatal O_2 insufficiency will occur. There are additional factors that further increase the toxic effects of CO: binding to intracellular heme proteins (e.g., myoglobin, cytochromes) further interfering with O_2 transport and utilization and likely oxidative stress causing cell damage.[25]

Finally, while inhalation of CO rapidly (seconds) causes CO poisoning through its uptake by and binding to red cells in the lung, the removal of CO from the body after the source of inhaled CO has been eliminated is very slow, with a half-time of about 5 hours if a subject is breathing ambient air. Because of the competitive binding of CO to the same heme sites as for O_2, administering high levels of inhaled O_2 substantially accelerates CO removal from the body, by about a factor of 4 if 100% O_2 is breathed.[26]

Standard P_{50} and In Vivo P_{50}

A final note on P_{50} is required. The preceding discussion makes it clear that the O_2Hb dissociation curve can shift left or right depending on factors other than the inherent P_{50} of Hb. This brings up the concepts of "standard" P_{50} and "in vivo" P_{50}. Standard P_{50} is the PO_2 at 50% O_2Hb saturation when temperature is 37°C, blood PCO_2 is 40 mm Hg, and blood pH is 7.40 (which are considered standard conditions). In vivo P_{50} is the actual P_{50} after dissociation curve shifts have occurred from all of the above five factors. By its definition, standard P_{50} remains constant (at 27 mm Hg) as blood circulates around the body. In vivo P_{50} in arterial blood normally equals the standard P_{50} because arterial blood is normally at 37°C, with PCO_2 of 40 mm Hg and pH of 7.40 units. However, the in vivo P_{50} in venous blood is higher because PCO_2 is higher, pH is lower, and during exercise, venous blood temperature is higher.

Finally, there are many known genetic mutations in Hb that can have major effects on O_2 affinity. This topic is beyond the scope of this chapter, and the interested reader is encouraged to seek articles describing the many mutations that have been discovered, and the corresponding effects they have on O_2 transport.

Carbon Dioxide Carriage in Blood

Overview

CO_2 is produced by the tissues as a byproduct of oxidative phosphorylation. It must be continuously eliminated from the body at the rate at which it is produced, so as to keep blood and tissue PCO_2 constant. Maintaining homeostasis of CO_2 is a major factor in keeping pH levels from fluctuating, which would disturb cellular function. At rest, a typical normal subject produces 240 mL CO_2/min. Elimination involves first moving, by diffusion, the CO_2 from the tissue cellular sites of production into the venous blood draining the tissues. That venous blood must then flow to the lungs where some of its CO_2 will diffuse from the capillaries into alveolar gas to be eliminated by ventilation. It is important to note that at rest, only about 10% of the CO_2 carried in the venous blood is eliminated, leaving 90% in the pulmonary venous (and thus also arterial) blood sent back to the tissues. CO_2 is a major player in acid–base regulation, and changing CO_2 levels by only 10% between venous and arterial locations means that acid–base balance is not continuously and seriously disrupted by the process of gas exchange.

Total CO_2 concentration in normal arterial blood is about 48 mL CO_2/100 mL blood, and 52 mL/100 mL in mixed venous blood. Correspondingly, arterial PCO_2 is normally 40 mm Hg, whereas mixed venous PCO_2 is about 45 mm Hg. Thus, whether looked at by concentration or partial pressure, these numbers comport with the statement that only 10% of the CO_2 carried in venous blood is eliminated at the lungs. While this may at first sight seem inefficient, (metaphorically akin to repeatedly filling a car's gas tank every time the indicator shows that only 10% of the fuel has been used) it means that the change in pH between arterial and venous blood is small, which contributes to cellular metabolic stability.

CO_2 is carried in blood in three forms:

- Physically dissolved, as for O_2.
- Bound to blood proteins as carbamino complexes, mostly with Hb (but not at the O_2 binding site within heme). Rather, CO_2 is chemically combined with terminal amine groups on the protein molecule.
- As bicarbonate ion, HCO_3^-.

All three forms and their underlying reactions/processes are rapidly reversible (albeit with enzymatic help in the case of bicarbonate formation, see below), such that the process of moving metabolically produced CO_2 from the tissues into blood perfusing the tissues is not considered to significantly impede CO_2 elimination from the body in health. So too, the diffusive process of moving CO_2 from the pulmonary capillary blood into the alveolar gas is not considered to impede CO_2 elimination.

Just as for O_2, CO_2 is not distributed uniformly within the blood. While both physically dissolved CO_2 and HCO_3^- ions are present in both plasma and the red cell interior, carbamino-Hb is limited to the red cell interior. Just as for O_2 added to the blood in the lungs, CO_2 added to the blood in the tissues must first dissolve in and diffuse through the plasma before moving into the red cell. These steps are reversed in the pulmonary capillaries as CO_2 is transferred from blood into alveolar gas. While there is but one chemical reaction in blood for O_2 (binding to [or release from] heme in Hb), two separate chemical processes take place when CO_2 is added to (or leaves) the blood. One is formation (or undoing) of carbamino-Hb, whereas the second is combination of CO_2 with water molecules in the blood to form carbonic acid, which rapidly dissociates into HCO_3^- and a proton (or the reverse reaction in the lung capillaries, where HCO_3^- and a proton combine to form carbonic acid and then CO_2 and H_2O). In round numbers, about 85 to 90% of the CO_2 in blood is present as HCO_3^- ion. Dissolved CO_2 accounts for only about 5% and carbamino-Hb the remaining 5 to 10%. Also, as for O_2, when the blood (arterial or venous) is in equilibrium such that the concentrations of dissolved CO_2, carbamino-Hb and HCO_3^- ion are constant in time, the PCO_2 is the same inside and outside the red cell, even as the concentrations of CO_2 are dissimilar inside versus outside the red cell.

The ability of CO_2 to combine with water in the blood to form a proton and a HCO_3^- ion makes CO_2 a major contributor to regulation of blood pH. Hyperventilation, as for example, occurs in hypoxia and in states of stress, acutely causes arterial PCO_2 and $[H^+]$ to fall, leading to alkalosis. Reciprocally, hypoventilation (which can rapidly accompany narcotic drug overdose, chest or head injury, and acute severe lung disease) causes arterial PCO_2 and $[H^+]$ to rise, leading to acidosis. It also means that a metabolic acidosis raising $[H^+]$ by nonrespiratory mechanisms can be in part countered by hyperventilation, and a metabolic alkalosis can be partly countered by hypoventilation, all with the objective of preventing large changes in blood pH. However, acid–base regulation and the role of CO_2 in that domain are well beyond the scope of this chapter and the interested reader will easily find articles and textbook chapters (referred to at the beginning of this chapter) describing the topic in considerable detail.

Carbon Dioxide in Physical Solution

The solubility of CO_2 in water within the blood at normal body temperature is about 0.067 mL CO_2/100 mL blood/mm Hg.[27] This is more than 20 times the solubility of O_2 described above, and as a result one might think dissolved CO_2 is a substantial contributor to overall CO_2 transport. However, with arterial blood normally having a PCO_2 of 40 mm Hg, the concentration of dissolved CO_2 is 40×0.067, or 2.7, mL/100 mL blood, equivalent to 27 mL/L. With total blood $[CO_2]$ at about 48 mL/100 mL blood, dissolved CO_2 therefore accounts for only about 5% of the CO_2 present. Mixed venous blood normally has a PCO_2 of 45 mm Hg, and therefore, its concentration of dissolved CO_2 is 45×0.067, or 3.0 mL/100 mL blood (30 mL/L). With a normal resting cardiac output of 6 L/min, the volume of CO_2 eliminated from the dissolved pool of CO_2 would be $6 \times (30 - 27)$ mL/min, which is just 18 mL/min. This is only 8% of the 240 mL/min in need of elimination. Physically dissolved CO_2 contributes an even smaller fraction of total CO_2 elimination during exercise, of the order of just 2%. The importance of physical solution of CO_2 is thus not for mass transport of CO_2, but as the means by which CO_2 molecules enter the red cell to take part in the other two forms of CO_2 transport mentioned above.

Carbon Dioxide Combined with Blood Proteins: Carbamino–Protein Complexes

CO_2 combines reversibly with terminal amine groups on amino acids within the plasma and red cells but most importantly with amine groups in the Hb molecule. This reaction is extremely quick in both directions and does not require enzymatic facilitation. However, it too accounts for only about 5% of the CO_2 present in arterial blood, similar to the physically dissolved component but plays a larger role in CO_2 elimination where, at rest, it accounts for about 30% of the amount eliminated from the lung per minute.

Carbon Dioxide Combined with Water: Carbonic Acid, Bicarbonate Ions, and Protons

The major form in which CO_2 is carried in the blood, and the pool from which most CO_2 eliminated by the lungs comes, is as HCO_3^- ions. To see how this happens, it is instructive to follow the journey of CO_2 molecules into the tissue bloodstream after generation by oxidative phosphorylation within a tissue cell. This is pictured in ►**Fig. 10**, which is quite complex. It will be described now, in a series of eight steps, with reference to the colors used at each step in the figure.

Step 1: CO_2 (yellow), dissolved in cellular fluid, diffuses out of the tissue cells and into the plasma in the capillary where some CO_2 molecules stay, still dissolved (small yellow arrow). However, most of the CO_2 continues to diffuse into the red cell interior (large green arrows). Diffusion results in net movement of CO_2 from cells to capillary because the cells produce CO_2, such that the intracellular PCO_2 exceeds that in the inflowing arterial blood (which has been previously partially cleared of CO_2 by the process of ventilation).

Step 2: some of the dissolved CO_2 molecules in the plasma react with water to form carbonic acid (H_2CO_3), which then dissociates into protons and bicarbonate ions (light green and small green arrow):

$$CO_2 + H_2O \rightleftharpoons H_2CO_3 \rightleftharpoons H^+ + HCO_3^- \qquad \textbf{Eq. 7}$$

A critical point in this chemical transformation is that without the enzyme carbonic anhydrase (CA),[28] which is not present in the plasma, the formation of carbonic acid from CO_2 and water, and the reverse reaction, are relatively slow, requiring many seconds to complete. Hence, the amount of CO_2 involved in this reaction in the plasma is small. However, as the arrows show, the reactions are reversible.

Step 3: also small in amount, some of the dissolved CO_2 reacts with terminal amines on plasma proteins rapidly forming carbamino compounds (pink).

Step 4: the majority of the CO_2 has diffused into the red cell (see step 1 above, large green arrows), where some remains as dissolved CO_2 in physical solution (yellow).

Step 5: a significant amount of CO_2 combines with the terminal amine groups in Hb, again rapidly and without the need for enzymatic facilitation (pink).

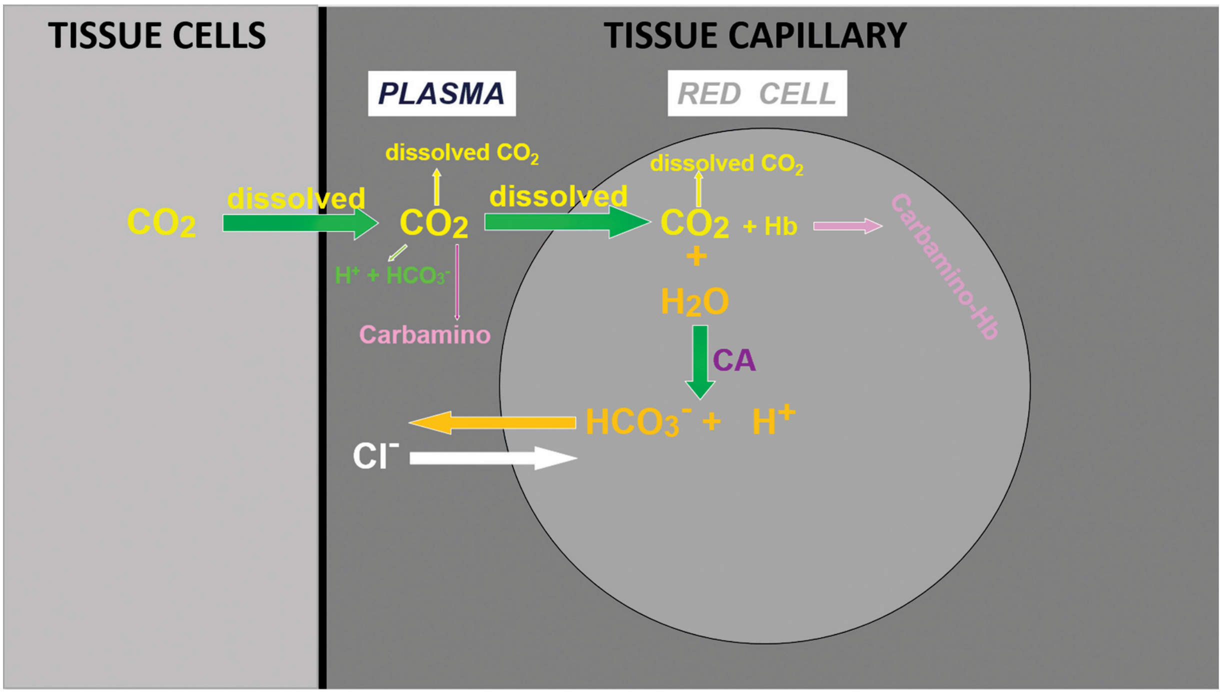

Fig. 10 Cartoon of the peripheral tissues showing a tissue cell and capillary with plasma and red cell compartments. The figure describes CO_2 movement from the tissue cell to the blood, and all three forms of CO_2 transport are included in the diagram. Arrows are sized to indicate general importance of each part of the pathway. CA, carbonic anhydrase; CO_2, carbon dioxide; Hb, hemoglobin.

Step 6: most of the CO_2 undergoes the above transformation (see **Eq. 7**, step 2) into carbonic acid and then into protons and bicarbonate ions (orange). The critical difference between this reaction in the plasma and the same reaction inside the red cell is that the enzyme CA (purple) is present inside the red cell, which speeds up the reaction some 10,000 fold or more.[29] The protons generated will reduce the pH of the blood: venous blood with more CO_2 is more acidic (pH ~ 7.37) than arterial blood (pH ~ 7.40) for this reason.

Step 7: thanks to the presence of CA within the red cell and its absence from the plasma, the intracellular $[HCO_3^-]$ exceeds the plasma $[HCO_3^-]$. This causes HCO_3^- ions to move from the red cell interior out into the plasma (large orange arrow).

Step 8: step 7 causes a net outward movement of negatively charged HCO_3^- ions, which sets up a charge inequality between plasma and red cell. Protons do not easily move out through the red cell wall to balance this net charge inequality, and so there is movement of negatively charged chloride ions (white) from the plasma into the red cell to balance the charge difference.

In this complex manner, CO_2 added to the tissue capillary blood ends up in all three transported forms (dissolved, carbamino bound, and as bicarbonate ions) both inside and outside the red cell.

The Composite Carbon Dioxide “Dissociation” Curve

Just as for O_2, it is useful to construct a total CO_2 binding curve showing concentration on the ordinate versus PCO_2 on the abscissa. This appears in ►**Fig. 11**, where the CO_2 concentration reflects the sum of all 3 forms of CO_2 in both plasma and red cell. To call this a “dissociation” curve is perhaps a stretch, but it has become the common term for the relationship. The concept of a P_{50} has never been applied to CO_2 the way it has to O_2 because, with the major form of carriage being as bicarbonate ions, there is no absolute limit to how much CO_2 can be carried in the blood. The concept of P_{50} is meaningful only for a chemical binding process with a defined number of binding sites.

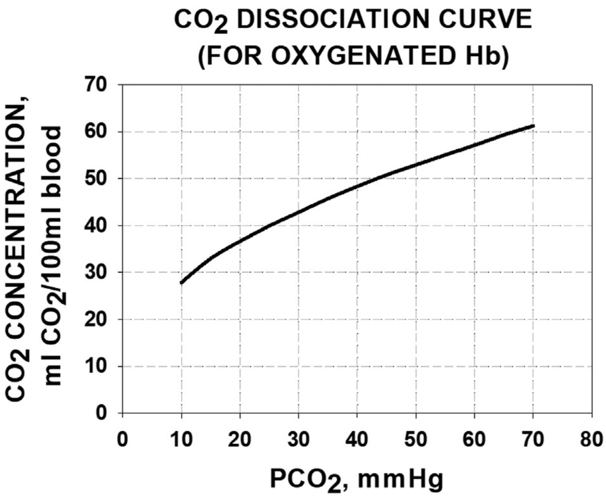

Fig. 11 The CO_2 dissociation curve: total CO_2 concentration (ordinate) plotted against PCO_2 (abscissa). The curve shows the sum of the contributions to CO_2 carriage that come from (A) physically dissolved CO_2 (about 5%); (B) CO_2 bound to terminal amine groups on blood proteins in plasma and red cells (also about 5%); and (C) CO_2 transformed into bicarbonate ion (about 90%). The CO_2 curve is both more nearly linear, and an order of magnitude steeper, than that for O_2. CO_2, carbon dioxide; Hb, hemoglobin; O_2, oxygen; PCO_2, partial pressure of carbon dioxide.

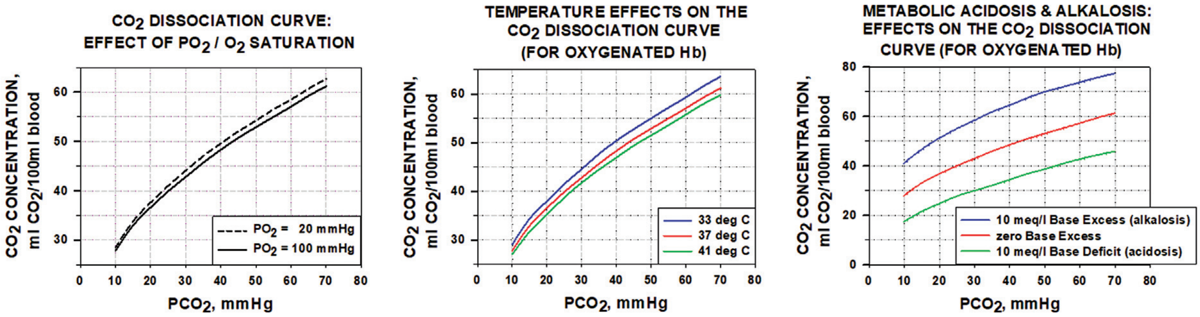

Fig. 12 Individual effects of Hb oxygenation level (left panel), blood temperature (middle panel), and pH (right panel) on the CO_2 dissociation curve. Metabolic acidosis and alkalosis cause the largest shifts in the CO_2 dissociation curve mostly through changes in bicarbonate ion concentration associated with more (acidosis) or less (alkalosis) proton availability. CO_2, carbon dioxide; Hb, hemoglobin; O_2, oxygen.

Factors Affecting the Carbon Dioxide Dissociation Curve

Just like the O_2Hb dissociation curve, that for CO_2 is not a static or unique relationship: The relationship between CO_2 concentration and partial pressure is affected by the O_2 saturation of Hb, by temperature, and by pH (i.e., acidosis and alkalosis). ►**Fig. 12** provides examples of how the CO_2 dissociation curve shifts with each of these factors one at a time. It is evident that blood pH has a major effect on how much CO_2 can be carried in the blood at any PCO_2, and (the chemical) **Eq. 7** above gives insight into why. Removal of protons by alkalosis drives the reaction in **Eq. 7** rightward by mass action. This causes the bicarbonate ion, the major CO_2 transport molecule, to increase in concentration. The reverse occurs during acidosis, where less bicarbonate exists as **Eq. 7** is driven leftward by an excess of protons. The effects of temperature and Hb oxygenation are also evident in ►**Fig. 12**, but the magnitude of their effects is much less than that of pH.

Interaction between Oxygen and Carbon Dioxide in Blood

Based on the preceding discussion of the factors that affect the O_2 and CO_2 dissociation curves, and as shown in ►**Figs. 9** and **12**, it is clear that the two gases affect each other in a complementary fashion. This means that when O_2 is added to the blood in the lungs, that action enhances the unloading of CO_2 in the lungs, and vice versa. Correspondingly, in the tissues, as O_2 is removed from the blood for use by the tissues, the addition of CO_2, produced by metabolism, to the blood is facilitated, and vice versa.

This may be understood chemically using ►**Fig. 13**, which extends ►**Fig. 10** to now include the simultaneous removal of O_2 from the blood for use by the tissues (using yellow and blue to represent O_2 details). In ►**Fig. 10**, it was noted that the main pathway for adding CO_2 to the blood in the tissue capillaries was conversion of CO_2 to bicarbonate ions inside the red cell (larger arrows in ►**Fig. 10**). Per **Eq. 7** above, this also produces protons, highlighted in the black dashed circle in ►**Fig. 13**. It turns out that as oxygenated Hb gives up O_2 for diffusion to the tissue cells it readily accepts a proton. Since this proton comes from CO_2 as shown, mass action then decrees that binding this proton reduces the proton number, which accelerates both the conversion of CO_2 to bicarbonate and the continued release of O_2 from Hb. In other words, through this proton, the two gases enhance each other's movement. Exactly the same scenario plays out in the pulmonary capillaries, the only difference being in direction (CO_2 moving out of the blood; O_2 moving into the blood). Thus, reverse the direction of the arrows and ►**Fig. 13** applies to the lungs. The enhancement of O_2 movement by CO_2 has become known as the Bohr effect,[30] whereas the enhancement of CO_2 movement by O_2 has become known as the Haldane effect.[31] ►**Fig. 14** shows the relative contribution of the Bohr effect to O_2 transport, both at rest and during exercise. Under both conditions, the Bohr effect plays only a small role in enhancing O_2 transport. That said, despite the relatively small effect during exercise (accounting for only about 10% of the total arteriovenous $[O_2]$ difference), the Bohr effect could be crucial in endurance athletic performance where races are commonly won and lost by inches. ►**Fig. 15** shows the relative contribution of the Haldane effect to CO_2 exchange both at rest and during exercise. At rest, with normal venous PCO_2 at about 45 mm Hg, about one-third of the CO_2 added to the blood in the tissues or removed from the blood in the lungs can be attributed to the Haldane effect. However, during exercise, the venous PCO_2 rises dramatically, and while the absolute Haldane effect is similar as at rest, it becomes a much smaller fraction of total CO_2 exchanged.

Overall Summary

This review of O_2 and CO_2 transport has attempted to provide not only the standard descriptions of how the two gases are carried in the blood, but also some conceptual foundations not only for how they are carried in blood, but also for the dynamics of how they exchange between alveolar gas and blood on the one hand and between tissue blood and tissue cells on the other hand. These dynamics are different for the two gases because of differences in their dissociation curves, especially in their different overall shapes and slopes. A companion chapter will use the information from the current chapter to explain how differences in the shape and slope of the O_2 and CO_2 dissociation curves affect O_2 and CO_2 exchange in both the lungs and tissues and their transport between them.

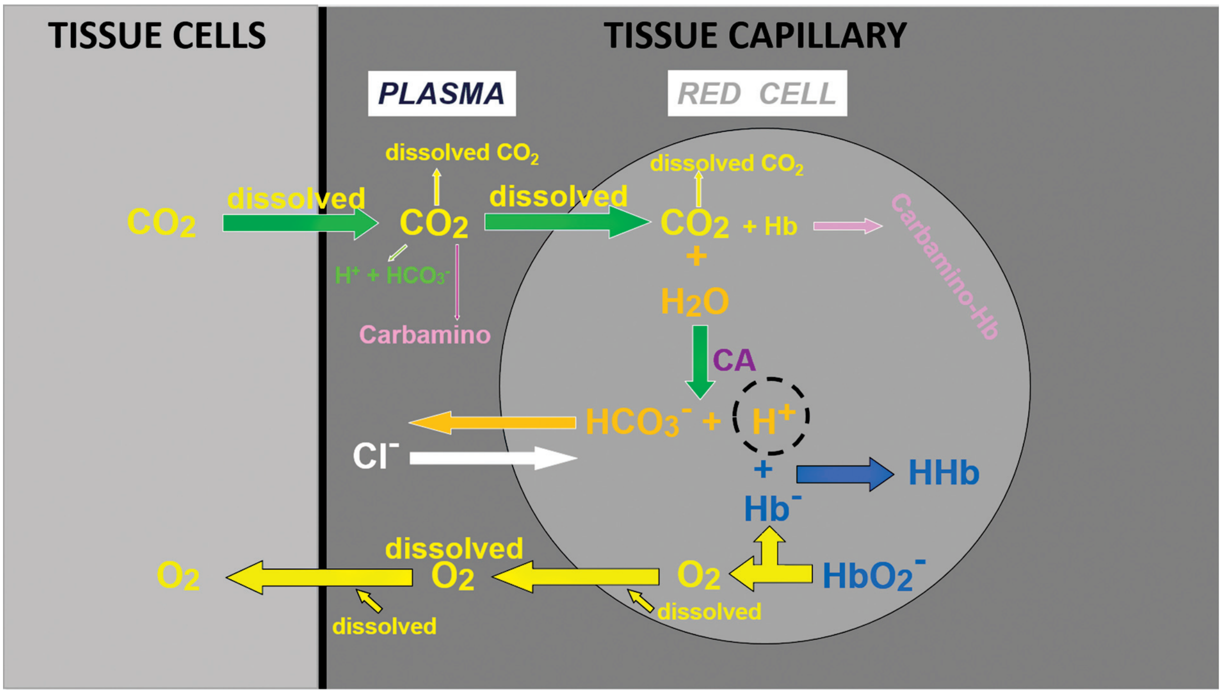

Fig. 13 Extension of ►**Fig. 10**, the cartoon of the peripheral tissues showing a tissue cell and capillary with plasma and red cell compartments, to now include both O_2 and CO_2 movement between the tissue cell and the blood. The key point is that protons (identified within the black dashed circle) become available from bicarbonate formation from CO_2 to enhance formation of reduced Hb (HHb) as O_2 is released. See text for full explanation and definition of terms and abbreviations. CA, carbonic anhydrase; CO_2, carbon dioxide; Hb, hemoglobin; O_2, oxygen.

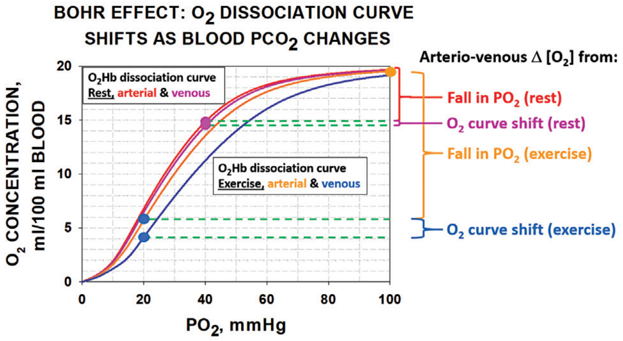

Fig. 14 O_2Hb dissociation curves for arterial and venous blood at rest and during exercise identifying both the arterial and venous $PO_2/[O_2]$ points for each. The main point of this figure is to show the quantitative effects of O_2Hb dissociation curve shifts from higher PCO_2 (and thus lower pH) in venous than arterial blood in augmenting O_2 unloading (i.e., the Bohr effect). While the shifts are the modest, small effects could have a large impact on endurance exercise success where events can be won or lost by inches. O_2, oxygen; O_2Hb, oxygen–hemoglobin; PCO_2, partial pressure of carbon dioxide; PO_2, partial pressure of O_2.

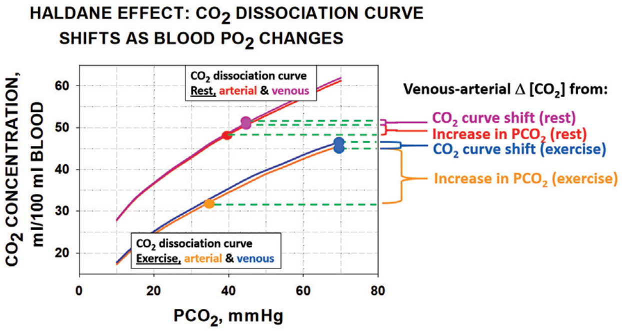

Fig. 15 In a format complementary to that of ►**Fig. 14** for O_2, CO_2 dissociation curves are shown for arterial and venous blood at rest and during exercise, identifying both the arterial and venous $PO_2/[O_2]$ points for each to illustrate the magnitude of the Haldane effect. Again, the effects are the modest. CO_2, carbon dioxide; Hb, hemoglobin; O_2, oxygen; PCO_2, partial pressure of carbon dioxide; PO_2, partial pressure of oxygen.

Conflict of Interest

None declared.

References

1 Barrett KE, Barman SM, Brooks HL, Yuan JX. Ganong's Review of Medical Physiology. 26th ed. New York: McGraw Hill; 2019
2 Boron WF, Boulpaep EL. Medical Physiology. 3rd ed. Philadelphia: Elsevier Health Sciences; 2017
3 Hall JE. Guyton and Hall Textbook of Medical Physiology. 14th ed. Philadelphia: Elsevier; 2021
4 Fox SI, Rompolski K. Human Physiology. 16th ed. New York: McGraw Hill; 2022
5 Koeppen BM, Stanton BA, Hall JM, Swiatecka-Urban A. Berne and Levy: Physiology. 8th ed. Philadelphia: Elsevier; 2024
6 Costanzo LS. BRS Series: Physiology. 8th ed. Philadelphia: Wolters Kluwer/Lippincott Williams Wilkins; 2023
7 Tandon OP, Tripathy Y. Best and Taylor's Physiological Basis of Medical Practice. 13th ed. Philadelphia: Wolters Kluwer/Lippincott Williams Wilkins; 2012
8 Widmaier EP, Raff H, Strang KT. Vander's Human Physiology. New York: McGraw Hill; 2022

9 Cloutier MM. Respiratory Physiology. 2nd ed. Philadelphia: Elsevier; 2018
10 Hlastala MP, Berger AJ. Physiology of Respiration. Oxford University Press; 2001
11 Levitzky MG. Pulmonary Physiology. 10th ed. New York: McGraw-Hill Education; 2022
12 Lumb AB, Thomas CR. Nunn's Applied Respiratory Physiology. 9th ed. Philadelphia: Elsevier Health Sciences; 2020
13 West JB, Luks AM. West's Respiratory Physiology. 11th ed. Philadelphia: Lippincott Williams & Wilkins; 2020
14 Weibel ER. The Pathway for Oxygen: Structure and Function in the Mammalian Respiratory System. Harvard University Press; 1984
15 Hedley-Whyte J, Laver MB. O2 solubility in blood and temperature correction factors for PO2. J Appl Physiol 1964;19(05):901–906
16 Hill AV. The possible effects of the aggregation of the molecules of haemoglobin on its dissociation curves. J Physiol 1910;40:4–7
17 Kaufman DP, Khattar J, Lappin SL. Physiology, Fetal Hemoglobin. StatPearls [Internet]: StatPearls Publishing; 2021
18 Benesch R, Benesch RE. The effect of organic phosphates from the human erythrocyte on the allosteric properties of hemoglobin. Biochem Biophys Res Commun 1967;26(02):162–167
19 Roughton F, Darling R. The effect of carbon monoxide on the oxyhemoglobin dissociation curve. Am J Physiol 1944;141(01):17–31
20 Kelman GR. Digital computer subroutine for the conversion of oxygen tension into saturation. J Appl Physiol 1966;21(04):1375–1376
21 Kelman GR. Digital computer procedure for the conversion of PCO2 into blood CO2 content. Respir Physiol 1967;3(01):111–115
22 Kelman GR. Computer program for the production of O2-CO2 diagrams. Respir Physiol 1968;4(02):260–269
23 Wagner PD. Insensitivity of VO2max to hemoglobin-P50 as sea level and altitude. Respir Physiol 1997;107(03):205–212
24 Wagner PD, Wagner HE, Groves BM, Cymerman A, Houston CS. Hemoglobin P(50) during a simulated ascent of Mt. Everest, Operation Everest II. High Alt Med Biol 2007;8(01):32–42
25 Nañagas KA, Penfound SJ, Kao LW. Carbon monoxide toxicity. Emerg Med Clin North Am 2022;40(02):283–312
26 Blumenthal I. Carbon monoxide poisoning. J R Soc Med 2001;94(06):270–272
27 Christmas KM, Bassingthwaighte JB. Equations for O_2 and CO_2 solubilities in saline and plasma: combining temperature and density dependences. J Appl Physiol 2017;122(05):1313–1320
28 Meldrum NU, Roughton FJ. Carbonic anhydrase. Its preparation and properties. J Physiol 1933;80(02):113–142
29 Kernohan JC, Forrest WW, Roughton FJ. The activity of concentrated solutions of carbonic anhydrase. Biochim Biophys Acta 1963;67:31–41
30 Bohr C, Hasselbalch K, Krogh A. Concerning a biologically important relationship - the influence of the carbon dioxide content of blood on its oxygen binding. Skand Arch Physiol 1904;16:401–412
31 Christiansen J, Douglas CG, Haldane JS. The absorption and dissociation of carbon dioxide by human blood. J Physiol 1914;48(04):244–271

Article published online: 2023-08-11

Blood Gas Transport: Implications for O_2 and CO_2 Exchange in Lungs and Tissues

Peter D. Wagner, MD[1]

[1] Department of Medicine, University of California San Diego, La Jolla, California

Address for correspondence Peter D. Wagner, MD, Department of Medicine, University of California San Diego, La Jolla, CA 92093 (e-mail: pdwagner@health.ucsd.edu).

Semin Respir Crit Care Med 2023;44:584–593.

Abstract

The well-known ways in which O_2 and CO_2 (and other gases) are carried in the blood were presented in the preceding chapter. However, what the many available texts about O_2 and CO_2 transport do not emphasize is why knowing how gases are carried in blood matters, and this second, companion, article specifically addresses that critical aspect of gas exchange physiology. During gas exchange, both at the lungs and in the peripheral tissues, it is the shapes and the slopes of the O_2 and CO_2 binding curves that explain almost all of the behaviors of each gas and the quantitative differences observed between them. This conclusion is derived from first principle considerations of the gas exchange processes. Dissociation curve shape and slope differences explain most of the differences between O_2 and CO_2 in both diffusive exchange in the lungs and tissues and convective exchange/transport in, and between, the lungs and tissues. In fact, each of the chapters in this volume describes physiological behavior that depends more or less directly on the dissociation curves of O_2 and CO_2.

Keywords
- ► inert gases
- ► solubility
- ► dissociation curves
- ► diffusive gas exchange
- ► convective gas transport
- ► O_2–CO_2 interactions

As presented in the preceding chapter, the O_2 and CO_2 dissociation curves differ in several physiologically important ways as follows:

- That for O_2 is more curvilinear in shape than that for CO_2 in the physiological and even pathophysiological range. It is steeper at low PO_2 and less steep at high PO_2.
- The average slope of the O_2 dissociation curve in the physiological range at rest at sea level is some 10-fold less than that for CO_2.
- About 2.5 times as much CO_2 as O_2 (mL/100 mL) is present in arterial blood.
- Other than for the minor contribution of physically dissolved O_2, there is a hard limit to how much O_2 can be carried per 100 mL blood because of the finite number of heme binding sites in hemoglobin (Hb). In contrast, the amount of CO_2 that can be carried in the blood in physical solution and as bicarbonate ion can, in concept, rise without limit as PCO_2 is increased, despite a limit on the number of terminal amine binding sites for CO_2.

How these differences affect gas exchange is now discussed. Recall that O_2 from the air reaches the tissue cells by a sequential series of four principal transport steps.[1] CO_2 moves from the cells to the air by the very same steps which are mentioned below:

- Pulmonary ventilation, mostly a convective process, that brings O_2 from the air to the alveoli and simultaneously returns CO_2 from the alveoli to the air.
- Alveolar-lung capillary diffusion. For both O_2 and CO_2, diffusion is responsible for their movement between the alveolar gas and the capillary blood.
- Circulation, a convective process, which transports blood containing O_2 and CO_2 from the lungs to the tissues and back to the lungs in a never-ending loop, powered of course by the heart as a pump.
- Tissue capillary-mitochondrial diffusion, that is responsible for gas movement between the tissue capillary blood and the tissue mitochondria, again for both O_2 and CO_2.

Physiological Significance of O_2 and CO_2 Dissociation Curve Characteristics in the *Diffusive* Steps of O_2 and CO_2 Transport

Both the shape and the slope of the dissociation curves play significant roles in the diffusive steps of O_2 and CO_2 transport, and these two characteristics explain the differences in

article published online
August 11, 2023

Issue Theme Pulmonary Physiology; Guest Editors: David A. Kaminsky, MD, Kathryn A. Hibbert, MD, and Andrew M. Luks, MD

Thieme Medical Publishers, Inc.,
333 Seventh Avenue, 18th Floor,
New York, NY 10001, USA

DOI https://doi.org/10.1055/s-0043-1771161.
ISSN 1069-3424.

diffusive equilibration for the two gases, and the greater vulnerability of O_2 than CO_2 to failure of complete diffusive equilibration across the capillary wall, be it in the lungs or tissues. The purpose of this section is to explain how these differences arise. While the process of diffusion is treated in depth in another chapter, it is necessary to provide here the quantitative foundation of diffusive movement to appreciate how and why the shape and slope of the dissociation curves play a role in the rate of diffusive equilibration.

It helps to visualize the diffusive process, and the example of O_2 diffusing from alveolar gas into pulmonary capillary blood will be used. However, the same principles apply to O_2 diffusion in the tissues and to CO_2 diffusion in both the lungs and tissues.

For O_2 diffusing from alveolar gas into the pulmonary capillaries, it helps to make the simplifying approximation that alveolar PO_2 is constant in time as long as tidal volume and respiratory frequency are constant. This means a steady state is assumed to exist, and that the minor differences in alveolar PO_2 (PAO_2) between inspiration and expiration are ignored. PAO_2 is normally about 100 to 110 mm Hg at rest at sea level. Next, it is recognized that red cells enter the alveolar capillaries with a PO_2 equal to that in the pulmonary arterial blood. This "mixed venous" PO_2 ($P_{\bar{v}}O_2$) is much lower than PAO_2, and is usually about 40 mm Hg. This too is taken to be constant in time. The next consideration is that a finite diffusion coefficient (equivalently called diffusing capacity, D_L) exists in the lung, defining the rate of movement of (dissolved) O_2 molecules through the alveolar blood:gas barrier from alveolar gas into capillary plasma. Note that D_L is proportional to the total pulmonary capillary surface area available for O_2 diffusion, and inversely proportional to the alveolar wall thickness (which is the distance O_2 has to move from gas to plasma). Of critical importance to the speed of net diffusive O_2 movement, D_L is also proportional to the physical solubility of O_2 in the alveolar wall (a solubility essentially equal to that in plasma, which is 0.003 mL O_2/100 mL blood/mm Hg PO_2 as discussed earlier).

Now to the diffusion process itself: as a red cell (with $PO_2 = P_{\bar{v}}O_2$, normally 40 mm Hg) enters the pulmonary capillary, the much higher alveolar PO_2 (normally 100 mm Hg) results in rapid diffusive flux of O_2 from gas to blood. That initial diffusive flux can be expressed by a simple diffusion equation, the Fick law of diffusion:

$$\text{Initial } O_2 \text{ flux} = D_L \times [PAO_2 - PO_2 = P_{\bar{v}}O_2] \qquad \textbf{Eq. 1}$$

D_L has units of mL O_2 diffusing/min/mm Hg PO_2 difference between gas and blood, while $[PAO_2 - PO_2 = P_{\bar{v}}O_2]$ has units of mm Hg. Thus, initial O_2 flux has units of mL/min, and is the mL/min of O_2 entering the pulmonary capillary from the alveolar gas at the start of the red cell's journey through the pulmonary capillary. As O_2 moves from alveolar gas into the capillary, it is replaced by more O_2 inhaled each breath, so that PAO_2 remains constant as stated. However, the initial O_2 flux immediately raises the O_2 concentration $[O_2]$ in the capillary, and thus also the capillary PO_2 (PcO_2). Thus, PcO_2 soon exceeds $PO_2 = P_{\bar{v}}O_2$, reducing the difference between alveolar and capillary PO_2. In turn, the O_2 flux rate is reduced, and as the red cell moves along the capillary, the flux rate continues to fall further as capillary PO_2 increases and its difference from PAO_2 becomes ever less. **Eq. 1** is generalizable to the entire capillary, making it able to capture this progressive change in PcO_2 as follows:

$$O_2 \text{ flux}(t) = D_L \times [PAO_2 - PcO_2(t)] \qquad \textbf{Eq. 2}$$

Eq. 2, a more general form of **Eq. 1**, recognizes that as the red cell moves along the capillary its PO_2 increases while at the same time, precisely because of this increase in PcO_2 the volumetric rate of addition of O_2 to the capillary is slowing down as the difference between PAO_2 and PcO_2 is decreasing.

O_2 flux can be thought of in terms of two components. These are capillary blood volume (Vc) and change in O_2 concentration ($[O_2]$). Because the *amount* of O_2 in the blood is the product of Vc and $[O_2]$, O_2 *flux* becomes the product of Vc (which is a constant) and the *rate of change* in $[O_2]$ at any time point, *t*:

$$O_2 \text{ flux}(t) = \text{Vc} \times [O_2] \text{ change / time} = \text{Vc} \times \text{d}[O_2]/\text{dt} \qquad \textbf{Eq. 3}$$

Eqs. 2 and **3** both provide expressions for O_2 flux(t) and can be equated (because they represent the same O_2 flux). They can then be rearranged to yield:

$$\text{d}[O_2]/\text{dt} = D_L \times [PAO_2 - PcO_2(t)]/\text{Vc} \qquad \textbf{Eq. 4}$$

As mentioned above, D_L is proportional to (1) capillary surface area (A), (2) O_2 solubility (often termed α) in the Hb-free alveolar wall, and (3) inversely proportional to alveolar wall thickness (T). Thus:

$$D_L = \text{k} \times A \times \alpha / T \qquad \textbf{Eq. 5}$$

where k is a constant of proportionality. **Eq. 4** can then be rewritten as:

$$\text{d}[O_2]/\text{dt} = [\text{k} \times A \times \alpha / (T \times \text{Vc})] \times [PAO_2 - PcO_2(t)] \qquad \textbf{Eq. 6}$$

Note that the O_2Hb dissociation curve is implicitly contained within **Eq. 6**, because $[O_2]$ appears on the left-hand side while PO_2 appears on the right-hand side (as PcO_2, the PO_2 corresponding to $[O_2]$ at the same time along the capillary). In other words, the shape and slope of the O_2Hb curve directly affects the solution to **Eq. 6** all along the capillary and thus, the rate of rise in both PO_2 and $[O_2]$ as the red cell moves along the capillary.

Importantly, if D_L is large enough that by the end of the red cell's transit through the pulmonary capillary, PcO_2 has equilibrated with PO_2 in alveolar gas (i.e., end-capillary $PO_2 = PAO_2$), it is stated that diffusion equilibration has occurred and therefore there is no diffusion limitation. But if end-capillary PO_2 is less than PAO_2, it is stated that there is failure of equilibration, such that diffusion limitation is present.

This can all be digested more readily by *approximating the dissociation curve as linear.* Recall from the first section of the preceding article (specifically, **Eq. 2** from "Blood Gas

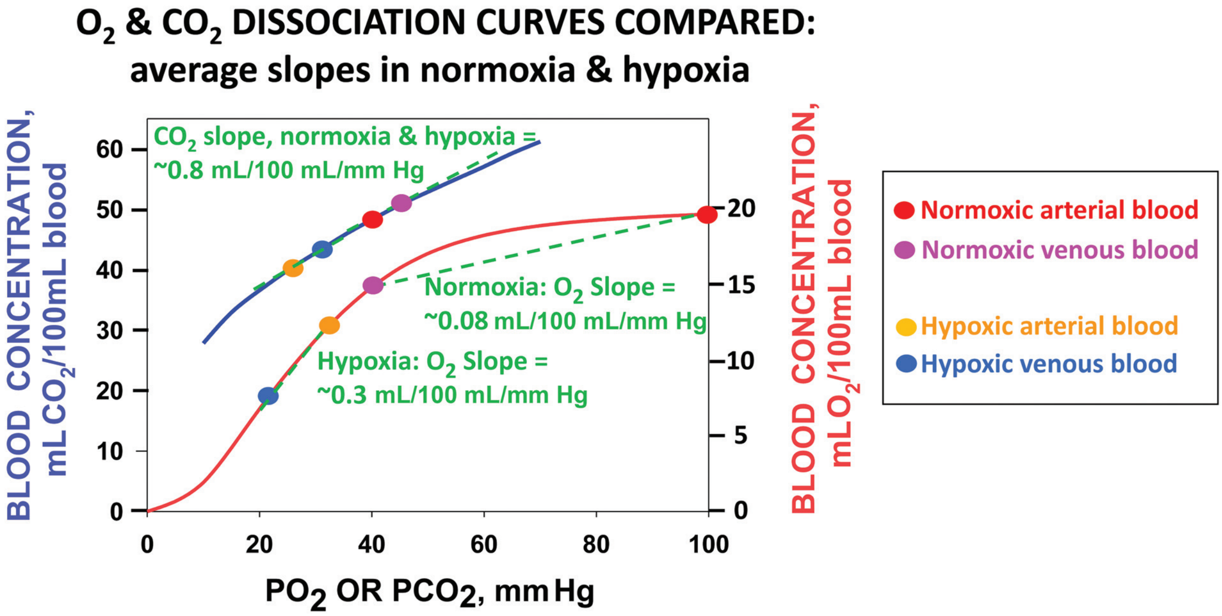

Fig. 1 The O_2Hb and CO_2 dissociation curves are compared on the same graph. Note the left ordinate scales CO_2 while the right ordinate applies to O_2. The main point of this graph is to illustrate the large differences between O_2 and CO_2 in the shapes and slopes of their respective dissociation curves, both in normoxia and hypoxia. The two properties (shape and slope) drive most of the differences between O_2 and CO_2 exchange at every step of the O_2 (and CO_2) transport pathway.

Transport: Carriage of Oxygen and Carbon Dioxide in Blood") that this makes concentration of a gas a linear function of partial pressure: concentration change = solubility × partial pressure change. This is not always justifiable for precise calculations for the respiratory gases, but is very helpful in concept. ►**Fig. 1** reproduces the dissociation curves for O_2 and CO_2, and over the normal physiological range, it is clear that this approximation is actually very good for CO_2 under all conditions. It is also good for O_2 in hypoxia but somewhat rough for O_2 in normoxia. Nonetheless, if linearity is assumed for both gases under all conditions, one can see a principle emerging by extending **Eq. 6**, using the average dissociation curve slope as expression of the functional "solubility" of each gas in any range of interest.

To avoid confusion, the average dissociation curve slope is given the abbreviation β, to distinguish it from the physical solubility mentioned above (α). Thus, β is the concentration difference divided by the partial pressure difference (over any desired range of the curves), and encompasses the sum of all forms of the gas present. **Eq. 6** can then be expressed using α and β:

$$d[O_2] / dt = d[\beta \times PcO_2] / dt = [k \times A \times \alpha \,/\, (T \times Vc)] \times [PAO_2 - PcO_2(t)]$$ **Eq. 6**

which (dropping the subscript (t) for clarity) simplifies to:

$$dPcO_2 / dt = k \times A \times \alpha \,/\, (\beta \times T \times Vc)] \times [PAO_2 - PcO_2]$$ **Eq. 7**

or

$$dPcO_2 / dt = [k \times A / (T \times Vc)] \times [\alpha / \beta] \times [PAO_2 - PcO_2]$$ **Eq. 8**

or

$$dPcO_2 / dt = L \times [\alpha/\beta] \times [PAO_2 - PcO_2]$$ **Eq. 9**

where $L = k \times A/(T \times Vc)$ is a compound constant with *components that all depend on lung structure and which are unrelated to which gas is under consideration. On the other hand, the compound term* α/β *is the ratio of the physical solubility of the gas in plasma (*α*) to its equivalent total blood "solubility" (*β*), that is, the ratio of arteriovenous concentration difference to arteriovenous partial pressure difference, summing all forms by which the gas is carried.*

Eq. 9 is important to understand. First, it is a simple first-order linear differential equation in PcO_2 as a function of time, *t*. Integration of this differential equation yields this solution for O_2 alveolar-capillary diffusion in the lung:

$$PecO_2 = PAO_2 - (PAO_2 - P\bar{v}O_2) \times \exp\,[- L \times \alpha / \beta \times tt]$$ **Eq. 10**

where $PecO_2$ is the final (i.e., end-capillary) PO_2 in the blood leaving the lungs on its way to the left atrium. The term *tt* is the total red cell transit time in the pulmonary capillary, given by the ratio of capillary blood volume (Vc) to *Q*, where *Q* is blood flow (here, cardiac output for the whole lung).

Eq. 10 can therefore now be rewritten as:

$$PecO_2 = PAO_2 - (PAO_2 - PvO_2) \times \exp\,[- L \times \alpha/\beta \times Vc/Q]$$ **Eq. 11**

or, since $L = k \times A / (T \times Vc)$

$$PecO_2 = PAO_2 - (PAO_2 - PvO_2) \times \exp\,[- (k \times A / (T \times Vc)) \times \alpha/\beta \times Vc/Q]$$ **Eq. 12**

or, cancelling out Vc which appears on the numerator and denominator,

$$PecO_2 = PAO_2 - (PAO_2 - PvO_2) \times \exp[-(k \times A/(T)) \times (\alpha/\beta)/Q] \quad \textbf{Eq. 13}$$

or, since $D_L = k \times A \times \alpha/T$

$$PecO_2 = PAO_2 - (PAO_2 - PvO_2) \times \exp[-D_L/(\beta \times Q)] \quad \textbf{Eq. 14}$$

Here is the bottom line of this drawn out analysis: **Eq. 14** *says that O_2 will not be diffusion limited* if $D_L >> (\beta \times Q)$ such that $\exp[-D_L/(\beta \times Q)]$ is (close to) zero. If so, $PecO_2 = PAO_2$ and diffusion equilibration is complete.

Note that D_L is the *diffusive conductance* for the gas across the blood:gas barrier while $(\beta \times Q)$ is the *perfusive conductance* for the gas in the capillary blood, both expressed as mL O_2 that can be moved (by diffusion and perfusion, respectively) per minute per mm Hg partial pressure.

The original premise of this analysis is the Fick law of diffusion (**Eq. 1**), and it applies to CO_2 as well, not just O_2. It describes both gas uptake and elimination by diffusion, since direction of gas flow does not change the principle. The principle also applies to both gas uptake into the blood and gas elimination from the blood in the tissues, and thus to O_2 diffusion out of the tissue capillaries and CO_2 diffusion into the tissue capillaries. It also applies to inert gas exchange in the lungs and tissues, as often occurs for anesthetic gases.

Eq. 10, in particular, is illuminating when used to compare the likelihood of diffusion limitation for any gas in its exchange across the pulmonary capillary:

$$PecO_2 = PAO_2 - (PAO_2 - PvO_2) \times \exp[-L \times \alpha/\beta \times tt] \quad \textbf{Eq. 10}$$

Removing reference to O_2 to acknowledge the generalizability of the equation, and rearranging its terms, yields this:

$$(PA - Pec)/(PA - Pv) = \exp[-L \times \alpha/\beta \times tt] = \exp[-D_L/(\beta \times Q)] \quad \textbf{Eq. 15}$$

Recall that L expresses factors based on lung structure and are gas-independent, as is also the case for transit time, tt. **Eqs. 1** to **15** embody a complicated sequence of operations, but allow the reader to see the analysis from first principles. If one equation is to be remembered, it is **Eq. 15**.

The left-hand side of **Eq. 15** is, by definition, fractional diffusion limitation: if the right-hand side is zero, this must mean PA = Pec and that there is full diffusion equilibration, while if the right-hand side took its maximal theoretical value of 1.0, implying that diffusing capacity D_L was zero, this would mean Pec = Pv and that there has been zero diffusive gas exchange, a fatal condition. Suppose that $\exp[-D_L/(\beta \times Q)]$ comes to 0.1: this means 10% diffusion limitation such that the difference between PA and Pec is 10% of the difference between PA and Pv. The concepts and equations laid out above are generally attributed to Johannes Piiper and Peter Scheid.[2–6]

Table 1 Vulnerability of O_2 to alveolar-capillary diffusion limitation in the lungs

$D_L/(\beta \times Q)$	$\exp[-D_L/(\beta \times Q)]$ **(fractional diffusion limitation)**
0	1.00 complete diffusion limitation
0.5	0.61
1.0	0.37 (altitude, exercise)
1.5	0.22
2.0	0.14
3.0	0.05 (sea level, exercise)
4.0	0.02
5.0	0.01 (altitude, rest)
8.0	0.00 (sea level, rest; full equilibration)

Note: This table is based on the theory developed by Piiper and Scheid.[2–6] Their approach approximates the O_2Hb dissociation curve by a straight line of slope β, which allows an analysis in which the ratio of pulmonary diffusive to perfusive conductances $[D_L/(\beta \times Q)]$ determines whether, and if so, how much, diffusion limitation of gas exchange results. Here, D_L is lung diffusing capacity and Q is cardiac output. The key message is that as a subject goes from rest to exercise and between sea level and altitude, arterial and/or venous PO_2 change, and as a result, β changes in accord with the shape of the O_2Hb dissociation curve. In essence, β determines the likelihood of diffusion limitation occurring for a given subject under different conditions. See text for details.

►**Table 1** gives, for oxygen, a range of values of $D_L/(\beta \times Q)$, and the corresponding numbers for $\exp[-D_L/(\beta \times Q)]$, which quantifies the fractional degree of diffusion limitation. The numbers in ►**Table 1** indicating rest/exercise and sea level/altitude conditions reflect typical values found in healthy young humans. There is of course considerable variability between individuals, and the table is therefore only a rough guide.

What ►**Table 1** tells us is that at rest, no significant (if any) diffusion limitation for O_2 is expected, even at high altitude. During exercise at sea level, some people may experience a small degree of diffusion limitation while others will not. Typically, it is athletes with high values for Q (cardiac output) who develop diffusion limitation on exercise. However, during exercise at high altitude, some degree of diffusion limitation is expected in all healthy humans.

Various gases can now be compared in terms of whether or not they will be subject to diffusion limitation in a given lung. Clearly, from **Eq. 15**, the ratio α/β is the critical factor that can vary between gases in any given lung, and thus answer this question in any given lung (or tissue) for which the compound parameter L is the same for all gases.

Inert Gases and Diffusion Equilibration in the Lungs

It is again instructive to first consider inert gases, defined earlier as gases being present in blood and tissues only in physical solution. For such gases, α and β are essentially the same, making their ratio nominally 1. In addition, poorly soluble gases, highly soluble gases, and those in between, will all have essentially the same ratio (of 1), since for every inert gases, $\alpha = \beta$, allowing the conclusion that absolute solubility of the gas does not affect diffusion equilibration. Given the large value of the normal alveolar-capillary surface area *A* (perhaps 80 square meters for the whole lung), the very small alveolar wall thickness *T* of less than 1 µm, and the available transit time at rest of about 0.75 seconds (calculated from typical resting values of Vc [75 mL], and cardiac output [6 L/min]), diffusion equilibration for inert gases must occur within about the first 0.05 seconds of the capillary transit, well within the available 0.75 seconds. Even during intense exercise, with the commonly accepted reduction in transit time to about 0.25 seconds, inert gases will fully equilibrate.

O_2 and Diffusion Equilibration in the Lungs

Unlike inert gases, for O_2, α is much less than β. At rest in normoxia, α/β is 0.003/0.08 (see ►**Fig. 1**) which is about 0.04. This means a 25-fold lower α/β ratio than for inert gases, making O_2 much more vulnerable to diffusion limitation than any inert gas. That said, given normal values for D_L, it takes roughly 0.25 seconds for O_2 to equilibrate with alveolar gas in the normal lung at rest. This is entirely sufficient given the total transit time of 0.75 seconds, and the outcome is that diffusion limitation for O_2 is not seen in normal subjects at rest at sea level.

►**Fig. 1** also allows insight into the likelihood of diffusion limitation during exercise in normoxia. Green dashed lines joining corresponding arterial to venous points during normoxic exercise were omitted from ►**Fig. 1** to avoid clutter, but they would join the red and blue points on the (red) O_2Hb dissociation curve. This yields a value for β of about 0.2, and an α/β ratio of approximately 0.02, 50 times smaller than for an inert gas, explaining why diffusion limitation may occur during normoxic exercise.[7] It is not generally seen, however, in untrained healthy subjects exercising in normoxia, likely because of the higher cardiac output and presumably lower red cell transit time in athletes.

The importance of the α/β ratio is especially evident in hypoxia of any cause, be it in lung disease or in healthy subjects at high altitude. The ratio falls in hypoxia because the slope of the O_2Hb dissociation curve, and thus β, is substantially higher when arterial and venous PO_2 values are low, while α does not change with PO_2. As implied by ►**Fig. 1**, the α/β ratio in hypoxia becomes 0.003/0.3 which is only 0.01, or 100 times smaller than for an inert gas. Under these conditions, O_2 exchange is susceptible to diffusion equilibration failure, but generally is not seen at rest, likely because of the transit time remaining at around 0.75 seconds. However, exercise in hypoxia is the "perfect storm" for diffusive transport of O_2 in the lungs. The α/β ratio remains at about 0.01, but now the red cell transit time is reduced (being similar to that at sea level, ~0.25 seconds). Essentially, all healthy subjects show evidence of alveolar-capillary diffusion limitation during exercise in hypoxia.[8]

An interesting question then is why patients with chronic lung disease resulting in arterial hypoxemia do not show significant alveolar-capillary diffusion limitation for O_2, even during exercise, especially when their diffusing capacity (D_L) is measurably reduced. There are several reasons for this. First, such patients cannot undertake much exercise due to lack of fitness, airways obstruction, reduced lung compliance, or cardiac failure (singly or in combination) such that peak cardiac output is usually low and red cell transit time in the pulmonary capillaries is thus not reduced as much as in an athlete. Second, the main physiological abnormality perturbing gas exchange in chronic lung diseases is ventilation/perfusion (V_A/Q) inequality. This means that some regions of the lung will be relatively normal and others will have low V_A/Q ratios (which are responsible for the hypoxemia) in which there is little gas exchange occurring anyway.

There is one additional factor that works to support diffusion equilibration for O_2 in the lungs but only in normoxia: the nonlinear shape of the O_2Hb dissociation curve. If one follows the trajectory from venous to arterial PO_2 along the O_2Hb dissociation curve in normoxia (►**Fig. 1**), $[O_2]$ at first rises rapidly with respect to PO_2. This means that early in red cell transit, rapid mass movement of O_2 occurs into the blood without a large rise in capillary PO_2. This works to preserve the alveolar-capillary PO_2 difference driving net diffusion, and in turn this means that diffusive flux is somewhat higher as the red cell moves along the capillary (compared to its time course had the O_2Hb dissociation curve been truly linear). Note that in hypoxia, as ►**Fig. 1** shows, the entire loading process occurs along the steep, linear portion of the O_2Hb curve, meaning that in hypoxia the curvature seen at higher PO_2 values is not there to be taken advantage of.

O_2 and Diffusion Equilibration in the Tissues

As stated earlier, the principles described above apply to both diffusive loading of O_2 in the lungs and O_2 unloading from the tissue capillaries, where the values of α and β remain essentially the same as in the consideration of pulmonary gas exchange.

For the lungs, the law of diffusion was written in this way:

$$\text{Initial } O_2 \text{ flux} = D_L \times [PAO_2 - PvO_2] \qquad \textbf{Eq. 1}$$

In the tissues, with a corresponding tissue diffusing capacity termed D_M, the equation becomes:

$$\text{Initial } O_2 \text{ flux} = D_M \times [PaO_2 - PmO_2] \qquad \textbf{Eq. 16}$$

PaO_2 (arterial PO_2) is the "upstream" PO_2 entering the tissue and PmO_2 (mitochondrial PO_2) is the "downstream" PO_2 at the end of the diffusion pathway, the difference between them driving the net diffusion of O_2 from capillaries to mitochondria.

One simple observation suggests that there is *no* diffusion limitation of O_2 unloading in the tissues at rest during normoxia, where α/β remains at $0.003/0.08 = 0.04$: resting O_2 consumption does *not* fall at high altitude (i.e., with hypoxia), while as indicated earlier (see ►**Fig. 1**) arterial PO_2, and presumably, also mitochondrial PO_2, do fall. Were there diffusion limitation in the resting tissue, O_2 flux (i.e., O_2 consumption) would fall at high altitude in concert with the reduction in PaO_2 and mitochondrial PO_2 per **Eq. 16**. This outcome parallels the absence of diffusion limitation at rest for O_2 uptake in the lungs. The structures enabling diffusion in both lungs and tissues are thus "overbuilt" for resting conditions, and are presumably matched to better meet the higher O_2 needs of exercise.

During normoxic exercise, it is generally believed that PmO_2 is less than 5 mm Hg,[9] and may even be in the astonishingly low range of 1 to 2 mm Hg, allowing PmO_2 to be essentially neglected in applying the Fick law of diffusion given that PaO_2 is of the order of 100 mm Hg.

Is there diffusion limitation of O_2 unloading in the tissues during normoxic exercise? Two observations taken together show that there must be a limit to unloading of O_2 in the tissues at peak exercise even during air breathing at sea level. One is that the venous blood draining the contracting muscles is never fully depleted of O_2 even during maximal exercise. In trained athletes, muscle venous O_2 saturation at peak exercise is around 20% or more[10] and thus venous PO_2 is in the 20 mm Hg range. It is even higher in untrained subjects at peak exercise. This means that some of the O_2 delivered by the circulation to the tissues is not used for muscle work, but is left in the veins to be returned to the lungs. The second observation is that when trained athletes undertake maximal exercise breathing 100% O_2, maximal external work and maximal O_2 uptake do increase, even if by only small amounts.[11] This observation can only mean that on ambient air the amount of O_2 consumed during maximal exercise does not push the mitochondria to their full capacity to use O_2—there must be some reserve in the ability of the mitochondria to use O_2 when exercising maximally in normoxia if more O_2 can be used in hyperoxia (when more O_2 is available). This raises the question of why more O_2 is not taken from the capillaries during exercise on air (where venous PO_2 does not fall below 15–20 mm Hg) to provide the mitochondria with additional usable O_2 that would enhance maximal exercise capacity. Research has shown that the primary explanation is indeed diffusion limitation of O_2 transfer from capillaries to tissue mitochondria.[12] The diffusive movement of O_2 from capillaries to mitochondria demands a sufficiently high capillary PO_2 to drive enough O_2 to the mitochondria. Thus, to achieve a high O_2 consumption, PO_2 in the tissue capillaries must not fall too low, and as a result, some O_2 remains in the capillary blood along its path from arterial to venous end to drive diffusion. Given that diffusion limitation exists during normoxic exercise, it is expected that this must also occur during hypoxic exercise, and research has shown this to be the case also.[12]

Importantly, in the tissues, there are mirror-image consequences of the nonlinearity of the O_2Hb dissociation curve in normoxia, again without these consequences in hypoxia (because here the dissociation curve is essentially linear). It was noted above that the nonlinearity of the O_2Hb dissociation curve provided a benefit to diffusive loading of O_2 in the lungs during normoxia. In the tissues, the very same nonlinearity means that as tissue blood PO_2 falls from arterial toward venous, there is initially a large fall in blood PO_2 with little loss of O_2 from Hb. So here, the driving PO_2 gradient is rapidly reduced before much O_2 has been unloaded from Hb. This is a clear disadvantage of the shape of the dissociation curve, and it likely contributes to the greater impact of diffusive limitation of movement of O_2 from blood to tissues than from alveolar gas to blood in the lungs at the same inspired PO_2 and exercise intensity.

CO_2 and Diffusion Equilibration in the Lungs and Tissues

For CO_2, α was previously indicated to be 0.067 mL CO_2/100 mL blood/mm Hg PCO_2. At rest, mixed venous PCO_2 is about 45 mm Hg while arterial PCO_2 is 40 mm Hg, also mentioned earlier. The corresponding CO_2 concentrations are about 52 and 48 mL CO_2/100 mL blood, respectively (see companion chapter fig. 11), yielding a value for β of $(52–48)/(45–40) = 0.8$ mL CO_2/100 mL blood/mm Hg PCO_2 while during exercise β is a little lower at about 0.5 mL CO_2/100 mL blood/mm Hg PCO_2 (see companion chapter fig. 15). These numbers change little with hypoxia because of the nearly linear shape of the CO_2 dissociation curve (see companion chapter fig. 11).

Thus, at rest, the α/β ratio for CO_2 is 0.08 which is about twice as high as for O_2, while during exercise the α/β ratio for CO_2 climbs to around 0.13, partially offsetting the shorter transit time in the capillaries. As a result, diffusion limitation for CO_2 has not been demonstrated either in pulmonary or tissue exchange. This is the case both at rest and during exercise, and in hypoxia as well as normoxia.

Carbon Monoxide and Diffusion Equilibration in the Lungs and Tissues

It was mentioned earlier that carbon monoxide (CO) has about 200 to 270 times the affinity for Hb as does O_2. That makes for a value of β that is 200 to 250 times as high as for O_2 when on the steep portions of their respective dissociation curves. From ►**Fig. 1**, β for O_2 on the steep portion of its curve was seen to be about 0.3 mL O_2/100 mL blood/mm Hg PO_2. Roughly, β for CO would then come to 200×0.3, or 60, mL CO/100 mL blood/mm Hg PCO. The physical solubility for CO in plasma is a little less than for O_2, at 0.0024 mL CO/100 mL plasma/mm Hg at 37°C.[13] This brings the α/β ratio for CO to 0.0024/60 or just 0.00004. It goes without saying that this incredibly low value for its α/β ratio means that CO exchange must be diffusion-limited in the lungs and tissues alike, even in health, and even at rest. This has of course been long recognized by the fact that the diffusing capacity of the lungs is measured using CO precisely because its uptake into the lung capillary blood is diffusion-limited. Measurement of diffusing capacity with an inert gas would not be possible because such a gas is not diffusion-limited.

►**Table 2** summarizes the α/β ratios for inert gases, O_2 and CO_2 at rest, and during exercise, in both normoxia and hypoxia, reflecting propensity for diffusion limitation in gas transport. That for CO, calculated only for rest in normoxia, is also provided for comparison. Any subject with significant CO poisoning would not voluntarily be exposed to hypoxia or undertake exercise, and so those conditions are not considered here. However, it is unlikely that the α/β ratio for CO during exercise or in hypoxia would differ significantly from that in normoxia at rest.

Table 2 The ratio of the physical solubility (α) for different gases in water/plasma to the average slope (β) of the dissociation curves in blood for each gas under conditions of rest and exercise in normoxia and hypoxia

Gas	Rest, normoxia	Exercise, normoxia	Rest, hypoxia	Exercise, hypoxia
Inert gases	1	1	1	1
Oxygen	0.04	0.02	0.01	0.01
Carbon dioxide	0.08	**0.13**	0.08	0.13
Carbon monoxide	0.00013	–	–	–

Notes: Color key: green = never diffusion-limited; orange = sometimes diffusion-limited; red = always diffusion-limited. Ratios of about 0.02 or less indicate vulnerability to diffusion limitation; color coding in the table associates gases, conditions, and α/β ratio to likelihood of diffusion limitation. Inert gases do not have a "dissociation curve" but their solubilities in blood and tissues are similar, so that in effect their α/β ratio will be about 1.

In summary, in a healthy subject, the followings will be present:

- Inert gas exchange in the lungs and tissues is never diffusion-limited at rest or during exercise.
- O_2 exchange in the lungs and tissues at rest is never reduced by diffusion limitation, whether in normoxia or hypoxia. This is true both in athletes and untrained subjects.
- O_2 exchange in the lungs during normoxic exercise is diffusion-limited in some athletes but not in untrained individuals. It is diffusion-limited in most healthy subjects during hypoxic exercise.
- O_2 exchange in the tissues during exercise is diffusion-limited in both normoxia and hypoxia in athletes, but mostly not diffusion-limited in untrained subjects.
- CO_2 is not seen to be diffusion-limited under any conditions (rest/exercise; normoxia/hypoxia; athletes/untrained individuals; lungs/tissues).
- CO is diffusion limited in all subjects under all conditions.

The different outcomes for the various gases considered result directly from differences in their respective dissociation curves and physical solubilities.

Physiological Significance of O_2 and CO_2 Dissociation Curve Characteristics in the Convective Steps of CO_2 and CO_2 Transport

Just as the shape and slope of the O_2 and CO_2 dissociation curves play critical roles in the diffusive steps of O_2 transport, they also affect the convective steps. In the lungs, the convective steps affected are those concerned with the intrapulmonary distribution of both ventilation (V_A) and blood flow (Q), and hence of their ratio, the ventilation/perfusion (or V_A/Q) ratio. In the tissues, the corresponding relationships are those of the intratissue distribution of both O_2 consumption (VO_2) and blood flow (Q), and their ratio, VO_2/Q. These will be discussed in turn.

Physiological Significance of O_2 and CO_2 Dissociation Curve Characteristics in Pulmonary V_A/Q Relationships

Some 75 years ago, pulmonary gas exchange was developed as a quantitative discipline.[14–16] Applying the fundamental principle that during transport between the air and the tissues the mass of O_2 (or CO_2) being transported was conserved across each step of the transport pathway, it was realized that the ventilation/perfusion (V_A/Q) ratio in any small homogeneous region of the lung determined the local values of alveolar PO_2 (and PCO_2) in that region. This topic is more fully treated in another chapter. Equations espousing the basic principle of conservation of mass were advanced as follows, with that for O_2 appearing as **Eqs. 17** and **18**:

$$VO_2 = V_I \times FIO_2 - V_A \times FAO_2 \qquad \textbf{Eq. 24}$$

$$VO_2 = Q \times [CecO_2 - C\bar{v}O_2] \qquad \textbf{Eq. 18}$$

In both equations, VO_2 is the amount of O_2 crossing per minute from the alveolar gas (**Eq. 17**) into the pulmonary capillary blood (**Eq. 18**). **Eq. 18** is the familiar equation defining the Fick principle. V_I and V_A represent inspired and expired alveolar ventilation of the region, while FIO_2 and FAO_2 represent inspired and expired alveolar fractional concentrations of O_2 for that region; Q is blood flow, $CecO_2$ is regional end-capillary O_2 concentration, and $C\bar{v}O_2$ is pulmonary arterial (i.e., mixed venous) O_2 concentration.

Note that V_I differs from V_A only when the respiratory exchange ratio is not 1.0: $V_A = V_I - VO_2 + VCO_2$. Given that, scaled for the whole lung at rest, V_I is about 6 L/min, VO_2 is about 300 mL/min, and VCO_2 is about 240 mL/min, V_A will almost equal V_I ($V_A = 99\%$ of V_I in this example). For simplicity, equality between V_I and V_A will now be assumed. Dalton's law of partial pressures allows FIO_2 and FAO_2 to be expressed as partial pressures: $PIO_2 = (PB - PH_2O) \times FIO_2$; $PAO_2 = (PB - PH_2O) \times FAO_2$.

Recognizing mass conservation such that VO_2 in these two equations are the same, the two equations can be combined as follows:

$$V_A \times (PIO_2 - PAO_2) \,/\, (PB - PH_2O) = Q \times [CecO_2 - CvO_2] \qquad \textbf{Eq. 19}$$

With V_A traditionally expressed in L/min BTPS and $CecO_2$ and CvO_2 usually expressed in mL O_2 STPD/100 mL blood, a correction for conversion of V_A to STPD must be made for the equation to hold true. When this is done, units reconciled, and the equation is rearranged, the outcome is this:

$$V_A/Q = 8.63 \times [CecO_2 - CvO_2] \,/\, [PIO_2 - PAO_2] \qquad \textbf{Eq. 20}$$

A further assumption is made for simplification of the analysis: that there is no diffusion limitation, such that PAO_2 equals $PecO_2$. This means that PAO_2 and $CecO_2$ correspond to the same point on the O_2Hb dissociation curve. In final form, the equation looks like this:

$$V_A/Q = 8.63 \times [CecO_2 - CvO_2] / [PIO_2 - PecO_2] \qquad \textbf{Eq. 21}$$

This analysis shows that the right-hand side numerator reflects blood O_2 concentrations while the denominator reflects partial pressures. The important conclusion in the present context is that the O_2Hb dissociation curve is implicit in, and a key component of, **Eq. 21**.

Exactly the same analysis for CO_2 yields this equation:

$$V_A/Q = 8.63 \times [CvCO_2 - CecCO_2] / [PecCO_2 - PICO_2] \qquad \textbf{Eq. 22}$$

Thus, the same conclusion applies for CO_2: its dissociation curve is firmly embedded in **Eq. 22**.

Both equations can be expressed in words: For any given set of boundary conditions (meaning inspired and mixed venous O_2 and CO_2 values) and dissociation curve configuration, the V_A/Q ratio of a homogeneous region of lung uniquely determines its alveolar PO_2 and PCO_2.

How does this play out in overall pulmonary gas exchange? It turns out that the very same approach to approximating the O_2 and CO_2 dissociation curves by a straight line joining arterial and venous values, thus defining their overall "solubility" as in ►**Fig. 1** provides much insight. The key point is that the average slope of the O_2Hb dissociation curve at 0.08 is some 10-fold less than that of CO_2 at 0.8 (mL gas/100 mL blood/mm Hg). Using **Eq. 3** (from "Blood Gas Transport: Carriage of Oxygen and Carbon Dioxide in Blood") above, these numbers translate to de facto blood:gas partition coefficients of around 0.6 and 6, respectively.

►**Fig. 2** shows an analysis[17] of the interference to overall gas exchange for gases across the range of blood:gas partition coefficients from very low (0.0001) to very high (10,000). The red and blue lines in each panel display the relative interference to gas exchange (on a scale from 0 interference to what amounts to a 50% reduction in total gas exchanged, scaled as 0.5 on the ordinate) for inert gases. The vertical green dashed lines and symbols refer to O_2 and CO_2 and where they would each be situated along the *x*-axis, given the slopes of their dissociation curves expressed as equivalent blood:gas partition coefficients. The two panels together display the patterns of gas exchange interference in four different scenarios.

The red line in panel (A) indicates how interference varies systematically with gas partition coefficient in a lung having half of its blood flow associated with normally ventilated alveoli and the other half perfusing regions that are very poorly ventilated. The pattern is smooth, and peaks in this example for a gas with a low partition coefficient of about 0.01. Gases of both lower and higher solubility are seen to be less affected. The important observation from this line is that O_2 exchange would be reduced by about 35% while that for CO_2 would be reduced by much less—by only about 10% (red solid circles). The blue line in panel (A) is the outcome when all ventilation to half the lung is eliminated, creating a 50% shunt. The solid blue circles (that for CO_2 is hidden behind the red circle) indicate the relative reductions in gas exchange for the two gases, and they are very similar between the two conditions.

The conclusions from panel (A) are that:

- O_2 exchange is affected more than 3× as much as that for CO_2 in this example, but both gases suffer significant reductions in their ability to be exchanged when areas of low or zero V_A/Q ratio develop in the lungs.
- The outcomes in each case are quantitatively similar for O_2, and also similar for CO_2.
- The explanation for the greater sensitivity of O_2 to shunt and low V_A/Q regions is the different slopes of the dissociation curves of the two gases.

Turning to panel (B), this mirror-image chart shows how O_2 and CO_2 exchange are reduced when very high, but still

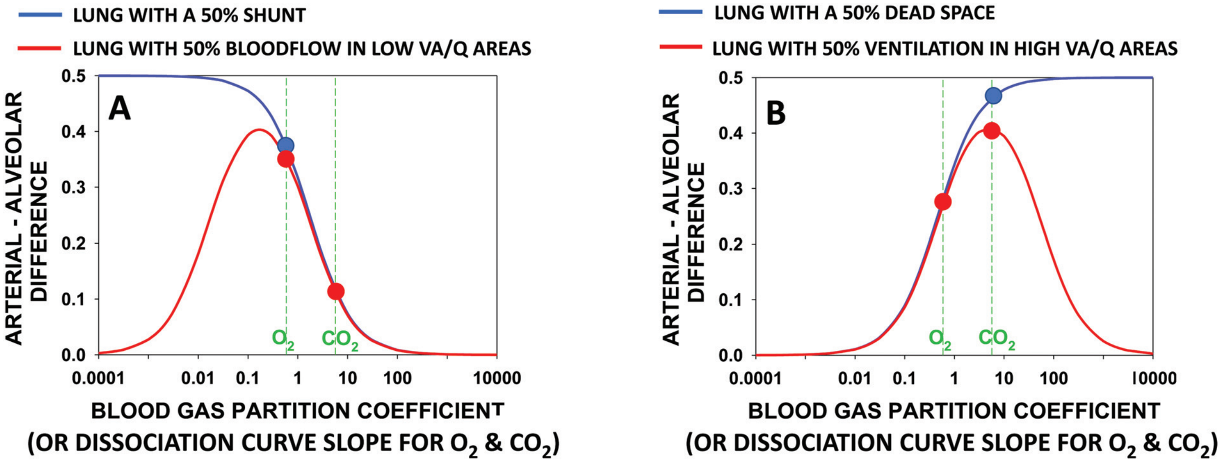

Fig. 2 How the solubility (or partition coefficient) of a gas affects its overall exchange in the lungs when poorly or unventilated regions exist (left, **A**) and when poorly or unperfused regions exist (right, **B**). The ordinate indicates fractional reduction in gas exchange (0 = no reduction; 1 = complete absence of gas exchange). The respiratory gases O_2 and CO_2 are positioned on the abscissa based on partition coefficients corresponding to the average slopes of their respective dissociation curves. See text for full analysis of this figure from reference 17.

slightly perfused, V_A/Q areas are present (red line) or when perfusion is eliminated and the V_A/Q ratio becomes infinite, known as dead space (blue line). In this type of abnormality, it is evident that CO_2 exchange is affected more than that of O_2.

The conclusions from panel (B) are that:

- CO_2 exchange is affected more that of O_2 by about 50 to 90% in this example, but again, both gases suffer significant reductions in their ability to be exchanged.
- The outcomes in each case are quantitatively similar for O_2, and also similar for CO_2.
- The explanation for the greater sensitivity of CO_2 to dead space and high V_A/Q regions is the different slopes of the dissociation curves of the two gases.

In summary, the slopes of the O_2 and CO_2 dissociation curves play a major role in determining the degree of interference to their exchange across the lungs. In lungs with poorly or unventilated regions (often from pneumonia, pleural effusion, or atelectasis), O_2 is affected more than is CO_2, while when poorly or unperfused regions develop (often from pulmonary thromboembolism, hypotension, or in ventilated patients, from high ventilator pressures) CO_2 is the more affected gas.

Physiological Significance of O_2 and CO_2 Dissociation Curve Characteristics in Tissue VO_2/Q Relationships

As mentioned above, the convective issue of interest in tissue gas transport is the relationship between regional VO_2 and blood flow (Q), and their ratio, VO_2/Q. In this circumstance, we can make use of the Fick principle of mass conservation which states that the VO_2 of a tissue in a steady state is given by the product of its blood flow and the arteriovenous O_2 concentration difference:

$$VO_2 = Q \times [CaO_2 - CvO_2] \qquad \textbf{Eq. 23}$$

This is basically the same as **Eq. 18** as used in the lungs. It applies equally well in the tissues, noting that while CaO_2 (arterial $[O_2]$) is the same for all tissue regions, VO_2, Q, and CvO_2 denote the specific (regional) tissue values for O_2 consumption, blood flow, and hence venous $[O_2]$ of that region.

Rearranging **Eq. 23** yields:

$$CvO_2 = CaO_2 - VO_2 / Q \qquad \textbf{Eq. 24}$$

This shows that the effluent regional tissue venous O_2 concentration is a simple function of the regional VO_2/Q ratio of that region and does not depend on the O_2Hb dissociation curve. However, using the linear approximation to the O_2Hb dissociation curve for simplicity, such that $[O_2] = \beta \times PO_2$ as discussed and used earlier,

$$PvO_2 = PaO_2 - VO_2 / (\beta \times Q) \qquad \textbf{Eq. 25}$$

This shows that the partial pressure of O_2 in the venous blood from a tissue (region) with a given VO_2/Q ratio does depend on the slope of the O_2Hb dissociation curve (β), which is, however, similar in all tissue regions. What potentially differs between tissue regions is VO_2, Q, and thus their ratio VO_2/Q.

For CO_2, the corresponding outcomes are these:

$$CvCO_2 = CaCO_2 + VCO_2 / Q \qquad \textbf{Eq. 26}$$

$$PvCO_2 = PaCO_2 + VCO_2 / (\beta \times Q) \qquad \textbf{Eq. 27}$$

The conclusions are qualitatively similar to those for O_2 in that the slope of the CO_2 dissociation curve plays a major role in establishing the venous PCO_2. The difference in β between the two gases explains why the fall in PO_2 from arterial to venous is generally much greater than the increase in PCO_2 from arterial to venous (for the same VO_2, VCO_2, and Q): Since β is higher for CO_2 than for O_2, the increase in $PvCO_2$ above $PaCO_2$ is smaller than is the fall in PO_2 from arterial to venous values (see companion chapter figs. 14 and 15).

These general conclusions will apply whether the exchange of O_2 and/or CO_2 is diffusion-limited or not as **Eqs. 24** to **27** simply reflect mass conservation, which will exist whether or not there is diffusion limitation for either gas.

At this point, there is very little known about regional inequality of VO_2/Q ratios in the tissues (in contrast to V_A/Q inequality in the lungs which has been well-studied). What data do exist suggests that there is minimal VO_2/Q heterogeneity across muscle regions, likely considerably less than in the normal lung for V_A/Q ratios.[18] Thus, the analysis presented for how the dissociation curve differences are important in the response of O_2 and CO_2 to different patterns of VO_2/Q inequality cannot be reliably done for the tissues as detailed estimates of inequality in VO_2/Q ratios are not available, and those which do exist reveal very little inequality.

Conclusion

This article has provided an extensive discussion of how the differences in the ways in which the two gases O_2 and CO_2 are carried in blood affect the fundamental transport processes of diffusion and convection that are at the core of the overall gas transport system responsible for exchanging both gases between the air and the tissues. In particular, the shapes and slopes of the two gases dictate many of their physiological properties in transport and exchange. The greater vulnerability of O_2 (compared to CO_2) to diffusion limitation in both lung and tissue exchange is directly attributable to differences in the dissociation curves. Similarly, the differences in vulnerability of the two gases to different patterns of ventilation/perfusion inequality in the lung are also attributable to the differences in their dissociation curves. In sum, differences in the shape and slope of the dissociation curves of O_2 and CO_2 explain the differences in their physiological behavior in gas transport and exchange, both at the lungs and in the tissues.

Conflict of Interest
None declared.

References

1 Weibel ER. The Pathway for Oxygen: Structure and Function in the Mammalian Respiratory System. Cambridge Mass: Harvard University Press; 1984

2 Piiper J, Scheid P. Blood-gas equilibration in the lungs. In: J.B W, ed. Pulmonary Gas Exchange Volume 1. Ventilation, Blood Flow and Diffusion. new York, NY: Academic press; 1980:131–173

3 Piiper J, Scheid P. Model for capillary-alveolar equilibration with special reference to O2 uptake in hypoxia. Respir Physiol 1981;46(03):193–208

4 Piiper J, Scheid P. Comparison of diffusion and perfusion limitations in alveolar gas exchange. Respir Physiol 1983;51(03):287–290

5 Piiper J, Scheid P. Diffusion limitation of O2 supply to tissue in homogeneous and heterogeneous models. Respir Physiol 1991;85(01):127–136

6 Piiper J, Scheid P. Modeling oxygen availability to exercising muscle. Respir Physiol 1999;118(2-3):95–101

7 Dempsey JA, Wagner PD. Exercise-induced arterial hypoxemia. J Appl Physiol 1999;87(06):1997–2006

8 Wagner PD, Gale GE, Moon RE, Torre-Bueno JR, Stolp BW, Saltzman HA. Pulmonary gas exchange in humans exercising at sea level and simulated altitude. J Appl Physiol (1985) 1986;61(01):260–270

9 Richardson RS, Noyszewski EA, Kendrick KF, Leigh JS, Wagner PD. Myoglobin O2 desaturation during exercise. Evidence of limited O2 transport. J Clin Invest 1995;96(04):1916–1926

10 Andersen P, Saltin B. Maximal perfusion of skeletal muscle in man. J Physiol 1985;366(01):233–249

11 Richardson RS, Grassi B, Gavin TP, et al. Evidence of O2 supply-dependent VO2 max in the exercise-trained human quadriceps. J Appl Physiol 1999;86(03):1048–1053

12 Roca J, Hogan MC, Story D, et al. Evidence for tissue diffusion limitation of VO2max in normal humans. J Appl Physiol (1985) 1989;67(01):291–299

13 Schmidt U. The solubility of carbon monoxide and hydrogen in water and sea-water at partial pressures of about 10-5 atmospheres. Tellus 1979;31(01):68–74

14 Rahn H, Fenn WO. Graphical Analysis of the Respiratory Gas Exchange. Bethesda, MD: American Physiological Society; 1955

15 Riley RL, Cournand A. Analysis of factors affecting partial pressures of oxygen and carbon dioxide in gas and blood of lungs; theory. J Appl Physiol 1951;4(02):77–101

16 Riley RL, Cournand A. Ideal alveolar air and the analysis of ventilation-perfusion relationships in the lungs. J Appl Physiol 1949;1(12):825–847

17 Wagner PD, Malhotra A, Prisk GK. Using pulmonary gas exchange to estimate shunt and deadspace in lung disease: theoretical approach and practical basis. J Appl Physiol (1985) 2022;132(04):1104–1113

18 Vogiatzis I, Habazettl H, Louvaris Z, et al. A method for assessing heterogeneity of blood flow and metabolism in exercising normal human muscle by near-infrared spectroscopy. J Appl Physiol (1985) 2015;118(06):783–793

Article published online: 2023-08-04

Tissue Perfusion and Diffusion and Cellular Respiration: Transport and Utilization of Oxygen

Connie C. W. Hsia, MD, FCCP, ATSF[1]

[1] Division of Pulmonary and Critical Care Medicine, Department of Internal Medicine, University of Texas Southwestern Medical Center, Dallas, Texas

Semin Respir Crit Care Med 2023;44:594–611.

Address for correspondence Connie C. W. Hsia, MD, FCCP, ATSF,
Division of Pulmonary and Critical Care Medicine, Department of
Internal Medicine, University of Texas Southwestern Medical Center,
5323 Harry Hines Boulevard., Dallas, TX 75390-8884
(e-mail: Connie.Hsia@utsouthwestern.edu).

Abstract

This article provides an overview of the journey of inspired oxygen after its uptake across the alveolar–capillary interface, and the interplay among tissue perfusion, diffusion, and cellular respiration in the transport and utilization of oxygen. The critical interactions between oxygen and its facilitative carriers (hemoglobin in red blood cells and myoglobin in muscle cells), and with other respiratory and vasoactive molecules (carbon dioxide, nitric oxide, and carbon monoxide), are emphasized to illustrate how this versatile system dynamically optimizes regional convective transport and diffusive gas exchange. The rates of reciprocal gas exchange in the lung and the periphery must be well-matched and sufficient for meeting the range of energy demands from rest to maximal stress but not excessive as to become toxic. The mobile red blood cells play a vital role in matching tissue perfusion and gas exchange by dynamically regulating the controlled uptake of oxygen and communicating regional metabolic signals across different organs. Intracellular oxygen diffusion and facilitation via myoglobin into the mitochondria, and utilization via electron transport chain and oxidative phosphorylation, are summarized. Physiological and pathophysiological adaptations are briefly described. Dysfunction of any component across this integrated system affects all other components and elicits corresponding structural and functional adaptation aimed at matching the capacities across the entire system and restoring equilibrium under normal and pathological conditions.

Keywords
- oxygen
- hemoglobin
- allosterism
- myoglobin
- electron transport
- oxidative phosphorylation
- mitochondrial coupling

Venous blood returning to the lung follows a hierarchical fractal pattern of branching blood vessels alongside a parallel network of airways. The stratified bronchovascular bundle extends into the acini and the alveolar–capillary units, ending in a web of capillaries covered by an extremely thin layer of tissue composed of cells, fibers, and matrix establishing an extensive surface area across which oxygen (O_2) diffuses from air to blood, enters the red blood cells (RBCs) and binds to hemoglobin (Hb). The oxygenated blood returns to the left heart via the pulmonary veins and is distributed to organs according to their metabolic needs. Within tissue capillaries, O_2 is unloaded from Hb in response to local metabolic signals and diffuses into cells along its concentration gradient. In muscle cells, $O_2 \geq 2$ diffusion is facilitated by myoglobin (Mb). Simultaneously, carbon dioxide (CO_2) produced as a metabolic byproduct is released into the blood, where it either dissolves in plasma, is converted to bicarbonate, or reacts with Hb; this reaction facilitates O_2 unloading from Hb, which in turn facilitates CO_2 uptake by Hb. The transport of vasoactive gases such as nitric oxide (NO) and carbon monoxide (CO) is also governed by their interactions with O_2 and Hb to modulate vascular function and gas and solute exchange. Within the end-organ cells, O_2 is consumed during oxidative phosphorylation to produce energy for cellular metabolism, while CO_2 is released into capillary blood and transported back to the lungs for elimination by

article published online
August 4, 2023

Issue Theme Pulmonary Physiology; Guest Editors: David A. Kaminsky, MD, Kathryn A. Hibbert, MD, and Andrew M. Luks, MD

Thieme Medical Publishers, Inc.,
333 Seventh Avenue, 18th Floor,
New York, NY 10001, USA

DOI https://doi.org/10.1055/s-0043-1770061.
ISSN 1069-3424.

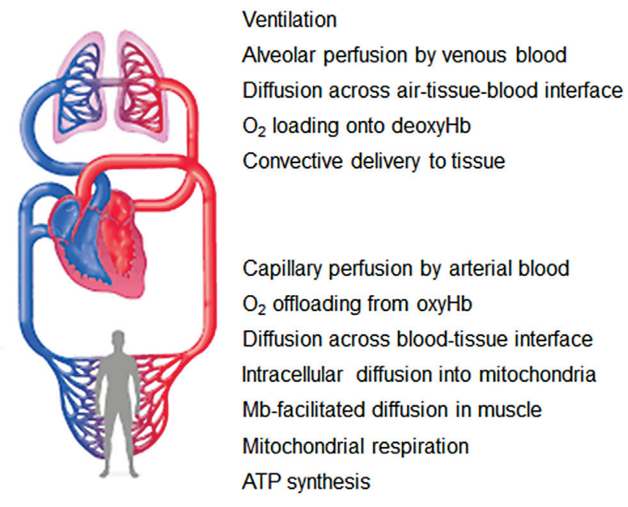
Ventilation
Alveolar perfusion by venous blood
Diffusion across air-tissue-blood interface
O_2 loading onto deoxyHb
Convective delivery to tissue
Capillary perfusion by arterial blood
O_2 offloading from oxyHb
Diffusion across blood-tissue interface
Intracellular diffusion into mitochondria
Mb-facilitated diffusion in muscle
Mitochondrial respiration
ATP synthesis

Fig. 1 Overview of the physiological processes during respiration in the lung and the extra-pulmonary tissue. ATP, adenosine triphosphate; deoxyHb, deoxyhemoglobin; Mb, myoglobin; oxyHb, oxyhemoglobin.

ventilation, thus completing the cycle of gas transport and exchange. These major physiological processes are shown in ►**Fig. 1**.

The rates of pulmonary and peripheral gas exchange must be well-matched and sufficient for meeting the range of energy demands from rest to peak exercise intensity. However, uptake and delivery must not be excessive as these gases are also potent toxins. To achieve this balance, precise feedback mechanisms evolved to monitor O_2 delivery to tissues and communicate their metabolic needs to the heart and lungs. The transport structures responsible for O_2 delivery, e.g., vascular size and tone, are anatomically and functionally adapted. The mobile RBCs play a vital role in gas exchange by dynamically regulating the controlled uptake and release of O_2 and communicating the metabolic signals between the lungs and the end organs. This article provides an overview of the interplay between tissue perfusion, diffusion, and respiration in the transport and utilization of O_2 following its uptake across the lung.

Tissue Perfusion

Whole body blood flow is the total volume of blood pumped by the heart through the systemic circulation per unit of time, expressed in (L.min^{-1}) or as a percentage of total cardiac output. *Tissue perfusion*, on the other hand, refers to the blood delivery to the tissue capillaries where gas and solute exchanges take place, expressed per unit tissue mass or volume (in mL.[min.mL of tissue]$^{-1}$ or mL.[min.g of tissue]$^{-1}$) in specific organs or regions. Inadequate perfusion predisposes to tissue hypoxia, cell damage, and eventually death. Hypo-perfusion or nonuniform distribution of perfusion impairs the overall efficiency of gas and solute exchange, leading to patchy regions of tissue hypoxia and damage. Hyper-perfusion can lead to hemodynamic compromise, tissue edema, and injury secondary to elevated mechanical and/or oxidative stress. *Tissue blood flow rate* is a primary determinant of tissue perfusion, and is modulated by multiple interrelated factors, including:

1. *Cardiac output* ($\dot{Q}c$; [liters of blood]·min^{-1}) = stroke volume (mL) × heart rate (beats/minute). The factors affecting cardiac output are shown in ►**Fig. 2**.[1] Cardiac systolic function is determined by the preload (the degree of ventricular stretch at end-diastole, or end-diastolic pressure), contractility (strength of muscle contraction during systole), and afterload (resistance or the total force needed to eject blood, or systemic vascular resistance). The systemic circulation returns deoxygenated venous blood to the right heart while the pulmonary circulation returns oxygenated blood to the left heart; both circulations are compliant, low pressure, and slow emptying. In contrast, the ventricles are less compliant with fast emptying rates that vary with myocardial contractility. Arterial pressures (systolic, diastolic, or mean) are commonly used as surrogate indices of afterload while systemic arterial resistance may be measured using invasive and noninvasive methods. Matching the mechanical outputs from the two compartments is a major determinant of cardiac output.[2] The pulsatile myocardial contractions accelerate ventricular emptying permitting an increase in stroke volume and cardiac output with sympathetic stimuli; however, pulsatile contractions also constrain peak stroke volume and cardiac output by reducing the time available for ventricular filling during diastole.[3] The relationship between stroke volume and left ventricular end-diastolic pressure is described by the Frank–Starling curve[3] (►**Fig. 2**).
2. *Systemic blood pressure and vascular tone*: tissue perfusion pressure depends on the transmission of mean arterial pressure (MAP; mm Hg) to the capillary level (**Eq. 1**):

$$\text{MAP} = \text{Systolic BP} + \left[\tfrac{2}{3} \cdot \text{Diastolic BP}\right] \qquad \textbf{Eq. 1}$$

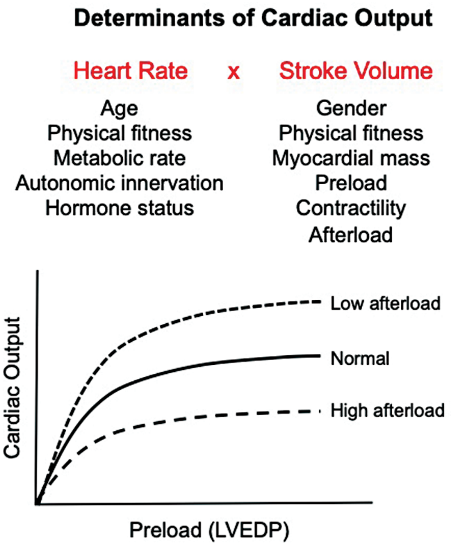

Fig. 2 The determinants of cardiac output (upper panel), the Frank–Starling curve, and the effects of afterload on the cardiac output (lower plot). LVEDP: left ventricular end-diastolic pressure.

An adequate perfusion pressure is essential to overcome blood flow resistance imposed by vessel diameter, luminal obstruction, hydrodynamic turbulence, blood viscosity, and RBC deformation. Capillary perfusion is also determined by the compliance of arterioles and precapillary sphincters, which may be altered by a plethora of neural, hormonal, and metabolic vasoregulatory factors. Stimuli that promote vasoconstriction, e.g., sympathetic nervous system activation, angiotensin-II agonists, or cold exposure, impede blood flow and central MAP transmission to the periphery, thereby reducing capillary perfusion. Administration of vasoconstrictors maintains central perfusion pressure at the expense of pressure transmission to the periphery, predisposing to capillary and tissue hypoperfusion. Stimuli that cause vasodilation, e.g., parasympathetic nervous system activation, NO release, hyperthermia, hypotension, calcium channel blockers, or smooth muscle relaxants, have the opposite effect by increasing capillary perfusion.[4,5] While smooth muscle in the arterioles and precapillary sphincters have been considered the main sites that regulate micro-vessel diameter and peripheral vascular resistance,[6] pericytes surrounding the capillaries are also contractile in response to stimuli such as ischemia and changes in O_2 and CO_2 tensions, and contribute to the regulation of local capillary diameter, blood flow, and resistance.[7–10] Capillary perfusion pressure is more effectively maintained via vasodilation than via vasoconstriction; the opposing and interacting vasoregulatory factors allow local modulation of gas exchange surface area and barrier distance for diffusion.

3. *Blood viscosity hemodilution* or *anemia* reduces hematocrit and viscosity, thereby reducing flow resistance and improving central MAP transmission and capillary perfusion at a given MAP. Hemodilution enhances blood flow and shear stress in arteriolar walls, associated with nitric oxide (NO) release from vascular endothelial and smooth muscle cells to mediate arteriolar vasodilation and increase capillary perfusion.[11,12] However, should shear stress-mediated vasodilatory capacity be exhausted as in extreme hemodilution, capillary perfusion pressure and the number of patent capillaries will be reduced.

Hemoconcentration due to dehydration, polycythemia, or pathological RBC rheology such as in sickle cell disease, increases blood viscosity and exerts biphasic effects on tissue perfusion. Increasing plasma viscosity initially stimulates arteriolar vasodilation to maintain a normal capillary perfusion pressure; however, an excessively high viscosity impedes capillary perfusion.[11,13]

Measurement of Blood Flow and Microvascular Perfusion

Multiple modalities are used to assess blood flow and tissue perfusion. Ultrasonography is commonly used to assess the flow direction, volume, and turbulence of blood cells in larger vessels, e.g., perfusion of the fetus during pregnancy or detecting venous thrombosis.[14] This method is enhanced by laser Doppler flowmetry (LDF) and imaging, utilizing dynamic light scattering to track soundwave of particles in blood to produce two-dimensional color images of their flow pattern.[15] Because LDF measures the flux of blood cells (flow rate per unit of area) rather than actual volumetric blood flow, it may over- or under-estimate real blood flow in conditions of low or high hematocrit, respectively, and cannot reliably compare perfusion among subjects.[16,17] Contrast-enhanced angiography follows the dynamic passage of a bolus of injected contrast agent, e.g., iodine in computed tomography (CT), gadolinium in magnetic resonance imaging (MRI), or radioactive tracers in scintigraphy, positron emission tomography (PET), and single-photon emission CT (SPECT).[18] Noninvasive imaging methods include arterial spin-labeling MRI where the magnetic field is transiently altered and used to tag the flowing RBCs and follow their transit.[19] In addition to imaging, indicator dilution techniques are used. In the thermodilution technique, cold saline is injected to alter blood temperature; the rate of downstream temperature change is measured to index the rate of blood flow.[17]

The anatomical capillary density may be directly measured ex vivo under light or electron microscopy from biopsy or surgical samples, e.g., muscle.[20,21] Capillary refill time is a bedside assessment used to ascertain peripheral perfusion in patients for an array of conditions.[22] In vivo capillary perfusion may be inferred by imaging microvascular blood flow in superficial sites, deriving the functional capillary density (FCD, cm^{-1}, length of capillaries with flowing RBCs per unit cross-sectional tissue area) as a surrogate indicator reflecting the quality of tissue perfusion and the mean path length for O_2 diffusion from capillaries to the cells.[23,24] LDF and darkfield videomicroscopy can visualize blood cells transiting through the cutaneous or sublingual microcirculation.[25,26] Fluorescein microangiography is commonly used to assess perfused retinal vessels.[27] Other modalities including radionuclide scintigraphy, CT angiography, and PET are also techniques employing tracer compounds to assess in vivo microvascular perfusion in different organs.[28]

Oxygen Delivery to the Tissue Capillaries

Total O_2 delivery, or more correctly the amount of O_2 available to the tissues (in [mL of O_2]·min^{-1}), is the product of cardiac output ($\dot{Q}c$, [liters of blood]·min^{-1}) and the O_2 concentration or content of arterial blood (CaO_2, [mL of O_2]·[dL of arterial blood]$^{-1}$; **Eq. 2**); the factor 10 reconciles the units.

$$\text{Total body } O_2 \text{ delivery} = \dot{Q}c \cdot CaO_2 \cdot 10 \qquad \textbf{Eq. 2}$$

These determinants of CaO_2 are discussed below:

1. *Oxygen delivery to and uptake by Hb in alveolar capillaries*: ventilatory delivery of O_2 to the distal lung may be compromised by ambient hypoxia, hypoventilation, or impaired matching of ventilation and perfusion. Diffusive uptake of O_2 across the alveolar–capillary barrier and binding to Hb may be altered by pathology of distal

lung parenchyma or microangiopathy. Normally the ratio of ventilation ($\dot{V}$) to alveolar perfusion ($\dot{Q}$) is well matched in the normal lung ($\dot{V}/\dot{Q}$ ratio = 1.0).[29] A reduced $\dot{V}/\dot{Q}$ ratio or shunt ($\dot{V}/\dot{Q}$ ratio = 0) reflects inadequate gas exchange due to blood flow through poorly ventilated or nonventilated lung regions (e.g., pneumonia, fibrosis), which reduces arterial O_2 tension and content and the total O_2 available to the periphery. An elevated $\dot{V}/\dot{Q}$ ratio reflects elevated or wasted ventilation (e.g., hyperventilation) or reduced perfusion (e.g., low cardiac output or vascular obstruction), which impairs carbon dioxide (CO_2) elimination, stimulates the respiratory center, and increases ventilatory effort and the work of breathing.[30] Derangement of $\dot{V}/\dot{Q}$ matching and shunt are the commonest physiological abnormalities in pulmonary diseases.

2. *The O_2 carrying capacity of Hb ($g.dL^{-1}$*; **Eq. 3**). Each gram of adult Hb A can bind 1.34 mL of O_2:

$$O_2 \text{ carrying capacity of Hb} = 1.34 \cdot [\text{Hb}] \qquad \textbf{Eq. 3}$$

3. *The saturation of O_2-binding sites on Hb (SaO_2, %)* according to the oxyhemoglobin dissociation curve (ODC; discussed below). Normal SaO_2 is approximately 97% at a normal arterial O_2 tension of 100 mm Hg, and mixed venous blood saturation is 60 to 80% at an O_2 tension (PO_2) of approximately 40 mm Hg.
4. A small amount of free O_2 is *dissolved in plasma*, determined by the solubility constant (= 0.0031 [mL of O_2]·[mm Hg of O_2·dL of blood]$^{-1}$) and the partial pressure of arterial O_2 (PaO_2, mm Hg; **Eqs. 4 and 5**).

$$\text{Dissolved } O_2 \text{ in plasma} = (0.0031 \cdot Pa_{O_2}) \qquad \textbf{Eq. 4}$$

Combining (2), (3), and (4), the total arterial O_2 content ([mm Hg of O_2·dL of blood]$^{-1}$) is

$$CaO_2 = \left(1.34 \cdot [\text{Hb}] \cdot \frac{Sa_{O_2}}{100}\right) + (0.0031 \cdot Pa_{O_2}) \qquad \textbf{Eq. 5}$$

In a normal adult male (resting cardiac output 5 L·min^{-1}), total body O_2 delivery is approximately 1 L·min^{-1}, distributed among organs in proportion to the size of their microvascular network and the magnitude of metabolic requirements. Total-body O_2 delivery alone cannot accurately reflect regional alterations or compensation. For example, in cardiopulmonary diseases during maximal exercise, an excessively elevated work of breathing mandates increased perfusion to respiratory muscles at a given cardiac output, thereby reducing the O_2 available to locomotive muscles and other organs, i.e., the "respiratory muscle steal" phenomenon.[31,32]

Oxygen Extraction

The amount of O_2 extracted by tissue is the difference in O_2 content between arterial (CaO_2) and mixed venous ($C\bar{v}O_2$) blood. The *Fick equation* describes total tissue O_2 consumption ($\dot{V}O_2$, in mL of O_2·min^{-1}) as the amount of O_2 removed from the total cardiac output ($\dot{Q}c$, L of blood·min^{-1}) during blood transit from the arteries to the veins, i.e., arterio-venous O_2 content difference ([CaO_2−$C\bar{v}O_2$], in mL O_2·dL blood^{-1}; **Eq. 6**). The factor of 10 reconciles the units.

$$\dot{V}O_2 = \dot{Q}c \cdot [CaO_2 - C\bar{v}O_2] \cdot 10 \qquad \textbf{Eq. 6}$$

The absolute arterio-venous O_2 content difference may also be expressed as a percentage of the arterial O_2 content (**Eq. 7**):

$$O_2 \text{ extraction } (\%) = \frac{[CaO2 - C\bar{v}O2]}{CaO2} \cdot 100 \qquad \textbf{Eq. 7}$$

The normal O_2 extraction ratio is approximately 25% at rest and may increase up to approximately 75% under extreme metabolic stress or heavy exercise. The amount of O_2 extracted from arterial blood by the tissues provides important neuro-chemical signals to the cardiopulmonary and vascular systems to elicit feedback adjustment of O_2 delivery. An elevated O_2 extraction by end-organs (e.g., with exercise, hyperthermia, infection, or inflammation) triggers compensatory mechanisms including hyperventilation, increased cardiac output, and vasodilation, aimed at restoring O_2 delivery, matching tissue perfusion to demand, and maintaining the O_2 supply–demand equilibrium. Total body O_2 extraction alone cannot describe the regional variations in O_2 extraction within or among organs.

Unloading Oxygen from Red Blood Cells

In tissue capillaries, O_2 bound to Hb is released for diffusion into cells. This is a highly orchestrated process as the RBCs dynamically sense the metabolic status and energy demands of surrounding tissue, differentially release O_2 in concert with the reciprocal uptake of CO_2 from tissue, react with nitrogenous compounds such as NO to effect vasoregulation, and carry the chemical signals via venous blood flow back to the lung, heart, and brainstem respiratory center, thereby coordinating neuro-humoral feedback adjustments in respiratory drive, pulmonary O_2 uptake, cardiovascular hemodynamics, and peripheral microvascular tone.[33,34]

At a given cardiac output and CaO_2, the size, shape, deformability, Hb content, distribution, and metabolic state of the RBCs determine their interaction with local microvasculature and consequently the efficiency of O_2 offloading. The metabolic state of the RBCs, and the allosteric interactions of O_2 and CO_2 with Hb, allow RBCs to gauge the metabolic needs of tissue and respond by fine-tuning the off-loading of O_2. In addition to O_2 and CO_2, allosteric interactions between Hb and vasoactive molecules such as NO and CO modulate local vasomotor tone.[35,36] These rapid Hb-mediated regional responses optimize both O_2 uptake in the lung and O_2 release in the periphery. The critical role of RBCs in regulating gas exchange is reviewed in detail elsewhere[33,34] and summarized below.

Physical Properties of Red Blood Cells

Free Hb has a short plasma half-life and is rapidly excreted via the kidney. Free Hb also avidly scavenges NO leading to

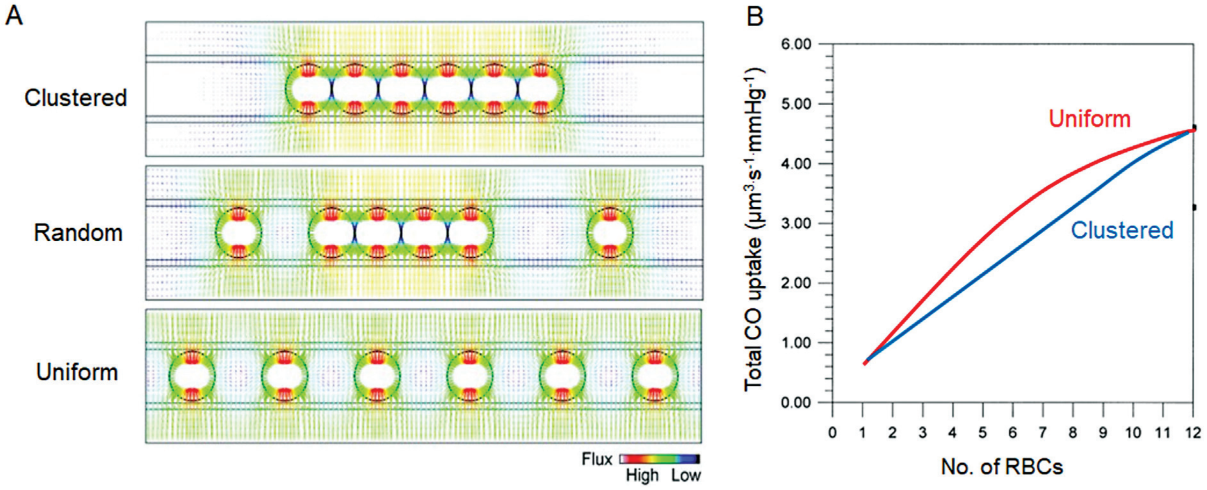

Fig. 3 RBC distribution alters gas exchange with Hb. (**A**) Simulated diffusive flux of carbon monoxide (CO) uptake by RBCs arranged in different distributions (clustered, random, and uniform) along the same length of the capillary. (**B**) The relationships of total gas uptake with respect to the number of RBCs are shown for CO. The uniform RBC distribution yields the highest and the clustered distribution the lowest uptake; random nonuniform distributions yield intermediate results. Adapted with permission from Hsia et al.[51]

widespread vasoconstriction.[37] Sequestering Hb within RBCs prevents undesirable vasoconstriction and facilitates controlled interactions among the four Hb subunits and with other blood constituents. However, compared with free Hb in the plasma, the RBC membrane adds resistance to diffusion[38] and increases the diffusion distance for O_2 to reach the endothelium while the mechanical stress and strain experienced by flowing RBCs add hemodynamic resistance. These caveats mandate that RBCs be sturdy and flexible, and not too large or too small.

Red Blood Cell Size, Shape, and Distribution

Tissue capillaries are approximately 4 to 5 µm in diameter. Blood flow velocity causes deformation and shear stress on RBCs and the endothelium. To minimize mechanical stress, the RBCs undergo drastic morphological changes during maturation by downsizing (to approximately 7 µm in diameter or 25–30% larger than capillary diameter[39]) and expelling their nuclei and most organelles[40] to maximize the Hb content per cell. Mature RBCs are devoid of a cytoskeleton and most metabolic machinery; waste products are incorporated into membrane vesicles and expelled.[41] With age, the RBCs become smaller, more rigid, and immunogenic,[42] eventually being eliminated by the reticuloendothelial system. Oxidative stress damage and apoptosis weaken the membrane, modify surface antigens, and hasten RBC senescence.

Compared with a sphere of the same volume, the biconcave RBCs possess a larger membrane surface-to-volume ratio, higher deformability (allowing up to a threefold change in linear dimension) and physical stability, and lower electrostatic energy,[43] flow rotation and turbulence, and mechanically induced inflammation.[44] The RBC membrane contains a unique spectrin–actin scaffold for greater deformability and low flow resistance.[45] Spectrin tetramers form hexagonal lattices with actin[46] reversibly dissociating and re-associating under mechanical stress, permitting viscoelastic changes in cell shape.[47] RBCs flowing through capillaries are tightly packed and often deform into a parabolic shape; deformation improves hydrodynamic efficiency but could reduce diffusive gas transfer efficiency.[38,48]

Both the RBC membrane and the plasma impede O_2 diffusion.[49] RBCs flow slower than plasma, and are nonuniformly distributed along the capillary; inflammation, leukocyte margination, and vasoconstriction accentuate the nonuniformity[50] and reduce gas exchange efficiency.[51] In anemia, capillary RBCs are farther apart; the mean O_2 diffusion path from RBC to endothelium surfaces is increased. As hematocrit increases, RBCs are closer together; more of the available RBC and endothelial surfaces are utilized and gas exchange efficiency (gas uptake per RBC) improves. In polycythemia, capillary RBCs are tightly squeezed together; large portions of RBC membrane are inaccessible to the plasma and endothelium, causing gas exchange efficiency to decline while the associated increases in viscosity and vascular resistance predispose to endothelial injury and thromboembolism (►**Fig. 3**).[51]

Sequestration and release of RBCs: erythropoiesis normally occurs in the fetal liver and bone marrow and the adult bone marrow. Extramedullary erythropoiesis can occur in the adult liver, spleen, or kidney when bone marrow erythropoiesis is impaired.[52] The spleen acts as a reservoir of RBCs. Splenic contraction under sympathetic and catecholamine stimulation releases RBCs into the circulation accompanied by increases in hematocrit and blood O_2-carrying capacity during exercise, hypoxia exposure, and metabolic stress.[53] Upon splenic relaxation, the extra RBCs are re-sequestered. The reversible demand-driven auto-transfusion has only mild effects on exercise performance in untrained subjects but contributes significantly to the exceptional aerobic capacity and hypoxia tolerance of athletic animals[53–55] and human apneic divers[56,57] who possess large spleens. Splenic release of RBCs effectively increases tissue O_2 delivery without the deleterious effects associated with persistent polycythemia. In contrast, the sustained increase in circulating

RBC mass and hematocrit in polycythemia rubra vera[58] and following autologous transfusion[59] heightens the risk of vascular complications.

Allosteric regulation of Hb function: the O_2 affinity of normal adult Hb A is indicated by its partial pressure at which 50% of the heme-binding sites are occupied (P_{50}, 26.5 mm Hg at sea level; ►**Fig. 4**). At a given alveolar O_2 tension, the pressure gradient from the alveolar air to capillary blood drives O_2 loading onto Hb; the pressure gradient from arterial blood to tissue mitochondria drives O_2 unloading from Hb. Shifts in P_{50} modulate the balance between O_2 loading and unloading. Allosterism refers to the interaction whereby a molecule at one location within a macromolecular complex influences the binding and function of the same or another molecule at another location of the same macromolecule.[60] Examples of allosteric interactions involving the RBCs include co-operativity, the Bohr–Haldane effects, temperature effects, the 2,3-bisphosphoglycerate (2,3-BPG) effect, and the coupled interactions of O_2 with CO_2, and NO and carbon monoxide (CO) within RBCs. These interactions are described below.

Cooperativity: cooperativity refers to interactions among the subunits of the Hb tetramer whereby O_2 binding to one heme group alters the conformation of the tetramer and increases the O_2 affinity of the remaining heme groups, making it easier for additional O_2 to bind to the same Hb molecule. Co-operativity is responsible for the sigmoidal shape of the ODC. A lack of cooperativity is exemplified by Mb which possesses only one heme group per molecule and exhibits a hyperbolic-shaped dissociation curve (►**Fig. 4**).

The Bohr–Haldane effects are shown in ►**Fig. 5**.[61]

The Bohr effect,[62] named after Christian Bohr, describes how increasing blood CO_2 concentration (or lowering the pH) reduces Hb affinity for O_2, leading to a right shift (higher P_{50}) of the ODC favoring O_2 unloading in tissue capillaries. Metabolic CO_2 produced by cells diffuse into capillaries dissolved in plasma or enters capillary RBCs to be converted via carbonic anhydrase (CA) to carbonic acid (H_2CO_3), which dissociates into bicarbonate (HCO_3^-) and hydrogen ion (H^+; ►**Fig. 6**).

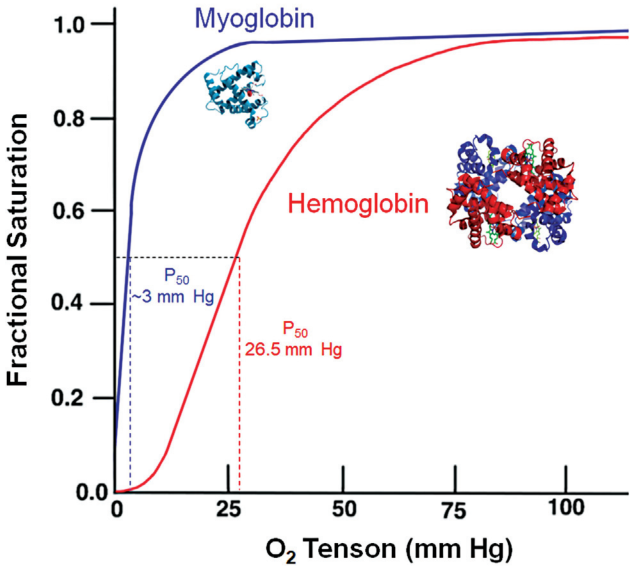

Fig. 4 Hemoglobin and myoglobin structure and O_2 dissociation curves. Each Hb molecule is a tetramer capable of allosteric interaction among the four subunits (i.e., co-operativity) and is adapted for enhanced intravascular gas transfer with 50% saturation at an O_2 tension (P_{50}) of 26.5 mm Hg. Each Mb molecule is a monomer with one heme and globin unit (no possibility of co-operativity) and is adapted for facilitated intracellular gas transfer with a very high O_2 affinity (p_{50} ~3 mm Hg).

$$CO_2 + H_2O \rightleftharpoons H_2CO_3 \rightleftharpoons HCO_3^- + H^+ \qquad \textbf{Eq. 8}$$

The H^+ ion binds to histidine residues on the globin chain and stabilizes the deoxyhemoglobin (deoxyHb, or the Tense) molecular conformation favoring O_2 unloading from Hb. Additionally, CO_2 binds to a nonheme site on oxyHb forming carbaminohemoglobin; this reaction also alters Hb conformation, reduces O_2 binding affinity, and facilitates O_2 release.

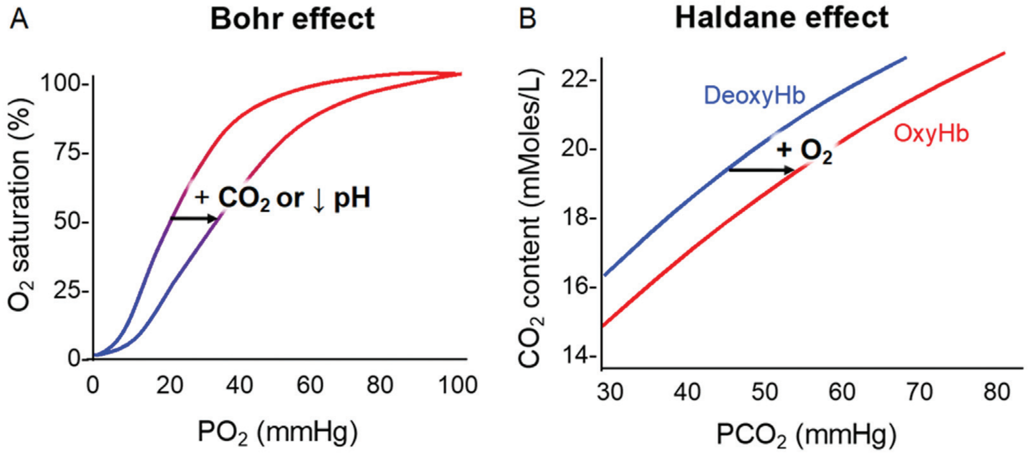

Fig. 5 The Bohr and Haldane effects. (**A**) Bohr effect: the addition of CO_2 or a lower pH reduces O_2 affinity of Hb, shifting the ODC to the right (higher P_{50}) and favoring O_2 release in tissue capillaries. Alkalosis has the opposite effects. (**B**) Haldane effect: the oxygenation of Hb reduces the CO_2 affinity of Hb, shifting the CO_2 dissociation curve to the right and favoring CO_2 release from Hb (a higher PCO_2 at a given CO_2 content of blood). Deoxygenation of Hb has the opposite effect. See text for discussion. ODC, oxyhemoglobin dissociation curve.

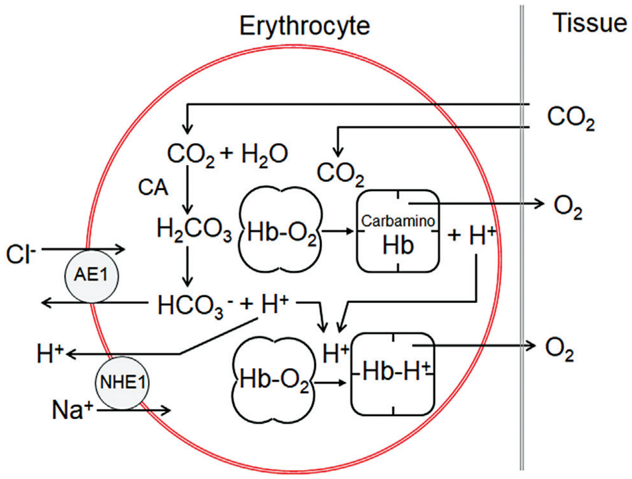

Fig. 6 Allosteric coupling of O_2 and CO_2 exchange in RBCs facilitates the transport of both gases. CO_2 released from tissue into capillaries is converted via carbonic anhydrase (CA) to carbonic acid (H_2CO_3) which dissociates into bicarbonate (HCO_3^-) and proton (H^+); the latter binds histidine residues on the globin to stabilize the deoxyHb conformation, facilitating unloading of O_2. CO_2 also directly binds oxyHb, forming carbaminohemoglobin (carbaminoHb), also facilitating O_2 release. H_2CO_3 diffuses out of the RBC. Excess HCO_3^- anions are removed from RBCs via the membrane anion exchanger-1 (AE-1).[63] Excess H^+ ions are removed from RBCs via the sodium–H^+ exchanger (NHE).[64,65] These reactions occur in reverse in pulmonary capillaries where CO_2 diffuses into alveolar air; the decrease in PCO_2 facilitates O_2 loading onto heme, stabilizing the oxyHb configuration and favoring unloading of CO_2 from Hb for elimination by ventilation. Adapted with permission from Hsia et al.[61]

The HCO_3^- anion is transported out of the RBC via the membrane anion exchanger-1 (AE-1).[63] The excess H^+ are transported out of the RBC via the sodium–hydrogen exchanger.[64,65] Intact H_2CO_3 may also diffuse across cell membranes[66] and act as a physiological buffer in plasma.[67] Furthermore, RBC membrane expresses the water channel protein aquaporin-1 (AQP1) and the ammonia (NH_3) channel protein rhesus-associated glycoprotein (RhAG); both proteins also conduct low-molecular-weight gases including CO_2 and NO,[68–71] and contribute to the extremely high gas permeability of the RBC membrane.

The opposite reactions occur in the lung. Dissolved CO_2 in venous blood diffuses along its pressure gradient into alveolar air; the drop in blood CO_2 tension stabilizes the oxyHb (relaxed) molecular conformation favoring O_2 loading onto deoxyHb, which in turn facilitates CO_2 unloading from Hb. A rightward shift of the ODC (lower O_2 affinity, higher P_{50}) is seen in conditions of elevated tissue O_2 demands mandating higher O_2 delivery, e.g., exercise, acidosis, hyperthermia, and acute hypoxia. A leftward shift of the ODC (higher O_2 affinity, lower P_{50}) is seen in alkalosis, hypothermia, and some native highland populations (discussed separately below). The coupled dynamic reciprocal uptake and release of CO_2 and O_2 by Hb via the Bohr–Haldane and the 2,3-BPG effects serve to optimize the transport of both gases in the lung and the periphery.[61]

The Haldane effect (►**Fig. 5**), named after John Scott Haldane, is the reciprocal counterpart of the Bohr effect and describes how O_2 binding to Hb reduces Hb affinity for CO_2, favoring CO_2 release in the lung. In peripheral capillaries as O_2 is unloaded from oxyHb, the drop in RBC O_2 tension leads to an increased Hb affinity for CO_2, thereby facilitating CO_2 loading onto Hb to be carried to the lung. In the lung the opposite effect occurs; O_2 loading onto Hb reduces Hb affinity for CO_2, thereby facilitating unloading of CO_2 from Hb for elimination by ventilation. The Haldane effect is commonly seen in patients breathing a high inspired O_2 concentration where the increase in arterial O_2 tension is accompanied by an increase in arterial CO_2 tension.

Temperature: resting core temperature is approximately 37°C. Skin temperature is 33°C or lower. Muscle temperature can rise above 39.5°C during heavy exercise; core temperature can be even higher in febrile illnesses. Hyperthermia increases molecular motion and reduces Hb–O_2 binding affinity (higher P_{50}), favoring O_2 release to meet the increased metabolic demand. Conversely, hypothermia increases Hb–O_2 binding affinity (lower P_{50}) and reduces O_2 release to match the reduction in tissue metabolic activity.[72–74]

The 2,3-bisphosphoglycerate (2,3-BPG) effect, shown in ►**Fig. 7**, describes how RBC metabolism modifies O_2 binding affinity with Hb. RBCs mainly rely on glycolysis for adenosine triphosphate (ATP) synthesis, producing the intermediary compound 2,3-BPG that binds to Hb between two globin subunits and stabilizes the deoxy- (tense) conformation with a higher P_{50} favoring O_2 unloading. Acidosis, hyperthermia, and moderate hypoxia increase glycolysis and 2,3-BPG synthesis leading to O_2 release. Alkalosis, low metabolic rate, and chronic extreme hypoxia exposure have the opposite effect on 2,3-BPG synthesis leading to reduced O_2 release. Approximately 35% of the change in Hb–O_2 affinity resulting from a change in RBC 2,3-BPG is explained by the effect of 2,3-BPG reducing the RBC pH.[75]

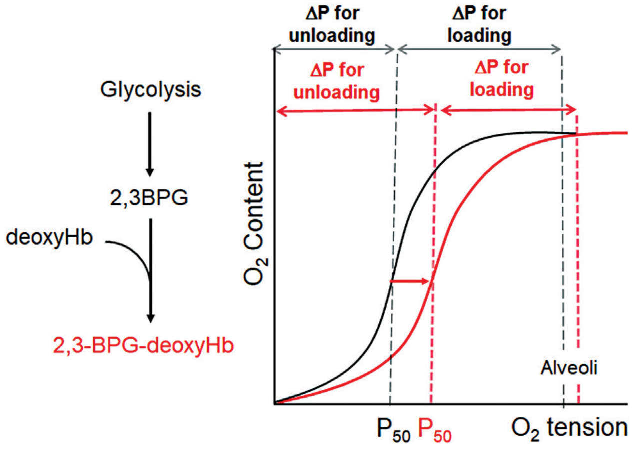

Fig. 7 Effects of 2,3-bisphosphoglycerate (2,3-BPG) on the oxyHb dissociation curve. The P_{50} balances partial pressure gradients (ΔP) for O_2 loading in the lung and O_2 unloading in tissue capillaries (curve in black). The intermediary product of RBC glycolysis, 2,3-BPG, binds to deoxyHb, which reduces both the O_2 affinity of Hb and the intra-RBC pH; the latter adds to the Bohr effect. The net result is a higher P_{50} and a larger mean ΔP for unloading O_2. In response, hyperventilation modestly increases alveolar PO_2 and maintains the ΔP for O_2 loading in the lung (curve and lines in red). See text for discussion.

Thus, 2,3-BPG alters O_2–Hb affinity by itself and also adds to the Bohr effect.[76] Linking the gas carrier function to its own metabolic state makes the RBC a mobile sensor of the local milieu and a versatile regulator of regional gas exchange.

Interactions among O_2 and CO_2, and 2,3-BPG: these interactions are integral to successful adaptation during high-altitude (HA) exposure. In lowlanders ascending to HA, the P_{50} is increased initially favoring O_2 release to tissue. During short-term acclimatization (3–7 days) the in vivo P_{50} (arterial blood) may be unchanged from baseline while standard P_{50} (pH 7.4, PCO_2 40 Torr) and 2,3-BPG are elevated, associated with abundant reticulocytes and young RBCs.[77,78] With longer HA exposure, fluid and metabolic shifts, erythropoiesis, and additional compensatory mechanisms are invoked to enhance the efficiency of O_2 delivery, tissue diffusion and cellular utilization, and the standard P_{50} also returns to baseline.[78] Native Tibetan highlanders and Han Chinese residing at HA for more than 10 years exhibit lower P_{50} compared with Han Chinese lowlanders.[78] The net change in P_{50} depends on the altitude, duration of exposure, extent of diffusion limitation, and the adequacy of compensatory mechanisms in the lung and the periphery.[79]

A wide range of P_{50} is seen among native highlanders. Some highland human populations[78] and animals[80,81] exhibit increased O_2–Hb affinity and enhanced O_2 transport in hypoxia relative to their lowland counterparts. The benefit of enhanced O_2 loading in the lung by high O_2–Hb affinity may be offset by the reduction in O_2 off-loading in the tissues. For example, human subjects with high O_2–Hb affinity genetic mutations show attenuated cardiorespiratory adjustments in hypoxia, but they also develop undesirable polycythemia suggesting inadequate tissue O_2 availability.[82,83] In a small study of long-term Tibetan and Han Chinese residing at HA (4,200 m), standard P_{50} was lower than in lowland subjects; there was no relationship between P_{50} and [Hb], alveolar-arterial O_2 tension difference, or peak O_2 uptake.[84] The adaptive advantages of a higher O_2–Hb affinity at HA is likely contingent upon other factors, e.g., a correspondingly increased capacity for tissue O_2 extraction and utilization[85] and concerted adaptation in every other step of the O_2 transport cascade without developing polycythemia.[86] Highlanders in Tibet and the Americas exhibit larger lung capacities,[87] and Sherpas exhibit a higher lung diffusing capacity, less pulmonary hypertension, and lower ventilatory responses than acclimatized lowlanders.[88] Native Tibetans exhibit superior pulmonary gas exchange efficiency and higher arterial O_2 tension and saturation during exercise at a lower total ventilation and respiratory effort than acclimatized lowlanders.[89] Tibetans also possess unique gene mutations associated with downregulation of the hypoxia-inducible factor (HIF) pathway that promotes hypoxia tolerance. An EGLN1 gain-of-function mutation is associated with increased O_2–Hb affinity suggesting lower sensitivity to hypoxia. An EPAS1 haplotype is associated with higher serum lactate levels suggesting heightened anaerobic metabolism, and a PPARA haplotype correlates with reduced fat oxidation.[80,90–92]

Intrinsic O_2 and NO interactions with Hb: deoxygenated Hb in tissue capillaries can react with nitrite, releasing bioactive NO into the microcirculation and facilitating vasodilation and O_2 delivery to tissue. Nitrogenous species react with Hb in multiple ways, outlined below and in ►**Fig. 8**.

1. Owing to the high NO affinity of heme, free circulating Hb, e.g., released during hemolysis, avidly scavenges NO, promoting vasoconstriction and causing tissue infarction and acute renal failure.[93]
2. NO binding to heme modifies the O_2-binding properties of Hb.[94] Under a high PO_2, NO oxidizes the heme iron from a ferrous (Fe^{+2}) to a ferric (Fe^{+3}) state, producing methemoglobin (metHb). MetHb cannot bind O_2 and increases the O_2–Hb affinity of the remaining ferrous heme-binding sites, thereby impairing both O_2 carrying capacity and O_2 release in tissue capillaries.
3. The reaction of NO donors (e.g., S-nitrocysteine) with oxyHb enhances O_2 affinity of Hb (i.e., lowers P_{50}).[94]
4. RBCs possess intrinsic NO synthase[95] and nitrite reductase[96] activities. Circulating NO can bind the Fe^{+2}-heme of deoxyHb forming nitrosylhemoglobin (Fe^{+2}NO-Hb).[97] In hypoxia, acidosis, or low perfusion states, the bound NO is released.[98,99] Other human globins, e.g., Mb,[100] cytoglobin,[101] and neuroglobin,[102] also possess intrinsic nitrite reductase activity and modulate diverse functions including hypoxic vasodilation,[103] platelet activation,[104] and mitochondrial respiration.[100]
5. NO covalently binds a β-93 cysteine residue on Hb, forming S-nitrosohemoglobin (SNO-Hb) in a reaction coupled to O_2 binding.[105] In hypoxia or during exercise, deoxygenation of SNO-Hb releases S-nitrosothiol into the microcirculation.[103,106,107] SNO-Hb is not a major source of bioavailable NO; however, the β93-cysteine is critical in sustaining Hb subunit cooperativity, protection of RBC and tissue from oxidative stress, and facilitation of respiration during recovery from acute hypoxia.[108–110]

Intrinsic O_2 and carbon monoxide (CO) interaction with Hb: endogenous CO, a natural byproduct of heme degradation, binds Hb with an affinity 240 times that of O_2. Binding of CO to Hb forming carboxyhemoglobin reduces not only the number of available heme binding sites on RBCs but also increases their O_2 binding affinity, leading to a leftward shift of the ODC (lower P_{50}) and severely impairing O_2 release to the tissues during CO poisoning. In addition, low levels of endogenous CO signal via various hemoproteins to mediate mitochondrial biogenesis, anti-inflammation, and antioxidative protection of hemoproteins (including Hb).[111]

RBC-mediated antioxidation: RBCs act as a mobile antioxidant depot containing multiple antioxidants, and are capable of regenerating redox equivalents via glutathione reductase and the pentose phosphate pathway to reduce inflammation and protect from damage inflicted by reactive O_2 species (ROS).[112,113] As ROS can directly bind NO, elimination of ROS by RBCs effectively increases NO bioavailability[114] for interaction with O_2 and enhanced vasoregulation. Human RBCs carry endothelial

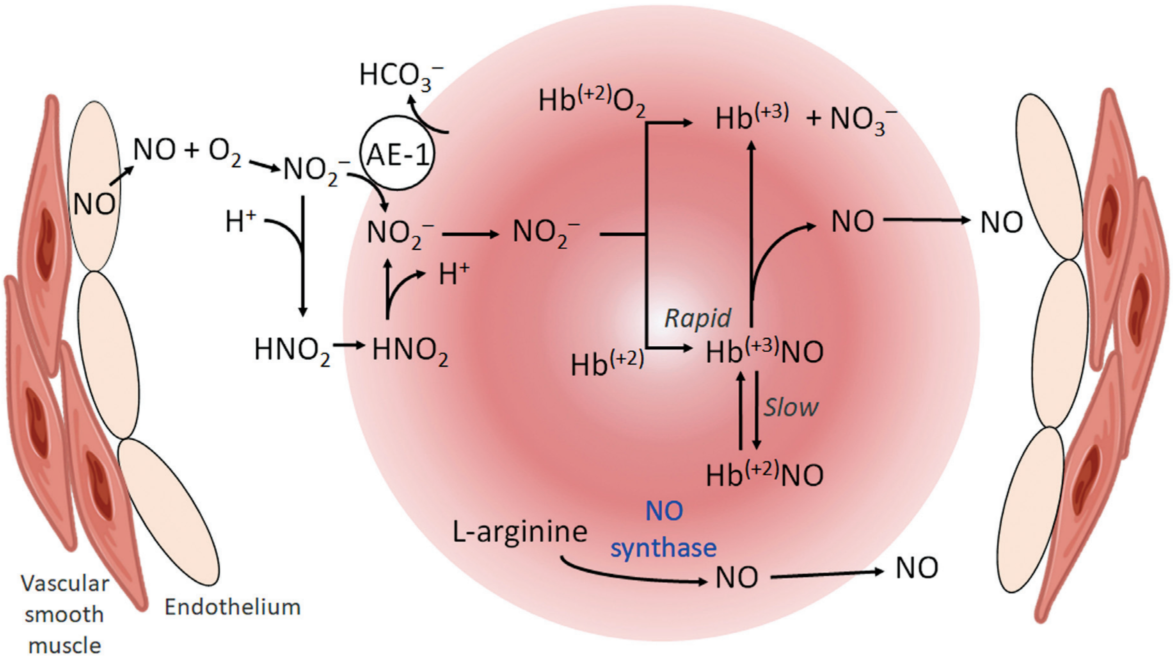

Fig. 8 NO–O_2 interactions. Nitric oxide synthesized in endothelium mediates vascular smooth muscle relaxation. Some NO diffuses into the blood and reacts with O_2 forming nitrite (NO_2^-), which enters RBCs via the anion exchanger-1 (AE-1) or diffuses as nitrous acid (HNO_2) to react with oxy- and deoxy-Hb. Reaction of nitrite with oxyHb ($Hb^{(+2)}O_2$) oxidizes Fe^{+2} to Fe^{+3} forming methemoglobin ($Hb^{(+3)}$) and converting nitrite to inert nitrate (NO_3^-). Reaction of nitrite with deoxyHb ($Hb^{(+2)}$) rapidly produces heme-nitrosylated methemoglobin ($Hb^{(+3)}NO$), a labile intermediate that slowly converts to stable heme-nitrosylated hemoglobin ($Hb^{(+2)}NO$). Hypoxia favors nitrite reaction with $Hb^{(+2)}$, leading to accumulation of the labile intermediate ($Hb^{(+3)}NO$) which serves as a reservoir capable of releasing bioactive NO into the circulation. Additional non-Hb nitrite reductases within RBCs also contribute to the NO reservoir.[109] Maximal RBC nitrite reductase activity occurs at a PO_2 near the in vivo P_{50}.[97] In addition, RBCs possess intrinsic NO synthase activity for generating bioactive NO. Adapted with permission from Hsia.[34]

NO synthase (eNOS) that constitutively converts L-arginine into NO, the activity of which is compromised in patients with coronary artery disease, potentially exacerbating cardiovascular complications.[115]

In summary, RBCs and their Hb content coordinate allosteric interactions with multiple respiratory gases and optimize their transport to and from the tissues via modulation of regional perfusion, vasomotor response, diffusive exchange, and antioxidation, leading to dynamic regional adjustments of O_2 and nutrient supply satisfying local tissue requirements.[33–35] The major functions of RBCs are listed in ►**Fig. 9**.

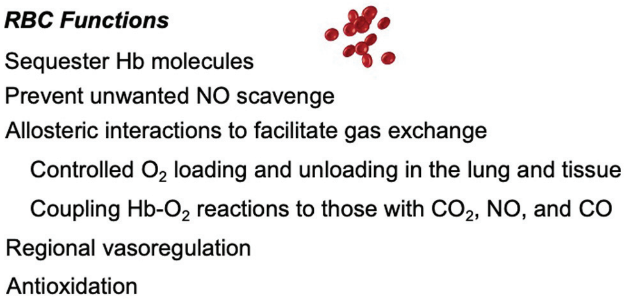
RBC Functions

- Sequester Hb molecules
- Prevent unwanted NO scavenge
- Allosteric interactions to facilitate gas exchange
  - Controlled O_2 loading and unloading in the lung and tissue
  - Coupling Hb-O_2 reactions to those with CO_2, NO, and CO
- Regional vasoregulation
- Antioxidation

Fig. 9 The major functions of the RBCs.

Tissue Respiration

The term *tissue respiration* refers to the exchange of gases between the capillaries and the end-organ cells, chiefly O_2 uptake and CO_2 elimination. The rate of O_2 diffusion from oxygenated capillary blood into individual end-organ cells is determined by several interrelated parameters discussed below.

O_2 Partial Pressure Gradient (ΔPO_2) between Arterial Blood and Cell Interior

The ΔPO_2 may be increased when pulmonary end-capillary or arterial O_2 tension is increased (e.g., hyperventilation in healthy subjects at a given O_2 consumption, CO_2 output and cardiac output,[30] or supplemental O_2 administration) or when intracellular O_2 tension is reduced (e.g., elevated O_2 consumption in exercise or hypermetabolic states, or in tissue hypoxia). Pulmonary pathology could blunt the effects of these maneuvers.

Regional O_2 Delivery (Discussed in an Earlier Section)

Local microvascular perfusion rate, oxyHb saturation, blood volume, hematocrit, and RBC transit time vary within and among organs and differ from those in larger vessels.[116] In the presence of inflammation, leukocytes and macrophages may reduce local perfusion by obstructing blood flow causing or exacerbating tissue hypoxia and releasing or recruiting mediators of cell injury.

Capillary Density, Patency, and the Perfused Surface Area

Anatomical capillary density may be assessed ex vivo in biopsy specimens using histological and immunohistochemical methods and quantified by morphometry, usually expressed as the number or length of capillary-to-muscle fiber ratio or the number of endothelial cell-to-muscle fiber ratio per unit of tissue volume.[20,117] In vivo FCD may be measured using imaging methods (*discussed in an earlier section*) to partially assess the quality of tissue diffusion. A high capillary density or FCD correlates with high aerobic energy turnover. Exercise training significantly increases angiogenic factors and capillary density in skeletal muscle,[118] correlating with an increased maximal O_2 uptake. Aging, deconditioning, chronic hypoxia, and disease states are associated with loss of muscle mass and capillary density, correlating with reduced O_2 transport.[118,119]

Path Length of the Diffusion Barrier

The average diffusion path length of O_2 across the RBC membrane, plasma layer, capillary endothelium, interstitium, and individual cell membrane and cytoplasm to the mitochondria is normally 1–5-µm. The path length is increased in the presence of inflammation, edema, fibrosis, low capillary density or capillary obliteration, leading to elevated resistance to O_2 diffusion. The path length is reduced in the presence of a high capillary density, e.g., in highly trained skeletal muscle. Theoretically the overall O_2 conductance (per unit of driving pressure) from capillary blood to tissue (D_{tissue}, mL O_2. [min.mmHg]^1) is directly proportional to the perfused capillary surface area (Sc, cm^2) and the tissue permeability to O_2, and inversely proportional to the mean diffusion path length (µm) from capillary to tissue mitochondria.[120] D_{tissue} may be facilitated by myoglobin in muscle but cannot yet be directly measured *in vivo* due to technical limitations, spatio-temporal constraints, the dependence of D_{tissue} on O_2 consumption, and the difficulty in separating convective from diffusive components of O_2 transport in different tissues.[121]

Myoglobin Facilitated O_2 Diffusion in Muscle

Mb is present in the cytoplasm and the sarcoplasm of skeletal, cardiac, and smooth muscle fibers, and some tumor cells. As the mean path length from the RBCs to the sarcolemma of muscle fibers imposes significant O_2 diffusion limitation upon exertion,[122] Mb plays a major role as an intracellular carrier for O_2 storage and facilitated transport from the sarcolemma to the mitochondria, and as a determinant of maximal muscle O_2 uptake.

Mb consists of a single heme and globin unit with a much higher O_2 affinity than Hb. The oxymyoglobin (oxyMb) dissociation curve has a hyperbolic shape following the typical Michaelis–Menten enzyme kinetics without cooperativity and with a very low P_{50} (2.5–3.0 mm Hg)[123] (►**Fig. 4**), i.e., optimized for the low intracellular PO_2 milieu. At the onset of muscle contraction, Mb releases its bound O_2 to the mitochondria, thereby maintaining the O_2 tension gradient from capillaries to the myocyte interior. The Mb molecules continuously combine with and dissociate from O_2 as the O_2 molecule diffuses along its partial pressure gradient. A given oxyMb molecule does not transverse the entire distance from sarcolemma to mitochondria and there is no direct transfer of O_2 from one Mb molecule to another.[124]

Like Hb, Mb also reacts with CO and NO, and possesses intrinsic nitrite reductase activity facilitating NO generation within myocytes.[125–127] Depending on intracellular O_2 tensions, Mb may also facilitate elimination of NO, which enhances muscle mitochondrial respiration efficiency. During periods of high energy demand, Mb can react with fatty acids to facilitate the removal of ROS.[128,129] Through these interactions, Mb actively regulates intracellular responses to hypoxia and reoxygenation, acting in tandem with Hb and optimizing O_2 availability to the mitochondria for oxidative respiration.

Homozygous Mb-knockout mice exhibit grossly normal exercise capacity and hypoxic ventilatory response,[130] but display low resting O_2 consumption, exercise endurance, heart rate and cardiac output, impaired systolic cardiac function and response to β1-adrenergic stimulation.[131] The reduction of nitrite to NO and the NO-mediated signal transduction pathways are impaired.[127] In response, circulating [Hb], coronary blood flow and reserve, and myocardial capillary density are elevated.[132] The HIFs, stress proteins, vascular endothelial growth factor, and NO synthase are upregulated.[133] Thus, in the absence of Mb multiple compensatory mechanisms are activated to increase capillary-to-tissue O_2 tension gradient and shorten O_2 diffusion path length, preserve NO homeostasis, and ensure adequate cellular O_2 delivery.[130,132,134]

In contrast to Mb deficiency, diving mammals exhibit 10- to 30-fold higher Mb content than nonathletic animals.[135] Exercise training increases oxidative slow-twitch type I muscle fibers that possess a Mb content approximately 1.6 times higher than the fast-twitch glycolytic type II fibers.[136] High-intensity training at HA induces additional muscle adaptations to compensate for a low O_2 availability, including higher capillary density and muscle Mb content, and upregulated glycolytic pathways favoring the use of carbohydrates instead of lipids as substrate.[137] Polymorphism of the human Mb gene is associated with an increased risk of exercise-induced skeletal muscle damage.[138] Excessive leakage of Mb into blood or urine indicates muscle damage following strenuous exercise,[139] trauma,[140] or myopathy,[141] often leading to acute kidney injury.[142]

Measurement of Tissue Respiration

The rate of O_2 consumption by peripheral tissue may be approximated from the O_2 uptake kinetics in response to a sudden increase in O_2 delivery. Changes in *whole-body O_2 uptake and CO_2 output*, in correlation with blood lactate threshold and hypoxanthine level as markers of anaerobic metabolism, have been measured to indirectly assess O_2 uptake kinetics[143]; however, the findings are not specific to any tissue groups. Near-infrared spectroscopy (NIRS) can estimate O_2 uptake kinetics in peripheral tissues and muscle groups by measuring the changes in tissue concentrations of oxyHb and deoxyHb, providing an indirect measure of O_2

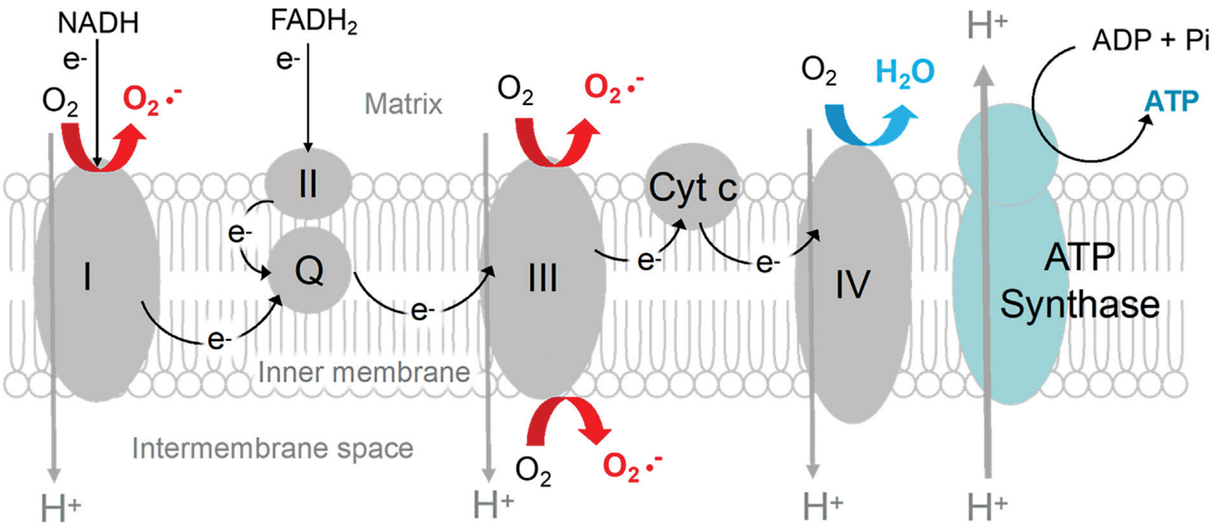

Fig. 10 The electron transport chain (ETC) and oxidative phosphorylation along the inner mitochondrial membrane. The reduced form of nicotinamide adenine dinucleotide (NADH) and the reduced form of flavin adenine dinucleotide ($FADH_2$) are products of the citric acid cycle donating electrons to the ETC. The electrons (e^-) are transferred from complexes I through IV, eventually accepted by O_2 which is reduced to water. The chain of reactions translocate protons (H^+, hydrogen ions) from the mitochondrial matrix across the inner membrane into the intermembrane space, creating a proton gradient. Potential kinetic energy stored in the proton gradient is used by ATP synthase to convert adenosine diphosphate (ADP) into adenosine triphosphate (ATP); free energy from the reaction is used to pump H^+ in the reverse direction from the intermembrane space back into the matrix; thereby sustaining the proton gradient and ATP synthesis. Free superoxide radicals ($O_2 \bullet^-$) are released at multiple sites along the ETC and are normally neutralized by endogenous antioxidants such as superoxide dismutase and glutathione. Increased rates of mitochondrial respiration, loss of enzymatic efficiency in electron transfer, or dissociation of electron transfer from ATP synthesis exacerbates the release of superoxide radicals and increases oxidative stress and cellular damage. Q, co-enzyme Q; Cyt. C, cytochrome C; Pi, inorganic phosphate.

uptake. NIRS has been shown to yield reliable measures of O_2 uptake kinetics in muscle during exercise.[144] Advanced imaging modalities, i.e., *nuclear magnetic resonance spectroscopy, PET, and SPECT*,[145] have also been used to assess muscle O_2 uptake kinetics by monitoring changes in blood flow and oxygenation status, providing high spatial resolution in select muscle groups.[146,147]

Cellular Respiration

The term cellular respiration refers to the breakdown of substrates for the generation of energy (ATP) to power cellular function.[5] The rate of cellular respiration is determined by the following factors:

1. O_2 availability for aerobic respiration (via tissue perfusion and diffusion, discussed above).
2. Substrate availability, e.g., tissue stores of glucose, fatty acid, redox equivalent, adenosine diphosphate (ADP), inorganic phosphate, calcium ion, among others.
3. Metabolic rate and enzyme activity, e.g., increased with physical activity, body temperature, or hyperthyroidism.
4. Biochemical and hormonal regulation, e.g., adrenaline broadly stimulates respiratory and heart rates, cardiac output, glucose release into the bloodstream, and enzymatic activities.

Cellular respiration begins with glycolysis in the cytoplasm, occurring in both aerobic and anaerobic respiration, followed by the citric acid cycle (aka the Krebs cycle), the electron transport chain (ETC) and finally oxidative phosphorylation in the mitochondria. In glycolysis, each glucose molecule is enzymatically converted producing two pyruvate molecules and a small amount of ATP. Pyruvate may be converted anaerobically to ethanol or lactic acid, or aerobically to oxaloacetate or acetyl-CoA. Acetyl-CoA enters the mitochondrial citric acid cycle, yielding electron donors that enter the ETC, eventually generating a proton (H^+ ion) gradient and driving oxidative phosphorylation in which ATP is synthesized. The ETC consists of protein complexes that transfer electrons from donors to acceptors in a series of redox reactions along the inner mitochondrial membrane[148] (►**Fig. 10**):

Complex I (ubiquinone oxidoreductase): in glycolysis and the citric acid cycle, the co-enzyme nicotinamide adenine dinucleotide (NAD^+) is reduced to NADH ($NAD^+ + H^+ + 2\ e^-$). NADH donates its electrons to Complex I, which transfers the electrons to a carrier co-enzyme Q (Co-Q) on the inner mitochondrial membrane while protons (H^+) are transferred from the mitochondrial matrix to the intermembrane space, generating an electrochemical proton gradient. Co-Q also has multiple other actions including antioxidation, support of lysosomal function, suppression of iron-dependent programmed cell death (ferroptosis), anti-inflammation, and gene regulation.[149]

Complex II (succinate dehydrogenase, SDH): SDH catalyzes the oxidation of succinate to fumarate, coupled to the reduction of flavin adenine dinucleotide (FAD) to $FADH_2$; the latter transfers electrons also to Co-Q. SDH is critical for cell growth and metabolism; mutations are associated with mitochondrial respiratory insufficiency and certain cancers.[150]

Complex III (cytochrome c reductase): this complex catalyzes the oxidation of ubihydroquinone and the reduction of cytochrome c. Electrons from Co-Q are transferred to Complex III while H^+ ions are released into the mitochondrial intermembrane space contributing to the proton gradient. ROSs are produced at multiple sites in these reactions and are normally neutralized by endogenous antioxidants such as superoxide dismutase and glutathione species.

Complex IV (cytochrome c oxidase): in this rate-limiting step, electrons from cytochrome c are sequentially transferred to iron and then copper moieties, eventually accepted by O_2 which is reduced to water. Free energy from the reactions moves more H^+ ions from the mitochondrial matrix to the intermembrane space contributing to the proton gradient across the inner membrane.

ATP synthase (aka Complex V): the energy stored in the proton gradient drives ATP synthase to phosphorylate ADP into ATP, i.e., ADP + phosphate → ATP,[151] while the H^+ ions are pumped from the intermembrane space back to the mitochondrial matrix. One ATP molecule is produced for every 4 H^+ ions.

Electron flow through the ETC is finely regulated to optimize ATP synthesis matched to ATP demand while limiting free ROS generation. During a maximal short sprint in normoxia, most of the ATP synthesis occurs via anaerobic metabolism as the demand for ATP exceeds what could be quickly supplied by aerobic respiration.[152,153] During repeated prolonged sprints or high-intensity sustained exercise, ROS production escalates and elicits the recruitment of endogenous antioxidant enzymes. The increased rate of ATP synthesis in skeletal muscle may be modulated by acidosis and ROS. Reactive nitrogen species may also be produced, contributing to nitro-oxidative stress, fatigue, and cellular damage[151] that in turn curtail ATP synthesis and exercise capacity.

Mitochondria function optimally at near anoxia.[154] The apparent O_2 affinity of mitochondria (P_{50mito}) is indexed by the PO_2 at which mitochondrial respiration is 50% of maximal; a high P_{50mito} reflects a low O_2 affinity and vice versa. Human P_{50mito} (approximately 0.2–0.4 mm Hg) measured from muscle biopsies shows significant interindividual variations correlated with individual basal metabolic rate and the O_2 cost during exercise.[155] The P_{50mito} is organ-specific, determined by the efficiency of mitochondrial coupling between electron transfer and ATP generation, the abundance and activity of cytochrome c oxidase, the flux through the ETC, and the mitochondrial membrane potential.[156–158] The P_{50mito} is typically lower in women and contributes to their higher O_2 extraction compared with men.[152]

Dysfunction of Mitochondrial Respiration

Mitochondrial disorders cause widespread abnormalities; they are the most common inherited neuromuscular-metabolic disorders with heterogeneous manifestations characterized by primary or secondary mitochondrial defects and abnormal aerobic metabolism.[159] Primary mitochondrial disorders refer to genetic abnormalities in the proteins encoded by mitochondrial DNA and other proteins encoded by nuclear DNA that are essential for mitochondrial respiration.[160] For example, Leber's hereditary optic neuropathy involves mutations in mitochondrial DNA encoding Complex I proteins causing degeneration of retinal ganglion cells, optic atrophy, and vision loss predominantly in young males due to maternal inheritance of mitochondrial DNA.[161] Primary Co-Q10 deficiencies are autosomal recessive disorders of any of the genes involved in Co-Q10 synthesis; the phenotypes include encephalopathy, cerebellar ataxia, myopathy, and nephropathy.[149] Co-Q deficiencies may also be acquired, e.g., in statin-induced myopathy.[149] Mutations of cytochrome c oxidase exacerbate oxidative stress by enhancing ROS production leading to DNA and protein damage, cellular aging, and myopathy.[162] Nonmitochondrial factors often modulate the expression of primary mitochondrial deficiencies.

Impaired ATP production in mitochondriopathies leads to a low aerobic energy state with often nonspecific clinical manifestations, e.g., failure to thrive, anemia, fatigue, exercise intolerance, muscle weakness, heart failure, and metabolic derangements such as pancreatic insufficiency and diabetes mellitus.[160] Mitochondrial dysfunction involving the respiratory system may manifest as abnormal control of breathing, dysphagia, respiratory muscle weakness, and airway hyperreactivity. Besides oxidative phosphorylation, mitochondria widely mediate cell signaling, calcium homeostasis, nitrooxidative stress, apoptosis, mitophagy senescence, initiation of inflammation, and tumorigenesis, among other vital processes.[163] Mitochondrial dysfunction has been proposed as a common root in the pathophysiology of chronic diseases including sepsis,[163] cardiovascular and metabolic diseases,[164–167] cystic fibrosis, chronic obstructive pulmonary disease, pulmonary fibrosis, and lung cancers.[168,169] Due to the extreme clinical variations, diagnosis is often delayed. Serum creatine kinase, lactic acid, and mitochondrial DNA levels may be elevated; tissue biopsy and/or genetic testing using next-generation sequencing techniques may be necessary for diagnosis. An increasing number of biomarkers and treatment options are under development.[159] For example, Co-Q10 deficiency is treatable with high-dose CoQ-10 supplementation,[170,171] making a definitive diagnosis extremely important.

Two dramatic examples of mitochondrial uncoupling, from salicylates and cyanide poisoning, are described below. High-dose salicylic acid and other nonsteroidal anti-inflammatory drugs that are monocarboxylic acids compete with ATP synthase as proton carriers, disrupting the proton gradient and reversing the normal proton flow across the inner mitochondrial membrane, thereby dissociating electron transport from oxidative phosphorylation,[172] preventing ATP production and inducing a shift to anaerobic metabolism with the generation of lactic acid and toxic metabolites.[173] Patients develop hyperthermia as heat is released from the ETC, and exhibit central ventilatory stimulation, dehydration, hypokalemia, mixed lactic acidosis and respiratory alkalosis, capillary hyperpermeability, and platelet dysfunction, culminating in cerebral and pulmonary edema, respiratory muscle fatigue, hemodynamic collapse, acute renal failure, and seizures.[174] There is no specific antidote. Treatment consists of aggressive ventilatory, volume and hemodynamic support, administration of activated charcoal to reduce plasma salicylate level, alkalinization of the urine to increase clearance, preventing and treating hypokalemia and other complications, and extracorporeal salicylate removal via hemodialysis.[175]

Cyanide (CN^-), the conjugate base of hydrogen cyanide (HCN) gas, is an innate gasotransmitter (like NO, CO, and hydrogen sulfide).[176] Low levels of endogenous cyanide stimulate cytochrome c oxidase and ATP generation, cell proliferation, calcium mobilization, enzymatic regulation, and neurotransmitter release.[176,177] High-dose cyanide blocks ATP synthesis by inhibiting cytochrome c oxidase, resulting in inadequate O_2 utilization, anaerobic metabolism, lactic acidosis, and tissue hypoxia. Cyanide is released by many plants and the seeds and pits of some fruits (cherry, apple, apricot), bitter almond, raw lima beans, and cassava. Cyanide salts are widely used in metallurgy and the production of paper, textiles, rubber and plastics, and are commonly found in industrial wastes and household solvents. Cyanide gas is used in pesticides and as a weapon of terrorism and warfare. Exposure is common in building fires from the combustion of carbon and nitrogen compounds; cyanide and CO poisoning synergistically exacerbate tissue hypoxia. Iatrogenic cyanide poisoning may develop with prolonged nitroprusside administration.[178] Nonspecific symptoms arise immediately following inhalational, oral, or blood-borne exposure, including chest pain, dyspnea, wheezing, nausea, vomiting, headache, confusion, weakness, mucus membrane irritation, tachycardia, hypertension, progressing rapidly to acute lung injury (if inhaled), circulatory collapse, coma, seizures, and death. Delayed symptoms may arise following dermal contact or exposure to cyanogenic compounds, e.g., amygdalin, that are metabolically converted to cyanide. Cherry red complexion, pupillary dilation, lactic acidosis, and supranormal venous O_2 tension are typical findings indicating O_2 accumulation in the blood and anaerobic cellular respiration. The specific antidote, hydroxycobalamin, converts cyanide to the nontoxic cyanocobalamin, which is excreted in urine.[179] A second-line countermeasure is combined sodium nitrite ($NaNO_2$) and sodium thiosulfate.[180,181] The nitrite (NO_2^-) anion oxidizes the iron of deoxyHb forming metHb, which binds cyanide with high affinity to produce the nontoxic cyanmethemoglobin. This reaction reduces blood O_2 carrying capacity and releases NO promoting vasodilation, which may benefit O_2 delivery but also cause hypotension.[178] Sodium thiosulfate is a sulfur donor catalyzing the enzymatic degradation of cyanide to the minimally toxic thiocyanate.[180,181] In addition to chemical countermeasures, adjunct hyperbaric oxygen therapy has shown efficacy in experimental models and is recommended especially for combined cyanide and CO poisoning.[182–184]

Conclusion

This review traces the journey of inspired O_2 after its uptake across the lung for cardiovascular delivery to peripheral tissue capillaries followed by diffusion into end-organ cells to reach the mitochondria. Along the way, O_2 interacts with facilitative carriers (Hb and Mb) and other respiratory and vasoactive molecules (CO_2, NO, and CO) to dynamically optimize both convective transport and diffusive gas exchange in accordance with regional metabolic demand. Within individual cells, O_2 serves as fuel for mitochondrial energy production via the ETC and oxidative phosphorylation, ultimately being transformed into water, another vital component of life. The components of O_2 transport are cooperative and interdependent: Hb and Mb are not solely O_2 carriers or storage molecules; they collaboratively regulate the local loading, release, and diffusion of O_2 and CO_2, the generation and scavenging of NO for vasoregulation, and the communication of physicochemical signals and metabolic feedback responses across distant organs and within individual cells. The mitochondria are not solely ATP production factories; they also modulate ROS levels and intracellular signal transduction of multiple metabolic pathways. Exercise increases tissue metabolic demands leading to concerted upregulation of O_2 uptake, delivery, diffusion, and utilization. Dysfunction of any component of this integrated system affects all other components and elicits corresponding structural and functional adaptation aimed at matching the capacities of all the components and restoring equilibrium albeit at a lower functional level. This concept of coordinated matching of adaptive responses across complex biological networks has been termed "*symmorphosis*"[185,186]; the concept applies throughout the biological hierarchy from molecules to tissue and the whole organism as a fundamental tenet of physiology and a prerequisite for survival under normal and pathological conditions.

Funding
This study was supported by the National Heart, Lung and Blood Institute grant (grant number: R01 HL157533).

Conflict of Interest
None declared.

References

1 Vincent JL. Understanding cardiac output. Crit Care 2008;12(04):174
2 Magder S, Famulari G, Gariepy B. Periodicity, time constants of drainage, and the mechanical determinants of peak cardiac output during exercise. J Appl Physiol 2019;127(06):1611–1619
3 LaCombe P, Tariq MA, Lappin SL. Physiology, Afterload Reduction. StatPearls. Treasure Island, FL: StatPearls Publishing; 2023
4 Sato K, Sogawa M, Namura O, Hayashi J. Deterioration of body oxygen metabolism by vasodilator and/or vasoconstrictor administration during cardiopulmonary bypass. ASAIO J 2006;52(01):96–99
5 Grote J. Tissue respiration. In: Schmidt RF, Thews G, eds. Human Physiology. Berlin, Heidelberg: Springer Berlin Heidelberg; 1989:598–612

6 Björnberg J, Grände PO, Maspers M, Mellander S. Site of autoregulatory reactions in the vascular bed of cat skeletal muscle as determined with a new technique for segmental vascular resistance recordings. Acta Physiol Scand 1988;133(02):199–210

7 Hall ET, Sá RC, Holverda S, et al. The effect of supine exercise on the distribution of regional pulmonary blood flow measured using proton MRI. J Appl Physiol 2014;116(04):451–461

8 Russell McEvoy GM, Wells BN, Kiley ME, Kaur KK, Fraser GM. Dynamics of capillary blood flow responses to acute local changes in oxygen and carbon dioxide concentrations. Front Physiol 2022;13:1052449

9 Korte N, Ilkan Z, Pearson CL, et al. The Ca2+-gated channel TMEM16A amplifies capillary pericyte contraction and reduces cerebral blood flow after ischemia. J Clin Invest 2022;132(09): e154118

10 Hirunpattarasilp C, Barkaway A, Davis H, Pfeiffer T, Sethi H, Attwell D. Hyperoxia evokes pericyte-mediated capillary constriction. J Cereb Blood Flow Metab 2022;42(11):2032–2047

11 Tsai AG, Acero C, Nance PR, et al. Elevated plasma viscosity in extreme hemodilution increases perivascular nitric oxide concentration and microvascular perfusion. Am J Physiol Heart Circ Physiol 2005;288(04):H1730–H1739

12 Cabrales P, Tsai AG, Intaglietta M. Microvascular pressure and functional capillary density in extreme hemodilution with low- and high-viscosity dextran and a low-viscosity Hb-based O2 carrier. Am J Physiol Heart Circ Physiol 2004;287(01): H363–H373

13 Cabrales P, Tsai AG, Intaglietta M. Balance between vasoconstriction and enhanced oxygen delivery. Transfusion 2008;48(10): 2087–2095

14 Baker M, Anjum F, dela Cruz J. Deep Venous Thrombosis Ultrasound Evaluation. StatPearls. Treasure Island, FL: StatPearls Publishing; 2023

15 de Graaff JC, Ubbink DT, Büller HR, Jacobs MJ. The diagnosis of deep venous thrombosis using laser Doppler skin perfusion measurements. Microvasc Res 2001;61(01):49–55

16 Jung F, Leithäuser B, Landgraf H, et al. Laser Doppler flux measurement for the assessment of cutaneous microcirculatio–critical remarks. Clin Hemorheol Microcirc 2013;55(04): 411–416

17 Bajwa A, Wesolowski R, Patel A, et al. Assessment of tissue perfusion in the lower limb: current methods and techniques under development. Circ Cardiovasc Imaging 2014;7(05): 836–843

18 Hsia CCW, Bates JHT, Driehuys B, et al. Quantitative imaging metrics for the assessment of pulmonary pathophysiology: an official American Thoracic Society and Fleischner Society Joint Workshop Report. Ann Am Thorac Soc 2023;20(02):161–195

19 Muir ER, Watts LT, Tiwari YV, Bresnen A, Shen Q, Duong TQ. Quantitative cerebral blood flow measurements using MRI. In: Milner R, ed. Cerebral Angiogenesis: Methods and Protocols. New York, NY: Springer New York; 2014:205–211

20 Duscha BD, Kraus WE, Keteyian SJ, et al. Capillary density of skeletal muscle: a contributing mechanism for exercise intolerance in class II-III chronic heart failure independent of other peripheral alterations. J Am Coll Cardiol 1999;33(07): 1956–1963

21 McGuire BJ, Secomb TW. Estimation of capillary density in human skeletal muscle based on maximal oxygen consumption rates. Am J Physiol Heart Circ Physiol 2003;285(06): H2382–H2391

22 Gillespie J, Hansen M, Samatham R, Baker SD, Filer S, Sheridan DC. Capillary refill technology to enhance the accuracy of peripheral perfusion evaluation in sepsis. J Intensive Care Med 2022;37(09):1159–1164

23 Virgini-Magalhães CE, Porto CL, Fernandes FF, Dorigo DM, Bottino DA, Bouskela E. Use of microcirculatory parameters to evaluate chronic venous insufficiency. J Vasc Surg 2006;43 (05):1037–1044

24 Nacul FE, Guia IL, Lessa MA, Tibiriçá E The effects of vasoactive drugs on intestinal functional capillary density in endotoxemic rats: intravital video-microscopy analysis. Anesth Analg 2010; 110(02):547–554

25 Langer S, Biberthaler P, Harris AG, Steinau HU, Messmer K. In vivo monitoring of microvessels in skin flaps: introduction of a novel technique. Microsurgery 2001;21(07):317–324

26 Wadowski PP, Steinlechner B, Zimpfer D, et al. Functional capillary impairment in patients with ventricular assist devices. Sci Rep 2019;9(01):5909

27 Silva PS, Marcus DM, Liu D, et al; DRCR Retina Network. Association of ultra-widefield fluorescein angiography-identified retinal nonperfusion and the risk of diabetic retinopathy worsening over time. JAMA Ophthalmol 2022;140(10):936–945

28 Michael Peters A. The precise physiological definition of tissue perfusion and clearance measured from imaging. Eur J Nucl Med Mol Imaging 2018;45(07):1139–1141

29 Wagner PD, Laravuso RB, Uhl RR, West JB. Continuous distributions of ventilation-perfusion ratios in normal subjects breathing air and 100 per cent O2. J Clin Invest 1974;54(01):54–68

30 Petersson J, Glenny RW. Gas exchange and ventilation-perfusion relationships in the lung. Eur Respir J 2014;44(04):1023–1041

31 Harms CA, Babcock MA, McClaran SR, et al. Respiratory muscle work compromises leg blood flow during maximal exercise. J Appl Physiol 1997;82(05):1573–1583

32 Olson TP, Joyner MJ, Dietz NM, Eisenach JH, Curry TB, Johnson BD. Effects of respiratory muscle work on blood flow distribution during exercise in heart failure. J Physiol 2010;588(Pt 13):2487–2501

33 Hsia CC. Respiratory function of hemoglobin. N Engl J Med 1998; 338(04):239–247

34 Hsia CCW. Respiratory function of hemoglobin: from origin to human physiology and pathophysiology. In: Magder S, Malhotra A, Hibbert KA, Hardin CC, eds. Cardiopulmonary Monitoring: Basic Physiology, Tools, and Bedside Management for the Critically Ill. Cham: Springer International Publishing; 2021:635–651

35 Premont RT, Reynolds JD, Zhang R, Stamler JS. Role of nitric oxide carried by hemoglobin in cardiovascular physiology: developments on a three-gas respiratory cycle. Circ Res 2020;126(01): 129–158

36 Perutz MF. Mechanisms regulating the reactions of human hemoglobin with oxygen and carbon monoxide. Annu Rev Physiol 1990;52:1–25

37 Cabrales P, Tsai AG, Intaglietta M. Isovolemic exchange transfusion with increasing concentrations of low oxygen affinity hemoglobin solution limits oxygen delivery due to vasoconstriction. Am J Physiol Heart Circ Physiol 2008;295(05):H2212–H2218

38 Betticher DC, Reinhart WH, Geiser J. Effect of RBC shape and deformability on pulmonary O2 diffusing capacity and resistance to flow in rabbit lungs. J Appl Physiol 1995;78(03): 778–783

39 Snyder GK, Sheafor BA. Red blood cells: centerpiece in the evolution of the vertebrate circulatory system. Am Zool 1999; 39:189–198

40 Lee JC, Gimm JA, Lo AJ, et al. Mechanism of protein sorting during erythroblast enucleation: role of cytoskeletal connectivity. Blood 2004;103(05):1912–1919

41 Gifford SC, Derganc J, Shevkoplyas SS, Yoshida T, Bitensky MW. A detailed study of time-dependent changes in human red blood cells: from reticulocyte maturation to erythrocyte senescence. Br J Haematol 2006;135(03):395–404

42 Kay M. Immunoregulation of cellular life span. Ann N Y Acad Sci 2005;1057:85–111

43 Adams KH. A theory for the shape of the red blood cell. Biophys J 1973;13(10):1049–1053

44 Uzoigwe C. The human erythrocyte has developed the biconcave disc shape to optimise the flow properties of the blood in the large vessels. Med Hypotheses 2006;67(05):1159–1163

45 Leterrier C, Pullarkat PA. Mechanical role of the submembrane spectrin scaffold in red blood cells and neurons. J Cell Sci 2022; 135(16):jcs259356

46 Mohandas N, Chasis JA. Red blood cell deformability, membrane material properties and shape: regulation by transmembrane, skeletal and cytosolic proteins and lipids. Semin Hematol 1993; 30(03):171–192

47 An X, Lecomte MC, Chasis JA, Mohandas N, Gratzer W. Shear-response of the spectrin dimer-tetramer equilibrium in the red blood cell membrane. J Biol Chem 2002;277(35):31796–31800

48 Hsia CC, Chuong CJ, Johnson RL Jr. Red cell distortion and conceptual basis of diffusing capacity estimates: finite element analysis. J Appl Physiol 1997;83(04):1397–1404

49 Geiser J, Betticher DC. Gas transfer in isolated lungs perfused with red cell suspension or hemoglobin solution. Respir Physiol 1989;77(01):31–39

50 Hogg JC, McLean T, Martin BA, Wiggs B. Erythrocyte transit and neutrophil concentration in the dog lung. J Appl Physiol 1988;65 (03):1217–1225

51 Hsia CC, Johnson RL Jr, Shah D. Red cell distribution and the recruitment of pulmonary diffusing capacity. J Appl Physiol 1999;86(05):1460–1467

52 Fan N, Lavu S, Hanson CA, Tefferi A. Extramedullary hematopoiesis in the absence of myeloproliferative neoplasm: Mayo Clinic case series of 309 patients. Blood Cancer J 2018;8(12):119

53 Hsia CC, Johnson RL Jr, Dane DM, et al. The canine spleen in oxygen transport: gas exchange and hemodynamic responses to splenectomy. J Appl Physiol 2007;103(05):1496–1505

54 Cabanac A, Folkow LP, Blix AS. Volume capacity and contraction control of the seal spleen. J Appl Physiol 1997;82(06):1989–1994

55 Dane DM, Hsia CC, Wu EY, et al. Splenectomy impairs diffusive oxygen transport in the lung of dogs. J Appl Physiol 2006;101 (01):289–297

56 Ilardo MA, Moltke I, Korneliussen TS, et al. Physiological and genetic adaptations to diving in sea nomads. Cell 2018;173(03): 569.e15–580.e15

57 Schagatay E, Richardson MX, Lodin-Sundström A. Size matters: spleen and lung volumes predict performance in human apneic divers. Front Physiol 2012;3:173

58 Podoltsev NA, Zhu M, Zeidan AM, et al. The impact of phlebotomy and hydroxyurea on survival and risk of thrombosis among older patients with polycythemia vera. Blood Adv 2018;2(20): 2681–2690

59 Cacic DL, Hervig T, Seghatchian J. Blood doping: the flip side of transfusion and transfusion alternatives. Transfus Apheresis Sci 2013;49(01):90–94

60 Strand K, Knapp JE, Bhyravbhatla B, Royer WE Jr. Crystal structure of the hemoglobin dodecamer from Lumbricus erythrocruorin: allosteric core of giant annelid respiratory complexes. J Mol Biol 2004;344(01):119–134

61 Hsia CC, Hyde DM, Weibel ER. Lung structure and the intrinsic challenges of gas exchange. Compr Physiol 2016;6(02):827–895

62 Sterner R, Decker H. Inversion of the Bohr effect upon oxygen binding to 24-meric tarantula hemocyanin. Proc Natl Acad Sci U S A 1994;91(11):4835–4839

63 McMurtrie HL, Cleary HJ, Alvarez BV, et al. The bicarbonate transport metabolon. J Enzyme Inhib Med Chem 2004;19(03): 231–236

64 Pedersen SF, Cala PM. Comparative biology of the ubiquitous Na+/H+ exchanger, NHE1: lessons from erythrocytes. J Exp Zoolog A Comp Exp Biol 2004;301(07):569–578

65 Matteucci E, Giampietro O. Electron pathways through erythrocyte plasma membrane in human physiology and pathology: potential redox biomarker? Biomark Insights 2007; 2:321–329

66 Wang KW, Deen WM. Chemical kinetic and diffusional limitations on bicarbonate reabsorption by the proximal tubule. Biophys J 1980;31(02):161–182

67 Aminov D, Pines D, Kiefer PM, Daschakraborty S, Hynes JT, Pines E. Intact carbonic acid is a viable protonating agent for biological bases. Proc Natl Acad Sci U S A 2019;116(42):20837–20843

68 Endeward V, Musa-Aziz R, Cooper GJ, et al. Evidence that aquaporin 1 is a major pathway for CO2 transport across the human erythrocyte membrane. FASEB J 2006;20(12):1974–1981

69 Endeward V, Cartron JP, Ripoche P, Gros G. RhAG protein of the Rhesus complex is a CO2 channel in the human red cell membrane. FASEB J 2008;22(01):64–73

70 Herrera M, Hong NJ, Garvin JL. Aquaporin-1 transports NO across cell membranes. Hypertension 2006;48(01):157–164

71 Michenkova M, Taki S, Blosser MC, et al. Carbon dioxide transport across membranes. Interface Focus 2021;11(02):20200090

72 Mairbäurl H, Weber RE. Oxygen transport by hemoglobin. Compr Physiol 2012;2(02):1463–1489

73 Kim KH, Chang TH, Kim SH, Kang SH, Kim JS. Changes of P50 during hypothermia for cardiopulmonary bypass surgery. Korean J Anesthesiol 1991;24(05):1006–1012

74 Wainwright MS, Sheng H, Sato Y, et al. Pharmacological correction of hypothermic P(50) shift does not alter outcome from focal cerebral ischemia in rats. Am J Physiol Heart Circ Physiol 2002; 282(05):H1863–H1870

75 Bellingham AJ, Detter JC, Lenfant C. Regulatory mechanisms of hemoglobin oxygen affinity in acidosis and alkalosis. J Clin Invest 1971;50(03):700–706

76 Duhm J. Dual effect of 2,3-diphosphoglycerate on the Bohr effects of human blood. Pflugers Arch 1976;363(01):55–60

77 Mairbäurl H, Schobersberger W, Oelz O, Bärtsch P, Eckardt KU, Bauer C. Unchanged in vivo P50 at high altitude despite decreased erythrocyte age and elevated 2,3-diphosphoglycerate. J Appl Physiol 1990;68(03):1186–1194

78 Li C, Li X, Liu J, et al. Investigation of the differences between the Tibetan and Han populations in the hemoglobin-oxygen affinity of red blood cells and in the adaptation to high-altitude environments. Hematology 2018;23(05):309–313

79 Bencowitz HZ, Wagner PD, West JB. Effect of change in P50 on exercise tolerance at high altitude: a theoretical study. J Appl Physiol 1982;53(06):1487–1495

80 Tashi T, Scott Reading N, Wuren T, et al. Gain-of-function EGLN1 prolyl hydroxylase (PHD2 D4E:C127S) in combination with EPAS1 (HIF-2α) polymorphism lowers hemoglobin concentration in Tibetan highlanders. J Mol Med (Berl) 2017;95(06): 665–670

81 Natarajan C, Jendroszek A, Kumar A, et al. Molecular basis of hemoglobin adaptation in the high-flying bar-headed goose. PLoS Genet 2018;14(04):e1007331

82 Dominelli PB, Wiggins CC, Baker SE, et al. Influence of high affinity haemoglobin on the response to normoxic and hypoxic exercise. J Physiol 2020;598(08):1475–1490

83 Webb KL, Dominelli PB, Baker SE, et al. Influence of high hemoglobin-oxygen affinity on humans during hypoxia. Front Physiol 2022;12:763933

84 Simonson TS, Wei G, Wagner HE, et al. Increased blood-oxygen binding affinity in Tibetan and Han Chinese residents at 4200 m. Exp Physiol 2014;99(12):1624–1635

85 Wearing OH, Ivy CM, Gutiérrez-Pinto N, et al. The adaptive benefit of evolved increases in hemoglobin-O_2 affinity is contingent on tissue O_2 diffusing capacity in high-altitude deer mice. BMC Biol 2021;19(01):128

86 Simonson TS, Wei G, Wagner HE, et al. Low haemoglobin concentration in Tibetan males is associated with greater high-altitude exercise capacity. J Physiol 2015;593(14):3207–3218

87 Droma T, McCullough RG, McCullough RE, et al. Increased vital and total lung capacities in Tibetan compared to Han residents of Lhasa (3,658 m). Am J Phys Anthropol 1991;86(03):341–351

88 Faoro V, Huez S, Vanderpool R, et al. Pulmonary circulation and gas exchange at exercise in Sherpas at high altitude. J Appl Physiol 2014;116(07):919–926

89 Zhuang J, Droma T, Sutton JR, et al. Smaller alveolar-arterial O2 gradients in Tibetan than Han residents of Lhasa (3658 m). Respir Physiol 1996;103(01):75–82

90 Hu H, Petousi N, Glusman G, et al. Evolutionary history of Tibetans inferred from whole-genome sequencing. PLoS Genet 2017;13(04):e1006675

91 Ge RL, Simonson TS, Gordeuk V, Prchal JT, McClain DA. Metabolic aspects of high-altitude adaptation in Tibetans. Exp Physiol 2015;100(11):1247–1255

92 Simonson TS, Huff CD, Witherspoon DJ, Prchal JT, Jorde LB. Adaptive genetic changes related to haemoglobin concentration in native high-altitude Tibetans. Exp Physiol 2015;100(11):1263–1268

93 Mack AK, Kato GJ. Sickle cell disease and nitric oxide: a paradigm shift? Int J Biochem Cell Biol 2006;38(08):1237–1243

94 Stepuro TL, Zinchuk VV. Nitric oxide effect on the hemoglobin-oxygen affinity. J Physiol Pharmacol 2006;57(01):29–38

95 Kleinbongard P, Schulz R, Rassaf T, et al. Red blood cells express a functional endothelial nitric oxide synthase. Blood 2006;107(07):2943–2951

96 Fens MH, Larkin SK, Oronsky B, Scicinski J, Morris CR, Kuypers FA. The capacity of red blood cells to reduce nitrite determines nitric oxide generation under hypoxic conditions. PLoS One 2014;9(07):e101626

97 Huang Z, Shiva S, Kim-Shapiro DB, et al. Enzymatic function of hemoglobin as a nitrite reductase that produces NO under allosteric control. J Clin Invest 2005;115(08):2099–2107

98 Stamler JS, Jia L, Eu JP, et al. Blood flow regulation by S-nitrosohemoglobin in the physiological oxygen gradient. Science 1997;276(5321):2034–2037

99 Gladwin MT, Ognibene FP, Pannell LK, et al. Relative role of heme nitrosylation and beta-cysteine 93 nitrosation in the transport and metabolism of nitric oxide by hemoglobin in the human circulation. Proc Natl Acad Sci U S A 2000;97(18):9943–9948

100 Shiva S, Huang Z, Grubina R, et al. Deoxymyoglobin is a nitrite reductase that generates nitric oxide and regulates mitochondrial respiration. Circ Res 2007;100(05):654–661

101 Reeder BJ, Ukeri J. Strong modulation of nitrite reductase activity of cytoglobin by disulfide bond oxidation: implications for nitric oxide homeostasis. Nitric Oxide 2018;72:16–23

102 Tiso M, Tejero J, Basu S, et al. Human neuroglobin functions as a redox-regulated nitrite reductase. J Biol Chem 2011;286(20):18277–18289

103 Gladwin MT, Shelhamer JH, Schechter AN, et al. Role of circulating nitrite and S-nitrosohemoglobin in the regulation of regional blood flow in humans. Proc Natl Acad Sci U S A 2000;97(21):11482–11487

104 Chamchoi A, Srihirun S, Paiboonsukwong K, et al. Decreased nitrite reductase activity of deoxyhemoglobin correlates with platelet activation in hemoglobin E/ß-thalassemia subjects. PLoS One 2018;13(09):e0203955

105 Gow AJ, Stamler JS. Reactions between nitric oxide and haemoglobin under physiological conditions. Nature 1998;391(6663):169–173

106 McMahon TJ, Moon RE, Luschinger BP, et al. Nitric oxide in the human respiratory cycle. Nat Med 2002;8(07):711–717

107 Bailey DM, Rasmussen P, Overgaard M, et al. Nitrite and S-nitrosohemoglobin exchange across the human cerebral and femoral circulation: relationship to basal and exercise blood flow responses to hypoxia. Circulation 2017;135(02):166–176

108 Sun CW, Yang J, Kleschyov AL, et al. Hemoglobin β93 cysteine is not required for export of nitric oxide bioactivity from the red blood cell. Circulation 2019;139(23):2654–2663

109 Schmidt HHHW, Feelisch M. Red blood cell-derived nitric oxide bioactivity and hypoxic vasodilation. Circulation 2019;139(23):2664–2667

110 Gaston B, May WJ, Sullivan S, et al. Essential role of hemoglobin beta-93-cysteine in posthypoxia facilitation of breathing in conscious mice. J Appl Physiol 2014;116(10):1290–1299

111 Motterlini R, Foresti R. Biological signaling by carbon monoxide and carbon monoxide-releasing molecules. Am J Physiol Cell Physiol 2017;312(03):C302–C313

112 Minetti M, Agati L, Malorni W. The microenvironment can shift erythrocytes from a friendly to a harmful behavior: pathogenetic implications for vascular diseases. Cardiovasc Res 2007;75(01):21–28

113 Nagababu E, Chrest FJ, Rifkind JM. Hydrogen-peroxide-induced heme degradation in red blood cells: the protective roles of catalase and glutathione peroxidase. Biochim Biophys Acta 2003;1620(1–3):211–217

114 Gow AJ, Luchsinger BP, Pawloski JR, Singel DJ, Stamler JS. The oxyhemoglobin reaction of nitric oxide. Proc Natl Acad Sci U S A 1999;96(16):9027–9032

115 Cortese-Krott MM, Kelm M. Endothelial nitric oxide synthase in red blood cells: key to a new erythrocrine function? Redox Biol 2014;2:251–258

116 Lücker A, Secomb TW, Barrett MJP, Weber B, Jenny P. The relation between capillary transit times and hemoglobin saturation heterogeneity. part 2: capillary networks. Front Physiol 2018;9:1296

117 Gavin TP, Kraus RM, Carrithers JA, Garry JP, Hickner RC. Aging and the skeletal muscle angiogenic response to exercise in women. J Gerontol A Biol Sci Med Sci 2015;70(10):1189–1197

118 Jensen L, Bangsbo J, Hellsten Y. Effect of high intensity training on capillarization and presence of angiogenic factors in human skeletal muscle. J Physiol 2004;557(Pt 2):571–582

119 Hawkins S, Wiswell R. Rate and mechanism of maximal oxygen consumption decline with aging: implications for exercise training. Sports Med 2003;33(12):877–888

120 Popel AS. Theory of oxygen transport to tissue. Crit Rev Biomed Eng 1989;17(03):257–321

121 Montero D, Diaz-Canestro C. Skeletal Muscle O(2) Diffusion and the Limitation of Aerobic Capacity in Heart Failure: A Clarification. Front Cardiovasc Med 2019;6:78

122 Richardson RS, Noyszewski EA, Kendrick KF, Leigh JS, Wagner PD. Myoglobin O2 desaturation during exercise. Evidence of limited O2 transport. J Clin Invest 1995;96(04):1916–1926

123 Wyman J. Facilitated diffusion and the possible role of myoglobin as a transport mechanism. J Biol Chem 1966;241(01):115–121

124 Gros G, Wittenberg BA, Jue T. Myoglobin's old and new clothes: from molecular structure to function in living cells. J Exp Biol 2010;213(Pt 16):2713–2725

125 Hendgen-Cotta UB, Merx MW, Shiva S, et al. Nitrite reductase activity of myoglobin regulates respiration and cellular viability in myocardial ischemia-reperfusion injury. Proc Natl Acad Sci U S A 2008;105(29):10256–10261

126 Kamga C, Krishnamurthy S, Shiva S. Myoglobin and mitochondria: a relationship bound by oxygen and nitric oxide. Nitric Oxide 2012;26(04):251–258

127 Totzeck M, Hendgen-Cotta UB, Luedike P, et al. Nitrite regulates hypoxic vasodilation via myoglobin-dependent nitric oxide generation. Circulation 2012;126(03):325–334

128 Christen L, Broghammer H, Rapöhn I, et al. Myoglobin-mediated lipid shuttling increases adrenergic activation of brown and white adipocyte metabolism and is as a marker of thermogenic adipocytes in humans. Clin Transl Med 2022;12(12):e1108

129 Totzeck M, Hendgen-Cotta UB, Kelm M, Rassaf T. Crosstalk between nitrite, myoglobin and reactive oxygen species to regulate vasodilation under hypoxia. PLoS One 2014;9(08):e105951

130 Garry DJ, Ordway GA, Lorenz JN, et al. Mice without myoglobin. Nature 1998;395(6705):905–908

131 Merx MW, Gödecke A, Flögel U, Schrader J. Oxygen supply and nitric oxide scavenging by myoglobin contribute to exercise endurance and cardiac function. FASEB J 2005;19(08): 1015–1017

132 Gödecke A, Flögel U, Zanger K, et al. Disruption of myoglobin in mice induces multiple compensatory mechanisms. Proc Natl Acad Sci U S A 1999;96(18):10495–10500

133 Meeson AP, Radford N, Shelton JM, et al. Adaptive mechanisms that preserve cardiac function in mice without myoglobin. Circ Res 2001;88(07):713–720

134 Park JW, Piknova B, Dey S, Noguchi CT, Schechter AN. Compensatory mechanisms in myoglobin deficient mice preserve NO homeostasis. Nitric Oxide 2019;90:10–14

135 Berenbrink M. The role of myoglobin in the evolution of mammalian diving capacity - the August Krogh principle applied in molecular and evolutionary physiology. Comp Biochem Physiol A Mol Integr Physiol 2021;252:110843

136 Jansson E, Sylvén C. Myoglobin concentration in single type I and type II muscle fibres in man. Histochemistry 1983;78(01): 121–124

137 Hoppeler H, Vogt M. Muscle tissue adaptations to hypoxia. J Exp Biol 2001;204(Pt 18):3133–3139

138 Cui T, Jiang MS. Myoglobin A79G polymorphism association with exercise-induced skeletal muscle damage. Genet Mol Res 2016; 15(02). Doi: 10.4238/gmr.15027506

139 Wichardt E, Mattsson CM, Ekblom B, Henriksson-Larsén K. Rhabdomyolysis/myoglobinemia and NSAID during 48 h ultra-endurance exercise (adventure racing). Eur J Appl Physiol 2011; 111(07):1541–1544

140 Zutt R, van der Kooi AJ, Linthorst GE, Wanders RJ, de Visser M. Rhabdomyolysis: review of the literature. Neuromuscul Disord 2014;24(08):651–659

141 Lovece S, Kagen LJ. Sensitive rapid detection of myoglobin in serum of patients with myopathy by immunoturbidimetric assay. J Rheumatol 1993;20(08):1331–1334

142 Zhang L, Kang Y, Fu P, et al. Myoglobin clearance by continuous venous-venous haemofiltration in rhabdomyolysis with acute kidney injury: a case series. Injury 2012;43(05):619–623

143 Zhang YY, Wasserman K, Sietsema KE, et al. O2 uptake kinetics in response to exercise. A measure of tissue anaerobiosis in heart failure. Chest 1993;103(03):735–741

144 Boushel R, Langberg H, Olesen J, Gonzales-Alonzo J, Bülow J, Kjaer M. Monitoring tissue oxygen availability with near infrared spectroscopy (NIRS) in health and disease. Scand J Med Sci Sports 2001;11(04):213–222

145 Rudroff T, Ketelhut NB, Kindred JH. Metabolic imaging in exercise physiology. J Appl Physiol 2018;124(02):497–503

146 Suminski RR, Robertson RJ, Goss FL, Arslanian S. Peak oxygen consumption and skeletal muscle bioenergetics in African-American and Caucasian men. Med Sci Sports Exerc 2000;32 (12):2059–2066

147 Murakami M, Katsumura T, Hamaoka T, et al. Effects of epinephrine and lactate on the increase in oxygen consumption of nonexercising skeletal muscle after aerobic exercise. J Biomed Opt 2000;5(04):406–410

148 Ahmad M, Wolberg A, Kahwaji CI. Biochemistry, Electron Transport Chain. StatPearls [Internet]. Updated 2022 Sep 5. Treasure Island, FL: StatPearls Publishing; 2023

149 Pallotti F, Bergamini C, Lamperti C, Fato R. The roles of coenzyme Q in disease: direct and indirect involvement in cellular functions. Int J Mol Sci 2021;23(01):128

150 Bandara AB, Drake JC, Brown DA. Complex II subunit SDHD is critical for cell growth and metabolism, which can be partially restored with a synthetic ubiquinone analog. BMC Mol Cell Biol 2021;22(01):35

151 Kadenbach B. Complex IV - The regulatory center of mitochondrial oxidative phosphorylation. Mitochondrion 2021;58:296–302

152 Calbet JAL, Martín-Rodríguez S, Martin-Rincon M, Morales-Alamo D. An integrative approach to the regulation of mitochondrial respiration during exercise: focus on high-intensity exercise. Redox Biol 2020;35:101478

153 Allen DG, Lamb GD, Westerblad H. Skeletal muscle fatigue: cellular mechanisms. Physiol Rev 2008;88(01):287–332

154 Nanadikar MS, Vergel Leon AM, Borowik S, et al. O_2 affects mitochondrial functionality ex vivo. Redox Biol 2019;22:101152

155 Larsen FJ, Schiffer TA, Sahlin K, Ekblom B, Weitzberg E, Lundberg JO. Mitochondrial oxygen affinity predicts basal metabolic rate in humans. FASEB J 2011;25(08):2843–2852

156 Verkhovsky MI, Morgan JE, Puustein A, Wikström M. Kinetic trapping of oxygen in cell respiration. Nature 1996;380 (6571):268–270

157 Gnaiger E, Lassnig B, Kuznetsov A, Rieger G, Margreiter R. Mitochondrial oxygen affinity, respiratory flux control and excess capacity of cytochrome c oxidase. J Exp Biol 1998;201 (Pt 8):1129–1139

158 Zhao RZ, Jiang S, Zhang L, Yu ZB. Mitochondrial electron transport chain, ROS generation and uncoupling (Review). Int J Mol Med 2019;44(01):3–15

159 Gorman GS, Chinnery PF, DiMauro S, et al. Mitochondrial diseases. Nat Rev Dis Primers 2016;2(01):16080

160 Chinnery PF. Primary mitochondrial disorders overview. University of Washington. Jul 29, 2021. Accessed May 29, 2023 at: https://www.ncbi.nlm.nih.gov/books/NBK1224/

161 Hage R, Vignal-Clermont C. Leber hereditary optic neuropathy: review of treatment and management. Front Neurol 2021; 12:651639

162 Crofts AR. The cytochrome bc1 complex: function in the context of structure. Annu Rev Physiol 2004;66:689–733

163 Arulkumaran N, Deutschman CS, Pinsky MR, et al;ADQI XIV Workgroup. Mitochondrial function in sepsis. Shock 2016;45 (03):271–281

164 Madamanchi NR, Runge MS. Mitochondrial dysfunction in atherosclerosis. Circ Res 2007;100(04):460–473

165 Pinti MV, Fink GK, Hathaway QA, Durr AJ, Kunovac A, Hollander JM. Mitochondrial dysfunction in type 2 diabetes mellitus: an organ-based analysis. Am J Physiol Endocrinol Metab 2019;316 (02):E268–E285

166 Zhunina OA, Yabbarov NG, Grechko AV, et al. The role of mitochondrial dysfunction in vascular disease, tumorigenesis, and diabetes. Front Mol Biosci 2021;8:671908

167 Diaz-Vegas A, Sanchez-Aguilera P, Krycer JR, et al. Is mitochondrial dysfunction a common root of noncommunicable chronic diseases? Endocr Rev 2020;41(03):bnaa005

168 Cloonan SM, Kim K, Esteves P, Trian T, Barnes PJ. Mitochondrial dysfunction in lung ageing and disease. Eur Respir Rev 2020;29 (157):200165

169 Zhang WZ, Rice MC, Hoffman KL, et al;SPIROMICS Investigators. Association of urine mitochondrial DNA with clinical measures of COPD in the SPIROMICS cohort. JCI Insight 2020;5(03): e133984

170 Yubero D, Montero R, Santos-Ocaña C, Salviati L, Navas P, Artuch R. Molecular diagnosis of coenzyme Q_{10} deficiency: an update. Expert Rev Mol Diagn 2018;18(06):491–498

171 Desbats MA, Lunardi G, Doimo M, Trevisson E, Salviati L. Genetic bases and clinical manifestations of coenzyme Q10 (CoQ 10) deficiency. J Inherit Metab Dis 2015;38(01):145–156

172 Mahmud T, Rafi SS, Scott DL, Wrigglesworth JM, Bjarnason I. Nonsteroidal antiinflammatory drugs and uncoupling of mitochondrial oxidative phosphorylation. Arthritis Rheum 1996;39 (12):1998–2003

173 Warrick BJ, King A, Smolinske S, Thomas R, Aaron C. A 29-year analysis of acute peak salicylate concentrations in fatalities reported to United States poison centers. Clin Toxicol (Phila) 2018;56(09):846–851

174 Ciejka M, Nguyen K, Bluth MH, Dubey E. Drug toxicities of common analgesic medications in the emergency department. Clin Lab Med 2016;36(04):761–776

175 Juurlink DN, Gosselin S, Kielstein JT, et al;EXTRIP Workgroup. Extracorporeal treatment for salicylate poisoning: systematic review and recommendations from the EXTRIP workgroup. Ann Emerg Med 2015;66(02):165–181

176 Randi EB, Zuhra K, Pecze L, Panagaki T, Szabo C. Physiological concentrations of cyanide stimulate mitochondrial Complex IV and enhance cellular bioenergetics. Proc Natl Acad Sci U S A 2021;118(20):e2026245118

177 Zuhra K, Szabo C. The two faces of cyanide: an environmental toxin and a potential novel mammalian gasotransmitter. FEBS J 2022;289(09):2481–2515

178 Gracia R, Shepherd G. Cyanide poisoning and its treatment. Pharmacotherapy 2004;24(10):1358–1365

179 Thompson JP, Marrs TC. Hydroxocobalamin in cyanide poisoning. Clin Toxicol (Phila) 2012;50(10):875–885

180 Bebarta VS, Brittain M, Chan A, et al. Sodium nitrite and sodium thiosulfate are effective against acute cyanide poisoning when administered by intramuscular injection. Ann Emerg Med 2017; 69(06):718.e4–725.e4

181 Sylvester DM, Hayton WL, Morgan RL, Way JL. Effects of thiosulfate on cyanide pharmacokinetics in dogs. Toxicol Appl Pharmacol 1983;69(02):265–271

182 Hansen MB, Olsen NV, Hyldegaard O. Combined administration of hyperbaric oxygen and hydroxocobalamin improves cerebral metabolism after acute cyanide poisoning in rats. J Appl Physiol 2013;115(09):1254–1261

183 Takano T, Miyazaki Y, Nashimoto I, Kobayashi K. Effect of hyperbaric oxygen on cyanide intoxication: in situ changes in intracellular oxidation reduction. Undersea Biomed Res 1980;7 (03):191–197

184 Smilkstein MJ, Bronstein AC, Pickett HM, Rumack BH. Hyperbaric oxygen therapy for severe hydrogen sulfide poisoning. J Emerg Med 1985;3(01):27–30

185 Weibel ER, Taylor CR, Hoppeler H. The concept of symmorphosis: a testable hypothesis of structure-function relationship. Proc Natl Acad Sci U S A 1991;88(22):10357–10361

186 Taylor CR, Weibel ER, Weber JM, et al. Design of the oxygen and substrate pathways. I. Model and strategy to test symmorphosis in a network structure. J Exp Biol 1996;199; (Pt 8):1643–1649

Article published online: 2023-06-27

Arterial Blood Gases and Acid–Base Regulation

Sarah F. Sanghavi, MD[1] Erik R. Swenson, MD[2]

[1] Division of Nephrology, Department of Medicine, University of Washington, Puget Sound Veterans Affairs Healthcare System, Seattle, Washington
[2] Division of Pulmonary, Critical Care and Sleep Medicine, Department of Medicine, University of Washington, Puget Sound Veterans Affairs Healthcare System, Seattle, Washington

Address for correspondence Sarah F. Sanghavi, MD, 1660 S. Columbian Way Seattle, Washington 98108 (e-mail: sanghavi@uw.edu).

Semin Respir Crit Care Med 2023;44:612–626.

Abstract

Disorders of acid–base status are common in the critically ill and prompt recognition is central to clinical decision making. The bicarbonate/carbon dioxide buffer system plays a pivotal role in maintaining acid–base homeostasis, and measurements of pH, PCO_2, and HCO_3^- are routinely used in the estimation of metabolic and respiratory disturbance severity. Hypoventilation and hyperventilation cause primary respiratory acidosis and primary respiratory alkalosis, respectively. Metabolic acidosis and metabolic alkalosis have numerous origins, that include alterations in acid or base intake, body fluid losses, abnormalities of intermediary metabolism, and renal, hepatic, and gastrointestinal dysfunction. The concept of the anion gap is used to categorize metabolic acidoses, and urine chloride excretion helps define metabolic alkaloses. Both the lungs and kidneys employ compensatory mechanisms to minimize changes in pH caused by various physiologic and disease disturbances. Treatment of acid–base disorders should focus primarily on correcting the underlying cause and the hemodynamic and electrolyte derangements that ensue. Specific therapies under certain conditions include renal replacement therapy, mechanical ventilation, respiratory stimulants or depressants, and inhibition of specific enzymes in intermediary metabolism disorders.

Keywords
- respiratory
- metabolic
- acidosis
- alkalosis
- anion gap
- lactate
- bicarbonate

Fundamental Concepts

Regulation of arterial and extracellular pH is critical in maintaining extracellular and intracellular acid–base homeostasis. Arterial pH is kept under tight control by the central nervous system (CNS) in combination with the lungs and kidneys. Although in most acid–base disorders deviations of arterial pH are mitigated by specific compensatory responses to maintain acid–base homeostasis, other physiologic priorities may take precedence. For example, hypoxemia stimulates the peripheral chemoreceptors, resulting in hyperventilation and respiratory alkalosis. In metabolic alkalosis due to severe vomiting, alkalosis is maintained by the overriding need for the kidneys to maintain sodium and extracellular volume. This article will review the basic concepts in acid–base balance, assessment of acid–base disturbances, their pathophysiology, and treatment.

Acid–Base Chemistry

pH versus [H^+]

In aqueous solutions, "free" hydrogen ions (protons) are associated with clusters of water molecules, but for convenience these are designated as H^+ or H_3O^+. Rather than expressing acidity in terms of H^+ concentration ([H^+], normally 35–45 nM in plasma), the logarithmic function ("pH," normally 7.35–7.45 in plasma) is $pH = -\log_{10}[H^+]$. pH is generally preferred for convenience in representing the broad range of concentrations existing in body fluids from

article published online
June 27, 2023

Issue Theme Pulmonary Physiology; Guest Editors: David A. Kaminsky, MD, Kathryn A. Hibbert, MD, and Andrew M. Luks, MD

Thieme Medical Publishers, Inc.,
333 Seventh Avenue, 18th Floor,
New York, NY 10001, USA

DOI https://doi.org/10.1055/s-0043-1770341.
ISSN 1069-3424.

a pH of 1 in gastric acid to 8 in urine, pancreatic and biliary secretions.

Conjugate Acids and Bases

As established by Bronsted and Lowry, an acid is a proton (H^+) donor, whereas a base is a H^+ acceptor. Ions that are completely ionized in water (e.g., Na^+, K^+, and Cl^-) are not considered bases or acids because they neither accept nor donate H^+ ions. Because the pH of the extracellular fluid (ECF) is normally approximately 7.4, some interpretations of acid–base chemistry categorize many organic acids (with dissociation constants below ≈ 4.0) as "strong" acids because these acids are more than 99.9% dissociated at an extracellular pH of 7.4.

Carbon Dioxide and Bicarbonate and Other Buffers

Buffer systems minimize changes in pH upon the addition of acid or base to defend normal enzymatic function, membrane voltage, and protein structure. The bicarbonate buffer system (**Eq. 1**) is quantitatively important in maintaining arterial pH at approximately 7.4 as demonstrated by the following relationship:

$$CO_2 + H_2O \overset{CA}{\leftrightarrow} H_2CO_3 \rightleftharpoons H^+ + HCO_3^- \quad \textbf{Eq. 1}$$

Pulmonary gas exchange maintains dissolved CO_2 concentrations approximately 20 times less than bicarbonate. A relatively low PCO_2 compared with HCO_3^- concentration makes for optimal function of the bicarbonate buffer system in vivo. The first reaction is slow, but catalytically accelerated by carbonic anhydrase (CA), which is present in erythrocytes and most other organs.[1,2]

Although HCO_3^- is a principal buffer, particularly in blood and the extracellular space, numerous other inorganic and organic compounds play a contributing role, including phosphates, titratable amino acids on proteins (e.g., albumin), and certain metabolites of glycolysis and oxidative metabolism. Their contribution varies depending on the nature of the acid–base disturbance, their dissociation constants, and the distribution between fast and slow exchanging spaces.

Arterial and Venous Blood Gas Analysis

Arterial blood gas analysis is the gold standard for assessing oxygenation, alveolar ventilation, and acid–base status. PO_2, PCO_2, and pH are readily measured with electrodes (maintained at 37°C) in blood, and plasma HCO_3^- is calculated from pH and PCO_2 values. Alternatively, HCO_3^- can be estimated from the total carbon dioxide content, which is measured as part of a basic metabolic profile in venous blood. Total venous CO_2 content is roughly 5% higher (2–3 mM) than arterial HCO_3^- because it includes all forms of CO_2 including H_2CO_3, dissolved CO_2, carbonate, and CO_2 bound to terminal amino acids on hemoglobin as carbamates. In addition, it is higher since it contains that amount of CO_2 not yet eliminated by the lungs from venous blood.

Changes in arterial plasma pH are assumed to reflect comparable changes within cells, but this simplification is frequently inappropriate. It is therefore better to refer to deviations from normal plasma pH as acidemia and alkalemia rather than as acidosis and alkalosis. The latter terms refer to processes and do not designate the actual pH or compartments. Intracellular pH, not clinically measurable, is regulated by an array of energy-dependent acid–base transporters.[3]

Blood pH, PCO_2, and PO_2 are prone to errors if blood samples are exposed to air or inadvertently diluted, analysis is delayed, or measurements are made without temperature correction for hypo- or hyperthermia. Air exposure decreases PCO_2 and raises pH and PO_2. Dilution of samples by saline or fluids in indwelling catheters causes both PCO_2 and HCO_3^- to fall equally. Hypothermic samples lead to spuriously higher PCO_2, lower pH, and higher PO_2.[4] The converse is true for hyperthermic samples. While it remains controversial as to whether temperature-corrected values should be used in clinical assessment of acid–base status, the calculation of the alveolar-arterial O_2 difference to assess pulmonary gas exchange efficiency is more accurate using the "in vivo" temperature-corrected values of PaO_2 and $PaCO_2$.

A venous blood gas sample drawn from a central venous catheter with its tip as close to the right atrium as possible, or more ideally a pulmonary artery catheter, offers an alternative way to assess acid–base status and may be used if one does not require information about arterial oxygenation. More peripheral venous sampling, particularly if a blood restricting tourniquet is employed, is not useful since these values are indicative of the local region's metabolic rate and blood flow, and not of the body in total. On average, central and mixed venous pH is lower by 0.05 units, and venous PCO_2 is higher by 5 mm Hg, than corresponding arterial values at basal metabolic rate and cardiac output. These differences will be lower if cardiac output is high. In states of low cardiac output, high CO_2 production (such as exercise), or red cell CA inhibition (e.g., high-dose acetazolamide), the arteriovenous differences can increase by as much as 10-fold.[5]

Nomenclature of Acid–Base Disorders

Procedures for naming acid–base disorders are simple if CO_2 and HCO_3^- are used as the respiratory and metabolic parameters. Ideally, the patient should be in a steady state with respect to compensations, but this is not always the case in a rapidly evolving clinical condition. An additional assumption is that compensations are never complete, especially with severe acid–base disturbances. If arterial pH is low, the primary disorder is an acidosis, and, if high, it is an alkalosis. Based on this approach, abnormal combinations of pH, PCO_2, and HCO_3^- can be designated in terms of a primary disorder and any compensation that might be present.

►**Fig. 1** indicates the ranges in which HCO_3^- and PCO_2 change in healthy people when undergoing acute or chronic respiratory and/or metabolic changes. The bands represent the known 95% confidence intervals for these disorders at their steady states. Baseline values for both PCO_2 and HCO_3^- help to clarify any compensatory responses. Blood gas values lying outside the 95% confidence bands represent either acid–base disorders that have not reached steady state or concurrent dual coexisting primary disorders. Occasionally, triple disorders may also be encountered, involving an anion gap acidosis, nonanion gap acidosis, or metabolic alkalosis, and a primary respiratory disorder.

Several caveats should be appreciated regarding both this and other approaches that classify acid–base disorders strictly based on pH, PCO_2, and a metabolic parameter. Distinctions between primary and compensatory disorders are based simply on which alteration is proportionately greater at the time blood was drawn rather than on the sequence of events involved. For example, it is common for patients with chronic obstructive pulmonary disease (COPD) to be admitted to the hospital with a compensated respiratory acidosis. With therapy, PCO_2 may decrease, leaving what might otherwise in the absence of the clinical history be taken as “a primary metabolic alkalosis with secondary respiratory compensation.” Winters[6] suggested that a distinction be made between the “physiologic” language commonly used by the physician and the “laboratory” terminology that is strictly based on blood parameters.

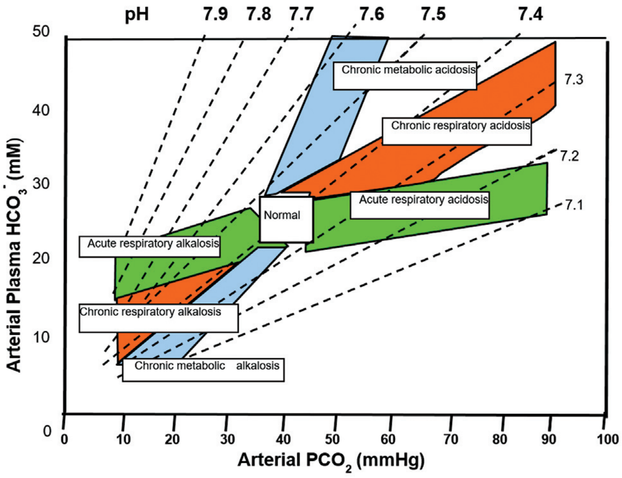

Fig. 1 The relation between HCO_3^- and PCO_2 in a variety of clinical disorders. For discussion, see text. (**A**) The 95% confidence levels for acute and chronic respiratory and metabolic abnormalities. (**B**) While in principle acute metabolic acidosis and alkalosis occur (no change in PCO_2) and would be seen as vertical bands above and below the “normal” box, respiratory compensations occur very quickly, in comparison to the renal response to a respiratory disturbance, that clinically only chronic metabolic acidosis and alkalosis are observed. The respiratory response to the onset of metabolic acidosis and alkalosis is rapid, and the metabolic bands rotate clockwise toward the chronic metabolic position within a matter of minutes. Compensatory metabolic responses to respiratory changes in arterial PCO_2 are much slower, making it easier to observe the acute respiratory bands before metabolic compensation.

Ventilatory Parameter: Arterial PCO_2

The Henderson–Hasselbalch equation (below) shows that pH (**Eq. 2**) can be calculated from two variables, PCO_2 and HCO_3^-, without consideration of other acid–base pairs in the plasma:

$$\mathrm{pH} = pK_a + \log\frac{[\mathrm{HCO_3^-}]}{\alpha \mathrm{PCO_2}} \quad \textbf{Eq. 2}$$

where pK_a is the dissociation constant of 6.1 at 37°C and α is the solubility constant of CO_2 (0.031 mM/mm Hg) to yield a molar concentration. Arterial PCO_2 can be interpreted as a “ventilatory” parameter that reflects the adequacy of alveolar ventilation relative to the rate of carbon dioxide production. If arterial PCO_2 exceeds the normal range (35–45 mm Hg), the patient is hypoventilating, and, conversely, if the arterial PCO_2 is lower, the patient is hyperventilating. These terms should be distinguished from hyperpnea and hypopnea, which refer to the increases or decreases in minute ventilation to meet respiratory requirements, and from tachypnea and bradypnea, which indicate rapid and slow respiratory rates.

Metabolic Parameters

Bicarbonate

Although HCO_3^- is the oldest and most popular metabolic parameter in assessing acid/base status, the magnitude of its change underestimates the amount of acid (or base) added to the body. This reflects the presence and participation of other buffer pairs that are titrated, which are generally nonvolatile and conserved. The second problem with using bicarbonate as a metabolic parameter is that it is influenced by changes in arterial PCO_2 and HCO_3^- that may be increased or decreased due to a preexisting condition. Thus, when relying only on HCO_3 concentration, deviations from normal will usually underestimate the severity of any metabolic acid–base abnormality.

Base Excess

The base excess (BE) concept was developed in response to some of above limitations, since it includes nonbicarbonate buffering and deals with the effects of PCO_2 changes (respiratory acid–base changes) on bicarbonate.[7] It estimates how much strong acid or alkali must be added to titrate fully oxygenated blood to a pH of 7.4 at 37°C and at the hemoglobin concentration in that sample. The “standard” BE uses a hemoglobin value of 5 g/dL (one-third of a normal hemoglobin of 15 g/dL) since buffering by hemoglobin occurs throughout the entire extracellular space (intravascular and interstitial) not just the intravascular compartment, which is only one-third of the total extravascular space. It has proven to be superior to the blood BE in vivo and normally is 0 ± 2 mEq/L.[8] Negative standard BE values indicate a metabolic acidosis and positive values indicate a metabolic alkalosis.

Strong Ion Difference

Another approach advocated to analyze acid–base disorders is to focus on the concentrations and dissociation constants of all strong and weak acids and bases present in the plasma, thereby avoiding either titration or the use of some of the approximations associated with earlier approaches. It calculates arterial plasma pH and HCO_3^- from (1) the difference between total concentrations of strong cations and strong anions in the plasma (strong ion difference [SID], which is normally 40–42 mEq/L), (2) the total concentration and dissociation constants of all nonvolatile weak acids and bases (primarily albumin and phosphates), and (3) the PCO_2. The SID is normally close to the charge difference between Na^+ and Cl^- concentrations, and albumin accounts for much of the weak nonbicarbonate anions in the SID. It is assumed that all the constituents in the plasma other than H^+, CO_2, HCO_3^-, and CO_3^{2-} are conserved and that the solution remains electroneutral. All organic anions with a pK_a below 4, such as lactate, are considered "strong" ions. The simultaneous equations for pH and HCO_3^- are then solved iteratively as a fourth-order polynomial using a computer program. "Metabolic" changes in acid–base balance are due to alterations in either SID or the total concentration of proteins with titratable amino acids in the physiologic range. If serum albumin concentrations are normal, then an increase in SID indicates a metabolic alkalosis and a decrease in SID indicates a metabolic acidosis.

In principle there is merit in defining the effects of all acid–base pairs upon plasma pH. However, it is difficult to make sufficiently precise measurements of the constituents of SID, and the plasma concentrations of weak acids and bases, many of which have not been identified or properly quantified, especially in patients with liver or kidney disease. Furthermore, the assumption of a single dissociation constant for all the weak acids and bases is questionable. Nor does the SID approach distinguish between acute and chronic disorders. The original suggestion that pH and HCO_3^- should be calculated rather than measured is particularly ungrounded because these two variables are much more easily and reliably measured than indirectly estimated from the strong ions and nonvolatile acids and bases in the blood, all of which have their own measurement errors.

None of the three metabolic parameters (bicarbonate, BE, and SID) provides a completely reliable estimate of the quantity of nonvolatile H^+ or OH^- that has been added to the body. Nor is it clear that either in vitro titration or SID calculations can provide a reliable guide to the in vivo acid–base status or the quantitative amount of administered base or acid that is needed for full correction. Consequently, frequent monitoring of arterial blood is essential in patients with metabolic acid–base disorders who are receiving infusions of acidic or alkaline fluids. Although the conventional approach of using bicarbonate changes suffices in cases of extreme acid–base disorders, we favor the BE approach as it deals with the problem of PCO_2 differences on HCO_3^- and contributions by other bases and acids in the ECF and may be more reliable in mixed disturbances and those of lesser severity.

Compensations

Respiratory Acidosis

The acute increase in HCO_3^- is relatively modest after the onset of hypercapnia from simple mass action chemical formation of H_2CO_3 and buffering of the H^+ produced by nonbicarbonate buffers. HCO_3^- continues to rise if hypercapnia persists and reaches a peak value after approximately 5 days (►**Table 1**) through renal bicarbonate generation. Increases in plasma HCO_3^- require an initial net loss of H^+, which occurs through increased excretion of NH_4^+ in the urine. Mechanisms mirror those that occur with an increase in exogenous acids. Data also suggests that chronic respiratory acidosis may downregulate activity of the apical HCO_3^-/Cl^- exchanger pendrin in the cortical collecting duct.[9] Once plasma HCO_3^- has reached a new steady state, NH_4^+ and H^+ excretion usually return to normal. An increase of approximately 4 mEq/L of HCO_3^- may be expected when PCO_2 increases by 10 mm Hg. Confidence bands for chronic compensation, along with the other acid–base disturbances are indicated in ►**Fig. 1**.

Respiratory Alkalosis

Hypocapnia results in a decrease in renal acid excretion and a fall in HCO_3^- that becomes fully evident within 2 to 3 days. As

Table 1 Rules of chronic compensation

		Examples	
Primary disorder	Compensation	Primary change	Compensation
↑ PCO_2	↑ HCO_3^-: 4 mEq/L for each 10-mm Hg increase in PCO_2 (± 3 mEq/L)	PCO_2: 40 → 80	HCO_3^-: 24 → 40pH: 7.1 → 7.32
↓ PCO_2	↓ HCO_3^-: 4 mEq/L for each 10-mm Hg decrease in PCO_2 (± 3 mEq/L)[a]	PCO_2: 40 → 20	HCO_3^-: 24 → 16pH: 7.70 → 7.53
↓ HCO_3^-	↓ PCO_2: 1–1.5 mm Hg for each mEq/L decrease in HCO_3^-	HCO_3^-: 24 → 9	PCO_2: 40 → 25pH: 7.00 → 7.20
↑ HCO_3^-	↑ PCO_2: 0.5–1.0 mm Hg for each mEq/L increase in HCO_3^-	HCO_3^-: 24 → 34	PCO_2: 40 → 50pH: 7.56 → 7.46

[a] HCO_3^- seldom falls below 18 mEq/L in acute and 16 mEq/L in chronic respiratory alkalosis.

indicated in ►**Table 1**, HCO_3^- decreases by 4 mEq/L for each decrease of 10 mm Hg in PCO_2[10] and does not generally fall much below 16 mEq/L in respiratory alkalosis unless there is an independent metabolic acidosis present. Both decreased reabsorption of HCO_3^- in the proximal tubule and decreased NH_4^+ excretion contribute to this process.

Metabolic Acidosis

Respiratory compensation for metabolic disorders is quite fast (within minutes) and reaches maximal values within 24 hours. As indicated in ►**Table 1**, a decrease in PCO_2 of 1 to 1.5 mm Hg should be observed for each mEq/L decrease of HCO_3^- in metabolic acidosis.[11] A simple rule for deciding whether the fall in PCO_2 is appropriate for the degree of metabolic acidosis is that the PCO_2 should be equal to the last two digits of the pH. For example, compensation is adequate if the PCO_2 decreases to 28 when the pH is 7.28. Another helpful formula is Winters' formula which can be used provided the pH is > 7.1 whereby the expected $PCO_2 = 1.5\,(HCO_3^-) + 8 \pm 2$.[12]

Metabolic Alkalosis

Compensation for metabolic alkalosis results in a decrease in minute ventilation and a rise of PCO_2 by approximately 0.6 to 0.7 mm Hg per mEq/L increase in HCO_3^- as indicated in ►**Table 1**. This compensatory hypoventilation generally does not exceed a PCO_2 of 55 mm Hg as the accompanying fall in PaO_2 evokes increased ventilation to defend arterial oxygenation. This general rule may not apply in severe metabolic alkalosis where compensatory PCO_2 increases greater than 60 mm Hg have been documented.[12] A variety of other factors have been reported that can increase PCO_2 with metabolic alkalosis.[13] Respiratory compensation for metabolic alkalosis, like that for metabolic acidosis, can have a counterproductive effect on renal H^+ transport: increases in PCO_2 associated with metabolic alkalosis decrease intracellular pH in the kidney, thereby promoting acid secretion and further increasing serum HCO_3^- levels.[14]

Clinical Acid–Base Disorders

Metabolic Acidosis

A metabolic acidosis may result from three processes: (1) addition of exogenous or endogenous acid, (2) bicarbonate loss, or (3) impaired renal acid excretion. Under physiologic conditions, the kidneys reclaim filtered HCO_3^- in the proximal tubule and secrete H^+ in the cortical collecting duct, thereby regenerating HCO_3^-. Any process that disrupts these activities causes a metabolic acidosis mediated by the kidney, as occurs in chronic kidney disease, acute kidney injury, and renal tubular acidosis (RTA).

Anion Gap

The anion gap measurement helps to determine whether the deficit of bicarbonate is due to buffering of an endogenous or exogenous acid. This calculated difference (**Eq. 3**) between serum cations and anions is roughly equal to the negative charge contributed by albumin and unmeasured anions including pyruvate, lactate, sulfate, and phosphate.

$$Anion\ \ Gap = [\mathrm{Na}^+] - ([\mathrm{Cl}^-] + [\mathrm{HCO}_3^-]) \ \ \textbf{Eq. 3}$$

Normally, the anion gap is between 8 and 16 mEq/L depending upon the type of electrodes used by the laboratory. Hypoalbuminemia decreases the anion gap by approximately 2.5 mEq/L for each 1 g/dL decrease in albumin concentration.[15]

When an acid is added to the serum and buffered by bicarbonate, the conjugate base, an unmeasured anion, remains, resulting in an elevated anion gap (**Eq. 4**).

$$\mathrm{HX + HCO_3^- \rightarrow H_2CO_3 + X^-} \ \ \textbf{Eq. 4}$$

The mnemonic "GOLD MARK" (**G**lycols including ethylene glycol and propylene glycol, 5-**O**xoproline (pyroglutamic acid), **L**actic acidosis, **D**- lactic acidosis, **M**ethanol, **A**spirin, **R**enal failure, and **K**etoacidosis) is useful for many causes of an anion gap acidosis.[16] A low anion gap reflects an increase in cations other than Na^+ (e.g., *calcium* [Ca^{2+}], *magnesium* [Mg^{2+}], *lithium* [Li^+], and abnormal cationic proteins, such as in multiple myeloma). A more extensive list of nonanion gap metabolic acidoses is provided in ►**Table 2**. Although the anion gap concept is used in the setting of a metabolic acidosis, a nonpathologic elevated anion gap may be seen in alkalotic conditions. Alkalemia decreases H^+ binding to albumin, thereby increasing the number of negatively charged groups.

Delta Gap

An anion gap acidosis may coexist with additional metabolic disturbances, which can be assessed using the delta gap (sometimes called the delta-delta). The delta gap is the difference between the calculated anion gap and a normal value of 12 or the patient's baseline value if known. When a new acid is added, the H^+ combines with HCO_3^- producing CO_2 and H_2O. The CO_2 is exhaled by the lungs resulting in the loss of bicarbonate and the equivalent gain of a conjugate base (anion) in the extracellular compartment (**Eqs. 5** and **6**).

$$\mathrm{HX + HCO_3^- \rightarrow H_2CO_3 + X^- \rightarrow H_2O + CO_2 + X^-} \ \ \textbf{Eq. 5}$$

$$\mathrm{HX + HCO_3 \rightarrow X^-} \ \ \textbf{Eq. 6}$$

In a pure anion gap acidosis, the delta gap would be expected to approximate the deficit in bicarbonate. Thus, when the delta gap is added to the total CO_2, the sum is 24. If the sum is much greater than 28, a concurrent metabolic alkalosis exists. A sum lower than 20 should prompt a search for a coexisting hyperchloremic acidosis. Either the H^+ or the conjugate base may leave the extracellular space, altering this 1:1 relationship. For example, in lactic acidosis, the delta gap often exceeds the decrease in bicarbonate whereas the opposite is true in diabetic ketoacidosis (DKA).[17]

Lactic Acidosis

Approximately 1,400 mEq of lactate are produced each day in normal metabolism.[18] In conditions of ischemia, profound hypoxemia, tissue hypoxia, and severe sepsis, lactate may be produced by anaerobic metabolism (nonoxidative glycolysis). Quantitative metabolism of lactate in the liver, skeletal muscle, and kidneys maintains a serum level of approximately 1 mEq/L. From a strict biochemical standpoint, the reduction of pyruvate to lactate consumes rather than produces a hydrogen ion (**Eq. 7**).

$$\text{Pyruvate} + \text{NADH} + \text{H}^+ \rightleftharpoons \text{Lactate} + \text{NAD}^+ \quad \textbf{Eq. 7}$$

The hydrogen ion that is formed in states of "lactic acidosis" arises from the hydrolysis of *adenosine triphosphate* (ATP; **Eq. 8**):

$$\text{ATP} + \text{H}_2\text{O} \rightleftharpoons \text{ADP} + \text{PO}_4^- + \text{H}^+ \quad \textbf{Eq. 8}$$

and other yet unknown reactions forming H^+ under states of metabolic stress. When *adenosine diphosphate* (ADP) is not rephosphorylated, H^+ accumulates.

The delta gap in lactic acidosis may exceed the decrease in bicarbonate. Lactate tends to remain in the extracellular space whereas hydrogen ions move intracellularly and are buffered by nonbicarbonate buffers. Intracellular buffering increases as the serum HCO_3^- decreases, leading to a more pronounced difference in severe acidosis.[17] Thus, when the delta gap is added to the total CO_2, the sum can be greater than 24. This occurs frequently in lactic acidosis and should not be misinterpreted as evidence for a coexisting metabolic alkalosis.[15]

Since lactic acidosis due to tissue hypoxia needs urgent attention, lactic acidosis is classified by the presence (type A) or absence (type B) of tissue hypoxia.[19] Type A disorders include all forms of shock, acute hypoxemia, carbon monoxide (CO) poisoning, methemoglobinemia, and severe anemia. Lactic acidosis is much more likely to appear when tissue hypoxia from poor perfusion is present than in hypoxemia, as compensatory increases in cardiac output and hematocrit minimize tissue hypoxia. Further, in acidotic conditions, a pH- mediated increase in 2,3-diphosphoglycerate production decreases oxygen-hemoglobin binding and increases offloading of O_2 to the tissues. In CO poisoning, oxygen delivery is impaired due to preferential hemoglobin binding by carbon monoxide. Carboxyhemoglobin induces an allosteric change increasing oxygen binding affinity, shifting the hemoglobin-dissociation curve to the left (lower P50) and impairing O_2 off-loading. Impaired oxygen utilization due to CO binding to myoglobin and mitochondrial cytochromes also contributes to the lactic acidosis. Methemoglobinemia, much like carboxyhemoglobin, also causes a loss of heme-O_2 binding sites as well as increasing the oxygen affinity of hemoglobin.

Type B disorders include congenital metabolic enzyme deficiencies, acquired disturbances in oxidative phosphorylation, and drug effects. Metformin-associated lactic acidosis (MALA) deserves special attention due to its high mortality rate of 30 to 35%.[20] Metformin decreases hepatic gluconeogenesis from lactate due to inhibition of mitochondrial respiratory chain complex 1.[21] Most cases involve standard metformin dosing in the setting of worsening renal function, while a minority of cases are due to overdoses. Patients with MALA often develop shock thought to be secondary to the negative inotropic effects of metformin.[22]

Salicylate overdose causes a lactic acidosis due to uncoupling of oxidative phosphorylation, which accounts for the anion gap seen in this condition. One of the defining features of salicylate intoxication is a primary respiratory alkalosis due to CNS stimulation. Therefore, a blood gas should be obtained if this diagnosis is plausible or if symptoms of tinnitus, nausea/vomiting, and vertigo are present.

5-Oxoproline, also known as pyroglutamic acid, is a metabolic byproduct that can accumulate in chronic

Table 2 Causes of elevated anion gap acidosis

Lactic acidosis
Type A: tissue hypoxia
Poor tissue perfusion: distributive shock, cardiogenic shock, obstructive shock
Severe hypoxemia
Increased oxygen requirement: strenuous exercise, seizures, shivering
Inadequate oxygen content: severe anemia, carbon monoxide poisoning, methemoglobinemia
Type B: altered lactate metabolism without hypoxia
Impaired clearance: liver disease, renal failure, diabetes mellitus, cancer (especially hematopoietic), sepsis
Drugs: β-agonists, biguanides, cocaine, cyanide, ethanol, diethyl ether, fluorouracil, halothane, salicylates, isoniazid, linezolid, propofol, zidovudine (AZT)
D-Lactic acidosis
Ketoacidosis
Diabetes mellitus, starvation, ethanol, SGLT2 inhibitors, inherited errors of metabolism
Uremia
Toxic anions
Ethylene glycol, methanol, paraldehyde (acetoacetate), aminocaproic acid

acetaminophen ingestion. Depletion of glutathione through the metabolism of acetaminophen upregulates enzymes such as γ-glutamyl cysteine synthase, which is involved in the conversion of glutamic acid to a glutathione precursor, γ-glutamyl phosphate. When cysteine levels are low, this precursor autocyclizes to form 5-oxoproline. Most patients who develop this disorder are malnourished or chronically ill, and serum concentrations of acetaminophen are normal.[23]

Malignancies, particularly lymphoproliferative and myeloproliferative disorders, may result in overproduction of lactic acid. This phenomenon may result from the preference of metabolically active and dividing cancer cells to rely on aerobic glycolysis as an ATP source rather than mitochondrial oxidative phosphorylation, even when oxygen is abundant,[24] and to generate 3-carbon intermediates for protein, fat, and nucleic acid synthesis. Furthermore, rapidly proliferating tumors may outgrow their blood supply causing localized ischemia.

Small increases in lactate may be seen with ethanol use, thiamine deficiency, and high-dose β-adrenergic agonist administration. The oxidation of ethanol generates NADH and shifts the NAD^+/NADH ratio to favor the conversion of pyruvate to lactate. Thiamine is a cofactor for pyruvate dehydrogenase complex, which converts pyruvate to acetyl-CoA allowing entry into the Krebs cycle. Deficiency of thiamine causes pyruvate to instead undergo anaerobic metabolism. In β-adrenergic stimulation, the production of pyruvate and free fatty acids are increased through glycolysis and lipolysis, respectively. These free fatty acids inhibit pyruvate dehydrogenase complex and therefore favor a shift to lactate.

One type of lactic acidosis that is not detected on routine assays is D-lactic acidosis.[25] Bacteria in the colon metabolize carbohydrates to D-lactic acid, which is absorbed systemically. Since D-lactate cannot be converted into pyruvate by L-lactate dehydrogenase, it may accumulate. This disorder is seen with conditions that predispose to delivery of starches and glucose to the colon such as short bowel syndrome.

Diabetic Ketoacidosis

Accumulation of acetoacetate, β-hydroxybutyrate, and acetone ("ketone bodies"), referred to as "ketoacidosis," requires both increased mobilization of free fatty acids from lipid stores and excessive hepatic conversion to ketones. Diabetes enhances the first process as lipase activity increases with a high glucagon-to-insulin ratio leading to increased lipolysis. Free fatty acids released from adipocytes are taken up by the liver where they combine with CoA to form acyl-CoA. When acyl-CoA enters hepatic mitochondria, it is converted into acetyl-CoA. Acetyl-CoA may then be(1) metabolized to CO_2 and water in the Krebs cycle or (2) converted to ketone bodies. In DKA, the quantities of acetyl-CoA produced exceed the capacity of the Krebs cycle and are converted to ketone bodies.[26]

It is common for a nonanion gap acidosis to develop during treatment for DKA. Volume resuscitation, particularly with saline, increases renal clearance of ketoacid anions as Na^+ and K^+ salts. This removes conjugate anions from the extracellular space decreasing the anion gap but does not consume hydrogen ions.

Euglycemic Ketoacidosis

Euglycemic ketoacidosis is defined as ketoacidosis with a serum glucose concentration less than 250 mg/dL. This presentation has become more common with the wide adoption of sodium-glucose-transporter-2 (SGLT2) inhibitors for diabetes.[27,28] SGLT2 inhibitors decrease serum glucose concentration by preventing reabsorption in the renal proximal tubule. This decrease in blood glucose stimulates glucagon secretion and inhibits insulin secretion. During fasting or surgical stress, the glucagon-to-insulin ratio rises and can precipitate ketoacidosis, particularly in people with type 1 diabetes. SGLT2 inhibitors may also directly stimulate glucagon secretion from pancreatic α cells.[29] The increase in the glucagon-to-insulin ratio accounts for the ketoacidosis seen in starvation. In ketoacidosis due to ethanol use, ketoacidosis worsens during withdrawal as catecholamine and cortisol levels rise, further increasing the glucagon-to-insulin ratio.

Toxic Alcohols

Ingestions of methanol and ethylene glycol raise the anion gap due to metabolism to formic acid, glycolic acid, and oxalic acid by alcohol dehydrogenase. Both methanol and ethylene glycol contribute to serum osmolarity, but are not represented in the calculated osmolarity equation (**Eq. 9**):

$$\text{Serum osmolality} = (2 \times [\text{Na}^+]) + (\text{BUN}/2.8) + (\text{glucose}/18) \qquad \textbf{Eq. 9}$$

Therefore, the difference in measured serum osmolarity and calculated serum osmolarity (osmolar gap) is greater than 10. However, as these alcohols are metabolized to acids, the osmolar gap may decrease as the anion gap increases.[30] Fomepizole[31] is an alcohol dehydrogenase inhibitor which prevents the accumulation of formic acid, glycolic acid, and oxalic acid. The parent drugs are ultimately cleared by the kidney, though this is exceedingly slow for methanol with a $t_{½}$ of 50 hours.[32]

Hyperchloremic Acidosis

Metabolic acidosis in the absence of an elevated anion gap is usually associated with hyperchloremia. Common causes include dilutional acidosis from large volume saline administration, diarrhea, and chronic kidney disease (►**Table 3**). RTA is a less prevalent cause of metabolic acidosis and should be diagnosed only when the acidosis is out of proportion to the reduction of the glomerular filtration rate (GFR). The cardinal feature of type 1 and type 4 RTA is a low rate of NH_4^+ excretion in the setting of a chronic metabolic acidosis. Direct measurement of urine ammonium is not widely available, but renal ammonium excretion can be qualitatively estimated using the urine anion gap ($UAG = U_{Na}{}^+ + U_{K+} - U_{Cl}{}^-$). Since the majority

Table 3 Causes of hyperchloremic acidosis

Renal tubular acidosis
Type 1 (distal) hypokalemic
Genetic mutations (anion exchanger, AE1 deficient)
Autoimmune disorders (e.g., Sjögren's syndrome, systemic lupus erythematosus)
Drug toxicity (e.g., amphotericin B, ifosfamide)
Nephrocalcinosis (e.g., primary hyperparathyroidism, vitamin D intoxication, hyperoxaluria, Fabry disease, Wilson disease)
Tubular and interstitial renal disease (e.g., pyelonephritis and obstructive renal disease, sickle cell anemia)
Type 2 (proximal) hypokalemic
Selective carbonic anhydrase inhibitors: topiramate, acetazolamide, methazolamide
Genetic (e.g., cystinosis, Wilson disease, tyrosinemia, galactosemia, Lowe syndrome)
Monoclonal gammopathy(e.g., multiple myeloma, AL amyloid, AA amyloid)
Drug or chemical toxicity (e.g., lead, cadmium, ifosfamide, tenofovir)
Secondary hyperparathyroidism with hypocalcemia (e.g., vitamin D deficiency or resistance)
Combined type 1 and 2 RTA
Carbonic anhydrase II deficiency
Type 4 hyperkalemic
Mineralocorticoid deficiency or inhibition: Addison disease, adrenal hemorrhage, angiotensin-converting enzyme inhibitors, spironolactone, heparin, azoles
Hyporeninemic states: diabetes mellitus, NSAID use
ENaC blockade: pseudohypoaldosteronism type 1, trimethoprim, amiloride, triamterene, pentamidine
Nonrenal hyperchloremic acidosis
Diarrhea
Pancreatic drainage
Ureterosigmoidostomy
Large volume saline administration
Toluene exposure (hippurate production)
Loss of ketoanions with Na^+ or K^+

Abbreviations: ENaC, epithelial Na channel; NSAID, nonsteroidal anti-inflammatory drug; RTA, renal tubular acidosis.

of NH_4^+ is excreted as NH_4Cl, U_{Cl}^- should exceed U_{Na}^+ and U_{K+} when the kidneys are excreting acid appropriately. A UAG > 20 in the setting of a normal GFR suggests a RTA as the cause of the hyperchloremic acidosis.[33]

Gastrointestinal Disorders

Diarrhea commonly causes hyperchloremic acidosis. In the normal bowel, Cl^- is selectively absorbed in exchange for HCO_3^-. Each liter of diarrheal fluid can result in the loss of 200 mEq of HCO_3^-. Passage of urine into the bowel after ureterosigmoidostomy or ureteroileostomy can also produce hyperchloremic acidosis, because of the high urine Cl^- concentration. The ensuing volume depletion and potassium losses result in low urine Na^+ and urine K^+. Since renal H^+ excretion increases in gastrointestinal causes of metabolic acidosis, the UAG should be < –20.

Type 1 Renal Tubular Acidosis

Type 1 RTA may be seen in autoimmune conditions such as Sjogren's disease, in which insufficient distal H^+ excretion results in a urine pH > 6.5. Most causes involve a defect in the luminal H^+-ATPase, but other mechanisms occur. For example, amphotericin B is thought to make pores in luminal cell membranes allowing back-leak of H^+ from the tubular fluid.[34] Hypokalemia is a prominent feature of type 1 RTA as Na^+ reabsorption in the collecting tubule is accompanied by excretion of K^+ in lieu of H^+.

Type 2 Renal Tubular Acidosis

Normally, the proximal tubule reabsorbs 80 to 90% of filtered bicarbonate. In type 2 or proximal RTA, HCO_3^- reabsorption is impaired resulting in significant bicarbonaturia. A typical patient will have a steady-state serum HCO_3^- value in the range of 12 to 20 mEq/L. When serum HCO_3^- is normalized to 24 mmol/L by HCO_3^- infusion, more than 15% of the filtered HCO_3^- is lost in the urine (fractional excretion of bicarbonate), compared with less than 5% under normal conditions.[35] Therefore, patients with type 2 RTA tend to have a urine pH of 5 to 6 under chronic steady-state conditions which rises with $NaHCO_3$ infusion. Hypokalemia may also worsen with $NaHCO_3^-$ infusion as Na^+ is delivered to the cortical collecting duct as $NaHCO_3$. When this Na^+ is reabsorbed, K^+ is excreted to maintain electroneutrality. Since NH_4^+ excretion is preserved, a proximal RTA may have an indeterminate UAG.[36] Often, the RTA presents with other proximal tubular defects that lead to loss of glucose, phosphate, amino acids, and low-molecular-weight proteins (Fanconi's syndrome). CA inhibitors are another cause for a type 2 RTA.

Type 4 Renal Tubular Acidosis

Type 4 RTA is distinguished from other RTAs by hyperkalemia and a less severe acidosis. Any cause of hyperkalemia may result in an acidosis due to inhibition of proximal tubule ammonia generation and consequent low NH_4^+ excretion.[37] Since NH_3 cannot buffer H^+ secreted by H^+- ATPase, urine pH may still be < 5.5. Potassium-sparing diuretics, angiotensin-converting enzyme inhibitors, hypoaldosteronism, and heparin (which can inhibit aldosterone production) may cause hyperkalemia and type 4 RTA.

Miscellaneous Causes of Hyperchloremic Acidosis

Respiratory alkalosis is normally compensated by a decrease in proximal HCO_3^- reabsorption. Correction of respiratory alkalosis may transiently produce a hyperchloremic acidosis. Toluene, inhaled with glue sniffing, is converted to hippuric acid. Hippurate is rapidly filtered and secreted by the kidney, resulting in a hyperchloremic acidosis with a positive urine anion gap.[38] In the setting of decreased renal blood flow, the renal excretion may be limited resulting in an elevated anion gap acidosis.

Clinical Manifestations

The clinical presentation is primarily determined by the underlying etiology of the metabolic acidosis. However, regardless of the cause, patients may experience dyspnea due to high compensatory ventilatory requirements. In severe metabolic acidosis, patients may demonstrate slow, deep breathing at rest known as Kussmaul respiration. This involuntary breathing technique of increasing tidal volume is more efficient than increasing the respiratory rate because the dead-space fraction is minimized. Acidosis has been shown to reduce myocardial contractility and inotropic responsiveness in vitro in some animal and human models. However, there is no convincing data that it decreases total peripheral resistance causing hypotension.

Therapy

Treatment of metabolic acidosis should focus primarily on correcting the cause and the hemodynamic and electrolyte derangements that ensue. $NaHCO_3$ administration for metabolic acidosis is clearly indicated in patients who have ongoing bicarbonate losses such as in diarrhea or RTAs. In acute severe metabolic acidosis due to endogenous acid production, HCO_3^- administration may not favorably alter clinical outcomes.[39] Potential negative consequences of alkalinization include a shift of the oxygen-hemoglobin dissociation curve to the left impairing oxygen delivery, decreases in ionized calcium, and generation of carbon dioxide from HCO_3^- with paradoxical intracellular acidosis. However, alkalinizing agents are indicated to enhance excretion of certain toxic ingestions and have been shown to decrease the requirement for hemodialysis in patients with metabolic acidosis and hyperkalemia.[40]

Metabolic Alkalosis

A metabolic alkalosis may arise from addition of base to the body or any condition that causes loss of acid. Because the kidney normally rapidly excretes excess bicarbonate if the patient is not volume depleted, for a metabolic alkalosis to persist, maintenance factors are required to prevent renal excretion. Aldosterone plays a key role by promoting sodium reabsorption via the epithelial Na channel (ENaC) in the cortical collecting duct. Aldosterone increases ENaC channel activity and increases its density on the luminal membrane. When sodium is reabsorbed, the tubular lumen becomes negatively charged, increasing the rate of H^+-ATPase H^+ excretion.[41,42] Other maintenance factors include hypochloremia and hypokalemia.

For both diagnostic and therapeutic reasons, it is helpful to divide causes of metabolic alkalosis into those associated with a decrease in the extracellular volume or chloride (chloride-sensitive) and those associated with a normal or increased extracellular volume (chloride-resistant)[43] (►**Table 4**). Urine chloride values < 20 mEq/L suggest a chloride-responsive process whereas levels > 40 mEq suggest a chloride-resistant process. Urine Na^+ is not used to assess effective arterial blood volume in a metabolic alkalosis because of its obligate excretion as $NaHCO_3$ when serum bicarbonate levels are high.

Chloride-Responsive Alkalosis

Emesis

Vomiting may generate a metabolic alkalosis due to loss of gastric HCl. However, maintenance of alkalosis is due to extracellular volume depletion stimulating aldosterone secretion. As noted above, aldosterone promotes H^+ excretion and HCO_3^- reabsorption, and alkalosis persists even after all initiating factors have abated. In these patients, Cl^- is avidly reabsorbed from the tubules, and urine chloride concentrations are less than 20 mEq/L. Correction of the metabolic alkalosis depends on replacement of Cl^- losses, and therefore saline is the fluid of choice.

Diuretics

All non-CA inhibiting diuretics acting proximal to the cortical collecting duct may cause a metabolic alkalosis. Blocking Na^+ reabsorption proximally promotes greater Na^+ delivery to the distal nephron. When this is coupled with extracellular volume depletion, there is considerable ENaC-mediated sodium reabsorption mediated by aldosterone. Loop diuretics, which inhibit the Na^+-K^+-$2Cl^-$ cotransporter (NKCC2), possess a unique mechanism of activating the renin-angiotensin-aldosterone system in the absence of volume depletion. In addition to blocking the NKCC2 channel in the loop of Henle, they block the NKCC2 sensor in the macula densa.[44] This sensor detects changes in distal tubular chloride to regulate GFR, a mechanism called tubuloglomerular feedback. Therefore, when this sensor is blocked, the macula densa senses a low volume state and upregulates renin. Renal disorders that mimic diuretics such as Bartter's and Gitelman's syndromes induce a metabolic alkalosis by the same mechanisms.

Recent studies have called into question the idea of "contraction alkalosis" in which the bicarbonate concentration increases due to contraction of the ECF. In a trial comparing ultrafiltration with diuretics, the bicarbonate concentration did not increase in the ultrafiltration arm despite significant fluid removal.[45] In a study in dogs, when urinary losses of water and electrolytes with furosemide were replaced to prevent volume contraction or electrolyte changes, continued administration of the drug led to progressive further increases in serum bicarbonate.[46]

Chloride-Resistant Alkalosis

Chloride-resistant alkalosis occurs in the absence of volume depletion due to direct stimulation of the ENaC channel, most commonly due to aldosterone excess. Unlike situations in which the ECF is decreased, Cl^- is lost in the urine and the urine $Cl^- > 40$ mEq/L. Maintenance of metabolic alkalosis is a result of persistent excess mineralocorticoid secretion and hypokalemia. Conditions that mimic the aldosterone actions such as Liddle's syndrome or activate the mineralocorticoid receptor, as in Cushing's disease or licorice ingestion, also result in metabolic alkalosis.

Alkali Intake

In patients with renal dysfunction, excessive intake of HCO_3^- or other anions that are metabolized to HCO_3^- can cause a metabolic alkalosis. The most common example is milk-alkali syndrome due to antacid ingestion, in which hypercalcemia potentiates the metabolic alkalosis. High serum calcium activates the calcium-sensing receptor in the thick ascending limb of the loop of Henle which blocks the NKCC2 channel. This results in a loop diuretic effect and volume depletion. Hypercalcemia also suppresses parathyroid hormone (PTH) secretion, and PTH normally inhibits the NHE3 transporter in the proximal tubule. As more H^+ is secreted into the tubule, more HCO_3^- is reclaimed. Volume depletion both increases proximal tubule bicarbonate reabsorption and increases aldosterone-mediated distal HCO_3^-reabsorption.[47] Finally, as hypercalcemic renal injury develops, GFR falls and bicarbonate filtration falls.

Clinical Manifestations

Metabolic alkalosis is often asymptomatic but may have consequences when $pH > 7.55$ and $[HCO_3^-] > 45$ mM.[48,49] Alkalosis increases hemoglobin O_2 affinity, thereby reducing off-loading of oxygen from hemoglobin. It also decreases ventilation by suppressing peripheral and central chemoreceptors and may constrict the peripheral vasculature, further limiting tissue oxygen supply. Neuromuscular hyperirritability may be observed and has been attributed in part to increased calcium binding to albumin. Twitching and tetany may be preceded by the Chvostek and Trousseau signs, and seizures can ensue. Myocardial irritability may also occur leading to ventricular arrythmias.[50]

Table 4 Causes of metabolic alkalosis

Loss of H^+ from the body
Chloride-responsive with urine $Cl^- < 20$ mEq/L
Gastrointestinal losses of chloride
Cystic fibrosis
Posthypercapnia: elevated HCO_3^- after overly rapid resolution of chronic respiratory acidosis
Chloride-resistant with urine $Cl^- > 40$ mEq/L with hypertension
Hyperaldosteronism: primary adrenal hyperplasia, aldosterone producing adenoma
Mineralocorticoid receptor activation: Cushing's syndrome, 11-β-HSD2 deficiency, glycyrrhetinic acid
Liddle syndrome: increased epithelial sodium channel (ENaC) expression in collecting duct
Chloride-resistant with urine $Cl^- > 40$ mEq/L without hypertension
Bartter syndrome: impaired reabsorption of sodium ions and chloride ions in the thick ascending loop of Henle (variants)
Gitelman syndrome: impaired thiazide-sensitive sodium/chloride transporter (NCCT) in the distal convoluted tubule
Administration of poorly absorbed anions (e.g., penicillin)
Excessive intake of bicarbonate or other bases
Milk-alkali syndrome, bicarbonate dialysis, massive blood transfusions (citrate)
Recovery from ketoacidosis or lactic acidosis after bicarbonate administration

Therapy

Treatment of metabolic alkalosis depends on ECF volume status. Patients with ECF volume loss can be distinguished from those with excess volume based on urine Cl^-. For patients who have sustained severe volume losses, fluids that contain Na^+, Cl^-, K^+, and Mg^{2+} are frequently indicated.

In volume overloaded patients, KCl may resolve metabolic alkalosis without Na^+ administration.[51] Spironolactone is useful in the presence of excessive mineralocorticoid secretion. The CA inhibitor, acetazolamide, may be particularly helpful in patients with heart failure, who develop loop-diuretic-induced metabolic alkalosis.[52] However, potassium should be repleted prior to administration in patients with borderline low potassium as it can increase K^+ excretion. Acetazolamide should be used judiciously in patients with severe hypercapnic lung disease, as high plasma concentrations can cause CO_2 retention due to red blood cell CA inhibition, and in patients with severe chronic liver disease.[53]

Infusions of HCl or NH_4Cl may be used, but these infusions require central access confirmed radiologically by location in the superior vena cava to minimize vascular wall necrosis and hemolysis by the acid infusion. In very severe cases, intubation and sedation or neuromuscular blockade may be used to control ventilation and, thereby, increase PCO_2.

Respiratory Acidosis

General Considerations

Respiratory acidosis (hypercapnia) is common in patients with severe respiratory insufficiency generally when lung function falls below 25% of predicted, particularly in COPD, and in those with ventilatory control disorders due to respiratory depressant drugs or CNS disease. PCO_2 is kept within narrow limits by the brainstem respiratory controller. Normally, arterial PCO_2 is sensed primarily by the central chemoreceptors, but their sensitivity is augmented with concomitant hypercapnic peripheral chemoreceptor input. However, both sites of CO_2 chemoreception may be suppressed by chronic hypercapnia due to renal compensation increasing bicarbonate and partially restoring pH. This is most common in patients with severe COPD or the obesity hypoventilation syndrome. Increases in PCO_2 result in an intracellular acidosis that acutely in renal tubular cells involves losses in chloride and bicarbonate retention; and over the next few days, acid excretion is accelerated by a rise in renal NH_3 generation and excretion as $NH_4{}^+$.[54]

Causes

Any process interfering with ventilation can lead to respiratory acidosis (►**Table 5**). COPD, acute severe asthma exacerbations, and opiate overdose are the most frequent causes, related primarily to increased airway resistance and work of breathing that decrease alveolar ventilation. Interstitial lung disease and pulmonary vascular diseases are less likely to increase PCO_2 values unless they become extremely severe and associated with respiratory muscle fatigue. Extensive infiltrative processes with little uninvolved lung (including pneumonias and pulmonary edema) and large pleural effusions can decrease alveolar ventilation. With significant acute pulmonary artery embolic obstruction, wasted ventilation due to increased alveolar dead space causes sudden increases in ventilation, or hypercapnia if ventilation cannot be increased. A paralyzed diaphragm or extensive rib fractures that lead to a unilateral flail chest may result in insufficient ventilation.

Hypoventilation is the most serious complication of neuromuscular disorders (see ►**Table 5**). The central respiratory centers may be depressed acutely or chronically by narcotics or by any process injuring the brainstem. A complex disturbance of the respiratory center may be encountered in patients with the obesity hypoventilation syndrome. Apneic episodes during sleep are common due to upper airway obstruction or a central failure to initiate ventilation when preceding hyperventilation drives the PCO_2 below the eucapnic threshold as can occur at high altitude and with severe right or left heart failure.

Rarely, when cardiac output is low, anemia is severe, and/or certain drugs are used that interfere with the normal high efficiency of red cell carbon dioxide transport and exchange such as acetazolamide (see ►**Table 5**), carbon dioxide retention in the tissues may develop and yet not be reflected in the arterial PCO_2.[53] In fact, as carbon dioxide rises in the vicinity of the central chemoreceptors, ventilation may be stimulated sufficiently to cause a paradoxical arterial hypocapnia that can be mistaken as evidence of a primary respiratory alkalosis. If PCO_2 is measured in the venous circulation (central or mixed venous PCO_2), one will find an elevated PCO_2 and lower pH, revealing the true state of carbon dioxide homeostasis.

Clinical Manifestations

If hypoventilation is caused by neuromuscular or mechanical problems, the patient will be dyspneic and tachypneic. In contrast, if the respiratory center is impaired, ventilation may be reduced without any sensation of dyspnea.

The physiologic and clinical consequences of respiratory acidosis tend to be more serious in acute than in chronic states. Elevations in PCO_2 cause systemic vasodilation that is particularly evident in the cerebral circulation. Cerebral blood flow and intracerebral pressures increase and may lead to a picture of pseudotumor cerebri with papilledema, retinal venous distention, and retinal hemorrhages. The patient may have dyspnea and manifest myoclonic jerks, asterixis, tremor, restlessness, and confusion. Coma may ensue at PCO_2 values of 70 to 100 mm Hg with abrupt onset of hypercapnia. Higher levels may be well tolerated with chronic respiratory acidosis, with much higher $HCO_3{}^-$ concentrations arising from renal compensation. Systemic vasodilation and increased cardiac output promote cerebral vasodilation and warm, flushed skin and a bounding pulse from sympathetic nervous system activation, although high sympathetic tone leads to renal vasoconstriction. Arrhythmias are observed occasionally. Mild increases in serum phosphate and K^+ and decreases in lactate and pyruvate

Table 5 Causes of respiratory acid–base disorders

Respiratory acidosis
Central nervous system depression
Drugs: opiates, sedatives, anesthetics
Excess oxygen in patients with COPD, chronic hypercapnia and acute decompensation (minor effect in relation to oxygen's detrimental effect on V/Q matching)
Obesity-hypoventilation syndrome
Central nervous system disorders (e.g., brainstem lesions)
Neuromuscular disorders
Neurologic: multiple sclerosis, poliomyelitis, phrenic nerve injuries, high spinal cord injury, Guillain–Barré syndrome, botulism, tetanus, amyotrophic lateral sclerosis
Myasthenia gravis, succinylcholine chloride, curare, aminoglycosides, organophosphorus
Muscle: hypokalemia, hypophosphatemia, muscular dystrophy, polio
Airflow obstruction
COPD, status asthmaticus, laryngospasm
Chest wall restriction
Pleural: effusions, empyema, fibrothorax
Chest wall: kyphoscoliosis, scleroderma, ankylosing spondylitis, very high body mass index
Severe pulmonary restrictive disorders
Severe fibrotic lung disease
Abnormalities in blood CO_2 transport
Decreased perfusion: severe heart failure, cardiac arrest with cardiopulmonary resuscitation, extensive pulmonary embolism with impaired ventilatory response, severe anemia
Carbonic anhydrase inhibition—high-dose acetazolamide
Respiratory alkalosis
Central nervous system stimulation
Hyperventilation syndrome, anxiety, pregnancy
Cerebrovascular disease, subarachnoid hemorrhage, traumatic brain injury
Meningitis, encephalitis
Sepsis, hypotension
Hepatic failure
Drugs: salicylates, nicotine, xanthines, quetiapine, progestational hormones
Excess CO_2 removal
Mechanical ventilators
Acetate hemodialysis, cardiopulmonary bypass, extracorporeal membrane oxygenation
Hypoxia
High altitude
Severe anemia, hemoglobinopathy
Decreased cardiac output
Pulmonary disease
Pneumonia, interstitial fibrosis, pulmonary fibrosis, embolism, edema
Right-to-left shunt
Decreased CO_2 production
Myxedema, hypothermia

Abbreviation: COPD, chronic obstructive pulmonary disease.

occur in acute respiratory acidosis, and serum Na^+ may increase modestly in both acute and chronic hypercapnia.

Therapy

Treatment of respiratory acidosis depends on restoration of adequate alveolar ventilation. In COPD and asthma, this focuses on bronchodilation, adequate but careful oxygen supplementation, and relief of anxiety to lower metabolic CO_2 production or other causes of an increased respiratory rate that may lead to reductions in expiratory time and dynamic hyperinflation. Indiscriminate administration of high oxygen concentrations should be avoided as this can lead to death. The phenomenon of oxygen-induced hypercapnia in these patients is usually observed in emergency department and intensive care unit settings when patients present with severe hypoxemia and are hypoxemic, hypercapnic, and fatigued. Sudden correction of arterial hypoxemia causes further hypercapnia by a combination of three mechanisms: (1) by relief of hypoxic pulmonary vasoconstriction in poorly ventilated lung regions that further reduces the ability of the lung to eliminate CO_2 as local perfusion to poorly ventilated regions increases, (2) by saturation of hemoglobin with oxygen that causes previously buffered protons on deoxyhemoglobin to be released with subsequent generation of new carbon dioxide from HCO_3^- stores (Haldane effect) and from hemoglobin carbamate, and (3) by depression of a hypoxia-driven peripheral chemoreceptor drive that causes more hypoventilation.[55] Low-flow oxygen generally suffices to increase Po_2 to satisfactory levels (60 mm Hg and arterial oxygen saturation [arterial SO_2] $\approx 90\%$); greater elevations are neither needed nor advisable. If the use of a ventilator becomes necessary, care must be taken that PCO_2 is not decreased by more than 10 mm Hg each hour to avoid complicating posttherapeutic metabolic alkalosis. If opiates are responsible for central respiratory depression, the respiratory acidosis may be relieved by naloxone. Bicarbonate is generally contraindicated because it tends to decrease respiratory drive and increases carbon dioxide levels in the tissues.

Respiratory Alkalosis

General Considerations

Although respiratory alkalosis is a common disorder and at times a serious prognostic sign, it seldom has a clinically significant effect on patients and generally requires little in the way of specific therapy to reverse the hyperventilation directly. Changes in pH related to hyperventilation are quickly moderated by tissue buffering. However, HCO_3^- concentrations do not usually fall below 18 mEq/L acutely, and even with renal compensation, a HCO_3^- concentration below 16 mEq/L should raise the possibility of an independent metabolic acidosis.

Causes

Respiratory alkalosis can be divided into three categories: hypoxia, pulmonary diseases, and CNS disorders (►**Table 5**). Both hypoxemia and tissue hypoxia cause hyperventilation. Decreases in arterial Po_2 stimulate peripheral chemoreceptors directly. In contrast, tissue hypoxia caused by decreased cardiac output, shock, severe anemia, or excessive hemoglobin oxygen affinity results in the production of lactic acid and other stimuli, which are sensed in blood by the carotid body chemoreceptors and by other less well-defined chemoreception in the affected tissues themselves. Ascent to high altitude predictably leads to hypocapnia because of increased ventilation mediated by the peripheral chemoreceptors in response to hypoxemia.

Many pulmonary disorders are associated with hyperventilation. Hypoxemia certainly plays a role but, additionally, receptors in lung tissue are activated by local irritant stimuli and fluid accumulation and remain activated even after hypoxemia has been corrected.

CNS disorders are among the most common causes of respiratory alkalosis. Anxiety can provoke hyperventilation (hyperventilation syndrome). Central stimulation of respiration is also common in a wide variety of intracerebral injuries. Many drugs and hormones (notably salicylates, theophylline, thyroxine, and progesterone) stimulate ventilation (see ►**Table 5**), and hyperventilation may be an early sign of both sepsis and hepatic insufficiency due to the accumulation of ammonia and amines that stimulate the respiratory controller.

Clinical Manifestations

Many manifestations of respiratory alkalosis may be related in part to a fall in free serum Ca^{2+} due to increased binding to serum proteins. Phosphate may also decline slightly and sometimes fall to rather low concentrations in patients who have prolonged severe respiratory alkalosis. It has been suggested that this decline in phosphate is related to activation of glycolysis and phosphorylation of the glucose metabolites thereby produced. Some of the CNS changes of acute respiratory alkalosis may be caused by hypocapnic cerebral vasoconstriction leading to reduced blood flow and hypoxia. Often, deliberate hyperventilation can be used to reduce cerebral blood flow acutely in states of impending brain herniation from high intracranial pressure; however, it is useful only for a few hours as a temporizing measure to allow more definitive pressure relief by other means.

Panic, weakness, and a sense of impending doom are common, as are paresthesias and muscle weakness or cramping. As in metabolic alkalosis, Trousseau and Chvostek signs can often be elicited, and overt tetany or seizures may follow. Vision and speech may become impaired, and syncope can occur. Transient electrocardiographic changes can resemble those of myocardial ischemia; this finding can be particularly misleading because it is not uncommon for hyperventilating patients to complain of chest discomfort. Indeed, acute hypocapnia, for example, with mechanical ventilation, can induce coronary artery vasospasm, angina, ominous cardiac arrhythmias, and ST elevations in patients with coronary artery disease. Acute respiratory alkalosis can increase lactate and reduce serum K^+ concentrations.

Therapy

Reassurance and rebreathing in a small paper bag are frequently all that is needed to control hyperventilation associated with anxiety attacks. In more severe cases, β-adrenergic inhibitors have proved useful, and specific therapy for anxiety may be indicated. Correction of respiratory alkalosis in other conditions, such as hepatic coma and pulmonary disorders, depends on treatment of the primary disorder. CO_2 inhalation by patients with hepatic coma or addition of dead space has not been helpful.

Conclusion

Arterial PCO_2 provides a suitable "respiratory" criterion for determining whether alveolar ventilation is appropriate for the rate at which carbon dioxide is produced in the body. Abnormalities in arterial PCO_2 may be "primary" causes of abnormal pH or "secondary" responses, which minimize pH disturbances. A "metabolic" disorder refers to a net accumulation or loss of nonvolatile acids and bases from the body and can be primary or secondary. Both the kidneys and other organs, including the gastrointestinal tract and skin, may be involved.

Incorporation of electrolyte concentrations into the analysis permits calculation of the anion gap and identification of various processes involved in both metabolic acidosis and alkalosis. However, these measurements must always be accompanied by measurement of conventional acid–base parameters (pH_a, arterial PCO_2, and HCO_3^-). Correction of the underlying metabolic or respiratory disorder represents the most effective way to treat the acid–base disorder.

Conflict of Interest
None declared.

References

1 Maren TH. Carbonic anhydrase: chemistry, physiology, and inhibition. Physiol Rev 1967;47(04):595–781
2 Effros RM, Chang RS, Silverman P. Acceleration of plasma bicarbonate conversion to carbon dioxide by pulmonary carbonic anhydrase. Science 1978;199(4327):427–429
3 Casey JR, Grinstein S, Orlowski J. Sensors and regulators of intracellular pH. Nat Rev Mol Cell Biol 2010;11(01):50–61
4 Albert TJ, Swenson ER. Circumstances when arterial blood gas analysis can lead us astray. Respir Care 2016;61(01):119–121
5 Adrogué HJ, Rashad MN, Gorin AB, Yacoub J, Madias NE. Assessing acid–base status in circulatory failure. Differences between arterial and central venous blood. N Engl J Med 1989;320(20):1312–1316
6 Winters RW. Terminology of acid–base disorders. Ann Intern Med 1965;63(05):873–884
7 Adrogué HJ, Tucker BM, Madias NE. Clinical approach to assessing acid–base status: physiological vs Stewart. Adv Chronic Kidney Dis 2022;29(04):343–354
8 Berend K. Diagnostic use of base excess in acid–base disorders. N Engl J Med 2018;378(15):1419–1428
9 de Seigneux S, Malte H, Dimke H, Frøkiaer J, Nielsen S, Frische S. Renal compensation to chronic hypoxic hypercapnia: downregulation of pendrin and adaptation of the proximal tubule. Am J Physiol Renal Physiol 2007;292(04):F1256–F1266
10 Gennari FJ, Goldstein MB, Schwartz WB. The nature of the renal adaptation to chronic hypocapnia. J Clin Invest 1972;51(07):1722–1730
11 Albert MS, Dell RB, Winters RW. Quantitative displacement of acid–base equilibrium in metabolic acidosis. Ann Intern Med 1967;66(02):312–322
12 Javaheri S, Kazemi H. Metabolic alkalosis and hypoventilation in humans. Am Rev Respir Dis 1987;136(04):1011–1016
13 Madias NE, Adrogué HJ, Cohen JJ. Maladaptive renal response to secondary hypercapnia in chronic metabolic alkalosis. Am J Physiol 1980;238(04):F283–F289
14 Feldman M, Alvarez NM, Trevino M, Weinstein GL. Respiratory compensation to a primary metabolic alkalosis in humans. Clin Nephrol 2012;78(05):365–369
15 Kraut JA, Madias NE. Serum anion gap: its uses and limitations in clinical medicine. Clin J Am Soc Nephrol 2007;2(01):162–174
16 Mehta AN, Emmett JB, Emmett M. GOLD MARK: an anion gap mnemonic for the 21st century. Lancet 2008;372(9642):892
17 Fernandez PC, Cohen RM, Feldman GM. The concept of bicarbonate distribution space: the crucial role of body buffers. Kidney Int 1989;36(05):747–752
18 Vernon C, Letourneau JL. Lactic acidosis: recognition, kinetics, and associated prognosis. Crit Care Clin 2010;26(02):255–283
19 Metcalfe HK, Monson JP, Welch SG, Cohen RD. Inhibition of lactate removal by ketone bodies in rat liver. Evidence for a quantitatively important role of the plasma membrane lactate transporter in lactate metabolism. J Clin Invest 1986;78(03):743–747
20 Blumenberg A, Benabbas R, Sinert R, Jeng A, Wiener SW. Do patients die with or from metformin-associated lactic acidosis (MALA)? Systematic review and meta-analysis of pH and lactate as predictors of mortality in MALA. J Med Toxicol 2020;16(02):222–229
21 Vecchio S, Giampreti A, Petrolini VM, et al. Metformin accumulation: lactic acidosis and high plasmatic metformin levels in a retrospective case series of 66 patients on chronic therapy. Clin Toxicol (Phila) 2014;52(02):129–135
22 Blough B, Moreland A, Mora A Jr. Metformin-induced lactic acidosis with emphasis on the anion gap. Proc Bayl Univ Med Cent 2015;28(01):31–33
23 Emmett M. Acetaminophen toxicity and 5-oxoproline (pyroglutamic acid): a tale of two cycles, one an ATP-depleting futile cycle and the other a useful cycle. Clin J Am Soc Nephrol 2014;9(01):191–200
24 Vander Heiden MG, Cantley LC, Thompson CB. Understanding the Warburg effect: the metabolic requirements of cell proliferation. Science 2009;324(5930):1029–1033
25 Oh MS, Uribarri J, Alveranga D, Lazar I, Bazilinski N, Carroll HJ. Metabolic utilization and renal handling of D-lactate in men. Metabolism 1985;34(07):621–625
26 Miles JM, Haymond MW, Nissen SL, Gerich JE. Effects of free fatty acid availability, glucagon excess, and insulin deficiency on ketone body production in postabsorptive man. J Clin Invest 1983;71(06):1554–1561
27 Palmer BF, Clegg DJ. Euglycemic ketoacidosis as a complication of SGLT2 inhibitor therapy. Clin J Am Soc Nephrol 2021;16(08):1284–1291
28 Mistry S, Eschler DC. Euglycemic diabetic ketoacidosis caused by SGLT2 inhibitors and a ketogenic diet: a case series and review of literature. AACE Clin Case Rep 2020;7(01):17–19
29 Saponaro C, Mühlemann M, Acosta-Montalvo A, et al. Interindividual heterogeneity of SGLT2 expression and function in human pancreatic islets. Diabetes 2020;69(05):902–914
30 Kraut JA, Mullins ME. Toxic alcohols. N Engl J Med 2018;378(03):270–280
31 Brent J. Fomepizole for ethylene glycol and methanol poisoning. N Engl J Med 2009;360(21):2216–2223
32 Zakharov S, Pelclova D, Navratil T, et al. Intermittent hemodialysis is superior to continuous veno-venous hemodialysis/hemodiafiltration to eliminate methanol and formate during treatment for methanol poisoning. Kidney Int 2014;86(01):199–207
33 Batlle DC, Hizon M, Cohen E, Gutterman C, Gupta R. The use of the urinary anion gap in the diagnosis of hyperchloremic metabolic acidosis. N Engl J Med 1988;318(10):594–599

34 Gil FZ, Malnic G. Effect of amphotericin B on renal tubular acidification in the rat. Pflugers Arch 1989;413(03):280–286

35 Haque SK, Ariceta G, Batlle D. Proximal renal tubular acidosis: a not so rare disorder of multiple etiologies. Nephrol Dial Transplant 2012;27(12):4273–4287

36 Brenes LG, Sanchez MI. Impaired urinary ammonium excretion in patients with isolated proximal renal tubular acidosis. J Am Soc Nephrol 1993;4(04):1073–1078

37 Harris AN, Grimm PR, Lee HW, et al. Mechanism of hyperkalemia-induced metabolic acidosis. J Am Soc Nephrol 2018;29(05):1411–1425

38 Carlisle EJ, Donnelly SM, Vasuvattakul S, Kamel KS, Tobe S, Halperin ML. Glue-sniffing and distal renal tubular acidosis: sticking to the facts. J Am Soc Nephrol 1991;1(08):1019–1027

39 Swenson ER. Metabolic acidosis. Respir Care 2001;46(04):342–353

40 Jaber S, Paugam C, Futier E, et al; BICAR-ICU Study Group. Sodium bicarbonate therapy for patients with severe metabolic acidaemia in the intensive care unit (BICAR-ICU): a multicentre, open-label, randomised controlled, phase 3 trial. Lancet 2018;392(10141):31–40

41 Roy A, Al-bataineh MM, Pastor-Soler NM. Collecting duct intercalated cell function and regulation. Clin J Am Soc Nephrol 2015;10(02):305–324

42 Pearce D, Soundararajan R, Trimpert C, Kashlan OB, Deen PMT, Kohan DE. Collecting duct principal cell transport processes and their regulation. Clin J Am Soc Nephrol 2015;10(01):135–146

43 Palmer BF, Alpern RJ. Metabolic alkalosis. J Am Soc Nephrol 1997;8(09):1462–1469

44 Castrop H, Lorenz JN, Hansen PB, et al. Contribution of the basolateral isoform of the Na-K-2Cl- cotransporter (NKCC1/BSC2) to renin secretion. Am J Physiol Renal Physiol 2005;289(06):F1185–F1192

45 Cooper LB, Mentz RJ, Gallup D, et al. Serum bicarbonate in acute heart failure: relationship to treatment strategies and clinical outcomes. J Card Fail 2016;22(09):738–742

46 Bosch JP, Goldstein MH, Levitt MF, Kahn T. Effect of chronic furosemide administration on hydrogen and sodium excretion in the dog. Am J Physiol 1977;232(05):F397–F404

47 Felsenfeld AJ, Levine BS. Milk alkali syndrome and the dynamics of calcium homeostasis. Clin J Am Soc Nephrol 2006;1(04):641–654

48 Galla JH. Metabolic alkalosis. J Am Soc Nephrol 2000;11(02):369–375

49 Anderson LE, Henrich WL. Alkalemia-associated morbidity and mortality in medical and surgical patients. South Med J 1987;80(06):729–733

50 Sliwiński M, Hoffman M, Biederman A, Wangin H, Holdrowicz M. Association between hypokaliaemic alkalosis and development of arrhythmia in early postoperative period. Anaesth Resusc Intensive Ther 1974;2(03):193–204

51 Luke RG, Galla JH. It is chloride depletion alkalosis, not contraction alkalosis. J Am Soc Nephrol 2012;23(02):204–207

52 Mullens W, Dauw J, Martens P, et al; ADVOR Study Group. Acetazolamide in acute decompensated heart failure with volume overload. N Engl J Med 2022;387(13):1185–1195

53 Swenson ER. Safety of carbonic anhydrase inhibitors. Expert Opin Drug Saf 2014;13(04):459–472

54 Schwartz WB, Cohen JJ. The nature of the renal response to chronic disorders of acid–base equilibrium. Am J Med 1978;64(03):417–428

55 Abdo WF, Heunks LMA. Oxygen-induced hypercapnia in COPD: myths and facts. Crit Care 2012;16(05):323

Article published online: 2023-07-11

Control of Breathing

Jerome A. Dempsey, PhD[1] Joseph F. Welch, PhD[2]

[1] John Rankin Laboratory of Pulmonary Medicine, Department of Population Health Sciences, University of Wisconsin, Madison, Wisconsin
[2] School of Sport, Exercise and Rehabilitation Sciences, University of Birmingham, Edgbaston, Birmingham, United Kingdom

Address for correspondence Jerome A. Dempsey, John Rankin Laboratory of Pulmonary Medicine, Department of Population Health Sciences, John Rankin Laboratory of Pulmonary Medicine, University of Wisconsin, 607 N. Walnut Street Room 700, Madison, WI 53706 (e-mail: jdempsey@wisc.edu).

Semin Respir Crit Care Med 2023;44:627–649.

Abstract

Keywords
- chemoreception
- exercise hyperpnea
- plasticity
- sleep-disordered breathing
- respiratory rhythm generation
- exertional dyspnea
- COPD
- CHF
- aging

Substantial advances have been made recently into the discovery of fundamental mechanisms underlying the neural control of breathing and even some inroads into translating these findings to treating breathing disorders. Here, we review several of these advances, starting with an appreciation of the importance of $\dot{V}_A$:$\dot{V}CO_2$:$PaCO_2$ relationships, then summarizing our current understanding of the mechanisms and neural pathways for central rhythm generation, chemoreception, exercise hyperpnea, plasticity, and sleep-state effects on ventilatory control. We apply these fundamental principles to consider the pathophysiology of ventilatory control attending hypersensitized chemoreception in select cardiorespiratory diseases, the pathogenesis of sleep-disordered breathing, and the exertional hyperventilation and dyspnea associated with aging and chronic diseases. These examples underscore the critical importance that many ventilatory control issues play in disease pathogenesis, diagnosis, and treatment.

The past three decades have seen an explosion of information on the neural control of breathing. The impetus for much of this expansion of both basic and applied research has been the key roles played by the neurochemical control system in several important clinical disorders. These include the highly prevalent problem of sleep apnea, exertional dyspnea in obstructive lung diseases and congestive heart failure (CHF), elevated sympathetic vasoconstriction in cardiorespiratory diseases, and the numerous ventilatory control problems facing intensive care unit practitioners with patients in dyssynchrony with mechanical ventilation, or with CO_2 retention.

In healthy humans, ventilation is tightly controlled by a system that is concerned with both the precise constancy of alveolar and arterial blood gases and acid–base status, as well as with minimizing the work and metabolic cost of breathing. Breathing must remain largely an involuntary act of which we are not made aware. To this end, a three-component system is required, consisting of a pontomedullary rhythm/pattern generator and integrator; extensive sensory and modulatory inputs from peripheral receptors and suprapontine circuits; and, finally, synchronous distribution of motor outputs to respiratory musculature of the upper airway, thorax, and abdominal wall (►**Fig. 1**).

In this review of ventilatory control, we begin with an appreciation of the fundamental relationships of alveolar ventilation ($\dot{V}_A$) and CO_2 production rate ($\dot{V}CO_2$) in the regulation of arterial CO_2 tension ($PaCO_2$). We then discuss key advances in our understanding of the respiratory central pattern generator and chemoreceptor feedback. The application of this basic knowledge is then made to sleep and to exercise, to the plasticity of ventilatory control, and to the failure of homeostatic control of breathing and sympathetic nerve activity in select chronic diseases.

$\dot{V}_A$:$\dot{V}CO_2$:$PaCO_2$ Relationships

Appreciating the role of $\dot{V}CO_2$ and its relationship to $\dot{V}_A$ in the regulation of $PaCO_2$ is fundamental to understanding breathing control, as shown in the following equation, where $\dot{V}_A$ is

article published online
August 11, 2023

Issue Theme Pulmonary Physiology; Guest Editors: David A. Kaminsky, MD, Kathryn A. Hibbert, MD, and Andrew M. Luks, MD

Thieme Medical Publishers, Inc.,
333 Seventh Avenue, 18th Floor,
New York, NY 10001, USA

DOI https://doi.org/10.1055/s-0043-1770342.
ISSN 1069-3424.

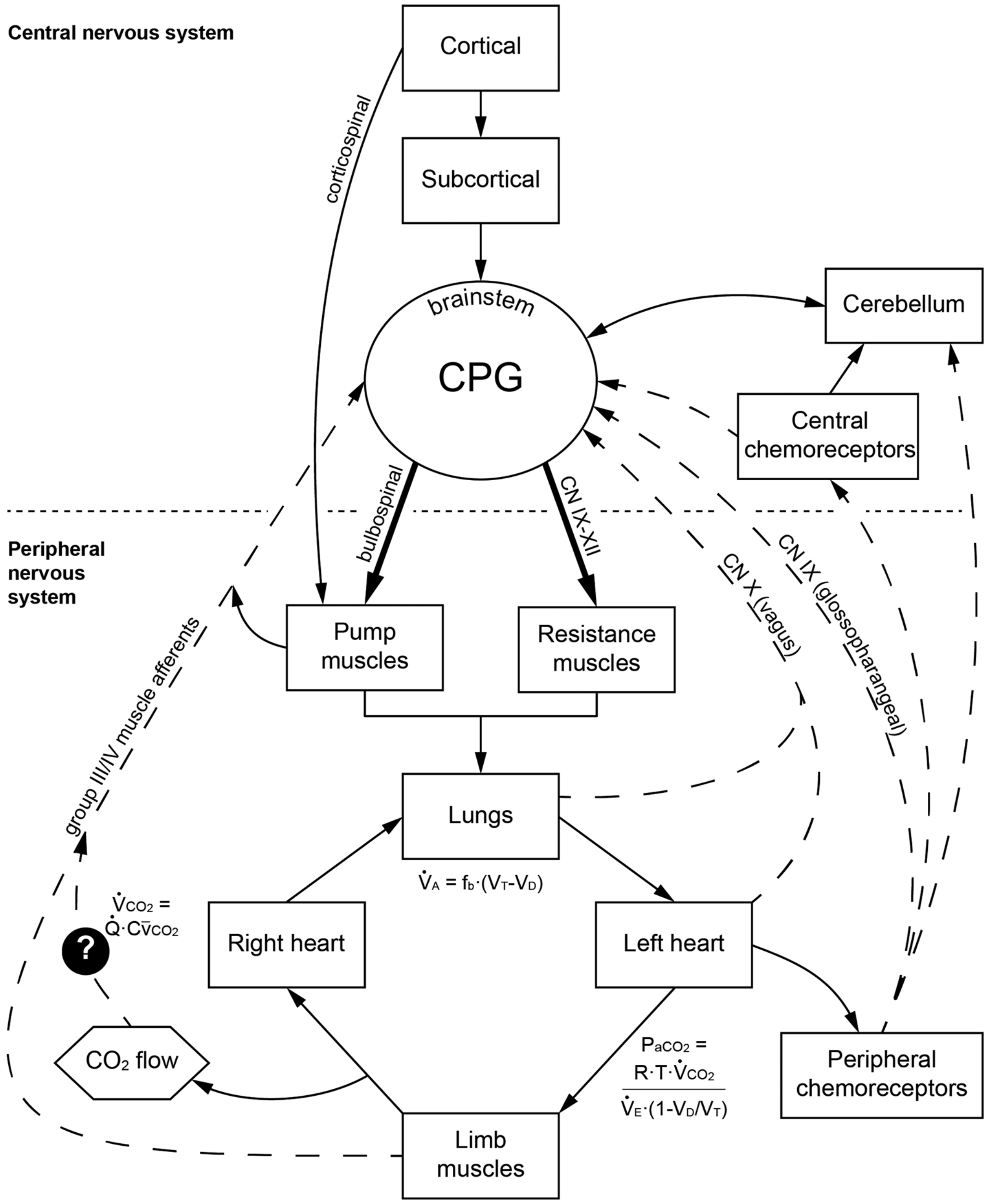
Central nervous system
Cortical
Subcortical
corticospinal
brainstem
CPG
Cerebellum
Central chemoreceptors
Peripheral nervous system
bulbospinal
CN IX-XII
CN X (vagus)
CN IX (glossopharangeal)
group III/IV muscle afferents
Pump muscles
Resistance muscles
Lungs
$\dot{V}_A = f_b \cdot (V_T - V_D)$
$\dot{V}_{CO_2} = \dot{Q} \cdot C\bar{v}_{CO_2}$
?
Right heart
Left heart
CO₂ flow
Peripheral chemoreceptors
$P_{aCO_2} = \frac{R \cdot T \cdot \dot{V}_{CO_2}}{\dot{V}_E \cdot (1 - V_D/V_T)}$
Limb muscles

Fig. 1 Schematic outlining of the three-component system for the neural control of breathing, consisting of a brainstem central pattern generator (CPG)/integrator, afferent sensory and modulatory inputs into the CPG, and efferent outputs to muscles of the respiratory pump and airways. The schema illustrates many concepts in the integrated neural control of breathing but is not intended to convey full pathways. Brainstem CPGs (e.g., ventral respiratory group) coordinate respiratory drives to spinal pump muscles (e.g., diaphragm) and upper airway resistance muscles (e.g., genioglossus). Alveolar ventilation ($\dot{V}_A$) is determined by the pattern of respiratory motor output which in turn regulates arterial CO_2 pressure ($PaCO_2$) for a given metabolic rate ($\dot{V}CO_2$). Contracting limb and respiratory muscles activate group III/IV muscle afferents which stimulate breathing. The "vascular distension" hypothesis posits that CO_2 flux to the lung may be detected by changes in cardiac output ($\dot{Q}$) which mechanically activates muscle afferents. Changes in $PaCO_2$ and arterial PO_2 are sensed by peripheral chemoreceptors (e.g., carotid body), whereas central chemoreceptors (e.g., retrotrapezoid nucleus) are sensitive to changes in $PaCO_2$. The respiratory CPG receives many inputs from suprapontine structures such as the periaqueductal gray of the midbrain and the dorsolateral prefrontal cortex. These central neurogenic inputs are associated with behavioral/voluntary control of respiration. The cerebellum receives an array of inputs from the cortex, brainstem, and spinal cord, including chemoafferent neurons, and may be an important site in respiratory learning and memory. $C\bar{v}CO_2$ = mixed-venous CO_2 content; f_b = breathing frequency; V_D = dead-space volume; V_T = tidal volume.

alveolar ventilation, $\dot{V}CO_2$ is the CO_2 exchange at the lung, $PaCO_2$ is the arterial PCO_2, and K is 0.863.

$$P_aCO_2 = \frac{\dot{V}CO_2}{\dot{V}_A} \cdot K$$

Consider the following observations which highlight the importance of these relationships (►**Fig. 2**). The hyperbolic shape of the $\dot{V}_A$:$PaCO_2$ relationship at any given $\dot{V}CO_2$ defines the "plant gain," which indicates system sensitivity to changes in $\dot{V}_A$ (i.e. $\Delta PaCO_2/\Delta \dot{V}_A$). Thus, a given change in

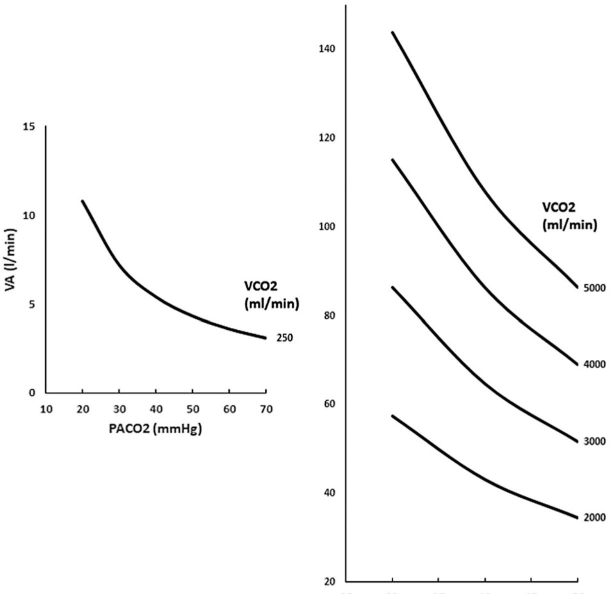

Fig. 2 Hyperbolic relationship of $\dot{V}_A$ to $PaCO_2$ at any given $\dot{V}CO_2$ dictates changing ventilatory requirements for regulating $PaCO_2$ at rest (left panel) and during exercise (right panel). At a normal resting $\dot{V}CO_2$ of 250 mL/min, a $\dot{V}_A$ of 5.4 L/min is required to maintain $PaCO_2$ at 40 mm Hg. $PaCO_2$ will increase to 50 mm Hg with a 1.1 L/min fall in $\dot{V}_A$ and to 60 and 70 mm Hg with only a further 0.7 and 0.6 L/min, respectively, further fall in $\dot{V}_A$. Conversely, lowering $PaCO_2$ by 20 mm Hg from normal requires a twofold increase in $\dot{V}_A$. These requirements for a changing $\dot{V}_A$ for raising and lowering $PaCO_2$ are magnified with increasing $\dot{V}CO_2$ as the hyperbolic slope of $PaCO_2$ to $\dot{V}_A$ steepens. So, for example, at maximal exercise in a normal untrained subject, the compensatory hyperventilatory response required to reduce $PaCO_2$ from 40 to 30 mm Hg would require an additional 21 L/min $\dot{V}_A$ at 3,000 mL/min $\dot{V}CO_2$ vs. 36 L/min at 5,000 mL/min $\dot{V}CO_2$ in a highly trained subject.

$\dot{V}_A$ will elicit relatively large changes in $PaCO_2$ when resting $PaCO_2$ is high (e.g., respiratory failure) and much smaller changes when resting $PaCO_2$ is low. Differences in plant gain of the respiratory control system have substantial clinical relevance. For example, a patient move readily in and out of severe CO_2 retention with only small changes in $\dot{V}_A$, whether these changes are made in total ventilation ($\dot{V}_E$) or in the ratio of dead-space to tidal volume (V_D/V_T). Thus, in severe chronic obstructive pulmonary disease (COPD), CO_2 retention is exacerbated by relatively small decreases in $\dot{V}_A$ resulting from nonuniform ventilation-perfusion ($\dot{V}_A$:$\dot{Q}$) distribution and high V_D/V_T, even at abnormally high levels of neural respiratory drive, tachypnea, and $\dot{V}_E$. Conversely, chronic stimulation of ventilatory drive can relieve all or most of the CO_2 retention via small increases in V_T and $\dot{V}_A$.[1–3] Transient increases in $\dot{V}_A$ during sleep will elicit sufficient transient reductions in $PaCO_2$ to reach the apneic threshold when the baseline, steady-state $PaCO_2$ is normal or high (i.e., high plant gain) but not when the baseline steady-state $PaCO_2$ is low (i.e., low plant gain; see section “Pathogenesis of Sleep-Disordered Breathing”). Third, the slope of the hyperbolic $\dot{V}_A$:$PaCO_2$ relationship steepens with rising $\dot{V}CO_2$ so that any compensatory reductions in $PaCO_2$ during exercise require a much larger increase in $\dot{V}_A$, the higher the exercise intensity and $\dot{V}CO_2$.

These few examples are intended to underscore the importance of considering $\dot{V}_A$:$\dot{V}CO_2$:$PaCO_2$ relationships when assessing the changing requirements placed on the ventilatory control system that have consequences for both the maintenance of blood–gas and acid–base homeostasis and the work of breathing. We will revisit these fundamental concepts as we discuss the mechanisms controlling breathing and breathing stability in various conditions.

Central Rhythm Generation and Integration

As with locomotion and other rhythmic behaviors, the basic breathing pattern is generated within the brainstem without the need for peripheral or suprapontine input. This central pattern generator always features active inspiration, commonly postinspiratory activity, and sometimes active expiration. At the core of the respiratory central pattern generator is the pre-Bötzinger complex (PBC),[4,5] where the inherent rhythm of breathing appears to be dependent on reciprocal synaptic inhibition, in which many PBC neurons become hyperpolarized following inspiratory bursts. In a network which relies on recurrent excitation for inspiratory burst initiation, any change in excitability during the refractory period determines the duration of periods between breaths. Inhibitory neurons active during inspiratory bursts are prevalent within the PBC.[5] Not acting in isolation, the PBC works with other rhythm generators located at the postinspiratory complex and retrotrapezoid nucleus (RTN) of the medulla to produce a synchronous and rhythmic breathing cycle. Importantly, vagal sensory feedback sensitive to lung stretch also shortens the refractory period of inspiratory neurons, thereby facilitating PBC inhibition. Accordingly, vagal blockade in a resting or exercising animal or human prolongs inspiratory time, reduces breathing frequency, and augments V_T.[6,7]

Research into how abnormalities or mutations of medullary neuronal networks responsible for rhythm and pattern generation may impact human disease is underway in animal models of select chronic diseases. Abnormal breathing patterns, often with CO_2 retention and especially during sleep, have been documented in neurodegenerative diseases such as Parkinson’s disease, amyotrophic lateral sclerosis, and post-polio syndrome with bulbar involvement, and are linked to deficits in neurons in the PBC, pontine raphe, and adjacent areas.[8,9] Furthermore, the PBC has been identified as a major site of action mediating the depressive effect of opiate agonists on respiratory rhythm and the reversal of depressive effects via µ-opiate antagonists.[10]

Chemoreceptors

Physiology

Chemoreceptors in both the central (CNS) and peripheral nervous systems serve primarily as feedback “error” detectors that “fine-tune” breathing, regulating arterial blood–gases and pH within normal limits. Carotid chemoreceptors are the body’s primary PaO_2 sensor and drive ventilation in a synergistic manner when hypoxemia is combined with hypercapnia.[11] Carotid chemoreceptors are polymodal receptors that also sense K^+, temperature, osmolarity, norepinephrine, and insulin.[12] Medullary chemoreceptors, principally the RTN, are highly sensitive to changes in brain extracellular fluid PCO_2 and pH.[13]

Both peripheral and central chemoreceptors regulate both sympathetic and phrenic motor nerve activity in response to hypoxemia and hypercapnia. Carotid body (CB) afferents project to multiple sites in the CNS via the nucleus of the solitary tract (NTS). Some NTS neurons relay to the respiratory central pattern generator that determines respiratory motor output, whereas other carotid chemoafferent neurons project to the rostral ventrolateral medulla (RVLM) that determines sympathetic outflow.[14] Additional evidence in rodents reveals differential regulation of respiratory *versus* sympathetic responses via the carotid chemoreceptor.[15] This differential regulation likely explains recent findings in healthy and hypertensive humans which revealed noncongruence in the sensitivity of sympathetic and ventilatory responses to hypoxia or to transient hyperoxia.[16,17]

The *PHOX2B* gene is expressed in an uninterrupted chain of neurons in a circuit that includes the CB, CB afferents, as well as the NTS and RTN; thus, CO_2-sensitive RTN neurons respond to CB stimulation.[18] Evidence obtained using an extracorporeal circuit to perfuse the CB in isolation from the CNS in the unanesthetized canine and goat revealed the functional nature of central and peripheral chemoreceptor interdependence. Inhibition of the isolated CB with hyperoxic, hypocapnic blood caused a marked depression of the central respiratory response to hypercapnia while hypoxemic or hypercapnic stimulation of the isolated CB increased the slope of the central CO_2 ventilatory response.[19–21] This interdependence was also shown in CB denervated humans and canines by a reduced slope of ventilatory responses to inhaled hyperoxic-hypercapnia[22,23] (►**Fig. 3A, B**). These isolated CB preparations revealed that exposing the extra-CB systemic circulation and the CNS to hypoxia (or hyperoxia) while maintaining normoxic/normocapnic tonic input from carotid chemoreceptors elicits hyperventilation in a dose–response manner.[24–27] Furthermore, in awake CB-denervated animals, hyperventilation increases with increasing levels of systemic hyperoxia with reductions in $PaCO_2$ that are likely sufficient to elicit CNS alkalosis.[22,28]

These collective findings have several implications for our understanding of human ventilatory control—especially attempts to quantify separately the sensitivities of central and peripheral chemoreceptors in humans with intact CBs. First, while the ventilatory response to hypoxia requires the presence of intact carotid chemoreceptors, extracarotid chemoreceptor hypoxic stimulation also contributes significantly to the total ventilatory response to hypoxia. Second,

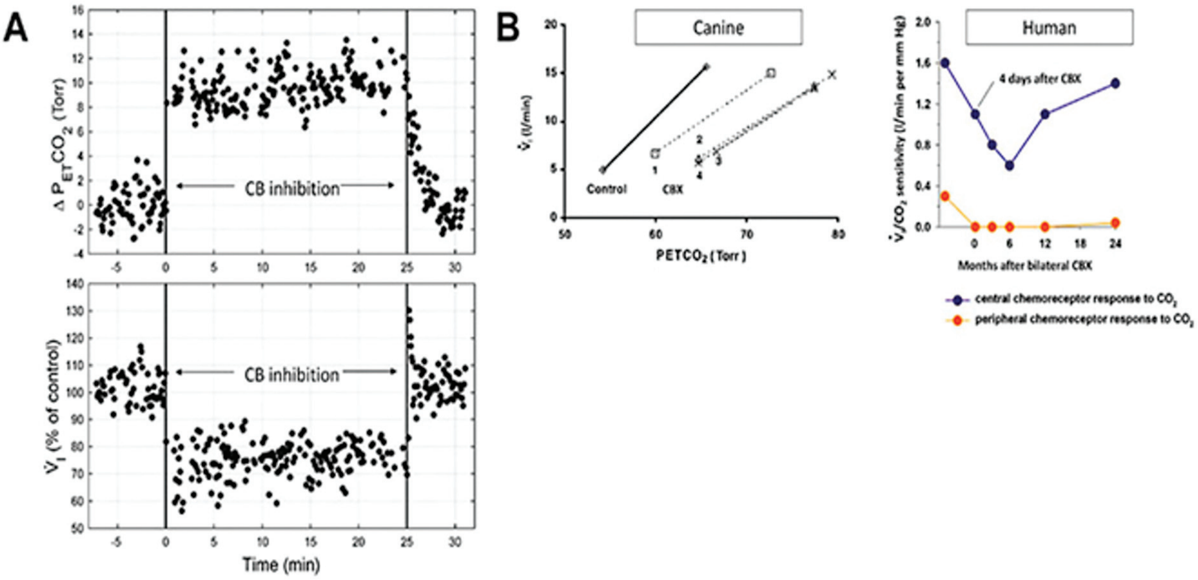

Fig. 3 The hyperadditive effect of carotid body (CB) sensory input on central CO_2 sensitivity is illustrated by two types of findings. (**A**) In awake (or sleeping) canines, one CB was denervated and the remaining CB vascularly isolated from the CNS and perfused extracorporeally. When the isolated CB was inhibited by hyperoxia plus hypocapnia, a marked alveolar hypoventilation and CO_2 retention occurred, which persisted despite substantial, sustained CNS acidosis. Note the immediate 60% increase in $\dot{V}_E$ at minute 25 when the tonic CB inhibition was removed, thereby further revealing the critical dependence of central CO_2 chemosensitivity on CB sensory input. Further experiments showed that the (extra-CB) central CO_2 ventilatory response slope was markedly depressed with CB inhibition and enhanced via CB stimulation using variations in CB PO_2, PCO_2, or their combination (not shown).[19,21] (**B**) In awake humans (right) and canines (left), bilateral CB denervation resulted in significantly reduced ventilatory response slopes to hyperoxic-hypercapnia as determined within a few days following CB denervation.[22,23] Several months following denervation, the "early" peripheral response to CO_2 remains eliminated, but the "late" central CO_2 response has risen to normal levels. These findings confirm those in other species and reveal the importance of quantifying the CB contribution to CO_2 chemosensitivity very early following CB denervation. To date, evidence for hyperadditive interdependence of central CO_2 chemosensitivity on CB input is limited to experimental preparations with physiologic levels of CO_2 chemosensitivity and in which the peripheral and central chemoreceptors are anatomically isolated (see explanation in Smith et al[21]). (Modified from Dempsey and Smith.[102])

the moderate hyperventilation associated with prolonged steady-state hyperoxia in intact animals and humans[28–30] likely reflects the effects of increased reactive oxygen species (ROS) in neural tissue, primarily the brainstem.[27] Third, the common use of hyperoxic CO_2 rebreathing tests to quantify chemoreflex sensitivity in humans reflects both the peripheral and central chemosensitivity, not just the latter as commonly presumed.

Extracarotid Body O_2 Sensors

Recent evidence points to three potential extra-CB sites of hypoxic sensing that might work cooperatively with varying levels of CB sensory input to impact the respiratory and sympathetic networks. First, release of ATP from PBC astrocytes contributes to hypoxic-induced ventilatory and sympathetic excitation via Ca^{2+}-dependent purinergic receptor mechanisms.[27] Second, in the kidney, hypoxia activates the cell bodies of renal afferent fibers which project to the ipsilateral horn of the spinal cord where they synapse with neurons projecting to the NTS and RVLM cardiorespiratory cells.[31] Further, erythropoietin released from the hypoxic kidney has been shown to stimulate the CB to increase ventilation.[32] Finally, sympathetic preganglionic neurons in the isolated thoracic spinal cord of the rodent responded to local hypoxia, triggering increases in sympathetic nerve activity.[33] Given that alterations in extra-CB PO_2 elicit bimodal stimulation of breathing i.e., in both hypoxia and hyperoxia, it is noteworthy that ROS also shows a similar bimodal response in many tissues, including the brainstem.[34,35] Increased ROS activates phospholipase-C and IP_3 receptors, thereby eliciting release of Ca^{2+} and enhancing vesicular release of ATP.[27]

Role of Chemoreceptors in Health

The chemoreceptors' principal role in the control of breathing is as feedback detectors of errors in PCO_2, pH, and PO_2 in the arterial blood, and, to a lesser extent, as contributors to the tonic control of breathing. Use of the isolated CB preparation in unanesthetized canines and humans (►**Fig. 3**) showed that acute, complete inhibition of the CB decreased the tonic steady-state drive to eupneic breathing by 25 to 35%, reflecting the effect of CB sensory input on the respiratory central controller plus its effect on central CO_2 chemosensitivity.

What stimuli comprise the large remaining drive to air-breathing ventilation that so precisely controls the link of $\dot{V}_A$ to $\dot{V}CO_2$ such that $PaCO_2$ varies little with changes in respiratory quotient or body mass, or even with several-fold increases in $\dot{V}CO_2$ and $\dot{V}_A$ during steady-state exercise?[36] Medullary CO_2 chemoreceptors are commonly viewed as major tonic inputs to eupnea, but there are several examples among rodents and other species or with pharmaco-genetic lesioning, in which the hypercapnic ventilatory response is reduced or even negligible while the eupneic air-breathing $PaCO_2$ is normal.[37–39] Acute optogenetic lesioning of RTN CO_2-sensitive neurons resulted in a significant CO_2 retention in the awake rodent, but this was due only to increased breathing frequency and dead-space ventilation with no significant reductions in V_T or $\dot{V}_E$.[40] This tachypneic response is not usually indicative of a chemoreceptor influence. Alternatively, perhaps pulmonary CO_2 exchange itself (i.e., $\dot{V}CO_2$) may be a major source of the "error-free" drive to breathe as is suggested by the precise link of $\dot{V}_A$ to $\dot{V}CO_2$ when venous CO_2 is raised or lowered.[41,42] While the mechanisms of $\dot{V}CO_2$ sensing is unknown, there is convincing evidence in anesthetized canines using separate pulmonary and systemic extracorporeal circulations to show the existence of a vagally innervated CO_2 sensor in the mammal's pulmonary circulation.[43] In this preparation, the ventilatory sensitivity to PCO_2 in the pulmonary circulation approximated that in the arterial systemic circulation. These CO_2 sensitive receptors exposed to mixed venous blood returning to the lung, might be sufficiently sensitive to account for modest changes in $\dot{V}_A$ due to changes in CO_2 flow to the lung.

Role of Chemoreceptors in Chronic Diseases

Accumulating evidence in animal models and human patients over the past two decades has demonstrated highly sensitized carotid chemoreceptors with augmented tonic activity—even in the presence of normal arterial oxygenation—in several disease states. In each of the following cases, this heightened tonic activity is associated with disease exacerbation.

Congestive Heart Failure

In humans with CHF, heightened chemoreflex sensitivity manifests as augmented sympathetic outflow, ventilatory instability, and augmented ventilatory responses to exercise.[44] Experimental heart failure in rats, canines, and rabbits produces carotid chemoreflex hypersensitivity leading to increased tonic levels of sympathetic outflow under normoxic conditions, enhanced sympathetic and ventilatory responses to acute hypoxemia, and vasoconstriction of locomotor muscle vasculature during exercise.[45,46] This form of CB plasticity is critically dependent on increases in locally produced angiotensin II, upregulation of angiotensin II type 1 receptors, increased expression of NADPH oxidase subunits, and enhanced superoxide production.[47] Thus, the CHF-induced increase in CB sensitivity is caused by a shift in redox balance toward oxidative stress. CHF-induced declines in CB blood flow, reduced shear stress, and resultant endothelial dysfunction are likely contributors to CB plasticity in this setting.[48,49]

Hypertension

In human hypertension, augmented neurocirculatory and ventilatory responses to transient hyperoxia provide evidence for tonically elevated chemoreflex drive.[50,51] Blood pressure elevation in the spontaneously hypertensive rat, an animal model of neurogenic hypertension, is dependent on excessive tonic input from the CB.[52] An important role for CB P2X3 receptors in causing chemoreflex hypersensitivity, heightened tonic sympathetic activity, and hypertension in this model has recently been demonstrated.[53] An interesting postulate is that the CB, via its own autonomic innervation, is a target of the widespread increase in sympathetic outflow observed in hypertensive states.[54] This local increase in sympathetic outflow could have an excitatory effect on the CB, caused at least, in part, by reductions in CB blood flow.[55]

Chronic Obstructive Pulmonary Disease

In patients with COPD, several findings provide evidence for CB hypersensitivity: (1) heightened basal sympathetic outflow, even in the absence of overt arterial hypoxemia[56–58]; (2) larger decreases in ventilation and sympathetic nerve activity during transient hyperoxia and during low-dose dopamine infusion; and (3) augmented increases in ventilation during exposure to acute hypoxia, relative to control subjects.[59] The origins of COPD-associated CB plasticity are unknown; however, COPD may impose an insult analogous to high altitude exposure—that is, continuous hypoxia-induced chemoreflex hypersensitivity leading to high tonic levels of sympathetic outflow and ventilatory instability, especially during sleep.[60,61]

In the chronically hypercapnic and hypoxemic COPD patient with acute exacerbation, even moderate amounts of supplemental O_2 will correct hypoxemia but often lead to worsening respiratory acidosis for multiple reasons. Reduced neural drives to breathe via suppression of high tonic levels of carotid chemoreceptor activity will reduce $\dot{V}_E$ transiently, but in the steady-state of hyperoxia, this reduction in ventilatory drive makes only a minor contribution to the reduced $\dot{V}_A$ and CO_2 retention. C˜ The major reason $\dot{V}_A$ is reduced and CO_2 retention occurs with hyperoxia is that hypoxic pulmonary vasoconstriction is inhibited in low $\dot{V}_A$:$\dot{Q}$ areas, thereby diverting blood flow from high $\dot{V}_A$:$\dot{Q}$ areas of the lung and increasing V_D/V_T.[2,62–64] Over reliance on oximetry monitoring of O_2 saturation (SpO_2) can contribute to this problem because respiratory acidosis can develop and worsen via small reductions in $\dot{V}_A$ (►**Fig. 2**) with little detectable change in SpO_2. Rather, frequent monitoring of $PaCO_2$ is important during gradual addition of supplemental O_2.[2]

Renal disease

Several sequelae of chronic kidney disease, such as metabolic acidosis and chronic anemia,[65,66] are potent chemoreflex stimuli. Patients with renal failure exhibit excessive basal sympathetic outflow[67,68] and augmented carotid chemoreflex-induced sympathoexcitation,[69,70] but the mechanisms leading to CB plasticity remain obscure. One potential instigator is increased vasoconstrictor sympathetic outflow to the CB, which is triggered reflexively by activation of renal afferents in response to hemodynamic and/or chemical derangements, including hypoxia in the failing kidney.[71]

Obstructive Sleep Apnea

The cyclical nature of sleep apnea elicits chronic intermittent hypoxemia (CIH; ►**Fig. 4**). ROS are generated primarily during the reoxygenation cycle of CIH, creating an imbalance in pro- versus antioxidant isoforms of the protein, hypoxia-inducible factor-1α (HIF-1α). The resultant oxidative stress increases [Ca^{2+}] which depolarizes CB glomus cells and triggers sensory neuronal activity.[72–74] Thus, in the CB, oxidative stress begets more oxidative stress, leading to enhanced sensory input and oxidative stress in other components of the extended chemoreflex pathway (e.g., NTS and RVLM) which results in increased sympathetic vasoconstrictor outflow and ventilation under baseline normoxic conditions and during hypoxia.

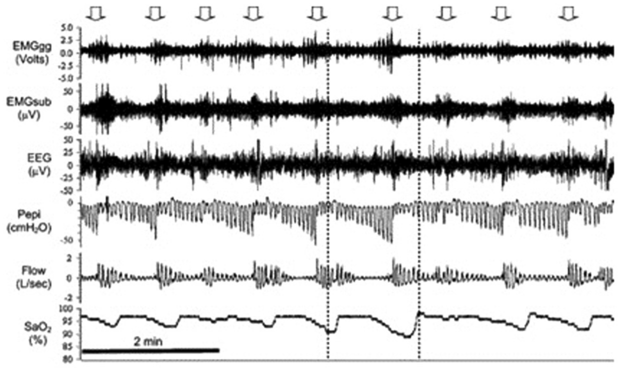

Fig. 4 Polysomnographic tracings of obstructive sleep apnea (OSA) in a patient with severe disease (apnea–hypopnea index = 56 events/hour). Note: (1) the reduction in the upper airway dilator genioglossus muscle EMG (EMG_{gg}) accompanying each airway obstruction; (2) the repeated O_2 desaturations as a result of severely impaired (hypopnea) or absent (apnea) airflow despite continued breathing efforts (P_{epi}); and (3) the cyclical breathing pattern that ensues as the patient oscillates between sleep and transient arousal (downward pointing arrows). (Reprinted with permission from Dempsey et al.[83])

Is Carotid Body Hypersensitization Reversible?

Studies in experimental animals point to potential benefits of strategies aimed at reducing chemoreflex hyperexcitability (e.g., CB resection, exercise training, statins, purinergic receptor blockade). In human CHF, surgical resection of the CB (both bilateral and unilateral) reduced muscle sympathetic nerve activity (MSNA) and produced a modest improvement in quality of life.[75] In patients with drug-resistant hypertension, unilateral CB resection reduced MSNA and blood pressure only in approximately 50% of individuals treated; moreover, these improvements were not maintained at 1-year follow-up.[76]

These observations in animals and humans demonstrate the capacity to eliminate, or at least suppress, excessive chemoreceptor drive, but is bilateral CB resection safe? In Japan,[63] extensive research in patients with asthma who underwent bilateral CB resection to relieve dyspnea suggests that the procedure is relatively benign; however, near-total suppression of the hypoxic ventilatory response persisted in some patients 30 years after resection.[77] Thus, of concern is the possibility that bilateral CB resection could lead to unsafe S_pO_2 levels with air travel, sojourns at high altitude, and via apnea prolongation during sleep-disordered breathing. A more pragmatic treatment would reduce tonic sympathetic hyperactivity while maintaining a normal ventilatory response to acute hypoxia. In this regard, one such treatment shown to be effective in rodents is selective pharmacologic blockade of ATP-gated ion channels (P2X3 receptors) in the CB.[53] The safety and efficacy of this treatment in humans with chronic disease has not been established.

Carotid Chemoreception and the "Silent Hypoxemia" of COVID-19

During the COVID-19 pandemic, many anecdotal reports surfaced of infected patients who were hypoxemic without dyspnea prior to hospitalization, leading to delayed treatment. While dyspnea perceptions have multiple causes with poorly defined central neural pathways, it is generally accepted that dyspnea occurs with dissociation between the "expectations" of the medullary control centers in terms of the ventilation produced for a given drive to breathe, and those outputs that the respiratory system is mechanically capable of producing. This concept of "neuromechanical uncoupling" is supported by experimental evidence demonstrating that when the spontaneous increase in V_T is mechanically constrained during rest or exercise in the face of increased chemostimulation, unpleasant sensations such as "air hunger" or "unsatisfied inspiration" are consistently provoked.[78] Thus, it is important to appreciate that moderate levels of hypoxemia (in the absence of coincident hypercapnia) and the attending hyperventilation, per se, are unlikely to elicit significant dyspneic sensations, as shown in healthy subjects at rest exposed acutely to hypoxic inspired gases or high altitudes.[79] It is more plausible that perceptions of dyspnea in the presence of COVID-19 infection would develop when the raised drive to breathe attending hypoxemia was combined with proinflammatory-induced lung injury which negatively impacts breathing mechanics and raises the work of breathing. Exacerbation of dyspnea might also be expected with lung vascular inflammation due to additional sensory stimulation of the drive to breathe and breathing frequency elicited through lung unmyelinated C-fibers via increases in pulmonary vascular pressures.[80] It has also been suggested that CB sensitivity might be enhanced via COVID-induced inflammation or immune reactions and/or an imbalance of ACE1/ACE2 (angiotensin-converting enzyme) occurring systemically or locally at the CB.[81] If the ventilatory response was coincidentally enhanced, this might be sufficient to promote dyspneic sensations, especially during exercise.

Pathogenesis of Sleep-Disordered Breathing

Sleep renders the ventilatory control system highly vulnerable to disordered breathing by removing the wakefulness drives to breathe, unmasking a critical dependence of ventilatory drive on chemoreception and reducing upper airway dilator muscle tonicity. These fundamental effects of sleep are manifested in cyclical sleep apnea when present in individuals with enhanced controller (i.e., $\Delta\dot{V}_A/\Delta PaCO_2$) and/or plant (i.e., $\Delta PaCO_2/\Delta\dot{V}_A$) gains, and pharyngeal airways susceptible to closure[82,83] (►**Fig. 4**).

Sleep-Induced Suppression of the Wakefulness Drive to Breathe and Ventilatory Stability: The Loss of Vigilance

Regulation of chemoresponsiveness, upper airway patency, and ventilatory stability is dependent on "wakefulness" drives to breathe.[84,85] The origins of these tonic facilitatory drives have been localized to several highly state-dependent areas of the CNS, including (1) orexinergic neurons in the hypothalamus[86,87]; (2) premotor cortex and supplementary motor area neurons[88]; and (3) parallel neuronal systems that link H^+ chemosensitivity to both breathing and arousal.[89,90]

Physiologically, the loss of tonic wakefulness neurogenic drives is manifest throughout sleep in the (1) increased collapsibility of the extrathoracic upper airway due to loss of pharyngeal dilator muscle tone; (2) varying degrees of alveolar hypoventilation secondary to both increased airway resistance and a resetting of the $PaCO_2$ set-point,[91] the latter likely due to NREM sleep-induced reductions in medullary inspiratory neuronal activity[92]; and (3) critical dependence on CO_2 chemosensitivity above and below eupnea on breathing stability. In turn, the breathing instability that occurs during NREM sleep is characterized by repeated, excessive ventilatory undershoots and overshoots (►**Fig. 4**), demonstrating a "loss of vigilance" of the respiratory control system for protecting stability and arterial blood gas homeostasis—characteristics it displays so precisely during wakefulness.

Transient Ventilatory Undershoots and Overshoots

During wakefulness, transient hyperventilation rarely culminates in apnea or hypopnea, but does so consistently and in a dose–response manner in NREM sleep.[93,94] DuBois et al[94] have associated maintained ventilation (i.e., absence of apnea) following active or passive hyperventilation with respiratory-related EEG activity—cortical activity that was absent when apnea was accompanied by hypocapnia. This association suggests a "cortical-subcortical cooperation" to preserve ventilation during wakefulness that would be lost during NREM sleep. Similarly, during wakefulness when inspiratory resistive or elastic loads are imposed on the airway, inspiratory drive is immediately augmented and inspiratory time prolonged to preserve V_T and $\dot{V}_A$. In contrast, during NREM sleep, this immediate load compensation is absent, precipitating a reduced V_T until CO_2 accumulates to such a degree that chemoreceptors stimulate inspiratory and expiratory muscle EMG activity to restore $\dot{V}_E$.[95] Studies in the sleeping canine have shown that apneas following transient hyperventilation require (1) intact carotid chemoreceptors[96]; (2) intact vagally mediated lung stretch receptors[97]; (3) transient hypocapnia acting at both peripheral and central chemoreceptor sites[98]; and (4) a hyperadditive interdependence of central CO_2 sensitivity on peripheral chemoreceptor sensory input.[21]

Transient ventilatory overshoots, on the other hand, commonly occur at the termination of an apnea or hypopnea during sleep due to the synergistic effect of hypercapnia plus hypoxemia acting at the CB and augmenting ventilatory drive. These effects of chemostimulation at apnea termination are further augmented because (1) the drive to breathe following cessation of respiratory rhythm is delayed until $PaCO_2$ rises to a value that exceeds the preapneic eupneic $PaCO_2$[99] and (2) the common occurrence of transient cortical arousals at end-apnea both restores upper airway patency (thereby reducing the resistive load on ventilation) and substantially augments the prevailing chemosensitive drive to breathe.

In summary, loss of wakefulness drives to breathe in NREM sleep unmask an apneic threshold sensitive to transient hypocapnia plus lung stretch. Equally, a sufficiently brisk synergistic responsiveness to hypercapnic/hypoxemic combinations is retained which, along with frequent transient arousals, mediates transient ventilatory overshoots at apnea termination. These combined effects above and below eupnea promote cyclical ventilatory instability. In phasic REM sleep, sporadic increases in medullary inspiratory neuronal activity augment breathing frequency[85] and oppose the occurrence of both hypocapnia-induced ventilatory undershoots/apneas and chemoreceptor-driven ventilatory overshoots.[100]

Loop Gain and Ventilatory Instability in Sleep

Excessive chemosensitivity to transient increases and decreases in CO_2 contributes importantly to central, obstructive, and mixed repeated apneas and hypopneas in health and in chronic diseases by enhancing the controller, plant, and "loop" gains of the respiratory control system. Loop gain is a dynamic measure of how close the respiratory control system is to instability[101–103] (see details in ►**Fig. 5** legend).

Lowering chemosensitivity/controller gain reduces sleep-disordered breathing instability, as shown via use of nocturnal hyperoxia in CHF patients,[104] and CB denervation or gaseous excitatory neurotransmitter blockade in rodent models of CHF.[105,106] Further, lowering of plant gain via acetazolamide-induced steady-state hypocapnic hyperventilation, or raising inspired CO_2 fraction and $PaCO_2$, reduces breathing instability and central apneas in CHF patients and in sojourners to high altitude, and even obstructive apneas in selected patients with OSA.[61,107–109]

Obstructive Sleep Apnea Links to a Declining Neural Drive to Breathe

Classically, OSA is thought to occur at sleep onset via a state-related decline in pharyngeal dilator muscle tone, precipitating pharyngeal/airway obstruction and hypoxemia. Obstructive apneas elicit a chemoreflex-induced rise in ventilatory drive which usually fails to reopen the airway until arousal occurs, resulting in transient ventilatory overshoots.[110,111] In contrast, several small physiologic studies have demonstrated that variations in neural ventilatory drive can have profound influences on upper airway patency and resistance, with complete airway obstruction occurring at the nadir of diaphragmatic EMG activity or during central apnea in subjects with airways susceptible to collapse[83,112–114] (►**Fig. 6A**). Furthermore, as shown in experimental studies with relatively small number of OSA patients, raising or preventing transient reductions or oscillations in ventilatory drive in many OSA patients (using supplemental CO_2, metabolic acidosis, or hyperoxia) significantly reduces airway obstruction.[109,115,116]

Most recently, Gell and colleagues[117] used multiple electrode high-resolution diaphragm EMG measurements to quantify neural inspiratory drive during sleep in a sample of 50 OSA patients, the majority of who had moderate-to-severe OSA. The authors demonstrated that most of the several hundred obstructive events studied exhibited drive-dependent event pathophysiology, whereby airflow was lost at the nadir of a gradually declining inspiratory drive (►**Fig. 6B**). A decline in genioglossus EMG was also shown to accompany the falling diaphragmatic EMG leading to airway obstruction. These data in a large OSA patient population confirm several prior physiologic studies supporting the importance of neural respiratory drive in the control of upper airway caliber in those with collapsible upper airways. Importantly, these data strongly reinforce the need for in-depth exploration of practical, patient-friendly ways to prevent ventilatory drive decline and instability in OSA without disrupting normal sleep states.

Control of Breathing during Exercise

The ventilatory response to steady-state exercise is characterized by proportional increases in $\dot{V}_A$ and $\dot{V}CO_2$[118–120] (►**Fig. 7**). The exercise ventilatory response must not only regulate $PaCO_2$ in the face of 10-fold increases in $\dot{V}CO_2$ but must also optimize respiratory mechanics to minimize the work, metabolic and circulatory costs of breathing. Below, we briefly describe the neural control of breathing with respect to respiratory muscle $\dot{V}O_2$ (mechanics) and $PaCO_2$ (hyperpnea) regulation during exercise.

Respiratory Mechanics

►**Fig. 8** shows ensemble averaged flow-volume and esophageal pressure-volume relationships during incremental exercise, which can be used to quantitatively assess respiratory mechanics.[118] The exercise ventilatory response is governed by the "principle of minimum effort." As workload increases, inspiratory pump muscles contract more forcefully, generating greater negative pleural pressures, and expiratory muscles are recruited to force air out of the lungs. Thus, increases in V_T are accomplished by lowering end-expiratory lung volume and increasing end-inspiratory lung volume[121,122] (►**Figs. 7** and **8**). This breathing strategy is important for two reasons: (1) increased V_T versus breathing frequency reduces V_D/V_T, thereby improving $\dot{V}_A$, and (2) breathing takes place on the linear portions of the lung and chest wall compliance curves which minimizes the increase in the elastic work of breathing as VT rises. In addition, relaxation of airway smooth muscle due to β_2-adrenergic receptor activation increases airway patency, reduces turbulent airflow, and lowers the resistive work of breathing as flow rate rises. Metaboreflexes from contraction of limb locomotor muscles contribute importantly to this exercise-induced bronchodilation.[123] Thus, in the healthy untrained individual, ventilatory demand rarely exceeds capacity to increase flow and volume, even at maximum exercise (►**Fig. 8**).

Exercise Hyperpnea

Exercise hyperpnea is $PaCO_2$ regulation about its set-point due to proportional changes in $\dot{V}_A$ and $\dot{V}CO_2$ ($\Delta\dot{V}_A \propto \Delta\dot{V}CO_2$). An important feature of exercise hyperpnea is that the gain of the exercise ventilatory response (i.e., $\Delta\dot{V}_E/\Delta\dot{V}CO_2$) is

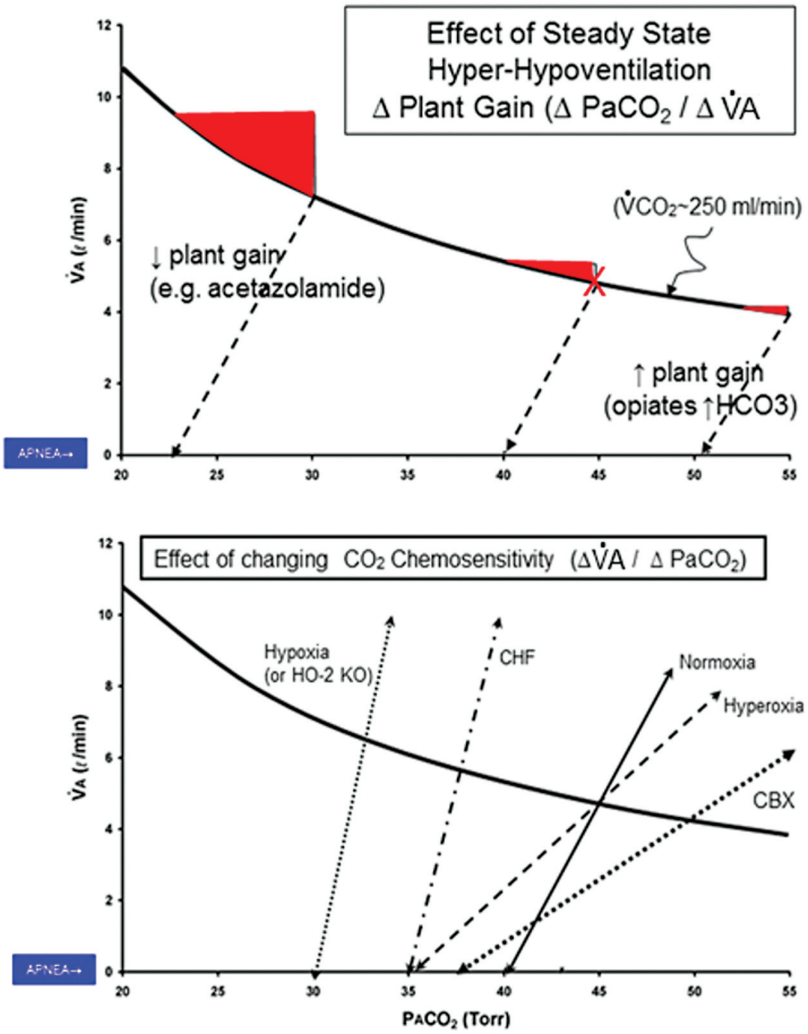

Fig. 5 Diagram of the alveolar gas equation to illustrate the effects of loop gain components on the propensity for apnea and ventilatory instability during NREM sleep. The equation is $PaCO_2 = \dot{V}CO_2/\dot{V}_A \cdot K$, where resting $\dot{V}CO_2 = 250$ mL/min. Each example shown is from an experimental study in sleeping humans or canines in which the apneic threshold and the slope of the CO_2 response below eupnea were measured during NREM sleep using a mechanical ventilator in the assist-control mode to gradually raise tidal volume and transiently lower partial pressure of end-tidal CO_2 ($P_{ET}CO_2$) until apnea occurred. The top panel shows effects of changing "plant" gain—low plant gain means low sensitivity of arterial PCO_2 ($PaCO_2$) response to changes in $\dot{V}_A$ ($\Delta PaCO_2/\Delta\dot{V}_A$) and the opposite is true of high plant gain. In these examples, we have changed plant gain by itself with steady-state hyper- or hypoventilation along the iso-metabolic hyperbola. The red filled-in areas indicate the magnitude of increase in alveolar ventilation needed to transiently reduce $PaCO_2$ sufficiently to reach the apneic threshold. For example, under control conditions in NREM sleep (eupneic $PaCO_2$ ~45 mm Hg, denoted by X), a transient ventilatory overshoot of ~1 L/min is required to reduce $PaCO_2$ ~5 mm Hg to the apneic threshold of 40 mm Hg. With steady-state hyperventilation (e.g., oral acetazolamide; $PaCO_2$, 30 mm Hg), the required transient ventilatory overshoot to achieve apnea ($PaCO_2$, 23 mm Hg) is approximately twice that of control; conversely, with steady-state hypoventilation (e.g., metabolic alkalosis, COPD, opiate use; $PaCO_2$ ~55 mm Hg), the required ventilatory overshoot to achieve apnea ($PaCO_2$ ~51 mm Hg) is about one-third that of control. Not illustrated here are: (1) the effects of transient arousal from sleep, which will increase the magnitude of the ventilatory overshoot above eupnea; (2) reductions in cerebral vasculature CO_2 responsivity as often occurs in congestive heart failure (CHF) which will increase the ventilatory response to transient changes in $PaCO_2$ by allowing changes in brain extracellular fluid PCO_2 to more closely reflect those in $PaCO_2$[210]; and (3) the dynamic effects of lung volume on plant gain. For example, at low lung volumes, plant gain is raised; thus, the CO_2 washout from the alveoli will occur more quickly and will require smaller transient increments in ventilation to reach the apneic threshold.[211] The lower panel shows effects of changing "controller" gain or chemoreceptor sensitivity to $PaCO_2$ ($\Delta\dot{V}_A/\Delta PaCO_2$) above eupnea (which affects the magnitude of the transient ventilatory overshoot) and below eupnea (which affects the CO_2 "reserve" or difference in $PaCO_2$ between eupneic breathing and the apneic threshold). Here the slope of the ventilatory response to CO_2 above and below eupnea represents the controller gain for each condition studied. Note the increased CO_2 response slopes above and below eupnea in CHF and with healthy subjects in hypoxic environments and the reduced CO_2 sensitivity in hyperoxia which is further reduced with carotid body denervation (CBX). K, constant 0.863; PCO_2, partial pressure of CO_2; $\dot{V}_A$, alveolar ventilation; $\dot{V}CO_2$, CO_2 production rate; $\dot{V}_E$, minute ventilation. (Modified from Dempsey.[103])

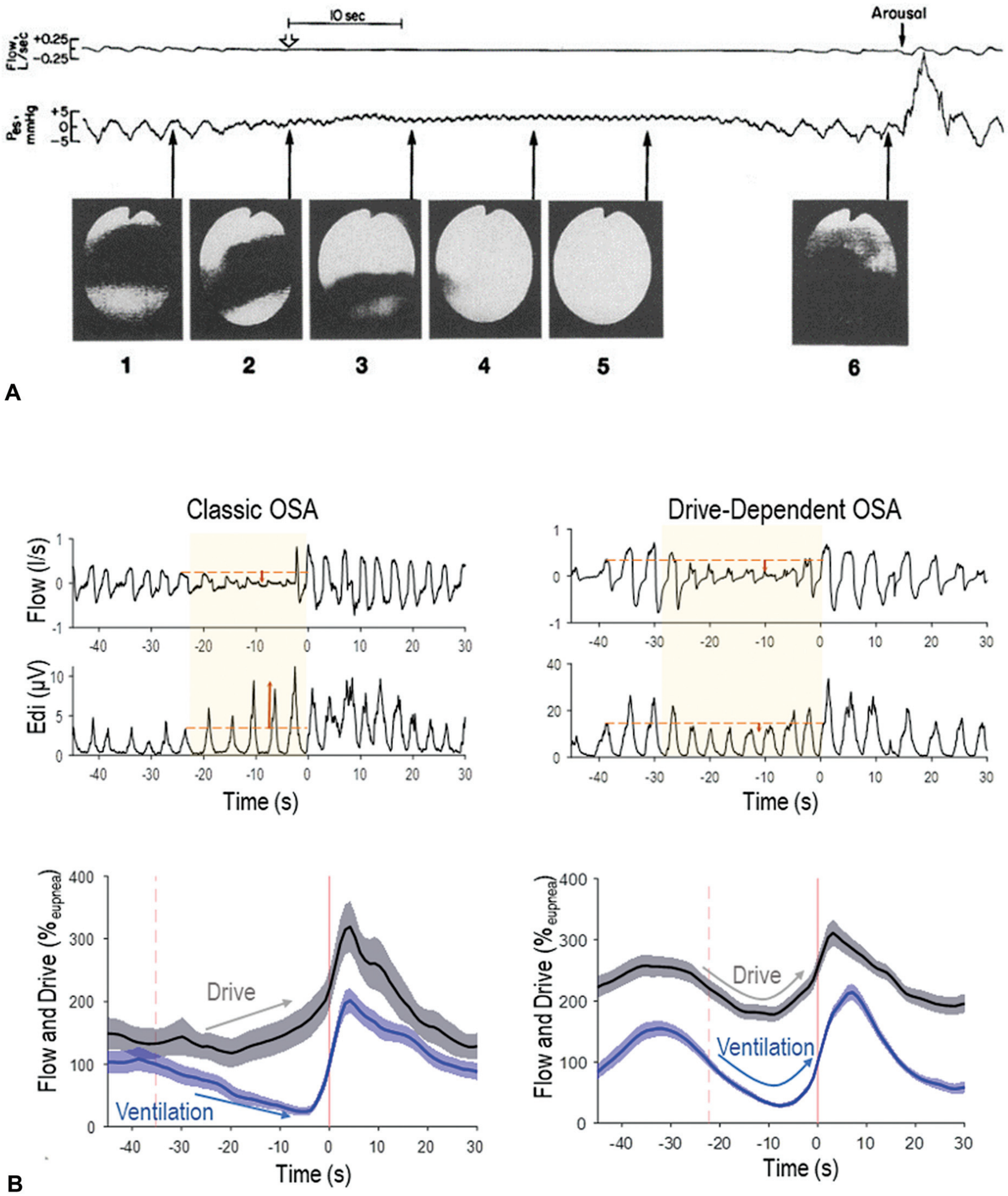

Fig. 6 (**A**) Effects of a spontaneous central apnea on upper airway patency during NREM sleep. Fiberoptic nasopharyngoscopy was used to determine airway dimensions at the level of the velopharynx or oropharynx. Initiation of central apnea occurred at the inverted open arrow with the cessation of both cyclical airflow and esophageal pressure. Complete airway occlusion occurred after ~15–20 seconds of airflow cessation and before an inspiratory effort occurred. Apnea continued and the airway remained closed for another ~35 seconds until inspiratory efforts began and then the airway opened completely with a ventilatory overshoot upon arousal from sleep.[113] (Reproduced with permission from Badr et al.[113]) (**B**) Illustrative examples of classic and drive-dependent obstructive sleep apnea (OSA). The patient with classic OSA (left) experiences a fall in flow to complete obstruction. Diaphragm EMG activity (E_{di}) is unchanged as ventilation falls leading to the obstruction and then rises in response to a falling O_2 saturation over the later stages of the apnea. In contrast, the patient with drive-dependent OSA (right) exhibits a characteristic fall in E_{di} during individual events, as seen in raw EMG signals (top) and in ensemble averaged data (below). Note that the drive-dependent patient shows a fall in drive that is in synchrony with the event-related loss in flow, ending in airway obstruction. Toward apnea termination, E_{di} rises in response to developing hypoxemia. At apnea termination, flow and E_{di} rise together, often augmented via transient arousals. (Modified from Gell et al.[117])

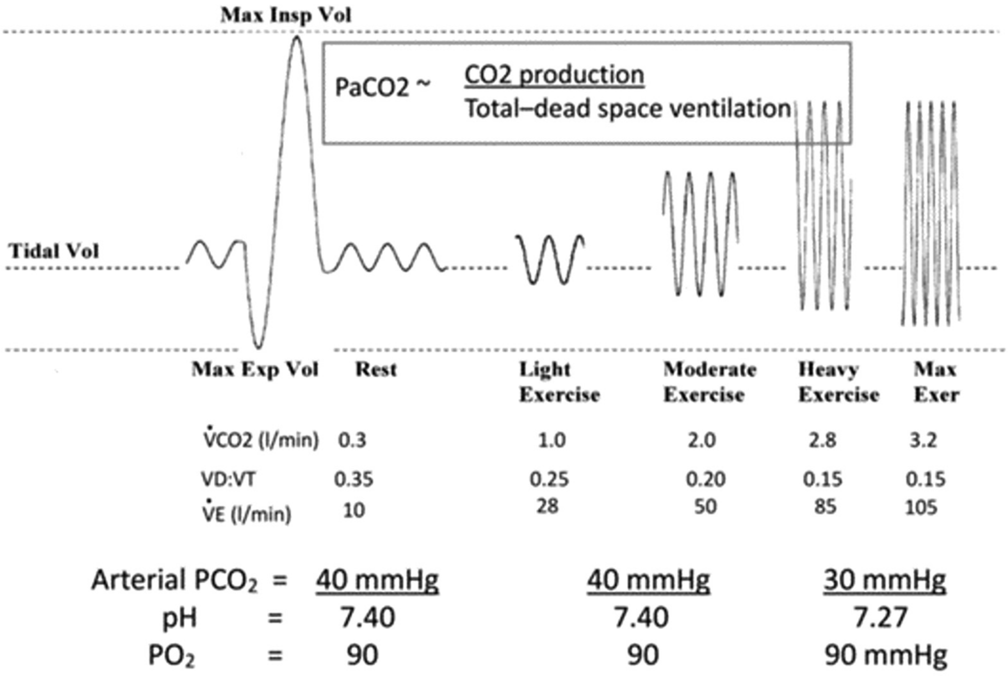
Max Insp Vol
PaCO2 ~ CO2 production / Total–dead space ventilation
Tidal Vol
Max Exp Vol
Rest
Light Exercise
Moderate Exercise
Heavy Exercise
Max Exer
V̇CO2 (l/min) 0.3 1.0 2.0 2.8 3.2
VD:VT 0.35 0.25 0.20 0.15 0.15
V̇E (l/min) 10 28 50 85 105
Arterial PCO₂ = 40 mmHg 40 mmHg 30 mmHg
pH = 7.40 7.40 7.27
PO₂ = 90 90 90 mmHg

Fig. 7 Description of typical ventilatory and arterial blood–gas responses to steady-state, incremental exercise in untrained young healthy adults (maximal oxygen consumption [$\dot{V}O_{2max}$] ~35–50 mL/kg/min; aged 20–35 years). Note: (1) the incremental rise in tidal volume (V_T) and then breathing frequency (f_b) with inspiratory time (T_i) remaining slightly less than expiratory time (T_e), and the reduction in end-expiratory lung volume; (2) the fall in the dead-space to tidal volume ratio (V_D/V_T) and ratio of minute ventilation to carbon dioxide production ($\dot{V}_E/\dot{V}CO_2$), which maintains the ratio of alveolar ventilation to carbon dioxide production ($\dot{V}_A/\dot{V}CO_2$) and partial pressure of carbon dioxide ($PaCO_2$) near resting values throughout moderate intensity exercise; and (3) the hyperventilatory response to heavy and maximum exercise intensities coincident with the onset of metabolic acidosis. (Reproduced with permission from Dempsey et al.[118])

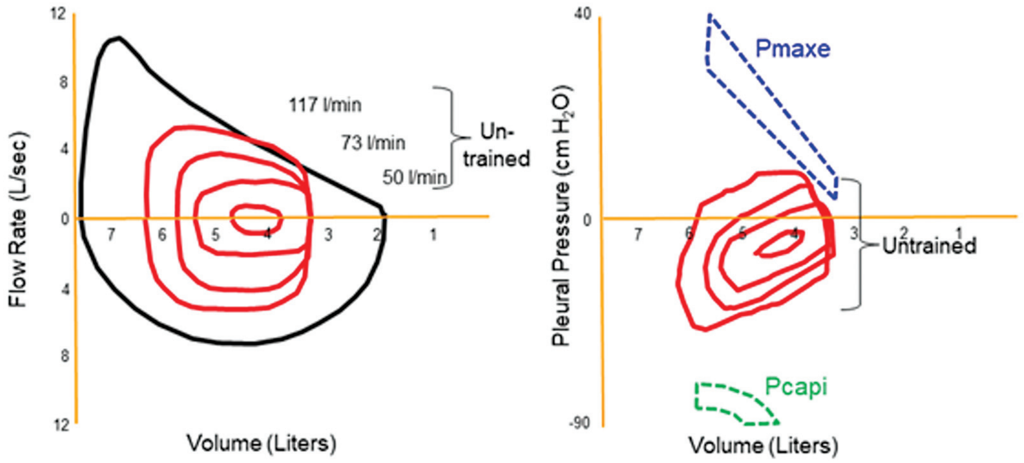

Fig. 8 Mean values for tidal flow-volume and esophageal (pleural) pressure-volume loops during incremental steady-state exercise in untrained young adult males. The maximum voluntary flow-volume loop (shown in black) was determined following exercise. The maximum effective pleural pressure on expiration (P_{maxe}) indicates a range of pressures at which further increases in pressure via expiratory muscle effort elicits dynamic airway compression and no further increase in flow rate. P_{capi} indicates maximum range of dynamic pressures capable of generation by the inspiratory muscles across the various lung volumes and flow rates experienced during exercise. Note that in these untrained individuals ($\dot{V}O_{2max}$ <50 mL/kg/min), (1) the maximum available flow-volume loop significantly exceeds the demand during maximal exercise; (2) the tidal expiratory pressures remain <P_{maxe}; (3) the maximum inspiratory muscle pressures developed during tidal breathing remain <50% of the maximum dynamic pressure available at the flow rates and lung volumes achieved during exercise; and (4) $\dot{V}_E$ averaged 50, 73, and 117 L/min at mild, moderate, and maximum exercise intensities. (Reproduced with permission from Dempsey et al.[118])

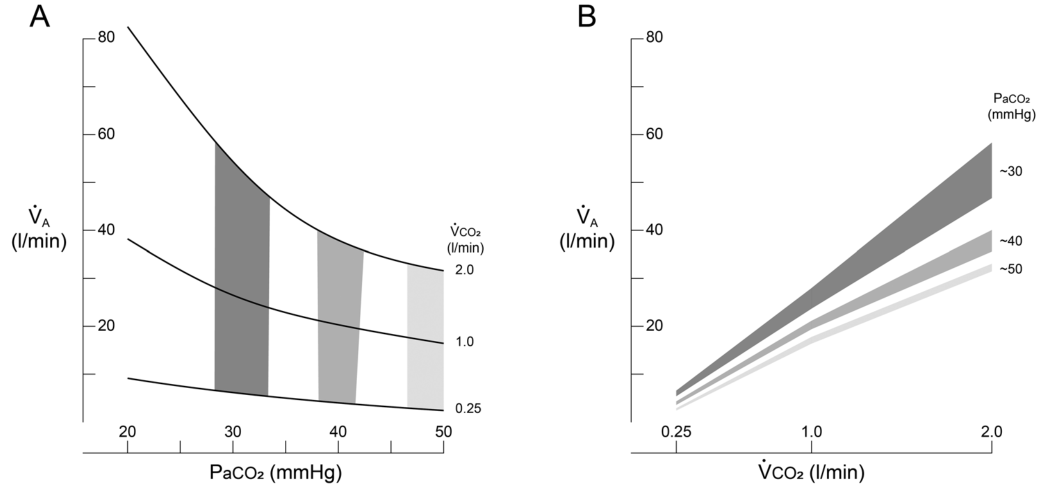

Fig. 9 The eucapnic ventilatory response to exercise is maintained when the resting $PaCO_2$ set-point is altered, by changing the gain of the ventilatory response to increasing $\dot{V}CO_2$. (**A**) The red X denotes the resting $PaCO_2$ (40 mm Hg) at resting $\dot{V}CO_2$ of 0.25 L/min in control and after steady-state hyperventilation secondary to metabolic acidosis or progesterone administration ($PaCO_2$, 30 mm Hg) and hypoventilation via metabolic alkalosis or carotid chemoreceptor denervation ($PaCO_2$, 50 mm Hg). Note (**A**) that during exercise at 2.0 L/min $\dot{V}CO_2$, $\dot{V}_A$ increases: (1) 40 L/min from rest to maintain $PaCO_2$ at its normal resting level of 40 mm Hg; (2) 50 L/min when resting $PaCO_2$ was 30 mm Hg; and (3) 30 L/min when resting $PaCO_2$ was 50 mm Hg. (**B**) The change in $\dot{V}_A$:$\dot{V}CO_2$ slope required to maintain eucapnia at the three resting set points for $PaCO_2$. These experimental results are an example of the strong, precise link of $\dot{V}_A$ to $\dot{V}CO_2$ which prevails in the face of a changing resting $PaCO_2$ and independently of any change in CO_2 chemosensitivity.[36,125]

dependent on the $PaCO_2$ set-point.[124] As shown in ►**Fig. 9**, a low resting $PaCO_2$ brings about a greater change in $\dot{V}_A$ *versus* a high resting $PaCO_2$ for any given $\dot{V}CO_2$ to maintain isocapnia during exercise.[125] These alterations in the slope of $\Delta\dot{V}_A/\Delta\dot{V}CO_2$ with changes in the resting $PaCO_2$ were not attributable to changes in the $\Delta\dot{V}_E/\Delta PaCO_2$ response and occurred even in the absence of carotid chemoreceptors.

It is widely held that the primary exercise stimulus during steady-state conditions is feedforward with respect to $PaCO_2$ regulation. This notion is based on evidence that (1) people with central congenital hypoventilation syndrome (dysfunctional central chemoreceptors) exhibit normal ventilatory responses to steady-state exercise compared with healthy controls[126] and (2) CB denervated humans and ponies exhibit blunted but not significantly impaired ventilatory responses, indicating that CB chemoreceptors "fine-tune" breathing only.[127,128] For the purposes of this review, we shall focus on two feedforward stimuli supported as obligatory to exercise hyperpnea. Further information can be found on this issue in a comprehensive review by Forster et al.[119]

Central Neurogenic

Commonly referred to as "central command," central neurogenic stimuli originate from suprapontine structures, both cortical and subcortical.[129,130] Demonstration of parallel increases in heart rate, blood pressure, and phrenic nerve activity during electrical stimulation of the hypothalamic locomotor region of paralyzed cats provided unequivocal evidence of a central neurogenic component to respiratory control.[131,132] Clever approaches to the study of central command in the genesis of exercise hyperpnea in humans stem from observations of hyperventilation during imagined exercise at rest under hypnosis.[133–135] When brain blood flow was estimated using positron emission tomography, activation of several cortical sites including the dorsolateral prefrontal cortex, supplemental motor area, and sensorimotor areas were markedly increased.[133] The cerebellum also shows increased activation and has been hypothesized to play a major role in respiratory modulation, memory, and learning.[134]

The periaqueductal gray matter region of the midbrain is believed to be an integration center of central neurogenic stimuli due to its functional connectivity to higher brain centers and the brainstem.[136–138] Electrodes implanted in the periaqueductal gray matter of patients who had undergone neurosurgery for pain or movement disorders showed increased activity during mild exercise coincident with small increases in ventilation and heart rate.[139] While there is a large body of evidence supporting central neurogenic stimuli as obligatory to exercise hyperpnea, counter evidence exists from studies in anaesthetized animals and in healthy humans during sinusoidal exercise,[140–142] discussed later.

Peripheral Neurogenic

Peripheral neurogenic stimuli originate from peripheral sensory receptors, not including receptors sensitive to changes in $PaCO_2$ that constitute feedback control. Electrical stimulation of S6-L1 elicits tetanic contractions of hind-limb muscles in anesthetized cats, which reflexly increases heart rate, blood pressure, and ventilation[143] by C-fiber activation.[144] In humans, intrathecal fentanyl (μ-opioid receptor agonist) injections to the lumbar cord partially blocks sensory inputs and blunts the exercise ventilatory response,[145] implying that group III/IV muscle afferents are obligatory to exercise hyperpnea. Alternatively, an argument is made that ventilation is coupled to $\dot{V}CO_2$.[140]

When exercise workload is altered in a sinusoidal fashion, the change in $\dot{V}_E$ and $\dot{V}CO_2$ during each sinusoid is attenuated as the duration of each sinusoid decreases. Because central command and presumably muscle afferent feedback are coalesced with exercise workload, the dissociation between workload and $\dot{V}_E/\dot{V}CO_2$ suggests that CO_2 flow to the lungs ($\dot{Q}.C\bar{v}CO_2$) is a primary, required stimulus to exercise hyperpnea.

In support of this notion, Phillipson et al[41] found that CO_2 loading or scrubbing from the venous circulation of sheep led to proportional changes in $\dot{V}_A$, such that $PaCO_2$ was maintained isocapnic during steady-state exercise. This impressive demonstration is not without limitations, such as the small range of $\dot{V}CO_2$ changes studied. Furthermore, only $C\bar{v}CO_2$ was altered, whereas during exercise $C\bar{v}CO_2$ changes very little, as the major increase in CO_2 flow is determined by an increase in venous return. A further difficulty is the absence of a mixed-venous CO_2 sensor in humans with sufficient gain to explain the substantial hyperpnea associated with exercise. The "vascular distention" hypothesis posits that $\dot{V}CO_2$ is not sensed through $C\bar{v}CO_2$, but via increased $\dot{Q}$, and simultaneous activation of group III/IV muscle afferents.[146,147]

Another plausible theory in support for CO_2 flow as obligatory to exercise hyperpnea was suggested by Yamamoto and Edwards, who also used extracorporeal perfusion in anesthetized rats to demonstrate proportional increases in $\dot{V}_A$ with the rate of femoral vein CO_2 loading, with no appreciable changes in the mean $PaCO_2$.[42] The authors concluded that "temporal fluctuations in the arterial PCO_2 can be sufficient information to signal for the required ventilation." Indeed, breath-to-breath oscillations in arterial pH can be detected at rest and during exercise in humans[148] and the slope of these oscillations increases during exercise in some but not all studies.[148,149] So arterial PCO_2/pH oscillations are amplified during exercise in the presence of constant mean arterial blood–gas values, but no evidence yet exists that any resultant sensitization of chemoreceptor gain will be sufficient to explain a significant fraction of the 10- to 12-fold increases in $\dot{V}_E$ above resting levels required during even moderate exercise.

In summary, the ventilatory response to steady-state mild to moderate intensity exercise is an excellent example of integrated systems symmorphosis. The tight coupling between $\dot{V}_A$ and $\dot{V}CO_2$ ensures arterial blood–gas and acid–base homeostasis, while the mechanics of breathing minimize respiratory muscle work and $\dot{V}O_2$. Exercise hyperpnea remains a phenomenon; however, strong evidence supports central and peripheral neurogenic stimuli, including stimuli linked to CO_2 flow to the lung, as obligatory to its control.

During heavy exercise in health, hyperventilation ensues in part due to chemoreceptor activation caused by metabolic acidosis, increased body temperature, and other humoral stimuli[150] (see ►**Fig. 7**). That locomotor muscle fatigue also contributes to this hyperventilatory response is suggested by the hyperventilation elicited during exercise in the face of partial neuromuscular blockade. This effect is likely due to the enhanced descending central motor drive required to maintain muscle force output in a fatiguing muscle.[151,152] Tonic and phasic activity of accessory inspiratory muscles increases[153] as respiratory muscle $\dot{V}O_2$ approaches 10% of whole-body maximum $\dot{V}O_2$.[154] Should exercise be of sufficient intensity and duration, accumulation of fatigue-inducing metabolites in the respiratory muscles will occur,[155,156] which elicits cardiovascular and hemodynamic adjustments known as the respiratory muscle metaboreflex.[157]

Exercise Hyperpnea: Pathophysiology

In the young healthy adult, the exercise ventilatory response is near perfect in terms of precision in the matching of $\dot{V}_A$ to $\dot{V}CO_2$ and in mechanical efficiency (i.e., work of breathing/respiratory muscle $\dot{V}O_2$; ►**Figs. 7–9**). The defining departures from this response with healthy aging or with chronic cardiorespiratory diseases include an imprecision in arterial blood–gas regulation, inefficient breathing mechanics, excessive drives to breathe, and heightened sensations of exertional dyspnea.

Healthy Aging

Normal aging beyond the second decade results in a reduction in the lung and airway's maximal available *capacity* for flow and volume (due primarily to a reduction in lung elastic recoil) together with an increased ventilatory *demand* (►**Fig. 10A**). High pulmonary capillary pressures at any given $\dot{Q}$ (due to an age-dependent reduction in pulmonary vascular compliance), together with a loss of alveolar capillary surface area, results in a rise in $\dot{V}_A/\dot{Q}$ nonuniformity and elevated V_D/V_T at rest and during exercise.[158,159] What are the consequences of this inefficient gas exchange to the healthy, exercising 70-year-old? On the one hand, remarkably, the high V_D/V_T is compensated as total $\dot{V}_E$ is elevated at any given $\dot{V}CO_2$ to maintain $\dot{V}_A$:$\dot{V}CO_2$ proportionality, nearly identical to that achieved in the 30-year-old with much lower V_D/V_T. How might the controller "determine" the fraction of the blood not properly exposed to gas exchanging alveoli and therefore gauge the extent of the V_D? Perhaps in the presence of a high V_D, the lower rate of CO_2 unloading from the pulmonary capillaries to the alveoli may lead to amplified intra- and inter-breath oscillations in $PaCO_2$ which in turn would sensitize chemoreceptor gain (see section "Exercise Hyperpnea"). Alternatively, plasticity in ventilatory control that "somehow" senses a gradually increasing V_D over time may occur with aging (see "Plasticity" section below). Note that concomitant age-associated changes in CO_2 chemosensitivity do not explain this adaptive increase in VE:VCO2 allowing the precise regulation of $\dot{V}_A$:$\dot{V}CO_2$ in the face of a rising V_D/V_T.

At any given exercise $\dot{V}CO_2$, the added ventilatory response combined with the reduced flow-volume capacity with age would appear to enhance the possibility of expiratory flow limitation leading to hyperinflation during exercise. This scenario appears unlikely in non-smoking, sedentary aging individuals whose lungs age coincidentally with reductions in cardiovascular and muscle metabolic capacities which dictate a reduction in maximum $\dot{V}O_2$ (~10%/decade) and, therefore, a similar decline in the maximal demand for ventilation and

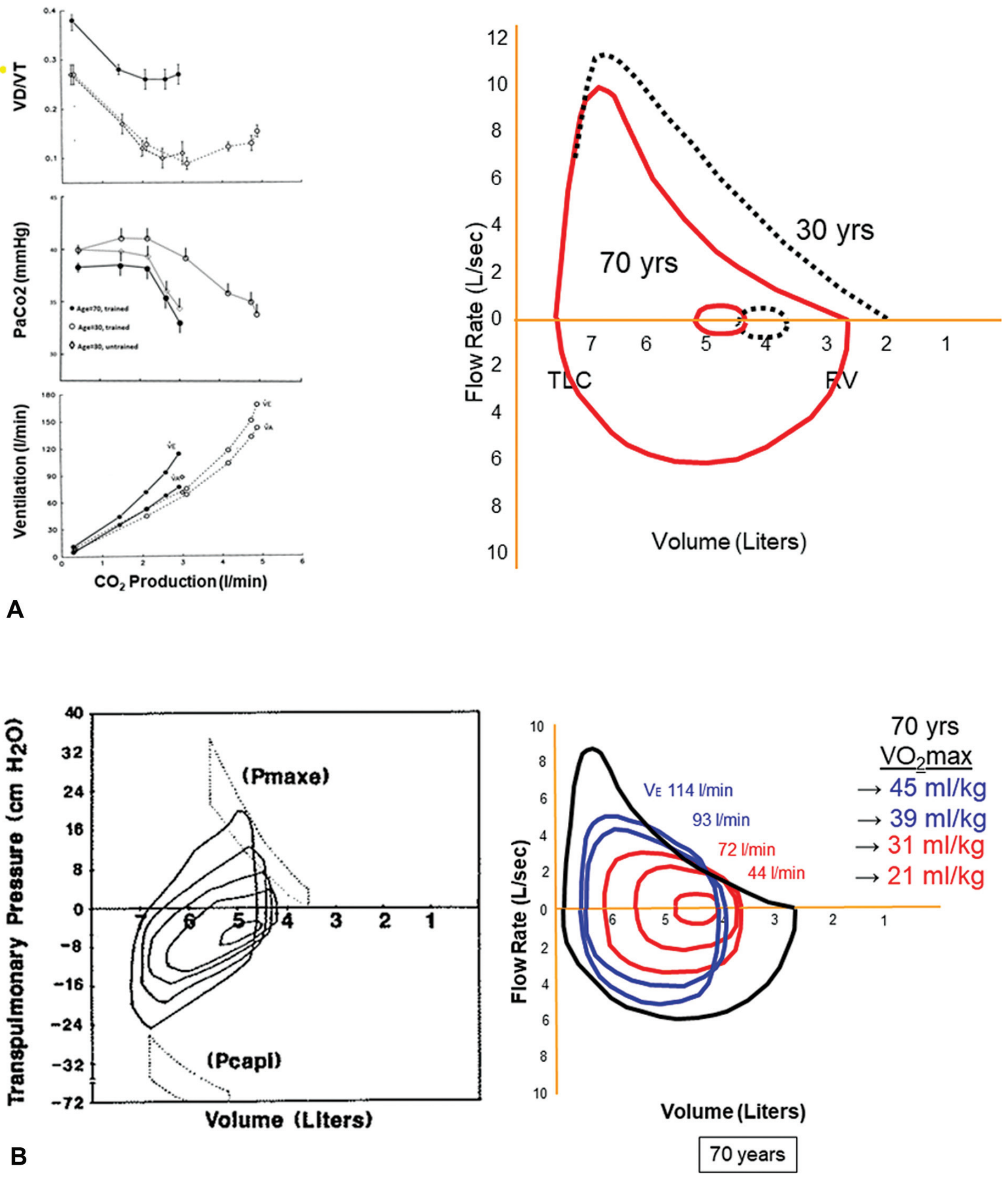

Fig. 10 (**A**) Decreased capacity for maximum flow-volume *vs.* increased ventilatory demand during exercise with healthy aging. The right-hand plot shows the reduced maximum flow-volume loop typical of a healthy, fit, 70-year-old *vs.* a 30-year-old male. The three left plots depict the plasticity in exercise hyperpnea which occurs with healthy aging. Note the higher dead-space to tidal volume ratio (V_D/V_T) at rest and throughout exercise in older *vs.* younger subjects, reflecting age-induced loss of lung elastic recoil and $\dot{V}_A/Q$ nonuniformity. Despite the higher V_D/V_T, alveolar ventilation to CO_2 production ($\dot{V}_A/\dot{V}CO_2$) and arterial CO_2 tension ($PaCO_2$) at rest and throughout exercise were essentially the same in young (untrained and trained) and older (trained) subjects, because minute ventilation to CO_2 production ($\dot{V}_E/\dot{V}CO_2$) was increased in the elderly to precisely compensate for their elevated V_D/V_T. (Modified from Johnson et al.[158]) (**B**) Effect of fitness level on expiratory flow limitation in healthy 70-year-old subjects. The maximum flow-volume loop (shown in black) is that from a healthy, active fit 70-year-old. The minute ventilation ($\dot{V}_E$) and tidal flow-volume loops are those achieved at four levels of maximum O_2 consumption ($\dot{V}O_{2max}$) of 21–31 mL/kg/min representative of sedentary untrained 70-year-olds (in red) and of 39–45 mL/mL/min in highly fit endurance-trained 70-year-old runners (in blue). Note that the maximum ventilatory demand is insufficient to induce flow limitation and hyperinflation in the sedentary 70-year-old but is sufficient in the highly trained 70-year-old. Also note the corresponding pressure-volume loops in the left diagram. Contrast these figures with the flow- and pressure-volume loops attained in young untrained subjects in ►**Fig. 8**, who are at similar $\dot{V}O_{2max}$ and $\dot{V}_E$ as are the trained 70-year-olds but have substantially greater capacities for maximum flow and volume.

pulmonary gas exchange. Accordingly, as shown in ►**Fig. 10B**, the ventilatory demands required at a maximum $\dot{V}O_2$ of 23 to 30 mL/kg/min in the sedentary 70-year-old are not sufficient to elicit flow limitation and excessive respiratory muscle work. However, the highly trained 70-year-old might differ because the age-dependent reductions in maximum $\dot{V}O_2$ (demand) can be markedly attenuated through a habitually active lifestyle. Another determining factor here is that some (but not all) longitudinal aging data show a 15 to 20% less aging-induced decline in forced expiratory volume and forced vital capacity in high *versus* low habitually active individuals.[160–162] Such a positive effect of lifelong activity on lung function would be somewhat protective in moderately fit older individuals, but in many highly trained endurance athletes, significant flow limitation with dynamic hyperinflation, high work of breathing, and severe dyspnea occurs at maximum levels of $\dot{V}O_2$ and $\dot{V}_E$ comparable to those experienced in the sedentary 30-year-old (►**Fig. 10B**). A significant portion of these highly trained older individuals also experience exercise-induced hypoxemia at maximum $\dot{V}O_2$ levels between 40 and 55 mL/kg/min.

Chronic Obstructive Pulmonary Disease

COPD represents an extreme example of a highly compliant lung and a compromised maximum expiratory flow-volume curve which leads to expiratory flow limitation with only modest increases in flow rates above resting levels. The ensuing progressive hyperinflation with mild to moderate exercise appears as the major contributor to dyspnea and exercise limitation.[163] Use of multielectrode diaphragm EMG measurements in patients with COPD of varying disease severity by O'Donnell and coworkers revealed that during exercise, the inspiratory neural drive to breathe and dyspnea ratings are augmented at any given $\dot{V}_E$, culminating in exercise limitation[150] (►**Fig. 11A, B**). The excessive neural drive to breathe during exercise in COPD has multiple well-documented sources, including augmented sensitivities of carotid chemoreceptors and limb and respiratory muscle afferents, plus engagement of pulmonary C-fiber afferents secondary to elevated pulmonary arterial pressures.[58,164,165] In addition, the limb muscle fatigue induced by even mild exercise in COPD[166] would be expected to elevate compensatory central neurogenic inputs to augment the drive to breathe and dyspnea during exercise as more motor units are recruited to maintain force in the failing limb locomotor musculature.[151,152]

Several approaches to reducing the excessive drive to breathe in COPD have resulted in less dyspnea, improved exercise performance, and decreased limb fatigue. First, inhalation of low-density He/O_2 mixtures expands the maximum expiratory flow-volume envelope in most patients, thereby reducing expiratory flow limitation and reducing the

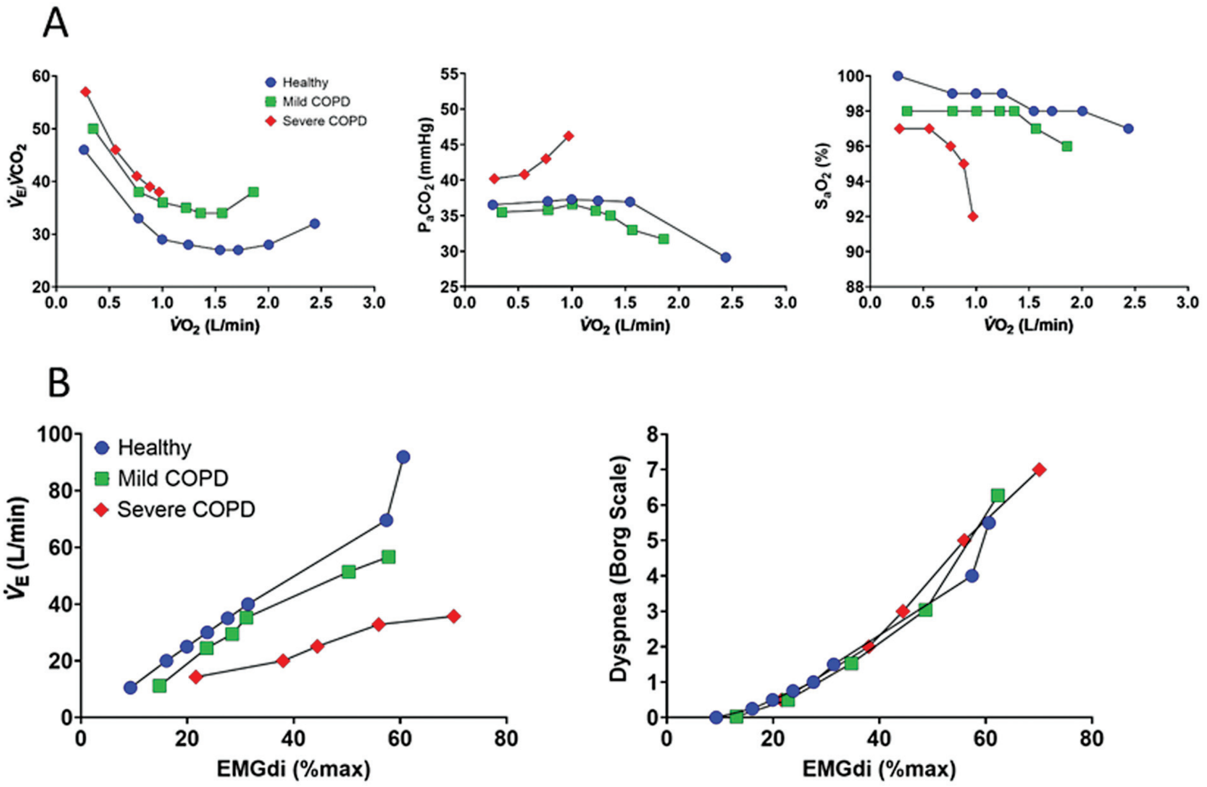

Fig. 11 (**A**) Elevated minute ventilation to CO_2 production ($\dot{V}_E/\dot{V}CO_2$) in mild and moderate chronic obstructive pulmonary disease (COPD) patients during exercise. Arterial CO_2 pressure ($PaCO_2$) is well controlled in most COPD patients, but CO_2 retention commonly occurs in more severe COPD patients as expiratory flow limitation and hyperinflation are exacerbated and the raised $\dot{V}_E/\dot{V}CO_2$ is insufficient to compensate for an elevated dead-space to tidal volume. (Modified from Dempsey et al.[150]) (**B**) Diaphragm EMG (EMGdi), a measure of neural inspiratory drive, is elevated along with dyspnea perception score for any given minute ventilation ($\dot{V}_E$) during exercise in mild and especially severe COPD. (Modified from Dempsey et al.[150]; Despite the differences in lung mechanics among the three groups, the fundamental relationship between the neural respiratory motor output [EMGdi] and dyspnea severity remains similar.)

rate of limb fatigue development during exercise.[166] In turn, the reduced limb fatigue likely results from a lowered work of breathing and attenuated respiratory muscle metaboreflex, thereby increasing blood flow availability to locomotor muscles.[167,168] Second, supplemental inspired O_2 reduced chemoreceptor drive and exercise $\dot{V}_{E,}$ slowed the rate of development of limb muscle fatigue and improved exercise performance.[163,166] Third, inspiratory muscle training was shown to reduce diaphragm EMG activity and dyspneic sensations during exercise.[169] Fourth, intrathecal fentanyl was used to reduce muscle afferent input in COPD patients, resulting in reduced breathing frequency, which in turn reduced dead-space ventilation and total $\dot{V}_E$, flow limitation, hyperinflation, and dyspnea.[165] So, as in healthy individuals, muscle afferent input in exercising COPD patients contributes significantly to exercise hyperpnea, but with a negative, rather than positive influence on exercise performance.[170] Given the diminished aerobic capacity and reduced fatigue resistance of limb locomotor muscles in the sedentary COPD patient,[166,171] specific resistance training of the legs[172] would be expected to reduce stimulation of muscle metaboreflexes and, thus, prevent excessive drives to breathe that evoke tachypneic, hyperpneic, and dyspneic responses to exercise.

Congestive Heart Failure

CHF patients also show excessive neural drives to breathe and occasionally, even oscillatory, periodic breathing during exercise. The severity, efficiency, and stability of their tachypneic hyperventilatory response to exercise is prognostic of morbidity and mortality.[173,174] As with COPD, the major sources of excessive ventilatory drive in CHF during exercise include chemoreceptor sensitization (see "Chemoreceptors" section above), muscle mechanoreceptor sensitization, and pulmonary C-fiber stimulation secondary to high pulmonary capillary pressures and interstitial pulmonary edema.[164] Intrathecal fentanyl administration in CHF patients was especially effective in reducing hyperventilatory responses, thereby demonstrating a major contribution from hypersensitized locomotor muscle afferents to the hyperventilatory response to exercise.[175]

Respiratory Neuroplasticity

Breathing is a vital behavior that must exhibit plasticity—defined as a persistent change in the neural control system (morphology and/or function) based on experience.[176] Plasticity is a fundamental property of robust neural systems to defend homeostasis against threats from recurrent and/or enduring physiological challenges across the lifespan (e.g., exposure to high altitude/hypoxia, injury/disease, aging, weight gain/loss, and pregnancy). Plasticity may occur at any level of respiratory control, including CB chemoreceptors, brainstem central pattern generators, and/or spinal α-motor neurons.[177] Below, we briefly discuss three models of respiratory neuroplasticity: (1) long-term modulation of the exercise ventilatory response, (2) ventilatory acclimatization/de-acclimatization, and (3) respiratory long-term facilitation.

Long-Term Modulation of the Exercise Ventilatory Response

Long-term modulation of the exercise ventilatory response is an example of respiratory neuroplasticity akin to associative learning. Repeated hypercapnic exercise in goats and humans with external CO_2 loading via increased respiratory dead-space or inspired CO_2 elicits hyperventilation during subsequent exercise when the hypercapnic stimulus is removed.[178,179] It stands to reason that error signals detected by chemoreceptors (including the CB and RTN) initiate changes within the CNS that encode the relationship between $\dot{V}_A$ and $PaCO_2$ for a given $\dot{V}CO_2$, possibly from birth.[180–182] Localization of a respiratory memory to the CNS that is developed during periods of learning has not been identified, although we speculate that localization may occur within the cerebellum. It should also be acknowledged that several researchers have failed to replicate long-term modulation in humans,[183,184] likely due to methodological inconsistencies, such as the number of training trials.

Ventilatory Acclimatization/Deacclimatization

Sojourn to high altitude elicits time-dependent hyperventilation over several days, known as ventilatory acclimatization; upon return to normoxia, hyperventilation persists, known as ventilatory deacclimatization.[185,186] Two mechanisms underlying ventilatory acclimatization/deacclimatization are (1) carotid chemoreceptor sensitization and (2) central/peripheral chemoreceptor interdependence.

CB denervation prevents ventilatory acclimatization[187] and isolated CB hypoxia alone (without systemic hypoxemia) elicits similar time-dependent hyperventilation to hypoxemia as in the animal exposed to whole body hypoxia,[188] demonstrating an obligatory role of the CB in ventilatory acclimatization to chronic sustained hypoxia. In anesthetized goats, carotid sinus nerve activity progressively increases during the first few hours of hypoxic exposure, suggesting that the CB undergoes changes in O_2 sensitivity.[189] CB plasticity is believed to be caused by a combination of factors, including upregulation of neuromodulators (e.g., dopamine, angiotensin-II, endothelin-I) and increased protein expression and proliferation of CB glomus cells.[190,191] Recently, HIF-1α has also been identified as a major player in CB plasticity induced by chronic sustained hypoxia exposure.[192]

Ventilatory deacclimatization, on the other hand, may partially be explained by central sensitization of phrenic nerve activity in response to carotid sinus nerve stimulation.[193] The carotid sinus nerve innervates the CB and relays sensory information to the NTS where second-order neurons extend to the RTN of the ventral medulla.[18,194] These CO_2 sensitive neurons increase their activity in response to systemic hypoxia and show no response following CB denervation.[185] Thus, central chemoreceptors located in the RTN are modulated by CB chemoafferent input. The net effect of carotid chemoreceptor activation on central chemoreceptor gain is argued to be hyper additive based on the observation that the CO_2 chemoreflex was enhanced by isolated CB stimulation via hypoxia and blunted by CB inhibition via hyperoxic–hypocapnia[20] (►**Fig. 3**).

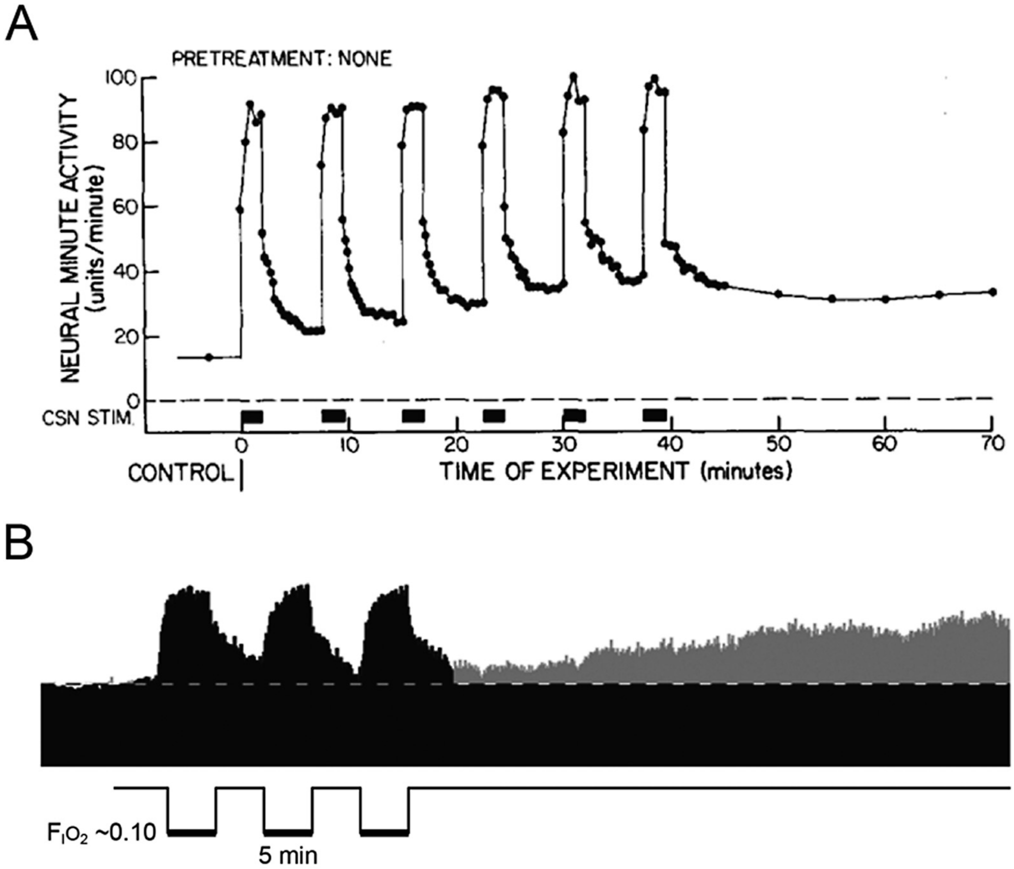

Fig. 12 (**A**) In a paralyzed, anesthetized or decerebrate cat, six 2-minute episodes of carotid sinus nerve (CSN) electrical stimulation were delivered (denoted by thick black bars) followed by 5-minute intervals. The increase in phrenic nerve activity that remained above baseline for ~5 minutes after each stimulation episode is known as phrenic "afterdischarge" or "short-term potentiation," whereas the persistent increase in integrated phrenic nerve activity that lasted up to 30 minutes after the final stimulation episode is a distinct mechanism of plasticity known as long-term facilitation. Modified from Millhorn et al.[186] (**B**) In anesthetized rats, three 5-minute episodes of acute intermittent hypoxia (AIH) were delivered with two 5-minute intervals. The inspired fraction of O_2 (FIO_2) is ~0.10 during episodes of hypoxia; normoxia (FIO_2 ~0.21), or hyperoxia (FIO_2 ~0.50) is often administered during intervals. Note the prolonged increase in raw phrenic nerve activity (shaded in gray), similar to that observed after CSN stimulation in the cat. Phrenic long-term facilitation is a pattern-sensitive, serotonin-dependent, and activity-independent form of spinal synaptic plasticity. (Modified from Devinney et al.[212])

Respiratory Long-Term Facilitation

First demonstrated in 1980 by Millhorn and colleagues,[186] repeated 2-minute episodes of electrical carotid sinus nerve stimulation in anesthetized cats elicited a prolonged increase in phrenic nerve activity that long outlasted the duration of its immediate effects. This form of respiratory motor plasticity, termed "phrenic long-term facilitation," can also be elicited by repeated brief exposures to hypoxia (i.e., acute intermittent hypoxia [AIH]), as shown in ►**Fig. 12**.[195] Moderate hypoxemia ($>$ 35 mm Hg PaO_2) stimulates CB chemoreceptors that activate brainstem raphe neurons to release the neurochemical serotonin. Serotonin binds to 5-HT_2 receptors on phrenic motor neurons which initiates an intracellular signaling cascade involving new protein (brain-derived neurotrophic factor) synthesis and protein kinase-Cθ activation.[196–199] Glutamatergic currents are potentiated through an undefined mechanism that strengthens synapses from pre-motor to α-motor neurons, possibly via NMDA receptor phosphorylation.[200] Consequently, phrenic, intercostal, hypoglossal, and other respiratory motor outputs are enhanced.[195]

Unlike chronic AIH associated with severe sleep apnea, which is known to elicit a plethora of cardiovascular maladaptations,[111] low doses of AIH may have therapeutic benefit.[201,202] While improvements in respiratory and non-respiratory motor function have been observed following therapeutic AIH in people with chronic spinal cord injury, the underlying mechanisms are poorly understood.[203,204] Poikilocapnic AIH does not appear to enhance corticospinal neurotransmission in respiratory nor limb muscles,[205–207] although this remains controversial.[208] Recent work shows that in healthy humans, AIH paired with concurrent hypercapnia (i.e., acute intermittent hypercapnic-hypoxia) enhances the amplitude diaphragmatic motor-evoked potentials induced by transcranial magnetic stimulation, without change in the amplitude of diaphragm potentials evoked by peripheral nerve stimulation.[209] Thus, a central neural mechanism of respiratory motor plasticity was identified. It is unclear if AIH is a viable therapeutic modality to harness respiratory neuroplasticity to restore or enhance breathing in humans.

Summary

We have examined a select few of the essential basic concepts and recent advances in our understanding of the control of breathing in health and disease:

- Quantifying the hyperbolic nature of $\dot{V}_A$:$\dot{V}CO_2$:$PaCO_2$ relationships revealed the importance of both the prevailing $PaCO_2$ and $\dot{V}CO_2$ (i.e., “plant gain”) in determining the relative magnitude of homeostatic ventilatory demands.
- Breathing and sympathetic nerve activity are influenced in a feedback fashion via disturbances in O_2 and/or CO_2 acting at the level of the carotid chemoreceptors, at several sites within the CNS and through the interdependence of medullary CO_2 responsiveness on carotid chemoreceptor sensory input.
- Hypersensitization of carotid chemoreceptors plays a significant role in chronically elevated tonic levels of sympathetic outflow and systemic vasoconstriction observed in many chronic diseases, such as CHF, COPD, hypertension, and OSA. Quantifying these increased chemosensitivities as well as constraining the elevated tonic sympathetic activity remains a challenge.
- Descending central neurogenic stimuli from suprapontine structures and ascending neurogenic stimuli from peripheral receptors (e.g., group III/IV muscle afferents) have been identified as obligatory feedforward mediators of the near eucapnic and highly mechanically efficient exercise hyperpnea in health; however, the mechanism(s) underlying the primary, underlying stimulus to breathe (i.e., $\dot{V}CO_2$) remains elusive.
- In healthy aging, COPD and CHF, augmented neural drives to breathe during exercise have been linked to performance-limiting dyspneic sensations and have been identified as originating in hypersensitized chemoreceptors, muscle afferents, and the pulmonary vasculature. Elevated dead-space ventilation in these conditions is also mysteriously linked to an added compensatory drive to breathe.
- The loss of wakefulness drives to breathe during sleep increases susceptibility to pharyngeal collapse and ventilatory instability. Elevated controller and/or plant gains in the system controlling breathing promote centrally mediated ventilatory instability, often leading to airway obstruction (OSA) during decrements in inspiratory neural drive.
- Neuroplasticity in respiratory control is common throughout life with important therapeutic implications and may provide mechanistic explanations for respiratory long-term facilitation and ventilatory acclimatization to hypoxic exposures, and maybe even for exercise hyperpnea.

Conclusion

While substantial insight has been gleaned over the past 30 years into the mechanisms governing respiratory control, several fundamental questions remain which are acknowledged throughout this review. We conclude with a few of these: (1) how is $\dot{V}CO_2$ sensed and how is this information transmitted to respiratory control centers; (2) what is the signal that allows the central controller to determine the fraction of blood leaving the lung not adequately exposed to alveolar gas exchange and then provide an appropriate adjustment to the drive to breathe; and (3) how can we adapt respiratory stimuli and stabilizers to be used in the treatment of OSA? Finally, motivation for further progress may be readily found in the realization that we are still unable to account for a great majority of the drive to breathe during wakefulness, sleep, and exercise, i.e., most of living!

Funding
Grant support for this study was provided by NHLBI.

Conflict of Interest
None declared.

Acknowledgments
The authors are indebted to Prof. Barbara Morgan for her invaluable assistance and to Profs. Patrice Guyenet, Thomas Clanton, and Joseph Santin for their insightful feedback.

References

1 Skatrud JB, Dempsey JA, Bhansali P, Irvin C. Determinants of chronic carbon dioxide retention and its correction in humans. J Clin Invest 1980;65(04):813–821
2 Malhotra A, Schwartz DR, Ayas N, Stanchina M, White DP. Treatment of oxygen-induced hypercapnia. Lancet 2001;357 (9259):884–885
3 Purro A, Appendini L, Polillo C, et al. Mechanical determinants of early acute ventilatory failure in COPD patients: a physiologic study. Intensive Care Med 2009;35(04):639–647
4 Del Negro CA, Funk GD, Feldman JL. Breathing matters. Nat Rev Neurosci 2018;19(06):351–367
5 Baertsch NA, Baertsch HC, Ramirez JM. The interdependence of excitation and inhibition for the control of dynamic breathing rhythms. Nat Commun 2018;9(01):843
6 Ainsworth DM, Smith CA, Johnson BD, Eicker SW, Henderson KS, Dempsey JA. Vagal modulation of respiratory muscle activity in awake dogs during exercise and hypercapnia. J Appl Physiol 1992;72(04):1362–1367
7 Phillipson EA, Hickey RF, Bainton CR, Nadel JA. Effect of vagal blockade on regulation of breathing in conscious dogs. J Appl Physiol 1970;29(04):475–479
8 Schwarzacher SW, Rüb U, Deller T. Neuroanatomical characteristics of the human pre-Bötzinger complex and its involvement in neurodegenerative brainstem diseases. Brain 2011;134(Pt 1):24–35
9 Alheid GF, Milsom WK, McCrimmon DR. Pontine influences on breathing: an overview. Respir Physiol Neurobiol 2004;143(2-3):105–114
10 Montandon G, Horner R. CrossTalk proposal: The preBotzinger complex is essential for the respiratory depression following systemic administration of opioid analgesics. J Physiol 2014;592 (06):1159–1162
11 Daristotle L, Berssenbrugge AD, Bisgard GE. Hypoxic-hypercapnic ventilatory interaction at the carotid body of awake goats. Respir Physiol 1987;70(01):63–72
12 Kumar P, Bin-Jaliah I. Adequate stimuli of the carotid body: more than an oxygen sensor? Respir Physiol Neurobiol 2007;157(01): 12–21
13 Guyenet PG, Stornetta RL, Bayliss DA. Central respiratory chemoreception. J Comp Neurol 2010;518(19):3883–3906

14 Guyenet PG. Regulation of breathing and autonomic outflows by chemoreceptors. Compr Physiol 2014;4(04):1511–1562

15 Zera T, Moraes DJA, da Silva MP, Fisher JP, Paton JFR. The logic of carotid body connectivity to the brain. Physiology (Bethesda) 2019;34(04):264–282

16 Keir DA, Duffin J, Millar PJ, Floras JS. Simultaneous assessment of central and peripheral chemoreflex regulation of muscle sympathetic nerve activity and ventilation in healthy young men. J Physiol 2019;597(13):3281–3296

17 Prasad B, Morgan BJ, Gupta A, et al. The need for specificity in quantifying neurocirculatory vs. respiratory effects of eucapnic hypoxia and transient hyperoxia. J Physiol 2020;598(21): 4803–4819

18 Takakura AC, Moreira TS, Colombari E, West GH, Stornetta RL, Guyenet PG. Peripheral chemoreceptor inputs to retrotrapezoid nucleus (RTN) CO2-sensitive neurons in rats. J Physiol 2006;572 (Pt 2):503–523

19 Blain GM, Smith CA, Henderson KS, Dempsey JA. Contribution of the carotid body chemoreceptors to eupneic ventilation in the intact, unanesthetized dog. J Appl Physiol 2009;106(05): 1564–1573

20 Blain GM, Smith CA, Henderson KS, Dempsey JA. Peripheral chemoreceptors determine the respiratory sensitivity of central chemoreceptors to CO(2). J Physiol 2010;588(Pt 13):2455–2471

21 Smith CA, Blain GM, Henderson KS, Dempsey JA. Peripheral chemoreceptors determine the respiratory sensitivity of central chemoreceptors to CO_2: role of carotid body CO_2. J Physiol 2015; 593(18):4225–4243

22 Rodman JR, Curran AK, Henderson KS, Dempsey JA, Smith CA. Carotid body denervation in dogs: eupnea and the ventilatory response to hyperoxic hypercapnia. J Appl Physiol 2001;91(01): 328–335

23 Dahan A, Nieuwenhuijs D, Teppema L. Plasticity of central chemoreceptors: effect of bilateral carotid body resection on central CO_2 sensitivity. PLoS Med 2007;4(07):e239

24 Curran AK, Rodman JR, Eastwood PR, Henderson KS, Dempsey JA, Smith CA. Ventilatory responses to specific CNS hypoxia in sleeping dogs. J Appl Physiol 2000;88(05):1840–1852

25 Smith CA, Engwall MJ, Dempsey JA, Bisgard GE. Effects of specific carotid body and brain hypoxia on respiratory muscle control in the awake goat. J Physiol 1993;460:623–640

26 Daristotle L, Engwall MJ, Niu WZ, Bisgard GE. Ventilatory effects and interactions with change in PaO_2 in awake goats. J Appl Physiol 1991;71(04):1254–1260

27 Gourine AV, Funk GD. On the existence of a central respiratory oxygen sensor. J Appl Physiol 2017;123(05):1344–1349

28 Olson EB Jr, Vidruk EH, Dempsey JA. Carotid body excision significantly changes ventilatory control in awake rats. J Appl Physiol 1988;64(02):666–671

29 Becker H, Polo O, McNamara SG, Berthon-Jones M, Sullivan CE. Ventilatory response to isocapnic hyperoxia. J Appl Physiol 1995; 78(02):696–701

30 Becker HF, Polo O, McNamara SG, Berthon-Jones M, Sullivan CE. Effect of different levels of hyperoxia on breathing in healthy subjects. J Appl Physiol 1996;81(04):1683–1690

31 Patinha D, Pijacka W, Paton JFR, Koeners MP. Cooperative oxygen sensing by the kidney and carotid body in blood pressure control. Front Physiol 2017;8:752

32 Soliz J, Joseph V, Soulage C, et al. Erythropoietin regulates hypoxic ventilation in mice by interacting with brainstem and carotid bodies. J Physiol 2005;568(Pt 2):559–571

33 Barioni NO, Derakhshan F, Tenorio Lopes L, et al. Novel oxygen sensing mechanism in the spinal cord involved in cardiorespiratory responses to hypoxia. Sci Adv 2022;8(12):eabm1444

34 Dean JB, Mulkey DK, Henderson RA III, Potter SJ, Putnam RW. Hyperoxia, reactive oxygen species, and hyperventilation: oxygen sensitivity of brain stem neurons. J Appl Physiol 2004;96 (02):784–791

35 Clanton TL. Hypoxia-induced reactive oxygen species formation in skeletal muscle. J Appl Physiol 2007;102(06):2379–2388

36 Whipp BJ. Control of the exercise hyperpnea: the unanswered question. Adv Exp Med Biol 2008;605:16–21

37 Santin JM. How important is the CO_2 chemoreflex for the control of breathing? Environmental and evolutionary considerations. Comp Biochem Physiol A Mol Integr Physiol 2018;215:6–19

38 Mouradian GC, Forster HV, Hodges MR. Acute and chronic effects of carotid body denervation on ventilation and chemoreflexes in three rat strains. J Physiol 2012;590(14):3335–3347

39 Hodges MR, Forster HV, Papanek PE, Dwinell MR, Hogan GE. Ventilatory phenotypes among four strains of adult rats. J Appl Physiol 2002;93(03):974–983

40 Souza GMPR, Kanbar R, Stornetta DS, Abbott SBG, Stornetta RL, Guyenet PG. Breathing regulation and blood gas homeostasis after near complete lesions of the retrotrapezoid nucleus in adult rats. J Physiol 2018;596(13):2521–2545

41 Phillipson EA, Bowes G, Townsend ER, Duffin J, Cooper JD. Role of metabolic CO_2 production in ventilatory response to steady-state exercise. J Clin Invest 1981;68(03):768–774

42 Yamamoto WS, Edwards MW Jr. Homeostasis of carbon dioxide during intravenous infusion of carbon dioxide. J Appl Physiol 1960;15:807–818

43 Sheldon MI, Green JF. Evidence for pulmonary CO2 chemosensitivity: effects on ventilation. J Appl Physiol 1982;52(05): 1192–1197

44 Ponikowski P, Banasiak W. Chemosensitivity in chronic heart failure. Heart Fail Monit 2001;1(04):126–131

45 Schultz HD, Sun SY. Chemoreflex function in heart failure. Heart Fail Rev 2000;5(01):45–56

46 Stickland MK, Miller JD, Smith CA, Dempsey JA. Carotid chemoreceptor modulation of regional blood flow distribution during exercise in health and chronic heart failure. Circ Res 2007;100 (09):1371–1378

47 Schultz HD, Marcus NJ, Del Rio R. Role of the carotid body chemoreflex in the pathophysiology of heart failure: a perspective from animal studies. Adv Exp Med Biol 2015;860:167–185

48 Ding Y, Li YL, Schultz HD. Role of blood flow in carotid body chemoreflex function in heart failure. J Physiol 2011;589(Pt 1):245–258

49 Marcus NJ, Del Rio R, Ding Y, Schultz HD. KLF2 mediates enhanced chemoreflex sensitivity, disordered breathing and autonomic dysregulation in heart failure. J Physiol 2018;596 (15):3171–3185

50 Siński M, Lewandowski J, Przybylski J, et al. Tonic activity of carotid body chemoreceptors contributes to the increased sympathetic drive in essential hypertension. Hypertens Res 2012;35 (05):487–491

51 Tafil-Klawe M, Trzebski A, Klawe J, Pałko T. Augmented chemoreceptor reflex tonic drive in early human hypertension and in normotensive subjects with family background of hypertension. Acta Physiol Pol 1985;36(01):51–58

52 Abdala AP, McBryde FD, Marina N, et al. Hypertension is critically dependent on the carotid body input in the spontaneously hypertensive rat. J Physiol 2012;590(17):4269–4277

53 Pijacka W, Moraes DJ, Ratcliffe LE, et al. Purinergic receptors in the carotid body as a new drug target for controlling hypertension. Nat Med 2016;22(10):1151–1159

54 Brognara F, Felippe ISA, Salgado HC, Paton JFR. Autonomic innervation of the carotid body as a determinant of its sensitivity - implications for cardiovascular physiology and pathology. Cardiovasc Res 2021;117(04):1015–1032

55 Acker H, O'Regan RG. The effects of stimulation of autonomic nerves on carotid body blood flow in the cat. J Physiol 1981; 315:99–110

56 Andreas S, Haarmann H, Klarner S, Hasenfuss G, Raupach T. Increased sympathetic nerve activity in COPD is associated with morbidity and mortality. Lung 2014;192(02):235–241

57 Heindl S, Lehnert M, Criée CP, Hasenfuss G, Andreas S. Marked sympathetic activation in patients with chronic respiratory failure. Am J Respir Crit Care Med 2001;164(04):597–601

58 Stickland MK, Fuhr DP, Edgell H, et al. Chemosensitivity, cardiovascular risk, and the ventilatory response to exercise in COPD. PLoS One 2016;11(06):e0158341

59 Phillips DB, Steinback CD, Collins SÉ, et al. The carotid chemoreceptor contributes to the elevated arterial stiffness and vasoconstrictor outflow in chronic obstructive pulmonary disease. J Physiol 2018;596(15):3233–3244

60 Hansen J, Sander M. Sympathetic neural overactivity in healthy humans after prolonged exposure to hypobaric hypoxia. J Physiol 2003;546(Pt 3):921–929

61 Berssenbrugge A, Dempsey J, Iber C, Skatrud J, Wilson P. Mechanisms of hypoxia-induced periodic breathing during sleep in humans. J Physiol 1983;343:507–524

62 Robinson TD, Freiberg DB, Regnis JA, Young IH. The role of hypoventilation and ventilation-perfusion redistribution in oxygen-induced hypercapnia during acute exacerbations of chronic obstructive pulmonary disease. Am J Respir Crit Care Med 2000;161(05):1524–1529

63 Nakayama K. Surgical removal of the carotid body for bronchial asthma. Dis Chest 1961;40:595–604

64 Abdo WF, Heunks LM. Oxygen-induced hypercapnia in COPD: myths and facts. Crit Care 2012;16(05):323

65 Chen TK, Knicely DH, Grams ME. Chronic kidney disease diagnosis and management: a review. JAMA 2019;322(13):1294–1304

66 Franchitto N, Despas F, Labrunee M, et al. Cardiorenal anemia syndrome in chronic heart failure contributes to increased sympathetic nerve activity. Int J Cardiol 2013;168(03):2352–2357

67 Converse RL Jr, Jacobsen TN, Toto RD, et al. Sympathetic overactivity in patients with chronic renal failure. N Engl J Med 1992; 327(27):1912–1918

68 Masuo K, Mikami H, Ogihara T, Tuck M. Hormonal mechanisms in blood pressure reduction during hemodialysis in patients with chronic renal failure. Hypertens Res 1995;18(Suppl 1):S201–S203

69 Despas F, Detis N, Dumonteil N, et al. Excessive sympathetic activation in heart failure with chronic renal failure: role of chemoreflex activation. J Hypertens 2009;27(09):1849–1854

70 Hering D, Zdrojewski Z, Król E, et al. Tonic chemoreflex activation contributes to the elevated muscle sympathetic nerve activity in patients with chronic renal failure. J Hypertens 2007;25(01): 157–161

71 Ye C, Qiu Y, Zhang F, et al. Chemical stimulation of renal tissue induces sympathetic activation and a pressor response via the paraventricular nucleus in rats. Neurosci Bull 2020;36(02):143–152

72 Semenza GL, Prabhakar NR. Neural regulation of hypoxia-inducible factors and redox state drives the pathogenesis of hypertension in a rodent model of sleep apnea. J Appl Physiol 2015;119 (10):1152–1156

73 Prabhakar NR, Semenza GL. Oxygen sensing and homeostasis. Physiology (Bethesda) 2015;30(05):340–348

74 Peng YJ, Yuan G, Ramakrishnan D, et al. Heterozygous HIF-1alpha deficiency impairs carotid body-mediated systemic responses and reactive oxygen species generation in mice exposed to intermittent hypoxia. J Physiol 2006;577(Pt 2):705–716

75 Niewinski P, Ponikowski P. The story of carotid body resection for HF: how an intriguing pathophysiology concept became a valid target for intervention. Eur Heart J 2017;38(47):3481–3482

76 Narkiewicz K, Ratcliffe LE, Hart EC, et al. Unilateral carotid body resection in resistant hypertension: a safety and feasibility trial. JACC Basic Transl Sci 2016;1(05):313–324

77 Honda Y. Respiratory and circulatory activities in carotid body-resected humans. J Appl Physiol 1992;73(01):1–8

78 Banzett RB, Lansing RW, Binks AP. Air hunger: a primal sensation and a primary element of dyspnea. Compr Physiol 2021;11(02): 1449–1483

79 Moosavi SH, Golestanian E, Binks AP, Lansing RW, Brown R, Banzett RB. Hypoxic and hypercapnic drives to breathe generate equivalent levels of air hunger in humans. J Appl Physiol 2003;94 (01):141–154

80 Simonson TS, Baker TL, Banzett RB, et al. Silent hypoxaemia in COVID-19 patients. J Physiol 2021;599(04):1057–1065

81 Porzionato A, Emmi A, Stocco E, et al. The potential role of the carotid body in COVID-19. Am J Physiol Lung Cell Mol Physiol 2020;319(04):L620–L626

82 Eckert DJ, Malhotra A. Pathophysiology of adult obstructive sleep apnea. Proc Am Thorac Soc 2008;5(02):144–153

83 Dempsey JA, Xie A, Patz DS, Wang D. Physiology in medicine: obstructive sleep apnea pathogenesis and treatment–considerations beyond airway anatomy. J Appl Physiol 2014;116(01):3–12

84 Horner RL. Emerging principles and neural substrates underlying tonic sleep-state-dependent influences on respiratory motor activity. Philos Trans R Soc Lond B Biol Sci 2009;364 (1529):2553–2564

85 Orem J, Lovering AT, Dunin-Barkowski W, Vidruk EH. Tonic activity in the respiratory system in wakefulness, NREM and REM sleep. Sleep 2002;25(05):488–496

86 Nakamura A, Zhang W, Yanagisawa M, Fukuda Y, Kuwaki T. Vigilance state-dependent attenuation of hypercapnic chemoreflex and exaggerated sleep apnea in orexin knockout mice. J Appl Physiol 2007;102(01):241–248

87 Gestreau C, Bévengut M, Dutschmann M. The dual role of the orexin/hypocretin system in modulating wakefulness and respiratory drive. Curr Opin Pulm Med 2008;14(06):512–518

88 Laviolette L, Niérat MC, Hudson AL, Raux M, Allard E, Similowski T. The supplementary motor area exerts a tonic excitatory influence on corticospinal projections to phrenic motoneurons in awake humans. PLoS One 2013;8(04):e62258

89 Williams RH, Jensen LT, Verkhratsky A, Fugger L, Burdakov D. Control of hypothalamic orexin neurons by acid and CO_2. Proc Natl Acad Sci U S A 2007;104(25):10685–10690

90 Benarroch EE. Control of the cardiovascular and respiratory systems during sleep. Auton Neurosci 2019;218:54–63

91 Simon PM, Dempsey JA, Landry DM, Skatrud JB. Effect of sleep on respiratory muscle activity during mechanical ventilation. Am Rev Respir Dis 1993;147(01):32–37

92 Orem J, Montplaisir J, Dement WC. Changes in the activity of respiratory neurons during sleep. Brain Res 1974;82(02): 309–315

93 Henke KG, Arias A, Skatrud JB, Dempsey JA. Inhibition of inspiratory muscle activity during sleep. Chemical and nonchemical influences. Am Rev Respir Dis 1988;138(01):8–15

94 Dubois M, Chenivesse C, Raux M, et al. Neurophysiological evidence for a cortical contribution to the wakefulness-related drive to breathe explaining hypocapnia-resistant ventilation in humans. J Neurosci 2016;36(41):10673–10682

95 Henke KG, Badr MS, Skatrud JB, Dempsey JA. Load compensation and respiratory muscle function during sleep. J Appl Physiol 1992;72(04):1221–1234

96 Nakayama H, Smith CA, Rodman JR, Skatrud JB, Dempsey JA. Carotid body denervation eliminates apnea in response to transient hypocapnia. J Appl Physiol 2003;94(01):155–164

97 Chow CM, Xi L, Smith CA, Saupe KW, Dempsey JA. A volume-dependent apneic threshold during NREM sleep in the dog. J Appl Physiol 1994;76(06):2315–2325

98 Smith CA, Chenuel BJ, Henderson KS, Dempsey JA. The apneic threshold during non-REM sleep in dogs: sensitivity of carotid body vs. central chemoreceptors. J Appl Physiol 2007;103(02): 578–586

99 Leevers AM, Simon PM, Xi L, Dempsey JA. Apnoea following normocapnic mechanical ventilation in awake mammals: a demonstration of control system inertia. J Physiol 1993; 472:749–768

100 Xi L, Smith CA, Saupe KW, Henderson KS, Dempsey JA. Effects of rapid-eye-movement sleep on the apneic threshold in dogs. J Appl Physiol 1993;75(03):1129–1139

101 Khoo MC. Determinants of ventilatory instability and variability. Respir Physiol 2000;122(2-3):167–182

102 Dempsey JA, Smith CA. Update on chemoreception: influence on cardiorespiratory regulation and pathophysiology. Clin Chest Med 2019;40(02):269–283

103 Dempsey JA. Central sleep apnea: misunderstood and mistreated! F1000Res. 2019;8. Doi: 10.12688/f1000research.18358.1

104 Bordier P, Lataste A, Hofmann P, Robert F, Bourenane G. Nocturnal oxygen therapy in patients with chronic heart failure and sleep apnea: a systematic review. Sleep Med 2016;17:149–157

105 Marcus NJ, Del Rio R, Schultz EP, Xia XH, Schultz HD. Carotid body denervation improves autonomic and cardiac function and attenuates disordered breathing in congestive heart failure. J Physiol 2014;592(02):391–408

106 Del Rio R, Marcus NJ, Schultz HD. Inhibition of hydrogen sulfide restores normal breathing stability and improves autonomic control during experimental heart failure. J Appl Physiol 2013; 114(09):1141–1150

107 Javaheri S. Acetazolamide improves central sleep apnea in heart failure: a double-blind, prospective study. Am J Respir Crit Care Med 2006;173(02):234–237

108 Khayat RN, Xie A, Patel AK, Kaminski A, Skatrud JB. Cardiorespiratory effects of added dead space in patients with heart failure and central sleep apnea. Chest 2003;123(05):1551–1560

109 Xie A, Teodorescu M, Pegelow DF, et al. Effects of stabilizing or increasing respiratory motor outputs on obstructive sleep apnea. J Appl Physiol 2013;115(01):22–33

110 Remmers JE, deGroot WJ, Sauerland EK, Anch AM. Pathogenesis of upper airway occlusion during sleep. J Appl Physiol 1978;44 (06):931–938

111 Dempsey JA, Veasey SC, Morgan BJ, O'Donnell CP. Pathophysiology of sleep apnea. Physiol Rev 2010;90(01):47–112

112 Onal E, Leech JA, Lopata M. Dynamics of respiratory drive and pressure during NREM sleep in patients with occlusive apneas. J Appl Physiol 1985;58(06):1971–1974

113 Badr MS, Toiber F, Skatrud JB, Dempsey J. Pharyngeal narrowing/occlusion during central sleep apnea. J Appl Physiol 1995;78(05):1806–1815

114 Warner G, Skatrud JB, Dempsey JA. Effect of hypoxia-induced periodic breathing on upper airway obstruction during sleep. J Appl Physiol 1987;62(06):2201–2211

115 Wellman A, Malhotra A, Jordan AS, Stevenson KE, Gautam S, White DP. Effect of oxygen in obstructive sleep apnea: role of loop gain. Respir Physiol Neurobiol 2008;162(02):144–151

116 Edwards BA, Sands SA, Eckert DJ, et al. Acetazolamide improves loop gain but not the other physiological traits causing obstructive sleep apnoea. J Physiol 2012;590(05):1199–1211

117 Gell LK, Vena D, Alex RM, et al. Neural ventilatory drive decline as a predominant mechanism of obstructive sleep apnoea events. Thorax 2022;77(07):707–716

118 Dempsey JA, La Gerche A, Hull JH. Is the healthy respiratory system built just right, overbuilt, or underbuilt to meet the demands imposed by exercise? J Appl Physiol 2020;129(06): 1235–1256

119 Forster HV, Haouzi P, Dempsey JA. Control of breathing during exercise. Compr Physiol 2012;2(01):743–777

120 Haldane JS, Priestley JG. The regulation of the lung-ventilation. J Physiol 1905;32(3-4):225–266

121 Aliverti A, Cala SJ, Duranti R, et al. Human respiratory muscle actions and control during exercise. J Appl Physiol 1997;83(04): 1256–1269

122 Grimby G, Goldman M, Mead J. Respiratory muscle action inferred from rib cage and abdominal V-P partitioning. J Appl Physiol 1976;41(5, Pt. 1):739–751

123 Kaufman MP, Forster HV. Reflexes controlling circulatory, ventilatory and airway responses to exercise. In: Rowell LB, Shepherd JT, eds. Handbook of Physiology. New York: Oxford University Press; 381–447

124 Oren A, Wasserman K, Davis JA, Whipp BJ. Effect of CO2 set point on ventilatory response to exercise. J Appl Physiol 1981;51(01): 185–189

125 Dempsey JA, Vidruk EH, Mitchell GS. Pulmonary control systems in exercise: update. Fed Proc 1985;44(07):2260–2270

126 Shea SA, Andres LP, Shannon DC, Banzett RB. Ventilatory responses to exercise in humans lacking ventilatory chemosensitivity. J Physiol 1993;468:623–640

127 Wasserman K, Whipp BJ, Koyal SN, Cleary MG. Effect of carotid body resection on ventilatory and acid-base control during exercise. J Appl Physiol 1975;39(03):354–358

128 Forster HV, Pan LG, Bisgard GE, Kaminski RP, Dorsey SM, Busch MA. Hyperpnea of exercise at various PIO_2 in normal and carotid body-denervated ponies. J Appl Physiol 1983;54(05):1387–1393

129 Goodwin GM, McCloskey DI, Mitchell JH. Cardiovascular and respiratory responses to changes in central command during isometric exercise at constant muscle tension. J Physiol 1972; 226(01):173–190

130 Krogh A, Lindhard J. The regulation of respiration and circulation during the initial stages of muscular work. J Physiol 1913;47(1-2):112–136

131 Eldridge FL, Millhorn DE, Waldrop TG. Exercise hyperpnea and locomotion: parallel activation from the hypothalamus. Science 1981;211(4484):844–846

132 Eldridge FL, Millhorn DE, Kiley JP, Waldrop TG. Stimulation by central command of locomotion, respiration and circulation during exercise. Respir Physiol 1985;59(03):313–337

133 Thornton JM, Guz A, Murphy K, et al. Identification of higher brain centres that may encode the cardiorespiratory response to exercise in humans. J Physiol 2001;533(Pt 3):823–836

134 Williamson JW, McColl R, Mathews D, Mitchell JH, Raven PB, Morgan WP. Brain activation by central command during actual and imagined handgrip under hypnosis. J Appl Physiol 2002;92 (03):1317–1324

135 Morgan W, Raven P, Drinkwater B, Horvath S. Perceptual and metabolic responsivity to standard bicycle ergometry following various hypnotic suggestions. Clin Exp Hypn 1973;21:86–101

136 An X, Bandler R, Ongür D, Price JL. Prefrontal cortical projections to longitudinal columns in the midbrain periaqueductal gray in macaque monkeys. J Comp Neurol 1998;401(04):455–479

137 Paterson DJ. Defining the neurocircuitry of exercise hyperpnoea. J Physiol 2014;592(03):433–444

138 Bandler R, Carrive P. Integrated defence reaction elicited by excitatory amino acid microinjection in the midbrain periaqueductal grey region of the unrestrained cat. Brain Res 1988;439(1-2):95–106

139 Basnayake SD, Hyam JA, Pereira EA, et al. Identifying cardiovascular neurocircuitry involved in the exercise pressor reflex in humans using functional neurosurgery. J Appl Physiol 2011;110 (04):881–891

140 Casaburi R, Whipp BJ, Wasserman K, Beaver WL, Koyal SN. Ventilatory and gas exchange dynamics in response to sinusoidal work. J Appl Physiol 1977;42(02):300–301

141 Tibes U. Reflex inputs to the cardiovascular and respiratory centers from dynamically working canine muscles. Some evidence for involvement of group III or IV nerve fibers. Circ Res 1977;41(03):332–341

142 Kao F. An experimental study of the pathway involved in exercise hyperpnea employing cross-circulation techniques. In: Cunningham DJC, Lloyd BB, eds. Regulation of Human Respiration. Oxford: Blackwell; 1963

143 Coote JH, Hilton SM, Perez-Gonzalez JF. The reflex nature of the pressor response to muscular exercise. J Physiol 1971;215(03): 789–804

144 McCloskey DI, Mitchell JH. Reflex cardiovascular and respiratory responses originating in exercising muscle. J Physiol 1972;224 (01):173–186

145 Amann M, Blain GM, Proctor LT, Sebranek JJ, Pegelow DF, Dempsey JA. Group III and IV muscle afferents contribute to ventilatory and cardiovascular response to rhythmic exercise in humans. J Appl Physiol 2010;109(04):966–976

146 Haouzi P. Tracking pulmonary gas exchange by breathing control during exercise: role of muscle blood flow. J Physiol 2014;592 (03):453–461

147 Haouzi P, Hill JM, Lewis BK, Kaufman MP. Responses of group III and IV muscle afferents to distension of the peripheral vascular bed. J Appl Physiol 1999;87(02):545–553

148 Band DM, Wolff CB, Ward J, Cochrane GM, Prior J. Respiratory oscillations in arterial carbon dioxide tension as a control signal in exercise. Nature 1980;283(5742):84–85

149 Murphy K, Stidwill RP, Cross BA, et al. Is hypercapnia necessary for the ventilatory response to exercise in man? Clin Sci (Lond) 1987;73(06):617–625

150 Dempsey J, Neder A, Phillips D, O'Donnell D. The physiology and pathophysiology of exercise hyperpnea. In: Chen R, Guyenet P, eds. Respiratory Neurology: Physiology and Clinical Disorders, Part I. Amsterdam: Elsevier; 2022

151 Asmussen E, Johansen SH, Jorgensen M, Nielsen M. On the nervous factors controlling respiration and circulation during exercise. Experiments with curarization. Acta Physiol Scand 1965;63:343–350

152 Amann M, Proctor LT, Sebranek JJ, Eldridge MW, Pegelow DF, Dempsey JA. Somatosensory feedback from the limbs exerts inhibitory influences on central neural drive during whole body endurance exercise. J Appl Physiol 2008;105(06):1714–1724

153 Vogiatzis I, Aliverti A, Golemati S, et al. Respiratory kinematics by optoelectronic plethysmography during exercise in men and women. Eur J Appl Physiol 2005;93(5-6):581–587

154 Aaron EA, Seow KC, Johnson BD, Dempsey JA. Oxygen cost of exercise hyperpnea: implications for performance. J Appl Physiol 1992;72(05):1818–1825

155 Johnson BD, Babcock MA, Suman OE, Dempsey JA. Exercise-induced diaphragmatic fatigue in healthy humans. J Physiol 1993;460:385–405

156 Mador MJ, Magalang UJ, Rodis A, Kufel TJ. Diaphragmatic fatigue after exercise in healthy human subjects. Am Rev Respir Dis 1993;148(6, Pt 1):1571–1575

157 Sheel AW, Boushel R, Dempsey JA. Competition for blood flow distribution between respiratory and locomotor muscles: implications for muscle fatigue. J Appl Physiol 2018;125(03):820–831

158 Johnson BD, Badr MS, Dempsey JA. Impact of the aging pulmonary system on the response to exercise. Clin Chest Med 1994;15 (02):229–246

159 Reeves J, Dempsey J, Grover R. Pulmonary circulation during exercise. In: Weir E, Reeves J, eds. Pulmonary Vascular Physiology and Pathophysiology. New York: Marcel Dekker; 1989:107–133

160 Pelkonen M, Notkola IL, Lakka T, Tukiainen HO, Kivinen P, Nissinen A. Delaying decline in pulmonary function with physical activity: a 25-year follow-up. Am J Respir Crit Care Med 2003; 168(04):494–499

161 McClaran SR, Babcock MA, Pegelow DF, Reddan WG, Dempsey JA. Longitudinal effects of aging on lung function at rest and exercise in healthy active fit elderly adults. J Appl Physiol 1995;78(05): 1957–1968

162 Garcia-Aymerich J, Lange P, Benet M, Schnohr P, Antó JM. Regular physical activity modifies smoking-related lung function decline and reduces risk of chronic obstructive pulmonary disease: a population-based cohort study. Am J Respir Crit Care Med 2007; 175(05):458–463

163 O'Donnell DE, Revill SM, Webb KA. Dynamic hyperinflation and exercise intolerance in chronic obstructive pulmonary disease. Am J Respir Crit Care Med 2001;164(05):770–777

164 Neder JA, Phillips DB, O'Donnell DE, Dempsey JA. Excess ventilation and exertional dyspnoea in heart failure and pulmonary hypertension. Eur Respir J 2022;60(05):x

165 Gagnon P, Bussières JS, Ribeiro F, et al. Influences of spinal anesthesia on exercise tolerance in patients with chronic obstructive pulmonary disease. Am J Respir Crit Care Med 2012; 186(07):606–615

166 Amann M, Regan MS, Kobitary M, et al. Impact of pulmonary system limitations on locomotor muscle fatigue in patients with COPD. Am J Physiol Regul Integr Comp Physiol 2010;299(01): R314–R324

167 Dominelli PB, Archiza B, Ramsook AH, et al. Effects of respiratory muscle work on respiratory and locomotor blood flow during exercise. Exp Physiol 2017;102(11):1535–1547

168 Harms CA, Babcock MA, McClaran SR, et al. Respiratory muscle work compromises leg blood flow during maximal exercise. J Appl Physiol 1997;82(05):1573–1583

169 Langer D, Ciavaglia C, Faisal A, et al. Inspiratory muscle training reduces diaphragm activation and dyspnea during exercise in COPD. J Appl Physiol 2018;125(02):381–392

170 Dempsey JA, Blain GM, Amann M. Are type III-IV muscle afferents required for a normal steady-state exercise hyperpnoea in humans? J Physiol 2014;592(03):463–474

171 Maltais F, Simard AA, Simard C, Jobin J, Desgagnés P, LeBlanc P. Oxidative capacity of the skeletal muscle and lactic acid kinetics during exercise in normal subjects and in patients with COPD. Am J Respir Crit Care Med 1996;153(01):288–293

172 Ribeiro F, Thériault ME, Debigaré R, Maltais F. Should all patients with COPD be exercise trained? J Appl Physiol 2013;114(09): 1300–1308

173 Johnson RL Jr. Gas exchange efficiency in congestive heart failure. Circulation 2000;101(24):2774–2776

174 Woods PR, Olson TP, Frantz RP, Johnson BD. Causes of breathing inefficiency during exercise in heart failure. J Card Fail 2010;16 (10):835–842

175 Olson TP, Joyner MJ, Eisenach JH, Curry TB, Johnson BD. Influence of locomotor muscle afferent inhibition on the ventilatory response to exercise in heart failure. Exp Physiol 2014;99(02): 414–426

176 Mitchell GS, Johnson SM. Neuroplasticity in respiratory motor control. J Appl Physiol 2003;94(01):358–374

177 Feldman JL, Mitchell GS, Nattie EE. Breathing: rhythmicity, plasticity, chemosensitivity. Annu Rev Neurosci 2003; 26:239–266

178 Martin PA, Mitchell GS. Long-term modulation of the exercise ventilatory response in goats. J Physiol 1993;470:601–617

179 Wood HE, Fatemian M, Robbins PA. A learned component of the ventilatory response to exercise in man. J Physiol 2003;553(Pt 3):967–974

180 Somjen G. The missing error signal-regulation beyond negative chemofeedback. News Physiol Sci 1992;7:184–185

181 Poon CS, Tin C, Yu Y. Homeostasis of exercise hyperpnea and optimal sensorimotor integration: the internal model paradigm. Respir Physiol Neurobiol 2007;159(01):1–13, discussion 14–20

182 Mitchell GS, Babb TG. Layers of exercise hyperpnea: modulation and plasticity. Respir Physiol Neurobiol 2006;151(2-3):251–266

183 Cathcart AJ, Herrold N, Turner AP, Wilson J, Ward SA. Absence of long-term modulation of ventilation by dead-space loading during moderate exercise in humans. Eur J Appl Physiol 2005; 93(04):411–420

184 Moosavi SH, Guz A, Adams L. Repeated exercise paired with "imperceptible" dead space loading does not alter VE of subsequent exercise in humans. J Appl Physiol 2002;92(03): 1159–1168

185 Basting TM, Abe C, Viar KE, Stornetta RL, Guyenet PG. Is plasticity within the retrotrapezoid nucleus responsible for the recovery of the PCO2 set-point after carotid body denervation in rats? J Physiol 2016;594(12):3371–3390

186 Millhorn DE, Eldridge FL, Waldrop TG. Prolonged stimulation of respiration by a new central neural mechanism. Respir Physiol 1980;41(01):87–103

187 Smith CA, Bisgard GE, Nielsen AM, et al. Carotid bodies are required for ventilatory acclimatization to chronic hypoxia. J Appl Physiol 1986;60(03):1003–1010

188 Busch MA, Bisgard GE, Forster HV. Ventilatory acclimatization to hypoxia is not dependent on arterial hypoxemia. J Appl Physiol 1985;58(06):1874–1880

189 Nielsen AM, Bisgard GE, Vidruk EH. Carotid chemoreceptor activity during acute and sustained hypoxia in goats. J Appl Physiol 1988;65(04):1796–1802

190 Wang ZY, Olson EB Jr, Bjorling DE, Mitchell GS, Bisgard GE. Sustained hypoxia-induced proliferation of carotid body type I cells in rats. J Appl Physiol 2008;104(03):803–808

191 Powell FL. The influence of chronic hypoxia upon chemoreception. Respir Physiol Neurobiol 2007;157(01):154–161

192 Moya EA, Go A, Kim CB, Fu Z, Simonson TS, Powell FL. Neuronal HIF-1α in the nucleus tractus solitarius contributes to ventilatory acclimatization to hypoxia. J Physiol 2020;598(10): 2021–2034

193 Dwinell MR, Powell FL. Chronic hypoxia enhances the phrenic nerve response to arterial chemoreceptor stimulation in anesthetized rats. J Appl Physiol 1999;87(02):817–823

194 Mulkey DK, Stornetta RL, Weston MC, et al. Respiratory control by ventral surface chemoreceptor neurons in rats. Nat Neurosci 2004;7(12):1360–1369

195 Hayashi F, Coles SK, Bach KB, Mitchell GS, McCrimmon DR. Time-dependent phrenic nerve responses to carotid afferent activation: intact vs. decerebellate rats. Am J Physiol 1993;265(4, Pt 2): R811–R819

196 Fuller DD, Zabka AG, Baker TL, Mitchell GS. Phrenic long-term facilitation requires 5-HT receptor activation during but not following episodic hypoxia. J Appl Physiol 2001;90(05):2001–2006, discussion 2000

197 Baker-Herman TL, Fuller DD, Bavis RW, et al. BDNF is necessary and sufficient for spinal respiratory plasticity following intermittent hypoxia. Nat Neurosci 2004;7(01):48–55

198 Baker-Herman TL, Mitchell GS. Phrenic long-term facilitation requires spinal serotonin receptor activation and protein synthesis. J Neurosci 2002;22(14):6239–6246

199 Devinney MJ, Fields DP, Huxtable AG, Peterson TJ, Dale EA, Mitchell GS. Phrenic long-term facilitation requires PKCθ activity within phrenic motor neurons. J Neurosci 2015;35(21):8107–8117

200 Ling L. Serotonin and NMDA receptors in respiratory long-term facilitation. Respir Physiol Neurobiol 2008;164(1-2):233–241

201 Vose AK, Welch JF, Nair J, et al. Therapeutic acute intermittent hypoxia: a translational roadmap for spinal cord injury and neuromuscular disease. Exp Neurol 2022;347:113891

202 Navarrete-Opazo A, Mitchell GS. Therapeutic potential of intermittent hypoxia: a matter of dose. Am J Physiol Regul Integr Comp Physiol 2014;307(10):R1181–R1197

203 Sutor T, Cavka K, Vose AK, et al. Single-session effects of acute intermittent hypoxia on breathing function after human spinal cord injury. Exp Neurol 2021;342:113735

204 Trumbower RD, Jayaraman A, Mitchell GS, Rymer WZ. Exposure to acute intermittent hypoxia augments somatic motor function in humans with incomplete spinal cord injury. Neurorehabil Neural Repair 2012;26(02):163–172

205 Welch JF, Perim RR, Argento PJ, et al. Effect of acute intermittent hypoxia on cortico-diaphragmatic conduction in healthy humans. Exp Neurol 2021;339:113651

206 Finn HT, Bogdanovski O, Hudson AL, et al. The effect of acute intermittent hypoxia on human limb motoneurone output. Exp Physiol 2022;107(06):615–630

207 Radia S, Vallence AM, Fujiyama H, et al. Effects of acute intermittent hypoxia on corticospinal excitability within the primary motor cortex. Eur J Appl Physiol 2022;122(09):2111–2123

208 Christiansen L, Urbin MA, Mitchell GS, Perez MA. Acute intermittent hypoxia enhances corticospinal synaptic plasticity in humans. eLife 2018;7:7

209 Welch JF, Nair J, Argento PJ, Mitchell GS, Fox EJ. Acute intermittent hypercapnic-hypoxia elicits central neural respiratory motor plasticity in humans. J Physiol 2022;600(10):2515–2533

210 Xie A, Skatrud JB, Barczi SR, et al. Influence of cerebral blood flow on breathing stability. J Appl Physiol 2009;106(03):850–856

211 Deacon-Diaz NL, Sands SA, McEvoy RD, Catcheside PG. Daytime loop gain is elevated in obstructive sleep apnea but not reduced by CPAP treatment. J Appl Physiol 2018;125(05):1490–1497

212 Devinney MJ, Huxtable AG, Nichols NL, Mitchell GS. Hypoxia-induced phrenic long-term facilitation: emergent properties. Ann N Y Acad Sci 2013;1279:143–153

Article published online: 2023-08-04

Heart–Lung Interactions

Natsumi Hamahata, MD[1] Michael R. Pinsky, MD, CM, Dr hc[1]

[1] Department of Critical Care Medicine, University of Pittsburgh, Pittsburgh, Pennsylvania

Address for correspondence Michael R. Pinsky, MD, Department of Critical Care Medicine, University of Pittsburgh, 638 Scaife Hall, 3550 Terrace Street, Pittsburgh, PA 15261 (e-mail: pinsky@pitt.edu).

Semin Respir Crit Care Med 2023;44:650–660.

Abstract

The pulmonary and cardiovascular systems have profound effects on each other. Overall cardiac function is determined by heart rate, preload, contractility, and afterload. Changes in lung volume, intrathoracic pressure (ITP), and hypoxemia can simultaneously change all of these four hemodynamic determinants for both ventricles and can even lead to cardiovascular collapse. Intubation using sedation depresses vasomotor tone. Also, the interdependence between right and left ventricles can be affected by lung volume-induced changes in pulmonary vascular resistance and the rise in ITP. An increase in venous return due to negative ITP during spontaneous inspiration can shift the septum to the left and cause a decrease in left ventricle compliance. During positive pressure ventilation, the increase in ITP causes a decrease in venous return (preload), minimizing ventricular interdependence and will decrease left ventricle afterload augmenting cardiac output. Thus, positive pressure ventilation is beneficial in acute heart failure patients and detrimental in hypovolemic patients where it can cause a significant decrease in venous return and cardiac output. Recently, this phenomenon has been used to assess patient's volume responsiveness to fluid by measuring pulse pressure variation and stroke volume variation. Heart–lung interaction is very dynamic and changes in lung volume, ITP, and oxygen level can have various effects on the cardiovascular system depending on preexisting cardiovascular function and volume status. Heart failure and either hypo or hypervolemia predispose to greater effects of ventilation of cardiovascular function and gas exchange. This review is an overview of the basics of heart–lung interaction.

Keywords
- heart–lung interactions
- ventricular interdependence
- right ventricular afterload
- pulmonary vascular resistance
- mechanical ventilation
- positive pressure ventilation
- hemodynamic monitoring

The significance of heart–lung interactions was described in antiquity as pulse paradoxus in patients with tuberculous pericardial effusions.[1] The impact of cardiovascular disease on gas exchange and lung disease on blood flow has been widely studied since the early 20th century.[2] Several fundamental concepts about heart–lung interactions are important in the care of the critically ill patients. First of all, spontaneous breathing can be considered a form of exercise.[3] Spontaneous breathing uses skeletal muscle to generate tension, is usually voluntary in frequency and tidal volume, consumes oxygen, and produces carbon dioxide relative to the work of breathing, and if cardiovascular reserve is inadequate to meet this metabolic demand, then the individual is unable to have unassisted breathing without going into circulatory shock. Ventilation normally requires less than 5% of the total oxygen delivery; however, if a patient is in respiratory distress, regardless of the etiology, spontaneous breathing with accessory muscles can take up 30% of the total oxygen delivery and cause ischemia to the vital organs[4–6] A spontaneous breathing trial in mechanically ventilated patients is a stress test for the heart, and providers have to be cautious removing positive pressure from patients with decompensated heart failure or myocardial ischemia.[3,7–9] On the contrary, positive pressure ventilation can impact the cardiovascular system negatively by decreasing venous return, especially in hypovolemic patients. Recently, several studies looked into the risk factors associated with hemodynamic collapse in the peri-intubation period, and

article published online
August 4, 2023

Issue Theme Pulmonary Physiology; Guest Editors: David A. Kaminsky, MD, Kathryn A. Hibbert, MD, and Andrew M. Luks, MD

Thieme Medical Publishers, Inc.,
333 Seventh Avenue, 18th Floor,
New York, NY 10001, USA

DOI https://doi.org/10.1055/s-0043-1770062.
ISSN 1069-3424.

positive pressure ventilation during preoxygenation (either with bag valve mask or noninvasive positive pressure ventilation) may be one of the risk factors for cardiopulmonary collapse during intubation.[10] Respiratory function and cardiovascular function are affected by each other very closely. For example, during spontaneous breathing, the venous return will increase and provide more pulmonary blood flow during inspiration improving ventilation and perfusion (V/Q) matching and gas exchange. On the contrary, positive pressure ventilation will decrease venous return and cardiac output negatively and decrease the pulmonary blood flow during inspiration, worsening V/Q mismatch. This is the reason why the A-a gradient during positive pressure ventilation is not equivalent to that of spontaneous breathing patients for the same level of lung pathology. To the extent possible without excessive ventilatory effort, intrathoracic pressure (ITP), or lung volume swings, we should maintain spontaneous breathing as much as possible.

Respiratory failure and applying positive pressure ventilation, by changing both lung volume and ITP, can affect the four determinants of cardiac function in both ventricles, which are heart rate, preload, contractility, and afterload. We will examine each of these contributing factors in detail. Similarly, pharmacological sedation during endotracheal intubation, by decreasing sympathetic tone, may worsen the decrease in venous return and blunt increased vasomotor tone, promoting cardiovascular collapse during the peri-intubation period.

Hemodynamic Effect of Change in Lung Volume

Autonomic Tone

Respiratory sinus arrhythmia (RSA) describes the changes in the heart rate associated with changing lung volume.[11] Inspiration cyclically causes vagal withdrawal causing cardiac acceleration, which slows during expiration. Since the R–R interval on EKG shortens during normal tidal volume inspiration and prolongs during expiration, RSA can be quantified by Fourier analysis of the R–R interval changes over time.[12] The physiologic role of RSA is unknown, but it may be a reaction to improve the V/Q matching by increasing blood flow to pulmonary capillaries during spontaneous inspiration through increasing the heart rate and cardiac output.[13]

However, when the lungs are hyperinflated with high tidal volumes, a lung inflation-vasodilation reflex occurs and causes blood pressure to drop. This reflex is owing to combined increased vagal tone and decreased sympathetic tone, mediated through intrapulmonary afferent vagal fibers.[14,15]

Hormonal Effects

There are several humoral effects that are triggered by lung distension. Positive pressure ventilation can induce the production of prostaglandin from the endothelial cells causing peripheral bronchodilation.[16–18] In obstructive sleep apnea patients, the application of continuous positive airway pressure (CPAP) significantly decreases the expression of endothelial cyclooxygenase level and increased nitric oxide level.[19] However, this humoral interaction does not seem to have a notable effect on the cardiovascular status.[20] Ventilation may also alter the intravascular fluid balance by affecting the natriuretic hormone level.[21,22] The sensor for effective circulating blood-volume exists in the right atrium, and right-atrial stretch, such as in heart failure, will trigger the elevation of circulating natriuretic peptides and promote sodium and water excretion from the kidneys. During positive pressure ventilation, decreased right atrial filling minimizes right-atrial stretch suppressing atrial natriuretic peptide release,[21] whereas norepinephrine and renin levels increase,[23] promoting fluid retention. This effect is especially seen in patients with heart failure and sleep-disordered breathing.[24]

Volume-Dependent Change in Pulmonary Vascular Resistance

During lung inflation, increasing transpulmonary pressure (Ptp), defined as the difference between airway pressure and pleural pressure (here called ITP), increases as a function of lung compliance. The increased Ptp causes mechanical compression of the alveolar vessels if the increase in Ptp exceeds pulmonary venous pressure. The resultant reduction in pulmonary capillary cross-sectional area results in increased pulmonary vascular resistance. Airway pressure during positive pressure breathing (i.e., plateau pressure) represents the input pressure distending the lungs and chest wall. The actual increase in lung volume will be a function of Ptp. For the same airway pressure, increased chest wall stiffness, as occurs with intra-abdominal hypertension, or decreased lung compliance, as occurs with acute lung injury, will result in a proportionally higher increase in airway pressure than lung volume. Thus, high airway pressures during positive-pressure breathing do not always equal lung overdistention or injurious breathing patterns. For example, in both obese patients and patients with pleural effusion, part of the airway pressure is dissipated to move the chest wall. However, for the same increase in lung volume, Ptp always increases by the same amount. Thus, Ptp is the important pressure that correlates with lung volume, pulmonary vascular resistance, and ventilator-induced lung injury.[25]

On the contrary, lung disease associated with decreased surfactant and increased interstitial lung water induces alveolar collapse which can increase pulmonary vascular resistance by the process of hypoxic pulmonary vasoconstriction (HPV). Lung recruitment maneuvers and positive end-expiratory airway pressure therapies, if associated with alveolar recruitment and increased alveolar oxygenation, should decrease pulmonary vascular resistance by reversing HPV (infra vide).[26,27]

Mechanical Compression of the Heart in the Fossa

The heart is in a pericardial chamber enclosed within a larger thoracic chamber. Pericardial volume restraint minimizes right ventricular (RV) over-distention during forced inspiratory efforts but also exaggerates ventricular interdependence. However, with lung over-expansion the heart can be compressed in the cardiac fossa, limiting biventricular cardiac filling in a fashion analogous to pericardial tamponade, when both pericardial and juxtacardiac intrathoracic pressure are equally increased. The compressive effect may be mainly on atrial compression, especially the right atrium[28] but the ventricular compression can cause biventricular dysfunction and mimic the pathophysiology of cardiac tamponade.[29] Importantly, fluid resuscitation alone during these conditions is often ineffective in restoring cardiovascular sufficiency.

Summary of How Lung Volume Affects Hemodynamics

- During normal tidal volume ventilation, RSA causes shortening of R-R interval during inspiration, which may increase cardiac output and improve the V/Q matching. In contrast, hyperinflation will cause blood pressure drop due to a hyperinflation-vasodilation reflex mediated by afferent vagal tone.
- Positive pressure ventilation can decrease the production of natriuretic hormone by preventing the right-atrial stretch promoting fluid retention.
- Lung volume change will impact the alveolar vessel resistance by the direct effect of alveolar pressure and extra-alveolar vessel resistance by increasing Ptp. The net effect on overall pulmonary vascular resistance has a biphasic change from residual volume to total lung capacity and is minimum at functional residual capacity.
- During hyperinflation, the heart is compressed in the cardiac fossa and can mimic tamponade physiology under significant hyperinflation.

Hemodynamic Effect of Elevated Pulmonary Vascular Resistance and Right Ventricular Afterload

Hypoxic vasoconstriction and volume-dependent change in pulmonary vascular resistance are the two main reversible mechanisms that cause elevated pulmonary vascular resistance and can increase RV afterload.

Hypoxic Pulmonary Vasoconstriction

From animal studies, pulmonary vasculature constricts when alveolar PO_2 (P_AO_2) decreases below 60 mm Hg[30] and reduces pulmonary blood flow to hypoxic regions of the lung, which will minimize shunt blood flow. The endothelium-derived vasoconstrictors/vasodilators (endothelin, thromboxane/nitric oxide, and prostacyclin) can modulate the HPV, but the core mechanism is due to the calcium influx to the pulmonary smooth muscle cells.[31]

HPV is normally seen in focal atelectasis or pneumonia where the alveolar hypoxia is localized to a lung segment and the pulmonary vascular tree surrounding these focal areas will vasoconstrict.[32] In most cases, the shift of the blood from these hypoxic lung regions to better-oxygenated regions of the lung will not cause elevation of the pulmonary arterial pressure.[33] However, when the hypoxic lung region is diffuse, such as in severe acute respiratory distress syndrome (ARDS), the degree of HPV is not negligible and also becomes generalized. This can cause elevation of the pulmonary artery pressure and can even impede RV ejection.[31,34]

Volume-Dependent Changes in Pulmonary Vascular Resistance

There are two distinct vascular domains in the pulmonary vascular system dependent upon their extravascular pressures: alveolar vessels and extra-alveolar vessels. Alveolar vessels are those vessels that sense alveolar pressure as their surrounding pressure and they include very small pulmonary arterioles, alveolar vessels, and venules surrounding the alveoli.[35] Extra-alveolar vessels are all the larger arteries and veins in the interstitial space and are sensitive to intrapleural pressure.[36] Increases in lung volume and maintaining lung inflation are associated with the change in Ptp and not the alveolar pressure itself. Ptp is defined as alveolar pressure minus pleural pressure or ITP. There are situations where the alveolar pressure is extremely elevated but the lung volume is unchanged, such as during a Valsalva maneuver, wherein airway pressure as high as 150 cm H_2O may occur during strain but this is matched by an equally high pleural pressure.[25] When Ptp exceeds pulmonary venous pressure, the alveolar vessels spontaneously collapse, and by decreasing their cross-sectional area, alveolar vascular resistance increases. On the contrary, the extra-alveolar vessels sense only intrapleural pressure as their surrounding pressure. During spontaneous breathing, negative pressure to increase the lung volume which will dilate both the extra-alveolar vessels and the airways and lower both extra-alveolar resistance and airway resistance.[37] In most forms of acute lung disease, end-expiratory lung volumes are decreased, which promotes alveolar collapse. Such alveolar collapse causes hypoxia and increases pulmonary vasomotor tone by HPV. The net effect on overall pulmonary vascular resistance of increasing lung volume from residual volume to total lung capacity is biphasic and the total resistance reaches its minimum level at about functional residual capacity (►**Fig. 1**).

Positive end-expiratory pressure (PEEP) only increases end-expiratory lung volume. When coupled with positive-pressure breathing, it can recruit collapsed alveolar units such that the positive-pressure breath will be on a lung with increased lung compliance and alveolar ventilation. This will be manifest by an increase in PaO_2 and a decrease in dead space ventilation, simultaneously decreasing pulmonary vascular resistance, by reversing HPV. Overdistention, with excessive PEEP, will only add to dead space ventilation and increase pulmonary vascular resistance.[38]

How Pulmonary Vascular Resistance Affects Right Ventricular Afterload

RV afterload is similar to that of the left ventricular (LV) afterload and determined by the wall tension of the RV. When pulmonary vascular resistance increases due to either increased pulmonary vasomotor tone or increased proportions of the vasculature in West zones 1 and 2, pulmonary artery pressure will also increase, increasing RV afterload.[39] Recent prospective physiologic study of postcardiac surgery

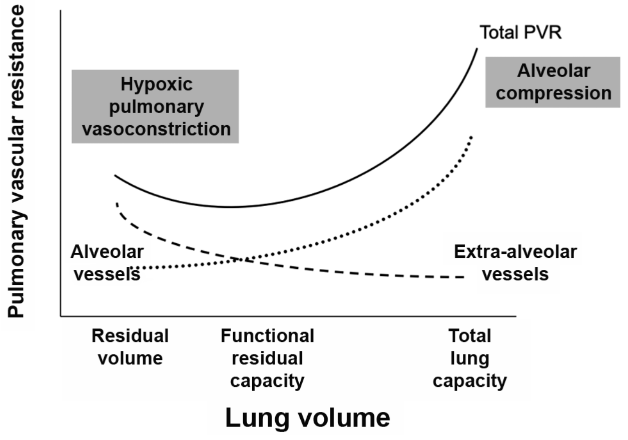

Fig. 1 Schematic diagram of the relation between changes in lung volume and pulmonary vascular resistance, where the extra-alveolar (dashed line) and alveolar vascular (dotted line) components are separated.

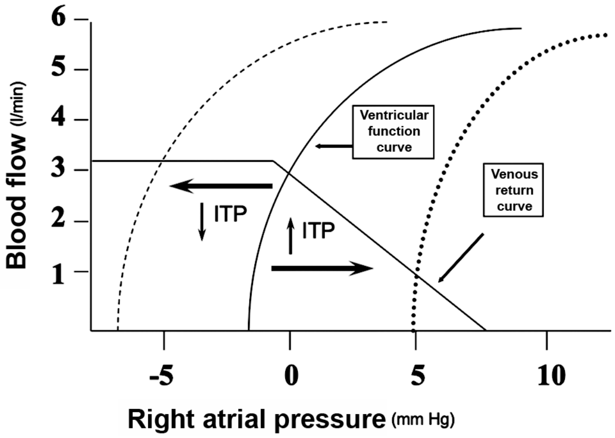

Fig. 2 Schematic representation of the effects of increasing intrathoracic pressure (ITP), as would occur during positive-pressure inspiration, or decreasing ITP, as would occur during spontaneous inspiratory efforts, on steady-state venous return as defined by the left ventricular (LV) function curve at that level of ITP. Note that decreases in ITP which decrease right atrial pressure to below zero relative to atmospheric pressure, will only increase venous return by a limited amount, whereas increases in ITP will progressively decrease venous return to a complete circulatory stand still.

patients showed more than 50% of the patients had nonzone 3 (aka zone 1 or 2) conditions at a tidal volume of 6 mL/kg,[40] and treating providers should be aware that positive pressure ventilation can cause increased pulmonary vascular resistance even during "lung protective strategy ventilation."

The pulmonary vascular system is a low-pressure, high-compliance system, as opposed to the systemic vasculature. During heavy exercise, in healthy subjects, the blood flow increases four to sixfold, but the pulmonary artery can distribute the increased amount of blood flow by opening more capillaries and by distending them. This is one of the reasons why pulmonary artery pressure does not change significantly during exercise with increased blood flow.[41] On the contrary, the RV is unable to handle acute increases in outflow pressure, such as those in acute pulmonary embolism or diffuse HPV. Even a small change in pulmonary artery pressure will rapidly reduce the stroke volume and cause RV strain.[42]

How Right Ventricular Afterload Can Affect the Left Ventricular Preload

RV and LV are linked in parallel through their common septum, circumferential fibers, and pericardium which limits the total cardiac volume. Thus, diastolic filling of the RV has direct influence on the shape and compliance of the LV. Investigators showed that if RV end-diastolic volumes (EDVs) were progressively increased in an asystolic canine heart, the LV compliance progressively decreases such that for the same LV pressure, LV volume was lower volume[43] (►**Fig. 2**). Increasing RV EDV induces intraventricular septal shift into the LV and has direct influence on the shape and compliance of the LV, which is called the "ventricular diastolic interdependence." Multiple clinical studies have documented that in the presence of significant increases in RV afterload (cor pulmonale, acute pulmonary embolism, pneumothorax, or diffuse HPV), by their associated increases in RV EDV, LV diastolic compliance decreases and can lead to cardiopulmonary collapse due to impaired LV diastolic filling.[40–42]

Summary of How Pulmonary Vascular Resistance Affects Hemodynamics

- Alveolar vessels directly sense the alveolar pressure and collapse when Ptp exceeds pulmonary venous pressure. Extra-alveolar vessels will dilate as lung volume increases and minimizes extra-alveolar resistance. At low lung volumes, the airways can be below their critical closing pressures causing alveolar deoxygenation and inducing HPV. Under most conditions, minimal pulmonary vascular resistance is achieved at functional residual capacity.
- Pulmonary vascular system is a low-pressure, high-compliance system. It is capable of accepting high blood flow but is unable to handle an acute rise in pulmonary pressure, which can be the result of severe HPV or mechanical compression of the vessels from increased lung volume.
- HPV and volume-dependent changes in pulmonary vascular resistance (owing to increases in Ptp) are the two main mechanisms that cause elevated pulmonary vascular resistance and can increase the RV afterload.
- When HPV is generalized, pulmonary artery pressure elevations can cause RV dysfunction.

Intrathoracic Pressure and Venous Return

Right atrium pressure (P_{RA}) is the downstream pressure for venous return, while the upstream reservoir for venous pressure is mean systemic pressure. Mean systemic pressure is the function of blood volume, peripheral vasomotor tone, and the distribution of blood within the vasculature, and it is basically the instantaneous pressure within the entire circulation when blood flow ceases. In reality, vascular pressure equilibrium during cardiac arrest requires approximately 15 seconds for this vascular pressure to become equalized across the arteries and veins. By extrapolation, the estimated zero flow P_{RA} seen when P_{RA} is artifactually increased during positive pressure ventilation approximates mean systemic pressure. Mean systemic filling pressure is affected by fluid volume and vessel compliance.[44] At fixed heart rate and arterial pressure, venous return equals cardiac output. If both are plotted relative to changing P_{RA}, with P_{RA} on the *x*-axis, the intersection of the venous return curve and cardiac function curve defines the "equilibrium point" (►**Fig. 2**). Since the heart is in the chest and senses ITP as its surrounding pressure and the rest of the body does not, increasing ITP will appear to shift the cardiac function curve to the left, with P_{RA} on the x-axis causing the cardiac output to transiently decrease.[45] Decreased ITP, as occurs with spontaneous inspiration, will shift the cardiac function curve to the right and increase and transiently increase cardiac output. This spontaneous inspiratory augmentation of venous return is limited, however, by venous collapse if ITP becomes subatmospheric. This process protects the RV from massive volume overload during forced spontaneous inspiratory efforts, as may occur with upper airway obstruction, bronchospasm, and decreased lung compliance.

Hemodynamic Effect of the Change in Intrathoracic Pressure in Different Breathing Patterns

Since the heart is in the chest and senses ITP as its surrounding pressure, both the pressure gradient for venous return to the heart and LV ejection from the heart are directly influenced by changes in ITP. Thus, changes in ITP can affect the pressure gradient of venous return altering RV preload and LV ejection pressure altering LV afterload (LV wall stress). When ITP increase, P_{RA} increases, decreasing the pressure gradient for venous return. Since the LV is also in the thorax and the aortic outflow passes into extrathoracic compartments, increases in ITP for the same arterial pressure must decrease LV transmural pressure, augmenting LV ejection. Opposite effects will be seen with decreases in ITP, as seen during spontaneous inspiration.

Spontaneous Breathing

Normal spontaneous breathing will cause negative ITP, resulting in diaphragmatic descent with increased intra-abdominal pressure and increased venous return. In healthy subjects, the pulmonary arterial inflow circuit is highly compliant and can accept large increase in RV stroke volume without increasing the RV end-diastolic pressure (EDP). Increase in RV stroke volume will increase the LV stroke volume a few beats later (serial interaction). However, this compensatory mechanism will fail if RV diastolic compliance decreases and the RV cannot tolerate the increase in venous return without increasing P_{RA}. An increase in RV volume and RV EDP will cause a parallel decrease in LV compliance and volume due to ventricular diastolic interdependence[46] (►**Fig. 3**).

Additionally, negative ITP will cause an increase in LV afterload. Both ventricular diastolic interdependence and increases in LV afterload will cause a simultaneous decrease in LV stroke volume[47] (parallel interaction) (►**Fig. 4**). In general, the slight increase in LV afterload is well tolerated

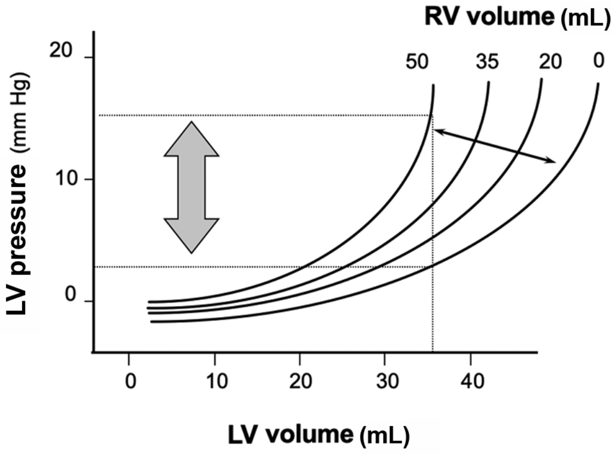

Fig. 3 Schematic diagram of the effect of changing right ventricular (RV) volumes on the left ventricular (LV) diastolic pressure–volume relationship. (Reproduced with permission from After Taylor et al. Dependence of ventricular distensibility on filling the opposite ventricle. Am J Physiol 1967;213:711–718.)

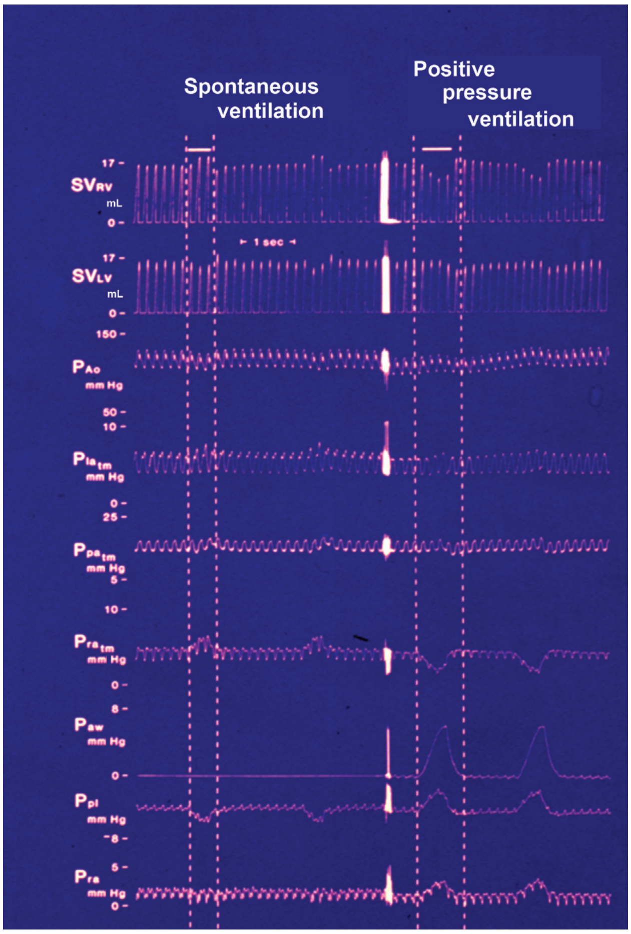

Fig. 4 Strip chart recoding of right and left ventricular stroke volumes (SVrv and SVlv, respectively), aortic pressure (P_{Ao}), left atrial. Pulmonary arterial and right atrial transmural pressures (Pla_{tm}, Ppa_{tm}, and Pra_{tm}, respectively), airway pressure (Paw), pleural pressure (Ppl), and right atrial pressure (Pra) during spontaneous ventilation (left) and similar tidal volume positive-pressure ventilation (right) in an anesthestized, intake canine model (Reproduced with permission from Pinsky et al. J Appl Physiol 1985;58:1189–1198.)

and the overall effect of spontaneous breathing is to increase cardiac output compared with an apneic baseline owing to the increase in venous return. However, with forced spontaneous inspiratory efforts against an occluded airway or during bronchospasm, ITP can become very negative, often exceeding −50 mm Hg. Such dramatic increases in LV afterload are presumed to be the cause of flash pulmonary edema in these clinical settings.[47,48] Using an automatic airway occlusion device immediately following chest compression to cause ITP to transiently become negative during chest recoil, then removing the airway obstruction during CPR, also augments venous return blood flow during cardiopulmonary resuscitation.[49]

Positive Pressure Ventilation

Positive pressure ventilation will increase both RA pressure and ITP and cause decreased venous return, which will subsequently decrease RV filling as well as RV stroke volume. However, in most cases, positive pressure ventilation itself does not induce profound hemodynamic insufficiency by a decrease in venous return. This venous return sparing effect is thought to be due to (1) the associated increase in intra-abdominal pressure owing to diaphragmatic descent during positive pressure ventilation and redistribution of the blood to the thoracic cavity,[50,51] minimizing the decreased venous return driving pressure and (2) increased sympathetic tone during positive pressure ventilation, increasing mean systemic pressure. These two mechanisms are usually effective when patients are euvolemic or hypervolemic, such as heart failure patients with elevated LV EDP.[52] Additionally, positive ITP will decrease the LV afterload and will maintain or increase the LV output.[47] However, when patients are hypovolemic, the venous return is not spared by the above mechanism and RV filling as well as RV stroke volume can diminish precipitously. This will subsequently cause a decrease in LV stroke volume, which usually occurs a few beats after the decrease in RV stroke volume[46] (serial interaction; ►**Fig. 4**) This is the reason why the institution of positive pressure ventilation or simply the use of CPAP is very effective in acute decompensated heart failure patients with volume overload since it decreases some degree of venous return (but not too much to cause collapse) and decrease the LV afterload which will optimize the LV output.[53]

Hyperinflation or Lung Recruitment Maneuver

During hyperinflation or a lung recruitment maneuver to 40 cm H_2O, ITP as well as RV afterload increases significantly as lung volumes are increased, and this causes immediate increases in RV EDP. The septum will shift toward the LV and both LV EDV and stroke volume diminish significantly. This effect will be more prominent in hypovolemic patients.[54] Thus, sustained lung recruitment maneuvers to high airway pressures should be avoided in hypovolemic patients.

Periintubation Hypotension

Tracheal intubation is a common procedure and hypotension is reported in 25 to 40% of tracheal intubations in the ICU.[10,55,56] The causes of this commonly seen cardiovascular collapse are complex, as described by the multiple mechanisms described above and the reality that emergent intubation is only done in patients with acute respiratory insufficiency. The potential primary factors causing peri-intubation cardiovascular insufficiency and hypotension include medication-induced decrease in sympathetic tone, positive-pressure induced increases in ITP, and P_{RA} and if too large tidal volumes are delivered, hyperinflation with its negative effects is described above. Importantly, peri-intubation sedation, by reducing the increased sympathetic tone present by the acute respiratory failure event, will cause mean systemic pressure to decrease as unstressed vascular volume increases. The circulating blood volume can be considered as comprising two separate physiologic volumes relative to its effect of distending pressure of the vasculature. Since most of the blood volume is in the venous capacitance systems and defines the upstream pressure for venous return, this blood volume and its distribution are more important in determining cardiac output. If one were to “fill” a completely empty venous vasculature with blood, more than 50% of the actual blood volume would fill this vasculature without causing distending pressure to rise. Once the vascular space has been filled such that the vessels start to distend against their walls, venous pressure rises. The volume in the vasculature needed to cause the initial venous pressure to rise is referred to as the unstressed volume. Increased sympathetic tone can reduce unstressed volume, moving it into the stressed volume space and increasing mean systemic pressure, the back pressure for venous return. The combined increase in P_{RA} from the increasing ITP, plus the decrease in mean systemic pressure, results in a marked decrease in venous return. Furthermore, the blunted sympathetic response limits reactive arterial vasoconstriction, allowing hypotension to persist. A small, randomized control study found a 500 mL fluid bolus during intubation prevented cardiovascular collapse in patients who received positive pressure ventilation with bag-mask device or non-invasive ventilator during the tracheal intubation procedure.[10] A subsequent randomized control study, which looked at the effect of fluid bolus particularly in patients receiving positive pressure ventilation, did not show a significant difference in the occurrence of cardiopulmonary collapse.[56] These negative results are not surprising because the contributing factors for peri-intubation hypotension are multifactorial, and providers should be cognizant about not only the effect of positive pressure ventilation to decrease venous return in patients with hypovolemia, but also the role of loss of sympathetic tone, vasoplegia, and potential ventilator-induced hyperinflation in this acute management setting.

Hemodynamic Effect of Different Ventilator Modes

The hemodynamic change seen between different ventilator modes is a result of differences in lung volume and ITP. Numerous studies documented cardiovascular equivalence when different ventilator modes are matched for tidal volume, level of PEEP, and mean airway pressure.[57,58] Pressure

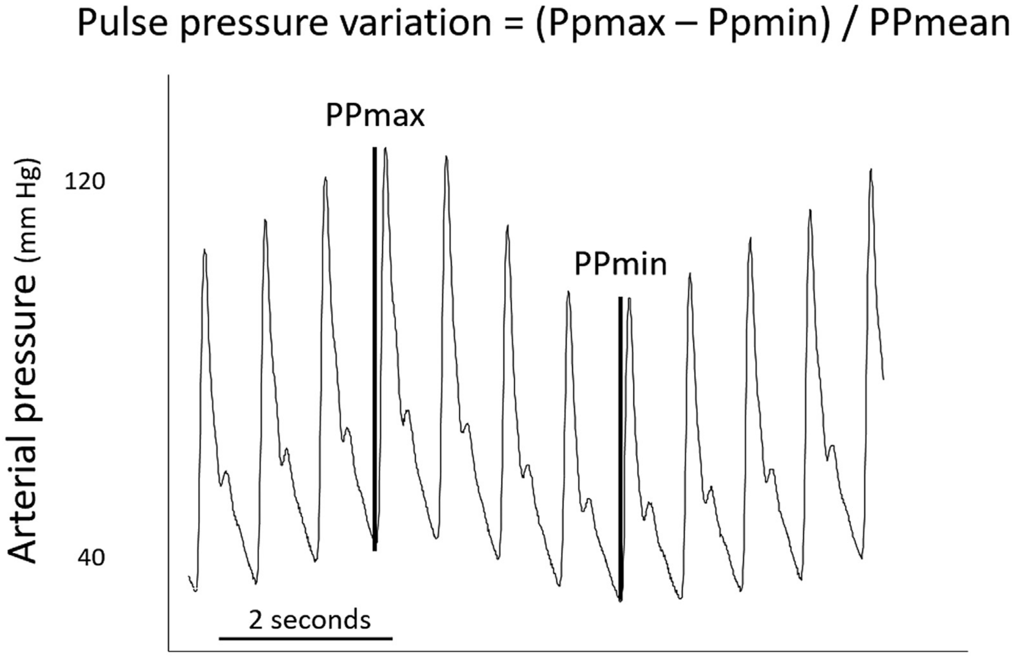

Fig. 5 Simultaneous recording of systemic arterial and airway pressure curves in a patient with large pulse pressure variations, which suggests fluid responsiveness in this patient. As the airway pressure and intrathoracic pressure increase, there is less venous return to the right atrium and the following stroke volume will decrease after few beats. In patients with hypovolemia or other fluid responsiveness conditions, this decrease in venous return and stroke volume will reflect on the pulse pressure variation. Pulse pressure is the difference between systolic and diastolic arterial pressure. Over a single respiratory cycle, the maximum pulse pressure (PP max) and minimum pulse pressure (PP min) are measured and pulse pressure is calculated as: pulse pressure (%) = 100 x {(PP max − PP min)/([PP max + PP min]/2)}. (Reproduced with permission from Michard F, et al Clinical use of respiratory changes in arterial pulse pressure to monitor the hemodynamic effects of PEEP. Am J Resp Crit Care 1999;**159**:935–939.)

control ventilation with inverse ratio (such as airway pressure release ventilation: APRV) will raise the mean airway pressure and may affect the cardiac output.[59]

Summary of Hemodynamic Effect of Intrathoracic Pressure in Different Breathing Patterns

- Spontaneous breathing can increase venous return due to negative ITP. With normal RV diastolic function, this will cause serial increase in LV stroke volume. When RV diastolic function is impaired, increase in RV volume will cause ventricular diastolic interdependence and LV volume will have a parallel decrease in parallel.
- Positive pressure ventilation can decrease venous return due to positive ITP. The degree of decrease in venous return will be altered based on their volume status and may be spared in hypervolemic patients such as heart failure patients but can be remarkable in patients with hypovolemia. Periintubation hypotension may partly be due to the effect of increased ITP causing decreased venous return. An increase in ITP will generally decrease LV afterload and increase LV stroke volume unless the venous return is significantly decreased due to hypovolemia.
- Different modes of mechanical ventilation, if matched for the same tidal volume and mean airway pressure, have similar hemodynamic effects.

How Can We Use Heart–Lung Interaction as Functional Hemodynamic Monitoring?

During positive pressure ventilation, the preload reducing effect becomes more prominent at end-inspiration as tidal volume increases. In euvolemic or hypervolemic patients, this effect may not be notable, but hypovolemic patients can drop their preload as well as their stroke volume significantly with positive pressure ventilation. This alteration of stroke volume with respiratory variation can be measured as stroke volume variation (SVV) or pulse pressure variation (PPV; ►**Fig. 5**),[60] and these dynamic changes are superior to static indices to monitor fluid responsiveness when patients are under controlled mechanical ventilation. Fluid responsiveness was traditionally considered as 15% increase in cardiac output with 500 mL of colloid fluid administration over 30 minutes.[61] PPV >12% suggests fluid responsiveness and is only reliable when patients do not have any spontaneous breathing or cardiac arrhythmia and are ventilated at least with 8 mL/kg. Recently, Myatra et al have looked into the change in SVV and PVV by increasing the tidal volume from 6 to 8 mL/kg (ΔSVV_{6-8}, ΔPVV_{6-8}), which they called a “tidal volume challenge.” The absolute change in SVV and PVV reliably predicted fluid responsiveness with cutoff values of 2.5 and 3.5%, respectively, whereas SVV and PVV at the tidal volume of 6 mL/kg did not.[62] For example, if PPV at a tidal volume of 6 mL/kg were 8% and 20 seconds later at a tidal volume of 8 mL/kg it was 12%, then the difference would be 4% and the patient would be volume responsive. The importance of this tidal volume challenge to assess volume responsiveness is that one does not need to estimate cardiac output or SVV to make the calculations. One requires only a continuous arterial pressure measure that allows the calculation of PPV. Since many of our ICU patients are on low tidal volume strategy, this "tidal volume challenge" may be a helpful measurement to estimate fluid responsiveness.

Summary of Heart–Lung Interaction and Hemodynamic Monitoring

- PPV and SVV are two reliable dynamic indices to assess fluid responsiveness in mechanically ventilated patients.

Heart–lung interactions in Specific Patient Populations

As we discussed earlier, a change in tidal volume and mean airway pressure will affect heart–lung interaction. As these factors remain the same, all forms of mechanical ventilator strategy will have a similar effect on hemodynamics.

Mechanical Ventilation Strategy for Patients with Obesity

Patients with obesity have increased pleural pressure and decreased lung capacity due to heavy chest wall and elevated intra-abdominal pressure causing cephalad displacement of the diaphragm.[63] The increase in pleural pressure (chest wall + intra-abdominal pressure) will increase the risk of developing negative Ptp (Ptp = airway pressure − pleural pressure), resulting in atelectasis.[64] Low functional residual capacity will increase the risk of expiratory flow limitation, which can result in decreased alveolar ventilation and impaired gas exchange and increased pulmonary vascular resistance. Thus, the application of adequate PEEP levels in mechanically ventilated obese patients to return Ptp to greater than zero is important to prevent atelectrauma and optimize respiratory mechanics. However, the optimal PEEP to maintain end-expiratory lung volume in these patients is difficult to estimate, and data suggest that the PEEP set by clinicians is often considerably less than what is required to prevent atelectasis.[65] Jong et al also looked into the impact of driving pressure on mortality in obese and nonobese patients with ARDS and found that contrary to nonobese patients, higher driving pressure was not associated with worse mortality.[66] This result suggests that much of the pressure applied from the ventilator is used to distend the chest wall rather than the lung itself, and monitoring Ptp will only differentiate the pressure being used to distend the lung. Fumagalli et al reported an animal study using healthy lung swine models, investigating the "optimal PEEP" by measuring the Ptp, lung mechanics, lung morphology, and hemodynamic parameter changes during decremental PEEP trial (PEEP starting at 25 cm H_2O and decreasing by 2 cm H_2O every 120 seconds. Optimal PEEP was defined as 2 cm H_2O above the PEEP level identifying the lowest lung and respiratory system elastance), preceded by a recruitment maneuver. In this animal study, low-to-negative values of Ptp predicted lung collapse and intratidal recruitment/derecruitment. Also, a decremental PEEP trial preceded by recruitment maneuver reversed atelectasis and improved lung mechanics, distribution of ventilation and oxygenation, and did not increase pulmonary vascular resistance.[67] Liou et al conducted a retrospective cohort study of Ptp-guided PEEP titration for mechanical ventilation in class II and III obese patients. The study used esophageal pressure (Pes) as the surrogate for pleural pressure and PEEP was titrated based on Ptp at end expiration until it approached 0 cm H_2O to minimize atelectasis. Patients with Ptp balancing ventilator settings had higher PEEP settings and smaller, lower driving pressures and improved oxygenation.[68] Another retrospective cohort study by Florio et al showed that individualized titration of mechanical ventilation by a lung recruitment maneuver and decremental PEEP trial, and monitoring of end-expiratory Ptp to choose the correct value of PEEP, was associated with decreased mortality compared with the use of the ARDSnet table PEEP titration in class III obese patients.[69] In reality, clinicians may be hesitant to raise the PEEP considerably above values associated with adequate oxygenation without monitoring the Ptp due to the concern of hyperinflation and hemodynamic compromise. Although the utility of esophageal manometry as a surrogate for pleural pressure for ARDS have shown mixed results,[70–72] recent studies in obese patients suggest the benefit of Ptp-guided titration of PEEP to prevent negative Ptp, and this "optimal" PEEP may actually improve lung mechanics as well as oxygenation.[67–69,73] Clinicians may consider the clinical benefit of using this strategy to safely optimize PEEP in obese population.

Chronic Obstructive Lung Disease

The progression of chronic obstructive lung disease (COPD) will result in the destruction of the lung parenchyma, vasculature, and airway obstruction. Expiratory flow limitation will cause intrinsic PEEP, hyperinflation, and increase negative ITP. Moreover, parenchymal destruction, alveolar hypoxia, and chronic vascular dysfunction will cause elevation in pulmonary vascular resistance. Dynamic lung hyperinflation, large increase in negative ITP, and increased PVR can all affect the heart–lung interaction. Cheyne et al conducted a study using healthy subjects to assess which of the three components (dynamic hyperinflation, negative ITP, and increased PVR) had the most effect on LV systolic function. The combination of dynamic hyperinflation and negative ITP reduced LV filling the most through significant septal flattening and the addition of PVR did not further reduce LV volume.[74] However, this study was performed in healthy subjects and many of the patients with severe COPD have chronic pulmonary vascular remodeling leading to pulmonary hypertension and RV dysfunction, which can certainly have an additional impact on the effect of negative ITP and dynamic hyperinflation.[75] To minimize intrinsic PEEP and hyperinflation, the application of adequate external PEEP and prolonged expiratory time are the essential parts of ventilator management.

Acute Respiratory Distress Syndrome

ARDS induces pulmonary vascular dysfunction (PVD) which includes both structural and functional pathophysiological changes to the pulmonary vessels affecting the vascular compartment and the RV, resulting in increased pulmonary arterial pressure and PVR. The main pathophysiology includes HPV, release of vasoactive inflammatory mediators, microvascular thrombosis, direct inflammatory endothelial damage, and vascular remodeling phenomena.[76] As the severity of ARDS progress, PVD can also advance to its most severe form, acute cor pulmonale with overt RV failure.[77] The main focus of ARDS ventilator management "lung protective strategy" is to prevent further damage to the alveolar compartment. Inspiratory driving pressure is the single most relevant independent factor affecting the outcome in ARDS.[78] The management to prevent vascular damage is not well established, but recently four factors promoting RV failure were reported, which include pneumonia as a cause of ARDS, PaO_2/FiO_2 ratio <150 mm Hg, driving pressure >18 cm H_2O, and $PaCO_2$ >48 mm Hg.

The optimal PEEP in ARDS ventilator management can be challenging. ARDS lungs are affected heterogeneously and aerated and collapsed lungs coexist. Applying lower PEEP to prevent further overdistension of the aerated lungs can also cause worsening collapse and atelectasis in dependent areas. How PEEP affects the overall lung volume (whether it reverses atelectasis or causes more hyperinflation) can also differ depending on the phenotype of the ARDS. Traditionally, ARDS was classified as either pulmonary ARDS (direct pulmonary insult causing ARDS) or extra-pulmonary ARDS (caused by acute systemic inflammatory response). Gattinoni et al reported the differences in lung mechanics for each class.[79] Extra-pulmonary ARDS patients tend to have higher intra-abdominal pressure due to intestinal edema and distension, which will cause higher elastance of the chest wall and diaphragm. On the other hand, lung elastance was higher in patients with pulmonary ARDS. Due to these differences in lung mechanics, applying high PEEP has an opposite effect on each patient subgroup. The elastance of the total respiratory system increases with high PEEP in pulmonary ARDS patients (due to overdistention) but decreases in extra-pulmonary ARDS patients (due to counterbalancing the high elastance of the chest wall). Thus, how PEEP affects the Ptp as well as lung volume will determine the effect of PEEP on afterload.

A recent study by Boissier et al showed that patients with PVD and acute cor pulmonale were ventilated more with lower levels of PEEP.[80] Lastly, the prone position is very effective in reducing the heterogeneity of the lung and improving the functional lung volume, which will result in unloading the RV. Pulmonary vasodilators, such as inhaled nitric oxide, phosphodiesterase-5 inhibitors, and endothelin-receptor agonists, are often used but the actual benefits are not well known. Thus, RV protective ventilation strategy in ARDS should include low driving pressure, limited hypercapnia, and PEEP adapted to lung recruitability.[80,81]

Conflict of Interest
None declared.

References

1 Wise RA, Robotham JL, Summer WR. Effects of spontaneous ventilation on the circulation. Lung 1981;159(04):175–186
2 Sette P, Dorizzi RM, Azzini AM. Vascular access: an historical perspective from Sir William Harvey to the 1956 Nobel prize to André F. Cournand, Werner Forssmann, and Dickinson W. Richards. J Vasc Access 2012;13(02):137–144
3 Pinsky MR. Breathing as exercise: the cardiovascular response to weaning from mechanical ventilation. Intensive Care Med 2000; 26(09):1164–1166
4 Lemaire F, Teboul JL, Cinotti L, et al. Acute left ventricular dysfunction during unsuccessful weaning from mechanical ventilation. Anesthesiology 1988;69(02):171–179
5 Jubran A, Mathru M, Dries D, Tobin MJ. Continuous recordings of mixed venous oxygen saturation during weaning from mechanical ventilation and the ramifications thereof. Am J Respir Crit Care Med 1998;158(06):1763–1769
6 Mohsenifar Z, Hay A, Hay J, Lewis MI, Koerner SK. Gastric intramural pH as a predictor of success or failure in weaning patients from mechanical ventilation. Ann Intern Med 1993;119 (08):794–798
7 Hurford WE, Lynch KE, Strauss HW, Lowenstein E, Zapol WM. Myocardial perfusion as assessed by thallium-201 scintigraphy during the discontinuation of mechanical ventilation in ventilator-dependent patients. Anesthesiology 1991;74(06):1007–1016
8 Chatila W, Ani S, Guaglianone D, Jacob B, Amoateng-Adjepong Y, Manthous CA. Cardiac ischemia during weaning from mechanical ventilation. Chest 1996;109(06):1577–1583
9 Srivastava S, Chatila W, Amoateng-Adjepong Y, et al. Myocardial ischemia and weaning failure in patients with coronary artery disease: an update. Crit Care Med 1999;27(10):2109–2112
10 Janz DR, Casey JD, Semler MW, et al; PrePARE Investigators. ; Pragmatic Critical Care Research Group. Effect of a fluid bolus on cardiovascular collapse among critically ill adults undergoing tracheal intubation (PrePARE): a randomised controlled trial. Lancet Respir Med 2019;7(12):1039–1047
11 Larsen PD, Tzeng YC, Sin PYW, Galletly DC. Respiratory sinus arrhythmia in conscious humans during spontaneous respiration. Respir Physiol Neurobiol 2010;174(1-2):111–118
12 Bernardi L, Calciati A, Gratarola A, Battistin I, Fratino P, Finardi G. Heart rate-respiration relationship: computerized method for early assessment of cardiac autonomic damage in diabetic patients. Acta Cardiol 1986;41(03):197–206
13 Yasuma F, Hayano J. Respiratory sinus arrhythmia: why does the heartbeat synchronize with respiratory rhythm? Chest 2004;125 (02):683–690
14 Shepherd JT. The lungs as receptor sites for cardiovascular regulation. Circulation 1981;63(01):1–10
15 Glick G, Wechsler AS, Epstein SE. Reflex cardiovascular depression produced by stimulation of pulmonary stretch receptors in the dog. J Clin Invest 1969;48(03):467–473
16 Vatner SF, Rutherford JD. Control of the myocardial contractile state by carotid chemo- and baroreceptor and pulmonary inflation reflexes in conscious dogs. J Clin Invest 1978;61(06): 1593–1601
17 Persson MG, Lönnqvist PA, Gustafsson LE. Positive end-expiratory pressure ventilation elicits increases in endogenously formed nitric oxide as detected in air exhaled by rabbits. Anesthesiology 1995;82(04):969–974
18 Berend N, Christopher KL, Voelkel NF. The effect of positive end-expiratory pressure on functional residual capacity: role of prostaglandin production. Am Rev Respir Dis 1982;126(04): 646–647

19 Jelic S, Padeletti M, Kawut SM, et al. Inflammation, oxidative stress, and repair capacity of the vascular endothelium in obstructive sleep apnea. Circulation 2008;117(17):2270–2278

20 Berglund JE, Haldén E, Jakobson S, Svensson J. PEEP ventilation does not cause humorally mediated cardiac output depression in pigs. Intensive Care Med 1994;20(05):360–364

21 Frass M, Watschinger B, Traindl O, et al. Atrial natriuretic peptide release in response to different positive end-expiratory pressure levels. Crit Care Med 1993;21(03):343–347

22 Payen DM, Brun-Buisson CJ, Carli PA, et al. Hemodynamic, gas exchange, and hormonal consequences of LBPP during PEEP ventilation. J Appl Physiol 1987;62(01):61–70

23 Farge D, De la Coussaye JE, Beloucif S, Fratacci MD, Payen DM. Interactions between hemodynamic and hormonal modifications during PEEP-induced antidiuresis and antinatriuresis. Chest 1995;107(04):1095–1100

24 Zhang X-B, Yuan Y-T, Du Y-P, Jiang X-T, Zeng H-Q. Efficacy of positive airway pressure on brain natriuretic peptide in patients with heart failure and sleep-disorder breathing: a meta-analysis of randomized controlled trials. Lung 2015;193(02):255–260

25 Slutsky AS, Ranieri VM. Ventilator-induced lung injury. N Engl J Med 2013;369(22):2126–2136

26 Dawson CA, Grimm DJ, Linehan JH. Lung inflation and longitudinal distribution of pulmonary vascular resistance during hypoxia. J Appl Physiol 1979;47(03):532–536

27 Hakim TS, Michel RP, Minami H, Chang HK. Site of pulmonary hypoxic vasoconstriction studied with arterial and venous occlusion. J Appl Physiol 1983;54(05):1298–1302

28 Marini JJ, Culver BH, Butler J. Mechanical effect of lung distention with positive pressure on cardiac function. Am Rev Respir Dis 1981;124(04):382–386

29 Butler J. The heart is in good hands. Circulation 1983;67(06): 1163–1168

30 Madden JA, Dawson CA, Harder DR. Hypoxia-induced activation in small isolated pulmonary arteries from the cat. J Appl Physiol 1985;59(01):113–118

31 Dunham-Snary KJ, Wu D, Sykes EA, et al. Hypoxic pulmonary vasoconstriction: from molecular mechanisms to medicine. Chest 2017;151(01):181–192

32 Marshall BE, Marshall C, Benumof J, Saidman LJ. Hypoxic pulmonary vasoconstriction in dogs: effects of lung segment size and oxygen tension. J Appl Physiol 1981;51(06):1543–1551

33 Sylvester JT, Shimoda LA, Aaronson PI, Ward JPT. Hypoxic pulmonary vasoconstriction. Physiol Rev 2012;92(01):367–520

34 Hughes JMB. Hypoxic pulmonary vasoconstriction: clinical implications. Eur Respir J 2016;47(01):31–34

35 Hakim TS, Michel RP, Chang HK. Effect of lung inflation on pulmonary vascular resistance by arterial and venous occlusion. J Appl Physiol 1982;53(05):1110–1115

36 Brower RG, Gottlieb J, Wise RA, Permutt S, Sylvester JT. Locus of hypoxic vasoconstriction in isolated ferret lungs. J Appl Physiol 1987;63(01):58–65

37 Howell JBL, Permutt S, Proctor DF, Riley RL. Effect of inflation of the lung on different parts of pulmonary vascular bed. J Appl Physiol 1961;16:71–76

38 Suter PM, Fairley B, Isenberg MD. Optimum end-expiratory airway pressure in patients with acute pulmonary failure. N Engl J Med 1975;292(06):284–289

39 West JB, Dollery CT, Naimark A. Distribution of blood flow in isolated lung; relation to vascular and alveolar pressures. J Appl Physiol 1964;19:713–724

40 Slobod D, Assanangkornchai N, Alhazza M, Mettasittigorn P, Magder S. Right ventricular loading by lung inflation during controlled mechanical ventilation. Am J Respir Crit Care Med 2022;205(11):1311–1319

41 Lewis GD, Bossone E, Naeije R, et al. Pulmonary vascular hemodynamic response to exercise in cardiopulmonary diseases. Circulation 2013;128(13):1470–1479

42 MacNee W. Pathophysiology of cor pulmonale in chronic obstructive pulmonary disease. Part One. Am J Respir Crit Care Med 1994; 150(03):833–852

43 Taylor RR, Covell JW, Sonnenblick EH, Ross J Jr. Dependence of ventricular distensibility on filling of the opposite ventricle. Am J Physiol 1967;213(03):711–718

44 Pinsky MR. Instantaneous venous return curves in an intact canine preparation. J Appl Physiol 1984;56(03):765–771

45 Goldberg HS, Rabson J. Control of cardiac output by systemic vessels. Circulatory adjustments to acute and chronic respiratory failure and the effect of therapeutic interventions. Am J Cardiol 1981;47(03):696–702

46 Pinsky MR, Matuschak GM, Klain M. Determinants of cardiac augmentation by elevations in intrathoracic pressure. J Appl Physiol 1985;58(04):1189–1198

47 Buda AJ, Pinsky MR, Ingels NB Jr, Daughters GT II, Stinson EB, Alderman EL. Effect of intrathoracic pressure on left ventricular performance. N Engl J Med 1979;301(09):453–459

48 Fletcher EC, Proctor M, Yu J, et al. Pulmonary edema develops after recurrent obstructive apneas. Am J Respir Crit Care Med 1999;160 (5 Pt 1):1688–1696

49 Lurie KG, Zielinski T, McKnite S, Aufderheide T, Voelckel W. Use of an inspiratory impedance valve improves neurologically intact survival in a porcine model of ventricular fibrillation. Circulation 2002;105(01):124–129

50 Takata M, Wise RA, Robotham JL. Effects of abdominal pressure on venous return: abdominal vascular zone conditions. J Appl Physiol 1990;69(06):1961–1972

51 Takata M, Robotham JL. Effects of inspiratory diaphragmatic descent on inferior vena caval venous return. J Appl Physiol 1992;72(02):597–607

52 De Hoyos A, Liu PP, Benard DC, Bradley TD. Haemodynamic effects of continuous positive airway pressure in humans with normal and impaired left ventricular function. Clin Sci (Lond) 1995;88 (02):173–178

53 Bradley TD, Holloway RM, McLaughlin PR, Ross BL, Walters J, Liu PP. Cardiac output response to continuous positive airway pressure in congestive heart failure. Am Rev Respir Dis 1992;145(2 Pt 1):377–382

54 Nielsen J, Østergaard M, Kjaergaard J, et al. Lung recruitment maneuver depresses central hemodynamics in patients following cardiac surgery. Intensive Care Med 2005;31(09):1189–1194

55 Russotto V, Myatra SN, Laffey JG, et al; INTUBE Study Investigators. Intubation practices and adverse peri-intubation events in critically ill patients from 29 countries. JAMA 2021;325(12): 1164–1172

56 Russell DW, Casey JD, Gibbs KW, et al; PREPARE II Investigators and the Pragmatic Critical Care Research Group. Effect of Fluid Bolus Administration On Cardiovascular Collapse Among Critically Ill Patients Undergoing Tracheal Intubation: A Randomized Clinical Trial. JAMA 2022;328(03):270–279

57 Lessard MR, Guérot E, Lorino H, Lemaire F, Brochard L. Effects of pressure-controlled with different I:E ratios versus volume-controlled ventilation on respiratory mechanics, gas exchange, and hemodynamics in patients with adult respiratory distress syndrome. Anesthesiology 1994;80(05):983–991

58 Mang H, Kacmarek RM, Ritz R, Wilson RS, Kimball WP. Cardiorespiratory effects of volume- and pressure-controlled ventilation at various I/E ratios in an acute lung injury model. Am J Respir Crit Care Med 1995;151(3 Pt 1):731–736

59 Chan K, Abraham E. Effects of inverse ratio ventilation on cardiorespiratory parameters in severe respiratory failure. Chest 1992; 102(05):1556–1561

60 Teboul J-L, Monnet X, Chemla D, Michard F. Arterial pulse pressure variation with mechanical ventilation. Am J Respir Crit Care Med 2019;199(01):22–31

61 Michard F, Boussat S, Chemla D, et al. Relation between respiratory changes in arterial pulse pressure and fluid responsiveness in

septic patients with acute circulatory failure. Am J Respir Crit Care Med 2000;162(01):134–138

62 Myatra SN, Prabu NR, Divatia JV, Monnet X, Kulkarni AP, Teboul JL. The changes in pulse pressure variation or stroke volume variation after a "tidal volume challenge" reliably predict fluid responsiveness during low tidal volume ventilation. Crit Care Med 2017;45(03):415–421

63 Hedenstierna G, Santesson J. Breathing mechanics, dead space and gas exchange in the extremely obese, breathing spontaneously and during anaesthesia with intermittent positive pressure ventilation. Acta Anaesthesiol Scand 1976;20(03):248–254

64 Jones RL, Nzekwu M-MU. The effects of body mass index on lung volumes. Chest 2006;130(03):827–833

65 Pirrone M, Fisher D, Chipman D, et al. Recruitment maneuvers and positive end-expiratory pressure titration in morbidly obese ICU patients. Crit Care Med 2016;44(02):300–307

66 De Jong A, Cossic J, Verzilli D, et al. Impact of the driving pressure on mortality in obese and non-obese ARDS patients: a retrospective study of 362 cases. Intensive Care Med 2018;44(07):1106–1114

67 Fumagalli J, Berra L, Zhang C, et al. Transpulmonary pressure describes lung morphology during decremental positive end-expiratory pressure trials in obesity. Crit Care Med 2017;45(08):1374–1381

68 Liou J, Doherty D, Gillin T, et al. Retrospective review of transpulmonary pressure guided positive end-expiratory pressure titration for mechanical ventilation in Class II and III Obesity. Crit Care Explor 2022;4(05):e0690

69 Florio G, Ferrari M, Bittner EA, et al; investigators of the lung rescue team. A lung rescue team improves survival in obesity with acute respiratory distress syndrome. Crit Care 2020;24(01):4

70 Beitler JR, Sarge T, Banner-Goodspeed VM, et al; EPVent-2 Study Group. Effect of titrating positive end-expiratory pressure (PEEP) with an esophageal pressure-guided strategy vs an empirical high PEEP-Fio2 strategy on death and days free from mechanical ventilation among patients with acute respiratory distress syndrome: a randomized clinical trial. JAMA 2019;321(09):846–857

71 Talmor D, Sarge T, Malhotra A, et al. Mechanical ventilation guided by esophageal pressure in acute lung injury. N Engl J Med 2008;359(20):2095–2104

72 Sarge T, Baedorf-Kassis E, Banner-Goodspeed V, et al; EPVent-2 Study Group. Effect of esophageal pressure-guided positive end-expiratory pressure on survival from acute respiratory distress syndrome: a risk-based and mechanistic reanalysis of the EPVent-2 Trial. Am J Respir Crit Care Med 2021;204(10):1153–1163

73 Umbrello M, Fumagalli J, Pesenti A, Chiumello D. Pathophysiology and management of acute respiratory distress syndrome in obese patients. Semin Respir Crit Care Med 2019;40(01):40–56

74 Cheyne WS, Williams AM, Harper MI, Eves ND. Heart-lung interaction in a model of COPD: importance of lung volume and direct ventricular interaction. Am J Physiol Heart Circ Physiol 2016;311(06):H1367–H1374

75 Chaouat A, Naeije R, Weitzenblum E. Pulmonary hypertension in COPD. Eur Respir J 2008;32(05):1371–1385

76 Price LC, McAuley DF, Marino PS, Finney SJ, Griffiths MJ, Wort SJ. Pathophysiology of pulmonary hypertension in acute lung injury. Am J Physiol Lung Cell Mol Physiol 2012;302(09):L803–L815

77 Sipmann FS, Santos A, Tusman G. Heart-lung interactions in acute respiratory distress syndrome: pathophysiology, detection and management strategies. Ann Transl Med 2018;6(02):27

78 Amato MBP, Meade MO, Slutsky AS, et al. Driving pressure and survival in the acute respiratory distress syndrome. N Engl J Med 2015;372(08):747–755

79 Gattinoni L, Pelosi P, Suter PM, Pedoto A, Vercesi P, Lissoni A. Acute respiratory distress syndrome caused by pulmonary and extrapulmonary disease. Different syndromes? Am J Respir Crit Care Med 1998;158(01):3–11

80 Boissier F, Katsahian S, Razazi K, et al. Prevalence and prognosis of cor pulmonale during protective ventilation for acute respiratory distress syndrome. Intensive Care Med 2013;39(10):1725–1733

81 Vieillard-Baron A, Matthay M, Teboul JL, et al. Experts' opinion on management of hemodynamics in ARDS patients: focus on the effects of mechanical ventilation. Intensive Care Med 2016;42(05):739–749

Article published online: 2023-07-10

Exercise Physiology and Cardiopulmonary Exercise Testing

Kathy E. Sietsema, MD[1] Harry B. Rossiter, PhD[1]

[1] Division of Respiratory and Critical Care Physiology and Medicine, The Lundquist Institute for Biomedical Innovation at Harbor-UCLA Medical Center, David Geffen School of Medicine at UCLA, Torrance, California

Address for correspondence Kathy E. Sietsema, MD, The Lundquist Institute for Biomedical Innovation at Harbor-UCLA Medical Center, 1124 W Carson St., CDCRC Building, Torrance, CA 90502 (e-mail: sietsema@ucla.edu).

Semin Respir Crit Care Med 2023;44:661–680.

Abstract

Aerobic, or endurance, exercise is an energy requiring process supported primarily by energy from oxidative adenosine triphosphate synthesis. The consumption of oxygen and production of carbon dioxide in muscle cells are dynamically linked to oxygen uptake ($\dot{V}O_2$) and carbon dioxide output ($\dot{V}CO_2$) at the lung by integrated functions of cardiovascular, pulmonary, hematologic, and neurohumoral systems. Maximum oxygen uptake ($\dot{V}O_{2max}$) is the standard expression of aerobic capacity and a predictor of outcomes in diverse populations. While commonly limited in young fit individuals by the capacity to deliver oxygen to exercising muscle, ($\dot{V}O_{2max}$) may become limited by impairment within any of the multiple systems supporting cellular or atmospheric gas exchange. In the range of available power outputs, endurance exercise can be partitioned into different intensity domains representing distinct metabolic profiles and tolerances for sustained activity. Estimates of both $\dot{V}O_{2max}$ and the lactate threshold, which marks the upper limit of moderate-intensity exercise, can be determined from measures of gas exchange from respired breath during whole-body exercise. Cardiopulmonary exercise testing (CPET) includes measurement of $\dot{V}O_2$ and $\dot{V}CO_2$ along with heart rate and other variables reflecting cardiac and pulmonary responses to exercise. Clinical CPET is conducted for persons with known medical conditions to quantify impairment, contribute to prognostic assessments, and help discriminate among proximal causes of symptoms or limitations for an individual. CPET is also conducted in persons without known disease as part of the diagnostic evaluation of unexplained symptoms. Although CPET quantifies a limited sample of the complex functions and interactions underlying exercise performance, both its specific and global findings are uniquely valuable. Some specific findings can aid in individualized diagnosis and treatment decisions. At the same time, CPET provides a holistic summary of an individual's exercise function, including effects not only of the primary diagnosis, but also of secondary and coexisting conditions.

Keywords

- oxygen uptake
- exercise intensity
- CPET
- respiration
- power–duration relationship

Exercise Physiology Overview

The ability to sustain physical activities, including those for daily living, recreation, occupation, or structured exercise depends on the capacity for oxygen transport and utilization. Endurance (or aerobic) exercise, such as walking or running, involves repeated muscle contraction that depends on oxidative energy provision in which oxygen is consumed and carbon dioxide is produced. Multiple organ systems link oxidative metabolism in involved tissues, predominantly exercising muscle (internal respiration), to gas exchange with the atmosphere at the lung (external respiration). Other

article published online
July 10, 2023

Issue Theme Pulmonary Physiology; Guest Editors: David A. Kaminsky, MD, Kathryn A. Hibbert, MD, and Andrew M. Luks, MD

Thieme Medical Publishers, Inc.,
333 Seventh Avenue, 18th Floor,
New York, NY 10001, USA

DOI https://doi.org/10.1055/s-0043-1770362.
ISSN 1069-3424.

articles in this publication detail the physiology of many processes fundamental to exercise, including tissue metabolism and gas exchange, gas transport in the circulation, the mechanics of breathing, control of ventilation, and pulmonary gas exchange. This article will touch briefly on muscle bioenergetics and the cardiovascular and pulmonary responses to exercise that support gas exchange. The range of endurance exercise is described in terms of discrete domains of intensity, characterized with respect to oxygen uptake, blood lactate, and sustainability. With this as background, the measurements for characterizing exercise function that are typically available from a cardiopulmonary exercise test (CPET) will be reviewed along with examples of their applications in clinical practice.

Skeletal Muscle Bioenergetics and Oxidative Metabolism

Skeletal muscle contraction, along with other cellular processes, is powered by energy from adenosine triphosphate (ATP). ATP in skeletal muscle is maintained at low concentration (approximately 8.2 mM), and ATP demand can increase >100-fold from the resting level (approximately 1 mM/min) at the onset of muscle contractions.[1] As such, muscle ATP could be depleted within seconds of exercise onset, if not for a parallel increase in ATP supply. Metabolic pathways for ATP synthesis are activated quickly, and in proportion to the metabolic demand of the exercise task. These pathways include substrate-level phosphorylation in the myocyte cytoplasm, i.e., breakdown of phosphocreatine and glycolysis/glycogenolysis that forms lactate, and oxidative phosphorylation in muscle mitochondria. These pathways are common to all muscle cells, although differing fiber types within and between active muscles vary in their metabolic profiles, some being oxidative in nature (slow, type I) and others glycolytic (fast, type IIx). Intermediate fibers (fast, type IIa) share features of fast contractile properties, but can be highly oxidative in their metabolism. Muscle also contains hybrid fibers that express more than one myosin heavy chain. Skeletal muscle thus presents a continuum of pure and hybrid fiber types that bridge the range of metabolic demand.[2]

Exercise intensities that can be well-sustained are characterized by the recruitment of motor units that have a high expression of oxidative metabolism. As exercise intensity and energy demand increase, more glycolytic and less fatigue resistant fibers are activated. Despite this, even at the highest levels of endurance exercise, the vast majority of ATP supply is still derived from oxidative phosphorylation, which depends on transport of oxygen from the mouth to muscle mitochondria where oxygen consumption occurs. Exercise can therefore be quantified by the corresponding rate of pulmonary oxygen uptake ($\dot{V}O_2$), and the capacity for exercise (or aerobic capacity) by the maximum rate of oxygen uptake ($\dot{V}O_{2max}$).

Substrate provision for exercise is predominately carbohydrates and fatty acids, with protein having little role except under conditions of starvation. The maximum rate of ATP supply from glycolysis/glycogenolysis (approximately 1.1 mM ATP/s) is approximately twice that of carbohydrate oxidation (0.6 mM ATP/s), which is in turn approximately twice that of fatty acid oxidation (0.3 mM ATP/s).[1] During the first minutes of exercise, bioenergetics initially relies on substrate-level phosphorylation (phosphocreatine breakdown and glycolysis/glycogenolysis), during which time carbohydrate oxidation is activated and rises to meet the energy demands of the task. With sustained moderate intensity exercise, there is progressive shift over time toward a higher proportion of fatty acid substrate. However, maximal rates of energy provision from fatty acid oxidation are limited, and therefore fatty acid oxidation contributions to ATP supply are at their greatest during sustained moderate exercise intensities. Reliance on carbohydrate oxidation and substrate-level phosphorylation increases as exercise intensity increases above moderate.

Maximum Oxygen Uptake ($\dot{V}O_{2max}$)

Among healthy persons, $\dot{V}O_{2max}$ has a wide range, varying by age, sex, muscle strength, and genomics, and is modifiable by exercise training. Average values can range from around 40 mL/min/kg in sedentary young adults to less than 20 mL/min/kg in older persons, and may be 60 to 80 mL/min/kg in conditioned endurance athletes. The normal limitation to $\dot{V}O_{2max}$ in trained young men is generally considered to lie in oxygen delivery processes, as aerobic capacity can be modified acutely by changes in arterial oxygen concentration.[3,4] This implies a metabolic reserve in skeletal muscle at maximal exercise in trained individuals. In very physically fit individuals, however, cardiovascular capacity for oxygen delivery may be sufficiently well-developed that constraints on pulmonary ventilation and gas exchange become evident, especially in endurance-trained women.[5] For older, or more sedentary individuals, peripheral limitations in muscle mass and/or metabolic capacity for oxidative energy supply may dictate aerobic capacity.[3,6] Determinants of aerobic capacity may thus vary across the spectrum of apparently healthy individuals, and of course pathologic dysfunction of any component can impose limitation constraining $\dot{V}O_{2max}$.[7–9]

Lactate Threshold

It has long been recognized that metabolic acidosis associated with lactate accumulation develops with strenuous exercise,[10] typically evident around 50% of $\dot{V}O_{2max}$.[11] The degree of lactate elevation portends intolerance for sustained activity.[12] The profile of arterial blood lactate concentration as a function of $\dot{V}O_2$ is therefore of great interest in characterizing cardiorespiratory fitness or severity of chronic disease (►**Fig. 1**)[12] and has been described and quantified in several ways.[13] It is most commonly characterized as a threshold phenomenon during a progressive exercise test (where power output, and therefore metabolic demand, increases linearly with time), and defined by a lactate threshold (LT). The well-recognized relationship between ischemia and metabolic acidosis (Pasteur effect), along with observations that experimentally induced changes in oxygen delivery can acutely shift the $\dot{V}O_2$–lactate relationship,[14–19] was originally interpreted to mean the LT identified a state above which oxygen delivery failed to fully meet the oxidative metabolic requirements of exercise. In the 1960s Wasserman and McIlroy thus proposed estimating LT based on

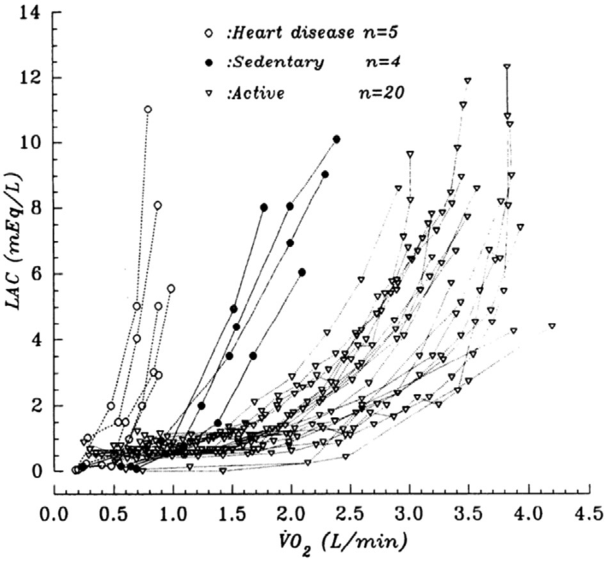

Fig. 1 Change in arterial lactate concentration (LAC) as a function of oxygen uptake ($\dot{V}O_2$) during incremental cycle ergometry. Data are for healthy sedentary (filled circles) and active (open triangles) individuals and patients with cardiovascular disease (open circles). Resting LAC is similar across groups. The $\dot{V}O_2$ at which LAC increases is reduced in patients and increased in active individuals, compared with sedentary individuals. mEq/L, milliequivalents per liter. (Reproduced with permission from Wasserman[12].)

pulmonary gas exchange (see below), as a means of identifying cardiovascular impairment, and termed this the anaerobic threshold (AT).[20] Studies using labeled tracers to track the dynamics of lactate metabolism[21] have since demonstrated that lactate is produced in muscle throughout the entire range of exercise, participates in numerous metabolic pathways, and is a preferred substrate for energy production in many tissues.[22] Rather than marking the onset of lactate *production*, therefore, the LT reflects the metabolic rate at which lactate accumulation in the arterial blood outstrips its clearance. The estimated LT derived from gas exchange measurements has since been given several names including the gas exchange threshold (GET), lactic acidosis threshold, and ventilatory threshold (VT), although the AT remains in common use.[22]

Cardiovascular Responses to Exercise

The circulatory system is a central component of the exercise response. Cardiac output and exercising muscle blood flow increase in close proportion with metabolic rate with a ratio of between 5 and 6 L/min increase in blood flow for each liter increase in $\dot{V}O_2$ (►**Fig. 2A, B, D**), mediated by increases in both cardiac stroke volume (SV) and heart rate (HR; ►**Fig. 2E, F**).[23–25] SV increases by approximately 50% between rest and moderate intensity during upright exercise; there is little additional increase in SV at higher intensities, and potentially a decline at very high HRs (►**Fig. 2F**).[26,27] HR increases progressively across the range of achievable exercise, with the peak value determined predominantly by age, independent of sex or level of conditioning.[28] In normal healthy individuals, HR and cardiac output approach or reach individual maximal values (±20 bpm) during a progressive exercise test. Endurance-trained individuals have higher than average SV at rest and during exercise, due

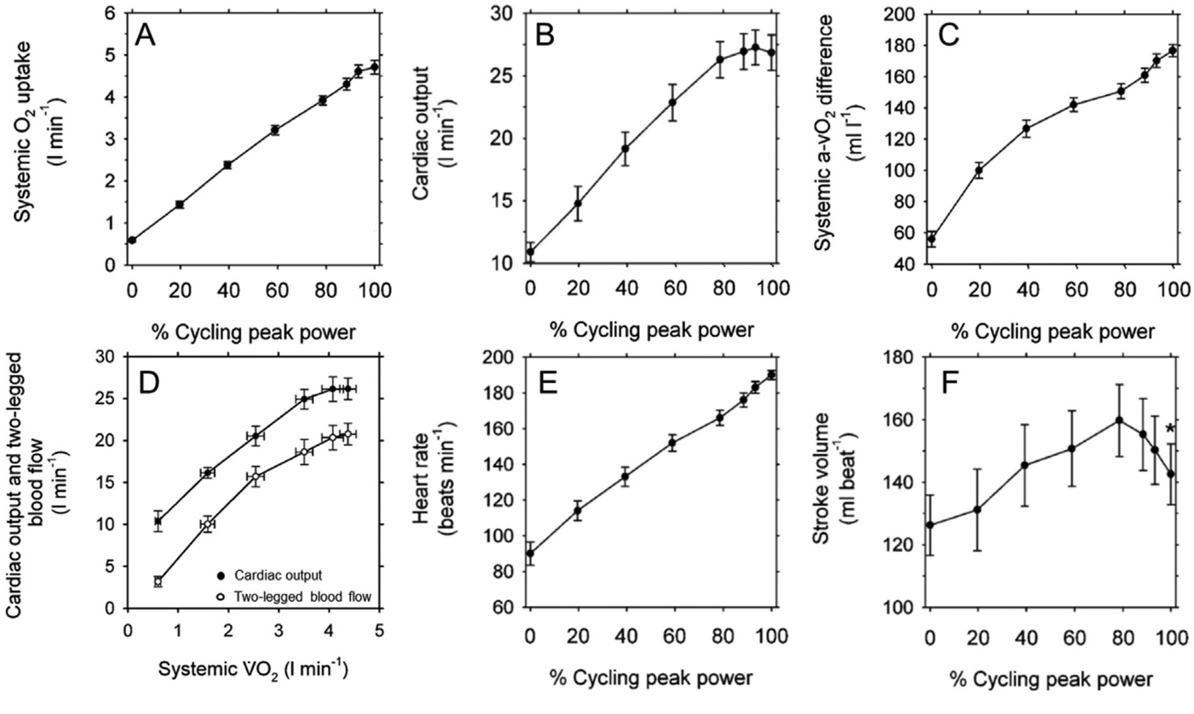

Fig. 2 Changes in cardiovascular variables during incremental cycle ergometry in endurance-trained young men ($n = 8$). $\dot{V}O_2$ increases essentially linearly relative to power output (**A**). The increase in cardiac output (**B**) is also linear through most of exercise, but plateaued in these subjects at approximately 80% peak power, corresponding to a decline in stroke volume (**F**), and is compensated by an increase in systemic O_2 extraction (C(a-v)O_2) (**C**) and heart rate (**E**). Essentially all the increase in cardiac output from rest to peak exercise is directed toward the legs during this cycling exercise (**D**). (Adapted with permission from Mortensen et al[25].)

to a combination of greater ventricular filling (end-diastolic volume) and faster diastolic filling time, increased left ventricular ejection time and contractility, decreased afterload, and/or greater blood volume. These adaptations are associated with lower resting HR and a shallower slope of relationship between HR and $\dot{V}O_2$, allowing these individuals to reach a greater $\dot{V}O_2$ peak at a similar peak HR during a progressive exercise test.[27]

The great majority of the increase of cardiac output during exercise is directed to the exercising muscle (►**Fig. 2D**), with concomitant reduction in flow to renal and splanchnic vascular beds.[26] The increase and redistribution of cardiac output in response to exercise result from a complex set of neural reflexes including both feedforward and feedback mechanisms. The feedforward component is termed central command,[29,30] referring to parallel afferent output from the central nervous system to both motor and cardiovascular structures. The effects include an abrupt increase in HR due to reduction of resting parasympathetic outflow to the heart, along with an increase in sympathetic outflow stimulating cardiac contractility, resulting in a near-instantaneous augmentation of HR, SV, and cardiac output at exercise onset. Essential to the cardiac output response is an increase in venous return to support preload.[31] This is mediated in part by the skeletal muscle pump, which translocates blood from dependent capacitance beds toward central venous vessels.[31,32] In health, thoracic pressure changes associated with ventilation also contribute to maintaining left ventricular preload.[33] Autonomic-mediated increases in venous tone of splanchnic and peripheral veins may also contribute to redistribution of blood flow, though the role of these mechanisms is debated.[34,35]

Simultaneously, afferent signals traveling in type III and IV fibers provide feedback from mechanoreceptors and metaboreceptors in skeletal muscle to activate the exercise pressor reflex.[36] The pressor reflex constitutes a diffuse increase in sympathetic outflow, to increase vascular resistance and decrease blood flow to regions with low metabolic needs. This is critical to maintenance of systemic blood pressure (BP), which would otherwise drop precipitously, compromising perfusion of both active muscle and vital organs. Titration of systemic BP during exercise is under the feedback control of the baroreflex, which operates at a higher pressure set point during exercise than rest,[37] such that mean arterial pressure rises.

The overall effect of these control mechanisms is that blood flow to the brain is preserved during exercise, and blood flow to active skeletal muscle and cardiac muscle is increased. Skin perfusion is also increased for heat dissipation, depending on exercise duration and environmental conditions. Blood flow to respiratory muscles increases in line with their oxygen consumption requirements, as ventilatory work increases.

A balance of central and peripheral mechanisms ultimately determines blood flow to the exercising muscle (►**Fig. 2D**). Local products of metabolism and/or responses triggered by metabo- or mechanosensing result in local vasodilation.[26,38] Titration of muscle blood flow to its metabolic needs reflects a balance of local vasodilating processes and persistent sympathetic tone, the results of which are reflected in systemic oxygen extraction (arterio-venous O_2 concentration difference, $C(a\text{-}v)O_2$; ►**Fig. 2C**). The locomotor muscles are the major contributor to increased oxygen extraction during exercise, and muscle venous PO_2 declines steeply with increasing work rate (WR) to a relatively stable nadir (approximately 15–20 mm Hg). The nadir muscle venous PO_2 differs little whether exercise is above or below LT, but muscle venous oxyhemoglobin saturation and oxygen content are lower at higher WRs, due to a shift in oxyhemoglobin dissociation curve as a result of increases in venous H^+ and CO_2 (the Bohr shift).[39] As a result, $C(a\text{-}v)O_2$ across exercising muscle (or the systemic circulation) increases progressively as $\dot{V}O_2$ rises (►**Fig. 2C**), even as average muscle capillary PO_2 remains relatively stable. The latter, together with longitudinal capillary recruitment to increase red blood cell apposition to muscle capillary endothelium, facilitates capillary to myocyte O_2 diffusion as WR increases.[40] Approaching peak exercise, vascular resistance toward the respiratory muscles may decline more than toward the exercising limbs, thereby diverting an increasingly greater fraction of the cardiac output away from the exercising limbs, potentially limiting peripheral muscle oxygen consumption.[41]

Ventilation and Pulmonary Mechanics

Similar to the cardiovascular responses, minute ventilation ($\dot{V}_E$) increases immediately at the onset of exercise. The increase in $\dot{V}_E$ at moderate-intensity exercise is predominately through increased tidal volume and, at higher intensities, by a progressive increase in breathing frequency (*f*). This pattern helps to ameliorate increases in the work of breathing by expanding tidal volume (V_T) over the most linear range of respiratory system compliance, constraining further increase where tissue compliance falls steeply. Breathing mechanics are generally viewed as not limiting to exercise in healthy non-athletes, as there is an apparent “breathing reserve” (BR) at peak exercise, i.e., maximum voluntary ventilation (MVV) considerably exceeds $\dot{V}_E$ at peak exercise (►**Fig. 3A**). Similarly, V_T as a fraction of inspiratory capacity (IC) does not typically exceed approximately 70%, so there is also an inspiratory reserve volume (IRV), and flow rates of spontaneous breaths remain below maximal forced flows (►**Fig. 3A**). This pulmonary reserve contrasts with cardiovascular responses, where a reserve in HR and cardiac output is typically absent in a progressive exercise test. Exceptions to the above pattern occur in endurance-trained individuals, and particularly trained females, whose capacity for oxygen delivery and utilization have increased to the point at which mechanical ventilatory reserves can be reduced or exhausted.[5] In these, the demand for high flow rates to service the ventilatory demand may cause dynamic hyperinflation (DH)—an increase in end-expiratory lung volume (EELV)—as flow rates at low lung volumes become limiting (►**Fig. 3B, C**).[42]

Control of $\dot{V}_E$ during exercise includes both feedforward and feedback neural processes. Central command is credited with an immediate increase in $\dot{V}_E$. Group III/IV metabo- and mechano-receptors in peripheral muscle,[43,44] and stretch receptors in the venous vasculature and cardiac muscle,[45] contribute afferent feedback input that may influence exercise ventilation, although considerable redundancy exists and the precise mechanism awaits discovery.[43] Titration of

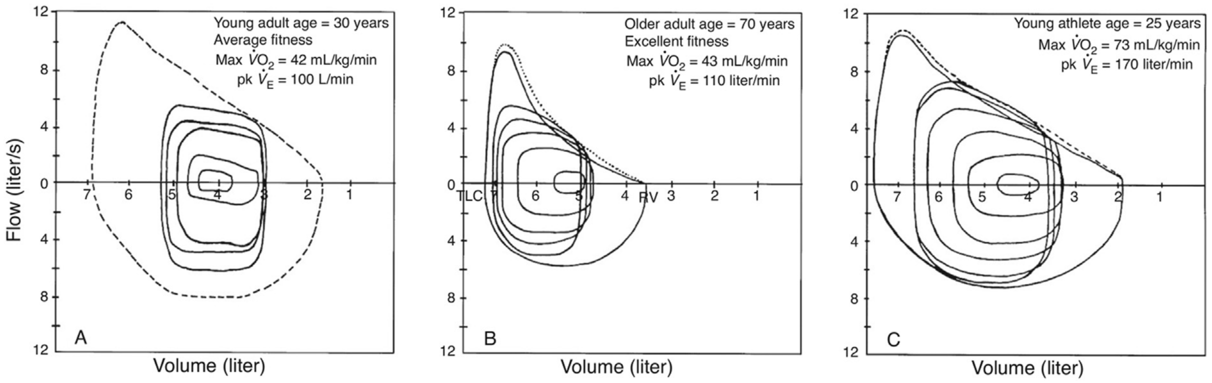

Fig. 3 Pulmonary flow volume loops in health. (**A**) Flow-volume response to exercise in the average fit healthy young adult during incremental exercise plotted within the maximal flow volume loop. In this population, end-expiratory lung volume (EELV) progressively decreases with exercise, and expiratory flow limitation is only present near EELV over a small portion of the tidal volume (V_T). Considerable room exists to increase ventilation even at peak exercise. Similar responses are also shown for the fit aged adult (**B**) and the young endurance athlete (**C**). The older adult (B) represents a group of individuals with a mild decline in lung function but maintenance of a high ventilatory demand. Flow limitation occurs at low work rates and $\dot{V}_E$ demand (40 L/min) and end-inspiratory lung volume at peak exercise reaches a higher percent of total lung capacity. This group has significant ventilatory constraint at peak exercise. The fit young athlete (C) represents a group of individuals with normal lung function but excessive ventilatory demands. EELV initially decreases during exercise like the average fit adult, but increases as significant expiratory flow limitation occurs. By peak exercise in the majority of these subjects, significant ventilatory constraint is observed similar to the aged, fit adult. (Reproduced with permission from Johnson et al[42].)

$\dot{V}_E$ after the initial hyperpnea is attributed to chemical responsiveness, evidenced by stability of arterial PCO_2 (P_aCO_2), which is maintained very close to resting values during exercise below LT. The mechanisms preserving P_aCO_2 in such a narrow range in the face of dynamic changes in $\dot{V}CO_2$ remain incompletely understood. For exercise above LT, there is an additional increment in $\dot{V}_E$, which compensates for the metabolic acidosis by reducing P_aCO_2, partially mitigating the increase in arterial H^+.

Pulmonary Gas Exchange

Pulmonary gas exchange is discussed in detail elsewhere in this series. In healthy individuals, alveolar ventilation ($\dot{V}_A$) increases considerably more than pulmonary perfusion ($\dot{Q}$) during exercise. Also, the relative dispersion of $\dot{Q}$ increases in heavy exercise in trained individuals, but to a lesser degree than for $\dot{V}_A$,[44] meaning that $\dot{V}_A/\dot{Q}$ mismatch increases in exercise, likely contributing to gas exchange inefficiency. Hyperventilation and $\dot{V}_A/\dot{Q}$ mismatch contribute to widening of the alveolar–arterial PO_2 difference ($P(A\text{-}a)O_2$) from approximately 5 mm Hg at rest to approximately 25 mm Hg in heavy-intensity exercise in trained individuals. In some athletes, high-intensity exercise leads to exercise-induced arterial hypoxemia, attributed to a combination of a relative hypoventilation (due to respiratory mechanical constraints in those with high ventilatory demand), diffusion limitation, $\dot{V}_A/\dot{Q}$ mismatch, and intrapulmonary shunting, although the contribution of each is still debated.[46–49] The increase in body temperature and metabolic acidosis above LT shift the oxyhemoglobin dissociation curve rightward, which also reduces S_aO_2 relative to P_aO_2. These effects are exacerbated by exercise training and may be marked in highly conditioned athletes.[50]

Despite the greater overall increase in $\dot{V}_A$ relative to $\dot{Q}$, the increased challenges to gas exchange efficiency during moderate- and high-intensity exercise, and the increased CO_2 concentration of the pulmonary perfusate, the ratio of $\dot{V}_E$ relative to $\dot{V}CO_2$ decreases with exercise. $\dot{V}_E/\dot{V}CO_2$ is reduced from values of around 40 at rest to 20 to 30 during moderate-intensity exercise, implying more efficient elimination of CO_2 per unit increase in $\dot{V}_E$. For exercise above LT, $\dot{V}_E/VCO_2$ values rise above their nadir values due to increased $\dot{V}_E$ that compensates for the metabolic acidosis. Standard expressions of gas exchange efficiency can be calculated during exercise using arterial blood gas measures and corresponding gas exchange data. For O_2 exchange, this is the $P(A\text{-}a)O_2$ for which the P_AO_2 is calculated from the alveolar gas equation:

$$P_AO_2 = F_IO_2 \times (P_B - 47) - P_aCO_2 / R$$

where P_B is barometric pressure, 47 is the partial pressure of water vapor at body temperature, and R is the simultaneously measured ratio of $\dot{V}CO_2/\dot{V}O_2$. As noted previously, in healthy individuals, $P(A\text{-}a)O_2$ increases progressively during exercise.

For CO_2 exchange, efficiency is calculated as the physiologic dead space volume to tidal volume ratio (V_D/V_T), using the Enghoff modification of the Bohr equation, which reflects the degree of difference in the partial pressures of CO_2 in exhaled breath compared with arterial blood:

$$V_D / V_T = [P_aCO_2 - (\dot{V}CO_2 / \dot{V}_E)] / P_aCO_2$$

where $\dot{V}CO_2/\dot{V}_E$ is used to quantify mixed expired PCO_2 ($P_{\bar{E}}CO_2$).

Using this approach, the calculated V_D/V_T reflects not only the truly unperfused portion of each breath (dead space), but also the effect on CO_2 elimination of areas that are underperfused relative to ventilation (e.g., high $\dot{V}_A/\dot{Q}$ regions).[51] In healthy individuals, V_D/V_T decreases progressively over the course of graded exercise.[52] The decrease in V_D/V_T is attributable in considerable part to the greater increase in V_T relative to the much smaller increase in anatomic dead space. While it would seem likely that recruitment of the pulmonary capillary circulation due to increased perfusion would also tend to reduce high $\dot{V}_A/\dot{Q}$ regions during exercise, analyses of $\dot{V}_A/\dot{Q}$ distribution using the multiple inert gas elimination techniques have not demonstrated a reduction in $\dot{V}_A/\dot{Q}$ mismatch from rest to moderate exercise in healthy people.[53]

Exercise Intensity

How long an exercise task can be maintained at a given power output, i.e., endurance or exercise tolerance, is clearly of importance with respect to sustaining personal, occupational, or athletic activities. While endurance athletic performance may be broadly correlated with $\dot{V}O_{2max}$, stratifying WRs into discrete domains of exercise intensity, defined by metabolic factors influencing exercise tolerance for the individual, affords more precise prediction of exercise tolerance. Key features of this are illustrated in ►**Fig. 4**, which shows changes in $\dot{V}O_2$, tolerable duration, and lactate concentration over time for four endurance WRs in healthy individuals.[54] These responses illustrate three discrete intensity domains: moderate, heavy, and very heavy (the latter has also been termed severe). It must be acknowledged that there are several models proposed to classify exercise intensity, and both the models and the distinctions derived from them have limitations.

Moderate-Intensity Exercise

Moderate-intensity exercise encompasses WRs below LT and is characterized by a $\dot{V}O_2$ response that increases from baseline to reach a new steady state (►**Fig. 4A**). This occurs within 2 to 3 minutes in healthy individuals. The increment in steady state $\dot{V}O_2$ relative to WR has a consistent relationship of 9 to 11 mL/min/watt. This relationship varies little between individuals by age, state of training, or even in chronic disease conditions, and reflects the intrinsic bioenergetics of skeletal muscle aerobic metabolism when carbohydrate is the primary substrate. In the moderate-intensity domain, there may be a transient rise in lactate concentration in the earliest minutes of exercise, but this intensity is characterized by the ability to stabilize lactate concentration at or below the resting value (►**Fig. 4C**). Moderate-intensity exercise can therefore be sustained for hours, and its energy demands met by wholly aerobic ATP supply. Endurance time for moderate-intensity exercise might well be dictated by factors external to the exercise itself.

It is perhaps worth noting that an intensity domain below moderate likely exists (light-intensity exercise), and would describe a range of power outputs that could be sustained functionally indefinitely, i.e., measured in units of months. The $\dot{V}O_2$ and blood lactate characteristics in this domain would be essentially the same as moderate-intensity exercise, but the maximum metabolic rate for light intensity would be much lower. It has been suggested, based on running data from the transcontinental Race Across the USA, that light-intensity exercise may be limited by the rate at which the alimentary system can provide nutrition to sustain exercise of this type; elite athletes being limited in this domain to metabolic rates of approximately 10 mL/min/kg.[55]

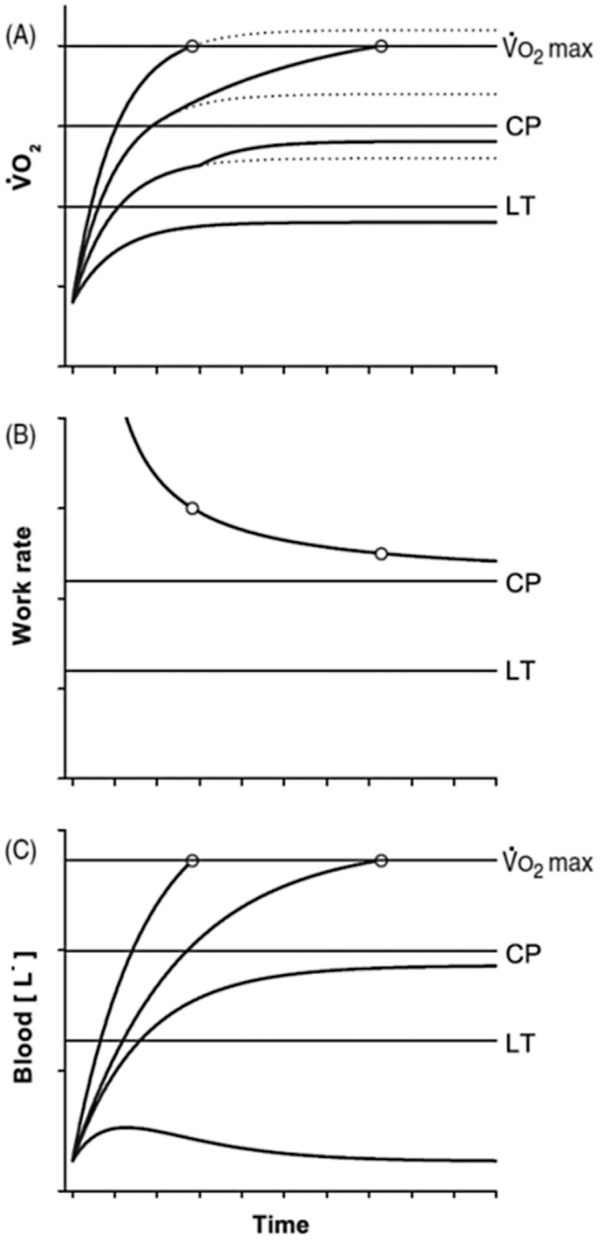

Fig. 4 Exercise intensity domains and the power–duration relationship. Schematic of characteristics of three different exercise intensity domains: moderate (<LT), heavy (>LT but <CP), and very heavy (>CP). In panels (**A**) and (**C**), physiologic responses are shown for one moderate, one heavy, and two very heavy intensity exercise bouts. Panel (**B**) shows the endurance time for the two very heavy intensity work rates connected by the individual power–duration relationship. (A) $\dot{V}O_2$ for heavy or very heavy exercise is higher than would be predicted (dotted lines) from steady-state increments in the moderate range, increasing to reach $\dot{V}O_{2max}$ in very intensity exercise. (B) Endurance time is a hyperbolic function of work rate, with an asymptote at critical power (CP). (C) Stable lactate concentration is reached for moderate and heavy intensity, but not in very heavy intensity exercise. CP, critical power; LT, lactate threshold. (Reproduced with permission from Rossiter[54].)

Heavy-Intensity Exercise

Exercise in the heavy-intensity domain (WRs above LT but below critical power [CP]; see below) is characterized by an elevated but stable lactate concentration (typically approximately 2–4 mM) and a $\dot{V}O_2$ response that may take up to 20 minutes after exercise onset to reach dynamic equilibrium (►**Fig. 4A, C**).[55] Exercise in the heavy-intensity domain has reduced efficiency, demonstrated by the attainment of a $\dot{V}O_2$ that is 0.5 mL/min/watt greater than the expected value of 9 to 11 mL/min/watt, i.e., an approximately 5% reduction in work efficiency. This additional $\dot{V}O_2$ is termed the $\dot{V}O_2$ "slow component" and is thought to relate to the effects of muscle fatigue on increasing the ATP demand to maintain mechanical output.[56–58] Exercise in this domain is terminated without reaching $\dot{V}O_{2max}$. Most exercise tasks in the heavy domain would be sustainable for approximately 1 hour, and potentially more, depending on factors such as muscle glycogen storage, body temperature or hydration status, or other environmental conditions.[59]

Very Heavy Intensity Exercise

WRs above CP are termed very heavy (or severe). The upper WR limit of this domain varies depending on the model used, but in any case, these WRs are characterized by the attainment of $\dot{V}O_{2max}$ at the tolerable limit. In the very heavy intensity domain, both $\dot{V}O_2$ and lactate concentration increase throughout exercise (►**Fig. 4A, C**).[60,61] Here, the $\dot{V}O_2$ slow component can cause $\dot{V}O_2$ increments to reach values of approximately 14 mL/min/watt, equivalent to an approximately 40% loss of work efficiency.[60] Exercise in the very heavy intensity domain illustrates the classical definition of $\dot{V}O_{2max}$,[62] because no matter the WR used in this domain, $\dot{V}O_2$ reaches the same value at the tolerable limit. Exercise in this domain is typically limited to less than approximately 30 minutes and is highly dependent on motivation.

Power–Duration Relationship and Exercise Tolerance

The inverse relationship between WR and tolerable duration in the very heavy intensity domain is termed the power–duration relationship and is hyperbolic in nature (►**Fig. 4B**). Extrapolation of this power–duration relationship identifies an asymptote, which is termed CP. CP demarks a metabolic rate above which a dynamic equilibrium in $\dot{V}O_2$, lactate concentration, and muscle metabolism can no longer be achieved, and is therefore the upper boundary of heavy-intensity exercise.[63–65] CP is typically about half way between WRs at LT and $\dot{V}O_{2max}$, but can vary widely (approximately 30–80%) by age or state of training.[11]

Summary of Exercise Intensity

The concept of distinct intensity domains (►**Fig. 4**) provides a framework for considering the capacity for various activities ranging from those that can be performed for hours at a time with minimal metabolic perturbation, to those having energy requirements above $\dot{V}O_{2\ max}$, but which can nevertheless be performed for a finite duration. Intensity domains may be demarked by LT, CP, and $\dot{V}O_{2max}$, which are each modifiable (both in absolute terms and in their relative proportions) by exercise training or chronic disease. LT and $\dot{V}O_{2max}$ can be assessed by gas exchange using incremental exercise tests, as discussed in the next section. CP demarcates heavy from very heavy intensities, and is relevant to exercise prescription and for optimizing athletic performance, but is more challenging to identify.

Cardiopulmonary Exercise Testing

Introduction to Cardiopulmonary Exercise Testing

CPET incorporates measurement of ventilation and pulmonary gas exchange along with electrocardiogram (ECG) and BP, during a standardized exercise stress. Here we describe elements of routine clinical CPET, commonly measured variables and their relevance to some common conditions, and applications of CPET in medical practice.

Protocols and Procedures

Most CPET utilizes graded (incremental), symptom-limited protocols, in which WR is increased progressively over a single uninterrupted test to the maximum tolerated level. Extensive experience has resulted in established practice standards[66–70] and a defined safety profile[71–73] for this kind of exercise stress.

Treadmill and cycle ergometer are most commonly used for CPET in clinical practice; both engage a large, although not identical, mass of skeletal muscle. Most individuals reach a higher $\dot{V}O_2$ on treadmill testing,[74,75] so this is arguably preferred for eliciting truly maximal responses. Also, patients with hypoxemic lung disease typically have more marked arterial oxygen desaturation on treadmill testing compared with cycle,[76,77] and patients dependent on rate-adaptive pacemakers may have a greater pacemaker response on treadmill. On the other hand, because the body weight is supported during cycling, it may be preferable for individuals with severe impairment, or with gait or balance difficulties. There is less body movement during cycling, which minimizes motion artifact in ECG or other signals, and the ergonomics of cycling are less variable than of walking in the face of changing WR, so cycle exercise allows more precise quantification of external WR.[78] In some circumstances, such as evaluation of competitive athletes or individuals in highly physical occupations, it may be desirable to customize exercise formats or ergometers to mimic the sport or occupation.

There are many eponymous graded exercise testing protocols in clinical use. While all may serve to elicit maximal responses, they may be less suited for discrimination of submaximal variables, e.g., LT. These are best identified from tests with gradual and linear transition of WRs through intensity domains. Recommended protocols for CPET thus begin, after a baseline of rest, with a nominal (moderate intensity) WR, continued for several minutes for establishment of a steady state, followed by increases in WR in frequent equal increments or as a continuous "ramp" function.[79,80] Conventional wisdom is that peak performance is optimized when the graded portion of a CPET is 8 to 12 minutes in duration,[80] but longer or shorter tests should have similar peak results in most cases.

The work profile represented by graded tests is designed to span the aerobic range in a short period of time, and not intended to mimic spontaneous daily activities. Responses to laboratory tests may thus not extrapolate directly to other modes of exercise. Routine CPET also does not measure all potential aspects of exercise pathophysiology. These limitations notwithstanding, graded, symptom-limited CPET protocols provide a meaningful profile of exercise function in a defined set of variables, and can be readily repeated for serial assessments. Other protocols, utilizing constant WRs, may be used, e.g., to mimic recreational or occupational conditions, for bronchoprovocation, or address other specific questions. Constant WR exercise protocols for determination of endurance time are especially useful for serial testing in studies of clinical interventions.[11] This is due to the shape of the power–duration curve (►**Fig. 4B**), for which small increments in peak or threshold values translate into substantial increases in endurance time over the asymptotic range of the relationship.[81,82]

Measurements

Primary physical measurements in CPET are respiratory flow rates, gas tensions in respired breath, and time. From these are calculated $\dot{V}_E$, V_T, f, $\dot{V}O_2$, $\dot{V}CO_2$, and end-tidal partial pressures of O_2 ($P_{ET}O_2$) and CO_2 ($P_{ET}CO_2$). Additional variables are derived from these, including slopes, quotients, or differences of the values. Typically, additional instrumentation is used to measure HR and ECG; pulse oximetry (SpO_2); BP; and WR, which can be measured when using a cycle ergometer, or estimated when using a treadmill. Widely available commercial instruments calculate $\dot{V}_E$ and gas exchange, most commonly on a breath-by-breath basis,[83] and include software that automates calibration, calculations, data storage, and reporting. This not only makes CPET readily adaptable to clinical settings, but also distances the user from the measurement processes, so attention to quality control and data validation remain essential to ensure accuracy.[83–85]

Cardiopulmonary Exercise TestingVariables

Variables typically reported from noninvasive CPET are grouped here under broad headings of those most related to: (1) oxygen delivery and utilization, i.e., cardiovascular and metabolic; (2) mechanics of breathing; and (3) efficiency of pulmonary gas exchange.[78] These processes are highly interdependent and interactive, so such grouping should be taken as a practical approach to organizing data rather than an implication that the underlying processes can be viewed in isolation.

Oxygen Delivery and Utilization

- *Peak oxygen uptake* ($\dot{V}O_{2peak}$): as identified earlier, $\dot{V}O_{2max}$ is a task-specific value which, in health, is primarily a reflection of the cardiovascular capacity for oxygen delivery, but may be limited by constraint or disease in other organ systems. The classical definition of $\dot{V}O_{2max}$ is rarely met during CPET, so the highest $\dot{V}O_2$ value, averaged over the last 20 to 30 seconds of the test, is termed the $\dot{V}O_{2peak}$ (►**Fig. 5A**). Adding a brief "confirmation" bout of high WR exercise at the end of the graded test has been proposed to determine if the definition of $\dot{V}O_{2\,max}$ is satisfied,[86–88] but this is not widely utilized.
- *Oxygen uptake to WR slope* ($\Delta\dot{V}O_2/\Delta WR$): for a linear increase WR over time (after a short lag related to $\dot{V}O_2$ kinetics), there is progressive increase of $\dot{V}O_2$ which has a slope similar to the 9 to 11 mL/min/watt established from moderate-intensity steady-state exercise measures. This

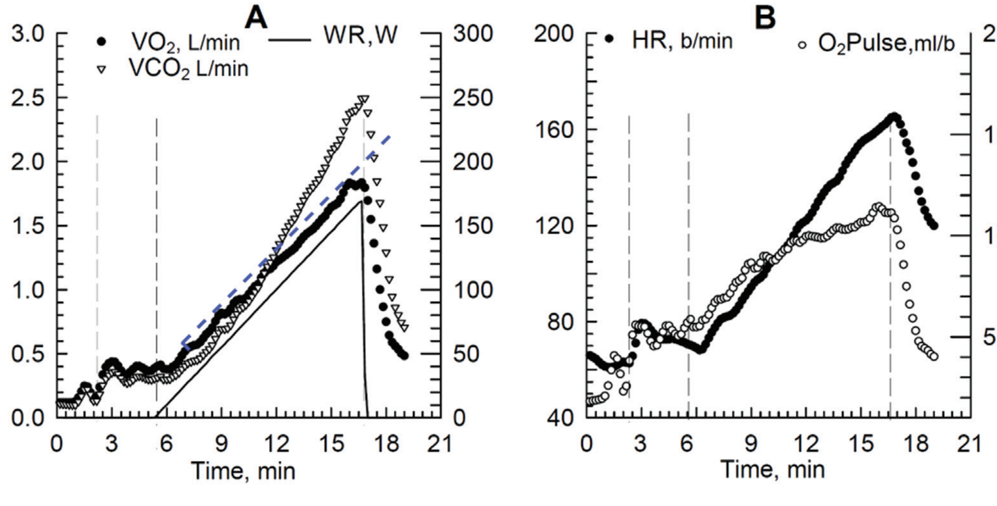

Fig. 5 $\dot{V}O_2$, $\dot{V}CO_2$, work rate (WR), and heart rate (HR) during incremental cycle exercise. Data are from a cycle ergometer CPET performed by a healthy 48-year-old woman. The protocol was 3 minutes of rest, 3 minutes of pedaling without resistance followed by incremental increase in WR at a rate of 15 W/min, and 2 minutes of active recovery without resistance; protocol phases are demarcated by vertical dotted lines. (**A**) $\dot{V}O_2$ (closed circle), $\dot{V}CO_2$ (open triangle), and work rate (solid line) plotted as a function of time in minutes. The diagonal dashed blue line parallels the $\dot{V}O_2$ data beginning shortly after onset of incremental work and has a slope of approximately 10 mL/min/watt (i.e., parallel with work rate when scaled appropriately). (**B**) HR (closed circle) and $\dot{V}O_2$/HR (open circle) plotted as a function of time in minutes. CPET, cardiopulmonary exercise testing.

slope is typically near-linear over the duration of a graded test, as shown in ►**Fig. 5A**. The apparent absence of the $\dot{V}O_2$ "slow component" in the upper range is attributable to the slow $\dot{V}O_2$ kinetics being obscured by the relatively rapid progression in WR.[89,90] Consistent with this, upward or downward deviation of the slope above LT is apparent with particularly slow or rapid WR incrementation, respectively.[91]

Abnormally low $\Delta\dot{V}O_2/\Delta WR$ slopes are sometimes evident in disorders of oxygen utilization, e.g., metabolic myopathy[92] or oxygen delivery, e.g., cardiovascular disease,[92] and downward deflection of an initially normal slope may mark the onset of exercise-induced myocardial ischemia.[93] These low slopes do not indicate higher metabolic efficiency, but rather failure to keep pace with rising oxygen requirements in the nonsteady-state conditions of the test.[94] This is mirrored in the recovery phase as a slow progression of $\dot{V}O_2$ to re-attain its baseline rate.[92]

Ergonomic factors can also alter the $\Delta\dot{V}O_2/\Delta WR$ slope, particularly during treadmill exercise as gait changes following adjustments in grade or speed can change economy of movement. Also, use of handrails to support the body weight can markedly reduce the actual work being performed. For these and other reasons, the $\Delta\dot{V}O_2/\Delta WR$ slope is usually only interpreted for cycle tests.

- *Peak HR*: HR is usually identified from the RR interval of the ECG signal, calculated over several cardiac cycles, and peak HR averaged over the same interval as other peak values (►**Fig. 5B**). Peak HR is age-dependent, but with a standard deviation of approximately 10 beats/min in healthy unmedicated individuals, it has a wide normal range.
- *Oxygen pulse ($\dot{V}O_2$/HR or O_2 pulse)*: the oxygen pulse[95] (►**Fig. 5B**) has units of mL of O_2 per heart beat. This variable is derived from expressing $\dot{V}O_2$ in terms of the Fick relationship, with each side of the equation divided by HR. This identifies that O_2 pulse, which is easily determined from noninvasive measures, and is numerically equal to the product of cardiac SV and O_2 extraction, important functions that are less readily measured:

$$\dot{V}O_2 = \dot{Q} \times C(a-v)O_2 \text{ (Fick relationship)}$$
$$\dot{V}O_2 / HR = SV \times C(a-v)O_2 \text{ (}O_2\text{ pulse)}$$

Peak O_2 pulse is increased in the setting of isolated chronotropic impairment, reflecting the associated augmentation of SV. Low values conversely might reflect reduced SV; however, constraint of $C(a\text{-}v)O_2$ due to anemia, hypoxemia, or impaired peripheral oxygen diffusion or utilization might also be responsible. A plateau of O_2 pulse at a low value, despite increasing WR, suggests a low maximal SV and/or $C(a\text{-}v)O_2$, or reciprocal changes in the two factors.

- *Chronotropic index ($\Delta HR/\Delta\dot{V}O_2$)*: HR is normally a linear function of $\dot{V}O_2$ (►**Fig. 6A**).[96] In endurance-trained individuals, the relationship is shifted downward due to greater resting and exercising SV. Shallow slopes can result from impaired chronotropy, and a steep or steepening slope can result from cardiovascular or muscle impairments.
- *GET*: noninvasive estimation of LT is made using combined gas exchange and ventilatory criteria.[97] The primary relationship to identify GET is the plot of $\dot{V}CO_2$ relative to $\dot{V}O_2$ (termed the "V-slope"), which inflects upward to exceed a baseline slope of approximately 1.0 (►**Fig. 6A**)

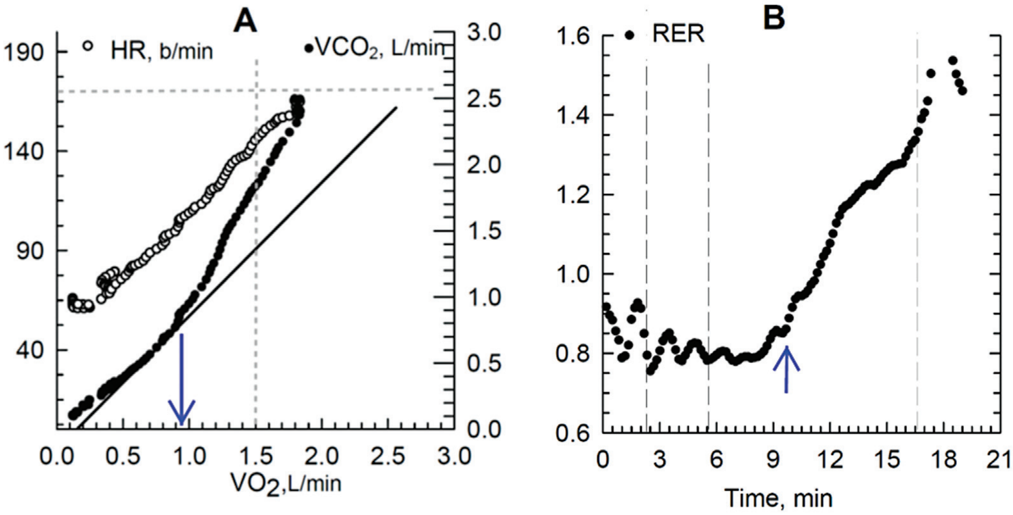

Fig. 6 Oxygen uptake ($\dot{V}O_2$), carbon dioxide output ($\dot{V}CO_2$), and heart rate (HR) relationships for the same CPET described in ►**Fig. 5**. (**A**) HR (open circle) increases linearly relative to $\dot{V}O_2$. The horizontal and vertical dashed lines indicate the predicted peak HR and $\dot{V}O_2$, respectively, for this individual. $\dot{V}CO_2$ (solid circle) as a function of $\dot{V}O_2$ ("V-slope"). Diagonal solid line references a slope of 1.0 for this relationship, and the blue arrow identifies the inflection point to a steeper slope, typical of the gas exchange threshold (GET). (**B**) Respiratory exchange ratio (RER) calculated as $\dot{V}CO_2/\dot{V}O_2$, plotted as a function of time. RER increases toward 1.0 during moderate exercise and more steeply above GET. Arrow indicates RER at time corresponding to GET identified from V-slope, at which RER typically is still below a value of 1.0. CPET, cardiopulmonary exercise testing.

(not to be confused with a respiratory exchange ratio (RER) value of 1.0; ►**Fig. 6B**). The acceleration of $\dot{V}CO_2$ relative to $\dot{V}O_2$ reflects the output of additional CO_2 from bicarbonate buffering of the metabolic acidosis, which augments the rate of CO_2 from oxidative metabolism.[11,92,97] Hyperventilation of any cause would also be associated with an inflection in the $\dot{V}CO_2$–$\dot{V}O_2$ relationship, and so is usually excluded by review of other variables. Specifically, in the absence of spurious hyperventilation, an inflection of $\dot{V}_E/\dot{V}O_2$ (also termed ventilatory equivalent for O_2) and $P_{ET}O_2$ precede changes in $\dot{V}_E/\dot{V}CO_2$ (ventilatory equivalent for CO_2) and $P_{ET}CO_2$, reflecting an immediate response of $\dot{V}_E$ to the excess CO_2 and delayed response to metabolic acidosis.[92]

- *RER ($\dot{V}CO_2/\dot{V}O_2$)*: under steady-state conditions of rest or moderate exercise, RER may range from 0.71 to 1.0 and is linearly proportional to the mix of substrate being oxidized by the whole body (fatty acids = 0.71; carbohydrates = 1.0). However, under nonsteady-state conditions—where a graded CPET is entirely nonsteady state—RER is also a function of differing kinetics of $\dot{V}O_2$ and $\dot{V}CO_2$, the progressive rise in the proportion of gas exchange arising from exercising muscle, and, in the range above LT, the additional CO_2 evolved from acid buffering and hyperventilation. These two latter responses cause RER to increase progressively from LT to peak exercise such that an end exercise value above approximately 1.1 is expected (►**Fig. 6B**). The exact value of RER attained on a maximal test is variable, however, it is affected by the test protocol.[86] So while end exercise RER is often used in the assessment of test adequacy, no single cut-off RER value identifies whether a test is maximal. In the immediate postexercise period, there is normally a further steep increase in RER, due to the more rapid kinetics of $\dot{V}O_2$ relative to $\dot{V}CO_2$ as they recover toward their resting baselines. Transient episodes of hyper- or hypoventilation can distort the normal pattern of RER during a CPET, as $\dot{V}CO_2$ is affected by these to a much greater extent than $\dot{V}O_2$.

Breathing Mechanics

- *Peak ventilation ($\dot{V}_E$) and BR*: BR refers to the absolute or percent difference of peak $\dot{V}_E$ (►**Fig. 7**) and the capacity for pulmonary ventilation, with the latter conventionally taken as MVV (►**Fig. 7**). A BR of less than 15% of MVV has been proposed as indicating ventilatory limitation,[70] resulting either from low breathing capacity and/or from high $\dot{V}_E$ demand. Because the MVV maneuver is not always performed, or not performed optimally, estimates of MVV from FEV_1 multiplied by a factor of 35 to 40 are often used to estimate MVV. As the MVV is itself a rough estimate of breathing capacity, and peak $\dot{V}_E$ may be affected by the test protocol, the BR is not a particularly a precise measure.
- *Tidal volume (V_T) and breathing frequency (f)*: initial increases in $\dot{V}_E$ are primarily by an increase in V_T up to a V_T approaching approximately 70% of IC, after which V_T remains relatively stable and breathing frequency rises (►**Fig. 7**; see also ►**Fig. 8**). Individuals' breathing patterns vary related to respiratory system compliance and other factors.[98] However, some notable patterns diverging from normal may be identified. An oscillatory breathing pattern is seen in some individuals with severe heart failure.[98] Oscillatory breathing is characterized by cyclic variations in $\dot{V}_E$, primarily due to V_T, but also affecting other variables, with a period of 50 to 100 seconds, and is recognized as an indicator of poor prognosis in heart failure. Other patterns observed in individuals with

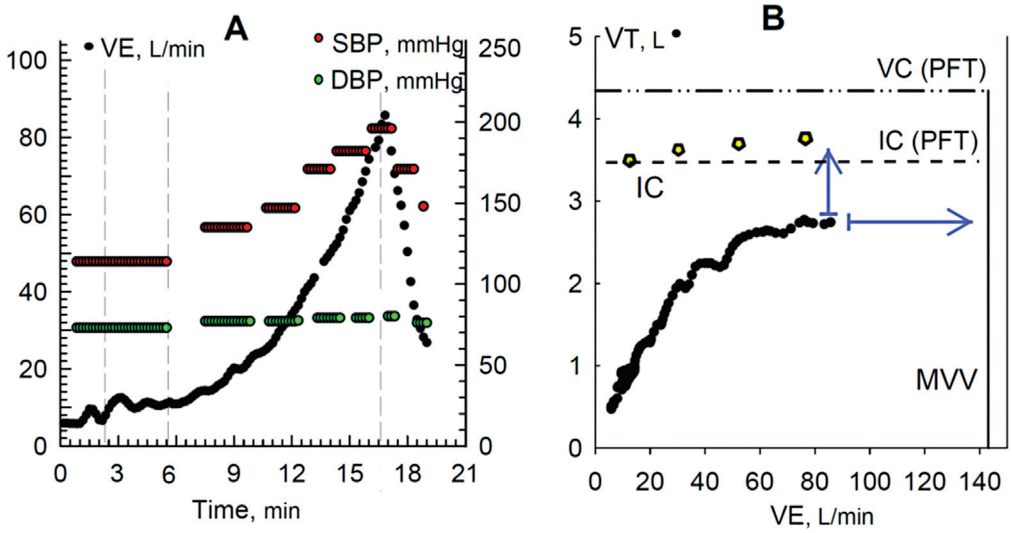

Fig. 7 Ventilation and breathing pattern from the same CPET described in ►**Fig. 5**. (**A**) Ventilation ($\dot{V}_E$) as a function of time in minutes (solid circle). Also plotted are systolic blood pressure (SBP; red circles) and diastolic blood pressure (DBP; green circles). (**B**) Tidal volume (V_T) as a function of $\dot{V}_E$ (solid circles) and periodic measurement of inspiratory capacity (IC) (yellow symbols). Horizontal dashed lines indicate resting measures of vital capacity [VC (PFT)] and inspiratory capacity [IC (PFT)]. Vertical solid line indicates maximal voluntary ventilation (MVV). The horizontal blue arrow indicates the breathing reserve defined by the difference between peak $\dot{V}E$ and MVV, and vertical blue arrow the inspiratory reserve volume, defined by the difference between V_T and IC. CPET, cardiopulmonary exercise testing.

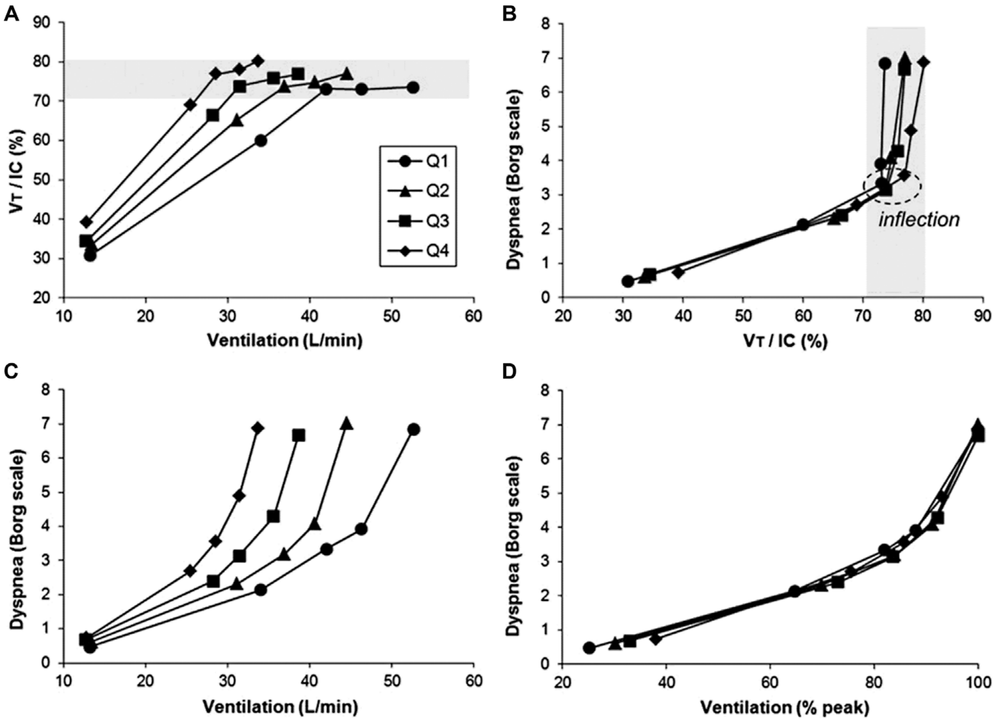

Fig. 8 Relationships of ventilation, operational lung volumes, and dyspnea during exercise across a spectrum of chronic obstructive lung disease (COPD) severity. Group mean values for quartiles of patients stratified by forced expiratory volume in 1 second (FEV_1) during constant work rate cycle exercise at 75% of incremental peak work rate. Values shown at matched time points in exercise, at individual V_T inflection points (defined by plateau of V_T as $\dot{V}_E$ continues to rise), and at peak exercise. (**A**) V_T/IC related to $\dot{V}_E$: all patients increase V_T up to a limit of $V_T/IC \approx 70–80\%$, regardless of severity of lung dysfunction, but the rate of rise is faster, and the threshold reached sooner, for progressively worse lung function. (**B**) Dyspnea related to V_T/IC: dyspnea increases markedly around a threshold of $V_T/IC \approx 70–80\%$ regardless of severity of lung dysfunction. (**C**) Dyspnea related to $\dot{V}_E$: dyspnea increases more quickly, and severe dyspnea is reached at lower levels of $\dot{V}_E$, with progressive severity of lung dysfunction. (**D**) Same relationship as in (C), but with $\dot{V}_E$ expressed as %peak: dyspnea rises equally for all severities of lung dysfunction. (Reproduced with permission from O'Donnell et al[125].)

unexplained dyspnea and termed "dysfunctional breathing," include highly irregular variation in tidal volumes or overt hyperventilation.[99,100] Another distinct cause of exertional dyspnea, exercise-induced laryngeal obstruction, is characterized by more subtle changes in inspiratory time and flow rates that may not overtly alter the V_T and *f* pattern.[101]

- *Expiratory flow limitation (EFL)*: mechanical constraints on breathing, in both health and disease, are most likely to occur during expiration.[102] EFL is often quantified as the percentage (%EFL) of exhaled tidal volume corresponding to maximal flow rates, based on analysis of flow volume loops (►**Fig. 9A**).[102] For this, spontaneous breaths are positioned within maximal loops[42] anchored on the volume axis by serial measures of IC (►**Fig. 9B**). To avoid errors related to exertional changes in airway tone, the maximal loop should ideally be measured immediately postexercise and, to avoid artifacts from thoracic gas and airway compression, should be constructed from a series of submaximal efforts.[103] Other approaches to detecting flow limitation include application of negative pressure at the mouth during exhalation[104] or geometric analysis of the spontaneous tidal expiratory flow volume relationships.[105] Identification of EFL is of significance as the factor leading to changes in operational lung volumes and DH, as described below.
- *Operational lung volumes*: increases in V_T during exercise are predominantly a result of increase in end-inspiratory lung volume (EILV; ►**Fig. 9B**), usually with an additional decrease in EELV due to active exhalation (also see ►**Fig. 3A**). Changes in IC measured during CPET are used to infer reciprocal changes in EELV, assuming, of course, that the IC maneuvers are consistently maximal, and not compromised by respiratory muscle fatigue or inspiratory airflow obstruction. These measures are of particular relevance to obstructive lung disease,[106] as a decrease in IC implies increased EELV, termed "dynamic hyperinflation" resulting from EFL and incomplete exhalation. With DH, V_T cycles over higher absolute lung volumes, which may include the flat portion of the respiratory compliance curve, and causes intrinsic positive end expiratory pressure, which increase work of breathing. These changes are associated with dramatic increase in dyspnea, occurring when IRV decreases below a critical value.[107] Importantly, DH can occur across a broad spectrum of chronic obstructive pulmonary disease (COPD) severity (►**Fig. 8**), making this a particularly valuable assessment when symptoms seem disproportionate to resting lung function impairment.

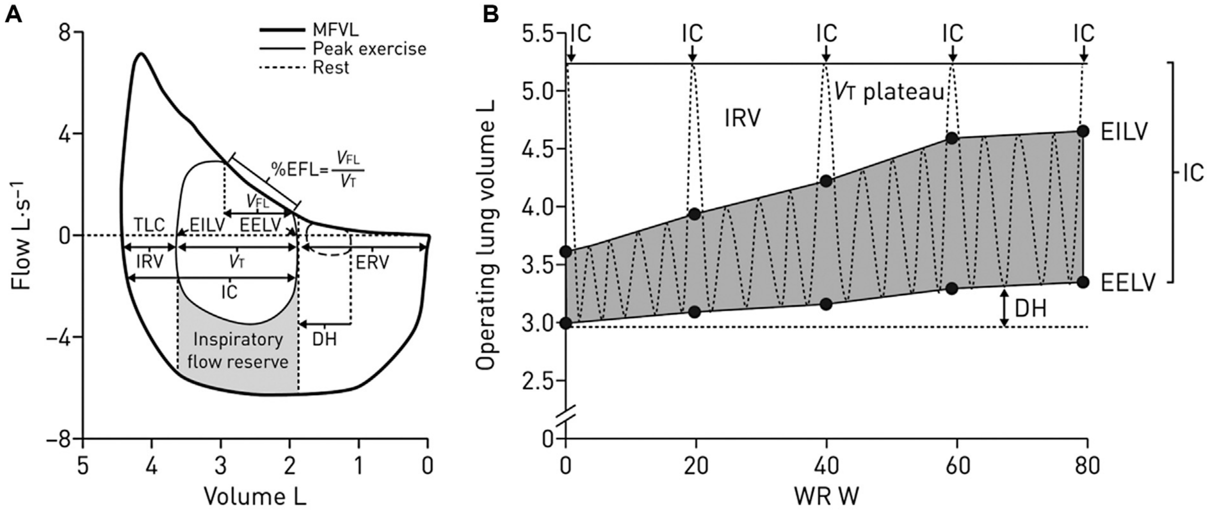

Fig. 9 Operational lung volumes during exercise. (**A**) Resting and peak exercise spontaneous flow volume loops within maximal flow volume loop (dark line) of an individual with chronic obstructive pulmonary disease. (**B**) Tidal volumes relative to total lung volume during graded exercise. DH, dynamic hyperinflation; EELV, end-expiratory lung volume; EFL, expiratory flow limitation; EILV, end-inspiratory lung volume; ERV, expiratory reserve volume; IC, inspiratory capacity; IRV, inspiratory reserve volume; MFVL, maximal flow volume loop; TLC, total lung capacity; V_{FL}, volume of flow limitation; V_T, tidal volume; W, watts; WR, work rate. (Reproduced with permission from O'Donnell et al[157].)

Pulmonary Gas Exchange Efficiency

- *Oxygen saturation by pulse oximetry (SpO_2)*: adequacy of oxygenation can be assessed noninvasively by pulse oximetry estimates of S_aO_2 (►**Fig. 10C**). Oximetry is most useful for tracking changes in hypoxemic patients during exercise. Because several factors affect the accuracy of exercise pulse oximetry,[108,109] unexpected low values may require verification.
- *Ventilatory efficiency ($\dot{V}_E/\dot{V}CO_2$ nadir and $\Delta\dot{V}_E/\Delta\dot{V}CO_2$ slope)*: the relationship of $\dot{V}_E$ to $\dot{V}CO_2$ has emerged as an important CPET outcome, reflecting disease severity, gas exchange inefficiency, and prognosis in both pulmonary[110] and cardiovascular[111] diseases. It is characterized either as the absolute ratio $\dot{V}_E/\dot{V}CO_2$ at its nadir shortly after GET (►**Fig. 10A**) or the slope of $\Delta\dot{V}_E/\Delta\dot{V}CO_2$ (►**Fig. 10B**). The slope is most appropriately measured over the linear portion of the relationship, prior to development of respiratory compensation for metabolic acidosis (as indicated in ►**Fig. 10B**). The $\dot{V}_E/\dot{V}CO_2$ relationship can be seen as determined by the set point for P_aCO_2 and the effective V_D / V_T:

$$\dot{V}_E / \dot{V}CO_2 = 863 / P_aCO_2 * (1 - V_D / V_T)$$

Elevation of $\dot{V}_E/\dot{V}CO_2$ thus occurs in diverse conditions associated with alterations in pulmonary $\dot{V}_A/\dot{Q}$, ventilatory drive, and/or acid–base balance.

Considerable attention has been given to $\dot{V}_E/\dot{V}CO_2$ in heart failure, and relating it to elevated V_D/V_T.[112] Elevated $\dot{V}_E/\dot{V}CO_2$ also, although not always,[113] results from some degree of hypocapnia, reflecting heightened ventilatory drive. The increased ventilatory drive has been linked to heightened stimulus from peripheral mechano- or ergo-receptors[114] and/or chemoreceptors in the carotid bodies.[115] The basis for the increased physiologic V_D/V_T in heart failure has eluded simple explanation. Reduced tidal volume may be a factor and was identified as the major determinant of elevated V_D/V_T in one analysis.[116] In a review of the physiology of respiratory dead space, Robertson[51] reminds us that well-established models of pulmonary gas exchange[117] predict that any increased $\dot{V}_A/\dot{Q}$ inhomogeneity (even in the absence of true dead space) will lead to an increase in calculated V_D/V_T, and that this effect will be amplified as the overall $\dot{V}_A/\dot{Q}$ ratio rises. Although overall $\dot{V}_A/\dot{Q}$ rises during exercise even in healthy individuals, in heart failure, augmented ventilatory drive, low resting cardiac output, and constraint of the exercise cardiac output response together can result in an exceptionally high overall $\dot{V}_A/\dot{Q}$. Several factors, therefore, including augmented ventilatory stimulation, impaired cardiac output, and constrained breathing mechanics, appear to contribute to high $\dot{V}_E/\dot{V}CO_2$ in heart failure.

- *End tidal gas tensions*: end tidal gas tensions are easily measured but challenging to interpret. End tidal PCO_2 ($P_{ET}CO_2$) at rest is normally 1 to 3 mm Hg less than P_aCO_2. With exercise $P_{ET}CO_2$ initially increases to values exceeding the arterial value. However, at the onset of respiratory compensation for a metabolic acidosis, $P_{ET}CO_2$ begins to decrease (►**Fig. 10C**). Thus, $P_{ET}CO_2$ cannot be equated to P_aCO_2; a resting $P_{ET}CO_2$ above the normal P_aCO_2 range strongly implies hypercapnia, but low values, whether at rest or exercise, can result from either low P_aCO_2 or elevated V_D/V_T.

Low $P_{ET}CO_2$ is one of multiple CPET findings with negative prognostic implication in cardiovascular conditions such as heart failure and pulmonary arterial hypertension. Comparison of $P_{ET}CO_2$ with $P_{\bar{E}}CO_2$ may help distinguish among potential underlying causes. Although $P_{\bar{E}}CO_2$ is always lower than $P_{ET}CO_2$ due to the diluting effect of physiologic dead

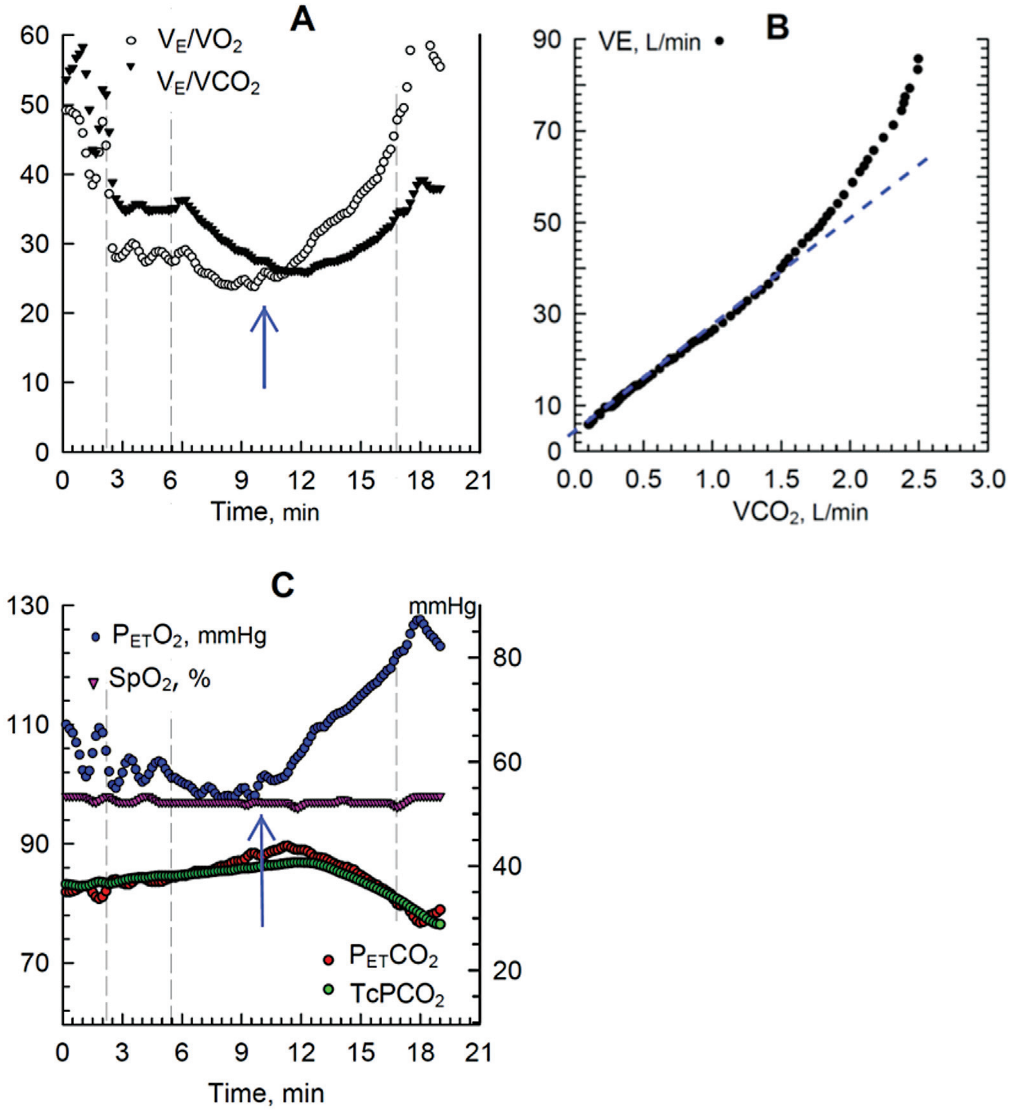

Fig. 10 Variables related to gas exchange efficiency for the same CPET described in ►**Fig. 5**. (**A**) Ventilatory equivalent for CO_2 ($\dot{V}_E/\dot{V}CO_2$; solid triangle) and for O_2 ($\dot{V}_E/\dot{V}O_2$; open circle). Blue arrow indicates typical finding of GET reflected in upward inflection of $\dot{V}_E/\dot{V}O_2$, without coincident increase in $\dot{V}_E/\dot{V}CO_2$. (**B**) $\dot{V}_E$ as a function of $\dot{V}CO_2$. The dashed blue line is the $\Delta\dot{V}_E/\Delta\dot{V}CO_2$ slope fit to the linear range of data, prior to respiratory compensation for metabolic acidosis. (**C**) Values of end tidal PCO_2 ($P_{ET}CO_2$; solid red circle), end tidal PO_2 ($P_{ET}O_2$; solid blue circle), transcutaneous PCO_2 ($TcPCO_2$; green circle), and pulse oximeter estimate of arterial oxygen saturation (SpO_2; purple triangle). Blue arrow indicates typical finding of GET reflected in upward inflection of $P_{ET}O_2$ without coincident decrease in $P_{ET}CO_2$. $TcPCO_2$ and SpO_2 signals are both subject to instrument delay times, so changes in values lag other variables and time axis. CPET, cardiopulmonary exercise testing; GET, gas exchange threshold.

space, both are reduced relative to normal when V_D/V_T is elevated. When elevated V_D/V_T is due to uneven ventilation (i.e., obstructive airways disease) as opposed to altered perfusion (e.g., heart failure or pulmonary vascular disease), the difference between $P_{\bar{E}}CO_2$ and $P_{ET}CO_2$ is particularly marked. This is postulated to result from the fact that $P_{ET}CO_2$ in airways disease reflects exhalate from those lung regions with the longest ventilatory time constants, which tend also to have low $\dot{V}_A/\dot{Q}$.[118]

End tidal PO_2 ($P_{ET}O_2$) at rest is also close to arterial P_aO_2. $P_{ET}O_2$ begins to rise before $P_{ET}CO_2$ starts to decline during incremental exercise due to ventilatory changes associated with the GET, so along with $\dot{V}_E/\dot{V}O_2$, the $P_{ET}O_2$ is used in identification of GET.[97]

A distinct pattern of end tidal gas tensions occurs during CPET when there is exercise-induced right to left shunt, evident in some congenital cardiac lesions[119] or pulmonary hypertension with coincident patent foramen ovale.[120] The onset of shunting results in acute augmentation of $\dot{V}_E$, preventing the hypercapnia that would otherwise result from the acute increase in venous admixture. This is marked by a decrease in $P_{ET}CO_2$ and a reciprocal increase in $P_{ET}O_2$, which is distinguished from pure hyperventilation by stability of P_aCO_2.[119]

- ***Alveolar arterial PO_2 difference ($P(A\text{-}a)O_2$) and dead space fraction of the tidal volume (V_D/V_T)***: as shown earlier, these expressions of gas exchange efficiency are calculated from measures of arterial blood gases and gas exchange. Substituting $P_{ET}CO_2$ or a derivative thereof for P_aCO_2 in the V_D/V_T calculation systematically overestimates the value when normal, and underestimates it when elevated.[121] Transcutaneous PCO_2 ($P_{tc}CO_2$) devices measure arterialized capillary PCO_2, which is a closer estimate of stable P_aCO_2, although, because of the long response time of the electrode, do not accurately track acute changes in P_aCO_2,[122,123] limiting their use over portions of a CPET, especially into recovery.

Additional Measurements

- *Symptoms*: the symptom(s) leading to termination of exercise during CPET, and how they correspond to symptoms in daily activities, are important to ascertain. Standard rating scales of symptoms, such as the Borg rating of perceived exertion or modified scales for intensity of dyspnea or leg fatigue, are readily administered during exercise and have high degrees of within-subject repeatability.[124] In obstructive lung disease, a marked increase in dyspnea is likely when mechanical limits of breathing are approached, such as a V_T/IC approximately 70 to 80% and $\dot{V}_E$/MVV exceeding approximately 80%, (►**Fig. 10**).[125] Other exertional symptoms such as chest pain or lightheadedness are of importance in both diagnostic and safety considerations.
- *ECG*: serial or continuous recording of ECG is used to identify cardiac rhythm and repolarization patterns as well as to calculate HR.
- *BP*: systolic and mean arterial pressures, typically measured by auscultation, rise with exercise. Diastolic pressure typically decreases during treadmill exercise and rises during cycle tests.

Interpretation of CPET measures includes their comparison with appropriately selected reference values, of which there are many.[126] Differences among reference values can reflect differences in study cohorts with respect to demographics, levels of fitness, genetic profile, testing procedures, and environmental (e.g., altitude) and other factors. There is also overlap in ranges of many variables in health and disease, which complicates strict demarcation of normal from abnormal ranges. For patients with known disease, comparisons may be more meaningfully made with data from relevant clinical cohorts for whom significance of particular variable values is known.

Applications of CPET

In clinical practice, CPET is used to measure integrated exercise function of individuals with known conditions, to aid in prognostic assessment, and to identify reasons for a particular individual's symptoms or limitations. CPET additionally has a role in diagnostic evaluation of symptomatic individuals in the absence of known or attributable disease.

Functional Assessment

$\dot{V}O_{2peak}$ quantifies cardiorespiratory fitness in healthy persons, and impairment in chronic disease. The latter is not necessarily predictable from static tests of organ function, which are largely insensitive to secondary systemic effects of disease, and to the confounding effects of additional comorbid conditions. Integrated functional assessment may be relevant to establishment of disability,[127] or for exercise training or rehabilitation prescription, among other uses. Objective measures of functional capacity is particularly valuable in complex or heterogenous conditions. Congenital heart diseases, for example, are a diverse set of life-long conditions with wide ranges of exercise capacity even within anatomic diagnoses.[128] Clinical guidelines for the care of adults with congenital heart diseases[129] recommend objective exercise testing for baseline and serial assessment of function for many of these due to the limitations of assessment by history and anatomy alone.[128]

Prognosis

Many clinical applications of CPET are based on the prognostic significance of exercise function, which can be demonstrated in virtually any clinical population.[130–135] A well-described example of this is chronic heart failure. Based on the recognized relationship between $\dot{V}O_{2peak}$ and prognosis, Mancini et al[136] reported using $\dot{V}O_{2peak}$ to prioritize heart transplantation, deferring transplant for candidates whose $\dot{V}O_{2peak}$ was above 14 mL/min/kg, due to it predicting low risk of near-term mortality. These and scores of subsequent observations not only confirm the prognostic relevance of $\dot{V}O_{2peak}$ in heart failure, but also support the feasibility of maximal exercise testing of individuals with chronic disease and demonstrate that CPET results have sufficient physiologic meaning to be valuable in clinical decision making. Other variables derived from CPET, including $\dot{V}_E/\dot{V}CO_2$, $P_{ET}CO_2$, and oscillatory breathing patterns, also have prognostic significance in heart failure and are recommended components of a multi-variable approach to risk stratification.[130,137–140] The absolute risk predicted by given values of these variables has changed with evolution of heart failure therapy, but they have remained relevant to the evaluation of patients with advanced disease.[141]

Another prognostic use of CPET is risk stratification for anticipated stresses, including high-risk elective surgery. While self-reported exercise capacity is a standard component of surgical risk assessment,[142] there is interest in using objective measures of function when circumstances permit.[143] Much of the data in this area identify GET as the primary predictive variable, with values of 9 to 11 mL/min/kg distinguishing between higher and lower risk of complications following major abdominal procedures.[144,145] In addition to informing risk–benefit discussions, this has potential to aid in resource management by identifying patients with a relatively favorable risk profile.[146]

Lung resection surgery presents a unique challenge in preoperative assessment, as it includes both procedural risk and the permanent loss of pulmonary function. Risk stratification algorithms include assessment of $\dot{V}O_{2peak}$ for selected individuals with anatomically resectable lung cancers.[147,148] Increased risks of perioperative complications are associated with preoperative $\dot{V}O_{2peak}$ less than 15 mL/min/kg, and concerns for unacceptable mortality with values below 10 mL/min/kg.[149] These criteria may be less predictive of complications with minimally invasive surgical approaches.[150]

Additional conditions for which use of CPET is reported in risk stratification include hypertrophic cardiomyopathy,[151] pulmonary arterial hypertension,[152] and individuals with structural heart disease considering sports participation[129] or pregnancy.[129,153,154]

Phenotyping

Many chronic diseases are systemic in nature and the cause of associated impairment may be heterogeneous and multifactorial. In heart failure, factors contributing to exercise limitation may include defects in chronotropy, SV, vascular endothelial function, pressor response, or skeletal muscle function; the relative importance of these varies among individuals even within clinical phenotypes based on ejection fraction.[144,155] Similarly, in COPD, individuals' limitations may differ with respect to the role of breathing mechanics,[156,157] cardiovascular responses,[158,159] or skeletal muscle function.[160,161] CPET can contribute to distinguishing critical factors of limitation which is central to the goal of individualizing therapy. Aspects of breathing mechanics are particularly amenable to noninvasive assessments, whereas defining hemodynamic and peripheral features and deciphering complex cardiopulmonary interactions[162] can require more specialized measures.[7]

Cardiopulmonary Exercise Testingfor Diagnostic Assessment

In clinical practice, CPET is often performed in individuals without known disease as part of the diagnostic evaluation of exertional dyspnea or other symptoms.[163] The distribution of conditions ultimately found to be responsible for dyspnea varies considerably,[164–169] and the diagnostic yield of CPET is thus likely to vary by clinical setting. Consensus among experienced users is that information gained from CPET is most helpful when part of a comprehensive assessment, including history, risk factors, and other clinical information.[70,170,171]

Performance of CPET for diagnostic purposes sometimes leads to a specific diagnosis, e.g., when the presenting symptoms are reproduced during testing and accompanied by a distinct finding such as stridor indicative of upper airway dysfunction. Of the myriad processes that can cause exertional dyspnea, however, few have completely unique findings on CPET, and the range of factors that can constrain exercise or precipitate symptoms can easily exceed simple algorithmic approaches to identifying them. More commonly, therefore, the goal of diagnostic CPET is to broadly distinguish among abnormalities such as outlined in the categories identified above.[170] Evidence for impairment in one or more of these areas can serve to narrow an otherwise extensive differential diagnosis and so aid in targeting additional specific diagnostics. Normal results can be useful as well, although do not necessarily exclude pathology, as normal ranges for some variables are wide, such that decrements from a previously trained state may occur without falling outside normal ranges. There are also aspects of the exercise response that are not measured in routine testing.

Diagnostic potential of CPET can be expanded by additional measurements based on pretest likelihood of diagnoses, for example, direct laryngoscopy for suspected upper airway dysfunction,[172] or echocardiography for structural or hypertensive heart disease.[173,174]

The addition of peripheral arterial and central venous catheterization to basic CPET procedures has been termed invasive CPET[175] and allows quantifying central vascular pressures, cardiac output, and $C(a\text{-}v)O_2$ during exercise. This extends diagnostic capability to several hemodynamically defined conditions,[176] including exercise-induced pulmonary arterial hypertension, or pulmonary venous hypertension due to left ventricular dysfunction. Other findings, while nonspecific, can significantly narrow diagnostic possibilities. For example, the finding of an excessively high slope of cardiac output relative to $\dot{V}O_2$ implies either failure of autonomic regulation of distribution of cardiac output[177] or impaired utilization of oxygen due to metabolic myopathy.[178]

Conclusion

Performance of exercise entails the interactive function of multiple organ systems. Exercise testing is unique among clinical tools in that it reflects the aggregate effects of impairment in those individual systems' functions along with effects of compensatory responses and/or secondary or co-existing conditions on overall aerobic capacity. Measures of $\dot{V}O_{2peak}$ peak and GET identify the ranges of attainable and sustainable exercise WRs for an individual, which can be considered in the context of those for healthy or clinical reference populations. While nonspecific, these are both functionally meaningful and also may have powerful predictive value of use in clinical decision making. Additional measurements from CPET characterize more specific aspects of cardiopulmonary exercise responses, which may offer insight into the basis of an individual's symptoms or limitations.

Funding

Harry B. Rossiter is supported by grants from National Institutes of Health (grant numbers: R01HL151452, R01HL153460, P50HD098593, R01DK122767) and the Tobacco Related Disease Research Program (grant number: T31IP1666).

Conflict of Interest

H.B.R. reports consulting fees from Omniox Inc., contributor royalties from Wasserman and Whipp's Exercise Testing and Interpretation textbook, and is involved in contracted clinical research with Boehringer Ingelheim, GlaxoSmithKline, Novartis, AstraZeneca, Astellas, United Therapeutics, Genentech, and Regeneron. He is a visiting Professor at the University of Leeds, United Kingdom.

K.E.S. reports royalties from Wasserman and Whipp's Exercise Testing and Interpretation textbook.

References

1 Bowen TS, Benson AP, Rossiter HB. The coupling of internal and external gas exchange during exercise. In: Zoladz JA, ed. Muscle and Exercise Physiology. New Amsterdam: Elsevier; 2018: 217–249

2 Pette D, Staron RS. Myosin isoforms, muscle fiber types, and transitions. Microsc Res Tech 2000;50(06):500–509

3 Roca J, Agusti AG, Alonso A, et al. Effects of training on muscle O2 transport at VO2max. J Appl Physiol 1992;73(03):1067–1076

4 Knight DR, Schaffartzik W, Poole DC, Hogan MC, Bebout DE, Wagner PD. Effects of hyperoxia on maximal leg O2 supply and utilization in men. J Appl Physiol 1993;75(06):2586–2594

5 McClaran SR, Harms CA, Pegelow DF, Dempsey JA. Smaller lungs in women affect exercise hyperpnea. J Appl Physiol 1998;84(06): 1872–1881

6 Rogers MA, Evans WJ. Changes in skeletal muscle with aging: effects of exercise training. Exerc Sport Sci Rev 1993;21:65–102

7 Cannon DT, Coelho AC, Cao R, et al. Skeletal muscle power and fatigue at the tolerable limit of ramp-incremental exercise in COPD. J Appl Physiol 2016;121(06):1365–1373

8 Ade CJ, Broxterman RM, Moore AD, Barstow TJ. Decreases in maximal oxygen uptake following long-duration spaceflight: Role of convective and diffusive O_2 transport mechanisms. J Appl Physiol 2017;122(04):968–975

9 Esposito F, Mathieu-Costello O, Shabetai R, Wagner PD, Richardson RS. Limited maximal exercise capacity in patients with chronic heart failure: partitioning the contributors. J Am Coll Cardiol 2010;55(18):1945–1954

10 Owles WH. Alterations in the lactic acid content of the blood as a result of light exercise, and associated changes in the co(2)-combining power of the blood and in the alveolar co(2) pressure. J Physiol 1930;69(02):214–237

11 van der Vaart H, Murgatroyd SR, Rossiter HB, Chen C, Casaburi R, Porszasz J. Selecting constant work rates for endurance testing in COPD: the role of the power-duration relationship. COPD 2014; 11(03):267–276

12 Wasserman K. Coupling of external to cellular respiration during exercise: the wisdom of the body revisited. Am J Physiol 1994; 266(4, Pt 1):E519–E539

13 Goodwin ML, Harris JE, Hernández A, Gladden LB. Blood lactate measurements and analysis during exercise: a guide for clinicians. J Diabetes Sci Technol 2007;1(04):558–569

14 Koike A, Weiler-Ravell D, McKenzie DK, Zanconato S, Wasserman K. Evidence that the metabolic acidosis threshold is the anaerobic threshold. J Appl Physiol 1990;68(06):2521–2526

15 Neill WA, Jensen PE, Rich GB, Werschkul JD. Effect of decreased O2 supply to tissue on the lactate: pyruvate ratio in blood. J Clin Invest 1969;48(10):1862–1869

16 Ekblom B, Wilson G, Astrand PO. Central circulation during exercise after venesection and reinfusion of red blood cells. J Appl Physiol 1976;40(03):379–383

17 Spriet LL, Gledhill N, Froese AB, Wilkes DL. Effect of graded erythrocythemia on cardiovascular and metabolic responses to exercise. J Appl Physiol 1986;61(05):1942–1948

18 van Hall G, Calbet JA, Søndergaard H, Saltin B. The re-establishment of the normal blood lactate response to exercise in humans after prolonged acclimatization to altitude. J Physiol 2001;536 (Pt 3):963–975

19 Benedetto D, Rao CM, Cefalù C, et al. Effects of blood transfusion on exercise capacity in thalassemia major patients. PLoS One 2015;10(05):e0127553

20 Wasserman K, McIlroy MB. Detecting the threshold of anaerobic metabolism in cardiac patients during exercise. Am J Cardiol 1964;14:844–852

21 Stanley WC, Gertz EW, Wisneski JA, Morris DL, Neese RA, Brooks GA. Systemic lactate kinetics during graded exercise in man. Am J Physiol 1985;249(6, Pt 1):E595–E602

22 Poole DC, Rossiter HB, Brooks GA, Gladden LB. The anaerobic threshold: 50+ years of controversy. J Physiol 2021;599(03): 737–767

23 Proctor DN, Koch DW, Newcomer SC, Le KU, Leuenberger UA. Impaired leg vasodilation during dynamic exercise in healthy older women. J Appl Physiol 2003;95(05):1963–1970

24 Proctor DN, Parker BA. Vasodilation and vascular control in contracting muscle of the aging human. Microcirculation 2006;13(04):315–327

25 Mortensen SP, Dawson EA, Yoshiga CC, et al. Limitations to systemic and locomotor limb muscle oxygen delivery and uptake during maximal exercise in humans. J Physiol 2005;566(Pt 1):273–285

26 Laughlin MH, Davis MJ, Secher NH, et al. Peripheral circulation. Compr Physiol 2012;2(01):321–447

27 Rowell LB. Human Circulation. New York, NY: Oxford University Press; 1986

28 Tanaka H, Monahan KD, Seals DR. Age-predicted maximal heart rate revisited. J Am Coll Cardiol 2001;37(01):153–156

29 Green AL, Wang S, Purvis S, et al. Identifying cardiorespiratory neurocircuitry involved in central command during exercise in humans. J Physiol 2007;578(Pt 2):605–612

30 Krogh A, Lindhard J. The regulation of respiration and circulation during the initial stages of muscular work. J Physiol 1913;47(1–2):112–136

31 Cornwell WK, Tran T, Cerbin L, et al. New insights into resting and exertional right ventricular performance in the healthy heart through real-time pressure-volume analysis. J Physiol 2020;598 (13):2575–2587

32 Rowell LB. Human Cardiovascular Control. New York, NY: Oxford University Press; 1993

33 Lalande S, Luoma CE, Miller AD, Johnson BD. Effect of changes in intrathoracic pressure on cardiac function at rest and during moderate exercise in health and heart failure. Exp Physiol 2012; 97(02):248–256

34 Hainsworth R, Drinkhill MJ. Counterpoint: active venoconstriction is not important in maintaining or raising end-diastolic volume and stroke volume during exercise and orthostasis. J Appl Physiol 2006;101(04):1264–1265, discussion 1265–1266, 1270

35 Rothe CF. Point: active venoconstriction is/is not important in maintaining or raising end-diastolic volume and stroke volume during exercise and orthostasis. J Appl Physiol 2006;101(04): 1262–1264, discussion 1265–1266, 1270

36 Fisher JP, Young CN, Fadel PJ. Autonomic adjustments to exercise in humans. Compr Physiol 2015;5(02):475–512

37 Miki K, Yoshimoto M. Exercise-induced modulation of baroreflex control of sympathetic nerve activity. Front Neurosci 2018; 12:493

38 Hearon CM Jr, Dinenno FA. Regulation of skeletal muscle blood flow during exercise in ageing humans. J Physiol 2016;594(08): 2261–2273

39 Stringer W, Wasserman K, Casaburi R, Pórszász J, Maehara K, French W. Lactic acidosis as a facilitator of oxyhemoglobin dissociation during exercise. J Appl Physiol 1994;76(04):1462–1467

40 Poole DC, Copp SW, Hirai DM, Musch TI. Dynamics of muscle microcirculatory and blood-myocyte O(2) flux during contractions. Acta Physiol (Oxf) 2011;202(03):293–310

41 Harms CA, Babcock MA, McClaran SR, et al. Respiratory muscle work compromises leg blood flow during maximal exercise. J Appl Physiol 1997;82(05):1573–1583

42 Johnson BD, Weisman IM, Zeballos RJ, Beck KC. Emerging concepts in the evaluation of ventilatory limitation during exercise: the exercise tidal flow-volume loop. Chest 1999;116(02):488–503

43 Gagnon P, Bussières JS, Ribeiro F, et al. Influences of spinal anesthesia on exercise tolerance in patients with chronic obstructive pulmonary disease. Am J Respir Crit Care Med 2012; 186(07):606–615

44 Morin D, Viala D. Coordinations of locomotor and respiratory rhythms in vitro are critically dependent on hindlimb sensory inputs. J Neurosci 2002;22(11):4756–4765
45 Haouzi P, Bell HJ. Respiratory effects of changing the volume load imposed on the peripheral venous system. Respir Physiol Neurobiol 2010;171(03):175–180
46 Lovering AT, Eldridge MW, Stickland MK. Counterpoint: exercise-induced intrapulmonary shunting is real. J Appl Physiol 2009;107(03):994–997
47 Hopkins SR, Olfert IM, Wagner PD. Point: exercise-induced intrapulmonary shunting is imaginary. J Appl Physiol 2009; 107(03):993–994
48 Constantini K, Tanner DA, Gavin TP, Harms CA, Stager JM, Chapman RF. Prevalence of exercise-induced arterial hypoxemia in distance runners at sea level. Med Sci Sports Exerc 2017;49 (05):948–954
49 Dempsey JA, Wagner PD. Exercise-induced arterial hypoxemia. J Appl Physiol 1999;87(06):1997–2006
50 Dominelli PB, Sheel AW. Exercise-induced arterial hypoxemia; some answers, more questions. Appl Physiol Nutr Metab 2019; 44(06):571–579
51 Robertson HT. Dead space: the physiology of wasted ventilation. Eur Respir J 2015;45(06):1704–1716
52 Wasserman K, Van Kessel AL, Burton GG. Interaction of physiological mechanisms during exercise. J Appl Physiol 1967;22(01): 71–85
53 Wagner PD, Gale GE, Moon RE, Torre-Bueno JR, Stolp BW, Saltzman HA. Pulmonary gas exchange in humans exercising at sea level and simulated altitude. J Appl Physiol 1986;61(01): 260–270
54 Rossiter HB. Exercise: kinetic considerations for gas exchange. Compr Physiol 2011;1(01):203–244
55 Thurber C, Dugas LR, Ocobock C, Carlson B, Speakman JR, Pontzer H. Extreme events reveal an alimentary limit on sustained maximal human energy expenditure. Sci Adv 2019;5(06): eaaw0341
56 Cannon DT, White AC, Andriano MF, Kolkhorst FW, Rossiter HB. Skeletal muscle fatigue precedes the slow component of oxygen uptake kinetics during exercise in humans. J Physiol 2011;589(Pt 3):727–739
57 Keir DA, Copithorne DB, Hodgson MD, Pogliaghi S, Rice CL, Kowalchuk JM. The slow component of pulmonary O2 uptake accompanies peripheral muscle fatigue during high-intensity exercise. J Appl Physiol 2016;121(02):493–502
58 de Almeida Azevedo R, Keir DA, Forot J, Iannetta D, Millet GY, Murias JM. The effects of exercise intensity and duration on the relationship between the slow component of $\dot{V}O_2$ and peripheral fatigue. Acta Physiol (Oxf) 2022;234(02):e13776
59 Coyle EF, Coggan AR, Hemmert MK, Ivy JL. Muscle glycogen utilization during prolonged strenuous exercise when fed carbohydrate. J Appl Physiol 1986;61(01):165–172
60 Ozyener F, Rossiter HB, Ward SA, Whipp BJ. Influence of exercise intensity on the on- and off-transient kinetics of pulmonary oxygen uptake in humans. J Physiol 2001;533(Pt 3):891–902
61 Coats EM, Rossiter HB, Day JR, Miura A, Fukuba Y, Whipp BJ. Intensity-dependent tolerance to exercise after attaining V(O2) max in humans. J Appl Physiol 2003;95(02):483–490
62 Hill AV, Lupton H. Muscular exercise, lactic acid, and the supply and utilization of oxygen. QJM 1923;16(62):135–171
63 Poole DC, Ward SA, Gardner GW, Whipp BJ. Metabolic and respiratory profile of the upper limit for prolonged exercise in man. Ergonomics 1988;31(09):1265–1279
64 Jones AM, Wilkerson DP, DiMenna F, Fulford J, Poole DC. Muscle metabolic responses to exercise above and below the “critical power” assessed using 31P-MRS. Am J Physiol Regul Integr Comp Physiol 2008;294(02):R585–R593
65 Barker T, Poole DC, Noble ML, Barstow TJ. Human critical power-oxygen uptake relationship at different pedalling frequencies. Exp Physiol 2006;91(03):621–632
66 Gibbons RJ, Balady GJ, Bricker JT, et al; American College of Cardiology/American Heart Association Task Force on Practice Guidelines. Committee to Update the 1997 Exercise Testing Guidelines. ACC/AHA 2002 guideline update for exercise testing: summary article. A report of the American College of Cardiology/American Heart Association Task Force on Practice Guidelines (Committee to Update the 1997 Exercise Testing Guidelines). J Am Coll Cardiol 2002;40(08):1531–1540
67 Balady GJ, Arena R, Sietsema K, et al; American Heart Association Exercise, Cardiac Rehabilitation, and Prevention Committee of the Council on Clinical Cardiology Council on Epidemiology and Prevention Council on Peripheral Vascular Disease Interdisciplinary Council on Quality of Care and Outcomes Research. Clinician’s Guide to cardiopulmonary exercise testing in adults: a scientific statement from the American Heart Association. Circulation 2010;122(02):191–225
68 Fletcher GF, Ades PA, Kligfield P, et al; American Heart Association Exercise, Cardiac Rehabilitation, and Prevention Committee of the Council on Clinical Cardiology, Council on Nutrition, Physical Activity and Metabolism, Council on Cardiovascular and Stroke Nursing, and Council on Epidemiology and Prevention. Exercise standards for testing and training: a scientific statement from the American Heart Association. Circulation 2013;128(08):873–934
69 Rodgers GP, Ayanian JZ, Balady G, et al. American College of Cardiology/American Heart Association Clinical Competence Statement on Stress Testing. A Report of the American College of Cardiology/American Heart Association/American College of Physicians-American Society of Internal Medicine Task Force on Clinical Competence. Circulation 2000;102(14):1726–1738
70 American Thoracic Society American College of Chest Physicians. ATS/ACCP statement on cardiopulmonary exercise testing. Am J Respir Crit Care Med 2003;167(02):211–277
71 Keteyian SJ, Isaac D, Thadani U, et al; HF-ACTION Investigators. Safety of symptom-limited cardiopulmonary exercise testing in patients with chronic heart failure due to severe left ventricular systolic dysfunction. Am Heart J 2009;158(4, Suppl):S72–S77
72 Myers J, Forman DE, Balady GJ, et al; American Heart Association Subcommittee on Exercise, Cardiac Rehabilitation, and Prevention of the Council on Clinical Cardiology, Council on Lifestyle and Cardiometabolic Health, Council on Epidemiology and Prevention, and Council on Cardiovascular and Stroke Nursing. Supervision of exercise testing by nonphysicians: a scientific statement from the American Heart Association. Circulation 2014;130(12):1014–1027
73 Nayor M, Shah RV, Tanguay M, et al. Feasibility, methodology, and interpretation of broad-scale assessment of cardiorespiratory fitness in a large community-based sample. Am J Cardiol 2021;157:56–63
74 Myers J, Buchanan N, Walsh D, et al. Comparison of the ramp versus standard exercise protocols. J Am Coll Cardiol 1991;17 (06):1334–1342
75 McKay GA, Banister EW. A comparison of maximum oxygen uptake determination by bicycle ergometry at various pedaling frequencies and by treadmill running at various speeds. Eur J Appl Physiol Occup Physiol 1976;35(03):191–200
76 Cockcroft A, Beaumont A, Adams L, Guz A. Arterial oxygen desaturation during treadmill and bicycle exercise in patients with chronic obstructive airways disease. Clin Sci (Lond) 1985; 68(03):327–332
77 Hsia D, Casaburi R, Pradhan A, Torres E, Porszasz J. Physiological responses to linear treadmill and cycle ergometer exercise in COPD. Eur Respir J 2009;34(03):605–615

78 Sietsema KE, Sue DY, Stringer WW, Ward SA. Wasserman and Whipp's Principles of Exercise Testing and Interpretation. Philadelphia, PA: Wolters Kluwer; 2021

79 Porszasz J, Casaburi R, Somfay A, Woodhouse LJ, Whipp BJ. A treadmill ramp protocol using simultaneous changes in speed and grade. Med Sci Sports Exerc 2003;35(09):1596–1603

80 Buchfuhrer MJ, Hansen JE, Robinson TE, Sue DY, Wasserman K, Whipp BJ. Optimizing the exercise protocol for cardiopulmonary assessment. J Appl Physiol 1983;55(05):1558–1564

81 Puente-Maestu L, Palange P, Casaburi R, et al. Use of exercise testing in the evaluation of interventional efficacy: an official ERS statement. Eur Respir J 2016;47(02):429–460

82 Casaburi R, Merrill DD, Harding G, et al; CBQC Constant Work Rate Exercise Working Group. A conceptual framework for use of increased endurance time during constant work rate cycle ergometry as a patient-focused meaningful outcome in COPD clinical trials. Chronic Obstr Pulm Dis (Miami) 2022;9(02): 252–265

83 Ward SA. Open-circuit respirometry: real-time, laboratory-based systems. Eur J Appl Physiol 2018;118(05):875–898

84 Roecker K, Prettin S, Sorichter S. Gas exchange measurements with high temporal resolution: the breath-by-breath approach. Int J Sports Med 2005;26(Suppl 1):S11–S18

85 Ramos-Álvarez JJ, Lorenzo-Capellá I, Calderón-Montero FJ. Disadvantages of automated respiratory gas exchange analyzers. Front Physiol 2020;11:19

86 Bowen TS, Cannon DT, Begg G, Baliga V, Witte KK, Rossiter HB. A novel cardiopulmonary exercise test protocol and criterion to determine maximal oxygen uptake in chronic heart failure. J Appl Physiol 2012;113(03):451–458

87 Rossiter HB, Kowalchuk JM, Whipp BJ. A test to establish maximum O2 uptake despite no plateau in the O2 uptake response to ramp incremental exercise. J Appl Physiol 2006;100(03): 764–770

88 Poole DC, Jones AM. Measurement of the maximum oxygen uptake $\dot{V}\mathrm{o}_{2\mathrm{max}}$: $\dot{V}\mathrm{o}_{2\mathrm{peak}}$ is no longer acceptable. J Appl Physiol 2017;122(04):997–1002

89 Wilcox SL, Broxterman RM, Barstow TJ. Constructing quasi-linear $\dot{V}$O2 responses from nonlinear parameters. J Appl Physiol 2016;120(02):121–129

90 Keir DA, Benson AP, Love LK, Robertson TC, Rossiter HB, Kowalchuk JM. Influence of muscle metabolic heterogeneity in determining the $\dot{V}$o2p kinetic response to ramp-incremental exercise. J Appl Physiol 2016;120(05):503–513

91 Iannetta D, de Almeida Azevedo R, Keir DA, Murias JM. Establishing the $\dot{V}\mathrm{o}_2$ versus constant-work-rate relationship from ramp-incremental exercise: simple strategies for an unsolved problem. J Appl Physiol 2019;127(06):1519–1527

92 Gimenes AC, Neder JA, Dal Corso S, et al. Relationship between work rate and oxygen uptake in mitochondrial myopathy during ramp-incremental exercise. Braz J Med Biol Res 2011;44(04): 354–360

93 Belardinelli R, Lacalaprice F, Tiano L, Muçai A, Perna GP. Cardiopulmonary exercise testing is more accurate than ECG-stress testing in diagnosing myocardial ischemia in subjects with chest pain. Int J Cardiol 2014;174(02):337–342

94 Tanabe Y, Nakagawa I, Ito E, Suzuki K. Hemodynamic basis of the reduced oxygen uptake relative to work rate during incremental exercise in patients with chronic heart failure. Int J Cardiol 2002; 83(01):57–62

95 Henderson Y, Prince AL. The oxygen pulse and the systolic discharge. Am J Physiol 1914;35:106–115

96 Sirichana W, Neufeld EV, Wang X, Hu SB, Dolezal BA, Cooper CB. Reference values for chronotropic index from 1280 incremental cycle ergometry tests. Med Sci Sports Exerc 2020;52(12): 2515–2521

97 Beaver WL, Wasserman K, Whipp BJ. A new method for detecting anaerobic threshold by gas exchange. J Appl Physiol 1986;60 (06):2020–2027

98 Blackie SP, Fairbarn MS, McElvaney NG, Wilcox PG, Morrison NJ, Pardy RL. Normal values and ranges for ventilation and breathing pattern at maximal exercise. Chest 1991;100(01):136–142

99 Boulding R, Stacey R, Niven R, Fowler SJ. Dysfunctional breathing: a review of the literature and proposal for classification. Eur Respir Rev 2016;25(141):287–294

100 Bansal T, Haji GS, Rossiter HB, Polkey MI, Hull JH. Exercise ventilatory irregularity can be quantified by approximate entropy to detect breathing pattern disorder. Respir Physiol Neurobiol 2018;255:1–6

101 Lie AH, Grønnevik I, Frisk B, et al. Breathing patterns in people with exercise-induced laryngeal obstruction. Physiol Rep 2021;9 (22):e15086

102 Babb TG. Exercise ventilatory limitation: the role of expiratory flow limitation. Exerc Sport Sci Rev 2013;41(01):11–18

103 Guenette JA, Dominelli PB, Reeve SS, Durkin CM, Eves ND, Sheel AW. Effect of thoracic gas compression and bronchodilation on the assessment of expiratory flow limitation during exercise in healthy humans. Respir Physiol Neurobiol 2010;170(03): 279–286

104 Koulouris NG, Dimopoulou I, Valta P, Finkelstein R, Cosio MG, Milic-Emili J. Detection of expiratory flow limitation during exercise in COPD patients. J Appl Physiol 1997;82(03):723–731

105 Ma S, Hecht A, Varga J, et al. Breath-by-breath quantification of progressive airflow limitation during exercise in COPD: a new method. Respir Med 2010;104(03):389–396

106 Milne KM, Domnik NJ, Phillips DB, et al. Evaluation of dynamic respiratory mechanical abnormalities during conventional CPET. Front Med (Lausanne) 2020;7:548

107 O'Donnell DE, Voduc N, Fitzpatrick M, Webb KA. Effect of salmeterol on the ventilatory response to exercise in chronic obstructive pulmonary disease. Eur Respir J 2004;24(01):86–94

108 Yamaya Y, Bogaard HJ, Wagner PD, Niizeki K, Hopkins SR. Validity of pulse oximetry during maximal exercise in normoxia, hypoxia, and hyperoxia. J Appl Physiol 2002;92(01):162–168

109 Ascha M, Bhattacharyya A, Ramos JA, Tonelli AR. Pulse oximetry and arterial oxygen saturation during cardiopulmonary exercise testing. Med Sci Sports Exerc 2018;50(10):1992–1997

110 Neder JA, Berton DC, Phillips DB, O'Donnell DE. Exertional ventilation/carbon dioxide output relationship in COPD: from physiological mechanisms to clinical applications. Eur Respir Rev 2021;30(161):200190

111 Robertson HT. Gas exchange consequences of left heart failure. Compr Physiol 2011;1(02):621–634

112 Van Iterson EH, Johnson BD, Borlaug BA, Olson TP. Physiological dead space and arterial carbon dioxide contributions to exercise ventilatory inefficiency in patients with reduced or preserved ejection fraction heart failure. Eur J Heart Fail 2017;19(12): 1675–1685

113 Sullivan MJ, Higginbotham MB, Cobb FR. Increased exercise ventilation in patients with chronic heart failure: intact ventilatory control despite hemodynamic and pulmonary abnormalities. Circulation 1988;77(03):552–559

114 Piepoli M, Clark AL, Volterrani M, Adamopoulos S, Sleight P, Coats AJ. Contribution of muscle afferents to the hemodynamic, autonomic, and ventilatory responses to exercise in patients with chronic heart failure: effects of physical training. Circulation 1996;93(05):940–952

115 Ponikowski P, Banasiak W. Chemosensitivity in chronic heart failure. Heart Fail Monit 2001;1(04):126–131

116 Woods PR, Olson TP, Frantz RP, Johnson BD. Causes of breathing inefficiency during exercise in heart failure. J Card Fail 2010;16 (10):835–842

117 West JB. Ventilation-perfusion inequality and overall gas exchange in computer models of the lung. Respir Physiol 1969;7 (01):88–110

118 Hansen JE, Ulubay G, Chow BF, Sun XG, Wasserman K. Mixed-expired and end-tidal CO2 distinguish between ventilation and perfusion defects during exercise testing in patients with lung and heart diseases. Chest 2007;132(03):977–983

119 Sietsema KE, Cooper DM, Perloff JK, et al. Control of ventilation during exercise in patients with central venous-to-systemic arterial shunts. J Appl Physiol 1988;64(01):234–242

120 Sun XG, Hansen JE, Oudiz RJ, Wasserman K. Gas exchange detection of exercise-induced right-to-left shunt in patients with primary pulmonary hypertension. Circulation 2002;105 (01):54–60

121 Lewis DA, Sietsema KE, Casaburi R, Sue DY. Inaccuracy of noninvasive estimates of VD/VT in clinical exercise testing. Chest 1994;106(05):1476–1480

122 Cao M, Stringer WW, Corey S, et al. Transcutaneous PCO_2 for exercise gas exchange efficiency in chronic obstructive pulmonary disease. COPD 2021;18(01):16–25

123 Hoffmann U, Essfeld D, Stegemann J. Comparison of arterial, end-tidal and transcutaneous PCO2 during moderate exercise and external CO2 loading in humans. Eur J Appl Physiol Occup Physiol 1990;61(1–2):1–4

124 Grant S, Aitchison T, Henderson E, et al. A comparison of the reproducibility and the sensitivity to change of visual analogue scales, Borg scales, and Likert scales in normal subjects during submaximal exercise. Chest 1999;116(05):1208–1217

125 O'Donnell DE, Guenette JA, Maltais F, Webb KA. Decline of resting inspiratory capacity in COPD: the impact on breathing pattern, dyspnea, and ventilatory capacity during exercise. Chest 2012; 141(03):753–762

126 Puente-Maestu L, García de Pedro J, Benedetti PA, López JJG, Giron-Matute WI. Reference values in adults. In: Palange P, Laveneziana P, Neder JA, Ward SA, eds. Clinical Exercise Testing. Lausanne: European Respiratory Society; 2018:82–106

127 Andersson GBJ, Cocchiarella L. Guides to the Evaluation of Permanent Impairment. 5th ed. Chigcao, IL: American Medical Association; 2000

128 Inuzuka R, Diller GP, Borgia F, et al. Comprehensive use of cardiopulmonary exercise testing identifies adults with congenital heart disease at increased mortality risk in the medium term. Circulation 2012;125(02):250–259

129 Stout KK, Daniels CJ, Aboulhosn JA, et al. 2018 AHA/ACC guideline for the management of adults with congenital heart disease: a report of the American College of Cardiology/American Heart Association Task Force on Clinical Practice Guidelines. Circulation 2019;139(14):e698–e800

130 Keteyian SJ, Patel M, Kraus WE, et al; HF-ACTION Investigators. Variables measured during cardiopulmonary exercise testing as predictors of mortality in chronic systolic heart failure. J Am Coll Cardiol 2016;67(07):780–789

131 Faselis C, Doumas M, Pittaras A, et al. Exercise capacity and all-cause mortality in male veterans with hypertension aged $\geq$70 years. Hypertension 2014;64(01):30–35

132 Myers J, Prakash M, Froelicher V, Do D, Partington S, Atwood JE. Exercise capacity and mortality among men referred for exercise testing. N Engl J Med 2002;346(11):793–801

133 Leeper NJ, Myers J, Zhou M, et al. Exercise capacity is the strongest predictor of mortality in patients with peripheral arterial disease. J Vasc Surg 2013;57(03):728–733

134 Sietsema KE, Amato A, Adler SG, Brass EP. Exercise capacity as a predictor of survival among ambulatory patients with end-stage renal disease. Kidney Int 2004;65(02):719–724

135 Nixon PA, Orenstein DM, Kelsey SF, Doershuk CF. The prognostic value of exercise testing in patients with cystic fibrosis. N Engl J Med 1992;327(25):1785–1788

136 Mancini DM, Eisen H, Kussmaul W, Mull R, Edmunds LH Jr, Wilson JR. Value of peak exercise oxygen consumption for optimal timing of cardiac transplantation in ambulatory patients with heart failure. Circulation 1991;83(03):778–786

137 Wagner J, Agostoni P, Arena R, et al. The role of gas exchange variables in cardiopulmonary exercise testing for risk stratification and management of heart failure with reduced ejection fraction. Am Heart J 2018;202:116–126

138 Gitt AK, Wasserman K, Kilkowski C, et al. Exercise anaerobic threshold and ventilatory efficiency identify heart failure patients for high risk of early death. Circulation 2002;106(24): 3079–3084

139 Cahalin LP, Chase P, Arena R, et al. A meta-analysis of the prognostic significance of cardiopulmonary exercise testing in patients with heart failure. Heart Fail Rev 2013;18(01):79–94

140 Nadruz W Jr, West E, Sengeløv M, et al. Prognostic value of cardiopulmonary exercise testing in heart failure with reduced, midrange, and preserved ejection fraction. J Am Heart Assoc 2017;6(11):e006000

141 Lewis GD, Zlotoff DA. Cardiopulmonary exercise testing-based risk stratification in the modern era of advanced heart failure management. JACC Heart Fail 2021;9(03):237–240

142 Fleisher LA, Fleischmann KE, Auerbach AD, et al. 2014 ACC/AHA guideline on perioperative cardiovascular evaluation and management of patients undergoing noncardiac surgery: executive summary: a report of the American College of Cardiology/American Heart Association Task Force on Practice Guidelines. Circulation 2014;130(24):2215–2245

143 Levett DZH, Jack S, Swart M, et al; Perioperative Exercise Testing and Training Society (POETTS) Perioperative cardiopulmonary exercise testing (CPET): consensus clinical guidelines on indications, organization, conduct, and physiological interpretation. Br J Anaesth 2018;120(03):484–500

144 Snowden CP, Prentis J, Jacques B, et al. Cardiorespiratory fitness predicts mortality and hospital length of stay after major elective surgery in older people. Ann Surg 2013;257(06):999–1004

145 Moran J, Wilson F, Guinan E, McCormick P, Hussey J, Moriarty J. Role of cardiopulmonary exercise testing as a risk-assessment method in patients undergoing intra-abdominal surgery: a systematic review. Br J Anaesth 2016;116(02):177–191

146 Older P, Hall A, Hader R. Cardiopulmonary exercise testing as a screening test for perioperative management of major surgery in the elderly. Chest 1999;116(02):355–362

147 Brunelli A, Kim AW, Berger KI, Addrizzo-Harris DJ. Physiologic evaluation of the patient with lung cancer being considered for resectional surgery: diagnosis and management of lung cancer, 3rd ed: American College of Chest Physicians evidence-based clinical practice guidelines. Chest 2013;143(5, Suppl): e166S–e190S

148 Brunelli A, Charloux A, Bolliger CT, et al; European Respiratory Society European Society of Thoracic Surgeons Joint Task Force on Fitness For Radical Therapy. The European Respiratory Society and European Society of Thoracic Surgeons clinical guidelines for evaluating fitness for radical treatment (surgery and chemoradiotherapy) in patients with lung cancer. Eur J Cardiothorac Surg 2009;36(01):181–184

149 Colice GL, Shafazand S, Griffin JP, Keenan R, Bolliger CTAmerican College of Chest Physicians. Physiologic evaluation of the patient with lung cancer being considered for resectional surgery: ACCP evidenced-based clinical practice guidelines (2nd edition). Chest 2007;132(3, Suppl):161S–177S

150 Chouinard G, Roy P, Blais MC, et al. Exercise testing and postoperative complications after minimally invasive lung resection: a cohort study. Front Physiol 2022;13:951460

151 Magrì D, Limongelli G, Re F, et al. Cardiopulmonary exercise test and sudden cardiac death risk in hypertrophic cardiomyopathy. Heart 2016;102(08):602–609

152 Wensel R, Francis DP, Meyer FJ, et al. Incremental prognostic value of cardiopulmonary exercise testing and resting haemodynamics in pulmonary arterial hypertension. Int J Cardiol 2013; 167(04):1193–1198
153 Ohuchi H, Tanabe Y, Kamiya C, et al. Cardiopulmonary variables during exercise predict pregnancy outcome in women with congenital heart disease. Circ J 2013;77(02):470–476
154 Lindley KJ, Bairey Merz CN, Asgar AW, et al; American College of Cardiology Cardiovascular Disease in Women Committee and the Cardio-Obstetrics Work Group. Management of women with congenital or inherited cardiovascular disease from pre-conception through pregnancy and postpartum: JACC Focus Seminar 2/5. J Am Coll Cardiol 2021;77(14):1778–1798
155 Houstis NE, Eisman AS, Pappagianopoulos PP, et al. Exercise intolerance in heart failure with preserved ejection fraction: diagnosing and ranking its causes using personalized O_2 pathway analysis. Circulation 2018;137(02):148–161
156 Phillips DB, Neder JA, Elbehairy AF, et al; Canadian Respiratory Research Network. Qualitative components of dyspnea during incremental exercise across the COPD continuum. Med Sci Sports Exerc 2021;53(12):2467–2476
157 O'Donnell DE, Elbehairy AF, Domnik NJ, et al. Patterns of cardiopulmonary response to exercise in COPD. In: Palange P, Laveneziana P, Neder JA, Ward SA, eds. Clinical Exercise Testing. Lausanne: European Respiratory Society; 2018:107–127
158 Boerrigter BG, Bogaard HJ, Trip P, et al. Ventilatory and cardiocirculatory exercise profiles in COPD: the role of pulmonary hypertension. Chest 2012;142(05):1166–1174
159 Simon M, LeBlanc P, Jobin J, Desmeules M, Sullivan MJ, Maltais F. Limitation of lower limb VO(2) during cycling exercise in COPD patients. J Appl Physiol 2001;90(03):1013–1019
160 Maltais F, Simard AA, Simard C, Jobin J, Desgagnés P, LeBlanc P. Oxidative capacity of the skeletal muscle and lactic acid kinetics during exercise in normal subjects and in patients with COPD. Am J Respir Crit Care Med 1996;153(01): 288–293
161 Broxterman RM, Hoff J, Wagner PD, Richardson RS. Determinants of the diminished exercise capacity in patients with chronic obstructive pulmonary disease: looking beyond the lungs. J Physiol 2020;598(03):599–610
162 Cheyne WS, Harper MI, Gelinas JC, Sasso JP, Eves ND. Mechanical cardiopulmonary interactions during exercise in health and disease. J Appl Physiol 2020;128(05):1271–1279
163 Waraich S, Sietsema KE. Clinical cardiopulmonary exercise testing: patient and referral characteristics. J Cardiopulm Rehabil Prev 2007;27(06):400–406
164 DePaso WJ, Winterbauer RH, Lusk JA, Dreis DF, Springmeyer SC. Chronic dyspnea unexplained by history, physical examination, chest roentgenogram, and spirometry. Analysis of a seven-year experience. Chest 1991;100(05):1293–1299
165 Pratter MR, Curley FJ, Dubois J, Irwin RS. Cause and evaluation of chronic dyspnea in a pulmonary disease clinic. Arch Intern Med 1989;149(10):2277–2282
166 Sandberg J, Ekström M, Börjesson M, et al. Underlying contributing conditions to breathlessness among middle-aged individuals in the general population: a cross-sectional study. BMJ Open Respir Res 2020;7(01):e000643
167 Pratter MR, Abouzgheib W, Akers S, Kass J, Bartter T. An algorithmic approach to chronic dyspnea. Respir Med 2011; 105(07):1014–1021
168 Martinez FJ, Stanopoulos I, Acero R, Becker FS, Pickering R, Beamis JF. Graded comprehensive cardiopulmonary exercise testing in the evaluation of dyspnea unexplained by routine evaluation. Chest 1994;105(01):168–174
169 Morris MJ, Grbach VX, Deal LE, Boyd SY, Morgan JA, Johnson JE. Evaluation of exertional dyspnea in the active duty patient: the diagnostic approach and the utility of clinical testing. Mil Med 2002;167(04):281–288
170 Palange P, Ward SA, Carlsen KH, et al; ERS Task Force. Recommendations on the use of exercise testing in clinical practice. Eur Respir J 2007;29(01):185–209
171 O'Donnell DE, Milne KM, Vincent SG, Neder JA. Unraveling the causes of unexplained dyspnea: the value of exercise testing. Clin Chest Med 2019;40(02):471–499
172 Tervonen H, Niskanen MM, Sovijärvi AR, Hakulinen AS, Vilkman EA, Aaltonen LM. Fiberoptic videolaryngoscopy during bicycle ergometry: a diagnostic tool for exercise-induced vocal cord dysfunction. Laryngoscope 2009;119(09):1776–1780
173 Nedeljkovic I, Banovic M, Stepanovic J, et al. The combined exercise stress echocardiography and cardiopulmonary exercise test for identification of masked heart failure with preserved ejection fraction in patients with hypertension. Eur J Prev Cardiol 2016;23(01):71–77
174 Laufer-Perl M, Gura Y, Shimiaie J, et al. Mechanisms of effort intolerance in patients with rheumatic mitral stenosis: combined echocardiography and cardiopulmonary stress protocol. JACC Cardiovasc Imaging 2017;10(06):622–633
175 Berry NC, Manyoo A, Oldham WM, et al. Protocol for exercise hemodynamic assessment: performing an invasive cardiopulmonary exercise test in clinical practice. Pulm Circ 2015;5(04):610–618
176 Huang W, Resch S, Oliveira RK, Cockrill BA, Systrom DM, Waxman AB. Invasive cardiopulmonary exercise testing in the evaluation of unexplained dyspnea: Insights from a multidisciplinary dyspnea center. Eur J Prev Cardiol 2017;24(11):1190–1199
177 Joseph P, Arevalo C, Oliveira RKF, et al. Insights from invasive cardiopulmonary exercise testing of patients with myalgic encephalomyelitis/chronic fatigue syndrome. Chest 2021;160(02):642–651
178 Taivassalo T, Jensen TD, Kennaway N, DiMauro S, Vissing J, Haller RG. The spectrum of exercise tolerance in mitochondrial myopathies: a study of 40 patients. Brain 2003;126(Pt 2):413–423

High Altitude

Marc Moritz Berger, MD, DESA[1] Andrew M. Luks, MD[2]

[1] Department of Anesthesiology and Intensive Care Medicine, University Hospital Essen, University Duisburg-Essen, Essen, Germany
[2] Division of Pulmonary, Critical Care and Sleep Medicine, University of Washington, Seattle, Washington

Address for correspondence Marc Moritz Berger, MD, DESA, Department of Anesthesiology and Intensive Care Medicine, University Hospital Essen, Hufelandstr. 55, 45147 Essen, Germany (e-mail: marcberger@hotmail.com).

Semin Respir Crit Care Med 2023;44:681–695.

Abstract

With ascent to high altitude, barometric pressure declines, leading to a reduction in the partial pressure of oxygen at every point along the oxygen transport chain from the ambient air to tissue mitochondria. This leads, in turn, to a series of changes over varying time frames across multiple organ systems that serve to maintain tissue oxygen delivery at levels sufficient to prevent acute altitude illness and preserve cognitive and locomotor function. This review focuses primarily on the physiological adjustments and acclimatization processes that occur in the lungs of healthy individuals, including alterations in control of breathing, ventilation, gas exchange, lung mechanics and dynamics, and pulmonary vascular physiology. Because other organ systems, including the cardiovascular, hematologic and renal systems, contribute to acclimatization, the responses seen in these systems, as well as changes in common activities such as sleep and exercise, are also addressed. While the pattern of the responses highlighted in this review are similar across individuals, the magnitude of such responses often demonstrates significant interindividual variability which accounts for subsequent differences in tolerance of the low oxygen conditions in this environment.

Keywords
- acclimatization
- cardiovascular system
- exercise
- gas exchange
- hematologic system
- hypoxic pulmonary vasoconstriction
- hypoxic ventilatory response
- respiratory system

Other articles of this series have primarily examined how the respiratory system functions under normal circumstances. The system changes in important ways, however, when various forms of stress including exercise and changes in barometric pressure are applied to the system. In this article, we consider the physiological changes that occur in response to one of those forms of stress—ascent to high altitude and a decrease in barometric pressure.

A variety of responses occur across multiple organ systems over varying time frames ranging from seconds to weeks following exposure to hypoxia and, in general, help the body adjust to the low oxygen conditions at high altitude, a process referred to as acclimatization. This article primarily focuses on the effects of hypobaric hypoxia on the respiratory system including its effects on control of breathing, ventilation, gas exchange, lung mechanics and dynamics, and pulmonary vascular physiology. Because other organ systems play a role in the coordinated response to hypobaric hypoxia and contribute to acclimatization, the article also addresses responses seen in the cardiovascular system, kidneys, and blood as well as at the tissue and cellular levels. Finally, the article examines alterations in common activities—sleep and exercise—in the setting of low barometric pressure and reduced oxygen tensions. The focus throughout the article will be on responses seen in unacclimatized lowlanders who ascend to high altitude rather than long-term residents at high elevation.

The Environment at High Altitude

The defining feature of the environment at high altitude is the nonlinear decrease in barometric pressure with

Issue Theme Pulmonary Physiology; Guest Editors: David A. Kaminsky, MD, Kathryn A. Hibbert, MD, and Andrew M. Luks, MD

Thieme Medical Publishers, Inc.,
333 Seventh Avenue, 18th Floor,
New York, NY 10001, USA

DOI https://doi.org/10.1055/s-0043-1770063.
ISSN 1069-3424.

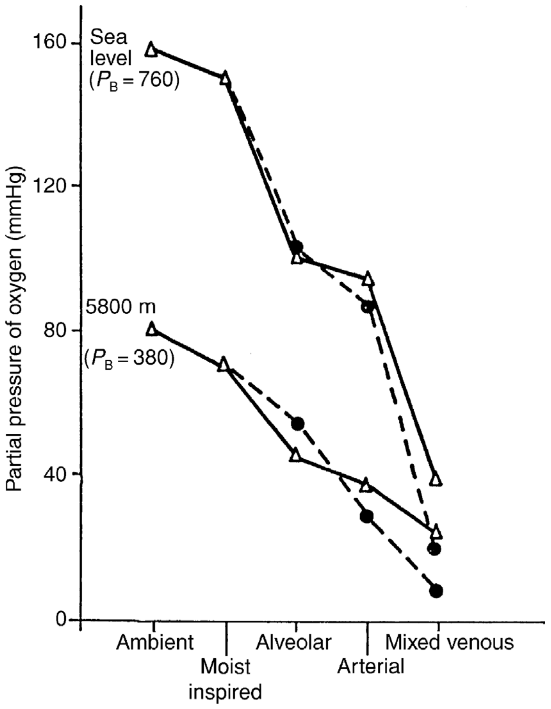

Fig. 1 Changes in the partial pressure of oxygen along the oxygen transport cascade from ambient air through the body at sea level and at an altitude of 5,800 m. Open triangles: rest; closed circles: maximum exercise. (Reproduced with permission from Pugh[153].)

increasing elevation, such that at the summit of Mount Everest (8,848 m), it is, on average, only about one-third the value at sea level or approximately 253 mm Hg. The decline in barometric pressure leads to a reduction in the partial pressure of oxygen (PO_2) at every point along the oxygen transport chain (►**Fig. 1**) from ambient air to the mitochondria which, in turn, sets in motion the series of physiologic responses that will be described in greater detail in the remainder of this article. The greater the gain in elevation, the lower the partial pressure at each point along this transport chain.

Due to a large mass of cold air in the stratosphere above the equatorial regions, the pressure for any given elevation is higher near the equator than at higher latitudes (►**Fig. 2A**).[1,2] Barometric pressure at any given elevation is also lower in the winter months (►**Fig. 2B**)[1] and can vary quite significantly during fluctuations in weather.[3] The magnitude of such changes in pressure is generally of little consequence from a physiologic standpoint at moderate elevations of 2,500 to 6,000 m but at the extremes of elevation (>8,000 m) can make a significant difference in the ability of a climber to perform physical work in the absence of supplemental oxygen.

Aside from the decline in barometric pressure and the reduction in PO_2, there are other important environmental changes that impact individuals at high altitude. Ambient temperature decreases with increasing elevation at a rate of approximately 1°C for every 150 m gain in elevation. Absolute humidity also decreases with increasing elevation and can contribute to excessive insensible fluid losses through the respiratory tract in the setting of increased minute ventilation, particularly with exercise. The amount of ultraviolet light exposure increases significantly with gains in altitude because absorption of solar radiation is reduced due to the less dense and drier air at higher elevations.

While air quality typically improves with travel into the mountains, poor air quality can still be seen at higher elevations. In addition to the fact that mountain valley systems can trap pollutants from nearby urban centers during temperature inversions, poor air quality can also be found in rural mountain communities with high use of wood and yak-burning heat sources and due to shifting smoke

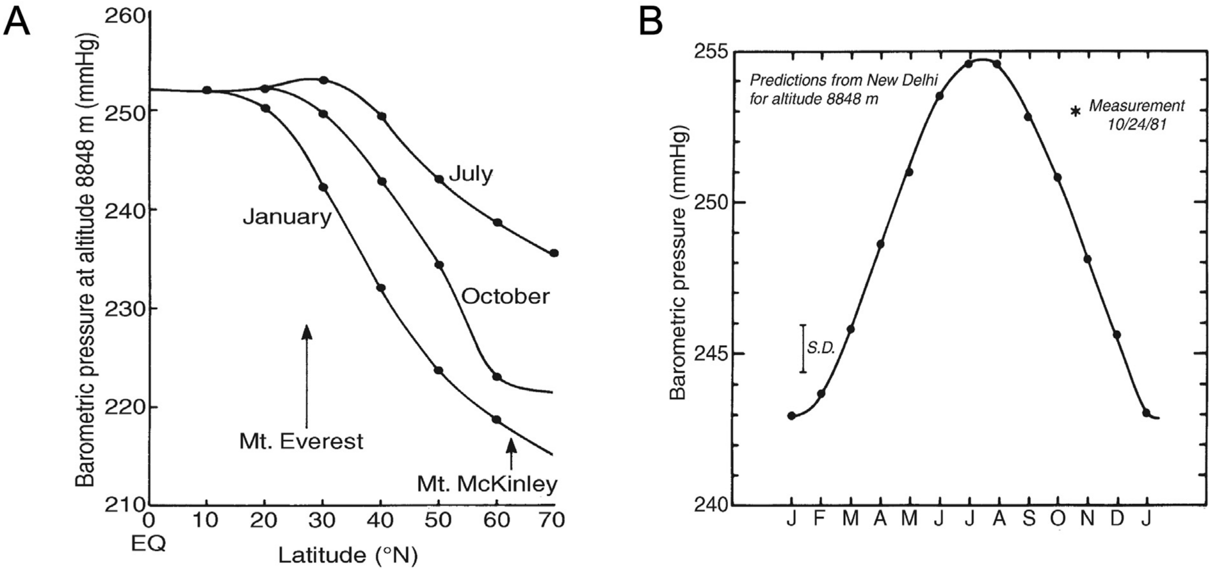

Fig. 2 **(A)** Relationship between latitude in the northern hemisphere and barometric pressure at an altitude of 8,848 m plotted for January, July, and October with the latter being one of two preferred climbing months for Mount Everest. **(B)** Mean monthly barometric pressure at an altitude of 8,848 m as obtained from data collected with weather balloons released from New Delhi, India, over a period of 15 years. During the summer months mean barometric pressure is higher than during the winter months. (Reproduced with permission from West et al[1].)

patterns from wildfires that are becoming more frequent in the era of climate change.

Acclimatization Versus Adaptation

The physiological responses that occur with acute exposure to hypobaric hypoxia are generally referred to as "acclimatization," the main purpose of which is to help individuals tolerate the reduction in barometric pressure and the subsequent reductions in the PO_2. While acclimatization does not restore the arterial and tissue PO_2 to sea-level values, particularly at the extremes of elevation, acclimatization protects against acute altitude illnesses—acute mountain sickness, high-altitude cerebral edema, and high-altitude pulmonary edema[4]—and improves cognitive and submaximal exercise performance.[5–7] The process of acclimatization should be distinguished from adaptation, a term used more commonly in regard to high-altitude residents which refers to phenotypic traits that have been acted upon by natural selection and, in particular, features of structure, function, and behavior that increase such residents' ability to survive and reproduce at high altitude.[8] The focus of the remainder of this article will be on acclimatization rather than adaptation.

Respiratory System Responses to High-Altitude Exposure

Although multiple systems participate in the response to hypobaric hypoxia, the respiratory system is clearly the center of this response and, as a result, warrants the greatest attention. The primary physiologic changes seen in the respiratory system are described below.

Control of Breathing

The rhythmic pattern of breathing is controlled by four separate respiratory centers located in the brain stem and is modulated by central and peripheral chemoreceptors, located in the ventrolateral surface of the medulla, and the carotid and aortic bodies, respectively.

Under sea-level conditions, ventilation is mainly modulated by the central chemoreceptors, which are sensitive to changes in PCO_2 and H^+ ion concentration in the extracellular fluid of the brain. Because the blood–brain barrier is highly permeable to dissolved CO_2, an increase in arterial PCO_2 ($PaCO_2$) increases the H^+ ion concentration in the brain's cerebrospinal fluid and neuronal tissue, mediating an increase in minute ventilation. The peripheral chemoreceptors are primarily sensitive to P_aO_2 but, to a lesser extent, also respond to changes in P_aCO_2 and H^+ ion concentration. The ventilatory drive of the peripheral chemoreceptors is assumed to be additive to the central chemoreflex drive that is already present,[9,10] with a relative contribution of about one-third when compared with the effect of the central chemoreceptors.[11]

With gains in altitude the contribution of the peripheral chemoreceptors increases, and eventually hypoxemia becomes the primary added stimulus to the basal breathing pattern.[12] Among the peripheral chemoreceptors, the carotid bodies are a more powerful regulator of the hypoxic ventilatory response (HVR) than the aortic bodies. The HVR is mediated by changes in the P_aO_2 rather than changes in arterial oxygen content and is not observed when the carotid bodies are denervated.[13] The characteristic sensing cells of the carotid bodies are the glomus cells, which synapse with peripheral, sensory endings of the glossopharyngeal nerve whose signals are then conducted to the brainstem, thereby regulating minute ventilation by changes in both respiratory rate and tidal volume.[12]

Ventilation

In what is perhaps the first and most important physiologic response to hypobaric hypoxia at high altitude, ventilation increases following ascent to high altitude to maintain adequate P_AO_2 and P_aO_2, with the magnitude of the response varying significantly between individuals. The increase in ventilation starts as the PO_2 falls,[14] becoming more prominent once the inspired PO_2 (P_IO_2) is below 100 mm Hg,[15] which corresponds to an altitude of approximately 3,000 m or a $P_aO_2 < \sim 60$ mm Hg. Upon acute exposure to high altitude the time course of the HVR is characterized by a rapid increase in ventilation followed by a secondary transient decrease, known as the "roll-off phenomenon."[16] After 30 to 60 minutes, ventilation increases again, eventually reaching a maximum after hours to days, weeks or even months depending on the absolute altitude attained, the duration of exposure, and the species.[17] The kinetic of the HVR is summarized in ►**Fig. 3**.

Hyperventilation is critical for defending the alveolar PO_2 (P_AO_2) in the face of the reduced barometric pressure and P_IO_2, particularly at the extremes of high elevation. At sea level, the normal alveolar ventilation results in a P_ACO_2 of approximately 40 mm Hg. If hyperventilation did not occur and ventilation and P_ACO_2 were maintained at sea-level values following ascent to the summit of Mount Everest where the P_IO_2 is approximately 43 mm Hg,[14] the P_AO_2 as calculated by the ideal alveolar gas equation using a respiratory exchange ratio of 0.8 would be about −7 mm Hg which, of course, is physiologically impossible. Yet, with an appropriate ventilatory response, an individual can maintain P_AO_2 and P_aO_2 to a degree sufficient to support metabolic activity.[18] By way of example, measurements during a simulated ascent of Mount Everest in a hypobaric chamber in Operation Everest II as well as measurements in a single mountaineer on the summit of Mount Everest have shown that hyperventilation decreases the P_ACO_2 to approximately 8 to 12 mm Hg yielding a P_aO_2 of approximately 30 mm Hg.[19,20]

At the same time that the P_AO_2 and P_aO_2 increase, the arterial partial pressure of CO_2 (P_aCO_2) decreases leading to a respiratory alkalosis. This, in turn, decreases central and peripheral chemoreceptor output, thereby acting as negative feedback mechanism and slowing the increase in ventilation. With ascent to the extremes of elevation and time to acclimatize, extreme degrees of hyperventilation and respiratory alkalosis can be seen. During the 1981 American Medical Research Expedition to Everest, for example, the mean minute ventilation of one of the mountaineers while

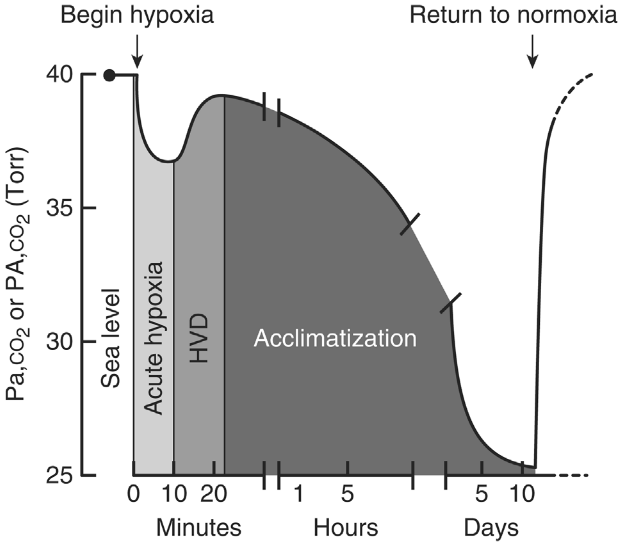

Fig. 3 Time course of the ventilatory response to a given degree of hypoxia. The acute rise in ventilation causes a decrease in PCO_2 that is followed by a transient increase in PCO_2 due to hypoxic ventilatory depression (roll-off phenomenon). After approximately 20 minutes of acclimatization ventilation increases again, causing a sustained decrease in PCO_2. (Reproduced with permission from Smith et al[154].)

climbing for nearly 7 minutes at an elevation of 8,300 m was approximately 108 L/min with a mean respiratory rate of approximately 86 breaths/min.[21] On the 2007 Xtreme Everest expedition, a mean P_aCO_2 of 13.3 mm Hg (range of 10.3–15.7 mm Hg) and pH >7.5 were observed when arterial blood gas measurements were performed on four subjects breathing ambient air at rest at 8,400 m.[22]

It is generally thought that a strong HVR helps in performing at the extremes of high altitude, as only those individuals with a strong HVR can tolerate exposure to such altitudes without supplemental oxygen.[23,24] At the same time, it has been suggested that individuals with very strong HVR may approach their ventilatory limit at relatively lower altitudes, whereas subjects with a strong but not excessive HVR can sustain high levels of ventilation at extreme altitudes while maintaining an adequate ventilatory reserve for the summit, particularly if a relatively lower minute ventilation is compensated by a higher ventilatory efficiency.[23]

HVR and Hypercapnic Ventilatory Response during Acclimatization

As time spent at a given elevation increases and acclimatization proceeds, the sensitivity of the peripheral chemoreceptors increases,[25–27] such that at a given altitude minute ventilation continues to rise.[25,28] After return to low altitude, the increased HVR persists for several days or weeks,[25] which, in turn, aids ventilatory acclimatization if the individual reascends to high altitude.[29]

As with HVR, the hypercapnic ventilatory response also evolves over time at high altitude. In particular, the sensitivity of the chemoreceptor response to CO_2 is increased with prolonged stay at high altitude,[25,26] such that ventilation rises in response to lower PCO_2 values at high altitude than would be the case at lower elevations.[30] The increased CO_2 sensitivity, which, as shown in ►**Fig. 4**, is reflected by a steepening and leftward shift in the ventilation–CO_2 response curve[31] results, in part, from elimination of bicarbonate ions (HCO_3^-) by the kidneys as they compensate for the sustained respiratory alkalosis.[32,33] This reduces the buffering capacity in the central compartment and increases the relative stimulation of central chemoreceptors by H^+ ions for a given PCO_2.[34]

Magnitude of Hypoxic Ventilatory Response

Measuring HVR is challenging because several different factors influence its regulation and must be controlled for

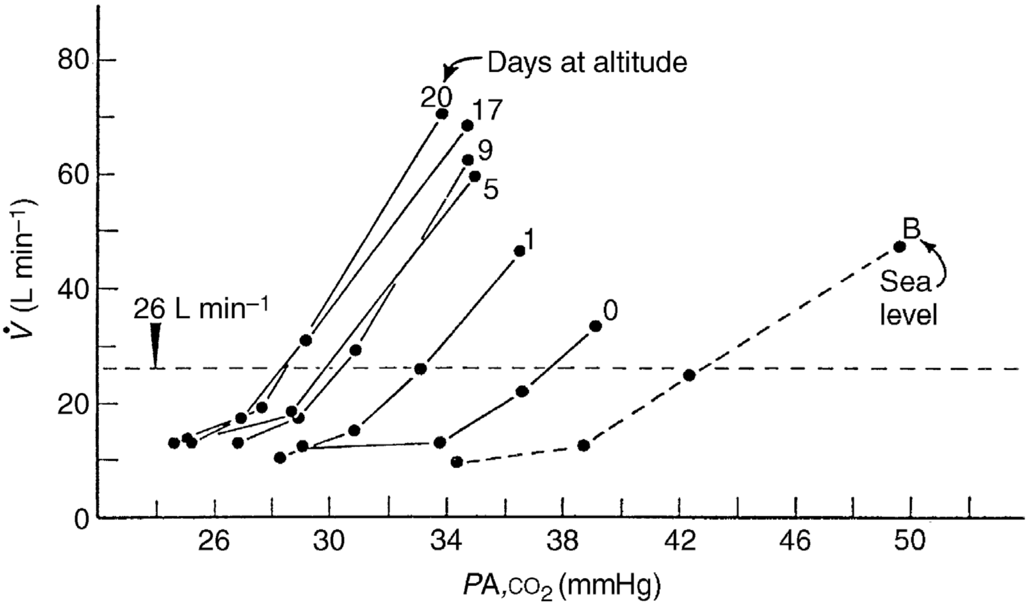

Fig. 4 Effect of acclimatization on the hypercapnic ventilatory response at an altitude of 4,340 m. (Reproduced with permission from Pace[155].)

in the measurement process. Since the change in ventilation at high altitude is mitigated by changes in P_aCO_2, the true magnitude of an individual's HVR can only be measured under isocapnic (i.e., constant P_aCO_2) conditions. If, in contrast, P_aCO_2 is allowed to decrease with an increase in minute ventilation, then the poikilocapnic HVR is measured.

Several methods are used to measure HVR. Both the rebreathing method, for which oxygen is consumed from a closed circuit to induce progressive hypoxemia, and the steady-state method, during which the ventilatory response is measured while hypoxia is progressively induced over 7 to 10 minutes, are used to quantify HVR as a change in ventilation for a given change in SO_2. Other approaches include single- or multiple breath methods in which several breaths of 100% nitrogen are made and the change in ventilation in the following few breaths is measured. If HVR is assessed in an environment that is already hypoxic, e.g., at high altitude, a 10-minute hyperoxic period ($F_IO_2 = 0.60$) should be administered before ventilatory response tests are performed to eliminate the hypoxic ventilatory depression caused by the ambient hypoxic atmosphere.[25]

As shown in ►**Fig. 5**, there are considerable interindividual differences in the magnitude of HVR,[35] in large part due to genetic factors.[36,37] This variability is also demonstrated by data from Milledge et al who reported an isocapnic HVR of 0.51 to 3.10 L/min/%SaO_2 (S_aO_2: arterial oxygen saturation) in 17 healthy male subjects with an age between 23 and 58 years.[38] Women appear to have a lower HVR compared with men,[36] while older individuals have lower HVR compared with a younger population.[39] At sea level, endurance athletes appear to have a lower HVR than age-matched controls[40,41] but this may not be the case following acclimatization to high altitude.[41]

Gas Exchange

Due to the reduction in the P_AO_2 following ascent, the pressure differential for diffusion across the alveolar capillary barrier (i.e., the difference between the alveolar and mixed venous PO_2) is reduced (►**Fig. 1**). The reduced pressure differential slows the rate of diffusion of oxygen across the alveolar–capillary barrier and increases the time required for equilibration between the alveolar and capillary PO_2. As long as an individual remains at rest, the red blood cells spend enough time in the pulmonary capillaries to allow full equilibration but with exercise, capillary transit time may fall to the point that an alveolar-end capillary PO_2 difference develops, thereby worsening hypoxemia. At the extremes of high elevation, however, an alveolar-end capillary PO_2 difference can be seen, even at rest, as the pressure differential and rate of diffusion are low enough to cause diffusion limitation to pulmonary gas exchange.[42]

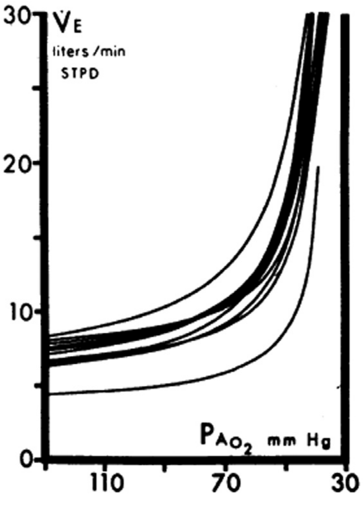

Fig. 5 Changes in minute ventilation ($\dot{V}_E$) with decreasing P_AO_2 in 10 normal subjects. (Reproduced with permission from Weil et al[35].)

Another important feature of pulmonary gas exchange at high altitude, especially during exercise, is the worsening of ventilation–perfusion matching, as demonstrated by Wagner et al,[43] who used the multiple inert gas elimination technique to measure ventilation–perfusion inequality during a simulated ascent of Mount Everest. At both rest and with increasing levels of work, the logarithmic standard deviation of perfusion, a marker of ventilation–perfusion inequality, increased with reductions in the barometric pressure (►**Fig. 6**). The mechanism for the rise in ventilation–perfusion inequality is not clear but may relate to the development of subclinical interstitial edema during physical activity on ascent,[44] uneven hypoxic pulmonary vasoconstriction (HPV) with regional overperfusion,[45] increased shunt caused by an open foramen ovale as seen in approximately 30% of the

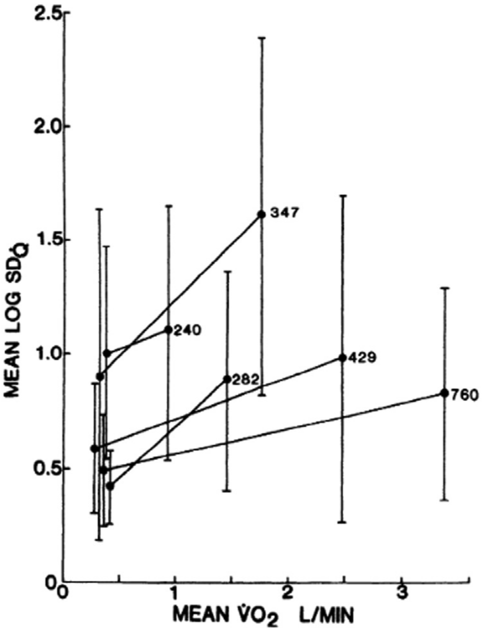

Fig. 6 Increasing ventilation–perfusion inequality with reductions in barometric pressure. The Log SD, obtained via the multiple inert gas elimination technique, is a marker of ventilation–perfusion matching with higher values representing greater degrees of inequality. For a given barometric pressure, represented by the number displayed to the right of each line, two points are shown, representing resting values and those measured at maximum exercise. Note that ventilation–perfusion inequality increases with decreasing barometric pressure and increasing levels of work. (Reproduced with permission from Wagner et al[43].)

population,[46] and/or by an increased right-to-left shunt due to intrapulmonary arterio-venous anastomoses.[47]

Lung Mechanics and Dynamics

Unlike many other aspects of respiratory system function for which there is clear evidence regarding the direction, magnitude, and timing of responses to hypobaric hypoxia, the situation is much less clear regarding changes in lung mechanics and dynamics following ascent. This problem likely relates not only to problems with small sample sizes in many studies but also to the extensive methodological differences across studies, such as whether a study was done at terrestrial high altitude or in a simulated high-altitude environment, the altitude at which the study was conducted, the timing of testing after arrival at that altitude, the ascent rate, and the activity level of the study participants.

Lung Mechanics

Of the parameters that have been repeatedly studied in hypoxia, the one for which there appears to be the most consistent data is the vital capacity. Multiple studies examining changes with acute[48,49] and subacute[50,51] exposures at both terrestrial[52] and simulated[53] high altitude have shown reductions in in this parameter, although several relatively large and more recent studies[44,54] have not shown any changes in vital capacity within 2 days of ascent to 4,559 m. There is no consensus as to why vital capacity is reduced but various mechanisms have been proposed including accumulation of interstitial fluid,[51] decreased respiratory muscle strength,[55] hypocapnia,[56] and increased pulmonary blood volume.[50] Inconsistent results have been reported regarding static lung compliance with studies reporting either a decrease,[57] an increase,[58] or no change[48] in this parameter at altitudes between 3,000 and 4,559 m.

The fact that minute ventilation increases at both rest and with any degree of physical exertion at high altitude compared with sea level raises the question as to whether respiratory muscle strength and the ability to sustain the increased work of breathing changes at high altitude are impaired. Inconsistent results have been reported regarding respiratory muscle strength at rest,[55,59,60] but studies performed during exercise do suggest that various markers of respiratory muscle strength including the force-generating capacity, time to exhaustion, and time to recovery of the diaphragm are impaired.[61,62] The clinical implications of these observed changes are not clear.

Lung Dynamics

When studied in isolation, some of the features of the high-altitude environment, including hypocapnia resulting from the HVR, have been shown to increase airway resistance,[63,64] while other factors such as the reduction in air density or increase in sympathetic nervous system activity[65] with ascent might be expected to reduce airway resistance. When an individual ascends to high altitude, however, all of these factors are acting on the airways at the same time. Given this, it is not necessarily surprising that variable results have been reported regarding changes in airway resistance following ascents to 3,400 to 5,300 m, with some studies reporting a decrease in resistance[48,52] and others reporting no change.[54,66] Despite the lack of clear changes in airway resistance, studies have consistently reported increases in peak expiratory flow at high altitude.[55,67] The magnitude of this change appears to increase with increasing altitude,[51] suggesting that further reductions in air density at high elevations may be responsible for the observed changes. Airway hyperresponsiveness has been shown to decrease following ascent to 4,559 to 5,050 m in both healthy individuals[68] and individuals with well-controlled asthma.[69]

Pulmonary Vascular Responses

The effect of hypoxia on the pulmonary vasculature, referred to as the von Euler–Liljestrand reflex or HPV,[70] has attracted considerable attention since the middle of the last century.[70] It is well known that alveolar hypoxia causes constriction of pulmonary arterioles to optimize ventilation–perfusion matching and alveolar gas exchange by diverting blood flow away from poorly ventilated regions of the lung. While HPV is beneficial in situations where alveolar hypoxia occurs on a local basis, as seen, for example, in patients with pneumonia, at high altitude alveolar hypoxia occurs on a global basis, resulting in more widespread HPV and subsequent increases in pulmonary vascular resistance. At altitudes above 1,600 to 2,500 m[71–73] and in conjunction with increases in cardiac output (see below), HPV increases pulmonary artery pressure and right ventricular afterload. The magnitude of HPV is not equivalent in all areas of the lung[45,74] and, like HVR, demonstrates significant inter-individual variability (►**Fig. 7**).[75] Due to the regional heterogeneity of HPV, some areas of the pulmonary vasculature receive more perfusion than others. In individuals with exaggerated HPV, this heterogeneity can contribute to the development of high-altitude pulmonary edema,[45,74] a noncardiogenic form of pulmonary edema seen in healthy individuals who ascend too quickly to altitudes above 3,000 m.

HPV occurs in several phases with the first beginning almost immediately upon exposure to hypoxia.[76,77] A second phase starts after approximately 2 hours, followed by a further increase in pulmonary artery pressure over another 6 to 8 hours.[78] The mechanisms underlying HPV are complex and intrinsic to the vascular smooth muscle. In the first phase, hypoxia induces the formation of free radicals and associated reactive oxygen species that increase intracellular Ca^{2+} concentration, leading to contraction of pulmonary vascular smooth muscle cells.[77] In the second phase, vasoconstriction is maintained by a sustained reduction in nitric oxide bioavailability combined with increased endothelium-derived vasoconstrictors, such as endothelin-1.[79–81] These processes are modulated by various factors, including pulmonary innervation, circulating hormones, acid–base status, and erythrocytes. Further details about these mechanisms can be found in several excellent reviews on this topic.[77,82,83]

With short exposures to hypoxia (hours to a few days), HPV can be completely reversed by administration of

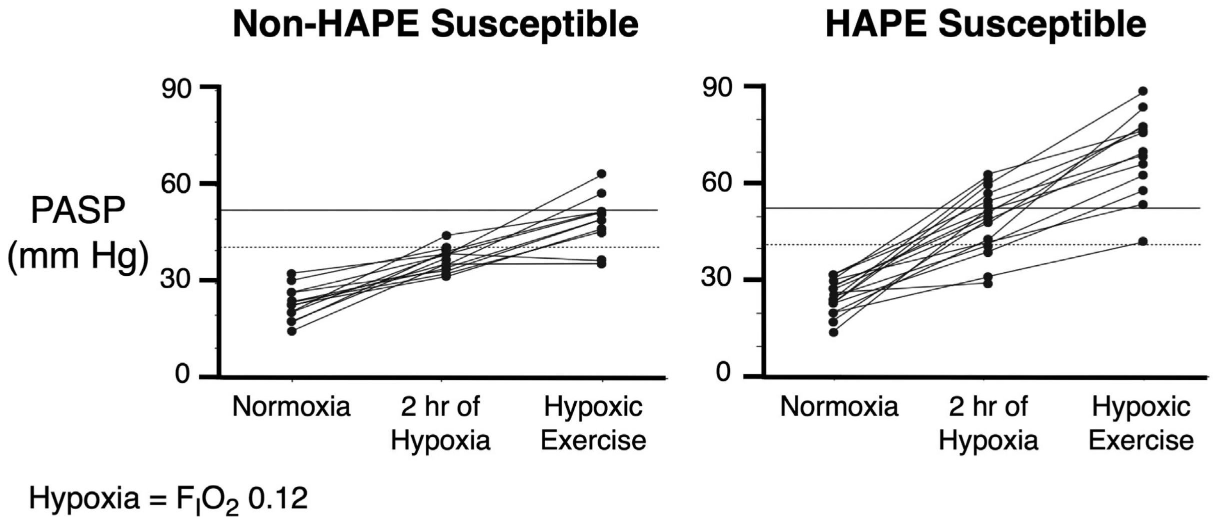

Fig. 7 Estimated pulmonary artery systolic pressure (PASP) values for subjects with and without susceptibility to high-altitude pulmonary edema (HAPE) measured with transthoracic echocardiography in normoxia, after 2 hours of normobaric hypoxia ($F_IO_2 = 0.12$), and during exercise in hypoxia. The lines indicate the cut-off levels for optimal differentiation between HAPE-susceptible and nonsusceptible subjects, i.e., 41 mm Hg after 2 hours in hypoxia (dotted line) and 52 mm Hg during hypoxic exercise (solid line). (Reproduced with permission from Dehnert et al[156].)

supplemental oxygen.[84] With prolonged hypoxia, however, vascular remodeling occurs, leading to structural changes in the pulmonary vasculature,[85] and progressive decreases in the reversibility of HPV with supplemental oxygen.[86] Remodeling results from a multistep process in which hypoxia-inducible factor (HIF) 1-α is considered to be the key player.[87,88] Hyperproliferation of endothelial cells, smooth muscle cells and fibroblasts, and accumulation of extracellular matrix lead to increased thickness of the vessel wall and vascular stiffening.[89] The precise time course for remodeling and blunted response to supplemental oxygen is not known but likely starts within a few days to several weeks.[84] If chronic and untreated, the increased pressure load of the right ventricle can progress to right heart failure in select individuals.[90]

Other Systems: Cardiovascular, Blood, Renal, and Tissue Responses

Other organ systems manifest changes in response to hypoxia which, together with the respiratory system responses noted above, play a large role in maintaining oxygen delivery and adequate PO_2 in the tissue.

The Cardiovascular System

Upon ascent to high altitude and exposure to acute hypoxia, cardiac output increases as a means of maintaining convective oxygen transport in the face of reduced arterial oxygen content. The observed changes in cardiac output are largely due to increases in heart rate[91,92] that are proportional to the degree of hypoxia and occur as a result of both β-sympathetic activation[93] and parasympathetic withdrawal.[94] Stroke volume does not change significantly with acute exposure to hypoxia but tends to fall as acclimatization proceeds, largely as a result of reductions in plasma volume,[95,96] due to a diuretic response to hypoxia and fluid shifts due to changes in plasma oncotic pressure.[97,98]

Myocardial contractility as assessed by echocardiography is preserved in acute hypoxia[95,99] although subtle changes such as more rapid diastolic untwisting velocity[100] have been reported. Systemic blood pressure increases to a limited degree following ascent to high altitude, although there can be a significant interindividual variability in the observed responses.[101] ►**Fig. 8** summarizes the average cardiovascular changes during the first 10 days of acute exposure to altitudes between 3,800 and 4,559 m in healthy subjects. These changes tend to normalize with exposures to moderate altitudes (approximately 2,500 m) but may remain elevated at higher elevations despite acclimatization to such altitudes.[102,103] Although myocardial ischemia is a well-known precipitant of arrhythmia in individuals with cardiac disease at sea level, clinically significant arrhythmias are uncommon at high altitude, even at the extremes of elevation (approximately 8,000 m) where the P_aO_2 may be as low as 30 to 35 mm Hg.[19,20,22] This is likely because coronary vasodilation occurs in the setting of hypoxemia and maintains sufficient myocardial perfusion and oxygen delivery.[104,105]

The Hematologic System

Along with the increase in cardiac output, another important physiologic response which helps maintain oxygen delivery in the face of arterial hypoxemia is an increase in the oxygen carrying capacity of the blood. Hemoglobin concentration increases following ascent, initially as a result of decreased plasma volume and hemoconcentration[106,107] and later as a result of increased red cell mass in response to the hypoxemia-mediated rise in the serum erythropoietin concentration. Erythropoietin secretion increases in the first 24 to

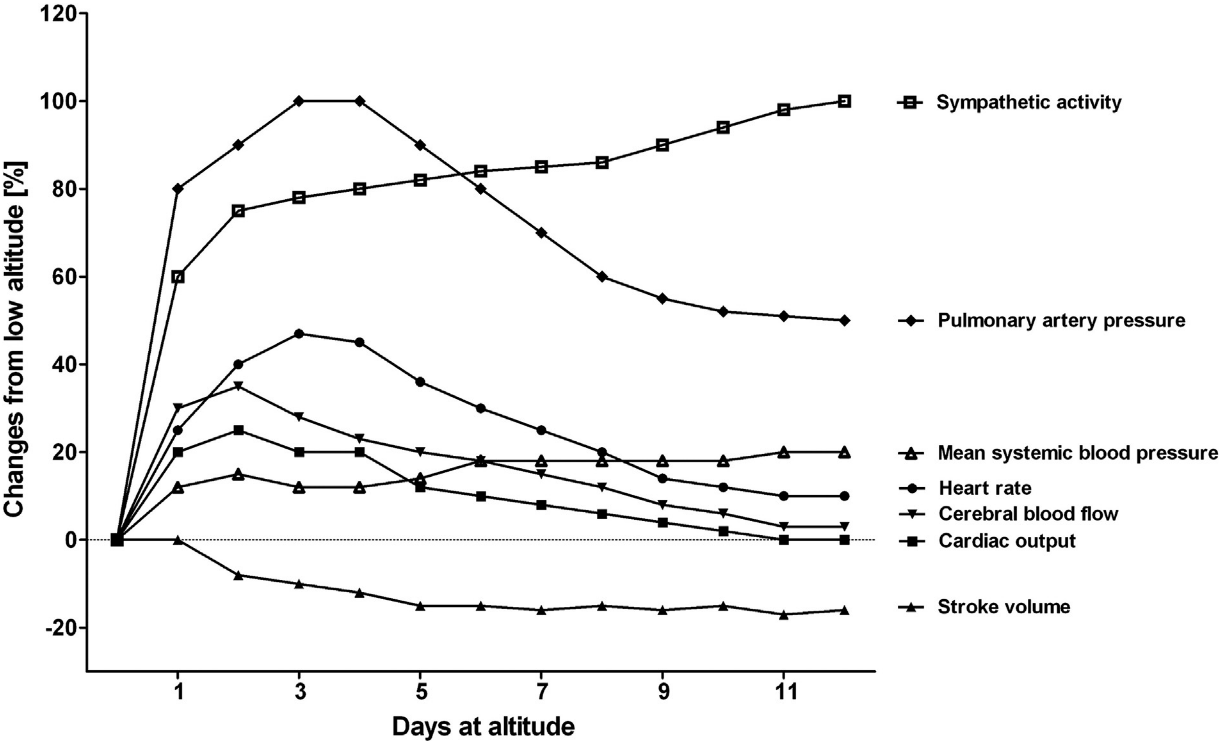

Fig. 8 Average cardiovascular and autonomic changes in healthy subjects during the first 10 days of acute exposure to altitudes between 3,800 and 4,559 m. Peak responses for the majority of cardiovascular system parameters are seen during the first few days of high-altitude exposure. (Reproduced with permission from Rimoldi et al[157].)

48 hours following ascent to a given elevation (►**Fig. 9**), declines as acclimatization proceeds, and increases further with subsequent gains in elevation.[108] The ultimate magnitude of the erythropoietic response varies significantly between individuals.

With ascent to a sufficiently high elevation, the P_aO_2 in healthy individuals falls along the steep portion of the hemoglobin–oxygen dissociation curve, whereby small changes in P_aO_2 lead to marked changes in the S_aO_2. The dissociation curve shifts to the left in the initial period following ascent due to the respiratory alkalosis that results from the HVR described above. Over time, however, the curve shifts back toward the right in response to increases in the serum 2,3-diphosphoglycerate concentration and renal compensation for the respiratory alkalosis. The ultimate position of the curve in a given individual is determined by the altitude attained and the duration of time spent at that elevation. For example, a rightward shift in the curve has been reported at a moderate altitude of 2,300 m,[109] whereas a leftward shift has been noted at 8,050 m,[110] likely due to the significant respiratory alkalosis at such elevations.

Based on numerous case reports of thromboembolic events at high altitude, there has long been suspicion that hypobaric hypoxia predisposes to coagulopathy, but systematic studies of the clotting cascade have never yielded consistent evidence of a hypercoagulable state. In fact, when thrombelastography, a technique which simultaneously investigates multiple aspects of the clotting cascade, was used to assess function of the coagulation system at high altitude, it appeared that coagulation was actually slowed at high elevation compared with low elevation.[111]

The Kidneys

Beyond renal compensation for the respiratory alkalosis described above, other important renal responses following ascent to high altitude include increased natriuresis and diuresis. These responses are not due to changes in renin, angiotensin, aldosterone, or atrial natriuretic peptide and, instead, are mediated by the peripheral chemoreceptors. Much like the HVR, which is also mediated by the peripheral chemoreceptors, the magnitudes of the diuretic and natriuretic responses vary significantly between individuals.[97] Along with the decreased humidity and increased insensible fluid losses through the respiratory tract with hyperventilation at high altitude, the diuretic and natriuretic responses increase the risk of dehydration, particularly when individuals do not maintain sufficient fluid intake.

The Central Nervous System

Even in the presence of severe reductions in arterial oxygen content with ascent to very high elevations, cerebral oxygen consumption remains constant due to the effects of hypoxic vasodilation in extra- and intracranial arteries and subsequent increases in cerebral blood flow.[112] The respiratory alkalosis noted above counteracts this vasodilation to some extent but the net response to high-altitude exposure is still a state of vasodilation. Increases in cerebral blood flow may play a role in the development of acute mountain sickness

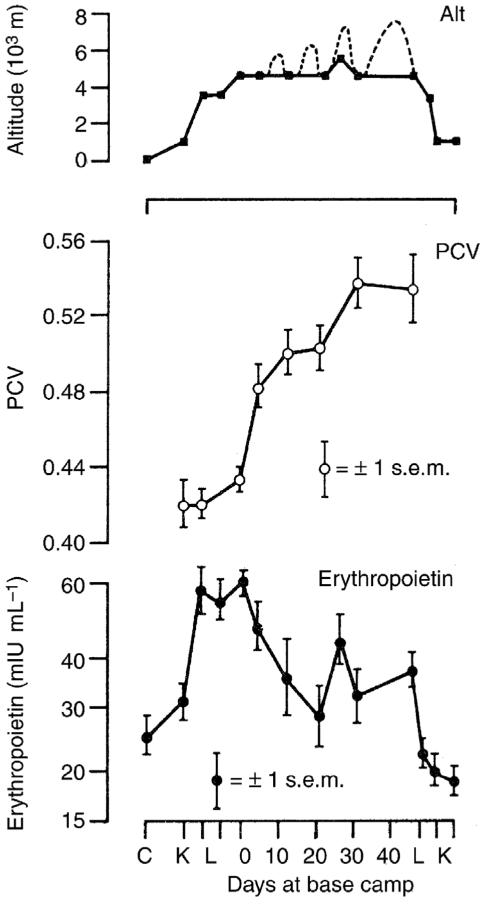

Fig. 9 Changes in mean packed cell volume (PCV, middle panel) and serum erythropoietin concentration (bottom panel) with gains in elevation (top panel). The dotted lines in the top panel indicate ascent above 4,500 m between collection of blood samples. (Reproduced with permission from Milledge and Cotes[108].)

and high-altitude cerebral edema, two of the primary forms of acute altitude illness, although the precise pathophysiology of those disorders remains unclear and many other factors contribute to their development. With continued stay at a given elevation, cerebral blood flow eventually declines toward baseline values due to increases in arterial oxygen content with acclimatization as well as changes in the sensitivity of the cerebral vasculature.[113,114]

Tissue and Cellular Level Responses

Multiple changes occur at the tissue level, particularly in skeletal muscle, which affect oxygen transport and utilization in the face of very low tissue PO_2. The degree of consensus around these changes is less than with other physiologic responses to hypoxia, due to the difficulties of studying many of these issues in humans. The diffusion distance from capillaries to mitochondria is reduced by an increase in capillary density that stems primarily from a reduction in muscle fiber size rather than angiogenesis.[115,116] There are no significant changes in muscle fiber type—slow versus fast twitch[117,118]—while mitochondrial volume density decreases with exposure to very high altitude.[117,119] Hypoxia likely decreases oxidative capacity in skeletal muscle but has little impact on glycolytic pathways.[14] Debate exists about whether expression of myoglobin, a monomeric globin protein that facilitates oxygen extraction from the blood and intracellular transport, is increased in hypoxia. Similar proteins, known as cytoglobins, may be upregulated in hypoxia and aid in adaptive responses.[120]

Many of the processes that occur at the cellular level are mediated by HIF-1 α. This transcription factor is normally degraded by prolyl-hydroxylases in normoxia but under hypoxic conditions avoids degradation and enters the cell nucleus where it binds HIF-1 β and other proteins to form complexes which initiate transcription of genes that subsequently affect a wide range of processes including angiogenesis, chemoreceptor function, energy utilization, erythropoiesis, and nitric oxide metabolism.[121]

Effects of High Altitude on Common Activities

In addition to the organ-specific physiologic responses to acute hypoxia, there are also changes in several common activities including sleep and exercise. These are described below.

Sleep

For people exposed to high altitude, one of the most noticeable changes they experience is disrupted sleep. The main driver of altered sleep at high altitude is periodic breathing, or what is commonly referred to as Cheyne–Stokes respirations, a form of central sleep apnea often seen at sea level in individuals with severe heart failure or various forms of neurologic injury. Periodic breathing is marked by a crescendo–decrescendo pattern of breathing movements and airflow punctuated by periods of absent respiratory effort and apnea lasting anywhere from 5 to 20 seconds. The S_aO_2 fluctuates in response to the apneas, with the nadir saturation determined by the duration of apnea and the altitude at which the individual is sleeping. One factor contributing to the significant fluctuations in S_aO_2 with periodic breathing at high altitude is the fact that the P_aO_2 typically resides on the steep portion of the hemoglobin–oxygen dissociation curve at high altitude, such that small changes in P_aO_2 with each apnea lead to marked changes in S_aO_2.[14] Periodic breathing tends to occur during non-rapid eye movement (non-REM) sleep and can even begin during the period of drowsiness that precedes sleep onset.[122,123] At moderate elevations (<3,000 m), it tends to diminish as acclimatization proceeds but at higher elevations (>4,500 m) it can persist despite acclimatization and even occupies a greater proportion of sleep time than earlier in the high-altitude sojourn.[124]

In addition to the transient fluctuations in S_aO_2, periodic breathing has several consequences. From a subjective standpoint, individuals report difficulty falling and/or remaining asleep, vivid dreams, frequent awakenings, and a feeling of not being refreshed upon awakening in the morning. In terms of more objective observations, studies using continuous recordings of electroencephalography

(EEG), electromyography, and eye movements have demonstrated an increased frequency of arousals,[122,125] although increased arousals can also be seen at high altitude in the absence of periodic breathing.[122,126] A variety of EEG studies have shown characteristic changes in sleep architecture including more time in the stages I and II of non-REM sleep and less time in the deeper sleep stages.[122,127] Conflicting data have been reported regarding the amount of time spent in REM sleep with some studies reporting a decrease[128] or even absence[129] of REM sleep and others reporting no change[130] in the time spent in this stage.

The mechanism underlying periodic breathing is best understood through the lens of control theory.[131,132] A control system is one in which disturbances are followed by corrective actions. In the case of respiratory system, a change in ventilation is followed by a change in the P_aCO_2 which acts through the central and peripheral chemoreceptors to counteract the initial change in ventilation as described in detail above. For example, increased ventilation lowers P_aCO_2 which, in turn, decreases central and peripheral chemoreceptor output, thereby reducing ventilation. Periodic breathing develops at high altitude due to several alterations in this negative feedback control system. When the ventilatory response to hypoxia is strong, large increases in ventilation easily drive the P_aCO_2 below the apnea threshold which resides within only 1 to 2 mm Hg of the eupneic PCO_2 during sleep at high altitude. In the setting of high chemosensitivity to CO_2 ($\Delta\dot{V}_E/\Delta PCO_2$, $\dot{V}_E$: minute ventilation), the drop in P_aCO_2 is followed by an excessive fall in ventilation and eventually apnea. In the absence of breathing, P_aCO_2 then rises above the apnea threshold. This eventually leads to an increase in ventilation but because chemoreceptor sensitivity is increased, the ventilatory response is excessive, leading the P_aCO_2 to fall below the apnea threshold leading again to cessation of respiratory efforts. An oscillatory pattern develops because the corrective changes in P_aCO_2 get out of phase with the changes in ventilation such that what would otherwise inhibit ventilation now augments it and vice versa. Further details on the mechanism of this phenomenon can be found in detailed reviews on the topic.[133,134]

Periodic breathing can be significantly reduced by supplemental oxygen administration[135] or sleeping in oxygen enrichment of the quarters in which people sleep.[136] The carbonic anhydrase inhibitor acetazolamide and phosphodiesterase inhibitor theophylline both reduce the extent of periodic breathing[137,138] although the latter is not used clinically due to its narrow therapeutic window. Other sedative-hypnotic agents such as zolpidem[139] and temazepam[140] improve subjective sleep quality at high altitude but have no effect on periodic breathing.

Exercise

Significant changes in exercise occur with exposure to high altitude, with the most important changes being a reduction in maximal exercise capacity ($\dot{V}_{O2max}$). As shown in ►**Fig. 10**, at altitudes above 1,500 m, $\dot{V}_{O2max}$ decreases from the sea level value by approximately 10% for every 1,000 m gain in altitude, and near the summit of Mount Everest, is just above the basal oxygen uptake.[14,141] For many years, the latter finding raised concerns that it was not possible to climb Mount Everest without supplemental oxygen because there would be insufficient oxygen available to support work above the basal metabolic rate. This debate was put to rest, however, when Peter Habeler and Reinhold Messner summitted the mountain without oxygen in 1978.

The decline in $\dot{V}_{O2max}$ occurs regardless of the individual's baseline level of fitness and differences in acclimatization status (i.e., during acute and chronic hypoxic exposure as well as in high-

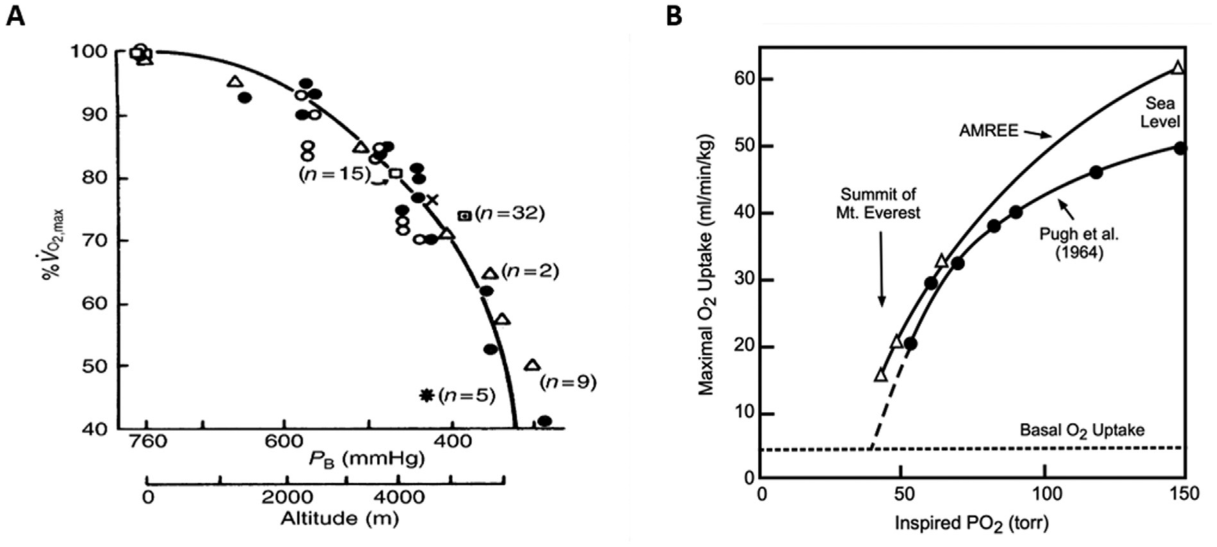

Fig. 10 (A) $\dot{V}_{O2max}$ as a percentage of the sea-level value plotted against barometric pressure and altitude based on several studies synthesized by Cerretelli.[141] Open circles and triangles (○, △): acute hypoxia; closed circles (●): chronic hypoxia; crosses (×): high-altitude natives. (Reproduced with permission from Cerretelli[141].) (B) Changes in maximal oxygen uptake with reductions in the inspired PO_2. Open triangles represent data from the 1981 American Medical Research Expedition to Everest (AMREE). Closed circles represent data from the 1961 Silver Hut Expedition and additional measurements on Mount Everest. (Reproduced with permission from West et al[150].)

altitude natives).[141,142] The clinical consequence of the decline is that exercise at the same absolute intensity becomes harder with increasing altitude. It is important to note that while acclimatization does not improve $\dot{V}_{O2max}$, submaximal exercise intensities improve with prolonged stay at high altitude.[6] The mechanisms underlying the decline in $\dot{V}_{O2max}$ are not entirely clear but likely relate to problems with oxygen transport to exercising muscles, such as redistribution of blood flow to nonlocomotor muscles,[143] and increased right ventricular afterload and reductions in right ventricular function due to increased pulmonary artery pressure.[144] Other evidence suggests hypoxia has effects on the central and peripheral nervous systems and perceptions of fatigue, which may also contribute to exercise limitation.[145,146]

In addition to the decline in $\dot{V}_{O2max}$, other important changes in exercise at high altitude include the fact that both heart rate and cardiac output are increased at any given submaximal work rate compared with sea-level conditions.[147,148] The increase in heart rate is related to increased sympathetic and decreased vagal activity[92] as described above. Importantly, because $\dot{V}_{O2max}$ is reduced, the maximum exercise heart rate is reduced compared with sea level.[95] The relationship between altitude and the reduction in maximal heart rate is almost linear, but like many of the responses described in this article demonstrates large interindividual variability.[149] As with heart rate, the minute ventilation for any given work rate is reduced at high altitude compared with sea level while the maximum exercise ventilation is lower at high elevation due to the reduction in maximum exercise capacity.

Whereas at sea level the P_aO_2 and S_aO_2 remain constant with progressive exercise, following ascent to high altitude both parameters decrease with increasing work rate.[150] As noted earlier in the section on gas exchange, this finding most likely relates to a combination of diffusion limitation and worsening ventilation–perfusion matching.

Because ascent to high altitude triggers physiologic responses across multiple organ systems that optimize the transport of oxygen to exercising muscle, multiple training concepts have been proposed to take advantage of these processes to improve sea-level exercise performance while avoiding the negative consequences of hypoxia. These paradigms include living at low altitude and training at high altitude, living and training at high altitude, living at high altitude and training at low altitude, and periods of intermittent hypoxia separated by time spent under sea-level conditions. There is currently no consensus regarding the best approach and significant debate exists regarding the required degree and duration of hypoxia as well as the timing of hypoxic training relative to competition at low elevation.[151]

Conclusion

With ascent to high altitude, barometric pressure declines and, as a result, the PO_2 falls at all points along the oxygen transport cascade from ambient air to tissue mitochondria. The lower oxygen tensions trigger a series of responses across multiple organ systems over varying time frames whose general role is to facilitate acclimatization to high altitude. While the respiratory system plays a primary role in these processes, other organ systems help to maintain oxygen delivery and preserve tissue and cellular level function. When sufficient time is provided for acclimatization, the majority of people traveling to high altitude tolerate ambient hypoxia without difficulty but in select cases; particularly in the setting of overly rapid ascent rates, maladaptive responses can occur which lead to one of three forms of acute altitude illness, acute mountain sickness, high-altitude cerebral edema, and high-altitude pulmonary edema, which have been alluded to at various points above. A full discussion of these entities is beyond the scope of this article but additional information on the pathophysiology and clinical features of these problems can be found in several detailed reviews on this topic.[4,152]

Conflict of Interest
None declared.

References

1 West JB, Lahiri S, Maret KH, Peters RM Jr, Pizzo CJ. Barometric pressures at extreme altitudes on Mt. Everest: physiological significance. J Appl Physiol 1983;54(05):1188–1194
2 Brunt D. Physical and Dynamical Meteorology. Cambridge: Cambridge University Press; 1952
3 Moore GWK, Semple JL. Weather and death on Mount Everest: an analysis of the into thin air storm. Bull Am Meteorol Soc 2006; 87:465–480
4 Bärtsch P, Swenson ER. Clinical practice: acute high-altitude illnesses. N Engl J Med 2013;368(24):2294–2302
5 Roach EB, Bleiberg J, Lathan CE, Wolpert L, Tsao JW, Roach RC. AltitudeOmics: decreased reaction time after high altitude cognitive testing is a sensitive metric of hypoxic impairment. Neuroreport 2014;25(11):814–818
6 Subudhi AW, Bourdillon N, Bucher J, et al. AltitudeOmics: the integrative physiology of human acclimatization to hypobaric hypoxia and its retention upon reascent. PLoS One 2014;9(03): e92191
7 Latshang TD, Turk AJ, Hess T, et al. Acclimatization improves submaximal exercise economy at 5533 m. Scand J Med Sci Sports 2013;23(04):458–467
8 Moore LG. Measuring high-altitude adaptation. J Appl Physiol 2017;123(05):1371–1385
9 Clement ID, Bascom DA, Conway J, et al. An assessment of central-peripheral ventilatory chemoreflex interaction in humans. Respir Physiol 1992;88(1–2):87–100
10 Clement ID, Pandit JJ, Bascom DA, Dorrington KL, O'Connor DF, Robbins PA. An assessment of central-peripheral ventilatory chemoreflex interaction using acid and bicarbonate infusions in humans. J Physiol 1995;485(Pt 2):561–570
11 Fatemian M, Nieuwenhuijs DJ, Teppema LJ, et al. The respiratory response to carbon dioxide in humans with unilateral and bilateral resections of the carotid bodies. J Physiol 2003;549(Pt 3):965–973
12 Powell FL, Milsom WK, Mitchell GS. Time domains of the hypoxic ventilatory response. Respir Physiol 1998;112(02):123–134
13 Timmers HJ, Karemaker JM, Wieling W, Marres HA, Folgering HT, Lenders JW. Baroreflex and chemoreflex function after bilateral carotid body tumor resection. J Hypertens 2003;21(03):591–599
14 Luks AM, Ainslie PN, Lawley JS, Roach RC, Simonson TS. Ward, Milledge and West's High Altitude Medicine and Physiology. Boca Raton, FL: CRC Press; 2021
15 Rahn H, Otis AB. Man's respiratory response during and after acclimatization to high altitude. Am J Physiol 1949;157(03): 445–462

16 Vizek M, Pickett CK, Weil JV. Biphasic ventilatory response of adult cats to sustained hypoxia has central origin. J Appl Physiol 1987;63(04):1658–1664
17 Pamenter ME, Powell FL. Time domains of the hypoxic ventilatory response and their molecular basis. Compr Physiol 2016;6 (03):1345–1385
18 Wagner PD. Gas exchange. In: Hornbein TF, Schoene RB, eds. High Altitude: An Exploration of Human Adaptation. New York, NY: Marcel Dekker Inc; 2001:199–234
19 West JB. Human physiology at extreme altitudes on Mount Everest. Science 1984;223(4638):784–788
20 Houston CS, Sutton JR, Cymerman A, Reeves JT. Operation Everest II: man at extreme altitude. J Appl Physiol 1987;63(02):877–882
21 West JB. American medical research expedition to Everest. High Alt Med Biol 2010;11(02):103–110
22 Grocott MP, Martin DS, Levett DZ, McMorrow R, Windsor J, Montgomery HECaudwell Xtreme Everest Research Group. Arterial blood gases and oxygen content in climbers on Mount Everest. N Engl J Med 2009;360(02):140–149
23 Bernardi L, Schneider A, Pomidori L, Paolucci E, Cogo A. Hypoxic ventilatory response in successful extreme altitude climbers. Eur Respir J 2006;27(01):165–171
24 Sharma S, Hashmi MF, Burns B. Alveolar Gas Equation. Treasure Island, FL: StatPearls; 2022
25 Sato M, Severinghaus JW, Powell FL, Xu FD, Spellman MJ Jr. Augmented hypoxic ventilatory response in men at altitude. J Appl Physiol 1992;73(01):101–107
26 Forster HV, Dempsey JA, Birnbaum ML, et al. Effect of chronic exposure to hypoxia on ventilatory response to CO 2 and hypoxia. J Appl Physiol 1971;31(04):586–592
27 Sorensen SC, Cruz JC. Ventilatory response to a single breath of CO2 in O2 in normal man at sea level and high altitude. J Appl Physiol 1969;27(02):186–190
28 Howard LS, Robbins PA. Ventilatory response to 8 h of isocapnic and poikilocapnic hypoxia in humans. J Appl Physiol 1995;78 (03):1092–1097
29 Subudhi AW, Fan JL, Evero O, et al. AltitudeOmics: cerebral autoregulation during ascent, acclimatization, and re-exposure to high altitude and its relation with acute mountain sickness. J Appl Physiol 2014;116(07):724–729
30 Tenney SM, Remmers JE, Mithoefer JC. Interaction of CO2 and hypoxic stimuli on ventilation at high altitude. Q J Exp Physiol Cogn Med Sci 1963;48:192–201
31 Fan JL, Burgess KR, Thomas KN, et al. Influence of indomethacin on ventilatory and cerebrovascular responsiveness to CO2 and breathing stability: the influence of PCO2 gradients. Am J Physiol Regul Integr Comp Physiol 2010;298(06):R1648–R1658
32 Krapf R, Beeler I, Hertner D, Hulter HN. Chronic respiratory alkalosis. The effect of sustained hyperventilation on renal regulation of acid-base equilibrium. N Engl J Med 1991;324 (20):1394–1401
33 Schoene RB, Roach RC, Hackett PH, Sutton JR, Cymerman A, Houston CS. Operation Everest II: ventilatory adaptation during gradual decompression to extreme altitude. Med Sci Sports Exerc 1990;22(06):804–810
34 Ainslie PN, Lucas SJ, Burgess KR. Breathing and sleep at high altitude. Respir Physiol Neurobiol 2013;188(03):233–256
35 Weil JV, Byrne-Quinn E, Sodal IE, et al. Hypoxic ventilatory drive in normal man. J Clin Invest 1970;49(06):1061–1072
36 Weil JV. Variation in human ventilatory control-genetic influence on the hypoxic ventilatory response. Respir Physiol Neurobiol 2003;135(2–3):239–246
37 Bird JD, Leacy JK, Foster GE, et al. Time course and magnitude of ventilatory and renal acid-base acclimatization following rapid ascent to and residence at 3,800 m over nine days. J Appl Physiol 2021;130(06):1705–1715
38 Milledge JS, Beeley JM, Broome J, Luff N, Pelling M, Smith D. Acute mountain sickness susceptibility, fitness and hypoxic ventilatory response. Eur Respir J 1991;4(08):1000–1003
39 Sharma G, Goodwin J. Effect of aging on respiratory system physiology and immunology. Clin Interv Aging 2006;1(03): 253–260
40 Byrne-Quinn E, Weil JV, Sodal IE, Filley GF, Grover RF. Ventilatory control in the athlete. J Appl Physiol 1971;30(01):91–98
41 Sareban M, Schiefer LM, Macholz F, et al. Endurance athletes are at increased risk for early acute mountain sickness at 3450 m. Med Sci Sports Exerc 2020;52(05):1109–1115
42 West JB, Wagner PD. Predicted gas exchange on the summit of Mt. Everest. Respir Physiol 1980;42(01):1–16
43 Wagner PD, Sutton JR, Reeves JT, Cymerman A, Groves BM, Malconian MK. Operation Everest II: pulmonary gas exchange during a simulated ascent of Mt. Everest. J Appl Physiol 1987;63 (06):2348–2359
44 Cremona G, Asnaghi R, Baderna P, et al. Pulmonary extravascular fluid accumulation in recreational climbers: a prospective study. Lancet 2002;359(9303):303–309
45 Dehnert C, Risse F, Ley S, et al. Magnetic resonance imaging of uneven pulmonary perfusion in hypoxia in humans. Am J Respir Crit Care Med 2006;174(10):1132–1138
46 Lovering AT, Kelly TS, DiMarco KG, Bradbury KE, Charkoudian N. Implications of a patent foramen ovale for environmental physiology and pathophysiology: do we know the 'hole' story? J Physiol 2022;600(07):1541–1553
47 Lovering AT, Duke JW, Elliott JE. Intrapulmonary arteriovenous anastomoses in humans–response to exercise and the environment. J Physiol 2015;593(03):507–520
48 Gautier H, Peslin R, Grassino A, et al. Mechanical properties of the lungs during acclimatization to altitude. J Appl Physiol 1982;52 (06):1407–1415
49 Senn O, Clarenbach CF, Fischler M, et al. Do changes in lung function predict high-altitude pulmonary edema at an early stage? Med Sci Sports Exerc 2006;38(09):1565–1570
50 Welsh CH, Wagner PD, Reeves JT, et al. Operation Everest. II: spirometric and radiographic changes in acclimatized humans at simulated high altitudes. Am Rev Respir Dis 1993;147(05): 1239–1244
51 Mason NP, Barry PW, Pollard AJ, et al. Serial changes in spirometry during an ascent to 5,300 m in the Nepalese Himalayas. High Alt Med Biol 2000;1(03):185–195
52 Mansell A, Powles A, Sutton J. Changes in pulmonary PV characteristics of human subjects at an altitude of 5,366 m. J Appl Physiol 1980;49(01):79–83
53 Finkelstein S, Tomashefski JF, Shillito FH. Pulmonary mechanics at altitude in normal and obstructive lung disease patients. Aerosp Med 1965;36:880–884
54 Dehnert C, Luks AM, Schendler G, et al. No evidence for interstitial lung oedema by extensive pulmonary function testing at 4,559 m. Eur Respir J 2010;35(04):812–820
55 Deboeck G, Moraine JJ, Naeije R. Respiratory muscle strength may explain hypoxia-induced decrease in vital capacity. Med Sci Sports Exerc 2005;37(05):754–758
56 Swenson ER. Con: most climbers do not develop subclinical interstitial pulmonary edema. High Alt Med Biol 2011;12(02): 125–128, discussion 129–130
57 Jaeger JJ, Sylvester JT, Cymerman A, Berberich JJ, Denniston JC, Maher JT. Evidence for increased intrathoracic fluid volume in man at high altitude. J Appl Physiol 1979;47(04):670–676
58 Raymond L, Severinghaus JW. Static pulmonary compliance of man during altitude hypoxia. J Appl Physiol 1971;31(05):785–787
59 Forte VA Jr, Leith DE, Muza SR, Fulco CS, Cymerman A. Ventilatory capacities at sea level and high altitude. Aviat Space Environ Med 1997;68(06):488–493

60 Sharma S, Brown B. Spirometry and respiratory muscle function during ascent to higher altitudes. Lung 2007;185(02):113–121

61 Babcock MA, Johnson BD, Pegelow DF, Suman OE, Griffin D, Dempsey JA. Hypoxic effects on exercise-induced diaphragmatic fatigue in normal healthy humans. J Appl Physiol 1995;78(01):82–92

62 Gudjonsdottir M, Appendini L, Baderna P, et al. Diaphragm fatigue during exercise at high altitude: the role of hypoxia and workload. Eur Respir J 2001;17(04):674–680

63 Newhouse MT, Becklake MR, MacKlem PT, McGregor M. Effect of alterations in end-tidal Co2 tension on flow resistance. J Appl Physiol 1964;19:745–749

64 van den Elshout FJ, van Herwaarden CL, Folgering HT. Effects of hypercapnia and hypocapnia on respiratory resistance in normal and asthmatic subjects. Thorax 1991;46(01):28–32

65 Mazzeo RS, Wolfel EE, Butterfield GE, Reeves JT. Sympathetic response during 21 days at high altitude (4,300 m) as determined by urinary and arterial catecholamines. Metabolism 1994;43(10):1226–1232

66 Pellegrino R, Pompilio P, Quaranta M, et al. Airway responses to methacholine and exercise at high altitude in healthy lowlanders. J Appl Physiol 2010;108(02):256–265

67 Pollard AJ, Mason NP, Barry PW, et al. Effect of altitude on spirometric parameters and the performance of peak flow meters. Thorax 1996;51(02):175–178

68 Pellegrino R, Viegi G, Brusasco V, et al. Interpretative strategies for lung function tests. Eur Respir J 2005;26(05):948–968

69 Cogo A, Basnyat B, Legnani D, Allegra L. Bronchial asthma and airway hyperresponsiveness at high altitude. Respiration 1997;64(06):444–449

70 von Euler US, Liljestrand G. Observations on the pulmonary arterial blood pressure in the cat. Acta Physiol Scand 1946;12:301–320

71 Levine BD, Zuckerman JH, deFilippi CR. Effect of high-altitude exposure in the elderly: the Tenth Mountain Division study. Circulation 1997;96(04):1224–1232

72 Smith TG, Talbot NP, Chang RW, et al. Pulmonary artery pressure increases during commercial air travel in healthy passengers. Aviat Space Environ Med 2012;83(07):673–676

73 Swenson ER, Robertson HT, Hlastala MP. Effects of inspired carbon dioxide on ventilation-perfusion matching in normoxia, hypoxia, and hyperoxia. Am J Respir Crit Care Med 1994;149(06):1563–1569

74 Hopkins SR, Garg J, Bolar DS, Balouch J, Levin DL. Pulmonary blood flow heterogeneity during hypoxia and high-altitude pulmonary edema. Am J Respir Crit Care Med 2005;171(01):83–87

75 Grünig E, Mereles D, Hildebrandt W, et al. Stress Doppler echocardiography for identification of susceptibility to high altitude pulmonary edema. J Am Coll Cardiol 2000;35(04):980–987

76 Talbot NP, Balanos GM, Dorrington KL, Robbins PA. Two temporal components within the human pulmonary vascular response to approximately 2 h of isocapnic hypoxia. J Appl Physiol 2005;98(03):1125–1139

77 Smith KA, Schumacker PT. Sensors and signals: the role of reactive oxygen species in hypoxic pulmonary vasoconstriction. J Physiol 2019;597(04):1033–1043

78 Vejlstrup NG, O'Neill M, Nagyova B, Dorrington KL. Time course of hypoxic pulmonary vasoconstriction: a rabbit model of regional hypoxia. Am J Respir Crit Care Med 1997;155(01):216–221

79 Bailey DM, Dehnert C, Luks AM, et al. High-altitude pulmonary hypertension is associated with a free radical-mediated reduction in pulmonary nitric oxide bioavailability. J Physiol 2010;588(Pt 23):4837–4847

80 Berger MM, Hesse C, Dehnert C, et al. Hypoxia impairs systemic endothelial function in individuals prone to high-altitude pulmonary edema. Am J Respir Crit Care Med 2005;172(06):763–767

81 Berger MM, Dehnert C, Bailey DM, et al. Transpulmonary plasma ET-1 and nitrite differences in high altitude pulmonary hypertension. High Alt Med Biol 2009;10(01):17–24

82 Swenson ER. Hypoxic pulmonary vasoconstriction. High Alt Med Biol 2013;14(02):101–110

83 Dunham-Snary KJ, Wu D, Sykes EA, et al. Hypoxic pulmonary vasoconstriction: from molecular mechanisms to medicine. Chest 2017;151(01):181–192

84 Subedi P, Gasho C, Stembridge M, et al. Pulmonary vascular reactivity to supplemental oxygen in Sherpa and lowlanders during gradual ascent to high altitude. Exp Physiol 2023;108(01):111–122

85 Berger MM, Bailey DM. On the mechanisms underlying activation and reversal of high altitude-induced pulmonary hypertension in humans - another piece in the pulmonary puzzle. Exp Physiol 2023;108(01):1–4

86 Sylvester JT, Shimoda LA, Aaronson PI, Ward JP. Hypoxic pulmonary vasoconstriction. Physiol Rev 2012;92(01):367–520

87 Pugh CW. Modulation of the hypoxic response. Adv Exp Med Biol 2016;903:259–271

88 Shimoda LA, Laurie SS. HIF and pulmonary vascular responses to hypoxia. J Appl Physiol 2014;116(07):867–874

89 Shimoda LA. Cellular pathways promoting pulmonary vascular remodeling by hypoxia. Physiology (Bethesda) 2020;35(04):222–233

90 Sydykov A, Mamazhakypov A, Maripov A, et al. Pulmonary hypertension in acute and chronic high altitude maladaptation disorders. Int J Environ Res Public Health 2021;18(04):18

91 Vogel JA, Harris CW. Cardiopulmonary responses of resting man during early exposure to high altitude. J Appl Physiol 1967;22(06):1124–1128

92 Koller EA, Drechsel S, Hess T, Macherel P, Boutellier U. Effects of atropine and propranolol on the respiratory, circulatory, and ECG responses to high altitude in man. Eur J Appl Physiol Occup Physiol 1988;57(02):163–172

93 Hansen J, Sander M. Sympathetic neural overactivity in healthy humans after prolonged exposure to hypobaric hypoxia. J Physiol 2003;546(Pt 3):921–929

94 Siebenmann C, Rasmussen P, Sørensen H, et al. Hypoxia increases exercise heart rate despite combined inhibition of β-adrenergic and muscarinic receptors. Am J Physiol Heart Circ Physiol 2015;308(12):H1540–H1546

95 Reeves JT, Groves BM, Sutton JR, et al. Operation Everest II: preservation of cardiac function at extreme altitude. J Appl Physiol 1987;63(02):531–539

96 Siebenmann C, Hug M, Keiser S, et al. Hypovolemia explains the reduced stroke volume at altitude. Physiol Rep 2013;1(05):e00094

97 Swenson ER. Renal function and fluid homeostasis. In: Hornbein TF, Schoene RB, eds. An Exploration of Human Adaptation. New York, NY: Marcel Dekker; 2001:525–568

98 Schlittler M, Gatterer H, Turner R, et al. Regulation of plasma volume in male lowlanders during 4 days of exposure to hypobaric hypoxia equivalent to 3500 m altitude. J Physiol 2021;599(04):1083–1096

99 Suarez J, Alexander JK, Houston CS. Enhanced left ventricular systolic performance at high altitude during Operation Everest II. Am J Cardiol 1987;60(01):137–142

100 Stembridge M, Levine BD. No heartbreak at high altitude; preserved cardiac function in chronic hypoxia. Exp Physiol 2019;104(05):619–620

101 Keyes LE, Sallade TD, Duke C, et al. Blood pressure and altitude: an observational cohort study of hypertensive and nonhypertensive Himalayan trekkers in Nepal. High Alt Med Biol 2017;18(03):267–277

102 Wolfel EE, Selland MA, Mazzeo RS, Reeves JT. Systemic hypertension at 4,300 m is related to sympathoadrenal activity. J Appl Physiol 1994;76(04):1643–1650

103 Parati G, Bilo G, Faini A, et al. Changes in 24 h ambulatory blood pressure and effects of angiotensin II receptor blockade during acute and prolonged high-altitude exposure: a randomized clinical trial. Eur Heart J 2014;35(44):3113–3122

104 Kaufmann PA, Schirlo C, Pavlicek V, et al. Increased myocardial blood flow during acute exposure to simulated altitudes. J Nucl Cardiol 2001;8(02):158–164

105 Wyss CA, Koepfli P, Fretz G, Seebauer M, Schirlo C, Kaufmann PA. Influence of altitude exposure on coronary flow reserve. Circulation 2003;108(10):1202–1207

106 Wolfel EE, Groves BM, Brooks GA, et al. Oxygen transport during steady-state submaximal exercise in chronic hypoxia. J Appl Physiol 1991;70(03):1129–1136

107 Singh MV, Rawal SB, Tyagi AK. Body fluid status on induction, reinduction and prolonged stay at high altitude of human volunteers. Int J Biometeorol 1990;34(02):93–97

108 Milledge JS, Cotes PM. Serum erythropoietin in humans at high altitude and its relation to plasma renin. J Appl Physiol 1985;59 (02):360–364

109 Mairbäurl H, Schobersberger W, Humpeler E, Hasibeder W, Fischer W, Raas E. Beneficial effects of exercising at moderate altitude on red cell oxygen transport and on exercise performance. Pflugers Arch 1986;406(06):594–599

110 Winslow RM, Samaja M, West JB. Red cell function at extreme altitude on Mount Everest. J Appl Physiol 1984;56(01): 109–116

111 Martin DS, Pate JS, Vercueil A, Doyle PW, Mythen MG, Grocott MPCaudwell Xtreme Everest Research Group. Reduced coagulation at high altitude identified by thromboelastography. Thromb Haemost 2012;107(06):1066–1071

112 Hoiland RL, Bain AR, Rieger MG, Bailey DM, Ainslie PN. Hypoxemia, oxygen content, and the regulation of cerebral blood flow. Am J Physiol Regul Integr Comp Physiol 2016;310(05): R398–R413

113 Ainslie PN, Subudhi AW. Cerebral blood flow at high altitude. High Alt Med Biol 2014;15(02):133–140

114 Lucas SJ, Burgess KR, Thomas KN, et al. Alterations in cerebral blood flow and cerebrovascular reactivity during 14 days at 5050 m. J Physiol 2011;589(Pt 3):741–753

115 Boutellier U, Howald H, di Prampero PE, Giezendanner D, Cerretelli P. Human muscle adaptations to chronic hypoxia. Prog Clin Biol Res 1983;136:273–285

116 Cerretelli P, Marconi C, Dériaz O, Giezendanner D. After effects of chronic hypoxia on cardiac output and muscle blood flow at rest and exercise. Eur J Appl Physiol Occup Physiol 1984;53(02): 92–96

117 Hoppeler H, Howald H, Cerretelli P. Human muscle structure after exposure to extreme altitude. Experientia 1990;46(11–12):1185–1187

118 Chaillou T. Skeletal muscle fiber type in hypoxia: adaptation to high-altitude exposure and under conditions of pathological hypoxia. Front Physiol 2018;9:1450

119 Levett DZ, Radford EJ, Menassa DA, et al; Caudwell Xtreme Everest Research Group. Acclimatization of skeletal muscle mitochondria to high-altitude hypoxia during an ascent of Everest. FASEB J 2012;26(04):1431–1441

120 Schmidt M, Gerlach F, Avivi A, et al. Cytoglobin is a respiratory protein in connective tissue and neurons, which is up-regulated by hypoxia. J Biol Chem 2004;279(09):8063–8069

121 Semenza GL. Hypoxia-inducible factors in physiology and medicine. Cell 2012;148(03):399–408

122 Reite M, Jackson D, Cahoon RL, Weil JV. Sleep physiology at high altitude. Electroencephalogr Clin Neurophysiol 1975;38(05): 463–471

123 Berssenbrugge A, Dempsey J, Iber C, Skatrud J, Wilson P. Mechanisms of hypoxia-induced periodic breathing during sleep in humans. J Physiol 1983;343:507–524

124 Bloch KE, Latshang TD, Turk AJ, et al. Nocturnal periodic breathing during acclimatization at very high altitude at Mount Muztagh Ata (7,546 m). Am J Respir Crit Care Med 2010;182(04): 562–568

125 Weil JV, Kryger MH, Scroggin CH. Sleep and breathing at high altitude. In: Guilleminault C, Dement, W. C., eds, ed. Sleep Apnea Syndromes. New York, NY: Alan R Liss; 1978:119–123

126 Wickramasinghe H, Anholm JD. Sleep and breathing at high altitude. Sleep Breath 1999;3(03):89–102

127 Joern AT, Shurley JT, Brooks RE, Guenter CA, Pierce CM. Short-term changes in sleep patterns on arrival at the South Polar Plateau. Arch Intern Med 1970;125(04):649–654

128 Anholm JD, Powles AC, Downey R III, et al. Operation Everest II: arterial oxygen saturation and sleep at extreme simulated altitude. Am Rev Respir Dis 1992;145(4, Pt 1):817–826

129 Pappenheimer JR. Sleep and respiration of rats during hypoxia. J Physiol 1977;266(01):191–207

130 Zieliński J, Koziej M, Mańkowski M, et al. The quality of sleep and periodic breathing in healthy subjects at an altitude of 3,200 m. High Alt Med Biol 2000;1(04):331–336

131 Cherniack NS, Longobardo GS. Mathematical models of periodic breathing and their usefulness in understanding cardiovascular and respiratory disorders. Exp Physiol 2006;91(02):295–305

132 Khoo MC, Kronauer RE, Strohl KP, Slutsky AS. Factors inducing periodic breathing in humans: a general model. J Appl Physiol 1982;53(03):644–659

133 Javaheri S, Dempsey JA. Central sleep apnea. Compr Physiol 2013;3(01):141–163

134 Burgess KR, Ainslie PN. Central sleep apnea at high altitude. Adv Exp Med Biol 2016;903:275–283

135 Lahiri S, Maret K, Sherpa MG. Dependence of high altitude sleep apnea on ventilatory sensitivity to hypoxia. Respir Physiol 1983; 52(03):281–301

136 Luks AM, van Melick H, Batarse RR, Powell FL, Grant I, West JB. Room oxygen enrichment improves sleep and subsequent daytime performance at high altitude. Respir Physiol 1998;113(03): 247–258

137 Hackett PH, Roach RC, Harrison GL, Schoene RB, Mills WJ Jr. Respiratory stimulants and sleep periodic breathing at high altitude. Almitrine versus acetazolamide. Am Rev Respir Dis 1987;135(04):896–898

138 Fischer R, Lang SM, Leitl M, Thiere M, Steiner U, Huber RM. Theophylline and acetazolamide reduce sleep-disordered breathing at high altitude. Eur Respir J 2004;23(01):47–52

139 Beaumont M, Goldenberg F, Lejeune D, Marotte H, Harf A, Lofaso F. Effect of zolpidem on sleep and ventilatory patterns at simulated altitude of 4,000 meters. Am J Respir Crit Care Med 1996;153(6, Pt 1):1864–1869

140 Nickol AH, Leverment J, Richards P, et al. Temazepam at high altitude reduces periodic breathing without impairing next-day performance: a randomized cross-over double-blind study. J Sleep Res 2006;15(04):445–454

141 Cerretelli P. Gas exchange at high altitude. In: West JB, ed. Pulmonary Gas Exchange. New York, NY: Academic Press; 1980:97–147

142 Fulco CS, Rock PB, Cymerman A. Maximal and submaximal exercise performance at altitude. Aviat Space Environ Med 1998;69(08):793–801

143 Calbet JA, Boushel R, Radegran G, Sondergaard H, Wagner PD, Saltin B. Why is VO2 max after altitude acclimatization still reduced despite normalization of arterial O2 content? Am J Physiol Regul Integr Comp Physiol 2003;284(02):R304–R316

144 Ghofrani HA, Reichenberger F, Kohstall MG, et al. Sildenafil increased exercise capacity during hypoxia at low altitudes and at Mount Everest base camp: a randomized, double-blind,

placebo-controlled crossover trial. Ann Intern Med 2004;141 (03):169–177
145 Amann M, Romer LM, Pegelow DF, Jacques AJ, Hess CJ, Dempsey JA. Effects of arterial oxygen content on peripheral locomotor muscle fatigue. J Appl Physiol 2006;101(01):119–127
146 Amann M, Romer LM, Subudhi AW, Pegelow DF, Dempsey JA. Severity of arterial hypoxaemia affects the relative contributions of peripheral muscle fatigue to exercise performance in healthy humans. J Physiol 2007;581(Pt 1):389–403
147 Bärtsch P, Gibbs JS. Effect of altitude on the heart and the lungs. Circulation 2007;116(19):2191–2202
148 Lundby C, Sander M, van Hall G, Saltin B, Calbet JA. Maximal exercise and muscle oxygen extraction in acclimatizing lowlanders and high altitude natives. J Physiol 2006;573(Pt 2):535–547
149 Mourot L. Limitation of maximal heart rate in hypoxia: mechanisms and clinical importance. Front Physiol 2018;9:972
150 West JB, Boyer SJ, Graber DJ, et al. Maximal exercise at extreme altitudes on Mount Everest. J Appl Physiol 1983;55(03):688–698
151 Chapman RF, Karlsen T, Ge RL, Stray-Gundersen J, Levine BD. Living altitude influences endurance exercise performance change over time at altitude. J Appl Physiol 2016;120(10): 1151–1158
152 Hackett PH, Luks AM, Lawley JS, Roach RC. High altitude medicine and pathophysiology. In: Auerbach PS, ed. Auerbach's Wilderness Medicine. Philadelphia, PA: Elsevier; 2017:8–29
153 Pugh LG. Man at high altitude: studies carried out in the Himalaya. Sci Basis Med Annu Rev 1964:32–54
154 Smith TG, Dempsey JA, Hornbein TF. Control of breathing at high altitude. In: Hornbein TF, Schoene RB, eds. High Altitude: An Exploration of Human Adaptation (Lung Biology in Health and Disease). New York, NY: Marcel Dekker; 2001:140–148
155 Pace Nello. Man at altitude. In: Farber SM. Wilson RHL, eds. The Air We Breathe: A Study of Man and His Environment. Springfield, MA: Charles C. Thomas; 1961:53–70
156 Dehnert C, Grünig E, Mereles D, von Lennep N, Bärtsch P. Identification of individuals susceptible to high-altitude pulmonary oedema at low altitude. Eur Respir J 2005;25(03):545–551
157 Rimoldi SF, Sartori C, Seiler C, et al. High-altitude exposure in patients with cardiovascular disease: risk assessment and practical recommendations. Prog Cardiovasc Dis 2010;52(06): 512–524

Article published online: 2023-07-17

Pulmonary Function in Human Spaceflight

Jan Stepanek, MD, MPH[1] Rebecca S. Blue, MD, MPH[2] Desmond Connolly, PhD, MA, MBBS, DAvMed[3]

[1] Aerospace Medicine Program, Department of Medicine, Mayo Clinic, Scottsdale, Arizona
[2] Aerospace Medicine Program, Aerospace Medicine and Vestibular Research Laboratory (AMVRL), Mayo Clinic, Scottsdale, Arizona
[3] Human Performance, Air & Space Division, QinetiQ Plc, Farnborough, United Kingdom

Address for correspondence Jan Stepanek, MD, MPH, Aerospace Medicine Program, Department of Medicine, Mayo Clinic, 13400 East Shea Boulevard, Scottsdale, AZ 85259
(e-mail: stepanek.jan@mayo.edu).

Semin Respir Crit Care Med 2023;44:696–704.

Abstract

Human spaceflight is entering a time of markedly increased activity fueled by collaboration between governmental and private industry entities. This has resulted in successful mission planning for destinations in low Earth orbit, lunar destinations (Artemis program, Gateway station) as well as exploration to Mars. The planned construction of additional commercial space stations will ensure continued low Earth orbit presence and destinations for science but also commercial spaceflight participants. The human in the journey to space is exposed to numerous environmental challenges including increased gravitational forces, microgravity, altered human physiology during adaptation to weightlessness in space, altered ambient pressure, as well as other important stressors contingent on the type of mission and destination. This chapter will cover clinically important aspects relevant to lung function in a normally proceeding mission; emergency scenarios such as decompression, fire, etc., will not be covered as these are beyond the scope of this review. To date, participation in commercial spaceflight by those with pre-existing chronic medical conditions is very limited, and hence, close collaboration between practicing pulmonary specialists and aerospace medicine specialists is of critical importance to guarantee safety, proper clinical management, and hence success in these important endeavors.

Keywords
- human spaceflight
- microgravity
- decompression sickness
- hypergravity
- ventilation/perfusion
- hypoxia
- hypocapnia
- hypercapnia
- commercial spaceflight participants

The recent emergence and growth of the commercial spaceflight industry signals a paradigm shift in prospective spaceflight participants (SFPs). Historically, astronauts have been a highly selected population with limited, well-controlled medical conditions and extensive training and preparation for spaceflight. As a result, many chronic medical conditions have not been common concerns for clinicians managing the health of this population. Future civilian SFPs are more likely to present with chronic medical conditions, including respiratory disorders, in varying states of control or progression, warranting heightened awareness by treating clinicians as to the potential impact of these chronic conditions during spaceflight and the related forces and environmental stressors that can impact human physiology.[1]

In the near-term future, commercial human spaceflight will likely include both suborbital and low-Earth orbit destinations, with the potential for few lunar sorties. The term “suborbital flight” is used for space vehicles that briefly reach an altitude of greater than 100 km (62 miles) and then return in a parabolic trajectory to the Earth; the term “orbital flight” is used when a space vehicle attains a velocity and distance from the Earth that allows it to stay in a stable orbit around the planet. For example, the International Space Station (ISS) is in an orbit on average 400 km (248 miles) above the Earth, traveling at a speed of 28,000 km/h (17,500 mph). The rapid velocity of an orbiting vehicle maintains a balance between centrifugal force and the force of Earth’s gravity, resulting in a constant “freefall” microgravity environment.

article published online
July 17, 2023

Issue Theme Pulmonary Physiology; Guest Editors: David A. Kaminsky, MD, Kathryn A. Hibbert, MD, and Andrew M. Luks, MD

Thieme Medical Publishers, Inc.,
333 Seventh Avenue, 18th Floor,
New York, NY 10001, USA

DOI https://doi.org/10.1055/s-0043-1770064.
ISSN 1069-3424.

Space vehicles constitute medically resource-constrained environments, and evacuation capabilities vary significantly between missions and vehicles. Return to definitive medical care is easily feasible within a short period of time (hours) from suborbital flights; even from low-Earth orbit, evacuation is typically feasible within 24 hours. For missions outside of low-Earth orbit, evacuation and return to a definitive medical care facility may require days to weeks, contingent on the phase of the flight. In contrast, it could take months to years to evacuate from Mars, if return is even possible.[2] Thus, careful understanding of the spaceflight environment, associated physiological changes, and application of this knowledge to mitigation strategies and preventive medicine are the primary means of maintaining the health of astronauts and commercial SFPs alike.

This review will focus on aspects particularly important for pulmonary and respiratory function during normally proceeding spaceflight missions rather than contingency events (such as spacecraft decompression, trauma, acute illness, or significant life support systems failure scenarios) and is intended to provide a basic understanding of the stressors unique to the space environment and the impact of those stressors on pulmonary physiology.

The Environment—Sustaining Life

The environment of a space vehicle or station needs to fulfill life support functions, including the provision of a normal temperature environment, adequate pressurization, and physiologically appropriate breathable atmosphere, while scrubbing metabolic waste gases and mitigating secondary risks, such as minimizing flammability and shielding against space radiation.[3,4] Adequate oxygenation is fundamental. Some vehicles maintain ground-level atmospheric conditions, for example, the ISS is pressurized to 14.7 psia (760 mm Hg) with an atmosphere composed of approximately 79% nitrogen and approximately 21% oxygen, and metabolically produced gasses such as carbon dioxide (CO_2), which are scrubbed from the environment.[5] In cabins pressurized to subatmospheric levels, the inspired partial pressure of oxygen (P_IO_2) in the trachea, saturated with water vapor at body temperature (P_{H2O}), is determined by the absolute ambient (barometric) pressure (P_B) and fractional inspired oxygen concentration (F_IO_2) in accordance with Eq. 1. At normal body temperature, saturated water vapor pressure is 47 mm Hg.

$$P_IO_2 = FIO_2 \times (P_B - P_{H2O}) \quad \textbf{Eq. 1}$$

The alveolar partial pressure of oxygen (P_AO_2) may then be estimated from the full alveolar air equation in the normal way, accounting for the alveolar partial pressure of carbon dioxide (P_ACO_2) and respiratory exchange ratio (R). The short form is shown at Eq. 2. Abrupt exposure over a few minutes, at rest, to a reduction in ambient pressure leads to hypobaric hypoxia, as the inspired and alveolar partial pressures of oxygen fall (e.g., in seated occupants in a decompression chamber). Under these circumstances, more typical of flight than terrestrial ascent, the acute hypoxic ventilatory response starts to promote a progressive reduction in P_ACO_2 once ambient pressure falls below 75% of sea level atmospheric pressure, equivalent to an altitude of approximately 8,000 ft (2,438 m) above mean sea level.[6] Below that pressure, F_IO_2 must be increased to prevent secondary hypocapnia

$$P_AO_2 = P_IO_2 - (P_ACO_2 / R) \quad \textbf{Eq. 2}$$

Excessive build-up of waste gasses or other atmospheric toxins poses a risk in a closed vehicular environment, particularly as the habitable atmosphere begins to deviate from terrestrial conditions. As an example, excessive build-up of CO_2 on the ISS has posed a persistent problem for space operations. While nominal ISS CO_2 concentrations are maintained at <3 mm Hg, even this concentration is substantially higher than the average concentration on Earth (0.3 mm Hg). When vehicle scrubbing capabilities are less rigorous, CO_2 concentration rises, and vehicle inhabitants can begin to feel symptoms of hypercapnia.[7,8] In an enclosed space vehicle, CO_2 can pose challenges that are not encountered on Earth. In the absence of gravity and natural air circulation, space vehicles require fans to mix air and ensure the circulation of otherwise stagnant gasses. When fans are insufficient to effectively circulate air, bubbles of stagnant gas can result; there have been incidents in spaceflight where crewmembers remained in an area of relatively stagnant ventilation and exhaled CO_2 collected in a bubble around crewmembers, leading to symptoms of hypercapnia.[7] Suboptimal air flow in areas of a space vehicle combined with the lack of gravity-induced settling can also be of relevance for exposure to airborne particles (e.g., dust) and toxic fumes (e.g., combustion by-products). Such concerns are exacerbated by planetary missions, for example, future lunar or Mars exploration missions will need to contend with dust tracked into the vehicle after extravehicular activity (EVA) and subsequent contamination of breathable air on return to microgravity conditions. Dust exposure during Apollo missions led to respiratory irritation[9]; careful engineering solutions to mitigate against dust contamination of future space vehicles are a focus of current habitat and exploration mission design efforts.[3]

In addition to atmospheric insults, an SFP's experience within, and reaction to, the space environment may contribute to a variety of clinical and pulmonary sequelae (►**Table 1**). Microgravity induces multiple changes in the human body, many of which can cause substantial discomfort. Notable immediate changes in the first days in microgravity include central fluid shifting, resulting in relative swelling soft tissues of the head and congestion of nasal and paranasal sinuses resulting in transient headache. The hydration of intervertebral discs results in spinal elongation and transient low back discomfort.[10] One notable early adaptive response is the impact of the microgravity environment on the neurovestibular system. The inner ear depends on gravity inputs (utricle, saccule, and semicircular canals) that are integrated with proprioceptive and visual input to the brain, providing humans clear orientation within a three-dimensional environment. The absence of gravity results in a mismatch with visual perception resulting in variable "space motion sickness" as a manifestation of space adaptation syndrome in the first approximately 72 hours in microgravity until adaptation to the new microgravity environment occurs (►**Table 1**).[11]

Table 1 Medical and environmental challenges according to the type of spaceflight (reproduced with permission from NEJM[1])

Mission profile	Medical challenges, short term	Medical challenges, long term	Environmental factors
Suborbital			
	Anxiety, psychological factors, space motion sickness, hypocapnia,	Minimal	Noise, vibration, acceleration forces, confinement, microgravity
Near earth orbit			
1. Short sojourn	Anxiety, psychological factors, space motion sickness, hypocapnia	Minimal	Microgravity adaptation: fluid shifts with headache, congestion; low back pain from spinal elongation
1. Sojourn $\geq$ 48 h	Altered T cell function, plasma volume shifts, neurovestibular, cardiovascular deconditioning, spaceflight-associated neuro-ocular syndrome	Mild, radiation induced changes, spaceflight-associated neuroocular syndrome risk in proportion to flight duration	Microgravity
Beyond low-earth orbit			
Lunar ($\geq$ weeks)	Neurovestibular deconditioning, cardiovascular deconditioning, plasma volume shifts, Spaceflight-associated neuroocular syndrome, radiation-induced changes	Radiation induced changes, spaceflight associated neuro-ocular syndrome	Microgravity, radiation, isolation
Planetary ($>$12 mo)	Radiation-induced changes, altered nutritional status, neurovestibular deconditioning, cardiovascular deconditioning, bone and muscle loss, renal stone formation, plasma volume shifts, spaceflight-associated neuroocular syndrome, isolation, alteration in immunity	Radiation induced changes, altered musculoskeletal system, spaceflight associated neuro-ocular syndrome	Microgravity, radiation, isolation

Note: SANS denotes spaceflight-associated neuroocular syndrome.

Overall, in professional astronauts, there are no significant changes in oxygen uptake or carbon dioxide output during initial exposure to microgravity. However, in conjunction with other spaceflight factors such as increased metabolic demands,[12] fear or anxiety, and the risk of ambient hypoxia or other atmospheric alterations, the unfamiliar environment of spaceflight for SFPs and these occasionally uncomfortable or painful adaptation responses may induce stress-related increases in ventilation that may exceed metabolic demands and cause hypocapnia. This, in turn, causes respiratory alkalosis, left shifting of the oxygen-hemoglobin dissociation curve, and resulting decrease in tissue oxygen delivery, and may manifest as clinically significant dyspnea, palpitations, fatigue, paresthesias, and decreased cerebral perfusion that ultimately impact human performance. Performance degradation in critical mission timeframes can have devastating consequences.

Hypergravity

Pulmonary physiology is challenged by unique spaceflight stressors in all phases of flight, though perhaps most dramatically during the acceleration of launch and reentry. Rapid acceleration leads to hypergravity or the experience of excess gravitational force, which is associated with symptoms and sequelae specific to the duration of exposure and the vector of acceleration applied to the body. Most spaceflight vehicle designs orient the human passengers such that gravitational forces are applied in a back-to-chest ($+G_x$) direction as this vector is best tolerated by the human body; however, in some circumstances, other vectors may be experienced, including toe-to-head ($+G_z$) or side-to-side ($\pm G_y$) acceleration. The force of acceleration on body tissues can result in tissue deformation and other physiological alterations. Here, we will focus on the most common sustained acceleration vectors, $+G_x$ and $+G_z$, and resultant pulmonary sequelae (►**Fig. 1**).

Sustained exposure to $+G_x$ acceleration, a transverse application of force to the body, leads to thoracic and abdominal compression that worsens with each G (multiple of Earth's gravitational force, 9.8 m/s^2). Thoracic compression leads to a reduction of vital capacity that is inversely proportional to $+G_x$ exposure. At $+6G_x$, vital capacity is reduced by 55 to 80% of normal, with increased functional dead space and a doubling of the work of breathing.[12] Sustained acceleration can result in dependent atelectasis[13,14] (in $+G_x$ exposures, the posterior lung would be dependent); in flight operations, the use of 100% oxygen is not uncommon, and hyperoxia combined with acceleration can worsen atelectasis and reduce arterial oxygen saturation.[15,16] Exposed individuals frequently report a notable increase in the work of breathing with increasing $+G_x$ acceleration and, additionally, report chest discomfort or cough during or after sustained exposure. Most individuals find exposure to $+6G_x$ or greater to cause significant chest discomfort; voluntary human tolerance limits are around $+15G_x$,[12] with tolerance limits generally influenced by chest discomfort and an increase in the work of breathing.

Sustained exposure to hypergravity in the $+G_z$ direction (toe-to-head) compresses pulmonary tissue in the inferior thoracic cavity and reduces lung compliance by approximately 15% for each G. Increasing acceleration additionally leads to inferior displacement of circulatory distribution, worsening ventilation-perfusion mismatch.[12,17] As with $+G_x$ exposure, sustained acceleration, particularly when accompanied by hyperoxia, can cause atelectasis in dependent regions,[13,15,18,19] and acceleration atelectasis can result in chest pain.[20] Simultaneously, hypergravity (generally in excess of $+3G_z$) can lead to dependent blood pooling in the lower extremity and a concurrent decrease of blood return to cerebral tissues, which can cause cerebral hypoxia and loss of consciousness. To prevent this, exposed individuals may make the use of an anti-G straining maneuver (AGSM), a combination of muscle contraction in the lower legs to increase peripheral blood return and a Valsalva maneuver to increase intra-abdominal pressure, improving circulatory return to the heart.[12,21,22] This maneuver requires breath-holding for 3 to 4 seconds during the Valsalva before a rapid exhalation and inhalation; however, altered breathing patterns, particularly concurrent with the use of a supplemental oxygen system, may contribute to poor gas exchange in excess of hypergravity-related stressors to pulmonary exchange.[23,24] Poor AGSM technique, including an excessively long breath hold or insufficient exchange during exhalation/inhalation, may worsen these issues and result in hyperventilation, lightheadedness, and higher likelihood of G-induced loss of consciousness.

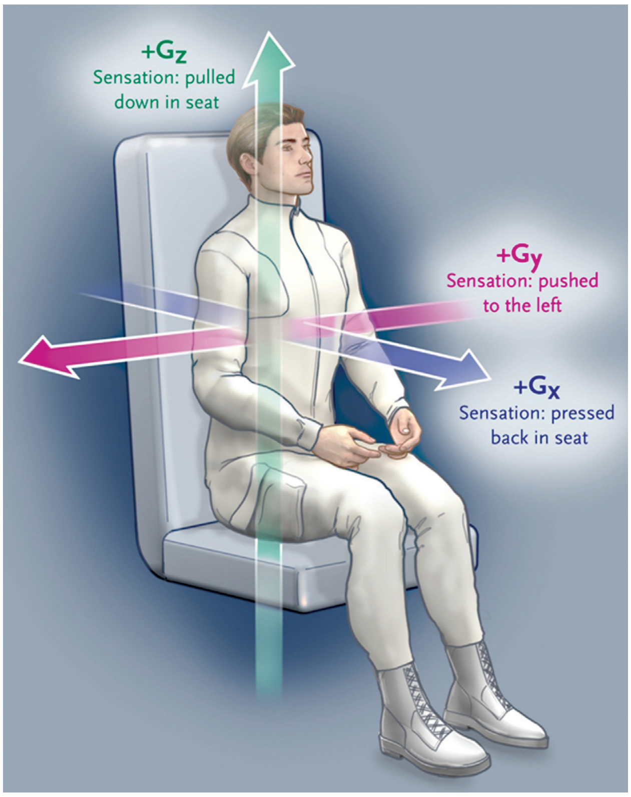
+Gz
Sensation: pulled down in seat
+Gy
Sensation: pushed to the left
+Gx
Sensation: pressed back in seat

Fig. 1 Cardinal acceleration vectors of relevance in human physiology (Reproduced with permission from NEJM[1]).

Recently, more invasive studies have attempted to quantify the effects of sustained acceleration on gas exchange. One study demonstrated a drop in peripheral oxygen saturation (S_PO_2) with sustained $+G_x$ acceleration, worsened by the addition of supplemental oxygen. In that study, oxygen supplementation reduced the S_PO_2 nadir in subjects breathing ambient air under $+G_x$ from 86 to 79% when subjects utilized 15% supplemental oxygen under the same conditions.[14] In the same study, arterial blood gas analysis demonstrated decreasing arterial partial pressure of oxygen and a widening alveolar-arterial gradient with increasing $+G_x$, exacerbated by supplemental oxygen.[14] Another study utilizing near-infrared spectroscopy to monitor cerebral oxygenation found that $+G_z$ exposures were associated with substantial cerebral hypoxia and correlated directly to the time in which hypergravity conditions were sustained.[25] Thus, sustained hypergravity exposure in $+G_x$ or $+G_z$ directions is sufficient to drive ventilation-perfusion mismatch and hypoxia at relevant magnitudes of exposure that are likely to be experienced in commercial spaceflight.

While astronauts and high-performance pilots have been historically capable of tolerating hypergravity conditions, even while completing complex operational tasks, there are limited data regarding the tolerance of laypersons to such forces. As the number of laypersons participating in spaceflight activities remains low, understanding of tolerance in individuals of varied medical history, age, and experience level is primarily based on studies in a human centrifuge. Such studies have identified many of the issues described above, including chest discomfort and increased work of breathing particularly under $+G_x$ strain and frequent cases of hyperventilation.[22,26–28] This research has involved individuals with pulmonary disease, including those with asthma, past or current cigarette smoking status, structural diseases including blebs, and prior surgeries.[22,26,27] In general, individuals with such medical history have done well, though authors have noted that some participants required coaching or similar interventions to manage hyperventilation and still others found chest discomfort painful enough to prompt their withdrawal from the studies.[22,26,29] These controlled conditions may not truly represent the space operational environment, particularly in the case of an emergency where coaching or dedicated assistance may not be readily available to the SFP.

Simple tolerance of hypergravity conditions may not be sufficient to ensure the enjoyment or even safety of the SFP in actual spaceflight. While individuals may be capable of surviving the experience, symptoms of chest pain or lightheadedness, or increasing respiratory rate due to poor ventilation, may negatively affect the SFP's experience. Simultaneously, discomfort, overt pain, or hypoxia and related symptoms may alter a participant's ability to appropriately respond to operational cues, particularly in the case of an emergency. Spaceflight emergency or contingency events may require that the SFP take critical actions, such as a safety procedure or vehicle evacuation; these actions could easily be negatively affected by pulmonary sequelae of hypergravity exposure. A hypoxic or hypocapnic individual, for example, may have delayed reaction time or may make more errors in completing a critical procedure. Studies evaluating hypergravity tolerance are unlikely to truly predict the effects of hypergravity-induced physiological alterations and subsequent impacts on operational performance.[30]

Microgravity

In orbit, or in transit to other bodies in the solar system, humans experience microgravity, potentially for many months at a time. As the gravitational influences on the pulmonary and cardiovascular systems are removed, there is an immediate central fluid shift, with blood volume redistributing throughout the body without gravity-dependent pooling in the lower extremities.[31] Similarly, gravity no longer influences the chest wall and the diaphragm and heart are not displaced "downwards." The mechanics of ventilation change and the abdominal contribution to tidal breathing increases.[32] The lungs no longer deform under their own weight, influencing pulmonary ventilation,[33] and hydrostatic pressure gradients within the lung vasculature disappear with resultant redistribution of pulmonary blood flow.[34]

The cephalad fluid shift rapidly redistributes a substantial volume of fluid from the lower body, distending central vessels which then sense fluid overload. Acute hemodynamic responses include a 35% increase in cardiac output due to a 60 to 70% increase in stroke volume, with reflex bradycardia.[35] Plasma volume later falls and cardiovascular homeostasis follows after 1 to 2 weeks in microgravity, with a net reduction in arterial blood pressure.[36] Counterintuitively, and contrary to bed rest and water immersion models of weightlessness, central venous pressure (CVP) falls immediately upon arrival in microgravity.[37] This may result from an increase in the overall volume of the chest cavity, as the relaxed chest wall rises and the rib cage becomes more circular at end-expiration. Intrapleural pressure falls and blood shifts into the vascular compartment within the chest, increasing cardiac transmural filling pressure and, despite the fluid shift, lowering CVP.[38] Data from transient microgravity during parabolic flight support this, with decreased CVP and esophageal pressure alongside an increase in left atrial diameter proportionate to the net increase in filling pressure.[39]

Central fluid shifts drive an initial reduction in pulmonary vital capacity on the order of 5 to 10%; this normalizes within a few days of exposure to microgravity.[40] Functional residual capacity decreases by approximately 500 mL (15%), compared with preflight standing baseline values, and remains decreased throughout exposure; expiratory reserve volume falls by 10 to 20% and residual volume by almost 20% (approximately 300 mL).[41] In microgravity, peak expiratory flow and forced expiratory volume in 1 second decrease slightly but recover after a few days of sustained microgravity exposure. Studies of forced expiration support transient changes due to vascular engorgement that subside quickly[42]; these changes are attributed to the cranial shift of the diaphragm, increased intrathoracic blood volume, and more uniform alveolar expansion and, hence, lung emptying.[41] Over time, resting tidal volume decreases by approximately 15% and breathing frequency increases by approximately 9%, reducing total ventilation by approximately 7%.[40] This is likely attributable to the reconfiguration of the chest wall following the removal of the weight of the shoulder girdle and abdominal contents, as there is no meaningful change in normal respiratory drive.[40] Microgravity effects on lung volumes, in particular, mirror those experienced during head-up water immersion, when the vascular hydrostatic pressure gradient is counterbalanced by the external water column, redistributing blood from the legs to the chest.[43]

On Earth, ventilation and perfusion of the lungs are regionally heterogeneous, with perfusion increasing from the apices to the bases in the upright position and inhomogeneity of ventilation-perfusion matching that is exaggerated under hypergravity as detailed above. In microgravity, both ventilation and perfusion become more uniformly distributed, the latter reducing physiological dead space as the entire pulmonary vasculature participates in gas exchange.[44,45] Sustained increases in pulmonary capillary blood flow, and the area of alveolar membrane available for gas exchange, raise pulmonary diffusion capacity by approximately 28% over time in microgravity conditions. Overall gas exchange remains effectively the same as on Earth, implying some residual ventilation-perfusion inhomogeneity.[40,46] Regional differences in the elastic properties of the lungs come to predominate in microgravity but are clinically insignificant.[47] Despite increased pulmonary perfusion and alveolar capillary blood volume, measurements of lung tissue volume suggest no tendency toward the development of interstitial edema.[48]

As described above, in the closed confines of a space vehicle there is, inevitably, some accumulation of CO_2 over time despite every effort to remove it from the atmosphere.

The effects of long-term exposure to higher-than-terrestrial CO_2 concentrations have been investigated.[49] Modest initial increases in ventilation subside after a few days in microgravity, with persistent elevation of end-tidal CO_2, though the hypercapnic ventilatory response remains essentially unaffected by microgravity.[50] In contrast, the hypoxic ventilatory response is blunted due to the loss of the hydrostatic pressure gradient between the heart and the carotid bodies, as when supine on Earth. Increasing blood pressure at the carotid bodies dampens the carotid chemoreceptor response to oxygen via a central pathway.[51]

Normobaric studies on Salyut-6, *Mir*, and the ISS indicate that exercise capacity is preserved in microgravity and aerobic deconditioning is not an inevitable consequence of spaceflight.[36] Maximal aerobic capacity, measured repeatedly in astronauts undertaking long-duration ISS missions, demonstrates an early 17% reduction that gradually recovered, with half of those tested regaining preflight levels either during flight or on the first recovery day postflight.[52] Astronauts with greater pre-flight aerobic capacity appear most affected by an initial decline in microgravity, while typically retaining greater aerobic capacity than their colleagues. Numerous factors may contribute to this, including a reduced opportunity to exercise in the first few days of spaceflight, space sickness, and cardiac deconditioning due to the central fluid shift.[51] In essence, however, lung function remains largely unperturbed following long-duration exposure to microgravity.[53]

Sleep disruption is common in spaceflight, as factors such as ambient noise, circadian dysregulation, work schedules, congestion, backache, and loss of gravitational proprioceptive input can all influence sleep quality onboard spacecraft.[1] However, altered ventilatory control is unlikely to contribute to sleep disruptions. In normal individuals, there is substantial reduction in the apnea–hypopnea index in microgravity, and sleep arousals due to respiratory causes almost disappear, presumably due to the removal of gravitational influences on the upper airway.[54] The increased abdominal contribution to tidal breathing in microgravity is maintained through all phases of sleep. The inspiratory flow rate increases while inspiratory time falls as a proportion of the respiratory cycle, preserving total ventilation (►**Fig. 2**).[55]

Extravehicular Activity

Astronauts who exit their vehicle to conduct "spacewalks," or EVA, must wear a full pressure suit to provide, among other things, adequate pressure to the respiratory tract to affect gas exchange. Low absolute suit pressures are a necessary compromise between conflicting requirements of engineering design, to contain adequate pressure and associated physiological protection while allowing movement and flexibility.[6] Frequently, spacesuits are maintained at a pressure altitude above 30,000 ft (4.3 psia). Under steady-state normobaric (760 mm Hg), normoxic (21% oxygen) ambient conditions, as employed on the ISS, the body contains approximately 1.0 to 1.5 L of nitrogen dissolved in the tissues. Decompression to suit pressure, therefore, presents a substantial risk of decompression sickness (DCS), with the potential for nitrogen evolution and bubble formation in tissues supersaturated with inert gas and the generation of venous gas emboli (VGE).[56] Even mild levels of activity will then substantially increase the risk of DCS and VGE.

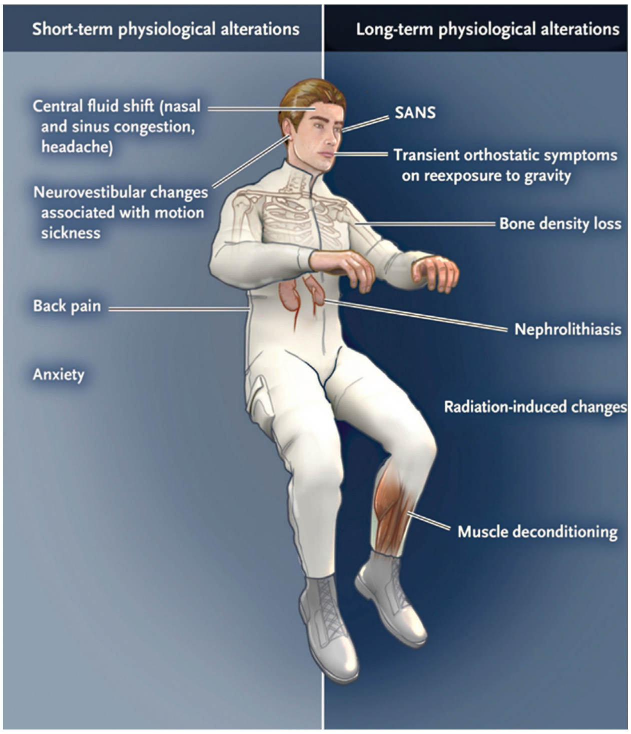
Short-term physiological alterations
Long-term physiological alterations
Central fluid shift (nasal and sinus congestion, headache)
Neurovestibular changes associated with motion sickness
Back pain
Anxiety
SANS
Transient orthostatic symptoms on reexposure to gravity
Bone density loss
Nephrolithiasis
Radiation-induced changes
Muscle deconditioning

Fig. 2 Short-term and long-term physiological alterations during human spaceflight (Reproduced with permission from NEJM[1]).

Respiratory DCS (the chokes) is rare,[57] though it is frequently severe and can rapidly progress to systemic illness and collapse. Early recompression and oxygen administration can be life-saving.[58] Initial symptoms may include some or all of the classic triad of inspiratory retrosternal chest pain, cough, and shortness of breath, attributed to overwhelming bubble loads entering the pulmonary circulation, interfering with gas exchange and promoting pulmonary edema. Normally, the lungs function as superb filters for VGE even when experiencing heavy bubble burden such that arterialized bubbles are not expected outside of cases involving right-to-left intracardiac (e.g., patent foramen ovale) or extra-alveolar pulmonary shunts.[59] Nonetheless, repeated animal experiments have demonstrated that it is possible for the pulmonary filtration capacity to be overwhelmed with massive bubble loads, resulting in arterialization.

Any preexisting lung disease with bullous elements warrants clinical review. Pulmonary bullae, especially if not freely communicating with the major airways, can present a risk for pulmonary barotrauma (including pneumothorax, pneumomediastinum, arterial gas embolization, and hemorrhage into a bulla) with alterations in ambient pressure. Cases have been described with commercial air travel (ambient pressure of 565 mm Hg equivalent to 8,000 ft altitude), which resulted in 38% increase in the volume of trapped gas.[60]

The cornerstone of prevention of DCS during EVA, and mitigation of VGE loading, is staged decompression with exercise-enhanced denitrogenation, breathing 100% oxygen prior to the EVA (prebreathe), and then continuing with 100% oxygen throughout EVA.[61] Nonetheless, the procedures are restrictive, burdensome, and time-consuming such that repeat or frequent EVA is impractical, while the residual risk of DCS and influence of VGE loads in microgravity remain incompletely understood.[62] After returning to the surface from hyperbaric conditions, saturation divers with heavy pulmonary VGE loads may experience increased ventilation-perfusion mismatch and compromised lung function.[63] In contrast, an ISS study indicated no disruption of gas exchange the day following EVA, suggesting that current preventive measures, including prebreathing activities, help protect the lungs.[64] It is possible that physiological responses to microgravity and weightlessness, particularly with respect to fluid distribution, somehow enhance the effectiveness of denitrogenation or otherwise mitigate the risk of DCS.[65] Nonetheless, alongside significant hyperoxic oxidative stress, any VGE that occur are liable to interact with and activate blood cells and pulmonary endothelium, promoting lung sequestration of neutrophils, further generation of reactive oxygen species, and increased microvascular permeability.[66] Every effort is made to minimize VGE when designing prebreathe denitrogenation protocols for current and future missions. This will be essential in future space exploration, particularly in missions where frequent EVA is necessary since some of these underlying acute pathophysiological responses may take time to normalize.

Exploration Atmospheres

As described above, human spaceflight activities require complex vehicles inclusive of pressurized habitats, life support systems, and extensive resources to sustain the mission and the crew. In general, travel to low-Earth orbit destinations such as the ISS enables relatively rapid return to Earth and ease of resupply. In contrast, exploration spaceflight, inclusive of travel to lunar orbit, the lunar surface, or destinations beyond such as Mars, pose additional unique challenges and risks. As destinations become more remote, vehicle and mission architecture must be capable of sustaining an autonomous crew with no prospect of timely resupply, delay in communications with support personnel on Earth, and prolonged journey time of 18 months or longer.

The physics of spaceflight dictates that mass, volume, power, and emanating costs are the determinants of what exploration vehicles can carry, particularly to destinations outside of low-Earth orbit.[67] Future vehicles may make use of an altered "exploration class atmosphere" designed to minimize consumables and payload, minimize the risk of DCS (while maximizing opportunity for multiple EVAs each day), and mitigate flammability concerns while still aiming to maintain performance and safety of the crew during their journey.[68] NASA is currently investigating a carefully chosen atmospheric composition of 8.2 psia and 34% oxygen content, resulting in a dry-inspired oxygen pressure of 144 mm Hg and nitrogen partial pressure of 280 mm Hg, for potential use in exploration missions.[69] While the pressure of 8.2 psia is equivalent to 15,000 ft pressure altitude, the addition of 34% oxygen results in oxygenation equivalent to breathing air at a pressure altitude of approximately 4,000 ft (equivalent air altitude model).

There is uncertainty about the clinical ramifications of the exploration atmosphere as hypobaria in and of itself is an important factor mediating physiologic responses.[70,71] It is unknown what effects the mild hypoxia with significant hypobaria, compensated by increased oxygen content in the inhaled air, will have on the incidence of altitude sickness and related phenomena[72–74] (e.g, periodic breathing at altitude and subsequent impact to sleep quality), exercise capacity,[75] T cell function and immune response, and alterations in cerebral blood flow and pressure,[76] specifically as it pertains to the vexing problem of spaceflight-associated neuroocular syndrome, a constellation of signs emanating from long-duration microgravity exposure including hyperopic shift in visual acuity, optic disc edema, cotton wool spots, and choroidal folds and at times elevated cerebrospinal fluid pressure on lumbar puncture.[77,78]

Additionally, intrapulmonary arterio-venous anastomoses contribute to physiological right-to-left shunts that can be demonstrated in health, particularly with exertion, but which tend to close when upright (normal gravity) or when breathing 100% oxygen.[79,80] The effect of this mildly hypoxic exploration atmosphere on potential right-to-left shunting under microgavity (transcardiac such as in patent foramen ovale or transpulmonary shunts[81]) has not been studied but may have relevance to repeated decompression for EVA, with respect to generating paradoxical gas emboli and risk of DCS.[82] Significant hypoxic stress has been shown to result in recruitment of shunting through patent foramen ovale compared with normoxic conditions.[83]

Conclusion

Ultimately, the advancing industry of commercial spaceflight will allow for the rapid expansion of our collective knowledge and experience in the space environment. Commercialization simultaneously engages medical practitioners even outside of the aerospace medical field of practice, as potential SFPs will undoubtedly pursue evaluation and insight from their physicians regarding preexisting conditions and potential sequelae in spaceflight activities. It is important for such practitioners to maintain awareness of the challenges posed by the space environment on cardiopulmonary physiology, adaptation, and response. As increasing numbers of individuals experience spaceflight, cumulative experience will continue to develop our understanding of the human body's ability to adapt to these unique environments and identify medical conditions that pose specific risk to SFPs or a particular mission architecture. Encouraging the interest and collaboration of clinicians with aerospace medical experts will help to protect both the future SFPs and the rapidly growing commercial spaceflight industry.

Conflict of Interest
None declared.

References

1 Stepanek J, Blue RS, Parazynski S. Space medicine in the era of civilian spaceflight. N Engl J Med 2019;380(11):1053–1060

2 Gillis DB, Hamilton DR. Estimating outcomes of astronauts with myocardial infarction in exploration class space missions. Aviat Space Environ Med 2012;83(02):79–91

3 Jerde EA. The Apollo program. In: Sample Return Missions. Elsevier; 2021: 9–36. Accessed May 26, 2023 at: https://linkinghub.elsevier.com/retrieve/pii/B9780128183304000021

4 Seedhouse E. International Space Station Life Support System. In: Life Support Systems for Humans in Space. Cham: Springer International Publishing; 2020 151–79. Accessed May 26, 2023 at: http://link.springer.com/10.1007/978-3-030-52859-1_5

5 Sherif, D. and Knox, J., "International Space Station Carbon Dioxide Removal Assembly (ISS CDRA) Concepts and Advancements," SAE Technical Paper 2005;01:2892

6 Jenkins DR Dressing for Altitude: U.S. Aviation Pressure Suits–Wiley Post to Space Shuttle. Washington, DC: National Aeronautics and Space Administration; 2012

7 Law J, Van Baalen M, Foy M, et al. Relationship between carbon dioxide levels and reported headaches on the international space station. J Occup Environ Med 2014;56(05):477–483

8 Frey MA, Sulzman FM, Oser H, Ruyters G. The effects of moderately elevated ambient carbon dioxide levels on human physiology and performance: a joint NASA-ESA-DARA study—. Aviat Space Environ Med 1998;69(03):282–284

9 James J, Lam C, Scully R, Meyers V, McCoy J Lunar dust toxicity final report. 2014. Accessed May 26, 2023 at: https://humanresearchroadmap.nasa.gov/Gaps/gap.aspx?i=295

10 Kerstman EL, Scheuring RA, Barnes MG, DeKorse TB, Saile LG. Space adaptation back pain: a retrospective study. Aviat Space Environ Med 2012;83(01):2–7

11 Buckey J. Effectively protecting astronauts from space motion sickness. Aviat Space Environ Med 2010;81(05):522–524

12 Banks R, Somers J, Chelette T, Wood R, Watson R. Human response to acceleration. In: Davis J, Stepanek J, Fogarty J, Blue R, eds. Fundamentals of Aerospace Medicine. Philadelphia: Wolters Kluwer; 2020

13 Pollock RD, Gates SD, Storey JA, Radcliffe JJ, Stevenson AT. Indices of acceleration atelectasis and the effect of hypergravity duration on its development. Exp Physiol 2021;106(01):18–27

14 Pollock RD, Jolley CJ, Abid N, et al. Pulmonary effects of sustained periods of high-G acceleration relevant to suborbital spaceflight. Aerosp Med Hum Perform 2021;92(08):633–641

15 Pollock RD, Gates SD, Radcliffe JJ, Stevenson AT. Indirect measurements of acceleration atelectasis and the role of inspired oxygen concentrations. Aerosp Med Hum Perform 2021;92(10): 780–785

16 Smith TG, Pollock RD, Britton JK, et al. Physiological effects of centrifuge-simulated suborbital spaceflight. Aerosp Med Hum Perform 2022;93(12):830–839

17 Glaister DH The Effects of Gravity and Acceleration on the Lung. Slough, [London]: [Published for] the Advisory Group for Aerospace Research and Development [of] N.A.T.O. [by] Technivision Services; [Distributed by Technical Press; 1970

18 Levy P, Jaeger E, Stone R, Doudna C. Clinical problems in aviation medicine: aeroatelectasis: a respiratory syndrome in aviators. Aerosp Med 1962;33(08):938–944

19 Haswell MS, Tacker WA Jr., Balldin UI, Burton RR. Influence of inspired oxygen concentration on acceleration atelectasis. Aviat Space Environ Med 1986;57(05):432–437

20 Green I, Burgess B An Investigation into the Major Factors Contributing to Post-Flight Chest Pain in Fighter Pilots. Farnborough, UK: RAF Institute of Aviation Medicine; 1962

21 Lyons TJ, Marlowe BL, Michaud VJ, McGowan DJ. Assessment of the anti-G straining maneuver (AGSM) skill performance and reinforcement program. Aviat Space Environ Med 1997;68(04):322–324

22 Blue RS, Pattarini JM, Reyes DP, et al. Tolerance of centrifuge-simulated suborbital spaceflight by medical condition. Aviat Space Environ Med 2014;85(07):721–729

23 White JT, Morin LM. Anti-G straining maneuver incompatibility with tactical aircraft oxygen systems. Aviat Space Environ Med 1988;59(02):176–177

24 Akparibo IY, Anderson J, Chumbley E Aerospace Gravitational Effects. StatPearls. Treasure Island, FL: StatPearls Publishing; 2022. Accessed May 26, 2023 at: http://www.ncbi.nlm.nih.gov/books/NBK430768/

25 Fresnel E, Dray G, Pla S, Jean P, Belda G, Perrey S. Cerebral oxygenation responses to aerobatic flight. Aerosp Med Hum Perform 2021;92(10):838–842

26 Blue R The effects of training on anxiety and task performance in simulated suborbital spaceflight. Presented at the 88th Annual Scientific Meeting of the Aerospace Medical Association, Denver, CO; 2017

27 Blue RS, Riccitello JM, Tizard J, Hamilton RJ, Vanderploeg JM. Commercial spaceflight participant G-force tolerance during centrifuge-simulated suborbital flight. Aviat Space Environ Med 2012;83(10):929–934

28 Mackenzie I, Viirre E, Vanderploeg JM, Chilvers ER. Zero G in a patient with advanced amyotrophic lateral sclerosis. Lancet 2007; 370(9587):566

29 Mulcahy RA, Blue RS, Vardiman JL, Mathers CH, Castleberry TL, Vanderploeg JM. Subject anxiety and psychological considerations for centrifuge-simulated suborbital spaceflight. Aviat Space Environ Med 2014;85(08):847–851

30 Blue RS, Bonato F, Seaton K, et al. The effects of training on anxiety and task performance in simulated suborbital spaceflight. Aerosp Med Hum Perform 2017;88(07):641–650

31 Moore TP, Thornton WE. Space shuttle inflight and postflight fluid shifts measured by leg volume changes. Aviat Space Environ Med 1987;58(9 Pt 2):A91–A96

32 Wantier M, Estenne M, Verbanck S, Prisk GK, Paiva M. Chest wall mechanics in sustained microgravity. J Appl Physiol 1998;84(06): 2060–2065

33 Bryan AC, Milic-Emili J, Pengelly D. Effect of gravity on the distribution of pulmonary ventilation. J Appl Physiol 1966;21 (03):778–784

34 West JB, Dollery CT, Naimark A. Distribution of blood flow in isolated lung; relation to vascular and alveolar pressures. J Appl Physiol 1964;19:713–724

35 Prisk GK, Guy HJ, Elliott AR, Deutschman RA III, West JB. Pulmonary diffusing capacity, capillary blood volume, and cardiac output during sustained microgravity. J Appl Physiol 1993;75 (01):15–26

36 Schneider V, Charles J, Conkin J, Prisk G Cardiopulmonary system: aeromedical considerations. In: Nicogossian AE, Williams RS, Huntoon CL, Doarn C, Polk JD, Schneider VS, eds. Space Physiology and Medicine: From Evidence to Practice. New York: Springer; 2016

37 Buckey J Central venous pressure. In: Prisk GK, Paiva M, West JB, eds. Gravity and the Lung. CRC Press; 2001. Available Accessed May 26, 2023 at: https://www.taylorfrancis.com/books/9781420026702

38 White RJ, Blomqvist CG. Central venous pressure and cardiac function during spaceflight. J Appl Physiol 1998;85(02):738–746

39 Videbaek R, Norsk P. Atrial distension in humans during microgravity induced by parabolic flights. J Appl Physiol 1997;83(06): 1862–1866

40 Prisk GK, Elliott AR, Guy HJ, Kosonen JM, West JB. Pulmonary gas exchange and its determinants during sustained microgravity on Spacelabs SLS-1 and SLS-2. J Appl Physiol 1995;79(04):1290–1298

41 Elliott AR, Prisk GK, Guy HJ, West JB. Lung volumes during sustained microgravity on Spacelab SLS-1. J Appl Physiol 1994; 77(04):2005–2014

42 Elliott AR, Prisk GK, Guy HJ, Kosonen JM, West JB. Forced expirations and maximum expiratory flow-volume curves during sustained microgravity on SLS-1. J Appl Physiol 1996;81(01):33–43

43 Agostoni E, Gurtner G, Torri G, Rahn H. Respiratory mechanics during submersion and negative-pressure breathing. J Appl Physiol 1966;21(01):251–258

44 Guy HJ, Prisk GK, Elliott AR, Deutschman RA III, West JB. Inhomogeneity of pulmonary ventilation during sustained microgravity as determined by single-breath washouts. J Appl Physiol 1994;76(04):1719–1729

45 Prisk GK, Guy HJ, Elliott AR, West JB. Inhomogeneity of pulmonary perfusion during sustained microgravity on SLS-1. J Appl Physiol 1994;76(04):1730–1738

46 Verbandt Y, Wantier M, Prisk GK, Paiva M. Ventilation-perfusion matching in long-term microgravity. J Appl Physiol 2000;89(06):2407–2412

47 Prisk GK, Fine JM, Cooper TK, West JB. Vital capacity, respiratory muscle strength, and pulmonary gas exchange during long-duration exposure to microgravity. J Appl Physiol 2006;101(02):439–447

48 Verbanck S, Larsson H, Linnarsson D, Prisk GK, West JB, Paiva M. Pulmonary tissue volume, cardiac output, and diffusing capacity in sustained microgravity. J Appl Physiol 1997;83(03):810–816

49 Prisk G Control of ventilation. In: Prisk GK, Paiva M, West JB, eds. Gravity and the Lung. CRC Press; 2001. Accessed May 26, 2023 at: https://www.taylorfrancis.com/books/9781420026702

50 Prisk GK, Elliott AR, West JB. Sustained microgravity reduces the human ventilatory response to hypoxia but not to hypercapnia. J Appl Physiol 2000;88(04):1421–1430

51 Prisk GK. Microgravity and the respiratory system. Eur Respir J 2014;43(05):1459–1471

52 Moore AD Jr, Downs ME, Lee SMC, Feiveson AH, Knudsen P, Ploutz-Snyder L. Peak exercise oxygen uptake during and following long-duration spaceflight. J Appl Physiol 2014;117(03):231–238

53 Prisk GK, Fine JM, Cooper TK, West JB. Lung function is unchanged in the 1 G environment following 6-months exposure to microgravity. Eur J Appl Physiol 2008;103(06):617–623

54 Elliott AR, Shea SA, Dijk DJ, et al. Microgravity reduces sleep-disordered breathing in humans. Am J Respir Crit Care Med 2001;164(03):478–485

55 Sá RC, Prisk GK, Paiva M. Microgravity alters respiratory abdominal and rib cage motion during sleep. J Appl Physiol 2009;107(05):1406–1412

56 Stepanek J, Connolly D, Pollock N Atmosphere, Hypoxia and Decompression Stress. In: Davis J, Stepanek J, Fogarty J, Blue R, editors. Fundamentals of Aerospace Medicine. Philadelphia: Wolters Kluwer; 2020

57 Balldin UI, Pilmanis AA, Webb JT. Pulmonary decompression sickness at altitude: early symptoms and circulating gas emboli. Aviat Space Environ Med 2002;73(10):996–999

58 Zwirewich CV, Müller NL, Abboud RT, Lepawsky M. Noncardiogenic pulmonary edema caused by decompression sickness: rapid resolution following hyperbaric therapy. Radiology 1987;163(01):81–82

59 Connolly DM, Lee VM, D'Oyly TJ. Decompression sickness risk at 6553 m breathing two gas mixtures. Aviat Space Environ Med 2010;81(12):1069–1077

60 Chen C-W, Perng W-C, Li M-H, Yan H-C, Wu C-P. Hemorrhage from an enlarged emphysematous bulla during commercial air travel. Aviat Space Environ Med 2006;77(12):1275–1277

61 Pendergast DR, Senf C, Lundgren CEG. Is the rate of whole-body nitrogen elimination influenced by exercise? Undersea Hyperb Med 2012;39(01):595–604

62 Conkin J, Norcross J, Abercromby A Evidence report: risk of decompression sickness (DCS) [Internet]. 2016. Accessed May 26, 2023 at: https://ntrs.nasa.gov/archive/nasa/casi.ntrs.nasa.gov/20150021491.pdf

63 Thorsen E, Segadal K, Kambestad BK. Mechanisms of reduced pulmonary function after a saturation dive. Eur Respir J 1994;7(01):4–10

64 Prisk GK, Fine JM, Cooper TK, West JB. Pulmonary gas exchange is not impaired 24 h after extravehicular activity. J Appl Physiol 2005;99(06):2233–2238

65 Karlsson LL, Blogg SL, Lindholm P, Gennser M, Hemmingsson T, Linnarsson D. Venous gas emboli and exhaled nitric oxide with simulated and actual extravehicular activity. Respir Physiol Neurobiol 2009;169(suppl 1):S59–S62

66 Norfleet W, Butler B Decompression Sickness in Extravehicular Activities [Internet]. In: Prisk GK, Paiva M, West JB, eds. Gravity and the Lung. CRC Press; 2001. Available May 26, 2023 at: https://www.taylorfrancis.com/books/9781420026702

67 Antonsen EL, Mulcahy RA, Rubin D, Blue RS, Canga MA, Shah R. Prototype development of a tradespace analysis tool for spaceflight medical resources. Aerosp Med Hum Perform 2018;89(02):108–114

68 Edwards LM, Murray AJ, Tyler DJ, et al; Caudwell Xtreme Everest Research Group. The effect of high-altitude on human skeletal muscle energetics: P-MRS results from the Caudwell Xtreme Everest expedition. PLoS One 2010;5(05):e10681

69 Norcross J, Norsk P, Law J, et al. Effects of the 8 psia / 32% O2 atmosphere on the human in the spaceflight environment. Houston, TX: NASA Johnson Space Center; 2013

70 Conkin J, Wessel JH III. Critique of the equivalent air altitude model. Aviat Space Environ Med 2008;79(10):975–982

71 Richard NA, Koehle MS. Differences in cardio-ventilatory responses to hypobaric and normobaric hypoxia: a review. Aviat Space Environ Med 2012;83(07):677–684

72 Imray C, Wright A, Subudhi A, Roach R. Acute mountain sickness: pathophysiology, prevention, and treatment. Prog Cardiovasc Dis 2010;52(06):467–484

73 Anderson PJ, Miller AD, O'Malley KA, et al. Incidence and symptoms of high altitude illness in south pole workers: Antarctic Study of Altitude Physiology (ASAP). Clin Med Insights Circ Respir Pulm Med 2011;5:27–35

74 Wilson MH, Newman S, Imray CH. The cerebral effects of ascent to high altitudes. Lancet Neurol 2009;8(02):175–191

75 Muhm JM, Signal TL, Rock PB, et al. Sleep at simulated 2438 m: effects on oxygenation, sleep quality, and postsleep performance. Aviat Space Environ Med 2009;80(08):691–697

76 Klokker M, Kharazmi A, Galbo H, Bygbjerg I, Pedersen BK. Influence of in vivo hypobaric hypoxia on function of lymphocytes, neutrocytes, natural killer cells, and cytokines. J Appl Physiol 1993;74(03):1100–1106

77 Mader TH, Gibson CR, Pass AF, et al. Optic disc edema, globe flattening, choroidal folds, and hyperopic shifts observed in astronauts after long-duration space flight. Ophthalmology 2011;118(10):2058–2069

78 Mader TH, Gibson CR, Pass AF, et al. Optic disc edema in an astronaut after repeat long-duration space flight. J Neuroophthalmol 2013;33(03):249–255

79 Elliott JE, Nigam SM, Laurie SS, et al. Prevalence of left heart contrast in healthy, young, asymptomatic humans at rest breathing room air. Respir Physiol Neurobiol 2013;188(01):71–78

80 Lovering AT, Duke JW, Elliott JE. Intrapulmonary arteriovenous anastomoses in humans—response to exercise and the environment. J Physiol 2015;593(03):507–520

81 Kerut EK, Norfleet WT, Plotnick GD, Giles TD. Patent foramen ovale: a review of associated conditions and the impact of physiological size. J Am Coll Cardiol 2001;38(03):613–623

82 Ljubkovic M, Zanchi J, Breskovic T, Marinovic J, Lojpur M, Dujic Z. Determinants of arterial gas embolism after scuba diving. J Appl Physiol 2012;112(01):91–95

83 Mojadidi MK, Ruiz JC, Chertoff J, et al. Patent foramen ovale and hypoxemia. Cardiol Rev 2019;27(01):34–40

Article published online: 2023-06-27

Pulmonary Physiology and Medicine of Diving

Kay Tetzlaff, MD[1]

[1] Department of Sports Medicine, University Hospital of Tuebingen, Tuebingen, Germany

Address for correspondence Kay Tetzlaff, MD, Department of Sports Medicine, University Hospital of Tuebingen, Tuebingen 72076, Germany (e-mail: Kay.tetzlaff@klinikum.uni-tuebingen.de).

Semin Respir Crit Care Med 2023;44:705–718.

Abstract

Keywords
- breath-hold diving
- immersion
- scuba-diving
- glossopharyngeal insufflation
- decompression illness
- pulmonary barotrauma
- pulmonary edema
- arterial gas embolism

Pulmonary physiology is significantly altered during underwater exposure, as immersion of the body and increased ambient pressure elicit profound effects on both the cardiovascular and respiratory systems. Thoracic blood pooling, increased breathing gas pressures, and variations in gas volumes alongside ambient pressure changes put the heart and lungs under stress. Normal physiologic function and fitness of the cardiovascular and respiratory systems are prerequisites to safely cope with the challenges of the underwater environment when freediving, or diving with underwater breathing apparatus. Few physicians are trained to understand the physiology and medicine of diving and how to recognize or manage diving injuries. This article provides an overview of the physiologic challenges to the respiratory system during diving, with or without breathing apparatus, and outlines possible health risks and hazards unique to the underwater environment. The underlying pathologic mechanisms of dive-related injuries are reviewed, with an emphasis on pulmonary physiology and pathophysiology.

Diving with self-contained underwater breathing apparatus (scuba) has become a popular leisure activity, with an estimated 3 million Americans participating in this sport.[1] Likewise, freediving (breath-hold diving) has gained traction more recently as a competitive sports activity, with athletes competing in several underwater disciplines.[2]

The underwater environment poses unique challenges and health risks to humans, due to altered physical conditions prevailing underwater. It is not, as layman's etiology often suspects, man-eating sharks or other dangerous sea creatures that cause dive-related injuries. Instead, disobeying physiological exposure limits under water, and the presence of predisposing pulmonary or cardiovascular conditions, account for most severe diving accidents.[3] Diving fatalities have been estimated at 3 to 6 per 100,000 divers for the United States, with an unknown error of estimation.[4] Remarkably, medical risk factors and fitness issues are present in many diving fatalities.[3,4]

Pulmonary physiology is significantly altered during underwater exposure, due to immersion in water and the physical effects of increased pressure on gases. Both hypoxia and hyperoxia may stress the respiratory system when freediving or breathing gas at depth, respectively. Inert gas narcosis and decompression stress may result from increased tissue nitrogen partial pressures. Rapid changes in ambient pressure may cause barotrauma of gas-filled cavities such as the lungs, and increased work of breathing combined with augmented cardiac filling may precipitate immersion pulmonary edema and cardiac failure. Thus, normal physiologic function of the respiratory and cardiovascular system is of particular importance to minimize serious health risks associated with underwater diving. In fact, respiratory diseases with functional impairment or parenchymal anomalies of the lung significantly increase the risk of serious injury from underwater diving.[5] To mitigate these health risks, medical clearance checks are recommended before subjects take on this activity. Consultation by the pulmonologist may be requested for the evaluation of medical fitness to dive, particularly for subjects presenting with pulmonary conditions.[6]

This article therefore provides an overview of the physiologic challenges to the respiratory system when freediving or diving with an underwater breathing apparatus. The underlying pathologic mechanisms of these hazards are reviewed, with an emphasis on pulmonary physiology and pathophysiology.

article published online
June 27, 2023

Issue Theme Pulmonary Physiology; Guest Editors: David A. Kaminsky, MD, Kathryn A. Hibbert, MD, and Andrew M. Luks, MD

Thieme Medical Publishers, Inc.,
333 Seventh Avenue, 18th Floor,
New York, NY 10001, USA

DOI https://doi.org/10.1055/s-0043-1770065.
ISSN 1069-3424.

The Physiology of Diving

Increased Pressure

In diving, ambient pressure has commonly been reported in absolute atmospheres (ata), where 1 ata equals sea-level pressure of 760 mm Hg. While atmospheric pressure decreases with altitude, pressure increases with depth below sea level due to hydrostatic pressure generated by water. For every meters sea water (msw) another 76 mm Hg is added. At 10 msw the ambient pressure eventually doubles compared with sea level, reaching 2 ata. Pressure continues to increase linearly with depth; at 20 msw it is 3 ata, etc. According to Boyle's law, pressure and volume are inversely proportional at constant temperature. Since gases are compressible, a given gas volume shrinks with increasing water depth. Conversely, gas expands with decreasing pressure upon ascent from depth. For a given gas, the total pressure exerted by a mixture of gases is the sum of the pressures exerted by each of the gases (Dalton's law). The partial pressure of each component gas depends on its fractional concentration and total pressure. For air, the total pressure of 760 mm Hg is constituted by the partial pressures of each gas in the mixture:

$$P_{\text{Air}} = P_{\text{Nitrogen}} + P_{\text{Oxygen}} + P_{\text{Argon}} + P_{\text{Carbon dioxide}} + P_{\text{Water vapor}} + P_x \quad \textbf{Eq. 1}$$

where x = trace gases with negligible fractional concentrations.

With the increase in ambient pressure, the partial pressures with the mixture rise; however, the fractional composition of a gas mixture such as air remains constant at depth. For example, alveolar oxygen partial pressure (P_AO_2) doubles at 10 msw according to the increase in total pressure, and when breathing air at 40 msw, arterial PO_2 (P_aO_2) reaches five times 160 mm Hg, a partial pressure that is comparable to breathing 100% oxygen at sea level (►**Table 1**).

The density of a given gas is determined by the mass of the gas occupying a certain volume at a specified pressure and temperature. Gas density is directly proportional to the pressure the gas is under, and as volume changes with ambient pressure, density changes accordingly. Gas density doubles at a depth of 10 m, and it increases fivefold at 40 msw. Thus, air breathed at 40 msw is five times as dense as compared with sea level.

Henry's law states that the amount of gas dissolved in a liquid is directly proportional to the partial pressure of the gas in equilibrium with that liquid. Thus, the main constituents of a breathing gas mixture dissolve in fluids proportionate to their partial pressures in the gas phase. When air is breathed at depth, nitrogen (N_2), being an inert gas, dissolves in blood and tissues until equilibrium with the gas phase is achieved, i.e., tissues are then saturated with N_2. The saturation follows a first-order exponential function; inert gas uptake in the blood and other tissues is mainly dependent on the speed and amount of elevation in ambient pressure, temperature, and inherent tissue perfusion. The saturation kinetics follow a pressure gradient that is determined by the difference between the ambient pressure of N_2 and a tissue's partial pressure of N_2.

When ambient pressure falls during the ascent from a dive, the dissolved tissue PN_2 may exceed ambient pressure, resulting in tissue supersaturation. During ascent or decompression from a dive, N_2 is eventually forced to leave solution and forms free gas bubbles, depending on the pressure gradient, temperature, and tissue perfusion. Haldane's concept of a tissue's half-times sets the basis for modern decompression algorithms limiting critical tissue N_2 supersaturation during descent from depth. While short single dives to shallow depths do not lead to significant tissue saturation with N_2, the risk of critical tissue supersaturation increases with depth and time at depth.

Immersion

Immersion in water leads to a redistribution of approximately 700 mL of blood into the thorax, since the pressure gradient between the lower and upper halves of the body of more than 97.5 mm Hg, normally caused by the hydrostatic pressure of the blood column, is neutralized.[7] This thoracic blood shift results in an increased end-diastolic filling of the right heart and pulmonary vessels, with an increase in pulmonary artery and capillary pressure. Cardiac output increases according to the water level of immersion in the erect posture; the reported 32 to 62% cardiac output increase is due to an enlarged stroke volume, dominating over a decrease in heart rate[8]; mean arterial pressure is unchanged. The increase in right heart end-diastolic volume increases myocardial wall tension and atrial stretching which augment release of the diuretically acting atrial natriuretic peptide; this phenomenon accounts for the so-called divers' diuresis.

Pulmonary function studies with head-out immersion showed that hydrostatic compression of the thorax with immersion-related cranial displacement of the diaphragm decreases inspiratory capacity and functional residual capacity, and reduces in pulmonary distensibility.[9,10]

The Diving Response

Immersion of the face causes a measurable decrease in heart rate and cardiac output, triggered by peripheral vasoconstriction via cutaneous receptors of the trigeminal nerve around the nose and mouth in the sense of a parasympathetically mediated reflex, called the diving response.[11] This response is a phylogenetically old protective mechanism of cardiovascular regulation and can be observed in all lung-breathing animals when immersed in water, including humans. Apnea, immersion, hypoxia, and other factors alone or in combination can trigger the dive reflex.

In humans, the diving response is characterized by synergistic sympathetic and parasympathetic activation and increased catecholamines,[12,13] redistribution of blood flow to maintain adequate oxygen supply to hypoxia-sensitive organs,[14,15] and reduced heart rate.[16,17] Active contraction of the spleen is also a characteristic of the human diving response.

Table 1 Relationship between depth, ambient pressure, corresponding oxygen and nitrogen partial pressures when breathing air, and relative reduction of a given gas volume

	Depth (msw)	Ambient pressure (ata)	Oxygen partial pressure (ata)	Nitrogen partial pressure (ata)	Gas volume
Sea level	0	1	0.21	0.79	1
	10	2	0.42	1.58	1/2
	20	3	0.63	2.37	1/3
	30	4	0.84	3.16	1/4
	40	5	1.05	3.95	1/5

Abbreviations: ata, atmosphere absolute; msw, meters sea water.

The human diving response is highly variable and can be modified by physiological as well as emotional factors. In trained breath-hold divers, the heart rate drops to values of 40 to 60 beats per minute.[18–20] Extreme bradycardia of 20 beats per min has been described in trained elite breath-hold divers.[21,22] Unlike in animals, bradycardia in humans is usually not accompanied by a similarly significant drop in cardiac output. Peripheral vasoconstriction subsequently results in an increase in blood pressure. Reflex bradycardia is augmented during cold water immersion. Additionally, a negative correlation between the drop in heart rate and arterial oxygen saturation can be demonstrated in humans, suggesting an overall oxygen-saving effect.[23]

Breath-Hold Diving

Breath-hold diving (synonyms: freediving, apnea diving, skin diving) is the original form of diving and has recently gained popularity as a competitive sport. The International Association for the Development of Apnea (AIDA) has published regulations on the various performance disciplines and organizes official competitions.[24] Records approved by AIDA have been set at 11:35 minutes for static apnea, a discipline where the diver floats on the surface of the water with the face immersed and holds their breath for as long as possible without moving. The depth record achieved in the extreme discipline where the freediver descends and ascends with the method of his or her choice has been set at 214 msw in 2007. The dive was performed with the help of technical descent and ascent aids such as sledge and balloon within a total breath-hold time of 4:24 minutes. ►**Fig. 1** shows an almost linear increase in breath-hold diving records over the past decades. However, more recently these trends appear to have stopped, possibly indicating that human pulmonary physiology has reached its limits.

For the pulmonologist, freediving offers interesting insights into the extremes of lung physiology. The physiological changes during the relatively short and deep breath-hold dives are enormous and are accompanied by significant cardiovascular and respiratory effects. Moreover, recent records could only be achieved by special physiologic

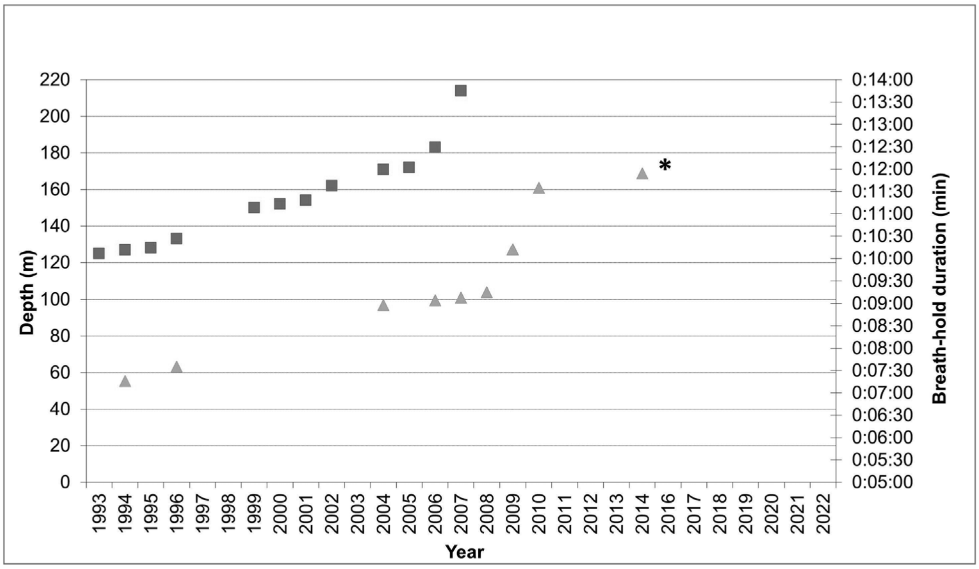

Fig. 1 Breath-hold diving records over time; squares indicate maximal diving depth achieved; triangles indicate breath-hold time records, asterisk indicates 2014 Guinness record not approved by AIDA. AIDA, Association for the Development of Apnea.

maneuvers to overcome challenges imposed by the physiologic limits of the respiratory system.

Total Lung Capacity/Residual Volume Ratio

When descending in apnea, the intrathoracic gas volume or total lung capacity (TLC) decreases according to Boyle's law, and is already halved at 10 m water depth. A reduction in intrathoracic gas volume with increasing diving depth in apnea stresses the lungs due to their anatomical suspension in the bony thorax and their rigid-walled large bronchi. For these reasons, there is a theoretical maximum diving depth after which the intrathoracic gas volume falls below the residual volume (RV). Below this critical volume, it is highly likely that pressure differences between the thoracic space and the rest of the body force blood redistribution into the chest with possible fluid extravasation into the airways and alveolar space (pulmonary barotrauma of descent). The TLC/RV ratio has therefore been considered the limiting factor for deep diving in apnea.[25,26]

With a TLC of, for example, 6 L and an RV of 1.5 L, corresponding to a ratio of 4/1, the point at which the intrathoracic gas volume reaches the RV at maximum inspiration is at 30 msw depth when ambient pressure corresponds to about four times the atmospheric pressure at sea level. This concept was compatible with the maximum diving depths achieved for many decades. Record divers often had a resting lung function with a relatively small RV and a large vital capacity, so that the TLC/RV ratio allowed visits to depths greater than 30 msw until reaching the point of pulmonary barotrauma of descent in individual divers.

Thoracic Blood Shift

When the Italian *Enzo Maiorca* and the French *Jacques Mayol* reached depths of 70 msw and more in the early 1970s, it was unclear as to how they survived these dives without negative pressure barotrauma of the lungs. Schaefer and colleagues[27] reported that U.S. Navy diver *Robert Croft* had a TLC of 6.9 L and an RV of 1.3 L, providing a ratio of 6.96. This would allow a maximum diving depth of approximately 60 msw. In fact, *Croft* reached a record depth of 70.4 msw without any problems. The authors were able to measure an accumulation of up to 1 L of blood in the chest during exploratory apnea dives.[27] With an assumed additional intrathoracic blood volume of 1 L, a reduction of the RV to 0.5 L instead of previously 1.5 L can be achieved. A compression of TLC from 6 L to 1/12 of the volume (instead of 1/4 of the volume before) would therefore correspond to a maximal depth of 110 msw.

Glossopharyngeal Insufflation

At the end of the last millennium, however, record depths of up to 200 msw were finally reached by athletes (►**Fig. 1**), which could no longer be explained by a favorable TLC/RV ratio and blood shift alone. It was subsequently reported that elite breath-hold divers perform a certain breathing technique to increase their available lung volume. The initial scientific report dates back to 1951 and describes the successful use of this technique in post-polio patients.[28] Even today, glossopharyngeal insufflation is still used by patients,[29,30] including those with amyotrophic lateral sclerosis, to extend the spontaneous breathing time from the ventilator and to increase cough strength. Only more recently, the use of glossopharyngeal insufflation has been reported in swimmers and elite freedivers.[31,32]

Breath-hold elite athletes employ glossopharyngeal insufflation to improve the TLC/RV ratio to penetrate to even greater depths and increase oxygen stores. When performing glossopharyngeal insufflation, the soft palate must close against the nose to minimize air escape. After maximum inhalation, the mouth–throat is filled with air and the mouth is closed. Meanwhile, the vocal folds are still closed. The air is compressed in the mouth by means of the buccal muscles and then pressed into the lungs by means of a swallowing technique with the vocal folds opening. Increased intrapulmonary pressure is maintained solely by the vocal fold occlusion. This buccal pumping cycle is repeated several times until a sensation of fullness occurs.[33,34] Elite breath-hold divers increase their TLC by an average 15 to 25%,[33,35–38] although extreme increases of up to 47% have been reported.[38] The increase in lung volume occurs through thoracic expansion and a downward shift of the diaphragm along with a displacement of the vascular mediastinum[39] (►**Fig. 2**).

When measuring mouth relaxation pressure versus plethysmographic volume change immediately and 5 minutes after glossopharyngeal insufflation, a mean increase of 69% in TLC was primarily attributable to overdistension of the lung, with the remainder due to air compression.[37] Since glossopharyngeal insufflation must overcome recoil pressure imposed by the lung and chest wall to increase lung volume above TLC, the authors speculated that recoil pressure at high lung volumes may be altered transiently, supported by the fact that TLC at 3 minutes after glossopharyngeal insufflation still was above expected normal variation. Indeed, there was a transient decline of static compliance over 5 minutes even when subjects had exhaled and returned to tidal breathing.[33]

Resting lung function in elite breath-hold divers does not differ from nondiving controls[33,37]; however, ventilatory volumes are higher than predicted.[35,36] With continued training including glossopharyngeal insufflation, a gradual increase in vital capacity could be demonstrated in swimmers over time.[40]

Blood Gases at Depth

The partial pressures of oxygen and carbon dioxide are subject to pronounced changes during a deep breath-hold dive and differ significantly from simple breath-holding in air at sea level. During descent, the alveolar partial pressures of nitrogen, oxygen, and carbon dioxide increase with depth. Since the mixed-venous partial pressures do not change, diffusion into the blood is augmented with increasing depth. P_aO_2 reaches 250 mm Hg at a depth of 20 msw.[31] Paradoxically, CO_2 is transferred from the alveolus into the blood during the descent due to an increase in P_ACO_2 with depth.

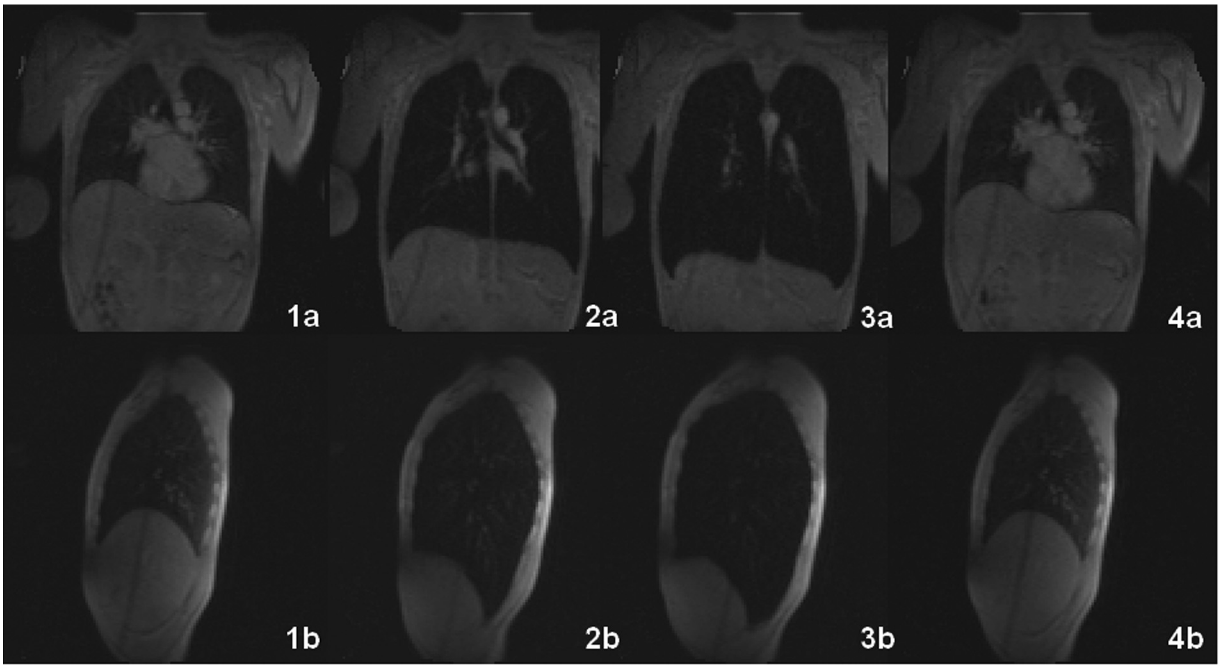

Fig. 2 Sequence of lung images in the magnetic resonance imaging scanner of an elite breath-hold diver before (1a), during (2a, 3a), and after (4a) glossopharyngeal insufflation (top = coronal view; bottom = sagittal view). The increase in lung volume is mainly achieved by widening of the thorax, flattening of the diaphragm, opening of the costodiaphragmatic recesses, and herniation of the lung below the xiphoid (Reproduced with permission from: S. Walterspacher S, Sorichter S, K. Tetzlaff. Extremes of respiratory physiology – apnea diving from our magazine. Respiratory and lung diseases2009;35(8):340–348).

Due to the high solubility of CO_2 in blood, immersion-related increases in intrathoracic blood volume and the subsequent increase in pulmonary blood flow redistribute CO_2 into well-perfused body tissues and increase CO_2 storage capacity.[41] P_ACO_2 values of approximately 50 mm Hg were measured at a simulated depth of 20 msw, although the P_ACO_2 should have risen to approximately 100 mm Hg according to an ambient pressure of 3 ata at that depth.[31,42] During ascent from depth the P_AO_2 decreases and may reach the mixed-venous value, eventually resulting in paradoxical diffusion of O_2 from the blood into the alveolar space, thereby aggravating tissue hypoxia.

Hypoxic Blackout

Hypoxemia accounts for the vast majority of incidents with breath-hold diving, with clinical signs ranging from temporary confusion, speech problems, spasms, transient nonresponsiveness to permanent cognitive deficits and impairment.[43,44] The incidence of these neurological disturbances has been reported in 10% of participants during breath-hold competitions.[43] The most serious hypoxia-related complication is unconsciousness, which obviously is life-threatening in the underwater environment.

Development of critical hypoxemia during underwater breath-hold diving usually is prevented by an urgency to breathe, the breath-hold breaking point, where P_aCO_2 exceeds approximately 45 to 55 mm Hg and involuntary inspiratory efforts such as contractions of the thorax and the diaphragm occur.[45,46] However, P_aCO_2 as the chief determinant of respiratory drive may be manipulated by hyperventilation, which prolongs breath-hold time. Shallow-water blackout may result from cerebral hypoxia toward the end of a breath-hold dive in shallow water. It is typically caused by hyperventilation immediately before a dive, which lowers the P_aCO_2 and thereby delays the diver's urge to breathe. However, when PO_2 falls below the critical level necessary to maintain consciousness, as P_aCO_2 rises from a substantially lower than normal level, the subject may drown when P_aCO_2 does not yet reach the critical level to signal breath-hold breaking.[47]

Another mechanism for loss of consciousness is the substantial fall of P_aO_2 during ascent from a deep breath-hold dive. Since P_aO_2 is elevated at depth and P_aCO_2 rises from a lower level following hyperventilation, the subjective assessment of time needed to return safely to surface may be inaccurate and confounded by a high P_aO_2 at depth and relatively low P_aCO_2. Oxygen consumption contributes to the decline in P_aO_2 that is aggravated by progressively falling P_AO_2 during ascent; the diffusion gradient for oxygen will decrease and P_AO_2 decreases until it equals the mixed venous PO_2. The direction of oxygen diffusion may even be reversed so that oxygen moves from the pulmonary capillary to the alveolar space. Unconsciousness occurs while the rising P_aCO_2 is still below the breath-stimulating threshold.

Decompression Illness

Extreme deep freediving is associated with an increased risk of decompression illness (DCI), an umbrella term encompassing diseases caused by gas bubbles in blood or tissue during or after a reduction in ambient pressure. Gas may evolve from inert gas microbubbles that are formed when critical tissue supersaturation is exceeded during rapid ascent from depth (decompression). Gas may also result from pulmonary barotrauma and creep into tissue or blood, depending on the location of tissue rupture.

Due to very high diffusion gradients between alveolar PN_2 and tissue PN_2 in the body tissues at great depths, nitrogen diffuses forcefully from the alveolar space into blood and tissues. Rapid decompression during an ascent from a deep breath-hold dive, however, may not allow sufficient time for N_2 to wash out of the tissues and diffuse into the alveolar space.

Evidence for decompression stress during breath-hold diving came from studies in subjects performing repeated breath-hold dives. According to Haldane's decompression theory, N_2 release is slower than uptake, so that repeated breath-hold dives with short surface intervals can lead to the accumulation of N_2 in the tissue. Corresponding clinical symptoms and neuroimaging findings have been reported from early experimental studies[48] and imaging studies in commercial Japanese breath-hold divers.[49] Decompression stress is likely present even during single deep breath-hold dives since the pressure gradient between intra-alveolar and tissue PN_2 becomes extreme during rapid descent to depth.[50] It is noteworthy to point out that the human lungs are predicted to fully collapse only at a depth of approximately 235 msw, which is much deeper than that of other diving mammals,[51] so that gas exchange between lungs and tissue is maintained until reaching that depth. There have been reports of stroke-like complications after extremely deep breath-hold dives.[52,53] It was hypothesized that N_2 bubbles passing through the heart (e.g., via a patent foramen ovale [PFO]) or through intrapulmonary arteriovenous anastomoses[53] may become arterialized and occlude vessels causing cerebral arterial gas embolism.

Pulmonary Barotrauma

Pulmonary barotrauma may occur during descent of a deep breath-hold dive when total intrapulmonary gas volume is compressed below RV and a critical negative intra-alveolar pressure is reached (see above). However, pulmonary barotrauma may also occur during the ascent from depth, although the risk of lung over-inflation in breath-hold diving is negligible since the diver does not add any gas to the intrapulmonary gas volume at depth. However, a few cases have been suspected and it was speculated that inhomogeneous ventilation and atelectasis may have contributed to local gas trapping and rupture of lung tissue.[54]

Finally, there is an increased risk of pulmonary barotrauma due to lung hyperinflation following glossopharyngeal breathing. In elite apnea divers, transpulmonary pressure values of 31.6 to 58.8 mm Hg have been measured during glossopharyngeal insufflation.[38] Cases of clinically asymptomatic radiologically detectable pneumomediastinum after this technique have been described.[55,56] It remains unclear whether the mediastinal gas is the result of pulmonary rupture or passes through the upper respiratory tract into the mediastinal space.

Hemoptysis and Pulmonary Edema

Hemoptysis due to alveolar hemorrhage induced by breath-hold diving may result from immense cardiovascular changes that occur during deep breath-hold dives. Immersion in water along with exposure to a cold environment induces an increase in intrathoracic blood volume and cardiac output, as well as pulmonary capillary pressure. The risk of alveolar hemorrhage is further increased by negative pressure that develops inside the alveoli due to involuntary breathing movements during late phase of a breath-hold dive just when reaching the breath-hold breaking point.

Hemoptysis has been self-reported in one-fifth of breath-hold divers.[43,57] Lindholm and coworkers could detect blood from the lower respiratory tract by laryngoscopy in apnea divers who, after complete exhalation to RV, dived to a depth of 6 m to simulate thoracic squeeze.[58] Although often reported as a single symptom, in many cases hemoptysis has been reported to occur together with cough and dyspnea, and pulmonary edema.[59–61]

Breathing Compressed Gas at Depth

There is a variety of technical methods that enable humans to breathe at depth, including surface gas supply, gas supply from an underwater habitat, or scuba-diving. Scuba allows the diver to breathe underwater independently of external air supply. Usually, scuba consists of a tank with compressed air, and a valve that is connected to a first-stage regulator and hose with a second-stage regulator and mouthpiece, allowing the diver to breathe at depth. The scuba is often attached to a buoyancy device (diving vest), and for safety reasons there is a mandatory alternative second-stage regulator connected to the gas tank that can be used by the dive buddy in an emergency out-of-air situation.

In sports scuba-diving, compressed air is most often used as breathing gas. However, there has recently been an increasing use of nitrogen–oxygen gas mixtures with enhanced fractional concentration of oxygen, with commonly used oxygen fractions of 0.32 to 0.36 instead of 0.21. A rather small percentage of recreational divers employ more special breathing gas and equipment, such as oxygen rebreathers, or several breathing gases with switch of gases during the dive (so-called technical diving). Technical factors of the breathing apparatus and the breathing gas need to be considered for safe dive planning, as these factors affect possible risks and complications. For example, the risk of nitrogen narcosis increases dramatically when diving with compressed air and descending to depths of 60 m or deeper. In case of an oxygen rebreather, acute oxygen toxicity may develop when exceeding shallow depths of 15 to 20 msw while there is virtually no risk of nitrogen narcosis or decompression sickness.

The following discussion reviews the most relevant mechanisms of dive-related injury for diving with compressed air, as this is the diving equipment used by the large majority of recreational scuba-divers. It should be noted that for scuba-diving the depth limit recommended by recreational diving organizations for diving with compressed air is 40 msw,[62] and lower depth limits may apply according to the skills and certified training level of the diver. Beyond 40 msw, it is necessary to make decompression stops during ascent and even use different gas mixtures, depending on the depth reached. Nitrogen may be replaced by other inert gases, such as helium, with less narcotic potency and less density to decrease the work of breathing at depth.

Decompression Illness

As outlined above, reduction in ambient pressure forces dissolved N_2 in tissues to form free gas when the sum of gas partial pressures in the tissue exceeds the ambient pressure. These N_2 bubbles arise from suitable nucleation sites and continue to grow if the tissues are sufficiently supersaturated and the diffusion of N_2 into the bubble exceeds the rate at which it diffuses back into solution. Bubble growth lasts if the excess pressure is greater than the pressure generated from the surface tension of the bubble.

Once nucleated, gas bubbles are subject to tissue diffusion and perfusion. The pressure gradient for the partial pressure of the inert gas toward alveolar gas eventually forces the inert gas to leave the tissues. Excess inert gas physiologically reaches the lungs by the venous return where it is trapped in the lung microvasculature and removed by diffusion into the alveolar space.[63] In fact, Intravascular gas bubbles are often present in the absence of symptoms after scuba dives,[64,65] and are associated with a decrease in diffusion capacity of the lungs for carbon monoxide.[66,67]

Even mild elevation of ambient pressure may cause decompression stress if tissues are allowed sufficient time to saturate with N_2. Venous gas bubbles could be detected by Doppler ultrasound a few hours after direct ascent from 1.38 ata ambient pressure (3.8 m) for 48 hours in 20% of asymptomatic subjects; bubbles were even detectable after 12 hours in subjects who ascended from 4.8 m depth.[68]

Illness may occur when a growing N_2 bubble distorts the surrounding tissue and damages cells, exerts pressure on nerves resulting in pain, and occludes blood vessels. In animal models intravascular air bubbles have been shown to exert diverse pathophysiological effects. Hemodynamic changes following venous gas embolism comprise a rise in both the pulmonary artery pressure and pulmonary vascular resistance and a decrease in arterial oxygen tension.[69–71] Humoral and cellular changes include activation of the complement system and of leukocytes.[72,73] These effects induce proinflammatory cascades that result in hemoconcentration and leakage of the vascular endothelium.[74] However, the magnitude of these changes depends on the amount of venous gas emboli and smaller bubble numbers are less likely to produce gross hemodynamic or fluid abnormalities.

Decompression sickness is defined as a clinical syndrome caused by gas bubble damage in body tissues during and after decompression. Clinical manifestations depend on the aforementioned mechanical and biochemical effects in situ and range from musculoskeletal pain (the bends) to severe neurological injury with paralyses of limbs if the spinal cord is affected. Cutis marmorata is a cutaneous manifestation that is thought to be due to endothelial damage to the skin with blood extravasation from cutaneous vessels[75] (►**Fig. 3**). Recently, it was suggested to use the term livedo racemosa to more accurately describe the pathology of thromboembolic obstruction of skin arterioles and capillaries.[76]

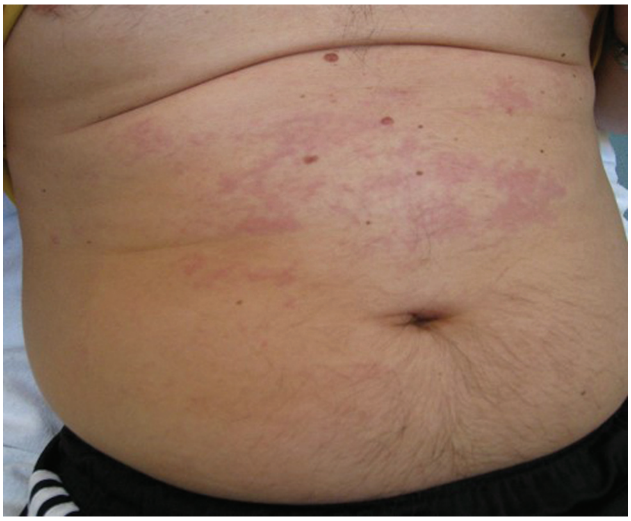

Fig. 3 Livedo racemosa as cutaneous manifestation of decompression sickness in a 57-year-old male diver. (Image courtesy: K. Hasmiller, MD, BG Unfallklinik Murnau, Germany.)

A rare but severe manifestation of decompression sickness is *the chokes* which is caused by massive occurrence of N_2 bubbles in the pulmonary circulation, leading to blockage of pulmonary arterioles and impaired pulmonary microcirculation and gas exchange.[77–79] In sheep it has been shown that the amount of lung microvascular injury could be controlled by the rate of venous gas embolism and is reversible within 1 to 2 days.[74] In another sheep model of experimental respiratory decompression sickness, animals were exposed to compressed air at 2.3 ata for 22 hours followed by simulated altitude at 570 mm Hg.[80] In that study, clinical findings were found to be correlated with pathophysiologic changes: an increased mean pulmonary artery pressure following the detection of high precordial bubble grades corresponded with the onset of restlessness and respiratory difficulty, and collapse. Radiography revealed interstitial pulmonary edema in five animals and patchy infiltrates as well as pleural effusions in two. It was concluded that massive embolization of the pulmonary capillary bed precipitates respiratory decompression sickness. While common dive profiles in scuba-diving usually prevent massive N_2 bubble generation, incidence of pulmonary decompression sickness in aviators has been reported as high as 6%.[81]

Another possible complication of DCI is *arterial gas embolism* which may occur when growing N_2 bubbles spill over to the arterial system through intracardiac or extracardiac shunts and embolize to small arteries. Postembolic pathology is caused by a reduction in perfusion distal to the obstruction and an inflammatory response to the bubble.[82] Arterial emboli may occlude end arteries throughout the body and cause serious morbidity or death if they occlude cardiac or cerebral vessels (i.e., cerebral arterial gas embolism). The latter is a frequent and serious dive-related injury in compressed air scuba-diving, which may possibly be precipitated by the diver's posture on ascent from depth. Notably, cerebral arterial gas embolism in divers has been linked to the presence of cerebral white matter lesions and, thus, may occur more frequently and in the absence of clinical symptoms (see below).

As discussed above, emerging N_2 microbubbles are usually filtered in the lung microcirculation where the gas diffuses into the alveolar space along a PN_2 gradient. The lungs' capacity to effectively filter N_2 bubbles, however, depends on size and number of bubbles trapped in the pulmonary circulation, and may be impaired by administration of pulmonary vasodilators.[77] In a dog model of respiratory decompression sickness, an overload threshold of the pulmonary vasculature could be determined at an infusion rate of 0.3 mL kg^{-1} min^{-1}.[83,84] Higher infusion doses of 0.35 mL kg^{-1} $minute^{-1}$ resulted in arterial bubbles as detected by Doppler ultrasound in more than 50% of the dogs. An elevation in pulmonary artery pressure was required before the spillover of venous gas bubbles occurred, with a pressure gradient between pulmonary artery pressure and left atrial pressure of approximately 52 mm Hg.[84] In a swine model, breakthrough of bubbles was already apparent at 0.1 mL kg^{-1} min^{-1} and was related to substantial reduction in mean arterial pressure and pulmonary artery pressure that had returned to normal at the time of spillover.[79] Although the time course of changes in mean pulmonary artery pressure in swine following rapid decompression from a 30-minute exposure to 500 kPa was related to the Doppler bubble counts in the pulmonary artery, there was great variation in the degree of bubble formation.[85]

Another route for N_2 bubbles to become arterialized is through extrapulmonary arterio-venous right-to-left shunts. PFO, the most common right-to-left shunt, has been demonstrated to be related to otherwise unexplained DCI in divers.[86,87] A PFO can be found in up to one-third of the general population and uncommonly poses a significant health risk in normal life because high left atrial pressure forces the interseptal valve against the septum. In divers, however, pressure equalization procedures during and after diving raise intra-abdominal pressure leading to a concomitant increase in right atrial pressure which enables passage of gas bubbles through the PFO. Accordingly, a shunt of venous bubbles could be shown by transcranial Doppler ultrasound in divers with a PFO who had developed venous gas emboli after two experimental chamber dives.[88] In a field study of recreational scuba-divers, arterial microembolic signals were detected by transcranial Doppler in 6 out of 40 asymptomatic divers who also had a significant venous bubble load.[64] Of note, in another field study using transcranial Doppler ultrasound, no arterial signals were detected after multiple dives in commercial divers with a PFO,[89] indicating that strict adherence to decompression procedures may prevent divers from significant bubble formation.

Recent data from a large prospective study in 148 divers with 66,859 collected dives revealed that a total of 8.3% of divers without and 28.6% of divers with a right-to-left shunt experienced a confirmed episode of DCI during the study period.[90] The incidence of DCI per 10,000 dives was 1.95 and 5.16, respectively, indicating a relative risk of 2.65 (confidence interval: 1.05–6.72, $p = 0.039$). This incidence is consistent with previous data derived from meta-analysis of three studies that reported incidences for DCI and echocardiographic presence of a PFO in different diving populations.[91] From these studies it can be concluded that the incidence of DCI in recreational scuba-divers averaged 0.02% and, thus, the absolute increase of risk in the presence of a PFO remains small. Of note, the size of PFO has been shown to be related to the risk of DCI with a 4.4-fold risk increase in divers with grade 2 PFO and a 6.6-fold increase in divers with grade 3 PFO.[92] PFO closure may successfully prevent from future DCI in scuba-divers with a high-grade PFO.[93]

There have been early reports of an increased prevalence of cerebral white-matter hyperintensities, even in asymptomatic divers, when compared with age-matched control subjects,[94] and it could be shown that multiple brain lesions in recreational scuba-divers with a PFO were associated with the presence of PFO.[95,96] These white matter hyperintensities as detectable on brain magnetic resonance imaging (MRI) were regarded as typical MRI expressions of cerebral small-vessel disease. Pathological correlates are varied with most pointing toward white-matter hyperintensities as a reflection of small-vessel ischemic burden. However, subsequent studies failed to show an increased prevalence of brain lesions in well-controlled cohorts of military scuba-divers without a history of DCI.[97,98] In a recent study[99] including strictly randomized recreational scuba-divers with no history of even mild DCI, a grade 2 PFO was found in 16 (38%) of the divers and brain lesions were identified using MRI in 5 (11.9%). There was no association between PFO and the presence or size of these lesions. A distinct and significant deterioration in neuro-psychometric test performance suggested a decrease of short-term memory and higher cognitive function, including visual-motor skills, which would be in line with previous findings in military and commercial divers.[100,101] However, it may be concluded that uneventful recreational diving, with or without PFO, does not seem to have any influence on the prevalence of MRI brain lesions, and whether there is a clear association between diving exposure and cognitive deficits remains to be established.

Pulmonary Barotrauma of Ascent

Deep-diving simulations in pressure chambers have shown that high absolute pressure, per se, can be well tolerated by the lungs; however, even small and abrupt changes in ambient pressure may elevate transpulmonary pressure and eventually cause barotrauma of the lungs.[102] Pulmonary barotrauma may occur during the ascent of a scuba-dive when ambient pressure is reduced and expanding air is not exhaled quickly enough. Studies in dogs with blocked trachea during ascent showed that pulmonary barotrauma occurred after rapid decompression of ambient pressures between 4.1 and 7.2 ata (corresponding to 31–62 m water depth) when the intratracheal pressure reached a critical level of approximately 80.3 mm Hg.[103] Interestingly, application of pressure bandages to the chest and abdomen could prevent pulmonary barotrauma, despite intratracheal pressure values of 180 mm Hg. Corresponding experiments on human corpses showed that pulmonary barotrauma occurred at intrapulmonary pressure values of approximately 73 to 80 mm Hg. For chest and abdominal pressure bandages, higher values of

133 to 190 mm Hg were necessary to cause barotrauma.[104] From these experiments, it could be concluded that the transpulmonary pressure, i.e., the difference between intratracheal and intrapleural pressure, was directly related to risk of barotrauma.

Air trapping may occur during ascent in any region in the airways and result in rupture of thin-walled structures, including alveoli or small bronchioles.[105] Further clinical complications are a function of the anatomic location of rupture and amount of escaped air: escaping gas may be sucked into the peribronchial space and cause interstitial emphysema; gas can continue to creep into the tissue and cause mediastinal or subcutaneous emphysema. It may also escape toward the lung periphery via ruptures of subpleural blisters into the pleural space and cause pneumothorax. Alternatively, mediastinal gas can rupture the mediastinal pleura and enter the pleural space. Furthermore, extra-alveolar gas can also pass through the esophageal hiatus and cause pneumoperitoneum.

The rate of decompression contributes to risk of pulmonary barotrauma as it reduces the time for expanding intrapulmonary air to escape through airways. In fact, the highest incidences of pulmonary barotrauma have been reported from submarine escape trainings or free emergency ascents[106,107]; any rapid or emergency ascent where the scuba-diver is not exhaling properly increases the risk of pulmonary barotrauma. Accordingly, pulmonary barotrauma has been reported less frequently from high-altitude exposures as ambient pressure changes within air cabins are modest compared with underwater diving. However, a case of fatal arterial gas embolism caused by rupture of a giant intrapulmonary air cyst has been reported from a commercial airplane passenger after a drop in cabin pressure by approximately 200 mm Hg.[108] Cases have also been reported during pilot training in negative pressure chambers[109–111] and after cabin pressure tests of aircraft.[112,113] Pre-existing lung pathology seems to have precipitated lung rupture in many cases of high-altitude pulmonary barotrauma where pressure change occurs at a slower pace during ascent.

The most serious clinical manifestation of pulmonary barotrauma of ascent is cerebral arterial gas embolism, a more frequent serious dive-related injury associated with high morbidity and mortality.[82] During ascent from a scuba-dive, expanding air may escape along the perivascular vascular bed of the pulmonary arterioles and enter such an arteriole, or escape during exhalation toward the pulmonary hila and enter the anatomically thin-walled pulmonary veins and enter the left heart. Arterial gas embolism actually is a frequent complication of pulmonary barotrauma in scuba-diving, in contrast to pulmonary barotrauma as a complication of mechanical ventilation, which typically only causes pneumothorax and/or mediastinal emphysema.[114] This may be due to the direction and the magnitude of the transpulmonary pressure elevation following decompression.

Of note, the risk of pulmonary barotrauma on ascent from depth is greatest in the last 10 m below sea level as the ambient pressure halves over this distance. Accordingly, cases of severe arterial air embolism have been reported after scuba-diving in a swimming pool or at shallow water ascents from depths of only 1 m.[115–117]

Next to an increased decompression rate, individual factors such as lung parenchymal abnormalities and airflow limitation due to obstructive airway diseases are associated with increased risk of pulmonary barotrauma. Poorly ventilated lung areas such as blisters or cysts can ultimately promote air trapping. Accordingly, valve mechanisms of emphysematous changes have been described, which explained an obstruction of the outflow of gas from these structures during exhalation.[108] Emphysematous bullae and lung cysts have indeed been described by thoracic imaging in scuba-divers suffering pulmonary barotrauma and in few cases proof could be presented that these abnormalities had been present even before the injury.[118–122] Obstructive airway changes or a history of asthma has also been reported more frequently among cases of pulmonary barotrauma of ascent.[116,117,123] In an autopsy study on 13 fatal diving accidents in which the primary cause of death was lung damage, the presence of pleural adhesions and lung bullae was reported, some of which were involved in causing tissue damage.[123] Decreased pulmonary distensibility may also increase risk of barotrauma.[124] In a retrospective analysis of cases of pulmonary barotrauma after submarine rescue ascents, a significant correlation between the occurrence of pulmonary barotrauma and a lower than predicted value of forced vital capacity was obtained. Both studies indicate that restrictive pulmonary disease or stiffer lungs in general could precipitate pulmonary barorotrauma.[125]

Immersion Pulmonary Edema

The occurrence of immersion pulmonary edema was initially reported from recreational scuba-divers after open sea dives in cold water.[126] An abnormal increase in vascular resistance to cold exposure was assumed to have precipitated edema by raising cardiac preload and afterload, since healthy controls did not show the same degree of increase in forearm vascular resistance to experimental cold exposure. However, subsequent studies reported pulmonary edema in subjects while scuba-diving or swimming in cold and in warm waters[127] with no evidence of abnormal vascular reactivity, and cases of immersion pulmonary edema were reported in competitive swimmers, triathletes, and during aqua jogging.[128–130] From more recent prospective cohort studies it became obvious that swimming-induced pulmonary edema occurs more frequently than previously thought and that there is some likelihood of recurrence in susceptible subjects (►**Table 2**).

While unique environmental conditions across these different exposures might have contributed to development of pulmonary edema, a common denominator was that the subject was immersed in water when the condition occurred. The stress generated by increased transalveolar pressure during immersion may lead to increasing leakage of the capillary endothelial layer. Increased accumulation of extravascular lung water without development of clinical signs of pulmonary edema can be detected even after scuba-dives without physical exercise.[131] Accumulation of extravascular

Table 2 Frequency of reported immersion pulmonary edema (IPE) cases according to study design and setting

Study	Design	Cohort	IPE frequency	Investigations	Recurrent events
Pons et al 1995[127]	Case reports and survey	460 respondents (divers and swimmers)	5 (1.1%)	Patient-reported data	1/4 (25%)
Weiler-Ravell et al 1995[128]	Prospective cohort	30 military trainees	8 (26.7%)	Symptoms, auscultation, SaO_2	2/8 (25%)
Adir et al 2004[142]	Prospective evaluation over 3 years	Military trainees (total not reported)	70 (1.8%)	CXR, symptoms, auscultation, SaO_2	16/70 (22%)
Miller et al 2010[129]	Online survey and case–control study	31/1,400 responders among U.S. triathletes	20 (1.4%)	Symptoms	Not reported
Smith et al 2018[143]	Retrospective analysis	68,557 triathletes	5 (0.007%)	Symptoms, patient records	2/5 (40%)
Hårdstedt et al 2020[144]	Prospective cohort	17,904 swimmers	102 (0.57%)	Lung ultrasound, auscultation, SaO_2, symptoms	Not reported
Volk et al 2021[145]	Prospective cohort	2,117 military trainees	106 (5%)	CXR, auscultation, symptoms	10/106 (9.43%)
Hårdstedt et al 2021[146]	Prospective cohort	45,913 recreational/competitive swimmers over 4 consecutive years	211 (0.44%)	Lung ultrasound, auscultation, symptoms	Not reported

Abbreviations: CXR, chest X-ray; S_aO_2, oxygen saturation.

lung water was associated with a significant increase in mean pulmonary artery pressure, a decrease in left ventricular contractility, and an augmented NT-proBNP release, suggesting significant cardiopulmonary strain. An increase in pulmonary artery pressure during repetitive dives suggested that there might exist a cumulative effect increasing the risk for development of pulmonary edema with repetitive scuba-dives.[131] Physical exercise was not a contributing factor in reported cases of diving-related immersion pulmonary edema.[132–134] Increased density of breathing gas at depth produces higher airway resistance and augments intrathoracic pressure swings between inspiration and expiration; greater negative intrathoracic pressure during inspiration increases right ventricular preload. It could be shown that negative pressure breathing combined with exercise resulted in much greater increases in right heart preload, pulmonary artery systolic pressure, and worsened interstitial edema formation as demonstrated by lung ultrasound.[135,136]

Exercise in water, however, places a unique set of stresses on the respiratory system due the effects of immersion on passive redistribution of venous blood from the extremities to the heart and pulmonary vessels, thereby increasing pulmonary artery systolic pressure. Exercise further increases thoracic blood volume and left atrial, pulmonary artery, and capillary pressures. Cold water immersion and exercise both increase mean arterial, pulmonary arterial, and pulmonary artery wedge pressures during prone immersion.[137] A two- to threefold variation in mean pulmonary artery pressure and pulmonary artery wedge pressure was reported from submersed exercise among study subjects, consistent with variation in individual susceptibility to immersion pulmonary edema[138] (►**Fig. 4**). Of note, pulmonary artery pressure even under dry exercise conditions may vary with age in subjects older than 50 years of age, and it has been suspected that high pulmonary artery pressure values during exercise in patients aged over 50 years might have been related partly to underlying diastolic

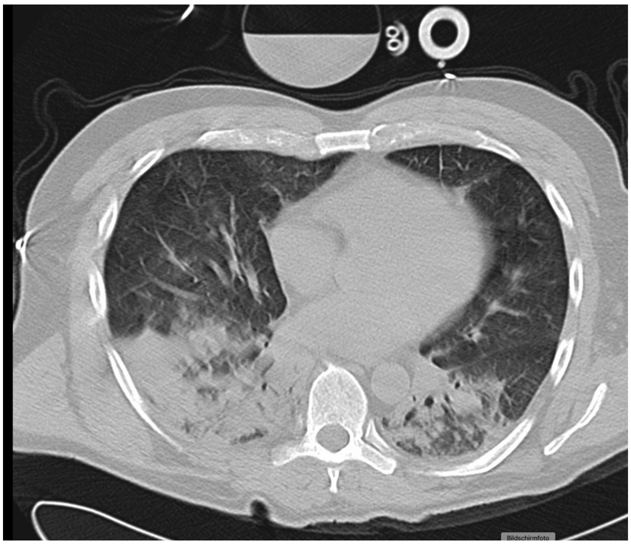

Fig. 4 Chest-computed tomography showing pulmonary edema in a 55-year-old male diver with a history of arterial hypertension. (Image courtesy: A. Koch, MD, German Naval Medical Institute, Kiel, Germany.)

dysfunction of the left ventricle.[139] Increased age has often been reported in cases of diving-related immersion pulmonary edema in otherwise healthy individuals.[132,133,140] It could finally be demonstrated that subjects with a history of immersion pulmonary edema developed higher mean pulmonary artery pressure and pulmonary artery wedge pressure during exercise in cold water in comparison with the general population,[141] and that these pressures could be reduced with a single 50-mg oral dose of sildenafil, a PDE-5 inhibitor.

In conclusion, diving-related pulmonary edema shares fundamental pathophysiologic mechanisms with swimming-induced pulmonary edema; however, factors related to diving apparatus and posture may play a key precipitating role next to immersion, and less so exercise and cold.

Conflict of Interest
None declared.

References

1 Number of participants in scuba diving in the United States from 2006 to 2020. Accessed April 20, 2023 at: https://www.statista.com/statistics/191304/participants-in-scuba-diving-in-the-us-since-2006/

2 Competitive freediving. Accessed April 20, 2023 at: https://usafreediving.com/competitive-freediving/

3 Tillmans F ed. DAN Annual Diving Report 2020 Edition - A Report on 2018 Diving Fatalities, Injuries, and Incidents. Durham, NC: Divers Alert Network; 2020

4 Vann RD, Lang MA eds. Recreational Diving Fatalities. Proceedings of the Divers Alert Network 2010 April 8–10. Workshop. Durham, NCDivers Alert Network2011

5 Bove AA. Diving medicine. Am J Respir Crit Care Med 2014;189 (12):1479–1486

6 British Thoracic Society Fitness to Dive Group, Subgroup of the British Thoracic Society Standards of Care Committee. British Thoracic Society guidelines on respiratory aspects of fitness for diving. Thorax 2003;58(01):3–13

7 Arborelius M Jr, Ballidin UI, Lilja B, Lundgren CE. Hemodynamic changes in man during immersion with the head above water. Aerosp Med 1972;43(06):592–598

8 Pendergast DR, Lundgren CE. The underwater environment: cardiopulmonary, thermal, and energetic demands. J Appl Physiol 2009;106(01):276–283

9 Prefaut C, Lupi-h E, Anthonisen NR. Human lung mechanics during water immersion. J Appl Physiol 1976;40(03):320–323

10 Guyatt AR, Newman F, Cinkotai FF, Palmer JI, Thomson ML. Pulmonary diffusing capacity in man during immersion in water. J Appl Physiol 1965;20(05):878–881

11 Foster GE, Sheel AW. The human diving response, its function, and its control. Scand J Med Sci Sports 2005;15(01):3–12

12 Heusser K, Dzamonja G, Tank J, et al. Cardiovascular regulation during apnea in elite divers. Hypertension 2009;53(04): 719–724

13 Eichhorn L, Erdfelder F, Kessler F, et al. Influence of apnea-induced hypoxia on catecholamine release and cardiovascular dynamics. Int J Sports Med 2017;38(02):85–91

14 Joulia F, Lemaitre F, Fontanari P, Mille ML, Barthelemy P. Circulatory effects of apnoea in elite breath-hold divers. Acta Physiol (Oxf) 2009;197(01):75–82

15 Eichhorn L, Doerner J, Luetkens JA, et al. Cardiovascular magnetic resonance assessment of acute cardiovascular effects of voluntary apnoea in elite divers. J Cardiovasc Magn Reson 2018;20 (01):40

16 Costalat G, Coquart J, Castres I, et al. The oxygen-conserving potential of the diving response: a kinetic-based analysis. J Sports Sci 2017;35(07):678–687

17 Perini R, Tironi A, Gheza A, Butti F, Moia C, Ferretti G. Heart rate and blood pressure time courses during prolonged dry apnoea in breath-hold divers. Eur J Appl Physiol 2008;104(01):1–7

18 Olsen CR, Fanestil DD, Scholander PF. Some effects of apneic underwater diving on blood gases, lactate, and pressure in man. J Appl Physiol 1962;17:938–942

19 Scholander PF, Hammel HT, Lemessurier H, Hemmingsen E, Garey W. Circulatory adjustment in pearl divers. J Appl Physiol 1962;17:184–190

20 Hansel J, Solleder I, Gfroerer W, et al. Hypoxia and cardiac arrhythmias in breath-hold divers during voluntary immersed breath-holds. Eur J Appl Physiol 2009;105(05):673–678

21 Ferrigno M, Grassi B, Ferretti G, et al. Electrocardiogram during deep breath-hold dives by elite divers. Undersea Biomed Res 1991;18(02):81–91

22 Ferrigno M, Ferretti G, Ellis A, et al. Cardiovascular changes during deep breath-hold dives in a pressure chamber. J Appl Physiol 1997;83(04):1282–1290

23 Lindholm P, Lundgren CEG. The physiology and pathophysiology of human breath-hold diving. J Appl Physiol 2009;106(01): 284–292

24 AIDA official World Records History. World Records. Accessed April 20, 2023 at: https://www.aidainternational.org/WorldRecords/History

25 Agostoni E Limitation to depths of diving mechanics of chest wall. In: Rahn H, Yokoyama T, eds. Physiology of Breath-Hold Diving and the Ama of Japan. Washington, DC: National Academy of Sciences; 1965:139–145

26 Craig AB Jr. Depth limits of breath hold diving (an example of Fennology). Respir Physiol 1968;5(01):14–22

27 Schaefer KE, Allison RD, Dougherty JHJ Jr, et al. Pulmonary and circulatory adjustments determining the limits of depths in breathhold diving. Science 1968;162(3857):1020–1023

28 Dail CW. “Glossopharyngeal breathing” by paralyzed patients; a preliminary report. Calif Med 1951;75(03):217–218

29 Bach JR, Bianchi C, Vidigal-Lopes M, Turi S, Felisari G. Lung inflation by glossopharyngeal breathing and “air stacking” in Duchenne muscular dystrophy. Am J Phys Med Rehabil 2007;86 (04):295–300

30 Bach JR, Tewfik G. Air doping: an exposé on “frog” insufflation in competitive sports. Am J Phys Med Rehabil 2007;86(04): 301–303

31 Muth CM, Radermacher P, Pittner A, et al. Arterial blood gases during diving in elite apnea divers. Int J Sports Med 2003;24(02): 104–107

32 Nygren-Bonnier M, Gullstrand L, Klefbeck B, Lindholm P. Effects of glossopharyngeal pistoning for lung insufflation in elite swimmers. Med Sci Sports Exerc 2007;39(05):836–841

33 Tetzlaff K, Scholz T, Walterspacher S, et al. Characteristics of the respiratory mechanical and muscle function of competitive breath-hold divers. Eur J Appl Physiol 2008;103(04): 469–475

34 Eichinger M, Walterspacher S, Scholz T, et al; Breath-hold Diving Study Group of Baden-Württemberg. Lung hyperinflation: foe or friend? Eur Respir J 2008;32(04):1113–1116

35 Lindholm P, Nyrén S. Studies on inspiratory and expiratory glossopharyngeal breathing in breath-hold divers employing magnetic resonance imaging and spirometry. Eur J Appl Physiol 2005;94(5–6):646–651

36 Overgaard K, Friis S, Pedersen RB, Lykkeboe G. Influence of lung volume, glossopharyngeal inhalation and P(ET) O2 and P(ET) CO2 on apnea performance in trained breath-hold divers. Eur J Appl Physiol 2006;97(02):158–164

37 Seccombe LM, Rogers PG, Mai N, Wong CK, Kritharides L, Jenkins CR. Features of glossopharyngeal breathing in breath-hold divers. J Appl Physiol 2006;101(03):799–801

38 Loring SH, O'Donnell CR, Butler JP, Lindholm P, Jacobson F, Ferrigno M. Transpulmonary pressures and lung mechanics with glossopharyngeal insufflation and exsufflation beyond normal lung volumes in competitive breath-hold divers. J Appl Physiol 2007;102(03):841–846

39 Seccombe LM, Chung SCS, Jenkins CR, et al. Lung perfusion and chest wall configuration is altered by glossopharyngeal breathing. Eur Respir J 2010;36(01):151–156

40 Nygren-Bonnier M, Lindholm P, Markström A, Skedinger M, Mattsson E, Klefbeck B. Effects of glossopharyngeal pistoning for lung insufflation on vital capacity in healthy women. Am J Phys Med Rehabil 2007;86(04):290–294

41 Schaefer KE, Carey CR. Alveolar pathways during 90-foot, breath-hold dives. Science 1962;137(3535):1051–1052

42 Linér MH, Linnarsson D. Intrapulmonary distribution of alveolar gas exchange during breath-hold diving in humans. J Appl Physiol 1995;78(02):410–416

43 Lindholm P. Loss of motor control and/or loss of consciousness during breath-hold competitions. Int J Sports Med 2007;28(04):295–299

44 Fitz-Clarke JR. Adverse events in competitive breath-hold diving. Undersea Hyperb Med 2006;33(01):55–62

45 Schagatay E, Andersson J. Diving response and apneic time in humans. Undersea Hyperb Med 1998;25(01):13–19

46 Schagatay E, van Kampen M, Emanuelsson S, Holm B. Effects of physical and apnea training on apneic time and the diving response in humans. Eur J Appl Physiol 2000;82(03):161–169

47 Boyd C, Levy A, McProud T, Huang L, Raneses E, Olson CCenters for Disease Control and Prevention (CDC) Fatal and nonfatal drowning outcomes related to dangerous underwater breath-holding behaviors - New York State, 1988-2011. MMWR Morb Mortal Wkly Rep 2015;64(19):518–521

48 Paulev P. Decompression sickness following repeated breath-hold dives. J Appl Physiol 1965;20(05):1028–1031

49 Kohshi K, Wong RM, Abe H, Katoh T, Okudera T, Mano Y. Neurological manifestations in Japanese Ama divers. Undersea Hyperb Med 2005;32(01):11–20

50 Schagatay E. Predicting performance in competitive apnea diving. Part III: deep diving. Diving Hyperb Med 2011;41(04):216–228

51 Fitz-Clarke JR. Mechanics of airway and alveolar collapse in human breath-hold diving. Respir Physiol Neurobiol 2007;159(02):202–210

52 Tetzlaff K, Schöppenthau H, Schipke JD. Risk of neurological insult in competitive deep breath-hold diving. Int J Sports Physiol Perform 2017;12(02):268–271

53 Schipke JD, Tetzlaff K. Why predominantly neurological decompression sickness in breath-hold divers? J Appl Physiol 2016;120(12):1474–1477

54 Laitila M, Eskola V. Spontaneous pneumomediastinum in an 11-year-old boy after a shallow breath-hold dive. Diving Hyperb Med 2013;43(04):235–236

55 Jacobson FL, Loring SH, Ferrigno M. Pneumomediastinum after lung packing. Undersea Hyperb Med 2006;33(05):313–316

56 Chung SC, Seccombe LM, Jenkins CR, Frater CJ, Ridley LJ, Peters MJ. Glossopharyngeal insufflation causes lung injury in trained breath-hold divers. Respirology 2010;15(05):813–817

57 Cialoni D, Sponsiello N, Marabotti C, et al. Prevalence of acute respiratory symptoms in breath-hold divers. Undersea Hyperb Med 2012;39(04):837–844

58 Lindholm P, Ekborn A, Oberg D, Gennser M. Pulmonary edema and hemoptysis after breath-hold diving at residual volume. J Appl Physiol 2008;104(04):912–917

59 Strauss MB, Wright PW. Thoracic squeeze diving casualty. Aerosp Med 1971;42(06):673–675

60 Boussuges A, Pinet C, Thomas P, Bergmann E, Sainty JM, Vervloet D. Haemoptysis after breath-hold diving. Eur Respir J 1999;13(03):697–699

61 Kiyan E, Aktas S, Toklu AS. Hemoptysis provoked by voluntary diaphragmatic contractions in breath-hold divers. Chest 2001;120(06):2098–2100

62 Training fundamentals: following recommended dive limits. Accessed April 20, 2023 at: https://scubadiverlife.com/training-fundamentals-following-recommended-dive-limits/

63 Butler BD, Hills BA. The lung as a filter for microbubbles. J Appl Physiol 1979;47(03):537–543

64 Gerriets T, Tetzlaff K, Liceni T, et al. Arteriovenous bubbles following cold water sport dives: relation to right-to-left shunting. Neurology 2000;55(11):1741–1743

65 Carturan D, Boussuges A, Vanuxem P, Bar-Hen A, Burnet H, Gardette B. Ascent rate, age, maximal oxygen uptake, adiposity, and circulating venous bubbles after diving. J Appl Physiol 2002;93(04):1349–1356

66 Dujić Z, Eterović D, Denoble P, Krstacić G, Tocilj J, Gosović S Effect of a single air dive on pulmonary diffusing capacity in professional divers. J Appl Physiol 1993;74(01):55–61

67 Thorsen E, Risberg J, Segadal K, Hope A. Effects of venous gas microemboli on pulmonary gas transfer function. Undersea Hyperb Med 1995;22(04):347–353

68 Eckenhoff RG, Olstad CS, Carrod G. Human dose-response relationship for decompression and endogenous bubble formation. J Appl Physiol 1990;69(03):914–918

69 Bove AA, Hallenbeck JM, Elliott DH. Circulatory responses to venous air embolism and decompression sickness in dogs. Undersea Biomed Res 1974;1(03):207–220

70 Neuman TS, Spragg RG, Wagner PD, Moser KM. Cardiopulmonary consequences of decompression stress. Respir Physiol 1980;41(02):143–153

71 Peterson BT, Grauer SE, Hyde RW, Ortiz C, Moosavi H, Utell MJ. Response of pulmonary veins to increased intracranial pressure and pulmonary air embolization. J Appl Physiol 1980;48(06):957–964

72 Levin LL, Stewart GJ, Lynch PR, Bove AA. Blood and blood vessel wall changes induced by decompression sickness in dogs. J Appl Physiol 1981;50(05):944–949

73 Ward CA, McCullough D, Fraser WD. Relation between complement activation and susceptibility to decompression sickness. J Appl Physiol 1987;62(03):1160–1166

74 Ohkuda K, Nakahara K, Binder A, Staub NC. Venous air emboli in sheep: reversible increase in lung microvascular permeability. J Appl Physiol 1981;51(04):887–894

75 Buttolph TB, Dick EJ Jr, Toner CB, et al. Cutaneous lesions in swine after decompression: histopathology and ultrastructure. Undersea Hyperb Med 1998;25(02):115–121

76 Hartig F, Reider N, Sojer M, et al. Livedo racemosa - the pathophysiology of decompression-associated cutis marmorata and right/left shunt. Front Physiol 2020;11:994

77 Butler BD, Hills BA. Transpulmonary passage of venous air emboli. J Appl Physiol 1985;59(02):543–547

78 Catron PW, Flynn ET Jr, Yaffe L, et al. Morphological and physiological responses of the lungs of dogs to acute decompression. J Appl Physiol 1984;57(02):467–474

79 Vik A, Brubakk AO, Hennessy TR, Jenssen BM, Ekker M, Slørdahl SA. Venous air embolism in swine: transport of gas bubbles through the pulmonary circulation. J Appl Physiol 1990;69(01):237–244

80 Atkins CE, Lehner CE, Beck KA, Dubielzig RR, Nordheim EV, Lanphier EH. Experimental respiratory decompression sickness in sheep. J Appl Physiol 1988;65(03):1163–1171

81 Wirjosemito SA, Touhey JE, Workman WT. Type II altitude decompression sickness (DCS): U.S. Air Force experience with 133 cases. Aviat Space Environ Med 1989;60(03):256–262

82 Muth CM, Shank ES. Gas embolism. N Engl J Med 2000;342(07):476–482

83 Butler BD, Luehr S, Katz J. Venous gas embolism: time course of residual pulmonary intravascular bubbles. Undersea Biomed Res 1989;16(01):21–29

84 Butler BD, Katz J. Vascular pressures and passage of gas emboli through the pulmonary circulation. Undersea Biomed Res 1988;15(03):203–209

85 Vik A, Jenssen BM, Eftedal O, Brubakk AO. Relationship between venous bubbles and hemodynamic responses after decompression in pigs. Undersea Hyperb Med 1993;20(03):233–248

86 Wilmshurst PT, Byrne JC, Webb-Peploe MM. Relation between interatrial shunts and decompression sickness in divers. Lancet 1989;2(8675):1302–1306

87 Moon RE, Camporesi EM, Kisslo JA. Patent foramen ovale and decompression sickness in divers. Lancet 1989;1(8637):513–514

88 Ries S, Knauth M, Kern R, et al. Arterial gas embolism after decompression: correlation with right-to-left shunting. Neurology 1999;52(02):401–404

89 Glen SK, Georgiadis D, Grosset DG, Douglas JDM, Lees KR. Transcranial Doppler ultrasound in commercial air divers: a field study including cases with right-to-left shunting. Undersea Hyperb Med 1995;22(02):129–135

90 Germonpré P, Lafère P, Portier W, Germonpré F-L, Marroni A, Balestra C. Increased risk of decompression sickness when diving with a right-to-left shunt: results of a prospective single-blinded observational study (the "Carotid Doppler" Study). Front Physiol 2021;12:763408

91 Bove AA. Risk of decompression sickness with patent foramen ovale. Undersea Hyperb Med 1998;25(03):175–178

92 Torti SR, Billinger M, Schwerzmann M, et al. Risk of decompression illness among 230 divers in relation to the presence and size of patent foramen ovale. Eur Heart J 2004;25(12):1014–1020

93 Honěk J, Šrámek M, Honěk T, et al. Patent foramen ovale closure is effective in divers: long-term results from the DIVE-PFO registry. J Am Coll Cardiol 2020;76(09):1149–1150

94 Reul J, Weis J, Jung A, Willmes K, Thron A. Central nervous system lesions and cervical disc herniations in amateur divers. Lancet 1995;345(8962):1403–1405

95 Knauth M, Ries S, Pohimann S, et al. Cohort study of multiple brain lesions in sport divers: role of a patent foramen ovale. BMJ 1997;314(7082):701–705

96 Schwerzmann M, Seiler C, Lipp E, et al. Relation between directly detected patent foramen ovale and ischemic brain lesions in sport divers. Ann Intern Med 2001;134(01):21–24

97 Cordes P, Keil R, Bartsch T, et al. Neurologic outcome of controlled compressed-air diving. Neurology 2000;55(11):1743–1745

98 Gerriets T, Tetzlaff K, Hutzelmann A, et al. Association between right-to-left shunts and brain lesions in sport divers. Aviat Space Environ Med 2003;74(10):1058–1060

99 Balestra C, Germonpré P Correlation between patent foramen ovale, cerebral "lesions" and neuropsychometric testing in experienced sports divers: does diving damage the brain? Front Psychol 2016;7:696

100 Slosman DO, De Ribaupierre S, Chicherio C, et al. Negative neurofunctional effects of frequency, depth and environment in recreational scuba diving: the Geneva "memory dive" study. Br J Sports Med 2004;38(02):108–114

101 Tetzlaff K, Friege L, Hutzelmann A, Reuter M, Höll D, Leplow B. Magnetic resonance signal abnormalities and neuropsychological deficits in elderly compressed-air divers. Eur Neurol 1999;42(04):194–199

102 Russi EW. Diving and the risk of barotrauma. Thorax 1998;53(suppl 2):S20–S24

103 Schaffer KE, McNULTY WP Jr, Carey C, Liebow AA. Mechanisms in development of interstitial emphysema and air embolism on decompression from depth. J Appl Physiol 1958;13(01):15–29

104 Malhotra MS, Wright HC. The effects of a raised intrapulmonary pressure on the lungs of fresh unchilled cadavers. J Pathol Bacteriol 1961;82:198–202

105 Liebow AA, Stark JE, Vogel J, Schaefer KE. Intrapulmonary air trapping in submarine escape training casualties. U S Armed Forces Med J 1959;10(03):265–289

106 Broome CR, Jarvis LJ, Clark RJ. Pulmonary barotrauma in submarine escape training. Thorax 1994;49(02):186–187

107 Lafère P, Germonpré P, Balestra C. Pulmonary barotrauma in divers during emergency free ascent training: review of 124 cases. Aviat Space Environ Med 2009;80(04):371–375

108 Zaugg M, Kaplan V, Widmer U, Baumann PC, Russi EW. Fatal air embolism in an airplane passenger with a giant intrapulmonary bronchogenic cyst. Am J Respir Crit Care Med 1998;157(5, Pt 1):1686–1689

109 Rudge FW. Altitude-induced arterial gas embolism: a case report. Aviat Space Environ Med 1992;63(03):203–205

110 Rios-Tejada F, Azofra-Garcia J, Valle-Garrido J, Pujante Escudero A. Neurological manifestation of arterial gas embolism following standard altitude chamber flight: a case report. Aviat Space Environ Med 1997;68(11):1025–1028

111 Cable GG, Keeble T, Wilson G. Pulmonary cyst and cerebral arterial gas embolism in a hypobaric chamber: a case report. Aviat Space Environ Med 2000;71(02):172–176

112 Lee CT. Cerebral arterial gas embolism in air force ground maintenance crew–a report of two cases. Aviat Space Environ Med 1999;70(07):698–700

113 Hickey MJ, Zanetti CL. Delayed-onset cerebral arterial gas embolism in a commercial airline mechanic. Aviat Space Environ Med 2003;74(09):977–980

114 Zwillich CW, Pierson DJ, Creagh CE, Sutton FD, Schatz E, Petty TL. Complications of assisted ventilation. A prospective study of 354 consecutive episodes. Am J Med 1974;57(02):161–170

115 Benton PJ, Woodfine JD, Westwood PR. Arterial gas embolism following a 1-meter ascent during helicopter escape training: a case report. Aviat Space Environ Med 1996;67(01):63–64

116 Raymond LW. Pulmonary barotrauma and related events in divers. Chest 1995;107(06):1648–1652

117 Weiss LD, Van Meter KW. Cerebral air embolism in asthmatic scuba divers in a swimming pool. Chest 1995;107(06):1653–1654

118 Mellem H, Emhjellen S, Horgen O. Pulmonary barotrauma and arterial gas embolism caused by an emphysematous bulla in a SCUBA diver. Aviat Space Environ Med 1990;61(06):559–562

119 Reuter M, Tetzlaff K, Warninghoff V, Steffens JC, Bettinghausen E, Heller M. Computed tomography of the chest in diving-related pulmonary barotrauma. Br J Radiol 1997;70(833):440–445

120 Toklu AS, Kiyan E, Aktas S, Cimsit M. Should computed chest tomography be recommended in the medical certification of professional divers? A report of three cases with pulmonary air cysts. Occup Environ Med 2003;60(08):606–608

121 Germonpré P, Balestra C, Pieters T. Influence of scuba diving on asymptomatic isolated pulmonary bullae. Diving Hyperb Med 2008;38(04):206–211

122 Tetzlaff K, Reuter M, Leplow B, Heller M, Bettinghausen E. Risk factors for pulmonary barotrauma in divers. Chest 1997;112(03):654–659

123 Calder IM. Autopsy and experimental observations on factors leading to barotrauma in man. Undersea Biomed Res 1985;12(02):165–182

124 Colebatch HJ, Ng CK. Decreased pulmonary distensibility and pulmonary barotrauma in divers. Respir Physiol 1991;86(03):293–303

125 Benton PJ, Francis TJR, Pethybridge RJ. Spirometric indices and the risk of pulmonary barotrauma in submarine escape training. Undersea Hyperb Med 1999;26(04):213–217

126 Wilmshurst PT, Nuri M, Crowther A, Webb-Peploe MM. Cold-induced pulmonary oedema in scuba divers and swimmers and subsequent development of hypertension. Lancet 1989;1(8629):62–65
127 Pons M, Blickenstorfer D, Oechslin E, et al. Pulmonary oedema in healthy persons during scuba-diving and swimming. Eur Respir J 1995;8(05):762–767
128 Weiler-Ravell D, Shupak A, Goldenberg I, et al. Pulmonary oedema and haemoptysis induced by strenuous swimming. BMJ 1995;311(7001):361–362
129 Miller CC III, Calder-Becker K, Modave F. Swimming-induced pulmonary edema in triathletes. Am J Emerg Med 2010;28(08):941–946
130 Wenger M, Russi EW. Aqua jogging-induced pulmonary oedema. Eur Respir J 2007;30(06):1231–1232
131 Marinovic J, Ljubkovic M, Obad A, et al. Assessment of extravascular lung water and cardiac function in trimix SCUBA diving. Med Sci Sports Exerc 2010;42(06):1054–1061
132 Hampson NB, Dunford RG. Pulmonary edema of scuba divers. Undersea Hyperb Med 1997;24(01):29–33
133 Slade JB Jr, Hattori T, Ray CS, Bove AA, Cianci P. Pulmonary edema associated with scuba diving : case reports and review. Chest 2001;120(05):1686–1694
134 Castagna O, de Maistre S, Schmid B, Caudal D, Regnard J. Immersion pulmonary oedema in a healthy diver not exposed to cold or strenuous exercise. Diving Hyperb Med 2018;48(01):40–44
135 Castagna O, Gempp E, Poyet R, et al. Cardiovascular mechanisms of extravascular lung water accumulation in divers. Am J Cardiol 2017;119(06):929–932
136 Castagna O, Regnard J, Gempp E, et al. The key roles of negative pressure breathing and exercise in the development of interstitial pulmonary edema in professional male SCUBA divers. Sports Med Open 2018;4(01):1
137 Wester TE, Cherry AD, Pollock NW, et al. Effects of head and body cooling on hemodynamics during immersed prone exercise at 1 ATA. J Appl Physiol 2009;106(02):691–700
138 Peacher DF, Pecorella SR, Freiberger JJ, et al. Effects of hyperoxia on ventilation and pulmonary hemodynamics during immersed prone exercise at 4.7 ATA: possible implications for immersion pulmonary edema. J Appl Physiol 2010;109(01):68–78
139 Kovacs G, Berghold A, Scheidl S, Olschewski H. Pulmonary arterial pressure during rest and exercise in healthy subjects: a systematic review. Eur Respir J 2009;34(04):888–894
140 Edmonds C, Lippmann J, Lockley S, Wolfers D. Scuba divers' pulmonary oedema: recurrences and fatalities. Diving Hyperb Med 2012;42(01):40–44
141 Moon RE, Martina SD, Peacher DF, et al. Swimming-induced pulmonary edema: pathophysiology and risk reduction with sildenafil. Circulation 2016;133(10):988–996
142 Adir Y, Shupak A, Gil A, et al. Swimming-induced pulmonary edema: clinical presentation and serial lung function. Chest 2004;126(02):394–399
143 Smith R, Ormerod JOM, Sabharwal N, Kipps C. Swimming-induced pulmonary edema: current perspectives. Open Access J Sports Med 2018;9:131–137
144 Hårdstedt M, Seiler C, Kristiansson L, Lundeqvist D, Klingberg C, Braman Eriksson A. Swimming-induced pulmonary edema: diagnostic criteria validated by lung ultrasound. Chest 2020;158(04):1586–1595
145 Volk C, Spiro J, Boswell G, et al. Incidence and impact of swimming-induced pulmonary edema on navy seal candidates. Chest 2021;159(05):1934–1941
146 Hårdstedt M, Kristiansson L, Seiler C, Braman Eriksson A, Sundh J. Incidence of swimming-induced pulmonary edema: a cohort study based on 47,600 open-water swimming distances. Chest 2021;160(05):1789–1798